LTR-LCPT-21-11-NP Attachment

Application for Certificate of Compliance for the Traveller PWR Fuel Shipping Package

NRC Certificate of Compliance
USA/9380/B(U)F-96
Docket 71-9380

Safety Analysis Report, Revision 2

©2021 Westinghouse Electric Company LLC
All Rights Reserved

Application for Certificate of Compliance for the Traveller PWR Fuel Shipping Package

NRC Certificate of Compliance
USA/9380/B(U)F-96
Docket 71-9380

Safety Analysis Report, Revision 2

Westinghouse

IMPORTANT NOTICE REGARDING CONTENTS OF THIS REPORT PLEASE READ CAREFULLY

The information contained in this document is furnished for the purpose of obtaining NRC approval of the Traveller radioactive material transport package. The use of this information by anyone other than that for which it is intended is not authorized.

RECORD OF REVISIONS

Rev. No.	Date	Description of Revision
0	September 2018	Original application. (Ref: LTR-LCPT-18-24)
1	November 2019	RAI incorporation (Ref: LTR-LCPT-19-32)
2	June 2021	Major changes detailed here, all changes marked by Revision number and change bars in margin. (Ref: LTR-LCPT-21-11) Chapter 1 changes: • Revised text under Sections 1.1, 1.2.2.1, and 1.2.2.2 to clarify the permissible enrichments of each content. • Section 1.2.1.5.3 revised to include details of new bottom support spacer design for four-legged, side-skirted nozzles. • Licensing drawings and safety-related part table updated for new Type B shoring component. Chapter 2 changes: • Added text to Section 2.1.1.2 and 2.12.4 for the new bottom support spacer design. • Revision of Section 2.2.18 to include total strain energy absorption evaluation and materials comparison of existing alloys with advanced variations of chromium coating, liner, and aluminum, and stainless steel alloys Chapter 3 changes: • Section 3.2.1 and Table 3.2-2 updated to include U_3Si_2 fuel and alloy thermal properties. • Section 3.2.1.1 added to address thermal comparison of advanced cladding variations and alloys. Chapter 5 changes: • Section 5.1.2 text added to define impact of the increase to 6.0 wt.% from 5.0 wt.% ^{235}U shielding analysis. • Section 5.2, Source Specification, clarified 5.0 wt.% ^{235}U in analysis Chapter 6 changes: • Section 6.1.2, 6.1.3, and 6.2 updated summary of contents to include new fuel content Group 4 added for 6.0 wt.% ^{235}U fuel assemblies and 7 wt.% ^{235}U UO_2 loose fuel rod content. • Section 6.1.2 and 6.8 – two new benchmark series added to supplement the addition of 6 wt.% Group 4 contents and 7 wt.% UO2 loose rod contents. New USL equation generated and USL values in Table 6-1 updated and Group 4 USL calculation added. • Fuel Group restrictions updated for advanced fuel features, including doped pellets and cladding features, in Section 6.2 subsections. • New fuel content Group 4 added for 6.0 wt.% ^{235}U fuel assemblies, including complete assessment of CFA (Section 6.9.4 and 6.3.4.1), summary of restrictions (Section 6.2.3), modeling (Section 6.3.1.2 and 6.3.4), sensitivity studies (Section 6.3.4.3) and single package NCT/HAC (Section 6.4), NCT package array (Section 6.5) and HAC package array (Section 6.6)

Rev. No.	Date	Description of Revision
2 (cont.)		Chapter 6 changes (cont.) • Revised UO_2 loose fuel rod content to increase to 7 wt.% ^{235}U, including complete assessment of CFA (Section 6.9.4), summary of restrictions (Section 6.2.4) and single package NCT/HAC (Section 6.4), NCT package array (Section 6.5) and HAC package array (Section 6.6) • Section 6.3.3, Material Properties, updated for enrichment levels per content, advanced cladding features, guide tubes/instrument tubes, and integral absorbers. • Section 6.3.3.2 added for application of SCALE code 6.1.3. • Section 6.3.4.3 updated to clarify the penalty criteria, and summary of sensitivity studies for PWR Group 4 content and UO2 fuel rods. Detail added for PWR Group 4 polyethylene packing material study (Section 6.3.4.3.5), tolerance studies (Section 6.3.4.3.8, 6.3.4.3.9, and 6.3.4.3.10), steel nozzle study (Section 6.3.4.3.11) and addition of ADOPT fuel sensitivity study (Section 6.3.4.3.13) • Section 6.3.4 and Sections 6.4, 6.5, and 6.6 throughout – text revised to genericize "Groups 1 and 2" to "PWR fuel assembly Groups". • Section 6.4.1, 6.5.1, and 6.6.1 – updated results based on total penalty with the statistical significance criteria added. Group 4 added. ADOPT fuel study added. • Section 6.4.2, 6.5.2, and 6.6.2 – updated results with the statistical significance criteria applied. Group 4 baseline and sensitivity study results added. All UO_2 loose rod baseline and sensitivity study results updated for 7 wt.% enrichment. Single package HAC fuel assembly shift study and ADOPT rod studies added. • Section 6.9.2 (6.9.2.6.11-6.9.2.6.16) – CFA analysis added for Group 4 contents. Text revised throughout for Group 4 contents • Section 6.9.3 – Group 4 results added. All UO_2 loose rod baseline results updated for 7 wt.%. Chapter 7 changes: • Sections 7.1.2.1 and 7.1.2.2, English unit torque value correction made for unit conversion error. Chapter 8 changes: • Section 8.1.2, reference added for ASME Code. • Sections 8.1.5.1.4 and 8.1.5.2.4 added in-text reference to in-section table. • Section 8.2.3.2 revised text from "weather seal" to "weather gasket". • Section 8.2.6 added for periodic weld examinations. • Section 8.2.7 added for acetate plug examinations.

TABLE OF CONTENTS

1.0 GENERAL INFORMATION 1-1

2.0 STRUCTURAL EVALUATION 2-1

3.0 THERMAL EVALUATION 3-1

4.0 CONTAINMENT 4-1

5.0 SHIELDING EVALUATION 5-1

6.0 CRITICALITY EVALUATION 6-1

7.0 PACKAGE OPERATIONS 7-1

8.0 ACCEPTANCE TESTS AND MAINTENANCE PROGRAM 8-1

TRAVELLER SAFETY ANALYSIS REPORT ACRONYM LIST

Acronym	Definition	Acronym	Definition
ASME	American Society of Mechanical Engineers	NCT	Normal Conditions of Transport
ANSI	American National Standards Institute	NFD	Nuclear Fuel Division of Westinghouse
ASTM	American Society for Testing and Materials	OD	Outer diameter
ATF	Accident Tolerant Fuel	OR	Outer radius
AWS	American Welding Society	OZL	Optimized ZIRLO liner
BORAL	Borated aluminum	PWR	Pressurized water reactor
BWR	Boiling water reactor	QC	Quality control
CFA	Categorized fuel assembly	QTC	Qualified test unit
CFR	Code of Federal Regulation	SAR	Safety Analysis Report
CG	Center of gravity	SS	Stainless steel
CS	Clamshell	SSR	Specific Safety Requirements
CSI	Criticality safety index	TE	Total energy
CTE	Coefficient of thermal expansion	UHMW	Ultra-high molecular weight
CTU	Certified test unit	UNC	Unified thread coarse
DFT	Directional flame thermometers	USL	Upper subcritical limit
DTE	Differential thermal expansion	WtF	Water-to-Fuel
EALF	Energy of average lethargy causing fission		
FA	Fuel assembly		
FAA	Federal Aviation Administration		
FEA	Finite Element Analysis		
FEM	Finite Element Model		
GT/IT	Guide tubes/instrument tubes		
HAC	Hypothetical Accident Conditions		
IAEA	International Atomic Energy Agency		
ICRP	International Commission on Radiological Protection		
ID	Inner diameter		
IE	Internal energy		
IR	Inner radius		
KE	Kinetic energy		
k_{eff}	Effective neutron multiplication factor		
LEU	Low-enriched uranium		
LWR	Light-water reactor		

TRAVELLER SAFETY ANALYSIS REPORT
LIST OF EFFECTIVE PAGES

Page	Rev.	Date	Page	Rev.	Date
i-viii	2	7/2021	6-42	1	11/2019
			6-43 - 6-109	2	7/2021
1-i - 1-iii	2	7/2021	6-110	1	11/2019
1-1 - 1-2	2	7/2021	6-111 - 6-113	2	7/2021
1-3 - 1-10	1	11/2019	6-114	1	11/2019
1-11 - 1-13	2	7/2021	6-115 - 6-123	2	7/2021
1-14 - 1-16	1	11/2019	6-124 - 6-133	1	11/2019
1-17 - 1-19	2	7/2021	6-134 - 6-148	2	7/2021
1-20	1	11/2019	6-149	1	11/2019
1-21 - 1-29	2	7/2021	6-150 - 6-152	2	7/2021
1-30	1	11/2019	6-153	1	11/2019
10004E58	9		6-154 - 6-162	2	7/2021
10071E36	3		6-163	1	11/2019
10006E58	7		6-164 - 6-168	2	7/2021
2-i - 2-v	2	7/2021	7-i	2	7/2021
2-1	1	11/2019	7-1 - 7-3	1	11/2019
2-2 - 2-3	2	7/2021	7-4	2	7/2021
2-4	1	11/2019	7-5 - 7-8	1	11/2019
2-5 - 2-6	2	7/2021			
2-7 - 2-18	1	11/2019	8-i - 8-ii	2	7/2021
2-19 - 2-34	2	7/2021	8-1	2	7/2021
2-35 - 2-128	1	11/2019	8-2 - 8-4	1	11/2019
2-129 - 2-145	2	7/2021	8-5	2	7/2021
			8-6	1	11/2019
3-i - 3-iii	2	7/2021	8-7	2	7/2021
3-1 - 3-2	1	11/2019	8-8 - 8-9	1	11/2019
3-3 - 3-6	2	7/2021	8-10 - 8-11	2	7/2021
3-7 - 3-29	1	11/2019	8-12	1	11/2019
4-i	1	11/2019			
4-1 - 4-4	1	11/2019			
5-i - 5-ii	2	7/2021			
5-1	1	11/2019			
5-2 - 5-3	2	7/2021			
5-4 - 5-12	1	11/2019			
6-i - 6-vii	2	7/2021			
6-1 - 6-6	2	7/2021			
6-7 - 6-8	1	11/2019			
6-9 - 6-13	2	7/2021			
6-14 - 6-17	1	11/2019			
6-18 - 6-32	2	7/2021			
6-33 - 6-34	1	11/2019			
6-35	2	7/2021			
6-36	1	11/2019			
6-37 - 6-41	2	7/2021			

TABLE OF CONTENTS

1.0 GENERAL INFORMATION 1-1
1.1 INTRODUCTION 1-1
1.2 PACKAGE DESCRIPTION 1-2
1.2.1 Packaging 1-2
1.2.1.1 Overall Dimensions and Weights of the Traveller Variants 1-2
1.2.1.2 Containment Features 1-2
1.2.1.3 Neutron and Gamma Shielding Features 1-3
1.2.1.4 Criticality Control Features 1-3
1.2.1.5 Structural Features 1-3
1.2.2 Contents 1-17
1.2.2.1 Type and Form 1-17
1.2.2.2 Maximum Quantity of Material per Package 1-19
1.2.3 Special Requirements for Plutonium 1-20
1.2.4 Operational Features 1-20
1.3 APPENDICES 1-21
1.3.1 References 1-21
1.3.2 Licensing Drawings for Packaging 1-21
1.3.3 Quality Categorization Tables 1-22

LIST OF TABLES

Table 1-1 Traveller Content Information 1-1
Table 1-2 Isotopic Content Specification 1-19
Table 1-3 Safety-Related Parts of Traveller Type A Configuration (Drawing 10004E58) 1-22
Table 1-4 Safety-Related Parts of Traveller Type B Configuration (Drawing 10071E36) 1-26
Table 1-5 Safety-Related Parts of Rod Pipe (Drawing 10006E58) 1-30

LIST OF FIGURES

Figure 1-1 Outerpack Closed Position (left) and Opened Position (right) 1-4
Figure 1-2 Outerpack and Clamshell Cross-Section View (typical) 1-4
Figure 1-3 Clamshell with Fixed Top Plate (FTP) 1-6
Figure 1-4 Clamshell with Removable Top Plate (RTP) 1-7
Figure 1-5 Clamshell Latch Locked Position (left) and Open Position (right) 1-7
Figure 1-6 Corner Post Axial Restraint – Removable Top Plate (left), Fixed Top Plate (right) 1-8
Figure 1-7 Center Plate Axial Restraint – Removable Top Plate (left), Fixed Top Plate (right) 1-9
Figure 1-8 Corner Post Axial Restraint 1-9
Figure 1-9 Clamshell Fuel Axial Bottom Spacer Assembly (length depends on fuel assembly type) 1-10
Figure 1-10 Clamshell Fuel Spacer Assembly 1-10
Figure 1-11A Bottom Support Spacer Installed – Bottom Nozzle with Four Corner Legs (Length depends on fuel assembly type) 1-12
Figure 1-11B Bottom Support Spacer Installed – Bottom Nozzle with Skirted Sides and Four Corner Legs (Length depends on fuel assembly type) 1-13
Figure 1-12 Bottom Support Plate Installed (on top of Fuel Axial Bottom Spacer) – Bottom Nozzle Features in Direct Contact with Rubber (Length depends on fuel assembly type) 1-14
Figure 1-13 Top Axial Restraint (left) and Center Base Plate Axial Restraint (right) 1-14
Figure 1-14 Rod Pipe 1-15
Figure 1-15 Generic Sketch of the Traveller Representing the Package as Prepared for Transport 1-16

1.0 GENERAL INFORMATION

1.1 INTRODUCTION

The Traveller is a shipping package designed to transport Type A and Type B fissile material in the form of uranium fuel assemblies or fuel rods. It will carry several types of pressurized water reactor (PWR) fuel assemblies with enrichments of up to 6.0 wt.% ^{235}U, as well as either PWR or boiling water reactor (BWR) fuel rods with uranium dioxide (UO_2) enrichments up to 7.0 wt.% ^{235}U and uranium silicide (U_3Si_2) enrichments up to 5.0 wt.% ^{235}U. The Traveller package is designed to carry one (1) fuel assembly or one (1) Rod Pipe for loose fuel rods. There are two packaging variants in the Traveller family: Traveller Standard (STD) and Traveller XL (XL).

In the criticality analysis, PWR fuel assemblies are organized with similar fuel assemblies into defined bins. Three PWR groups define the allowable fuel assembly contents, with each group containing like bins. The bounding parameters of the fuel assembly contents in a bin are represented by categorized fuel assemblies (CFA), for the criticality analyses. All CFAs among the PWR groups are evaluated and organized by Criticality Safety Indices (CSI) and Traveller packaging variants. This is described further in Section 6, with contents parameter details in Section 6.2, Fissile Material Contents.

The CSI and quantity of radioactive content for the Traveller packages are provided in Table 1-1. The following chapters describe the package design and testing program in detail. Licensing drawings are presented in Section 1.3.2. A generic sketch of the Traveller representing the package as prepared for transport is provided in Figure 1-15.

Table 1-1 Traveller Content Information

Content	Traveller Packaging Variant	Max wt.% ^{235}U	CSI	Quantity[1]
PWR Group 1	Traveller STD/XL	5.0	1.0	Type A or B
PWR Group 2	Traveller XL	5.0	4.2	Type A or B
PWR Group 4	Traveller STD/XL	6.0	2.5	Type B
Rod Pipe	Traveller STD/XL	7.0 UO_2 5.0 U_3Si_2	0.7	Type A

NOTE: [1] Quantity of radioisotopes in the contents determined based on Section 1.2.2.2, and limited based on Table 1-2.

The analyses and testing are performed under an NRC-approved quality assurance program, which specifically complies with Title 10 of the Code of Federal Regulations, Part 50 (10 CFR 50) Appendix B requirements and is adopted to meet the requirements of 10 CFR 71, Subpart H for transportation of radioactive material.

1.2 PACKAGE DESCRIPTION

1.2.1 Packaging

The packaging is made up of two basic components: 1) an Outerpack and 2) a Clamshell. The package is made up of the packaging and the contents, which consist of either a fuel assembly or Rod Pipe with loose fuel rods. The Outerpack and Clamshell are connected together with a suspension system that reduces the forces applied to the contents during transport. The contents, either a fuel assembly or Rod Pipe, are positively secured inside the Clamshell during transport.

1.2.1.1 Overall Dimensions and Weights of the Traveller Variants

There are two packaging variants in the Traveller family: Traveller STD and Traveller XL. General parameters for each packaging variant are as defined in the following subsections. Dimensions represent an as manufactured outer-most measurement. Weights represent a bounding maximum weight.

1.2.1.1.1 Traveller STD

- Gross Weight = 4,500 lb (2,041 kg)
- Tare Weight = 2,850 lb (1,293 kg)
- Outer Dimensions = LxWxH- 197.0 in. x 27.1 in. x 39.3 in. (5004 mm x 688 mm x 998 mm)
- Accommodates standard length fuel assemblies and Rod Pipe

1.2.1.1.2 Traveller XL

- Gross Weight = 5,230 lb (2,372 kg)
- Tare Weight = 3,260 lb (1,479 kg)
- Outer Dimensions = LxWxH- 226.0 in. x 27.1 in. x 39.3 in. (5740 mm x 688 mm x 998 mm)
- Accommodates standard and long length fuel assemblies and Rod Pipe

1.2.1.2 Containment Features

The Containment System is described in both IAEA Regulations for the Safe Transport of Radioactive Material, Specific Safety Requirements No. SSR-6 para. 213 [1] and 10 CFR 71.4 [2] as, "the assembly of components of the packaging intended to retain the radioactive material during transport." The Containment System for the Traveller is the alloy clad and end plugs of the fuel rods. Containment as required for Type B contents is described further in Chapter 4.

The fuel rod is assembled by loading the uranium dioxide (UO_2) or uranium silicide (U_3Si_2) pellets into a cladding tube. The tubes are pressurized with helium and end plugs are welded or bonded to the tube which effectively seals and contains the radioactive material. Welds and bonds of the fuel rods are verified for integrity by non-destructive methods such as radiographic or ultrasonic testing. As the containment boundary is welded or bonded closed, it cannot be opened unintentionally. Thus, the requirements of 10 CFR 71.43(c) are satisfied.

1.2.1.3 Neutron and Gamma Shielding Features

The Traveller packaging does not contain neutron or gamma shielding features because neutron and gamma radiation emitted from the allowable contents is negligible in quantity, as discussed in Chapter 5. Due to insignificant decay heat of the allowable contents, payload personnel barriers are not necessary. The Traveller packaging meets the requirements of 10 CFR 71.47.

1.2.1.4 Criticality Control Features

The confinement system for the Traveller consists of the fuel rods, the fuel assembly (or Rod Pipe), the Clamshell assembly including the neutron absorber plates, and the Outerpack. The Traveller features a flux trap system that reduces neutron communication between packages in an array. This system features BORAL® neutron absorber plates located at each lateral side of the Clamshell that act in conjunction with ultra-high molecular weight (UHMW) polyethylene moderator blocks, which are affixed to the walls of the Outerpack inner cavity. Neutrons leaving one package must pass through two regions of moderator blocks and then BORAL neutron absorber plates before reaching the contents of another package. In addition, the structural materials of the Traveller for which credit is taken in the criticality safety analysis provide additional neutron absorption.

1.2.1.5 Structural Features

1.2.1.5.1 Outerpack

The Outerpack is a structural component that serves as the primary impact and thermal protection for the contents. It also includes components that provide for lifting, stacking, and tie down during transportation. The Outerpack is a long tubular design consisting of a top and bottom half, as shown in Figure 1-1. Each half consists of a stainless steel outer shell, a layer of rigid 10-pcf polyurethane foam, and an inner stainless steel shell. The stainless steel provides structural strength and acts as a protective covering to the foam. A typical cross-section showing key elements of the package is depicted in Figure 1-2.

The Outerpack also has independent impact limiters at the top and lower ends. Each Endcap Impact Limiter system contains an Inner Pillow Impact Limiter adjacent to 20-pcf polyurethane foam. The 20-pcf foam is encased by the package Outerpack stainless steel skins. The top Inner Pillow Impact Limiter consists of 6-pcf foam encased between two stainless steel plates to allow mating with the upper Outerpack. The lower Inner Pillow Impact Limiter consists of 6-pcf foam encased in a stainless steel circular housing, which allows mating with the lower Outerpack. Details of the top and lower Inner Pillow Impact Limiters are also shown on Sheet 6 of 10071E36 and 10004E58 for the Traveller STD and XL, Type A and Type B configurations, respectively.

The foam is a rigid, closed-cell polyurethane that is an excellent impact absorber and thermal insulator, and has well-defined characteristics that make it ideal for this application. The steel-foam-steel “sandwich” is the primary fire protection and is described in more detail in Chapter 3.

The inside of the Outerpack is lined with UHMW polyethylene moderator blocks. The polyethylene provides a conformal cavity for the Clamshell and fuel assembly to fall into during low-angle drops. The Clamshell is fastened to the lower Outerpack using shock absorbing rubber mounts. Polyethylene foam sheeting may be positioned between the Clamshell and lower Outerpack to augment the shock absorbing characteristics for

transport. A weather gasket between the mating surfaces of the upper and lower Outerpack is used to mitigate water and debris from entering the package.

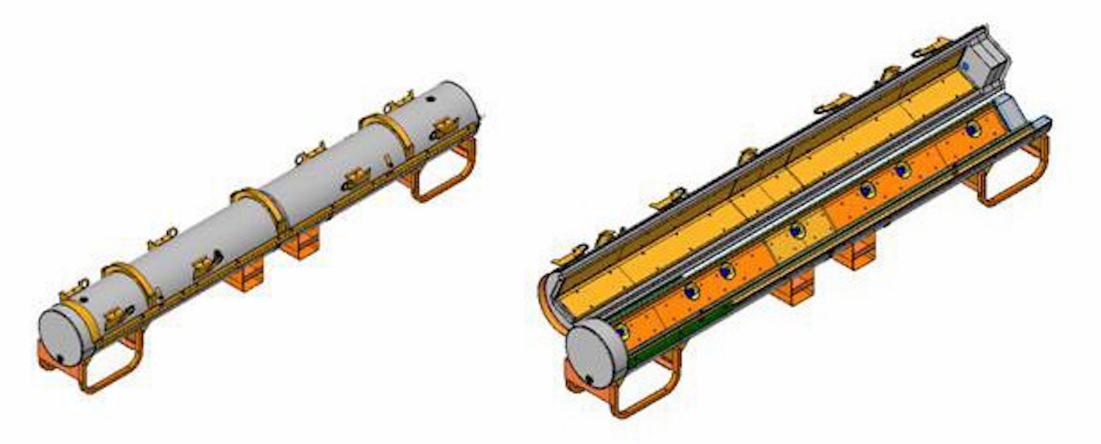

Figure 1-1 Outerpack Closed Position (left) and Opened Position (right)

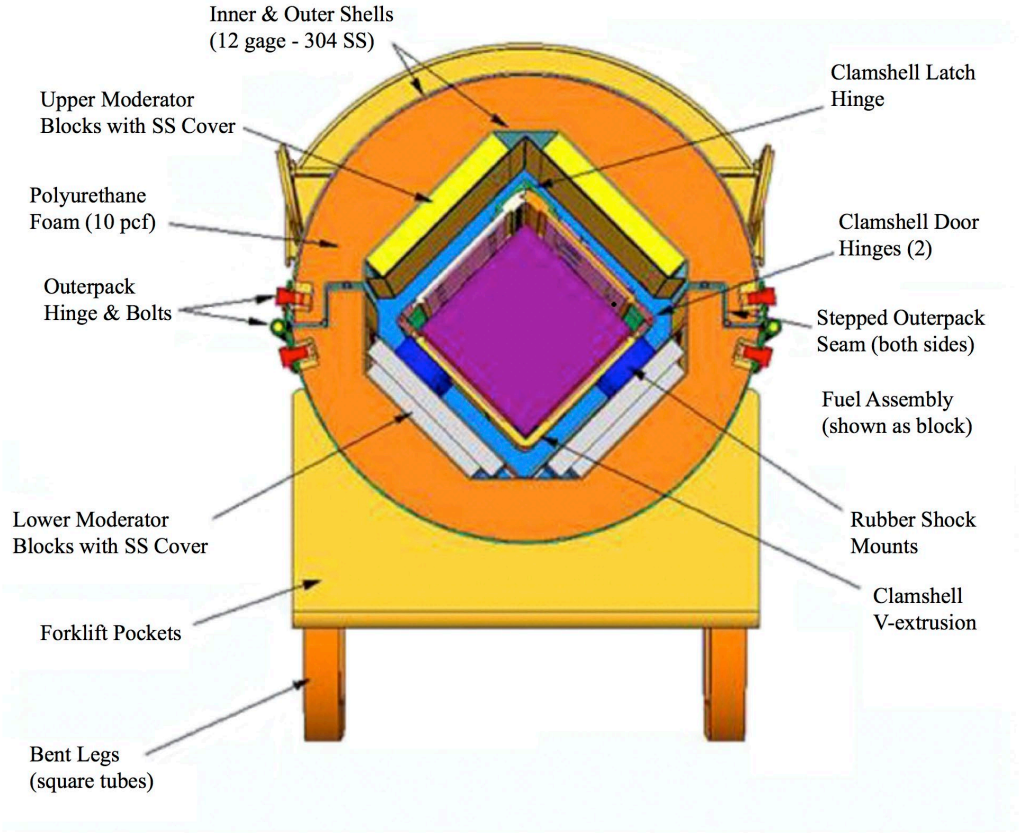

Figure 1-2 Outerpack and Clamshell Cross-Section View (typical)

1.2.1.5.2 Clamshell

The purpose of the Clamshell is to protect the contents during routine handling and to limit rearrangement of the contents in the event of a transport accident. During routine handling, the Clamshell main doors open to load the contents and are secured with multi-point cammed latches and hinge pins. The Clamshell protects and restrains the fuel assembly or Rod Pipe contents during all transport conditions. During accident transport conditions, the Clamshell remains closed and its structure limits rearrangement of the fuel assembly. Neutron absorber plates are installed on the inside surface of the Clamshell along the full length of each side.

A rectangular Clamshell is used in both the Traveller STD and XL packages as two slightly different Clamshell variants, with these differences between the STD and XL Clamshells described below.

The Clamshell structural components consist of an aluminum "V" base, two aluminum main doors, a small top "V" access door, bottom and top end plates, and multi-point cammed latch closure mechanisms. Piano type hinges (continuous hinges) connect each main door and the small top "V" access door to the "V" base. The BORAL neutron absorber plates are secured to the Clamshell with threaded fasteners and do not provide any structural strength to the Clamshell. The "V" base and bottom plate are lined with a cork rubber pad to cushion the contents and prevent damage during normal handling and routine transport conditions.

The top plate of the Clamshell has two configurations in order to accommodate different fuel types. Each uses a combination of flat head cap screws and tongue and groove joints in order to be fastened securely to the Clamshell. The Fixed Top Plate (FTP), shown in Figure 1-3, is secured directly to the top access door with cap screws. It has a tongue edge that fits into grooved shear bars that are attached directly to both faces of the Clamshell base with cap screws. The Removable Top Plate (RTP), shown in Figure 1-4, has grooved edges all around, and mates with shear bars that are fastened to all four faces of the Clamshell base. The bottom plate is secured to the Clamshell base with cap screws. Closure is provided by tongue and groove joining with the Clamshell doors.

Multi-point cammed latches that are spaced along the length of the Clamshell secure the main doors. These mechanical fasteners consist of a cam latch on the right main door that engages a keeper on the left main door. The cam latch is rotated a quarter-turn to engage the keeper as shown in Figure 1-5. A wave spring washer prevents inadvertent movement of the cam latch. There are nine (9) cam latches on the Traveller STD Clamshell and eleven (11) cam latches on the Traveller XL Clamshell. The top access door is secured with a short hinge pin inserted into the hinge knuckles when the small top access door is closed.

Clamping mechanisms that interface with the contents provide axial and lateral restraint during all transport conditions. An adjustable, threaded rod-clamping device provides axial restraint at the top of the fuel assembly or Rod Pipe. The design of the top axial restraint components, as shown in Figure 1-6, Figure 1-7, and Figure 1-8, depends on the Clamshell top plate configuration (FTP or RTP) and the fuel assembly type. An additional restraint may be added to secure non-fissile, non-radioactive reactor core components when shipped within the fuel assembly. Rubber pads are positioned at axial locations along the inside of the Clamshell doors to restrain lateral movement. These restraints, referred to as grid pads, are positioned to match the structural grid locations for each fuel assembly type.

Some fuel assemblies require an axial or lateral spacer to ensure proper axial fit into the Clamshell. The Clamshell is adapted axially for shorter fuel assemblies by adding an aluminum spacer component, as shown in Figure 1-9. The spacer is placed on the bottom end plate to elevate the fuel assembly in the longer Clamshell so it can be secured with the axial restraints at the top of the Clamshell. The larger cross-section dimension may be adapted for fuel assemblies with smaller cross sections by adding lateral fuel spacers in the aluminum "V" base, as shown in Figure 1-10.

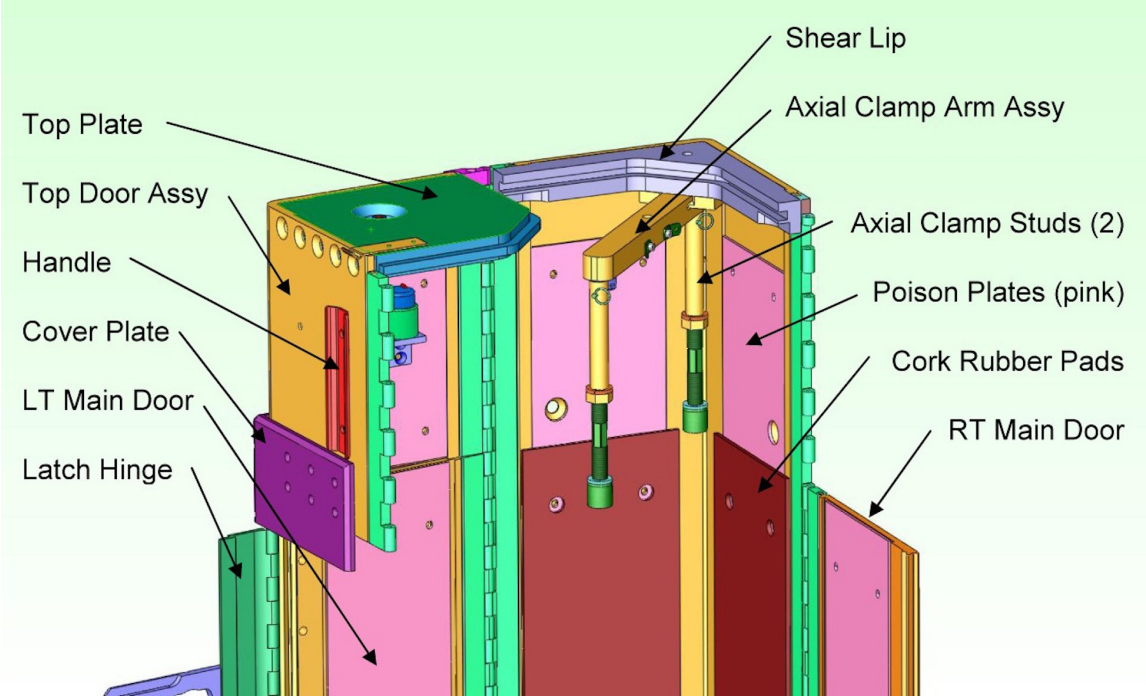

Figure 1-3 Clamshell with Fixed Top Plate (FTP)

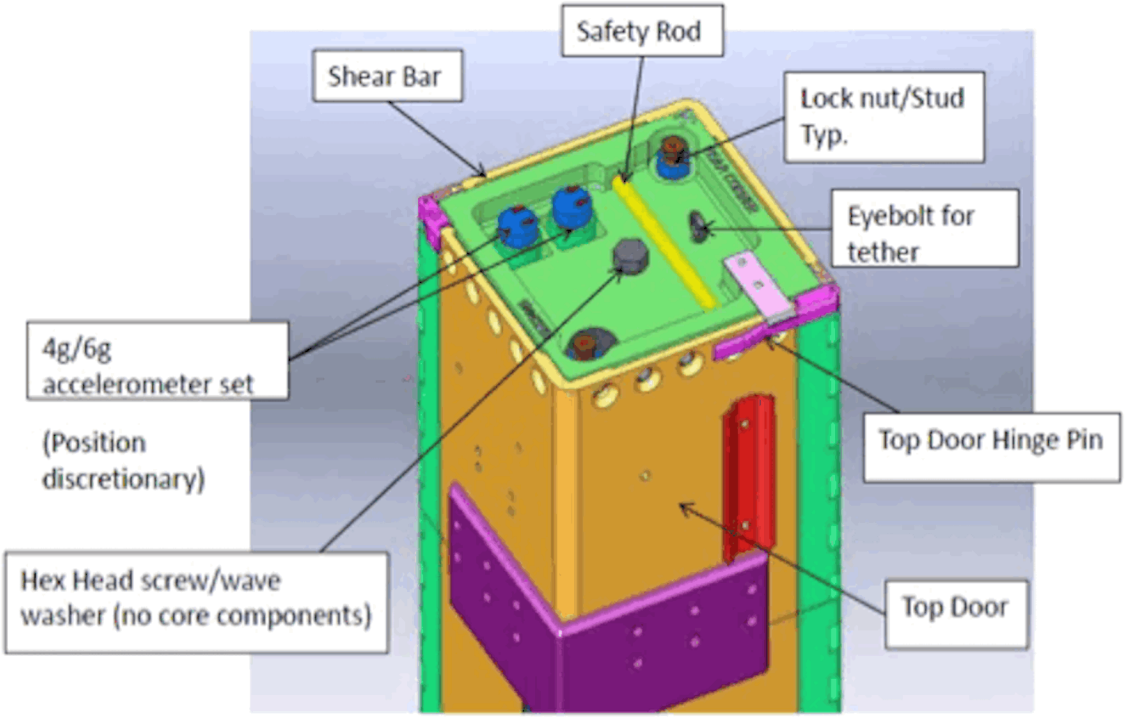

Figure 1-4 Clamshell with Removable Top Plate (RTP)

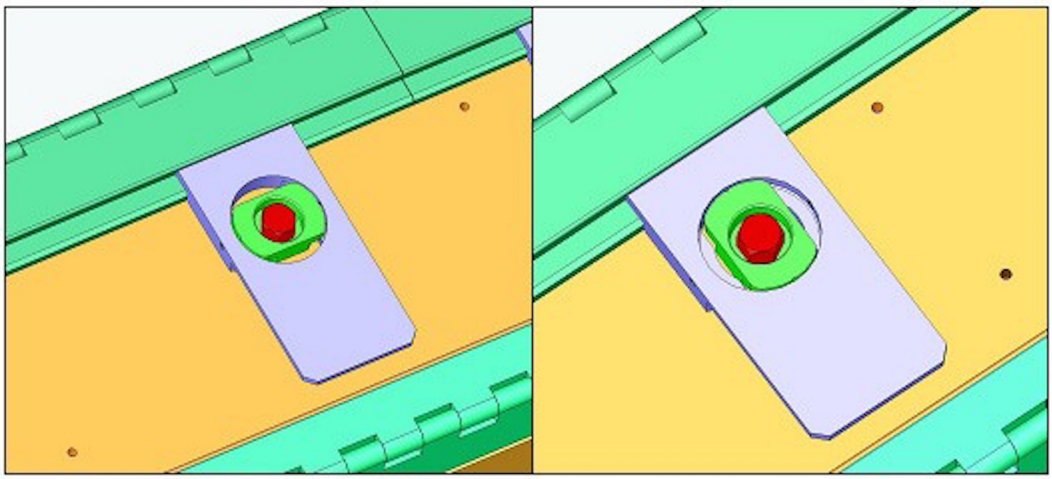

Figure 1-5 Clamshell Latch Locked Position (left) and Open Position (right)

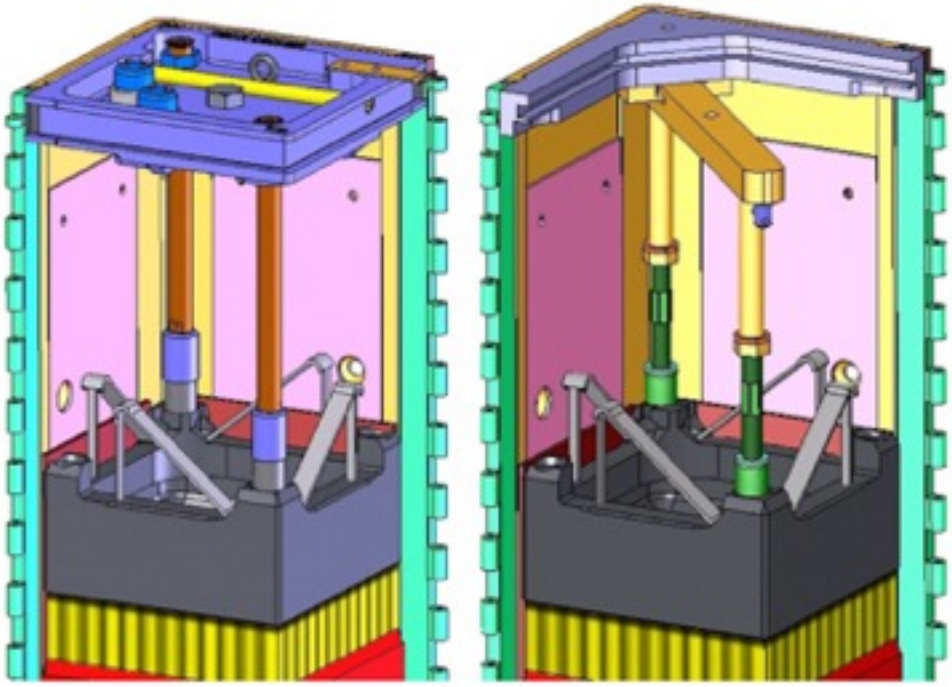

Fuel Assembly

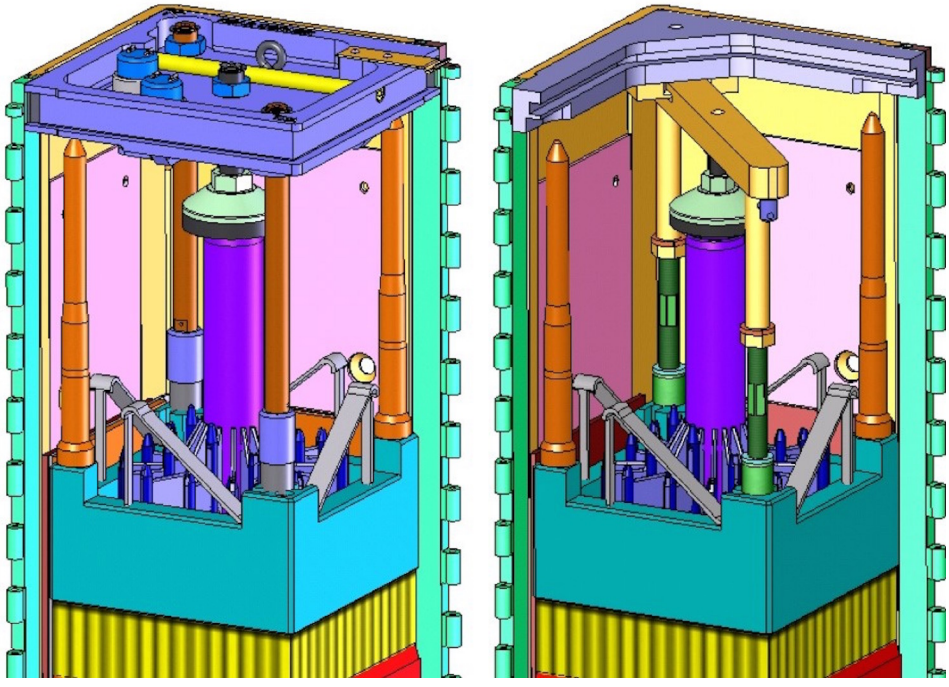

Fuel Assembly with Reactor Core Component

Figure 1-6 Corner Post Axial Restraint – Removable Top Plate (left), Fixed Top Plate (right)

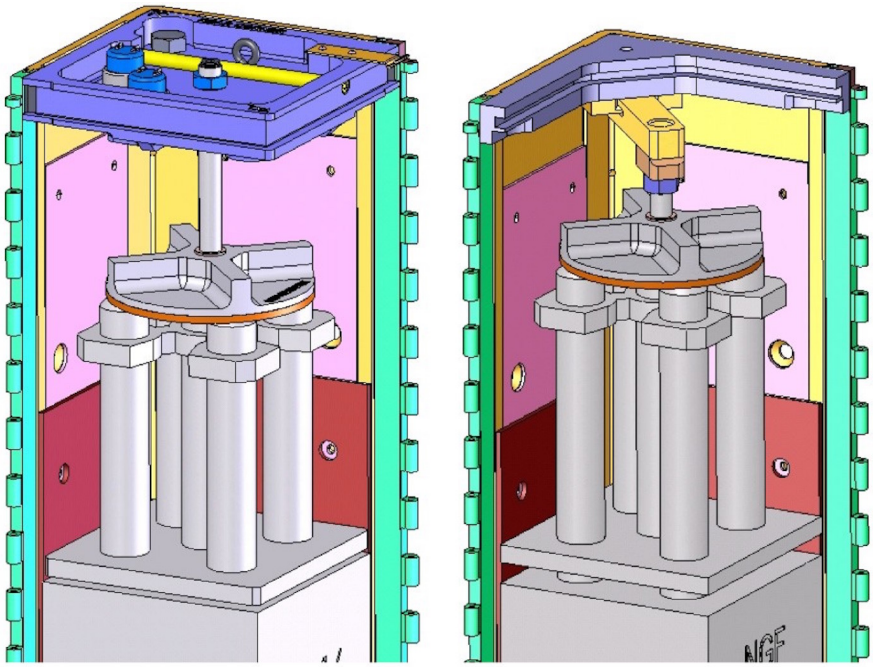

Figure 1-7 Center Plate Axial Restraint – Removable Top Plate (left), Fixed Top Plate (right)

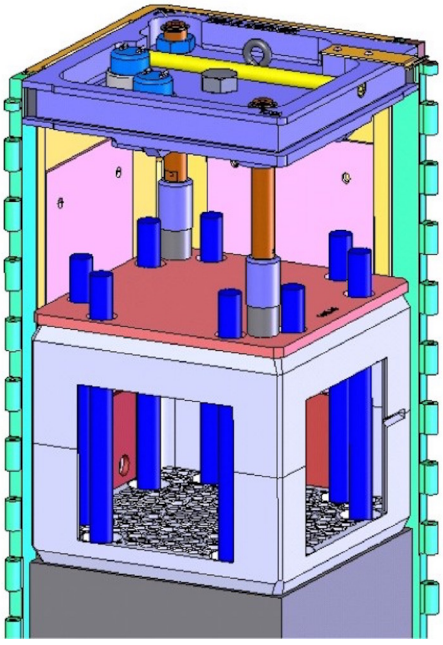

Figure 1-8 Corner Post Axial Restraint

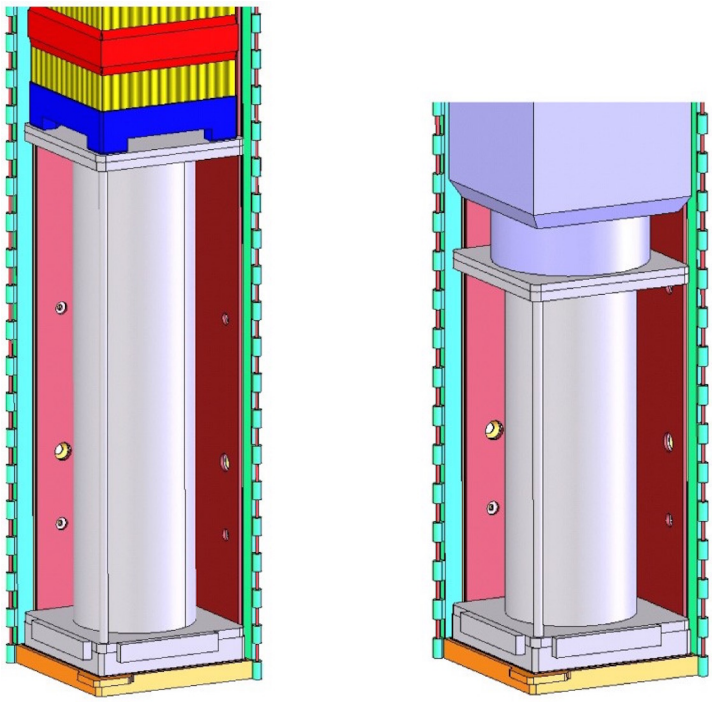

Figure 1-9 Clamshell Fuel Axial Bottom Spacer Assembly (length depends on fuel assembly type)

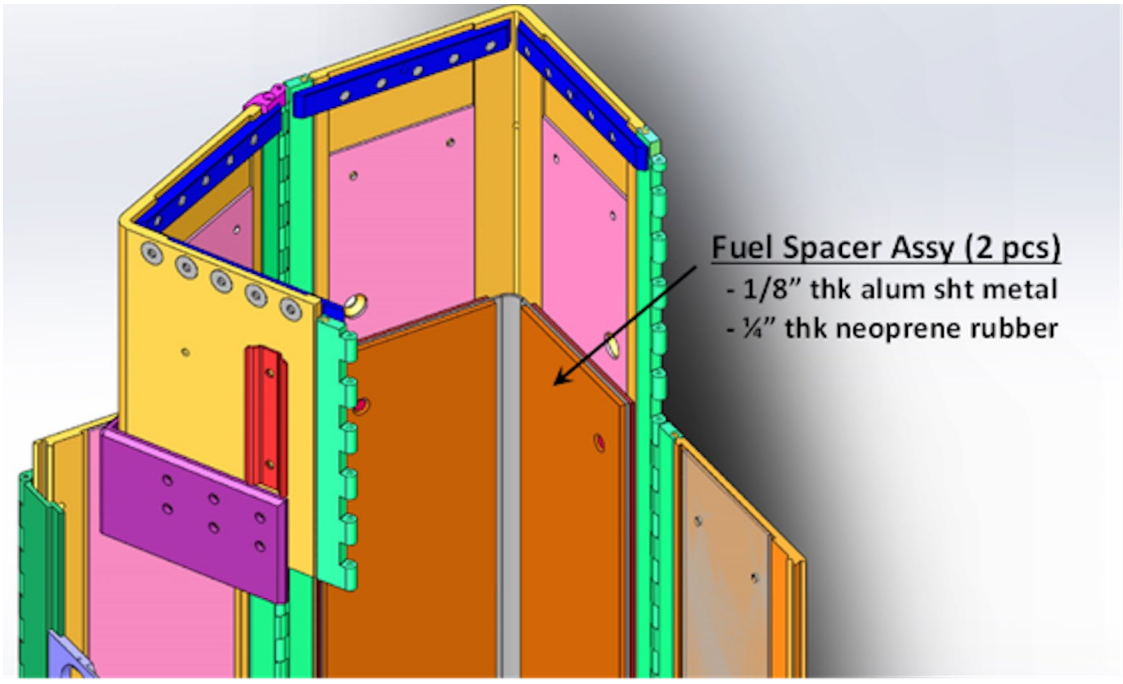

Figure 1-10 Clamshell Fuel Spacer Assembly

1.2.1.5.3 Type B Configuration Shoring Components

For any shipment of contents that are classified as Type B material (see discussion in Section 1.2.2.2), axial restraints are required to ensure proper structural support for the fuel assembly during a free drop. For the Type B configuration, the axial restraints required include a bottom support (spacer or plate) along with the top axial clamping mechanism.

For fuel assemblies with four corner support legs on the bottom nozzle, the fuel assembly is positioned on top of a reusable aluminum bottom support spacer, as shown in Figure 1-11A. The bottom support spacer rests on top of the Clamshell bottom plate and fits under the fuel assembly bottom nozzle structure. The bottom support spacer is a stiff structure with full length sides, void center, and sufficient top thickness to ensure the fuel assembly bottom nozzle flow plate is supported during all transport conditions. For fuel assemblies with bottom nozzles having both four corner legs and side skirts, the fuel assembly is positioned on top of a two-tiered aluminum spacer as shown in Figure 1-11B. The two-tiered bottom support spacer is a stiff structure with a solid upper portion and a stiff, voided, lower portion. The lower tier provides structural support for the four corner legs, and the upper tier provides clearance for the side skirts as well as sufficient thickness to ensure the fuel assembly bottom nozzle flow plate is supported during all transport conditions. The dimensions of the bottom support spacer for each fuel design ensure a maximum nominal remaining axial free space of 3/32 in. (2.38 mm) between the flow plate lower surface of the fuel assembly bottom nozzle structure and the upper rigid (metal) bottom support spacer surface for both support spacer design types. This free space above the bottom support spacer and the underside of the fuel assembly bottom nozzle structure is occupied by the 1/8 in. (3.175 mm) thick compressible rubber pad for both support spacer design types. The rubber pad is glued to the top of the support spacer to avoid surface scratching (as shown in Figure 1-11A and Figure 1-11B). The allowable tolerance on the rubber pad thickness is 0.010 in. (0.254 mm), ensuring that there is rubber compression even at the minimum manufacturing thickness. Each bottom support spacer assembly has the same geometry and is a combination of the aluminum base with rubber pads, but the length is designed specifically for each fuel assembly type to ensure there is a conforming fit between the fuel assembly bottom nozzle and the bottom support spacer. The bottom support spacer is required for the transport of Type B fuel assemblies with four corner support legs on the bottom nozzle (as shown in Figure 1-11A), and for fuel assemblies with both four corner support legs and side skirts on the bottom nozzle (as shown in Figure 1-11B).

For fuel assemblies that have a bottom nozzle without corner support legs, the fuel assembly is positioned on top of a reusable axial bottom spacer and solid aluminum bottom support plate, as shown in Figure 1-12. The fuel axial bottom spacer rests on top of the Clamshell bottom plate and the solid bottom support plate fits under the fuel assembly bottom nozzle structure. This bottom support plate ensures the fuel assembly bottom nozzle flow plate is supported during all transport conditions. A 1/16 in. (1.588 mm) thick pad is glued to the top of the support spacer to avoid surface scratching (as shown in Figure 1-12). The overall axial bottom spacer length is designed specifically for each fuel assembly type. The bottom support plate is a solid plate that the bottom nozzle rests upon. The combination of the fuel axial bottom spacer and bottom support plate is required for the transport of fuel assemblies with a bottom nozzle without corner support legs (as shown in Figure 1-12).

Clamping mechanisms that interface with the contents provide axial and lateral restraint during all transport conditions. An adjustable, threaded rod-clamping device provides axial restraint at the top of the fuel assembly. There are two top axial clamping mechanism configurations, as shown in licensing drawing 10071E36 sheet 9:

1) circular/square base plate plus clamping stud (items 140 and 141) for flat top nozzles (Figure 1-13)
   or
2) top axial restraint (i.e. center post) plus two axial clamping studs (items 133 and 139) for top nozzles with an open center (Figure 1-13)

The design of the top axial clamping mechanisms, as shown in Figure 1-13, includes either a center base plate for flat top nozzles or a top axial restraint and two (2) axial clamping studs for top nozzles with an open center. The axial restraints are threaded through the RTP. The length of the top axial clamping mechanisms depends on the fuel assembly type. The axial restraint may contact non-fissile, non-radioactive reactor core components when shipped within the fuel assembly by varying the threaded rod length. In all cases, the top axial clamping mechanisms provide positive axial hold down during normal transport conditions. Grid pads are positioned at axial locations along the inside of the Clamshell doors to match the structural grid locations for each fuel assembly type, providing lateral movement restraint.

When shipping in the Type B configuration, the combination of a top axial clamping mechanism and bottom support spacer or plate assembly is always required. For each fuel assembly design, the axial restraint configurations (i.e. top axial clamping mechanism and bottom support spacer/plate) are designed to ensure that the fuel assembly is secure prior to Clamshell door closure. The specific axial restraint and fuel assembly design configuration is controlled by site operational procedure. A tight fit of the fuel assembly and axial restraints is verified prior to each shipment, as discussed in Section 7.1.2.

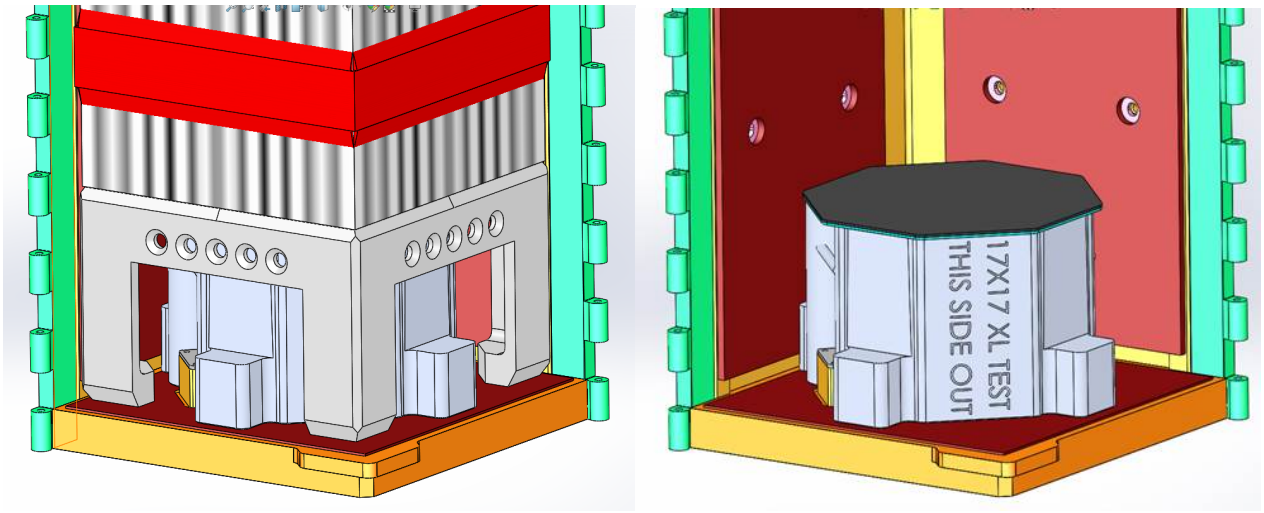

Figure 1-11A Bottom Support Spacer Installed – Bottom Nozzle with Four Corner Legs (Length depends on fuel assembly type)

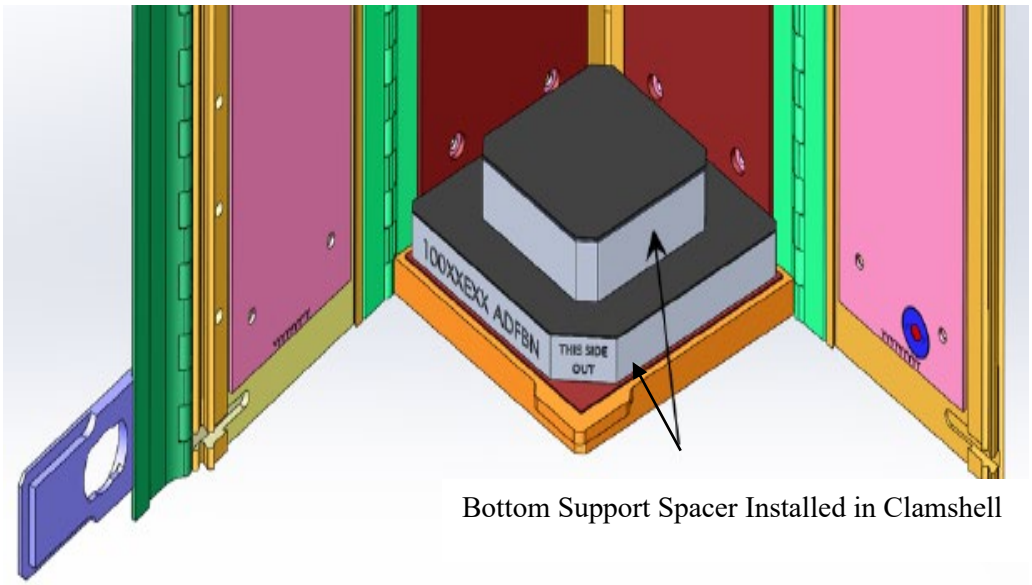

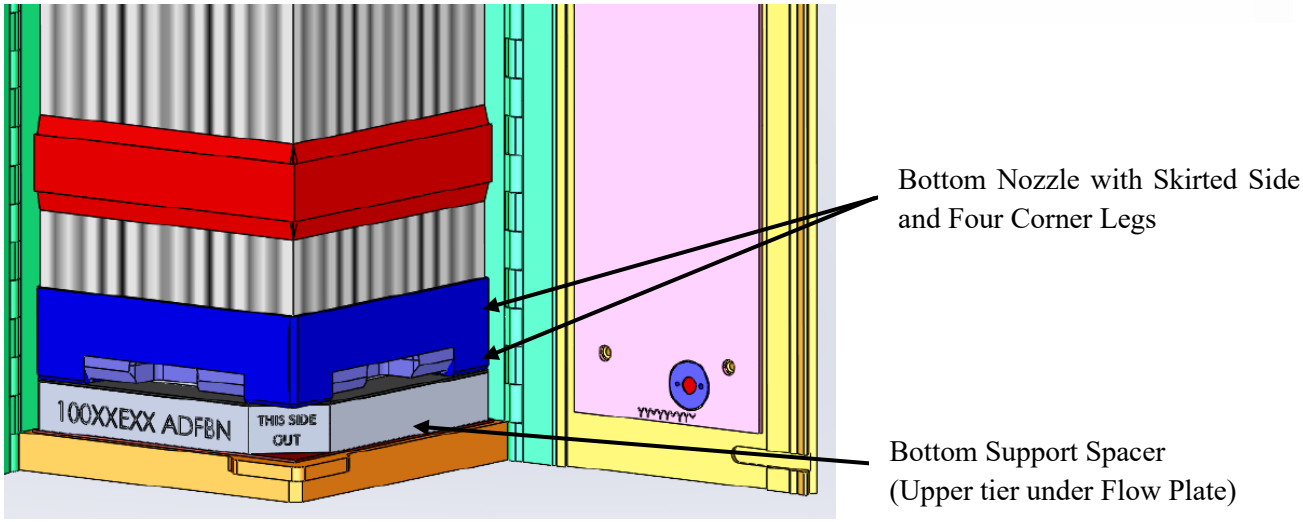

Figure 1-11B Bottom Support Spacer Installed – Bottom Nozzle with Skirted Sides and Four Corner Legs (Length depends on fuel assembly type)

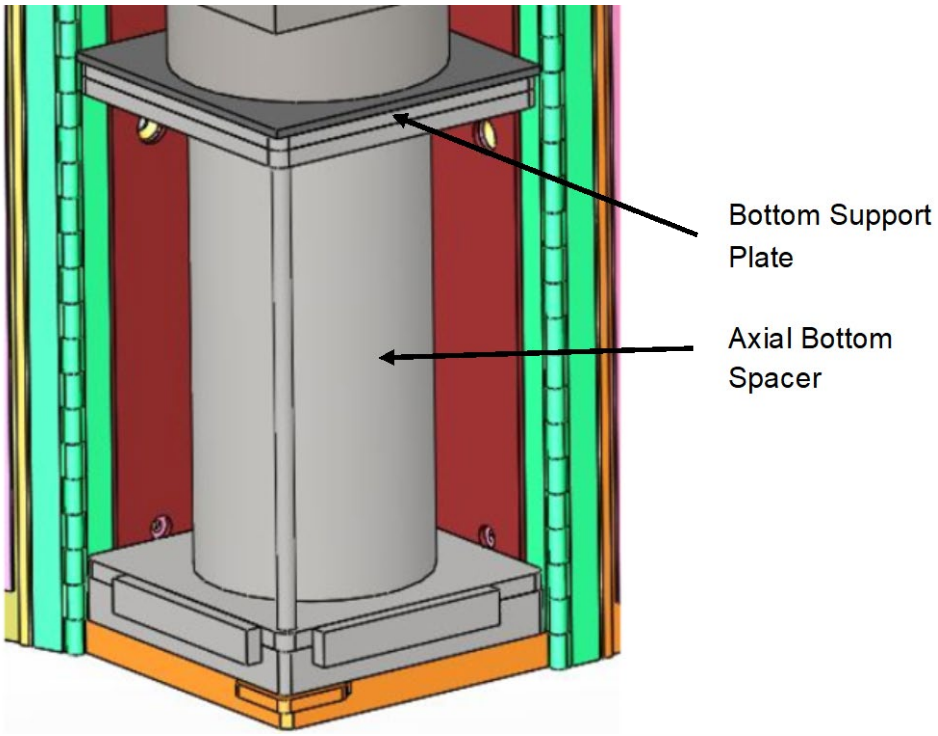

Figure 1-12 Bottom Support Plate Installed (on top of Fuel Axial Bottom Spacer) – Bottom Nozzle Features in Direct Contact with Rubber (Length depends on fuel assembly type)

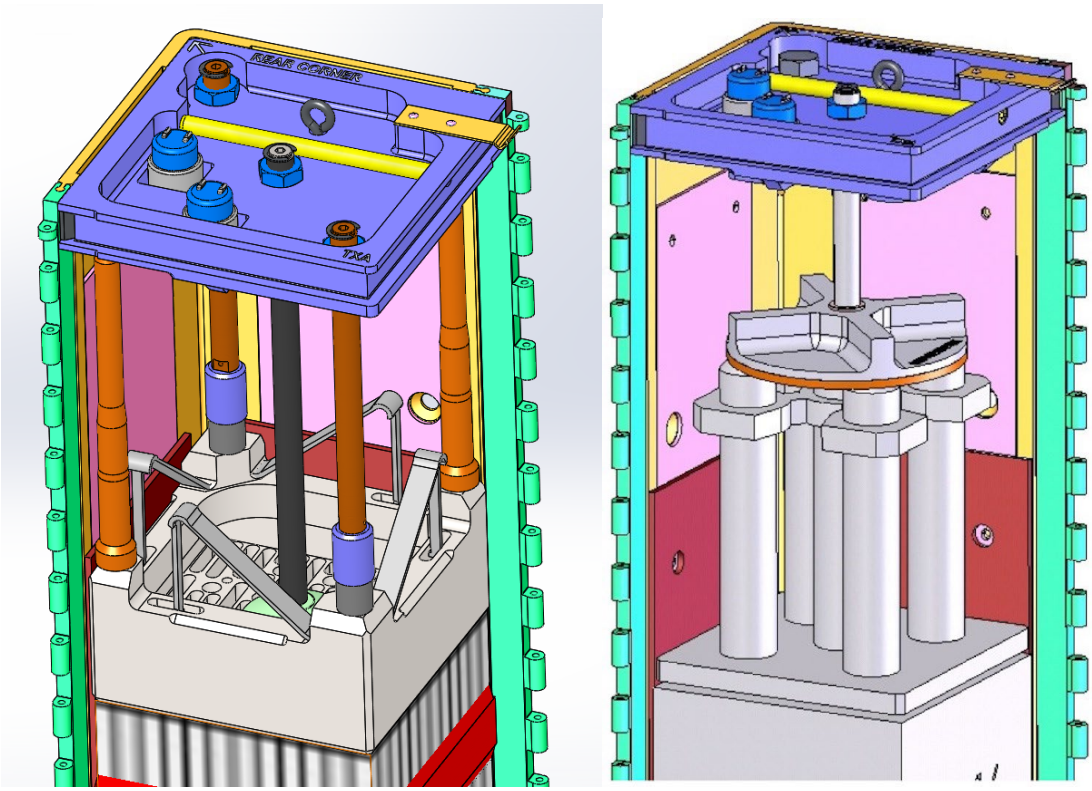

Figure 1-13 Top Axial Restraint (left) and Center Base Plate Axial Restraint (right) (Length depends on fuel assembly type)

1.2.1.5.4 Rod Pipe

The Traveller is designed to carry loose fuel rods using the Rod Ripe shown in Figure 1-14. The Rod Pipe consists of a 6 in. (15.2 cm) 304 stainless steel, Schedule 40 pipe with 304 stainless steel closures at each end. The end closures are a 0.25 in. (6.35 mm) thick cover secured to a flange fabricated from 0.25 in. (6.35 mm) thick plate.

The Rod Ripe is held in place inside the Clamshell with positive restraining devices. The axial clamp assembly provides axial restraint for the Traveller XL. The axial clamp arm is bolted into the top shear lip and contacts the Rod Pipe by means of an adjustable jackscrew. For Traveller STD, the Clamshell top plate provides the axial restraint, and contact between the Clamshell top plate and the Rod Pipe is achieved by means of a conformal shipping insert/spacer. Lateral and vertical restraint is accomplished through the use of removable rubber pads located inside the Clamshell door lip in conjunction with the latch assemblies on the Clamshell doors. The rubber pads are of varying thickness to accommodate the Rod Pipe in the Traveller variants. The Rod Pipe design has a maximum loaded weight of 1650 lb. (748 kg).

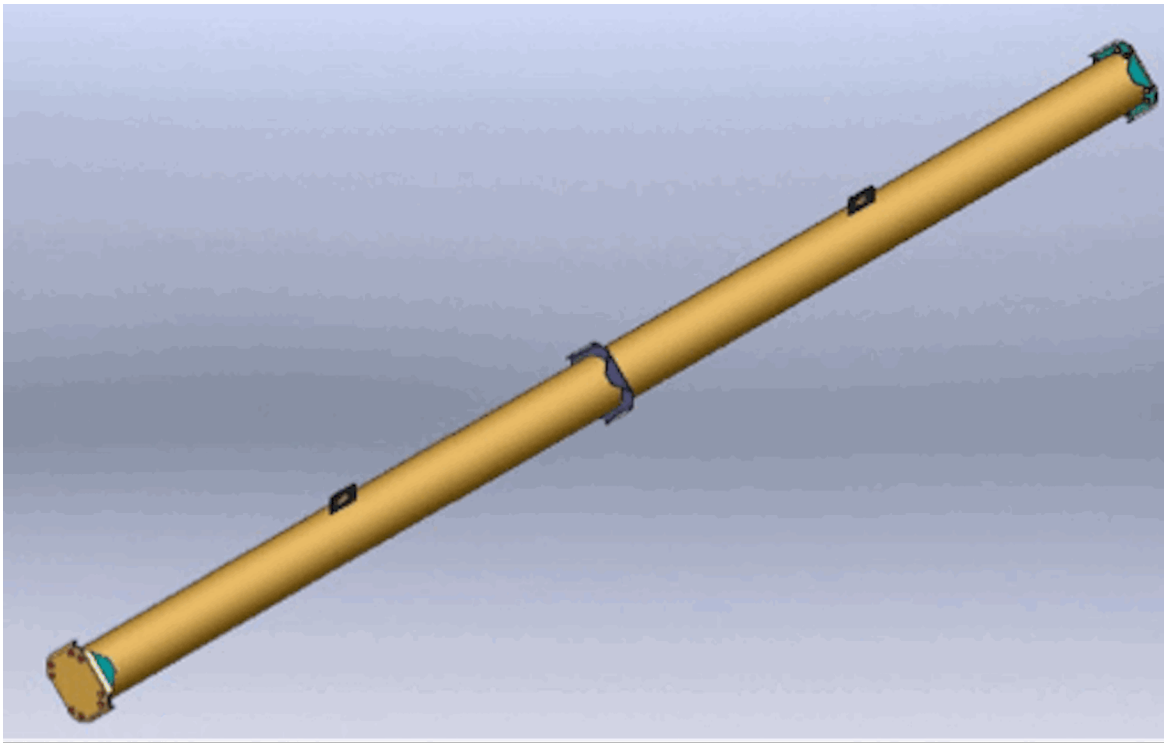

Figure 1-14 Rod Pipe

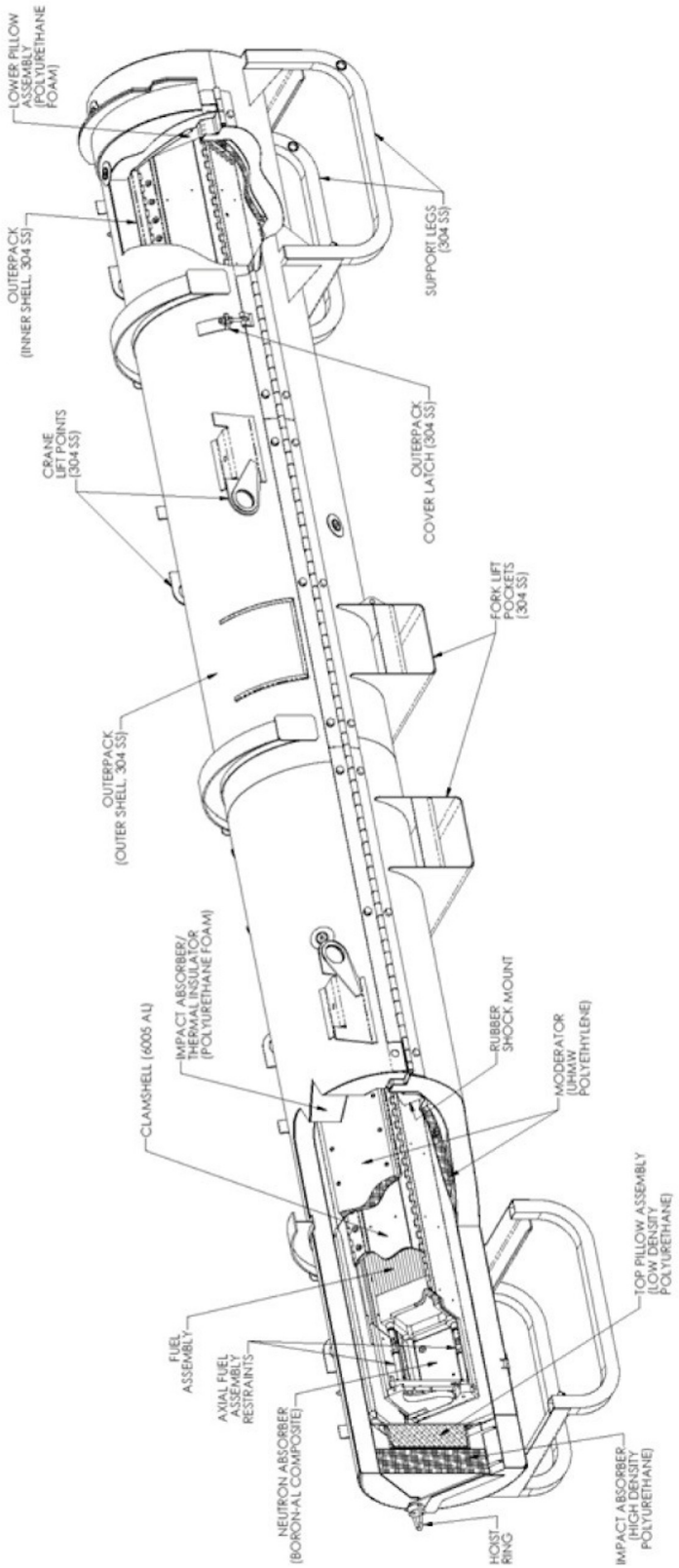

Figure 1-15 Generic Sketch of the Traveller Representing the Package as Prepared for Transport

1.2.2 Contents

1.2.2.1 Type and Form

The contents consist of either a single PWR fuel assembly or loose fuel rods. Fissile material is in the form of ^{235}U. For UO_2 contents, fuel assemblies are limited to an enrichment of 6 wt.% ^{235}U and loose fuel rods are limited to an enrichment of 7 wt.% ^{235}U. For U_3Si_2 contents, loose fuel rods are limited to an enrichment of 5 wt.% ^{235}U. Additionally, UO_2 contents in the form of loose fuel rods or fuel assemblies under PWR Group 1, Group 2, or Group 4 may be Advanced Doped Pellet Technology (ADOPT™) rods, doped with up to 700 ppm Cr_2O_3 and up to 200 ppm Al_2O_3. A single fuel assembly or a single Rod Pipe is transported in a package.

Any number of loose UO_2 fuel rods or 60 loose U_3Si_2 fuel rods may be transported in a Rod Pipe at a time. Fuel rods in the Rod Pipe include designs for both PWR and BWR. For the range of fuel rod diameters, ≥0.308 in. (0.7823 cm), the theoretical maximum number of fuel rods that can fit inside the Rod Pipe is ~250 fuel rods. The physical number of fuel rods placed in the Rod Pipe is less than the theoretical maximum value as some space is required to accommodate the packing materials and allow for the handling of fuel rods.

The PWR fuel assembly may be transported with non-fissile, non-radioactive reactor core components, as discussed in Section 1.2.2.1.3. In addition, a solid stainless steel rod may replace any of the fuel rods in a fuel assembly. The maximum contents weight for the two Traveller variants is:

- Traveller STD: 1,650 lb (748 kg)
- Traveller XL: 1,971 lb (894 kg)

1.2.2.1.1 Fuel Rods

Uranium Dioxide (UO_2) or Uranium Silicide (U_3Si_2) pellets are inserted into an alloy tube and end plugs are welded or bonded to seal each end of the tube, which together forms a fuel rod. The pellets are prevented from shifting during handling and shipment by a compression spring located between the top of the fuel pellet stack and the top end plug. Loose fuel rod shipments in the Rod Pipe are restricted to Type A contents and may have aluminum or stainless steel cladding with welded or bonded end plugs, per Section 2.2.1.8; see Section 6.2.4 for additional limitations and requirements for fuel rod shipments in the Rod Pipe.

The fuel rod is designed as a pressure vessel, which significantly reduces the number and extent of cyclic stresses experienced by the cladding. The result is a marked extension of the fatigue life margin of cladding with enhanced cladding reliability. The rods are pressurized with helium and end plugs are welded or bonded to the rod which effectively seals and contains the radioactive material. The maximum backfill pressure of fuel rods at room temperature conditions is 460 psig (3.17 MPa gauge) for the Type A configuration and 275 psig (1.90 MPa gauge) for the Type B configuration. The maximum normal operating pressure (MNOP) for the Type A and Type B fuel rods is 509 psig (3.51 MPa gauge) and 305 psig (2.10 MPa gauge), respectively. There is no pressure relief device that would allow radioactive contents to escape. Cladding may include a chromium coating of 25 μm thick, nominally and/or include an Optimized ZIRLO Liner (OZL) per Section 2.2.1.8.

The ASME Boiler and Pressure Vessel Code, Section III, is used as a guide in the mechanical design and stress analysis of the fuel rod. The rod is designed to withstand the applied loads, both external and internal. Welds and bonds of the fuel rods are verified for integrity by non-destructive methods such as radiographic or

ultrasonic testing, and process controls. As the containment boundary is welded or bonded closed, it cannot be opened unintentionally.

1.2.2.1.2 Fuel Assembly

A fuel assembly is a square array of fuel rods of UO_2 pellets in zirconium alloy tubes with welded end plugs that are structurally bound together in a skeleton, which consists of thimble tubes, grids, a top nozzle, a bottom nozzle, and other hardware (i.e. springs, nuts, etc.). A reactor core component may be inserted into the fuel assembly and is fastened to the top and bottom nozzles of the assembly. Grid assemblies are mechanically fastened to the guide thimbles along the height of the fuel assembly to provide support for the fuel rods. The fuel rods are contained and supported, and the rod-to-rod centerline spacing is maintained within the skeletal framework. See Section 6.2 for the limitations and requirements for fuel assembly contents in the Traveller variants.

1.2.2.1.3 Non-Fissile, Non-Radioactive Reactor Core Components

Reactor core components that may be shipped with the radioactive/fissile contents of the Traveller are non-fissile, non-radioactive components that have specific functions within a reactor core but have no primary function in a transport scenario. As a result, these components are not represented in transport analyses and no credit is taken for their presence in transport evaluations. Reactor core components include various types of rod control assemblies, base plate-mounted core components, spider-body core components, burnable absorbers, and secondary neutron sources.

A reactor core component is fitted into the guide/instrument tube locations of a fuel assembly. The core component may function as a flux suppressant, flow by-pass, or as a neutron absorber during reactor operation and does not alter the design of the fuel assembly. As such, it is not evaluated in the package criticality safety analysis because its function as a neutron absorber decreases the reactivity of the system.

Various components may include integral absorbers/poisons including, but not limited to, gadolinium, boron, erbium, and hafnium. For example, aluminum oxide-boron carbide burnable absorber material may be integrated in the fuel assembly in order to provide additional reactivity control during reactor operation. This material depletes during the reactor cycle in the same manner as ^{235}U. Fuel assembly integral burnable absorbers are not credited in the package criticality safety analysis, because its function as a neutron absorber decreases the reactivity of the system.

Startup neutron sources are typically of two types: 1) primary sources and 2) secondary sources. Primary sources are not an acceptable content for the Traveller package. Secondary sources are an acceptable content for the Traveller package. Secondary sources typically contain a mixture of antimony and beryllium (Sb-Be), and are used for restart of the reactor, which require in-core neutron activation to become a source.

1.2.2.2 Maximum Quantity of Material per Package

The maximum quantity of radioisotopes in the contents of the package is limited to the quantity contained in a single fuel assembly or in the maximum number of fuel rods that can be transported in the Rod Pipe. The only fissile material is low-enriched uranium that is:

- ≤ 5.0 wt.% ^{235}U for PWR Group 1 and 2 fuel assemblies and U_3Si_2 loose rods,
- ≤ 6.0 wt.% ^{235}U for PWR Group 4 fuel assemblies,
- ≤ 7.0 wt.% ^{235}U for UO_2 loose fuel rods.
- ≤ 5.0 wt.% ^{235}U for U_3Si_2 loose fuel rods

The maximum quantity of fissile material is approximately 32 kg of ^{235}U for the largest fuel assembly. The fuel pellets adhere to the isotopic content specified by ASTM C996 [3] or the contaminated uranium content limits defined in Table 1-2. Table 1-2 is applicable to both UO_2 and U_3Si_2 fuel rods.

In the Rod Pipe configuration, individual fuel rods are wrapped in a protective polyethylene sleeve. When the Rod Pipe is filled with a desired number of rods, a plastic disc is inserted to protect the ends of the fuel rods. The space between the plastic disc and the Rod Pipe is filled with packing materials, such as "bubble wrap", so that the rods are secured axially. Fuel assemblies are also wrapped in a protective polyethylene sleeve.

Table 1-2 Isotopic Content Specification

Content	Enriched Commercial Grade [1]	Contaminated [2]
^{232}U	0.0001 μg/gU	0.0500 μg/gU
^{234}U	11.0×10^3 μg/g^{235}U	2000 μg/gU
^{236}U	250 μg/gU	25,000 μg/gU
^{99}Tc	0.01 μg/gU	5 μg/gU
Alpha Activity from Np and Pu	Expected to be below the detection limits of commonly used measurement methodology	3300 Bq/kgU
Total Gamma Activity [3]	Expected to be below the detection limits of the measurement methodology	4.4×10^5 MeV-Bq/kgU

NOTE: [1] As defined in ASTM C996 [3].

[2] Limits for contaminated uranium contents with trace amounts of materials. Note that these limits apply at the time of transport.

[3] Gamma emissions resulting from any isotope, excluding those from ^{99}Tc and the actinides listed in this table.

For contents to be acceptable for shipment in the Traveller package as Type A material, without the additional configuration requirements for Type B, the requirements of (a) or (b) shall be met:

a. The uranium content meets the "unirradiated uranium" definition of SSR-6 para. 527 [1] and 10 CFR 71.4 [2]:

> *Unirradiated uranium* means uranium containing not more than 2 x 10^3 Bq of plutonium per gram of uranium-235, not more than 9 x 10^6 Bq of fission products per gram of uranium-235, and not more than 5 x 10^{-3} g of uranium-236 per gram of uranium-235.

b. If the ^{236}U requirement of the unirradiated definition is not met, the content may still be shipped if the following criteria are met:

1) The contents meet the requirements of the Enriched Commercial Grade specification of ASTM C996 [3], specifically the ^{236}U limit (250 $\mu g^{236}U/gU$), as outlined in Table 1-2.
2) There is less than a Type A quantity of material in the content.
   - For an A_2 calculation, the *U (enriched to 20% or less) - Unlimited* value may not be used.
   - The A_2 calculation must be completed using the A_2 values in 10 CFR 71 Appendix A Table A-1 for the individual isotopes in the fuel content, using the "slow lung absorption" values for uranium isotopes (i.e. for a UO_2 or U_3Si_2 compound).

Contents that exceed the quantities defined as Type A material shall be transported as Type B material, given the limits of contaminated uranium, as defined in Table 1-2, are not exceeded. Any contents transported as Type B material are subject to the Type B material requirements outlined in Chapters 4, 7, and 8 of this document.

Loose fuel rods in the Rod Pipe may only be transported in the Type A configuration.

Packing materials that have a moderating effectiveness greater than water, such as polyethylene sleeves and dunnage used to protect the fuel assembly or fuel rod contents during transport, are limited as follows:

- Such hydrogen-dense packing materials must have a moderating effectiveness which is less than or equal to a hydrogen density of 0.1325 g/cm^3;
  - For PWR fuel assemblies, packing material is limited to a maximum of 4.5 lb (2.0 kg) in the Clamshell per package;
  - For loose fuel rods, packing material is unlimited inside the Rod Pipe per package.

1.2.3 Special Requirements for Plutonium

Per the maximum radionuclide concentration calculations in Section 5.2, the maximum possible quantity of plutonium, based on the contaminated uranium limits, as defined in Table 1-2, is 5.19E-05 Ci (1.92 MBq). This is well below the 20 Ci (740 GBq) limitations for special requirements for plutonium in 10 CFR 71.63. However, all contents are fuel rods or assemblies, and thus are in solid form.

1.2.4 Operational Features

Forklift pockets and tubular legs are attached to the bottom half of the Outerpack. Stacking brackets, which double as lift points, are attached to the top half of the Outerpack and are located in eight (8) locations. The package must be up righted on one end for loading and unloading of contents. Two lifting points are attached to the top half of the Outerpack. Chapter 7 further describes the operation of the Traveller packages. A generic sketch of the Traveller representing the package as prepared for transport is provided in Figure 1-15.

1.3 APPENDICES

1.3.1 References

[1] International Atomic Energy Agency, "Regulations for the Safe Transport of Radioactive Material," SSR-6, 2012.

[2] U.S. Nuclear Regulatory Commission Code of Federal Regulations, Title 10 Part 71, "Packaging and Transport of Radioactive Material," 10 CFR 71, 2018.

[3] American Society for Testing and Materials, "Standard Specification for Uranium Hexafluoride Enriched to Less Than 5% 235U," ASTM C996-15, 2015.

1.3.2 Licensing Drawings for Packaging

Traveller Type A Design (RTP and FTP) – Licensing Drawings
10004E58, Rev. 9 (Sheets 1-9)

Traveller Type B Design (RTP) – Licensing Drawings
10071E36, Rev. 3 (Sheets 1-9)

Rod Pipe – Licensing Drawing
10006E58, Rev. 7

1.3.3 Quality Categorization Tables

Table 1-3 Safety-Related Parts of Traveller Type A Configuration (Drawing 10004E58)

ITEM	SAFETY CLASS	PART NAME	(SIZE) REFERENCE INFORMATION
01	B	HEX HEAD SCREW (3/4-10 X 1" LONG)	ASTM A193, CLASS 1, B8
02	B	FHCS (1/2-13 UNC X .75" LONG)	304 STAINLESS STEEL
03	B	LOCK WASHER (3/4)	304 STAINLESS STEEL
04	B	UPPER OUTER SHELL (SXN. 1)	ASTM A240 304 STAINLESS STEEL
05	B	UPPER OUTER SHELL (SXN.2, BACK)	ASTM A240 304 STAINLESS STEEL
06	B	UPPER INNER SHELL	ASTM A240 304 STAINLESS STEEL
07	B	UPPPER OUTER HEAD (SXN. 1)	ASTM A240 304 STAINLESS STEEL
08	B	UPPPER OUTER HEAD (SXN. 2)	ASTM A240 304 STAINLESS STEEL
09	B	LIMITER END CAP	ASTM A240 304 STAINLESS STEEL
10	B	END SEAM COVER	ASTM A240 304 STAINLESS STEEL
11	B	END SEAM COVER SPACER	ASTM A240 304 STAINLESS STEEL
12	B	BOTTOM SEAM COVER	ASTM A240 304 STAINLESS STEEL
13	B	BOTTOM SEAM COVER SPACER	ASTM A240 304 STAINLESS STEEL
14	B	LIMITER END CAP (SXN. 1)	ASTM A240 304 STAINLESS STEEL
15	B	LIMITER END CAP (SXN.2)	ASTM A240 304 STAINLESS STEEL
16	B	BOTTOM INNER COVER	ASTM A240 304 STAINLESS STEEL
17	B	MODERATOR END COVER (RH)	ASTM A240 304 STAINLESS STEEL
18	B	MODERATOR END COVER (LH)	ASTM A240 304 STAINLESS STEEL
19	B	UPPER MODERATOR COVER - LG.	ASTM A240 304 STAINLESS STEEL
20	B	UPPER MODERATOR COVER - SH0RT	ASTM A240 304 STAINLESS STEEL
21	B	CERAMIC FIBER BLANKET	CERAMIC FIBER
22	B	OUTER SHELL BACKING BAR - LG.	ASTM A240 304 STAINLESS STEEL
23	B	10 PCF FOAM (UPPER)	POLYURETHANE
24	B	20 PCF FOAM (UPPER)	POLYURETHANE
25	B	CERAMIC PAPER	CERAMIC FIBER
26	B	MODERATOR - UPPER UNIT	UHMW POLYETHYLENE
27	B	WELD STUD	304 STAINLESS STEEL
28	B	WELD STUD HEX NUT	304 STAINLESS STEEL
29	--	NOT USED	--
30	B	LOWER INNER SHELL	ASTM A240 304 STAINLESS STEEL
31	B	LOWER OUTER SHELL - BACK	ASTM A240 304 STAINLESS STEEL
32	B	LOWER OUTER SHELL - FRONT	ASTM A240 304 STAINLESS STEEL
33	B	LOWER IMPACT LIMITER COVER	ASTM A240 304 STAINLESS STEEL
34	B	BACKER BAR - SHORT	ASTM A240 304 STAINLESS STEEL
35	B	LOWER IMPACT LIMITER COVER	ASTM A240 304 STAINLESS STEEL
36	B	FRONT CLOSURE LIP	ASTM A240 304 STAINLESS STEEL
37	B	FRONT HEAD	ASTM A240 304 STAINLESS STEEL
38	B	BACK HEAD	ASTM A240 304 STAINLESS STEEL
39	B	SHOCK MOUNT COVER	ASTM A240 304 STAINLESS STEEL
40	B	GUSSET PLATE	ASTM A240 304 STAINLESS STEEL
41	B	BACK FOAM COVER	ASTM A240 304 STAINLESS STEEL

Table 1-3 Safety-Related Parts of Traveller Type A Configuration (Drawing 10004E58)

ITEM	SAFETY CLASS	PART NAME	(SIZE) REFERENCE INFORMATION
42	B	MODERATOR - LOWER SXN. 1	UHMW POLYETHYLENE
43	B	MODERATOR - LOWER SXN. 2	UHMW POLYETHYLENE
44	B	MODERATOR - LOWER SXN. 3	UHMW POLYETHYLENE
45	B	MODERATOR - LOWER SXN. 4	UHMW POLYETHYLENE
46	B	MODERATOR - LOWER SXN. 5	UHMW POLYETHYLENE
47	B	MODERATOR - LOWER SXN. 6	UHMW POLYETHYLENE
48	B	END RIB MODERATOR COVER (RH)	ASTM A240 304 STAINLESS STEEL
49	B	MODERATOR CENTER COVER	ASTM A240 304 STAINLESS STEEL
50	B	MODERATOR END COVER - LG.	ASTM A240 304 STAINLESS STEEL
51	B	MODERATOR END COVER - SHORT	ASTM A240 304 STAINLESS STEEL
52	B	CERAMIC PAPER (LOWER)	CERAMIC FIBER
53	B	WELD STUD	304 STAINLESS STEEL
54	B	WELD STUD HEX NUT	304 STAINLESS STEEL
55	--	NOT USED	--
56	B	10 PCF FOAM (LOWER)	POLYURETHANE
57	B	20 PCF FOAM (LOWER)	POLYURETHANE
58	B	CERAMIC FIBER BLANKET	CERAMIC FIBER
59	B	STIFFENER WEB	ASTM A240 304 STAINLESS STEEL
60	B	BOTTOM STIFFENER FLANGE	ASTM A240/A276 304 STAINLESS STEEL
61	B	TOP STIFFNER FLANGE	ASTM A240/A276 304 STAINLESS STEEL
62	B	BUMPER PLATE	ASTM A240/A276 304 STAINLESS STEEL
63	C	CROSS MEMBER	ASTM A240 304 STAINLESS STEEL
64	C	LEG	ASTM A240 304 STAINLESS STEEL
65	B	LOWER PILLOW BASE PLATE	ASTM A240 304 STAINLESS STEEL
66	B	LOWER PILLOW LIP	ASTM A240 304 STAINLESS STEEL
67	B	LOWER PILLOW SPUN HEAD - MIDDLE	ASTM A240 304 STAINLESS STEEL
68	B	LOWER PILLOW SOFT FOAM	POLYURETHANE
69	B	LOWER PILLOW INSULATION	CERAMIC FIBER
70	B	LOWER PILLOW SPUN HEAD - BASE	ASTM A240 304 STAINLESS STEEL
71	B	LOWER PILLOW SPUN HEAD - TOP	ASTM A240 304 STAINLESS STEEL
72	B	INSULATION - TOP	CERAMIC FIBER
73	B	VENT PORT COUPLING	304 STAINLESS STEEL
74	B	VENT PORT NPT PLUG	ACETATE
75	B	FLAT VENT PORT PLATE	ASTM A240 304 STAINLESS STEEL
76	B	BENT VENT PORT PLATE	ASTM A240 304 STAINLESS STEEL
77	B	BOLTING BLOCK BASE	ASTM A240/A276 304 STAINLESS STEEL
78	B	BOLTING BLOCK CAP	ASTM A240 304 STAINLESS STEEL
79	B	SHELF SUPPORT PLATE	ASTM A240 304 STAINLESS STEEL
80	B	SHELF DOUBLER	ASTM A240 304 STAINLESS STEEL
81	C	LOCATOR PIN	ASTM A276 304 STAINLESS STEEL
82	B	TOP PILLOW COVER PLATE	ASTM A240 304 STAINLESS STEEL
83	B	TOP PILLOW SPUN HEAD - INNER	ASTM A240 304 STAINLESS STEEL
84	B	TOP PILLOW FOAM	POLYURETHANE

Table 1-3 Safety-Related Parts of Traveller Type A Configuration (Drawing 10004E58)

ITEM	SAFETY CLASS	PART NAME	(SIZE) REFERENCE INFORMATION
85	B	TOP PILLOW BACK PLATE	ASTM A240 304 STAINLESS STEEL
86	B	HINGE	304 STAINLESS STEEL
87	B	BASE EXTRUSION / MACHINING	ASTM B209/B221 6005-T5 ALUMINUM
88	B	BOTTOM PLATE	ASTM B209/B221 6061-T6 ALUMINUM
89	B	BASE DOOR HINGE MACHINED	ASTM B209/B221 6005-T5 ALUMINUM
90	C	FHCS (1/2-13 X 1.25" LONG)	304 STAINLESS STEEL
91	C	SPRING PLUNGER/WAVE WASHER	304 STAINLESS STEEL
92	A	POISON PLATE - UPPER LEFT SIDE BASE	COMPOSITE BORON PLATE
93	A	POISON PLATE - LOWER LEFT SIDE BASE	COMPOSITE BORON PLATE
94	A	POISON PLATE - UPPER RIGHT SIDE BASE	COMPOSITE BORON PLATE
95	A	POISON PLATE - LOWER RIGHT SIDE BASE	COMPOSITE BORON PLATE
96	B	HINGE PIN SHORT	304 STAINLESS STEEL
97	B	LATCH EXTRUSION SHORT / MACHINING	ASTM B209/B221 6005-T5 ALUMINUM
98	B	LATCH EXTRUSION SHORT W/HOLES MACH.	ASTM B209/B221 6005-T5 ALUMINUM
99	B	LATCH HANDLE	ASTM B209/B221 6061-T6 ALUMINUM
100	B	HINGE PIN LONG	304 STAINLESS STEEL
101	B	LATCH EXTRUSION LONG / MACHINING	ASTM B209/B221 6005-T5 ALUMINUM
102	B	LATCH EXTRUSION LONG W/HOLES MACH.	ASTM B209/B221 6005-T5 ALUMINUM
103	B	LEFT DOOR EXTRUSION MACHINING	ASTM B209-B221 6005-T5 ALUMINUM
104	B	LEFT DOOR HINGE MACHINED	ASTM B209-B221 6005-T5 ALUMINUM
105	C	FHCS (7/16-14 X 3/4" LONG)	304 STAINLESS STEEL
106	B	RIGHT DOOR EXTRUSION/MACHINING	ASTM B209/B221 6005-T5 ALUMINUM
107	B	TOP DOOR EXTRUSION/MACHINING	ASTM B209/B221 6005-T5 ALUMINUM
108	B	DOOR HINGE RIGHT MACHINED	ASTM B209/B221 6005-T5 ALUMINUM
109	B	DOOR HINGE MACHINED	ASTM B209/B221 6005-T5 ALUMINUM
110	B	TOP DOOR COVER	ASTM B209/B221 6061-T6 ALUMINUM
111	C	TOP DOOR HINGE PIN HANDLE-LEFT	304 STAINLESS STEEL
112	C	TOP DOOR HINGE PIN HANDLE-RIGHT	304 STAINLESS STEEL
113	C	TOP DOOR HINGE PIN	304 STAINLESS STEEL
114	C	LATCH NUT	304 STAINLESS STEEL
115	C	LATCH KEEPER	304 STAINLESS STEEL
116	C	LATCH HEX BOLT (1/2-20 X 3/4" LG.)	304 STAINLESS STEEL
117	B	TOP PLATE	ASTM B209/B221 6061-T6 ALUMINUM
118	B	TOP SHEAR LIP	ASTM B209/B221 6061-T6 ALUMINUM
119	A	POISON PLATE - UPPER LEFT DOOR	COMPOSITE BORON PLATE
120	A	POISON PLATE - LOWER LEFT DOOR	COMPOSITE BORON PLATE
121	A	POISON PLATE - UPPER RIGHT DOOR	COMPOSITE BORON PLATE
122	A	POISON PLATE - LOWER RIGHT DOOR	COMPOSITE BORON PLATE
123	C	SPRING CLIP	304 STAINLESS STEEL
124	C	TOP DOOR HANDLE	304 STAINLESS STEEL
125	C	POISON PLATE FASTENER (1/4-28 X 3/8" LONG)	304 STAINLESS STEEL
126	C	BHCS (6-32 X 3/8" LONG)	304 STAINLESS STEEL
127	C	BHCS (5/16-24 X 3/8" LONG)	304 STAINLESS STEEL

Table 1-3 Safety-Related Parts of Traveller Type A Configuration (Drawing 10004E58)

ITEM	SAFETY CLASS	PART NAME	(SIZE) REFERENCE INFORMATION
128	B	FHCS (1/2-13 X 1-1/4" LONG)	304 STAINLESS STEEL
129	B	FHCS (1/2-13 X 7/8" LONG)	304 STAINLESS STEEL
130	B	HINGE PIN	304 STAINLESS STEEL
131	C	MODIFIED SET SCREW (3/8-24)	304 STAINLESS STEEL
132	C	REACTION PAD	ASTM B209/B221 6061-T6 ALUMINUM
133	C	FHCS (1/4-20 X 7/8" LONG)	304 STAINLESS STEEL
134	C	SHEAR LIP PLUNGER	304 STAINLESS STEEL
135	B	AXIAL CLAMP ARM	304 STAINLESS STEEL
136	C	AXIAL CLAMP STUD	304 STAINLESS STEEL
137	C	TOGGLE/RUBBER PAD	304 STAINLESS STEEL
138	C	JAM NUT (5/8-11)	304 STAINLESS STEEL
139	C	SPLUT LOCK WASHER (5/8)	304 STAINLESS STEEL
140	C	AXIAL CLAMP EXTENSION SLEEVE	304 STAINLESS STEEL
141	C	SHCS (3/8-16 X 1.0" LONG)	304 STAINLESS STEEL
142	C	DOG POINT SCREW (3/8-16 X 1.25" LONG)	304 STAINLESS STEEL
143	C	JAM NUT (3/8-16)	304 STAINLESS STEEL
144	C	FHCS (1/2-13 X 3/4" LONG)	304 STAINLESS STEEL
145	C	AXIAL CLAMP PINS A & B	304 STAINLESS STEEL
146	A	POISON PLATE - TOP DOOR LEFT	COMPOSITE BORON PLATE
147	A	POISON PLATE -TOP DOOR RIGHT	COMPOSITE BORON PLATE
148	C	FHCS (1/2-13 X .75")	304 STAINLESS STEEL
149	C	AXIAL CLAMP RET - LEFT	304 STAINLESS STEEL
150	C	AXIAL CLAMP RET - RIGHT	304 STAINLESS STEEL
151	C	SHCS (3/8-16 X 0.5" LONG)	304 STAINLESS STEEL
152	B	ALT TOP AXIAL RESTRAINT	ASTM B209/B221 6061-T6 ALUMINUM
153	B	AXIAL SPACER	ASTM B209/B221 6061-T6, 6063-T6, OR 6082-T6 ALUMINUM
154	B	REMOVABLE TOP SHEAR PLATE	ASTM B209/B221 6061-T6 ALUMINUM
155	B	JAM NUT (3/4-10)	304 STAINLESS STEEL
156	C	WAVE WASHER	300 SERIES STAINLESS STEEL
157	B	SHEAR BARS (.495)	304 STAINLESS STEEL
158	B	AXIAL CLAMPING STUDS (3/4-10)	300 SERIES STAINLESS STEEL
159	B	CIRCULAR BASE PLATE	ASTM B209/B221 6061-T6 ALUMINUM
160	B	CIRCULAR PLATE CLAMPING STUD (3/4-10)	300 SERIES STAINLESS STEEL
161	C	MODIFIED HHCS (1/4-28 X 3/4" LG.)	304 STAINLESS STEEL

Table 1-4 Safety-Related Parts of Traveller Type B Configuration (Drawing 10071E36)

ITEM	SAFETY CLASS	PART NAME	(SIZE) REFERENCE INFORMATION
01	B	HEX HEAD SCREW (3/4-10 X 1" LONG)	ASTM A193, CLASS 1, B8
02	B	FHCS (1/2-13 UNC X .75" LONG)	304 STAINLESS STEEL
03	B	LOCK WASHER (3/4)	304 STAINLESS STEEL
04	B	UPPER OUTER SHELL (SXN. 1)	ASTM A240 304 STAINLESS STEEL
05	B	UPPER OUTER SHELL (SXN.2, BACK)	ASTM A240 304 STAINLESS STEEL
06	B	UPPER INNER SHELL	ASTM A240 304 STAINLESS STEEL
07	B	UPPPER OUTER HEAD (SXN. 1)	ASTM A240 304 STAINLESS STEEL
08	B	UPPPER OUTER HEAD (SXN. 2)	ASTM A240 304 STAINLESS STEEL
09	B	LIMITER END CAP	ASTM A240 304 STAINLESS STEEL
10	B	END SEAM COVER	ASTM A240 304 STAINLESS STEEL
11	B	END SEAM COVER SPACER	ASTM A240 304 STAINLESS STEEL
12	B	BOTTOM SEAM COVER	ASTM A240 304 STAINLESS STEEL
13	B	BOTTOM SEAM COVER SPACER	ASTM A240 304 STAINLESS STEEL
14	B	LIMITER END CAP (SXN. 1)	ASTM A240 304 STAINLESS STEEL
15	B	LIMITER END CAP (SXN.2)	ASTM A240 304 STAINLESS STEEL
16	B	BOTTOM INNER COVER	ASTM A240 304 STAINLESS STEEL
17	B	MODERATOR END COVER (RH)	ASTM A240 304 STAINLESS STEEL
18	B	MODERATOR END COVER (LH)	ASTM A240 304 STAINLESS STEEL
19	B	UPPER MODERATOR COVER - LG.	ASTM A240 304 STAINLESS STEEL
20	B	UPPER MODERATOR COVER - SH0RT	ASTM A240 304 STAINLESS STEEL
21	B	CERAMIC FIBER BLANKET	CERAMIC FIBER
22	B	OUTER SHELL BACKING BAR - LG.	ASTM A240 304 STAINLESS STEEL
23	B	10 PCF FOAM (UPPER)	POLYURETHANE
24	B	20 PCF FOAM (UPPER)	POLYURETHANE
25	B	CERAMIC PAPER	CERAMIC FIBER
26	B	MODERATOR - UPPER UNIT	UHMW POLYETHYLENE
27	B	WELD STUD	304 STAINLESS STEEL
28	B	WELD STUD HEX NUT	304 STAINLESS STEEL
29	--	NOT USED	--
30	B	LOWER INNER SHELL	ASTM A240 304 STAINLESS STEEL
31	B	LOWER OUTER SHELL - BACK	ASTM A240 304 STAINLESS STEEL
32	B	LOWER OUTER SHELL - FRONT	ASTM A240 304 STAINLESS STEEL
33	B	LOWER IMPACT LIMITER COVER	ASTM A240 304 STAINLESS STEEL
34	B	BACKER BAR - SHORT	ASTM A240 304 STAINLESS STEEL
35	B	LOWER IMPACT LIMITER COVER	ASTM A240 304 STAINLESS STEEL
36	B	FRONT CLOSURE LIP	ASTM A240 304 STAINLESS STEEL
37	B	FRONT HEAD	ASTM A240 304 STAINLESS STEEL
38	B	BACK HEAD	ASTM A240 304 STAINLESS STEEL
39	B	SHOCK MOUNT COVER	ASTM A240 304 STAINLESS STEEL
40	B	GUSSET PLATE	ASTM A240 304 STAINLESS STEEL
41	B	BACK FOAM COVER	ASTM A240 304 STAINLESS STEEL
42	B	MODERATOR - LOWER SXN. 1	UHMW POLYETHYLENE

Table 1-4 Safety-Related Parts of Traveller Type B Configuration (Drawing 10071E36)

ITEM	SAFETY CLASS	PART NAME	(SIZE) REFERENCE INFORMATION
43	B	MODERATOR - LOWER SXN. 2	UHMW POLYETHYLENE
44	B	MODERATOR - LOWER SXN. 3	UHMW POLYETHYLENE
45	B	MODERATOR - LOWER SXN. 4	UHMW POLYETHYLENE
46	B	MODERATOR - LOWER SXN. 5	UHMW POLYETHYLENE
47	B	MODERATOR - LOWER SXN. 6	UHMW POLYETHYLENE
48	B	END RIB MODERATOR COVER (RH)	ASTM A240 304 STAINLESS STEEL
49	B	MODERATOR CENTER COVER	ASTM A240 304 STAINLESS STEEL
50	B	MODERATOR END COVER - LG.	ASTM A240 304 STAINLESS STEEL
51	B	MODERATOR END COVER - SHORT	ASTM A240 304 STAINLESS STEEL
52	B	CERAMIC PAPER (LOWER)	CERAMIC FIBER
53	B	WELD STUD	304 STAINLESS STEEL
54	B	WELD STUD HEX NUT	304 STAINLESS STEEL
55	--	NOT USED	--
56	B	10 PCF FOAM (LOWER)	POLYURETHANE
57	B	20 PCF FOAM (LOWER)	POLYURETHANE
58	B	CERAMIC FIBER BLANKET	CERAMIC FIBER
59	B	STIFFENER WEB	ASTM A240 304 STAINLESS STEEL
60	B	BOTTOM STIFFENER FLANGE	ASTM A240/A276 304 STAINLESS STEEL
61	B	TOP STIFFNER FLANGE	ASTM A240/A276 304 STAINLESS STEEL
62	B	BUMPER PLATE	ASTM A240/A276 304 STAINLESS STEEL
63	C	CROSS MEMBER	ASTM A240 304 STAINLESS STEEL
64	C	LEG	ASTM A240 304 STAINLESS STEEL
65	B	LOWER PILLOW BASE PLATE	ASTM A240 304 STAINLESS STEEL
66	B	LOWER PILLOW THERMAL PLATE	ASTM A240 304 STAINLESS STEEL
67	B	LOWER PILLOW SPUN HEAD - MIDDLE	ASTM A240 304 STAINLESS STEEL
68	B	LOWER PILLOW SOFT FOAM	POLYURETHANE
69	B	LOWER PILLOW INSULATION	CERAMIC FIBER
70	B	LOWER PILLOW SPUN HEAD - BASE	ASTM A240 304 STAINLESS STEEL
71	B	LOWER PILLOW SPUN HEAD - TOP	ASTM A240 304 STAINLESS STEEL
72	B	INSULATION - TOP	CERAMIC FIBER
73	B	VENT PORT COUPLING	304 STAINLESS STEEL
74	B	VENT PORT NPT PLUG	ACETATE
75	B	FLAT VENT PORT PLATE	ASTM A240 304 STAINLESS STEEL
76	B	BENT VENT PORT PLATE	ASTM A240 304 STAINLESS STEEL
77	B	BOLTING BLOCK BASE	ASTM A240/A276 304 STAINLESS STEEL
78	B	BOLTING BLOCK CAP	ASTM A240 304 STAINLESS STEEL
79	B	SHELF SUPPORT PLATE	ASTM A240 304 STAINLESS STEEL
80	B	SHELF DOUBLER	ASTM A240 304 STAINLESS STEEL
81	C	LOCATOR PIN	ASTM A276 304 STAINLESS STEEL
82	B	TOP PILLOW COVER PLATE	ASTM A240 304 STAINLESS STEEL
83	B	TOP PILLOW SPUN HEAD - INNER	ASTM A240 304 STAINLESS STEEL
84	B	TOP PILLOW FOAM	POLYURETHANE
85	B	TOP PILLOW BACK PLATE	ASTM A240 304 STAINLESS STEEL

Table 1-4 Safety-Related Parts of Traveller Type B Configuration (Drawing 10071E36)

ITEM	SAFETY CLASS	PART NAME	(SIZE) REFERENCE INFORMATION
86	B	HINGE	304 STAINLESS STEEL
87	B	BASE EXTRUSION / MACHINING	ASTM B209/B221 6005-T5 ALUMINUM
88	B	BOTTOM PLATE	ASTM B209/B221 6061-T6 ALUMINUM
89	B	50 IN.DOOR HINGE MACHINED	ASTM B209/B221 6005-T5 ALUMINUM
90	C	FHCS (1/2-13 X 1.25" LONG)	304 STAINLESS STEEL
91	C	SPRING PLUNGER/WAVE WASHER	304 STAINLESS STEEL
92	A	POISON PLATE - UPPER LEFT SIDE BASE	COMPOSITE BORON PLATE
93	A	POISON PLATE - LOWER LEFT SIDE BASE	COMPOSITE BORON PLATE
94	A	POISON PLATE - UPPER RIGHT SIDE BASE	COMPOSITE BORON PLATE
95	A	POISON PLATE - LOWER RIGHT SIDE BASE	COMPOSITE BORON PLATE
96	B	HINGE PIN SHORT	304 STAINLESS STEEL
97	B	LATCH EXTRUSION SHORT / MACHINING	ASTM B209/B221 6005-T5 ALUMINUM
98	B	LATCH EXTRUSION SHORT W/HOLES MACH.	ASTM B209/B221 6005-T5 ALUMINUM
99	B	LATCH HANDLE	ASTM B209/B221 6061-T6 ALUMINUM
100	B	HINGE PIN LONG	304 STAINLESS STEEL
101	B	LATCH EXTRUSION LONG / MACHINING	ASTM B209/B221 6005-T5 ALUMINUM
102	B	LATCH EXTRUSION LONG W/HOLES MACH.	ASTM B209/B221 6005-T5 ALUMINUM
103	B	LEFT DOOR EXTRUSION MACHINING	ASTM B209-B221 6005-T5 ALUMINUM
104	B	LEFT DOOR HINGE MACHINED	ASTM B209-B221 6005-T5 ALUMINUM
105	C	FHCS (7/16-14 X 3/4" LONG)	304 STAINLESS STEEL
106	B	RIGHT DOOR EXTRUSION/MACHINING	ASTM B209/B221 6005-T5 ALUMINUM
107	B	TOP DOOR EXTRUSION/MACHINING	ASTM B209/B221 6005-T5 ALUMINUM
108	B	DOOR HINGE RIGHT MACHINED	ASTM B209/B221 6005-T5 ALUMINUM
109	B	DOOR HINGE MACHINED	ASTM B209/B221 6005-T5 ALUMINUM
110	B	TOP DOOR COVER	ASTM B209/B221 6061-T6 ALUMINUM
111	C	TOP DOOR HINGE PIN HANDLE-LEFT	304 STAINLESS STEEL
112	C	TOP DOOR HINGE PIN HANDLE-RIGHT	304 STAINLESS STEEL
113	C	TOP DOOR HINGE PIN	304 STAINLESS STEEL
114	C	LATCH NUT	304 STAINLESS STEEL
115	C	LATCH KEEPER	304 STAINLESS STEEL
116	C	LATCH HEX BOLT (1/2-20 X 3/4" LG.)	304 STAINLESS STEEL
117	A	POISON PLATE - UPPER LEFT DOOR	COMPOSITE BORON PLATE
118	A	POISON PLATE - LOWER LEFT DOOR	COMPOSITE BORON PLATE
119	A	POISON PLATE - UPPER RIGHT DOOR	COMPOSITE BORON PLATE
120	A	POISON PLATE - LOWER RIGHT DOOR	COMPOSITE BORON PLATE
121	C	SPRING CLIP	304 STAINLESS STEEL
122	C	TOP DOOR HANDLE	304 STAINLESS STEEL
123	C	POISON PLATE FASTENER (1/4-28 X 3/8" LONG)	304 STAINLESS STEEL
124	C	BHCS (6-32 X 3/8" LONG)	304 STAINLESS STEEL
125	C	BHCS (5/16-24 X 3/8" LONG)	304 STAINLESS STEEL
126	B	FHCS (1/2-13 X 1-1/4" LONG)	304 STAINLESS STEEL
127	B	FHCS (1/2-13 X 7/8" LONG)	304 STAINLESS STEEL
128	B	HINGE PIN	304 STAINLESS STEEL

Table 1-4 Safety-Related Parts of Traveller Type B Configuration (Drawing 10071E36)			
ITEM	**SAFETY CLASS**	**PART NAME**	**(SIZE) REFERENCE INFORMATION**
129	B	FHCS (1/2-13 X 1/2" LONG)	304 STAINLESS STEEL
130	A	POISON PLATE - TOP DOOR LEFT	COMPOSITE BORON PLATE
131	A	POISON PLATE -TOP DOOR RIGHT	COMPOSITE BORON PLATE
132	B	FHCS (1/2-13 X .75" LONG)	304 STAINLESS STEEL
133	B	TOP AXIAL RESTRAINT	ASTM B209/B221 6061-T6 ALUMINUM
134	B	AXIAL BOTTOM SPACER	ASTM B209/B221 6061-T6, 6063-T6, OR 6082-T6 ALUMINUM
135	B	REMOVABLE TOP PLATE	ASTM B209/B221 6061-T6 ALUMINUM
136	B	JAM NUT (3/4-10)	304 STAINLESS STEEL
137	C	WAVE WASHER	300 SERIES STAINLESS STEEL
138	B	SHEAR BARS (.495)	304 STAINLESS STEEL
139	B	AXIAL CLAMPING STUDS (3/4-10)	300 SERIES STAINLESS STEEL
140	B	CIRCULAR BASE PLATE	ASTM B209/B221 6061-T6 ALUMINUM
141	B	CIRCULAR PLATE CLAMPING STUD (3/4-10)	300 SERIES STAINLESS STEEL
142	C	MODIFIED HHCS (1/4-28 X 3/4" LG.)	304 STAINLESS STEEL
143	B	BOTTOM SUPPORT SPACER (NOZZLE)	ASTM B209/B221 6061-T6 ALUMINUM BASE / 1/8" RUBBER PAD
144	B	BOTTOM SUPPORT PLATE (NOZZLE)	ASTM B209/B221 6061-T6 ALUMINUM BASE / 1/16" RUBBER PAD
145	B	BOTTOM SUPPORT SPACER (SKIRTED NOZZLE)	ASTM B209/B221 6061-T6 ALUMINUM BASE / 1/8" RUBBER PAD

Table 1-5 Safety-Related Parts of Rod Pipe (Drawing 10006E58)

ITEM	SAFETY CLASS	PART NAME	(SIZE) REFERENCE INFORMATION
01	B	6" PIPE	SCHED 40, 304 STAINLESS STEEL
02	B	END FLANGE	304 STAINLESS STEEL
03	B	SOLID FLANGE	304 STAINLESS STEEL
04	B	END PLATE	304 STAINLESS STEEL
05	B	BOLT (1/2"-13 X 1.25" LG)	304 STAINLESS STEEL
06	B	NUT (1/2"-13)	304 STAINLESS STEEL
07	C	LIFTING LUG	304 STAINLESS STEEL
08	C	TOP SHIM PLATE	304 STAINLESS STEEL
09	NQ	SHIPPING PAD	N/A
10	NQ	PACKING FOAM	N/A
11	NQ	GASKET	N/A
12	NQ	BOTTOM PLATE SPACER	N/A

DOCUMENT OF RECORD Electronically approved records are authenticated in the electronic document management system. (ENOVIA) Thursday, September 24, 2015 9:43:47 AM PE Document Product Design Engineer: Brian Hempy; ProductDraftsman: Greg Hill; ProductChecker: Todd Rodgers;

Withheld under 10CFR2.390 a,c

1	SO 752255 ECN 61148-0		
7	ZNE QC DESCRIPTION PKGSUPPORT ECN 0002409-0		
	ZNE QC DESCRIPTION - - SEE SHEETS 2 - 5 FOR CHANGES.		
	DWN BY C. GIBBS 2012/07/06		
8	USPKGSUPPORT ECN 0002769-0		
	ZNE QC DESCRIPTION B3 - EDITED NOTE.		
	DWN BY C. GIBBS 2013/08/19		
9	BUD128779 ECN 0003155-0		
	ZNE QC DESCRIPTION - - ADDED NOTE F.		
	- - EDITED BILL OF MATERIAL.		
	DWN BY C. GIBBS 2015/09/22		

SEE PRODUCT SPECIFICATION
PDINFO00 FOR SUPPLEMENTAL
PRODUCT INFORMATION

DIMENSIONS ARE IN INCHES

DWG REF -
NEXT ASSY -

THIRD ANGLE PROJECTION

DCTM	-
CHKD	-
DES ENG	-
MFG ENG	-
PA ENG	-
QES ENG MGR	-
APVD	-
APVD	-
APVD	-

Westinghouse ELECTRIC COMPANY LLC - NUCLEAR FUEL
COLUMBIA, SC USA

SAFETY RELATED ITEMS TRAVELLER XL & STD

SIZE	FSCM NO	DWG NO	REV
E		10004E58	9
SCALE 1:1	WEIGHT(LBS)	SHEET 1 OF 9	

SOLIDWORKS DRAWING
DO NOT REVISE MANUALLY

© 2015 Westinghouse Electric Company LLC
All Rights Reserved

DOCUMENT OF RECORD Electronically approved records are authenticated in the electronic document management system. (ENOVIA) Thursday, September 24, 2015 9:43:47 AM PE Document Product Design Engineer: Brian Hempy; ProductDraftsman: Greg Hill; ProductChecker: Todd Rodgers;

Withheld under 10CFR2.390 a,c

SO	752255		
ECN	61148-0		
ZNE	QC	DESCRIPTION	
		PKGSUPPORT	
		ECN 0002409-0	
ZNE	QC	DESCRIPTION	
C2	-	DIM (2.741) WAS 2.739	

DWN BY	C. GIBBS	2012/07/06	
		USPKGSUPPORT	
		ECN 0002769-0	
ZNE	QC	DESCRIPTION	
-	-	SEE SHEET 1 FOR CHANGES.	

DWN BY	C. GIBBS	2013/08/1	
		BUD1128779	
		ECN 0003155-0	
ZNE	QC	DESCRIPTION	
-	-	SEE SHEET 1 FOR CHANGES.	

DWN BY	C. GIBBS	2015/09/22	

SEE PRODUCT SPECIFICATION
PDINFO00 FOR SUPPLEMENTAL
PRODUCT INFORMATION

DIMENSIONS ARE IN INCHES

DWG REF	-
NEXT ASSY	-

THIRD ANGLE PROJECTION

CHKD	-
DES ENG	-
MFG ENG	-
PA ENG	-
DES ENG MGR	-
APVD	-
APVD	-
APVD	-

Westinghouse

ELECTRIC COMPANY LLC - NUCLEAR FUEL
COLUMBIA, SC USA

SAFETY RELATED ITEMS TRAVELLER XL & STD

SIZE	FSCM NO	DWG NO	REV
E		10004E58	9
SCALE 1:8		WEIGHT(LBS)	SHEET 2 OF 9

SOLIDWORKS DRAWING
DO NOT REVISE MANUALLY

© 2015 Westinghouse Electric Company LLC
All Rights Reserved

DOCUMENT OF RECORD Electronically approved records are authenticated in the electronic document management system. (ENOVIA) Thursday, September 24, 2015 9:43:48 AM PE Document Product Design Engineer: Brian Hempy; ProductDraftsman: Greg Hill; ProductChecker: Todd Rodgers;

Withheld under 10CFR2.390 a,c

1	SO 752255 ECN 61148-0		
7	ZNE QC DESCRIPTION PKGSUPPORT ECN 0002409-0	DWN BY C. GIBBS	2012/07/06
8	ZNE QC DESCRIPTION C3 - EDITED WELD SYMBOL.	USPKGSUPPORT ECN 0002769-0	
9	ZNE QC DESCRIPTION - - SEE SHEET 1 FOR CHANGES.	DWN BY C. GIBBS	2013/08/16
		BUD1128779 ECN 0003155-0	
	ZNE QC DESCRIPTION - - SEE SHEET 1 FOR CHANGES.	DWN BY C. GIBBS	2015/09/22

SEE PRODUCT SPECIFICATION
PDINFO00 FOR SUPPLEMENTAL
PRODUCT INFORMATION

DIMENSIONS ARE IN INCHES

DWG REF -	THIRD ANGLE PROJECTION
NEXT ASSY -	

DCM	-
CHKD	-
DES ENG	-
MFG ENG	-
PA ENG	-
QES ENG MGR	-
APVD	-
APVD	-
APVD	-

Westinghouse ELECTRIC COMPANY LLC - NUCLEAR FUEL
COLUMBIA, SC USA

SAFETY RELATED ITEMS TRAVELLER XL & STD

SIZE	FSCM NO	DWG NO	REV
E		10004E58	9
SCALE 1:8	WEIGHT(LBS)	SHEET 3 OF 9	

SOLIDWORKS DRAWING
DO NOT REVISE MANUALLY

© 2015 Westinghouse Electric Company LLC
All Rights Reserved

DOCUMENT OF RECORD Electronically approved records are authenticated in the electronic document management system. (ENOVIA) Thursday, September 24, 2015 9:43:48 AM PE Document Product Design Engineer: Brian Hempy; ProductDraftsman: Greg Hill; ProductChecker: Todd Rodgers;

Withheld under 10CFR2.390 a,c

SO 752255	1		
ECN 61148-0			
ZNE	OC	DESCRIPTION	
PKGSUPPORT			7
ECN 0002409-0			
ZNE	OC	DESCRIPTION	
H7/ H8	-	REMOVED WELD CALL OUTS.	
DWN BY	C. GIBBS	2012/07/06	
USPKGSUPPORT			8
ECN 0002769-0			
ZNE	OC	DESCRIPTION	
-	-	SEE SHEET 1 FOR CHANGES.	
DWN BY	C. GIBBS	2013/08/19	
BUD1128779			9
ECN 0003155-0			
ZNE	OC	DESCRIPTION	
-	-	SEE SHEET 1 FOR CHANGES.	
DWN BY	C. GIBBS	2015/09/22	

SEE PRODUCT SPECIFICATION PDINFO00 FOR SUPPLEMENTAL PRODUCT INFORMATION

DIMENSIONS ARE IN INCHES

DWG REF -	THIRD ANGLE PROJECTION
NEXT ASSY -	

DRTN -	-
CHKD -	-
DES ENG -	-
MFG ENG -	-
PA ENG -	-
DES ENG MGR -	-
APVD -	-
APVD -	-
APVD -	-

Westinghouse ELECTRIC COMPANY LLC - NUCLEAR FUEL COLUMBIA, SC USA

SAFETY RELATED ITEMS TRAVELLER XL & STD

SIZE	FSCM NO	DWG NO	REV
E		10004E58	9
SCALE 1:1		WEIGHT(LBS)	SHEET 4 OF 9

SOLIDWORKS DRAWING DO NOT REVISE MANUALLY

© 2015 Westinghouse Electric Company LLC All Rights Reserved

DOCUMENT OF RECORD Electronically approved records are authenticated in the electronic document management system. (ENOVIA) Thursday, September 24, 2015 9:43:48 AM PE Document Product Design Engineer: Brian Hempy; ProductDraftsman: Greg Hill; ProductChecker: Todd Rodgers;

Withheld under 10CFR2.390 a,c

SO 752255 ECN 61148-0	1		
ZNE	QC	DESCRIPTION	
PKGSUPPORT ECN 0002409-0	7		
ZNE	QC	DESCRIPTION	
BB	-	ADDED WELD SYMBOL CALLOUT.	
DWN BY C. GIBBS			2012/07/06
USPKGSUPPORT ECN 0002769-0	8		
ZNE	QC	DESCRIPTION	
-	-	SEE SHEET 1 FOR CHANGES.	
DWN BY C. GIBBS			2013/08/1
BUD1128779 ECN 0003155-0	9		
ZNE	QC	DESCRIPTION	
-	-	SEE SHEET 1 FOR CHANGES.	
DWN BY C. GIBBS			2015/09/22

SEE PRODUCT SPECIFICATION PDINFO00 FOR SUPPLEMENTAL PRODUCT INFORMATION

DIMENSIONS ARE IN INCHES

DWG REF -	THIRD ANGLE PROJECTION
NEXT ASSY -	

CHKD	-
DES ENG	-
MFG ENG	-
PA ENG	-
DES ENG MGR	-
APVD	-
APVD	-
APVD	-

Westinghouse ELECTRIC COMPANY LLC - NUCLEAR FUEL COLUMBIA, SC USA

SAFETY RELATED ITEMS TRAVELLER XL & STD

SIZE	FSCM NO	DWG NO	REV
E		10004E58	9
SCALE 1:1	WEIGHT(LBS)	SHEET 5 OF 9	

SOLIDWORKS DRAWING DO NOT REVISE MANUALLY

© 2015 Westinghouse Electric Company LLC All Rights Reserved

DOCUMENT OF RECORD Electronically approved records are authenticated in the electronic document management system. (ENOVIA) Thursday, September 24, 2015 9:43:49 AM PE Document Product Design Engineer: Brian Hempy; ProductDraftsman: Greg Hill; ProductChecker: Todd Rodgers;

Withheld under 10CFR2.390 a,c

1	SO 752255 ECN 61148-0		
7	ZNE QC DESCRIPTION PKGSUPPORT ECN 0002409-0		
	ZNE QC DESCRIPTION - - SEE SHEETS 2 - 5 FOR CHANGES.		
	DWN BY C. GIBBS	2012/07/06	
8	USPKGSUPPORT ECN 0002769-0		
	ZNE QC DESCRIPTION - - SEE SHEET 1 FOR CHANGES.		
	DWN BY C. GIBBS	2013/08/16	
9	BUD128779 ECN 0003155-0		
	ZNE QC DESCRIPTION - - SEE SHEET 1 FOR CHANGES.		
	DWN BY C. GIBBS	2015/09/22	

SEE PRODUCT SPECIFICATION
PDINFO00 FOR SUPPLEMENTAL
PRODUCT INFORMATION

DIMENSIONS ARE IN INCHES

DWG REF -
NEXT ASSY -

THIRD ANGLE PROJECTION

DCM	-	-
CHKD	-	-
DES ENG	-	
MFG ENG	-	-
PA ENG	-	-
DES ENG MGR	-	-
APVD	-	
APVD	-	-
APVD	-	-

Westinghouse ELECTRIC COMPANY LLC - NUCLEAR FUEL
COLUMBIA, SC USA

SAFETY RELATED ITEMS TRAVELLER XL & STD

SIZE	FSCM NO	DWG NO	REV
E		10004E58	9
SCALE 1:1		WEIGHT(LBS)	SHEET 6 OF 9

SOLIDWORKS DRAWING
DO NOT REVISE MANUALLY

© 2015 Westinghouse Electric Company LLC
All Rights Reserved

DOCUMENT OF RECORD Electronically approved records are authenticated in the electronic document management system. (ENOVIA) Thursday, September 24, 2015 9:43:49 AM PE Document Product Design Engineer: Brian Hempy; ProductDraftsman: Greg Hill; ProductChecker: Todd Rodgers;

Withheld under 10CFR2.390 a,c

1	SO 752255 ECN 61148-0	ZNE	OC
7	PKGSUPPORT ECN 0002409-0	ZNE	OC
	-	-	
8	USPKGSUPPORT ECN 0002769-0	ZNE	OC
	-	-	
9	BUD1128779 ECN 0003155-0	ZNE	OC
	-	-	

DESCRIPTION	DWN BY	
SEE SHEETS 2 - 5 FOR CHANGES.	C. GIBBS	2012/07/06
SEE SHEET 1 FOR CHANGES.	C. GIBBS	2013/08/19
SEE SHEET 1 FOR CHANGES.	C. GIBBS	2015/09/22

SEE PRODUCT SPECIFICATION PDINFO00 FOR SUPPLEMENTAL PRODUCT INFORMATION

DIMENSIONS ARE IN INCHES

DWG REF	-
NEXT ASSY	-

THIRD ANGLE PROJECTION

DWN	-
CHKD	-
DES ENG	-
MFG ENG	-
PA ENG	-
DES ENG MGR	-
APVD	-
APVD	-
APVD	-

Westinghouse ELECTRIC COMPANY LLC - NUCLEAR FUEL COLUMBIA, SC USA

SAFETY RELATED ITEMS TRAVELLER XL & STD

SIZE	FSCM NO	DWG NO	REV
E		10004E58	9
SCALE 1:6		WEIGHT(LBS)	SHEET 7 OF 9

SOLIDWORKS DRAWING
DO NOT REVISE MANUALLY

© 2015 Westinghouse Electric Company LLC
All Rights Reserved

DOCUMENT OF RECORD Electronically approved records are authenticated in the electronic document management system. (ENOVIA) Thursday, September 24, 2015 9:43:49 AM PE Document Product Design Engineer: Brian Hempy; ProductDraftsman: Greg Hill; ProductChecker: Todd Rodgers;

Withheld under 10CFR2.390 a,c

1	SO 752255 ECN 61148-0		
7	ZNE QC DESCRIPTION PKGSUPPORT ECN 0002409-0		
	ZNE QC DESCRIPTION - - SEE SHEETS 2 - 5 FOR CHANGES.	DWN BY C. GIBBS	2012/07/06
8	USPKGSUPPORT ECN 0002769-0		
	ZNE QC DESCRIPTION - - SEE SHEET 1 FOR CHANGES.	DWN BY C. GIBBS	2013/08/19
9	BUD1287779 ECN 0003155-0		
	ZNE QC DESCRIPTION - - SEE SHEET 1 FOR CHANGES.	DWN BY C. GIBBS	2015/09/22

SEE PRODUCT SPECIFICATION
PDINFO00 FOR SUPPLEMENTAL
PRODUCT INFORMATION

DIMENSIONS ARE IN INCHES

DWG REF -	THIRD ANGLE PROJECTION
NEXT ASSY -	

-	-
CHKD -	-
DES ENG -	-
MFG ENG -	-
PA ENG -	-
DES ENG MGR -	-
APVD -	-
APVD -	-
APVD -	-

Westinghouse ELECTRIC COMPANY LLC - NUCLEAR FUEL
COLUMBIA, SC USA

SAFETY RELATED ITEMS TRAVELLER XL & STD

SIZE	FSCM NO	DWG NO	REV
E		10004E58	9
SCALE 1:7.5		WEIGHT(LBS)	SHEET 8 OF 9

SOLIDWORKS DRAWING
DO NOT REVISE MANUALLY

© 2015 Westinghouse Electric Company LLC
All Rights Reserved

DOCUMENT OF RECORD Electronically approved records are authenticated in the electronic document management system. (ENOVIA) Thursday, September 24, 2015 9:43:49 AM PE Document Product Design Engineer: Brian Hempy; ProductDraftsman: Greg Hill; ProductChecker: Todd Rodgers;

Withheld under 10CFR2.390 a,c

SO	752255		1
ECN	61148-0		
ZNE	QC	DESCRIPTION	
PKGSUPPORT			7
ECN 0002409-0			
ZNE	QC	DESCRIPTION	
-	-	SEE SHEETS 2 - 5 FOR CHANGES.	
DWN BY	C. GIBBS	2012/07/06	
USPKGSUPPORT			8
ECN 0002769-0			
ZNE	QC	DESCRIPTION	
-	-	SEE SHEET 1 FOR CHANGES.	
DWN BY	C. GIBBS	2013/08/1	
BUD1128779			9
ECN 0003155-0			
ZNE	QC	DESCRIPTION	
-	-	SEE SHEET 1 FOR CHANGES.	
DWN BY	C. GIBBS	2015/09/22	

SEE PRODUCT SPECIFICATION
PDINFO00 FOR SUPPLEMENTAL
PRODUCT INFORMATION

DIMENSIONS ARE IN INCHES

DWG REF	-
NEXT ASSY	-

THIRD ANGLE PROJECTION

CHKD	-
DES ENG	-
MFG ENG	-
PA ENG	-
DES ENG MGR	-
APVD	-
APVD	-
APVD	-

Westinghouse

ELECTRIC COMPANY LLC - NUCLEAR FUEL
COLUMBIA, SC USA

SAFETY RELATED ITEMS TRAVELLER XL & STD

SIZE	FSCM NO	DWG NO	REV
E		10004E58	9
SCALE 1:2		WEIGHT(LBS)	SHEET 9 OF 9

SOLIDWORKS DRAWING
DO NOT REVISE MANUALLY

© 2015 Westinghouse Electric Company LLC
All Rights Reserved

DOCUMENT OF RECORD Electronically approved records are authenticated in the electronic document management system. (ENOVIA) Wednesday, 16 June, 2021 11:44:38 AM PE Document Product Design Engineer: Brian Hempy; ProductDraftsman: Charles Gibbs; ProductChecker: Greg Hill;

Withheld under 10CFR2.390 a,c

	ZNE	OC	DESCRIPTION
1	SO	NFOSEUP	
	ECN	0003518-0	
2	NFOSEUP		
	ECN 0003725-0		
	ZNE	OC	DESCRIPTION
	-	-	REVISED ITEM 143 IN BOM. ADDED ITEM 144 TO BOM.
	DWN BY	C. GIBBS	2019/08/26
3	BUD128779		
	ECN 0003957-0		
	ZNE	OC	DESCRIPTION
	-	-	ADDED ITEM 145 TO BILL OF MATERIAL.
	DWN BY	C. GIBBS	2021/06/08

SEE PRODUCT SPECIFICATION PDINFO00 FOR SUPPLEMENTAL PRODUCT INFORMATION

DIMENSIONS ARE IN INCHES

DWG REF -

NEXT ASSY -

THIRD ANGLE PROJECTION

DFTM	C. GIBBS	2018/04/12
CHKD	W. RODGERS	2018/04/13
DES ENG	B. HEMPY	2018/03/21
MFG ENG	S. PALMER	2018/03/21
PA ENG	B. JOYNER	2018/04/11
DES ENG MGR	C. AMICK	2018/04/11
APVD	G. PHELPS	2018/03/22
APVD	R. MAURER	2018/03/27
APVD	J. HALLIGAN	2018/03/21

Westinghouse ELECTRIC COMPANY LLC - NUCLEAR FUEL COLUMBIA, SC USA

SAFETY RELATED ITEMS TRAVELLER TYPE B XL & STD

SIZE	FSCM NO	DWG NO	REV
E		10071E36	3
SCALE 1:1	WEIGHT(LBS)	SHEET 1 OF 9	

SOLIDWORKS DRAWING
DO NOT REVISE MANUALLY

© 2021 Westinghouse Electric Company LLC
All Rights Reserved

DOCUMENT OF RECORD Electronically approved records are authenticated in the electronic document management system. (ENOVIA) Wednesday, 16 June, 2021 11:44:38 AM PE Document Product Design Engineer: Brian Hempy; ProductDraftsman: Charles Gibbs; ProductChecker: Greg Hill;

Withheld under 10CFR2.390 a,c

	ZNE	QC	DESCRIPTION
1	SO	NFOSEUP	
	ECN	0003518-0	
2	ZNE	QC	DESCRIPTION
	NFOSEUP		
	ECN 0003725-0		
	-	-	NO CHANGES THIS SHEET.
	DWN BY	C. GIBBS	2019/08/26
3	ZNE	QC	DESCRIPTION
	BUD128779		
	ECN 0003957-0		
	-	-	SEE SHEETS 1, 4 & 7 FOR CHANGES.
	DWN BY	C. GIBBS	2021/06/08

SEE PRODUCT SPECIFICATION PDINFO00 FOR SUPPLEMENTAL PRODUCT INFORMATION

DIMENSIONS ARE IN INCHES

DWG REF -

NEXT ASSY -

THIRD ANGLE PROJECTION

DFTM	C. GIBBS	2018/04/12
DWD	W. RODGERS	2018/04/13
DES ENG	B. HEMPY	2018/03/21
MFG ENG	S. PALMER	2018/03/21
PA ENG	B. JOYNER	2018/04/11
DES ENG MGR	C. AMICK	2018/04/11
APVD	G. PHELPS	2018/03/22
APVD	R. MAURER	2018/03/27
APVD	J. HALLIGAN	2018/03/21

Westinghouse

ELECTRIC COMPANY LLC - NUCLEAR FUEL
COLUMBIA, SC USA

SAFETY RELATED ITEMS TRAVELLER TYPE B XL & STD

SIZE	FSCM NO	DWG NO	REV
E		10071E36	3
SCALE 1:8		WEIGHT(LBS)	SHEET 2 OF 9

SOLIDWORKS DRAWING
DO NOT REVISE MANUALLY

© 2021 Westinghouse Electric Company LLC
All Rights Reserved

DOCUMENT OF RECORD Electronically approved records are authenticated in the electronic document management system. (ENOVIA) Wednesday, 16 June, 2021 11:44:38 AM PE Document Product Design Engineer: Brian Hempy; ProductDraftsman: Charles Gibbs; ProductChecker: Greg Hill;

Withheld under 10CFR2.390 a,c

	ZNE	QC	DESCRIPTION
1			NFOSEUP SO 0003518-0 ECN 0003725-0
2			NFOSEUP ECN 0003957-0 BUD128779
3			NO CHANGES THIS SHEET. SEE SHEETS 1, 4 & 7 FOR CHANGES.

	DWN BY	DATE
1	C. GIBBS	2019/08/26
2		
3	C. GIBBS	2021/06/08

SEE PRODUCT SPECIFICATION PDINFO00 FOR SUPPLEMENTAL PRODUCT INFORMATION

DIMENSIONS ARE IN INCHES

DWG REF -
NEXT ASSY -
THIRD ANGLE PROJECTION

DFTM	C. GIBBS	2018/04/12
DWD	W. RODGERS	2018/04/13
DES ENG	B. HEMPY	2018/03/21
MFG ENG	S. PALMER	2018/03/21
PA ENG	B. JOYNER	2018/04/11
DES ENG MGR	C. AMICK	2018/04/11
APVD	G. PHELPS	2018/03/22
APVD	R. MAURER	2018/03/27
APVD	J. HALLIGAN	2018/03/21

Westinghouse

ELECTRIC COMPANY LLC - NUCLEAR FUEL
COLUMBIA, SC USA

SAFETY RELATED ITEMS TRAVELLER TYPE B XL & STD

SIZE	FSCM NO	DWG NO	REV
E		10071E36	3
SCALE 1:8		WEIGHT(LBS)	SHEET 3 OF 9

SOLIDWORKS DRAWING
DO NOT REVISE MANUALLY

© 2021 Westinghouse Electric Company LLC
All Rights Reserved

DOCUMENT OF RECORD Electronically approved records are authenticated in the electronic document management system. (ENOVIA) Wednesday, 16 June, 2021 11:44:38 AM PE Document Product Design Engineer: Brian Hempy; ProductDraftsman: Charles Gibbs; ProductChecker: Greg Hill;

Withheld under 10CFR2.390 a,c

	ZNE	QC	DESCRIPTION
1	SO	NFOSEUP	
	ECN	0003518-0	
2	ZNE	QC	DESCRIPTION
	NFOSEUP		
	ECN 0003725-0		
	ZNE	QC	DESCRIPTION
	-	-	NO CHANGES THIS SHEET.
	DWN BY	C. GIBBS	2019/08/26
3	BUD128779		
	ECN 0003957-0		
	ZNE	QC	DESCRIPTION
	HIS	-	ADDED ITEM 145 BALLOON.
	DWN BY	C. GIBBS	2021/06/08

SEE PRODUCT SPECIFICATION PDINFO00 FOR SUPPLEMENTAL PRODUCT INFORMATION

DIMENSIONS ARE IN INCHES

DWG REF	-
NEXT ASSY	-

THIRD ANGLE PROJECTION

DFTM	C. GIBBS	2018/04/12
DWD	W. RODGERS	2018/04/13
DES ENG	B. HEMPY	2018/03/21
MFG ENG	S. PALMER	2018/03/21
PA ENG	B. JOYNER	2018/04/11
DES ENG MGR	C. AMICK	2018/04/11
APVD	G. PHELPS	2018/03/22
APVD	R. MAURER	2018/03/27
APVD	J. HALLIGAN	2018/03/21

Westinghouse ELECTRIC COMPANY LLC - NUCLEAR FUEL COLUMBIA, SC USA

SAFETY RELATED ITEMS TRAVELLER TYPE B XL & STD

SIZE	FSCM NO	DWG NO	REV
E		10071E36	3
SCALE 1:1		WEIGHT(LBS)	SHEET 4 OF 9

SOLIDWORKS DRAWING
DO NOT REVISE MANUALLY

© 2021 Westinghouse Electric Company LLC
All Rights Reserved

DOCUMENT OF RECORD Electronically approved records are authenticated in the electronic document management system. (ENOVIA) Wednesday, 16 June, 2021 11:44:38 AM PE Document Product Design Engineer: Brian Hempy; ProductDraftsman: Charles Gibbs; ProductChecker: Greg Hill;

Withheld under 10CFR2.390 a,c

	ZNE	QC	DESCRIPTION
1	SO	NFOSEUP	
	ECN	0003518-0	
2	ZNE	QC	DESCRIPTION
	NFOSEUP		
	ECN 0003725-0		
	ZNE	QC	DESCRIPTION
	-	-	NO CHANGES THIS SHEET.
	DWN BY	C. GIBBS	2019/08/26
3	BUD128779		
	ECN 0003957-0		
	ZNE	QC	DESCRIPTION
	-	-	SEE SHEETS 1, 4 & 7 FOR CHANGES.
	DWN BY	C. GIBBS	2021/06/08

SEE PRODUCT SPECIFICATION PDINFO00 FOR SUPPLEMENTAL PRODUCT INFORMATION

DIMENSIONS ARE IN INCHES

DWG REF -	THIRD ANGLE PROJECTION
NEXT ASSY -	

	C. GIBBS	2018/04/12
DWD	W. RODGERS	2018/04/13
DES ENG	B. HEMPY	2018/03/21
MFG ENG	S. PALMER	2018/03/21
PA ENG	B. JOYNER	2018/04/11
DES ENG MGR	C. AMICK	2018/04/11
APVD	G. PHELPS	2018/03/22
APVD	R. MAURER	2018/03/27
APVD	J. HALLIGAN	2018/03/21

Westinghouse ELECTRIC COMPANY LLC - NUCLEAR FUEL COLUMBIA, SC USA

SAFETY RELATED ITEMS TRAVELLER TYPE B XL & STD

SIZE	FSCM NO	DWG NO	REV
E		10071E36	3
SCALE 1:1		WEIGHT(LBS)	SHEET 5 OF 9

SOLIDWORKS DRAWING DO NOT REVISE MANUALLY

© 2021 Westinghouse Electric Company LLC All Rights Reserved

DOCUMENT OF RECORD Electronically approved records are authenticated in the electronic document management system. (ENOVIA) Wednesday, 16 June, 2021 11:44:38 AM PE Document Product Design Engineer: Brian Hempy; ProductDraftsman: Charles Gibbs; ProductChecker: Greg Hill;

Withheld under 10CFR2.390 a,c

1	SO	NFOSEUP	
	ECN	0003518-0	
	ZNE	QC	DESCRIPTION
	-	-	NO CHANGES THIS SHEET.
	DWN BY	C. GIBBS	2019/08/26
2	BUD128779		
	ECN	0003957-0	
	ZNE	QC	DESCRIPTION
	-	-	SEE SHEETS 1, 4 & 7 FOR CHANGES.
	DWN BY	C. GIBBS	2021/06/08
2	NFOSEUP		
	ECN	0003725-0	
	ZNE	QC	DESCRIPTION
	-	-	NO CHANGES THIS SHEET.
	DWN BY	C. GIBBS	2019/08/26

SEE PRODUCT SPECIFICATION PDINFO00 FOR SUPPLEMENTAL PRODUCT INFORMATION

DIMENSIONS ARE IN INCHES

DWG REF	-
NEXT ASSY	-

THIRD ANGLE PROJECTION

DFTM	C. GIBBS	2018/04/12
DWD	W. RODGERS	2018/04/13
DES ENG	B. HEMPY	2018/03/21
MFG ENG	S. PALMER	2018/03/21
PA ENG	B. JOYNER	2018/04/11
DES ENG MGR	C. AMICK	2018/04/11
APVD	G. PHELPS	2018/03/22
APVD	R. MAURER	2018/03/27
APVD	J. HALLIGAN	2018/03/21

Westinghouse

ELECTRIC COMPANY LLC - NUCLEAR FUEL
COLUMBIA, SC USA

SAFETY RELATED ITEMS TRAVELLER TYPE B XL & STD

SIZE	FSCM NO	DWG NO	REV
E		10071E36	3
SCALE	1:1	WEIGHT(LBS)	SHEET 6 OF 9

SOLIDWORKS DRAWING
DO NOT REVISE MANUALLY

© 2021 Westinghouse Electric Company LLC
All Rights Reserved

DOCUMENT OF RECORD Electronically approved records are authenticated in the electronic document management system. (ENOVIA) Wednesday, 16 June, 2021 11:44:38 AM PE Document Product Design Engineer: Brian Hempy; ProductDraftsman: Charles Gibbs; ProductChecker: Greg Hill;

Withheld under 10CFR2.390 a,c

SO	NFOSEUP	1	
ECN	0003518-0		
ZNE	QC	DESCRIPTION	
NFOSEUP		2	
ECN 0003725-0			
ZNE	QC	DESCRIPTION	
G4-G8, D1-D3	-	ADDED VIEWS FOR ITEM 143.	
		DELETED VIEWS.	
B4		REVISED NOTE.	
DWN BY	C. GIBBS	2019/08/26	
BUD128779		3	
ECN 0003957-0			
ZNE	QC	DESCRIPTION	
	-	ADDED ITEM 145 VIEWS.	
B2	-	ADDED NOTE AND ITEM 145 BALLOON.	
DWN BY	C. GIBBS	2021/06/08	

SEE PRODUCT SPECIFICATION PDINFO00 FOR SUPPLEMENTAL PRODUCT INFORMATION

DIMENSIONS ARE IN INCHES

DWG REF	-
NEXT ASSY	-

THIRD ANGLE PROJECTION

DFTM	C. GIBBS	2018/04/12
DWD	W. RODGERS	2018/04/13
DES ENG	B. HEMPY	2018/03/21
MFG ENG	S. PALMER	2018/03/21
PA ENG	B. JOYNER	2018/04/11
DES ENG MGR	C. AMICK	2018/04/11
APVD	G. PHELPS	2018/03/22
APVD	R. MAURER	2018/03/27
APVD	J. HALLIGAN	2018/03/21

Westinghouse

ELECTRIC COMPANY LLC - NUCLEAR FUEL
COLUMBIA, SC USA

SAFETY RELATED ITEMS TRAVELLER TYPE B XL & STD

SIZE	FSCM NO	DWG NO	REV
E		10071E36	3
SCALE 1:2		WEIGHT(LBS)	SHEET 7 OF 9

SOLIDWORKS DRAWING
DO NOT REVISE MANUALLY

© 2021 Westinghouse Electric Company LLC
All Rights Reserved

DOCUMENT OF RECORD Electronically approved records are authenticated in the electronic document management system. (ENOVIA) Wednesday, 16 June, 2021 11:44:38 AM PE Document Product Design Engineer: Brian Hempy; ProductDraftsman: Charles Gibbs; ProductChecker: Greg Hill;

Withheld under 10CFR2.390 a,c

	ZNE	QC	DESCRIPTION
1	SO	NFOSEUP	
	ECN	0003518-0	
2	NFOSEUP		
	ECN	0003725-0	
	ZNE	QC	DESCRIPTION
	-	-	NO CHANGES THIS SHEET.
	DWN BY	C. GIBBS	2019/08/26
3	BUD128779		
	ECN	0003957-0	
	ZNE	QC	DESCRIPTION
	-	-	SEE SHEETS 1, 4 & 7 FOR CHANGES.
	DWN BY	C. GIBBS	2021/06/08

SEE PRODUCT SPECIFICATION PDINFO00 FOR SUPPLEMENTAL PRODUCT INFORMATION

DIMENSIONS ARE IN INCHES

DWG REF -	THIRD ANGLE PROJECTION
NEXT ASSY -	

	C. GIBBS	2018/04/12
DWD	W. RODGERS	2018/04/13
DES ENG	B. HEMPY	2018/03/21
MFG ENG	S. PALMER	2018/03/21
PA ENG	B. JOYNER	2018/04/11
DES ENG MGR	C. AMICK	2018/04/11
APVD	G. PHELPS	2018/03/22
APVD	R. MAURER	2018/03/27
APVD	J. HALLIGAN	2018/03/21

Westinghouse ELECTRIC COMPANY LLC - NUCLEAR FUEL COLUMBIA, SC USA

SAFETY RELATED ITEMS TRAVELLER TYPE B XL & STD

SIZE	FSCM NO	DWG NO	REV
E		10071E36	3
SCALE 1:7.5	WEIGHT(LBS)	SHEET 8 OF 9	

SOLIDWORKS DRAWING DO NOT REVISE MANUALLY

© 2021 Westinghouse Electric Company LLC All Rights Reserved

DOCUMENT OF RECORD Electronically approved records are authenticated in the electronic document management system. (ENOVIA) Wednesday, 16 June, 2021 11:44:38 AM PE Document Product Design Engineer: Brian Hempy; ProductDraftsman: Charles Gibbs; ProductChecker: Greg Hill;

Withheld under 10CFR2.390 a,c

ZNE	OC	DESCRIPTION
	1	
SO	NFOSEUP	
ECN	0003518-0	
	2	
NFOSEUP		
ECN 0003725-0		
B5	-	REVISED NOTES.
D7		
	3	
BUD128779		
ECN 0003957-0		
-	-	SEE SHEETS 1, 4 & 7 FOR CHANGES.

DWN BY	C. GIBBS	2019/08/26
DWN BY	C. GIBBS	2021/06/08

SEE PRODUCT SPECIFICATION PDINFO00 FOR SUPPLEMENTAL PRODUCT INFORMATION

DIMENSIONS ARE IN INCHES

DWG REF -	THIRD ANGLE PROJECTION
NEXT ASSY -	

DFTM	C. GIBBS	2018/04/12
CHKD	W. RODGERS	2018/04/13
DES ENG	B. HEMPY	2018/03/21
MFG ENG	S. PALMER	2018/03/21
PA ENG	B. JOYNER	2018/04/11
DES ENG MGR	C. AMICK	2018/04/11
APVD	G. PHELPS	2018/03/22
APVD	R. MAURER	2018/03/27
APVD	J. HALLIGAN	2018/03/21

Westinghouse ELECTRIC COMPANY LLC - NUCLEAR FUEL COLUMBIA, SC USA

SAFETY RELATED ITEMS TRAVELLER TYPE B XL & STD

SIZE	FSCM NO	DWG NO	REV
E		10071E36	3
SCALE 1:2		WEIGHT(LBS)	SHEET 9 OF 9

SOLIDWORKS DRAWING
DO NOT REVISE MANUALLY

© 2021 Westinghouse Electric Company LLC
All Rights Reserved

DOCUMENT OF RECORD Electronically approved records are authenticated in the electronic document management system. (ENOVIA) Thursday, 13 August, 2020 09:46:47 AM PE Document Product Design Engineer: Brian Hempy; ProductDraftsman: Charles Gibbs; ProductChecker: Christopher Myers;

Withheld under 10CFR2.390 a,c

SO	752255		
ECN	61146-0		
ZNE	QC	DESCRIPTION	1
-	-	SEE ECN FOR CHANGES.	
DWN BY	C. GIBBS		2019/08/22
ZNE	QC	DESCRIPTION	6
-	-	NOSEUP ECN 0003725-0	
DWN BY	C. GIBBS		2020/08/11
ZNE	QC	DESCRIPTION	7
-	-	SEE SHEET 2 FOR CHANGES.	
DWN BY	C. GIBBS		2020/08/11

SEE PRODUCT SPECIFICATION PDINFO00 FOR SUPPLEMENTAL PRODUCT INFORMATION

DIMENSIONS ARE IN INCHES

DWG REF -

NEXT ASSY -

THIRD ANGLE PROJECTION

ALL TOLERANCES +/- 1/8" UNLESS OTHERWISE NOTED

DETM	-
CHKD	-
DES ENG	-
MFG ENG	-
PA ENG	-
QES ENG MGR	-
APVD	-
APVD	-
APVD	-

Westinghouse

ELECTRIC COMPANY LLC - NUCLEAR FUEL
COLUMBIA, SC USA

SHIPPING PACKAGE LOOSE ROD PIPE

SIZE	FSCM NO	DWG NO	REV
E	-	10006E58	7
SCALE 1:6	WEIGHT(LBS) SEE DWG	SHEET 1 OF 2	

SOLIDWORKS DRAWING
DO NOT REVISE MANUALLY

©2020 Westinghouse Electric Company LLC
All Rights Reserved

DOCUMENT OF RECORD Electronically approved records are authenticated in the electronic document management system. (ENOVIA) Thursday, 13 August, 2020 09:46:47 AM PE Document Product Design Engineer: Brian Hempy; ProductDraftsman: Charles Gibbs; ProductChecker: Christopher Myers;

Withheld under 10CFR2.390 a,c

SO	752255		
ECN	61146-0		
ZNE	QC	DESCRIPTION	1
		NOSEUP	
		ECN 0003725-0	6
ZNE	QC	DESCRIPTION	
-	-	SEE ECN FOR CHANGES.	
DWN BY	C. GIBBS	2019/08/22	7
		BUD128779	
		ECN 0003884-0	
ZNE	QC	DESCRIPTION	
B8	-	REMOVED "4G/6G" FROM NOTE.	
DWN BY	C. GIBBS	2020/08/11	

SEE PRODUCT SPECIFICATION PDINFO00 FOR SUPPLEMENTAL PRODUCT INFORMATION

DIMENSIONS ARE IN INCHES

DWG REF -

NEXT ASSY -

THIRD ANGLE PROJECTION

ALL TOLERANCES +/- 1/8" UNLESS OTHERWISE NOTED

DNTM	-
CHKD	-
DES ENG	-
MFG ENG	-
PA ENG	-
QES ENG MGR	-
APVD	-
APVD	-
APVD	-

Westinghouse

ELECTRIC COMPANY LLC - NUCLEAR FUEL
COLUMBIA, SC USA

SHIPPING PACKAGE LOOSE ROD PIPE

SIZE	FSCM NO	DWG NO	REV
E	-	10006E58	7
SCALE 1:8	WEIGHT(LBS) SEE DWG	SHEET 2 OF 2	

SOLIDWORKS DRAWING
DO NOT REVISE MANUALLY

©2020 Westinghouse Electric Company LLC
All Rights Reserved

TABLE OF CONTENTS

2.0 STRUCTURAL EVALUATION 2-1
2.1 DESCRIPTION OF STRUCTURAL DESIGN 2-1
2.1.1 Discussion 2-1
2.1.1.1 Packaging Configuration 2-1
2.1.1.2 Type B Configuration 2-2
2.1.2 Design Criteria 2-8
2.1.2.1 Basic Design Criteria 2-8
2.1.2.2 Miscellaneous Structural Failure Modes 2-10
2.1.3 Weights and Centers of Gravity 2-10
2.1.4 Identification of Codes and Standards for Package Design 2-12
2.2 MATERIALS 2-12
2.2.1 Material Properties and Specifications 2-12
2.2.1.1 ASTM A240/A276 Type 304 Stainless Steel 2-12
2.2.1.2 6005-T5 and 6061-T6 Aluminum 2-14
2.2.1.3 Polyurethane Foam 2-16
2.2.1.4 Neoprene 2-19
2.2.1.5 Ultra-High Molecular Weight Polyethylene 2-19
2.2.1.6 Borated Aluminum Laminate Composite 2-19
2.2.1.7 Ceramic Insulation (Paper and Felt) 2-19
2.2.1.8 Zirconium and Other Metal Alloy Performance 2-19
2.2.2 Chemical, Galvanic, or Other Reactions 2-35
2.2.3 Effects of Radiation on Materials 2-35
2.3 FABRICATION AND EXAMINATION 2-36
2.3.1 Fabrication 2-36
2.3.2 Examination 2-36
2.4 GENERAL REQUIREMENTS FOR ALL PACKAGES 2-37
2.4.1 Minimum Package Size 2-37
2.4.2 Tamper-Indicating Feature 2-37
2.4.3 Positive Closure 2-37
2.5 LIFTING AND TIE-DOWN STANDARDS FOR ALL PACKAGES 2-38
2.5.1 Lifting Devices 2-38
2.5.1.1 Traveller XL Four Point Lift 2-38
2.5.1.2 Traveller STD Four-Point Lift 2-41
2.5.1.3 Forklift Analysis 2-42
2.5.1.4 Weld Shear 2-45
2.5.1.5 Bolts 2-46
2.5.1.6 Coupling Nut 2-46
2.5.1.7 Hoist Ring 2-47
2.5.2 Tie-Down Devices 2-47
2.5.2.1 Leg Assembly 2-48
2.5.2.2 Weld Shear Analysis 2-49
2.5.2.3 Lift Eyes 2-50
2.5.2.4 Wind Shear Analysis – Vertical Direction 2-51
2.5.2.5 Weld Shear Analysis – Combined Shear 2-52
2.6 NORMAL CONDITIONS OF TRANSPORT 2-53
2.6.1 Heat 2-53
2.6.1.1 Summary of Pressures and Temperatures 2-53
2.6.1.2 Differential Thermal Expansion 2-53
2.6.1.3 Stress Calculations 2-55
2.6.1.4 Comparison with Allowable Stresses 2-55
2.6.2 Cold 2-56
2.6.3 Reduced External Pressure 2-56
2.6.4 Increased External Pressure 2-56
2.6.5 Vibration 2-56
2.6.6 Water Spray 2-58

2.6.7 Free Drop 2-58
2.6.8 Corner Drop 2-58
2.6.9 Compression – Stacking Test 2-58
2.6.9.1 Stacking Bracket 2-60
2.6.9.2 Outerpack Section 2-61
2.6.9.3 Leg Support 2-64
2.6.10 Penetration 2-65
2.7 HYPOTHETICAL ACCIDENT CONDITIONS 2-67
2.7.1 Free Drop 2-67
2.7.1.1 QTU Test Sequence 2-69
2.7.1.2 CTU Test Sequence 2-73
2.7.1.3 Summary of QTU and CTU Drop Testing 2-91
2.7.1.4 Type B Full Scale Drop Testing 2-91
2.7.2 Crush 2-103
2.7.3 Puncture 2-103
2.7.3.1 Technical Basis for the Puncture Drop Tests 2-103
2.7.3.2 Summary of Results from the Puncture Drop Test 2-104
2.7.4 Thermal 2-104
2.7.4.1 Summary of Pressures and Temperatures 2-105
2.7.4.2 Differential Thermal Expansion 2-105
2.7.4.3 Stress Calculations 2-105
2.7.4.4 Comparison with Allowable Stresses 2-105
2.7.5 Immersion – Fissile Material 2-105
2.7.6 Immersion – All Packages 2-105
2.7.7 Deep Water Immersion Test (for Type B Packages Containing More than 10^5 A_2) 2-106
2.7.8 Summary of Damage 2-106
2.8 ACCIDENT CONDITIONS FOR AIR TRANSPORT OF PLUTONIUM 2-106
2.9 ACCIDENT CONDITIONS FOR FISSILE MATERIAL FOR AIR TRANSPORT 2-106
2.10 SPECIAL FORM 2-106
2.11 FUEL RODS 2-107
2.11.1 Type A Configuration 2-107
2.11.2 Type B Configuration 2-107
2.11.3 Rod Pipe 2-108
2.11.3.1 Drop Test Basis 2-108
2.11.3.2 Drop Test Results 2-109
2.12 APPENDICES 2-112
2.12.1 References 2-113
2.12.2 Clamshell Axial Bottom Spacer Structural Evaluation 2-114
2.12.2.1 Background 2-114
2.12.2.2 Conclusions 2-115
2.12.2.3 Detailed Calculations and Evaluations 2-115
2.12.3 Clamshell Removable Top Plate Structural Evaluation 2-122
2.12.3.1 Background 2-122
2.12.3.2 Conclusions 2-123
2.12.3.3 Detailed Calculations and Evaluations 2-124
2.12.3.4 Method 2-124
2.12.3.5 Calculation Results 2-125
2.12.3.6 Validation 2-128
2.12.4 Side Skirted/Four Legged Bottom Nozzle Support Spacer Structural Evaluation 2-129
2.12.4.1 Background 2-129
2.12.4.2 Conclusions 2-131
2.12.4.3 Detailed Calculations and Evaluations 2-132
2.12.4.4 Method 2-132
2.12.4.5 Calculation Results 2-135
2.12.4.6 Validation 2-138

LIST OF TABLES

Table 2.1-1 Summary of Regulatory Requirements 2-8
Table 2.1-2 Summary of Traveller Mechanical Analysis and Impact 2-9
Table 2.1-3 Summary of Traveller STD and Traveller XL Design Weights 2-11
Table 2.2-1 Type 304 Stainless Steel Properties 2-13
Table 2.2-2 6005-T5 and 6061-T6 Aluminum Properties 2-15
Table 2.2-3 Crushable Foam Properties 2-16
Table 2.2-4 Neoprene (Rubber, 60 durometer) Properties 2-19
Table 2.2-5 Fuel Rod Strain Energy Absorption Using Minimum Tensile Mechanical Properties 2-20
Table 2.2-6 Fuel Cladding Yield Stress Values vs. Temperature 2-21
Table 2.2-7 Fuel Cladding Ultimate Stress Values vs. Temperature 2-21
Table 2.7-2 Test Weights 2-76
Table 2.7-3 CTU Drop Test Orientations 2-77
Table 2.7-4 CTU Fuel Assembly Key Dimensions Before Drop Test 2-87
Table 2.7-5 CTU Fuel Assembly Grid Envelope Dimensions After Testing 2-88
Table 2.7-6 CTU Fuel Assembly Rod Envelope Data After Testing 2-88
Table 2.7-7 CTU Fuel Assembly Rod Envelope After Testing 2-89
Table 2.7-8 CTU Fuel Rod Gap and Pitch Inspection After Testing 2-89
Table 2.7-9 Traveller Maximum Fuel Assembly and Core Component Weights 2-93
Table 2.7-10 Type B Drop Test Licensing Weight Summary 2-97
Table 2.7-11 Type B Design Weight Summary 2-97
Table 2.7-12 Post-test Fuel Assembly Measured Maximum and Minimum Envelope Characterization Dimensions (in) 2-102
Table 2.7-13 Post-test Fuel Assembly Measured Maximum and Minimum Gap Characterization Dimensions (in) 2-103
Table 2.11-1 Rod Pipe Evaluations for Vertical End Drop Test 2-110
Table 2.12-1 Dimension and Material Properties of Axial Bottom Spacer 2-118
Table 2.12-2 Aluminum 6005-T5 and 6061-T6 Aluminum at 75 degrees F Properties 2-133
Table 2.12-3 Annealed Type 304 Stainless Steel Properties 2-133

LIST OF FIGURES

Figure 2.1-1 Traveller Package 2-4
Figure 2.1-2 Traveller STD Package Exploded View 2-4
Figure 2.1-3 STD Clamshell Details 2-5
Figure 2.1-4A Bottom Support Spacer Installed – Bottom Nozzle with Corner Support Legs (Length depend on fuel assembly type) 2-5
Figure 2.1 4B Bottom Support Spacer Installed – Bottom Nozzle with Skirted Side and Four Corner Legs (Length depends on fuel assembly type) 2-6
Figure 2.1-5 Bottom Support Spacer Installed (on top of Fuel Axial Bottom Spacer) – Bottom Nozzle Features in Direct Contact with Rubber (Length depends on fuel assembly type) 2-7
Figure 2.1-6 Top Axial Restraint (left) and Center Base Plate Axial Restraint (right) (Length depends on fuel assembly type) 2-7
Figure 2.1-7 Traveller XL and Traveller STD Dimensions and Centers of Gravity (Note: End View is Common to Both Models) 2-11
Figure 2.2-1 Temperature Dependent Tensile Properties for 304 SS 2-14
Figure 2.2-2 Annealed 304 Stainless Steel Stress-Strain Characteristics 2-14
Figure 2.2-3 Typical Temperature Dependent Tensile Properties for Tempered 6000 Series Al 2-15
Figure 2.2-4 Temperature Dependent Crush Strength for 6 PCF Polyurethane Foam 2-16
Figure 2.2-5 Temperature Dependent Crush Strength for 10 PCF Polyurethane Foam 2-17
Figure 2.2-6 Temperature Dependent Crush Strength for 20 PCF Polyurethane Foam 2-17
Figure 2.2-7 Temperature Dependent Crush Strength for Traveller Foam at 10% Strain 2-18
Figure 2.2-8 Dynamic Crush Strengths for Foam Materials Utilized in the Traveller 2-18
Figure 2.2-9 Resilience and Toughness (Strain Area) 2-22
Figure 2.2-10 ZIRLO Cladding Stress-Strain Plot 2-23
Figure 2.5-1 Traveller XL Lifting Configurations 2-38
Figure 2.5-2 Lifting Hole Force Detail 2-39
Figure 2.5-3 Lifting Bracket Fabrication Detail 2-39
Figure 2.5-4 Hole Tear-out Model and Mohr's Circle Stress State 2-40
Figure 2.5-5 Traveller STD Stacked Lifting Configuration 2-41
Figure 2.5-6 Forklift Handling XL Model and Assumed Cross Section 2-43
Figure 2.5-7 Forklift Pocket Weld Detail 2-43
Figure 2.5-8 Leg Assembly Loading Condition During Inadvertent Tie-Down 2-48
Figure 2.5-9 Welding Depiction at Representative Gusset Plate 2-49
Figure 2.5-10 Welding Depiction at Cross Member 2-49
Figure 2.5-11 Lift Eye Loading Assumed Conditions During Inadvertent Tie-Down 2-50
Figure 2.5-12 Vertical Lift Eye Welding Configuration 2-51
Figure 2.5-13 Combined Shear Lift Eye Welding Configuration 2-52
Figure 2.6-1 Sample of Clamshell Accelerations Measured During Road Test (May 11, 2004) 2-57
Figure 2.6-2 Compression/Stacking Requirement Analysis Model 2-59
Figure 2.6-3 Stacking Force Model on Stacking Bracket 2-60
Figure 2.6-4 Outerpack Section Compression Model 2-62
Figure 2.6-5 Leg Support Section Compression Model 2-64
Figure 2.7-1 Traveller QTU-1 Test Series Drop Sequence 2-70
Figure 2.7-2 Traveller QTU-1 Test Series Worst-Case Cumulative Damage 2-70
Figure 2.7-3 Traveller QTU-2 Test Series Drop Sequence 2-72
Figure 2.7-4 Traveller QTU-2 Test Series Bottom End Damage 2-72
Figure 2.7-5 Traveller CTU Test Article Internal View 2-74
Figure 2.7-6 Traveller CTU External View 2-75
Figure 2.7-7 CTU Drop Test Orientations 2-76
Figure 2.7-8 Top Nozzle End Outerpack Impact Damage 2-78
Figure 2.7-9 CTU Outerpack Stiffener After Test 1 2-78
Figure 2.7-10 CTU Outerpack After Test 2 2-79
Figure 2.7-11 Hinge Separation at Bottom Nozzle End from Test 2 2-79
Figure 2.7-12 CTU Outerpack After Test 3 2-80
Figure 2.7-13 CTU Clamshell After Drop and Fire Tests 2-81
Figure 2.7-14 Outerpack Lid Moderator After Testing 2-81

Figure 2.7-15 Fuel Assembly Damage Sketch and Pre-test Assembly 2-83
Figure 2.7-16 CTU Fuel Assembly After Testing (top end) 2-84
Figure 2.7-17 CTU Fuel Assembly Top End After Testing 2-84
Figure 2.7-18 Cracked Rod from CTU Fuel Assembly 2-85
Figure 2.7-19 Cracked Rod Locations on CTU Fuel Assembly 2-85
Figure 2.7-20 Measurements Made on CTU Fuel Assembly Before and After Drop Tests 2-86
Figure 2.7-21 Type B Bottom Support Spacer/Fuel Assembly Interface Pre-test 2-94
Figure 2.7-22 Type B Center RTP Fit-up Pre-test 2-95
Figure 2.7-23 Type B Drop Test Final Set-up 2-96
Figure 2.7-24 Impact Limiter Post-test Condition 2-98
Figure 2.7-25 Clamshell Exterior Post-test Condition (Bottom End) 2-99
Figure 2.7-26 Clamshell RTP Post-test Condition 2-99
Figure 2.7-27 Global Fuel Assembly Post-test Condition 2-100
Figure 2.7-28 Localized Fuel Rod Expansion and Grid Buckling Post-test 2-101
Figure 2.11-1 Rod Pipe Characteristics for Evaluation 2-109
Figure 2.11-2 Flange 3 Pre-test 2-110
Figure 2.11-3 Flange 3 Post-test 2-110
Figure 2.11-4 Rubber Spacer and Impact Limiter Post-test Conditions 2-111
Figure 2.12-1 Axial Bottom Spacer Below Fuel Assembly in Traveller XL Clamshell 2-114
Figure 2.12-2 FEA Model – Axial Spacer 2-117
Figure 2.12-3 Deformed Model with Axial Spacer at 23 ms (the end of the impact) 2-119
Figure 2.12-4 Predicted Total End Crushing (mm) with Axial Spacer 2-120
Figure 2.12-5 Kinetic Energy History (MJ) of the Axial Spacer Model 2-120
Figure 2.12-6 Fuel Handling Tool Grappled to a 17×17 Top Nozzle (in blue) within the Opened Outerpack and Clamshell 2-123
Figure 2.12-7 Fuel Handling Tool Shown Attached to a 17×17 Fuel Assembly and Behind the Overhanging Shear Lip 2-123
Figure 2.12-8 Traveller Top End Plate FEA Model 2-125
Figure 2.12-9 RTP Model at Beginning of Impact (0 ms) and End of Impact (33 ms) 2-126
Figure 2.12-10 Rigid Wall Impact Force History of RTP Model 2-127
Figure 2.12-11 Kinetic Energy History of RTP Model (MJ vs. s) 2-127
Figure 2.12-12 Comparison of Simulated Top Nozzle Damage (left) to Drop Test (right) 2-128
Figure 2.12-13 Bottom Support Spacer for Side Skirted/Four Legged Bottom Nozzles 2-130
Figure 2.12-14 Fuel Assembly Fully Seated on Two-Tiered Bottom Support Spacer 2-130
Figure 2.12-15 FEA 9-meter Drop Simulation at Peak Load for Side Skirted/Four Legged Bottom Nozzle with Two-Tiered Bottom Support Spacer (~12 ms) 2-131
Figure 2.12-16 True Stress-Strain Curve for Traveller 304 Stainless Steel Components (MPa) 2-134
Figure 2.12-17 Bi-linear Stress-Strain Curve for ZIRLO Fuel Clad (MPa) 2-134
Figure 2.12-18 6 PCF Pillow (Curve B) & 20 PCF Limiter (Curve A) Dynamic Crush Strength 2-135
Figure 2.12-19 Kinetic Energy Plot of Type B Simulated Impact for Side Skirted/Four Legged Bottom Support Spacer 2-136
Figure 2.12-20 Y-Displacement of Pillow Crush Plate (mm vs sec) 2-137
Figure 2.12-21 Traveller CTU Model Developed for FEA (Clamshell Walls Removed for Clarity) 2-139
Figure 2.12-22 CTU Model and Actual Bottom Nozzle Deformed Shape After Impact 2-140
Figure 2.12-23 CTU Model and Actual Bottom Nozzle Deformed Shape After Impact (Bottom View) 2-140
Figure 2.12-24 Type B Model for XL Fuel Assembly with Four Legged Bottom Nozzle Including Bottom Support Spacer 2-141
Figure 2.12-25 Type B Model for Drop Simulation (Support Spacer not Shown) 2-142
Figure 2.12-26 Kinetic Energy Plot of Type B Simulated Impact (J vs sec) 2-143
Figure 2.12-27 Y Displacement of Nodes on Pillow Crush Plate (mm vs sec) 2-143
Figure 2.12-28 Fuel Assembly After Drop (Left) and Type B Model After Simulated Drop 2-145

2.0 STRUCTURAL EVALUATION

This section presents the structural design criteria, weights, mechanical properties of materials, and structural evaluations that demonstrate the Traveller series of packages meet all applicable structural criteria for transportation as defined in 10 CFR 71 [1] and SSR-6 [2].

2.1 DESCRIPTION OF STRUCTURAL DESIGN

The structural evaluation of the standard length Traveller (Traveller STD) and longer length Traveller (Traveller XL) packages is qualified through testing, standard engineering hand calculations, and computer simulations using finite element analysis. The results of the computer simulations and testing are provided in the following sections. Figure 2.1-1 displays the Traveller package, while Figure 2.1-2 shows an exploded view of the Traveller STD, and Figure 2.1-3 displays the Clamshell detail.

The Traveller shipping package consists of two major fabricated components: 1) an Outerpack assembly, and 2) a Clamshell assembly. The Outerpack consists of a stainless steel outer shell for structural strength, a layer of rigid polyurethane foam for thermal and impact protection, and a stainless steel inner shell for structural strength. Polyethylene blocks are affixed to the inner shell of the Outerpack for criticality safety. See Section 6, Criticality Evaluation, for the full criticality safety description. The Clamshell consists of an aluminum container to structurally enclose the contents. Neutron absorber panels are affixed to the inner faces of the Clamshell. Rubber shock mounts separate and isolate the Clamshell from the Outerpack assembly.

2.1.1 Discussion

There are two packaging variants in the Traveller family: Traveller STD and Traveller XL. The Traveller packagings have a Type A and Type B configuration. Except where differentiated in Section 2.1.1.2, the Type B configuration of the Traveller is identical to the Type A configuration.

2.1.1.1 Packaging Configuration

The designs of the Traveller STD and Traveller XL fuel shipping packages are the same except for length (and therefore weight). Details of the packages, including dimensions and materials, can be found in Section 1, General Information. Section 1.2.1.5 provides additional details of the structural features of the package. Both packages consist of an Outerpack and a Clamshell.

Positive closure of the two halves of the Outerpack is accomplished by means of high strength stainless steel bolts. The number of bolts is the same for the XL and STD designs, which results in lower loading per bolt for the STD design. The design loadings for both packages are below the ultimate design loads for the Outerpack bolts. There are 48, ¾-10 UNC hex head bolts total in the Outerpack: 24 attaching the hinge sections to the lower Outerpack and 24 attaching the upper Outerpack to the hinge sections. To remove the upper Outerpack horizontally, the 24 upper bolts must be removed. In the preferred approach, the Outerpack is opened and closed when it is in a vertical orientation by removing the 12 bolts attaching the upper Outerpack to the hinges on one side. This allows the upper Outerpack to swing open on the hinge like a door. The Outerpack top half or “door” may be opened in either direction, depending on which side the 12 bolts are removed.

Closure of the Traveller STD and Traveller XL Clamshells is provided by latch assemblies that are secured by mechanical fasteners consisting of a cam latch on the right main door that engages a keeper on the left main door. The cam latch is rotated a quarter-turn to engage the keeper. A wave spring washer prevents inadvertent movement of the cam latch. There are nine (9) cam latches on the Traveller STD Clamshell and eleven (11) cam latches on the Traveller XL Clamshell. The Clamshell is closed using ¼-turn nuts, which lock the cam latches on the doors of the assembly. Piano type hinges (continuous hinges) connect each main door and the small top "V" access door to the "V" shape-base of the Clamshell. Connected with the top access door, the top plate of the Clamshell has two configurations, Fixed Top Plate (FTP) and Removable Top Plate (RTP), in order to accommodate different fuel types. Each uses a combination of flat head cap screws and tongue and groove joints in order to be fastened securely to the Clamshell.

The Outerpack bolts and the Clamshell closure mechanisms have been subjected to the drop conditions of 10 CFR 71 and SSR-6 without failure. Therefore, these designs are more than adequate to withstand the loads experienced during transport conditions.

Clamping mechanisms that interface with the contents provide axial and lateral restraint during all transport conditions. The design of the top axial restraint components, described in Section 1.2.1.5.2, depends on the Clamshell top plate configuration (FTP or RTP) and the fuel assembly type. Rubber pads are positioned at axial locations along the inside of the Clamshell doors to restrain content lateral movement.

The Traveller packages are not pressure sealed from the ambient environment, therefore, no differential pressures can occur within the package. A weather gasket is used on the Outerpack to mitigate water and debris ingress.

Handling of the packages is performed using the forklift pockets on the lower Outerpack. Handling may also utilize the lifting holes in the stacking brackets on the upper Outerpack.

Standard fabrication methods are utilized to fabricate the Traveller series of packages. Visual weld examinations are performed on all welds of the Traveller packages in accordance with AWS D1.6 [3] and ASME Section III, Subsection NF [4], or engineering-approved equivalents, for stainless steel and aluminum respectively.

2.1.1.2 Type B Configuration

The Type B configuration of the Traveller is similar to the Type A configuration, except as defined in this section. The Type B configuration requires the RTP Clamshell configuration.

For any shipment of contents that are classified as Type B quantity material (see discussion in Section 1.2.2.2), a bottom support component is required to be used along with the top axial clamping mechanism to ensure proper structural support for the fuel assembly during a free drop. If this bottom support spacer is not in place, the contents to be shipped may not exceed a Type A quantity.

For fuel assemblies with four corner support legs on the bottom nozzle, the fuel assembly is positioned on top of a reusable aluminum bottom support spacer, as shown in Figure 2.1-4A. For fuel assemblies with bottom nozzles having both four corner legs and side skirts, the fuel assembly is positioned on top of a two-tiered

aluminum spacer as shown in Figure 2.1-4B. The bottom support spacer rests on top of the Clamshell bottom plate and fits under the fuel assembly bottom nozzle structure. The bottom support spacer is a stiff structure with full length sides, void center, and sufficient top thickness to ensure the fuel assembly bottom nozzle flow plate is supported during all transport conditions. The two-tiered bottom support spacer is a stiff structure with a solid upper portion and a stiff, voided, lower portion. The lower tier provides structural support for the four corner legs, and the upper tier provides clearance for the side skirts as well as sufficient thickness to ensure the fuel assembly bottom nozzle flow plate is supported during all transport conditions. A rubber pad is glued to the top of the bottom support component to avoid surface scratching. The overall bottom support spacer has the same geometry, but the length is designed specifically for each fuel assembly type to ensure there is a conforming fit between the fuel assembly bottom nozzle and the bottom support spacer. The bottom support spacer is required for the transport of Type B fuel assemblies with four corner support legs on the bottom nozzle.

For fuel assemblies that have a bottom nozzle without corner support legs, the fuel assembly is positioned on top of a reusable axial bottom spacer and solid aluminum bottom support plate, as shown in Figure 2.1-5. The fuel axial bottom spacer rests on top of the Clamshell bottom plate and the solid bottom support plate fits under the fuel assembly bottom nozzle structure. This bottom support plate ensures the fuel assembly bottom nozzle flow plate is supported during all transport conditions. A rubber pad is glued to the top of the bottom support component to avoid surface scratching. The overall axial bottom spacer length is designed specifically for each fuel assembly type. The bottom support plate is a solid plate that the bottom nozzle rests upon. The combination of the fuel axial bottom spacer and bottom support plate is required for the transport of fuel assemblies with a bottom nozzle without corner support legs.

Clamping mechanisms that interface with the contents provide axial and lateral restraint during all transport conditions. An adjustable, threaded rod-clamping device provides axial restraint at the top of the fuel assembly. The design of the top axial clamping mechanisms, as shown in Figure 2.1-6, includes either a center base plate for flat top nozzles or a top axial restraint and two (2) axial clamping studs for top nozzles with an open center. The axial restraints are threaded through the RTP. The length of the top axial clamping mechanisms depends on the fuel assembly type. The axial restraint may contact non-fissile, non-radioactive reactor core components when shipped within the fuel assembly by varying the threaded rod length. In all cases, the top axial clamping mechanisms provide positive axial hold down during normal transport conditions. Grid pads are positioned at axial locations along the inside of the Clamshell doors to match the structural grid locations for each fuel assembly type, provide lateral movement restraint.

When shipping in the Type B configuration, the combination of a top axial clamping mechanism and bottom support (spacer or plate) is always required. For each fuel assembly design, the axial restraint configurations (i.e. top axial clamping mechanism and bottom support spacer/plate) are designed to ensure that the fuel assembly is secure prior to Clamshell door closure. The specific axial restraint and fuel assembly design configuration is controlled by site operational procedure. A tight fit of the fuel assembly and axial restraints is verified prior to each shipment.

The primary containment for the Type B quantity radioactive material in the Traveller is the fuel rod cladding, which is manufactured to high standards for use in nuclear reactors. The fabrication standards for the fuel are in excess of what is needed to provide containment for shipping of the fuel. The fuel rod cladding is designed

to provide containment throughout the life of the fuel, prior to loading, in transportation, and while used in the reactor where it operates at higher pressures and temperatures than transport conditions, and must contain fission products, gases, as well as the fuel itself.

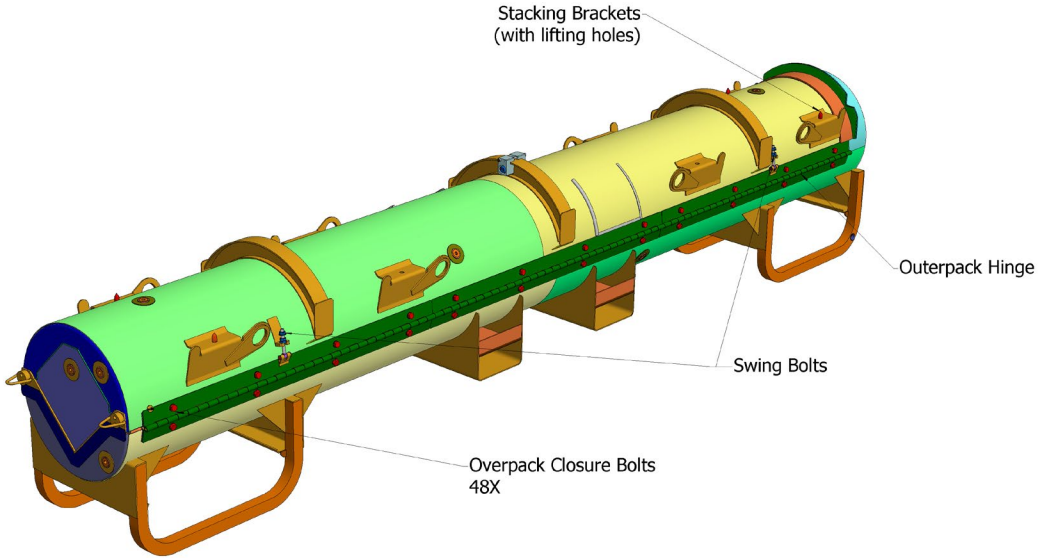

Figure 2.1-1 Traveller Package

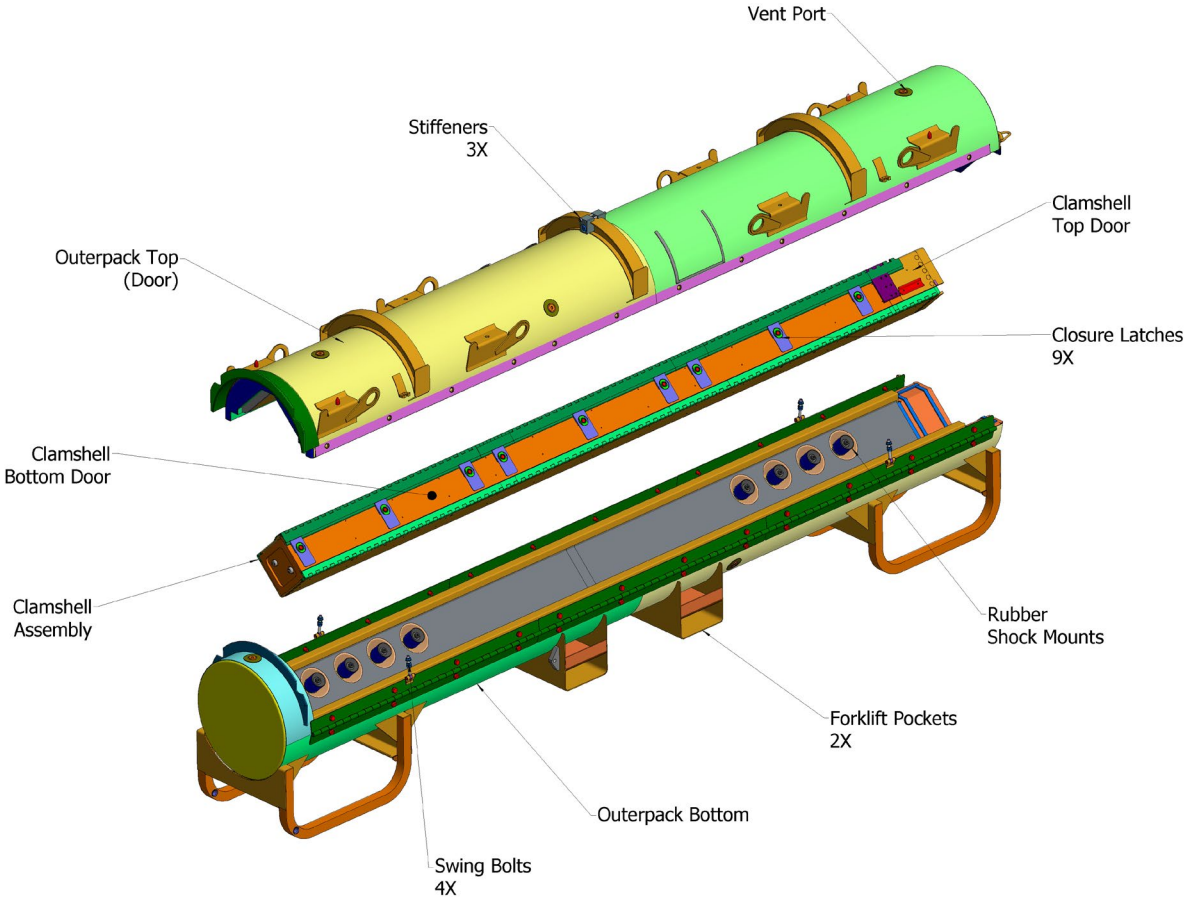

Figure 2.1-2 Traveller STD Package Exploded View

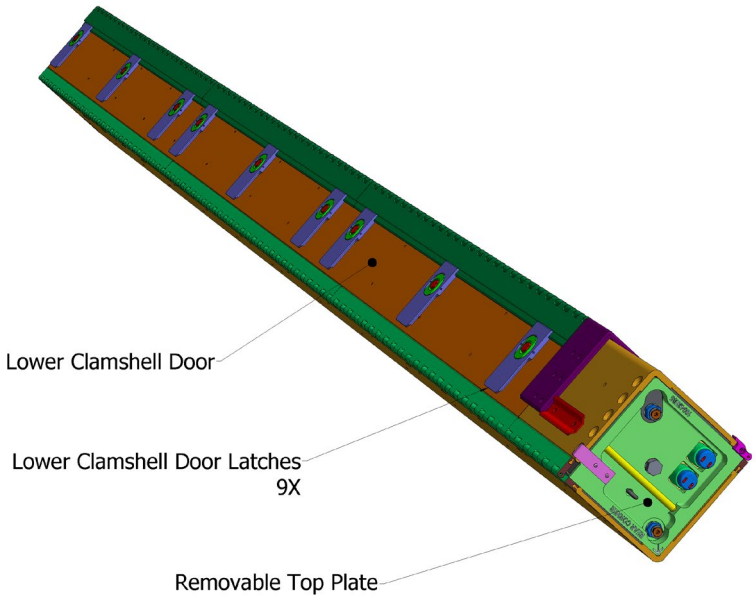

Figure 2.1-3 STD Clamshell Details

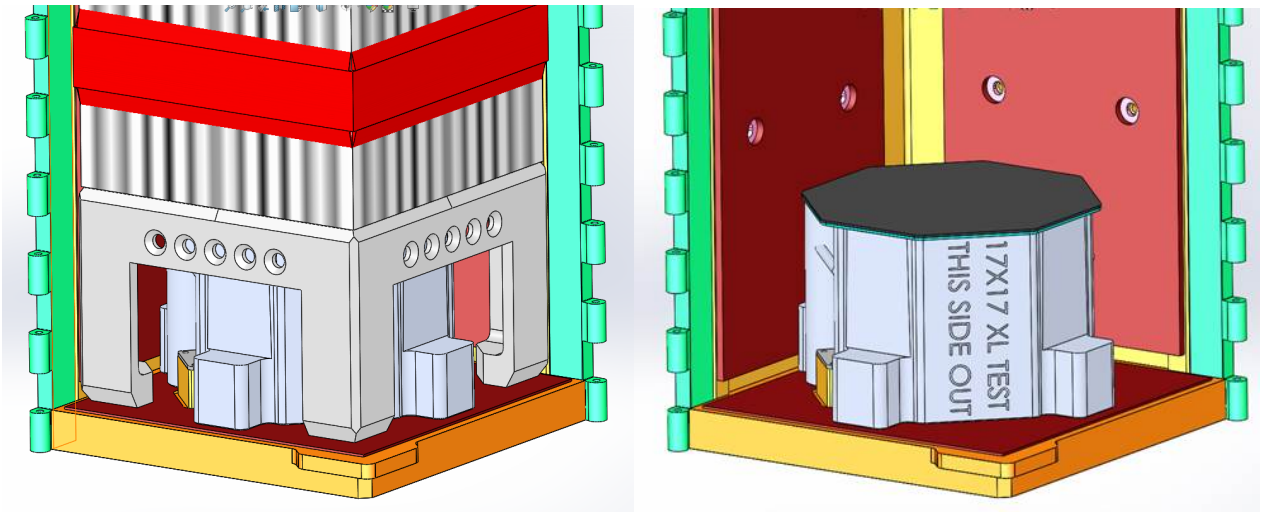

Figure 2.1-4A Bottom Support Spacer Installed – Bottom Nozzle with Corner Support Legs (Length depend on fuel assembly type)

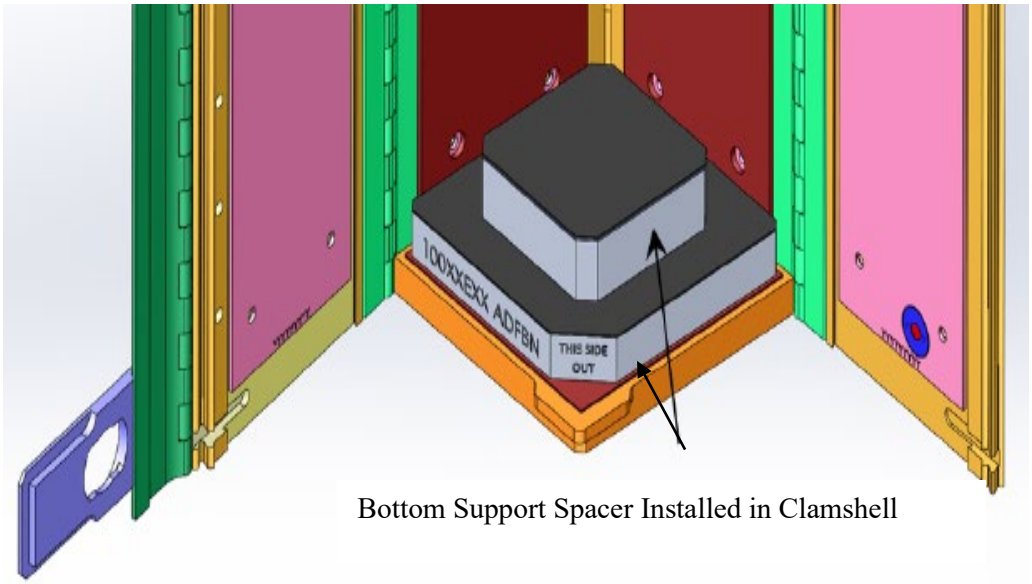

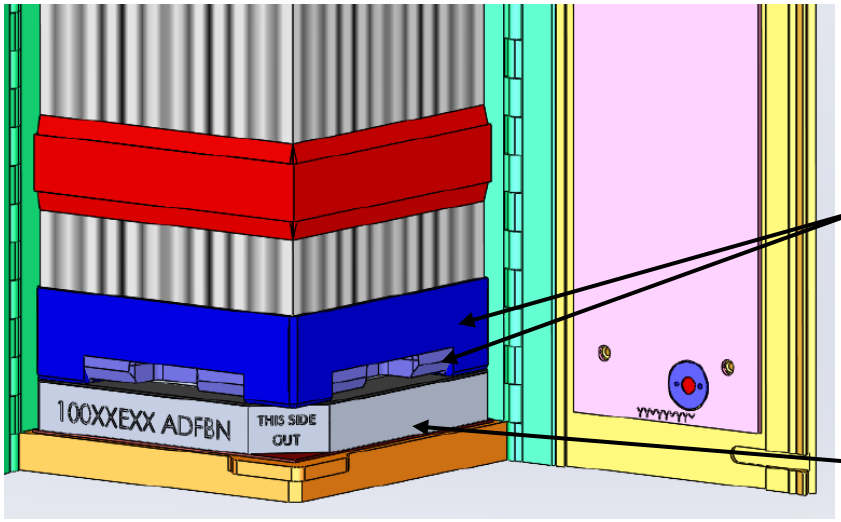

Figure 2.1-4B Bottom Support Spacer Installed – Bottom Nozzle with Skirted Side and Four Corner Legs (Length depends on fuel assembly type)

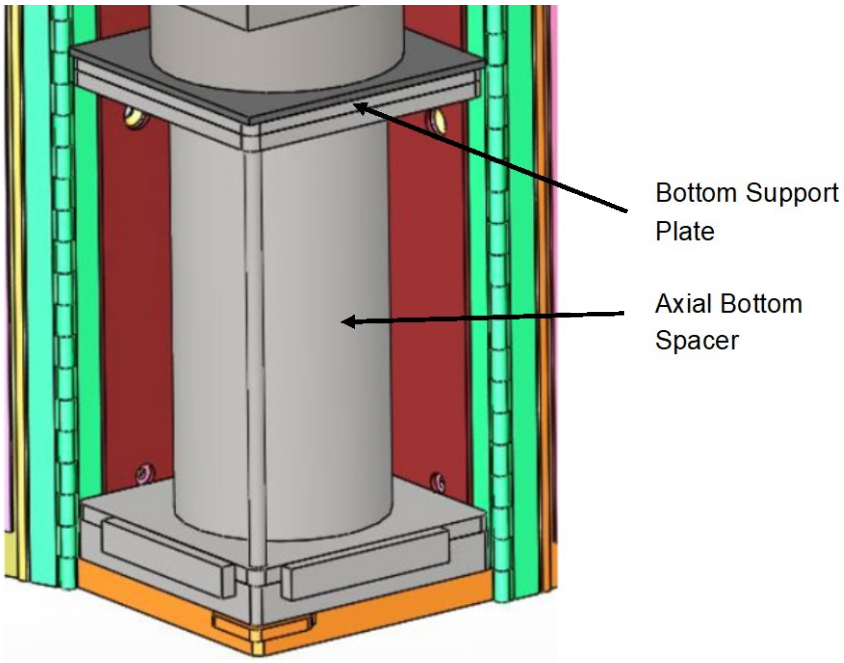

Figure 2.1-5 Bottom Support Spacer Installed (on top of Fuel Axial Bottom Spacer) – Bottom Nozzle Features in Direct Contact with Rubber (Length depends on fuel assembly type)

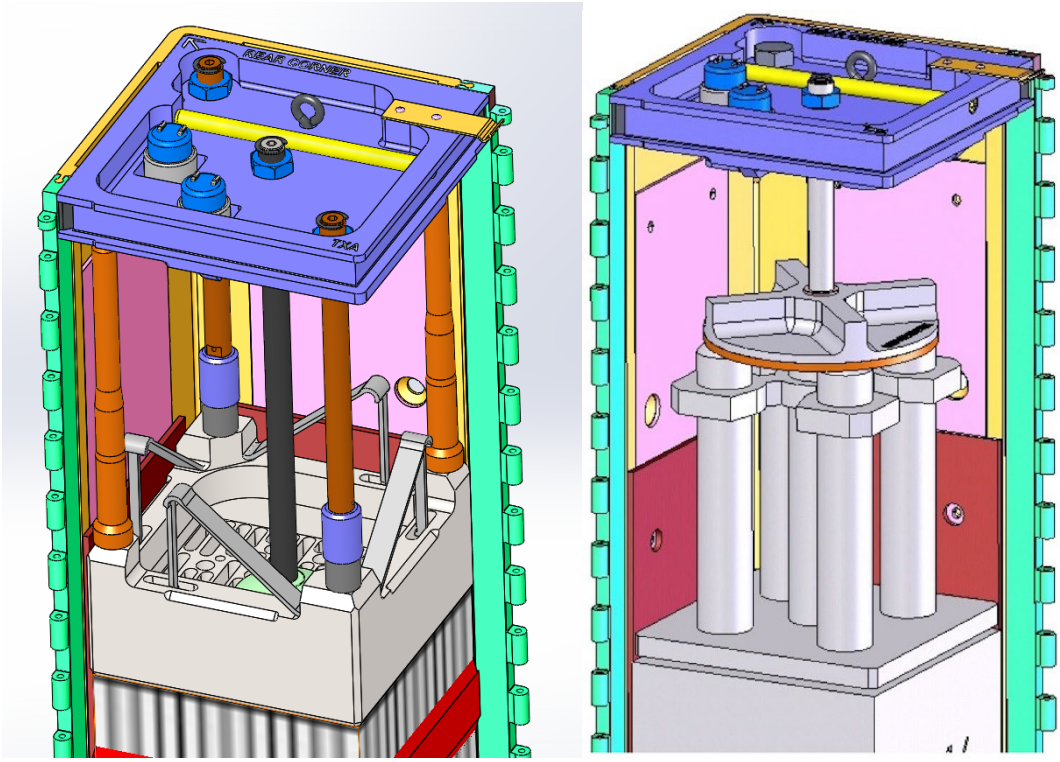

Figure 2.1-6 Top Axial Restraint (left) and Center Base Plate Axial Restraint (right) (Length depends on fuel assembly type)

2.1.2 Design Criteria

2.1.2.1 Basic Design Criteria

Evidence of performance for the Traveller XL package is achieved by (1) empirical evaluations using full-scale packages and (2) large-strain capable Finite Element Analysis (FEA). The Traveller XL is bounding of the Traveller STD due to its increased weight and length. The criteria used for the impact evaluation is a demonstration that the containment and confinement systems maintain integrity throughout Normal Conditions of Transport (NCT) and Hypothetical Accident Condition (HAC) certification testing. That is, it is necessary to demonstrate that there is no release of material, no loss of moderator or neutron absorber, no gross decrease in Outerpack geometry, and no gross increase in Clamshell geometry. The as-found condition of the package (packaging and contents) is the baseline configuration for the criticality safety evaluation that can be found in Chapter 6. Table 2.1-1 shows the regulatory requirements and how satisfactory compliance was demonstrated. Table 2.1-2 provides a summary of the mechanical analyses and impact for the regulatory requirements.

Table 2.1-1 Summary of Regulatory Requirements

Requirement Description	US NRC	IAEA	Applicable Condition	Means Demonstrated
Lifting attachments	10 CFR 71.45(a)	SSR-6 para. 608	General Package Standard	Mech. Design Calc.
Tie-Down devices	10 CFR 71.45(b)(1,2)	SSR-6 para. 638	General Package Standard	Mech. Design Calc.
Design temperatures between –40°F (-40°C) and 158°F (70°C)	10 CFR 71.71(c)(1,2)	SSR-6 para. 639 and 679	General Package Standard	Mech. Design Calc.
Reduced/Increased External Pressure	10 CFR 71.71(c)(3,4)	SSR-6 para. 616	Normal transport condition	Mech. Design Calc.
Vibration	10 CFR 71.71(c)(5)	SSR-6 para. 613	Normal transport condition	Mech. Design Calc. and Testing
Water spray	10 CFR 71.71(c)(6)	SSR-6 para. 721	Normal transport condition	Mech. Design Evaluation
Free drop	10 CFR 71.71(c)(7)	SSR-6 para. 722	Normal transport condition	Testing
Compression/Stacking test	10 CFR 71.71(c)(9)	SSR-6 para. 723	Normal transport condition	Mech. Design Calc.
Penetration	10 CFR 71.71(c)(10)	SSR-6 para. 724	Normal transport condition	Mech. Design Calc.
Free drop	10 CFR 71.73(c)(1)	SSR-6 para. 727(a)	Accident transport condition	Testing
Pin puncture	10 CFR 71.73(c)(3)	SSR-6 para. 727(b)	Accident transport condition	Testing
Thermal test	10 CFR 71.73(c)(4)	SSR-6 para. 728	Accident transport condition	Testing
Immersion—fissile material	10 CFR 71.73(c)(5)	SSR-6 para. 733	Accident transport condition	Criticality Design Calc.
Immersion—all packages	10 CFR 71.73(c)(6)	SSR-6 para. 729	Accident transport condition	Mech. Design Calc.
Deep water immersion	10 CFR 71.61	SSR-6 para. 730	Accident transport condition	Not Applicable

Table 2.1-2 Summary of Traveller Mechanical Analysis and Impact

Requirement Description	Allowable Design Value(s) or Acceptance Criteria	Resultant Component Calculated Value vs. Allowable and/or Impact
Lifting attachments, ksi (MPa)	Tensile Yield Stress, σ_y < 30 (207) Shear Yield Stress, σ_y < 18 (124) Weld shear Yield Stress, σ_y < 12 (83) Hoist Screw Shear Stress, τ < 72 (496) Coupling Nut Shear Stress, τ < 18 (124) Hoist Ring Tensile Stress, τ < 130 (896)	**Hole tear-out (4-pt. lifting), ksi (MPa):** XL: τ = 5.23 < 18 (36 < 124) STD: τ = 6.364 < 18 (44 < 124) **Weld shear (4-pt. lifting), ksi (MPa):** XL: τ = 7.565 < 12 (52 < 83) STD: τ = 9.205 < 12 (63 < 83) **Forklift, ksi (MPa):** XL Bending: τ = 17.528 < 30 (121 < 207) STD Bending: τ = 26.26 < 30 (181 < 207) XL Weld Shear: τ = 3.533 < 12 (24 < 83) STD Weld Shear: τ = 6.08 < 12 (42 < 83) **Hoist Ring Assembly, ksi (MPa):** Bolt Shear: τ = 50.619 < 72 (349 < 496) Coupling Nut Shear: τ = 17.671 < 18 (122 < 124) Hoist Ring Tensile: τ = 35.659 < 130 (246 < 896)
Tie-Down ksi (MPa)	Weld shear Yield Stress, σ_y < 12 (83)	**Leg Assembly, ksi (MPa):** Weld Shear: τ = 11.648 < 12 (80 < 83) **Lift Eyes** Weld Shear (vertical): τ = 7.158 < 12 (49 < 83) Weld Shear (combined): τ = 7.173 < 12 (49 < 83)
Temperatures Effects	No brittle fracture No impact from Differential Thermal Expansion (DTE)	No brittle fracture No DTE Impact
Reduced/Increased External Pressure	Compressive Yield Stress, σ_y < 30 ksi (207 MPa)	No stress developed
Vibration	No impact on structural performance, $f_{natOP} > f_{natTRANS}$	No impact, 23 Hz > 3.7 - 8 Hz
Water spray	No impact on structural performance	No impact
NCT Free drop	Geometric form of the package contents would not be substantially altered	No impact
Compression/ Stacking	Weld Shear Yield Stress, σ_y < 12 ksi (83 MPa) Compressive Yield Stress, σ_y < 30 ksi (207 MPa) Elastic Stability (Critical Buckling), F < Pcr	**Stacking Bracket, ksi (MPa):** Weld Shear: τ = 4.729 < 12 (33 < 83) Bending: σ = 1.827 << 30 (13 << 207) **Outerpack Buckling, lbf (kN):** Buckling: 26,150 < 78,583 (116 < 350) **Leg Support Buckling, lbf (kN):** Buckling: 3,269 < 71,978 (14.5 < 320)
Penetration	No perforation of outer skin	Bounded by 3.3 ft (1.0 m) HAC pin-puncture; No perforation of outer skin.
HAC Free drop Pin puncture Thermal test	Type A - Package damage not significant and remains subcritical Type B – Type A requirements and containment maintained	Package damage documented and evaluated in criticality analysis Containment verified post-testing
Immersion—fissile material	N/A, inleakage assumed in criticality safety analysis	Inleakage evaluated in criticality analysis
Immersion—all packages	Compressive Yield Stress, σ_y < 30 ksi (207 MPa)	No stress developed
Deep water immersion	Evaluation of increased external pressure	Package not authorized for >10^5 A_2.

2.1.2.2 Miscellaneous Structural Failure Modes

2.1.2.2.1 Brittle Fracture

The primary structural materials of the Traveller packages are austenitic stainless steel (ASTM A240 Type 304 SS) and 6000 Series aluminum (extruded components 6005-T5, all else 6061-T6). These materials do not undergo a ductile-to-brittle transition in the temperature range of interest [i.e. down to -40°F (-40°C)], and thus do not require evaluation for brittle fracture. See Section 2.2.1 for additional material property detail.

2.1.2.2.2 Fatigue

Because the shells of the Outerpack are constructed of ductile stainless steel and they are formed into a very stiff body with low resulting stresses, no structural failures of the Outerpack due to fatigue will occur. Because the Clamshell is structurally isolated from the Outerpack through the rubber shock mounts, no Clamshell fatigue will occur. The Clamshell is, for practical purposes, decoupled from the Outerpack through the rubber shock mounts. These rubber shock mounts also provide excellent damping to the Clamshell.

2.1.2.2.3 Buckling

For normal and hypothetical accident conditions, the Clamshell, which structurally encloses the fuel, will not buckle due to free or puncture drops. This behavior has been demonstrated via full-scale testing of the bounding Traveller XL package.

2.1.3 Weights and Centers of Gravity

The Traveller XL weight bounds the Traveller STD weight, as shown in Table 2.1-3. The calculated weight breakdown for the major individual subassemblies, including the shipping components for both packages, is listed below. For licensing purposes, the maximum bounding Traveller XL design weight is assumed to be 5,230 lb (2,372 kg). The Traveller structural analysis, applicable to STD and XL, is located in Sections 2.5 through 2.7.

The center of gravity of both Traveller packages is approximately at the geometric center of the Outerpack, i.e. approximately 23 in (0.58 m) above ground level, at the axial mid-station for both packages. Figure 2.1-7 shows the overall dimensions and locations of the centers of gravity for both empty Traveller XL and Traveller STD packages.

Table 2.1-3 Summary of Traveller STD and Traveller XL Design Weights		
Package Variant	**Traveller STD**	**Traveller XL**
Nominal Outerpack Weight, lb (kg)	2368 (1074)	2670 (1211)
Max. Fuel Assembly Weight, lb (kg)	1650 (748)	1971 (894)
Nominal Clamshell Weight, lb (kg)	378 (171)	467 (212)
Nominal Total Weight, lb (kg)	4396 (1994)	5108 (2317)
Design and Licensing Basis Gross Weight, lb (kg)	4500 (2041)	5230 (2372)
Design Tare Weight, lb (kg)	2850 (1293)	3260 (1479)

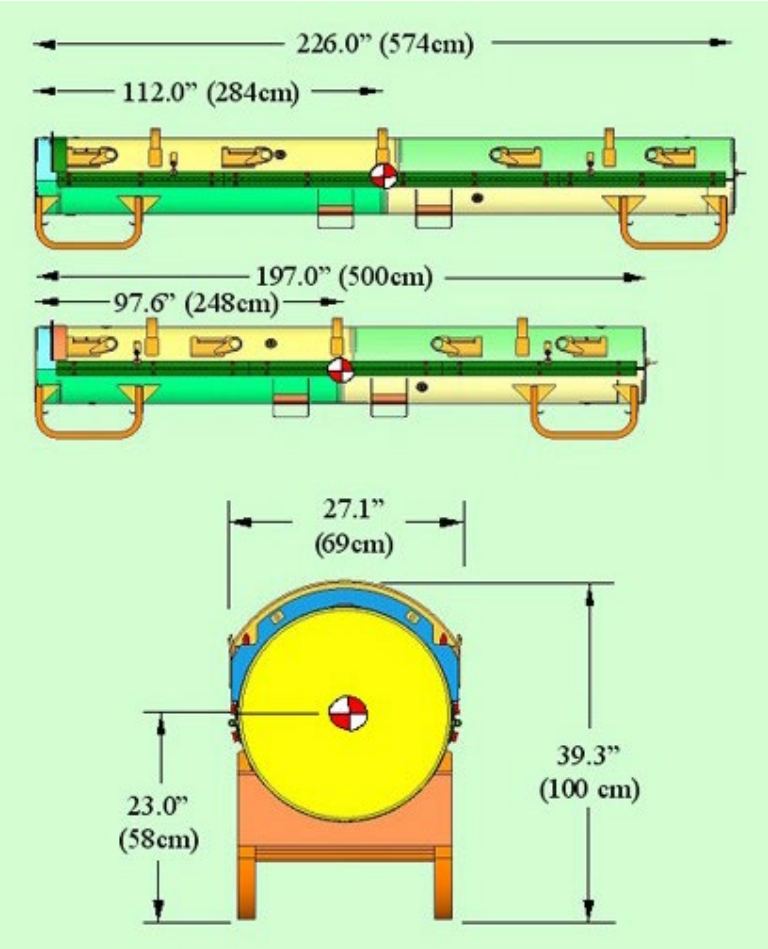

Figure 2.1-7 Traveller XL and Traveller STD Dimensions and Centers of Gravity (Note: End View is Common to Both Models)

2.1.4 Identification of Codes and Standards for Package Design

The Traveller packages are evaluated with respect to the general standards for all packaging specified in 10 CFR 71.43, and SSR-6 paras. 607 – 651, as applicable. The fabrication, assembly, testing, maintenance, and operation will be accomplished with the use of generally accepted codes and standards, such as ASME, ASTM, and/or AWS noted on engineering drawings or in engineering product specifications. Special processes will be documented with procedures that will be evaluated and approved per Westinghouse procedures.

2.2 MATERIALS

2.2.1 Material Properties and Specifications

Mechanical properties for the materials used for the structural components of the Traveller packages are provided in this section. Temperature-dependent material properties for structural components are primarily obtained from Section II, Part D, of the ASME Boiler and Pressure Vessel (B&PV) Code [5]. The analytic evaluation of the Traveller packages is via computer simulation (ANSYS [6]/LS-DYNA® [7]), only the material properties specific to the analysis portion and computer simulation portion of the evaluation are given. Section 2.2 lists the materials used in the Traveller packages and summarized key properties and specifications.

All materials used in the fabrication of the Certification Test Unit (CTU) and Type B test components meet 10 CFR 71 and SSR-6 requirements. However, for CTU testing, simulated neutron absorber plates were affixed to the inner faces of the Clamshell. These were fabricated from 1100-T0 aluminum ("dead soft" aluminum). These component plates did not contain boron and were used to simulate the mechanical and thermal properties of the neutron absorber plates. The 1100-T0 aluminum was used due to its low mechanical properties. In production units, the actual neutron absorber plates will have insignificant differences in the material properties compared to the material used in the CTU package.

The materials of construction of the Traveller Outerpack include ASTM A240/A276 Type 304 stainless steel for the shells and low density, closed cell polyurethane impact limiter/thermal insulator [10 pcf (0.16 g/cm^3) along the axis, 6 pcf (0.096 g/cm^3) inside the top and lower pillows, and 20 pcf (0.32 g/cm^3) between the top and lower pillows]. The Clamshell is comprised of ASTM B209/B221 Type 6005-T5 aluminum. The moderator blocks are comprised of ultra-high molecular weight (UHMW) polyethylene. Ceramic insulation (paper and felt) is used as a thermal brake for the polyurethane foam of the Outerpack and between the moderator blocks and their stainless steel covering. The top and bottom spacer pads for the axial spacers are made of neoprene rubber. As demonstrated in this section, the package is suitable for transport operations over the required design temperature range.

The containment system is the fuel rods in the fuel assembly; the cladding is comprised of zirconium alloy for fuel assemblies.

2.2.1.1 ASTM A240/A276 Type 304 Stainless Steel

The Outerpack structure is composed of ASTM A240/A276 Type 304 stainless steel. The calculations to determine the maximum Outerpack allowable stresses for yield, shear, and weld shear are based on the properties of ASTM A240 Type 304 stainless steel. It is further assumed that the weld consumable possesses

greater mechanical properties than that of the base metal. Hence, the mechanical properties of the base metal will be employed for weld stress analysis. The reference drawings used in mechanical analysis represent the Certification Test Unit (CTU) Traveller XL, which was fabricated for the drop and fire tests.

The range of tensile and yield strength of 304 stainless steel over the design temperature range will not preclude the package from performing its intended design function. Figure 2.2-1 provides the temperature-dependent yield and tensile strengths for 304 stainless steel up to approximately 194°F (90°C). Figure 2.2-2 shows the stress-strain curve of the 304 stainless steel properties used in the LS-DYNA simulation.

Austenitic steels such as 304 stainless steel have a face-centered cubic (FCC) structure and consequently exhibit a ductile-to-brittle transition at cryogenic temperatures near -297°F (-183°C). Thus, brittle fracture of the stainless steel components is not expected.

The mechanical properties of ASTM A240 Type 304 stainless steel are listed below:

- Tensile strength (UTS), Minimum: 75 ksi (517 MPa)
- Yield strength (YLD), Minimum: 30 ksi (207 MPa)

For mechanical analyses where tensile, shear, or weld shear stresses were determined, the acceptance criteria were as follows:

- Maximum allowable tensile yield stress, σ_y = 30 ksi (207 MPa)
- Maximum allowable shear stress, τ_{max} (τ_{allow}) = $0.6\sigma_y$ = 18 ksi (124 MPa)
- Maximum allowable weld shear stress, τ_{weld} = $0.4\sigma_y$ = 12 ksi (83 MPa)

Table 2.2-1 Type 304 Stainless Steel Properties

Property	Symbol	Value	Units
Density	RO	8.00E-09	Mg/mm^3
Modulus of Elasticity	E	29.4E06 (203)	psi (GPa)
Poisson's Ratio	PR	0.30	dimensionless

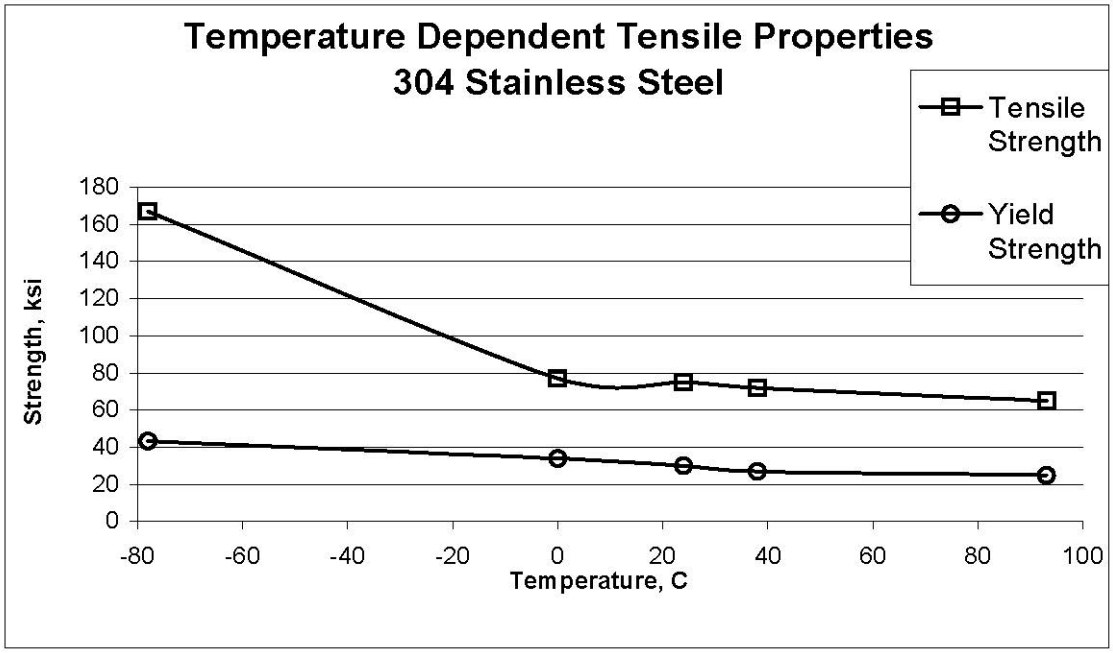

Figure 2.2-1 Temperature Dependent Tensile Properties for 304 SS

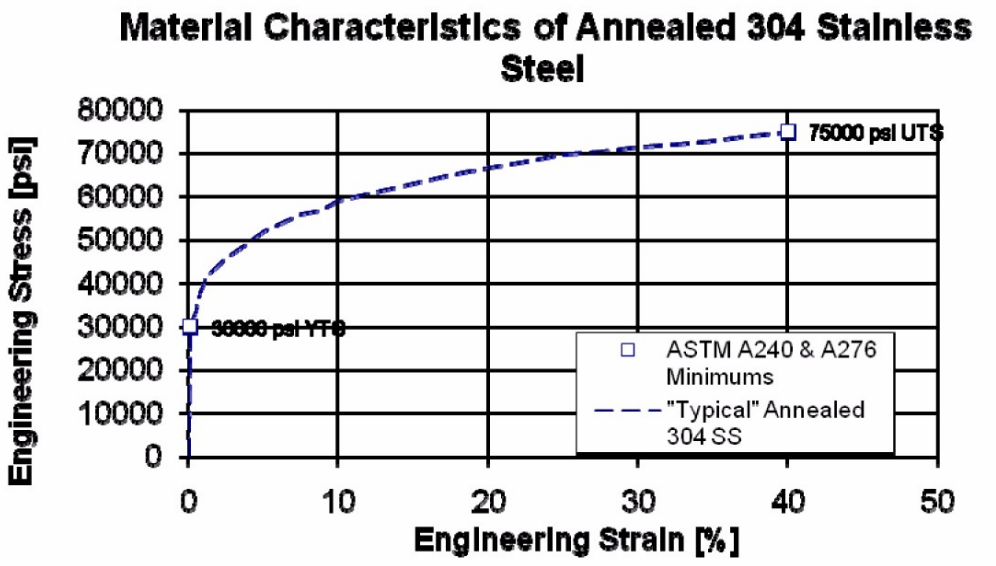

Figure 2.2-2 Annealed 304 Stainless Steel Stress-Strain Characteristics

2.2.1.2 6005-T5 and 6061-T6 Aluminum

The material properties assumed for the aluminum are summarized in Table 2.2-2. The range of tensile and yield strengths of 6005 series aluminum over the design temperature range will not preclude the package from performing its intended design function. Figure 2.2-3 provides the temperature-dependent yield and tensile strengths typical for 6000-series aluminum up to approximately 212°F (100°C). Furthermore, the recommended operating temperature of aluminum alloys for structural applications is up to a temperature of 400°F (204°C), which is well below the maximum design temperature of 158°F (70°C).

Aluminum alloys, including 6005-T5 aluminum, do not exhibit a ductile-to-brittle temperature transition; consequently, neither ASTM nor ASME specifications require low temperature Charpy or Izod tests of aluminum alloys. Thus, brittle fracture of the aluminum components is not expected.

Table 2.2-2 6005-T5 and 6061-T6 Aluminum Properties

Property	Symbol	Value (at 75°F)	Units
Density	RO	2.71E-09	Mg/mm^3
Modulus of Elasticity	E	69	GPa
Poisson's Ratio	PR	0.30	dimensionless
Tensile Strength	SIGT	0.262	GPa
Yield Strength	SIGY	0.241	GPa
Allowable Shear Stress	0.6 SIGY	0.145	GPa
Hardening Modulus	ETAN	0.25	GPa
Failure Strain	FAIL	0.35	In compression

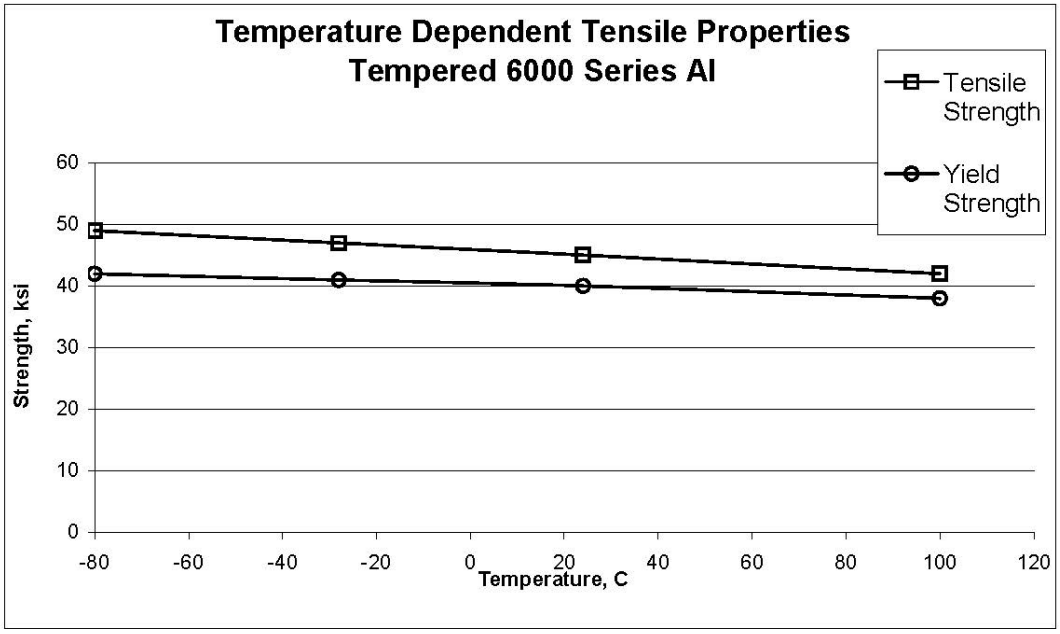

Figure 2.2-3 Typical Temperature Dependent Tensile Properties for Tempered 6000 Series Al

2.2.1.3 Polyurethane Foam

The material properties assumed in the LS-DYNA analysis for the crushable foams are summarized in Table 2.2-3. The compressive strength difference between the crushable foams is shown in Figure 2.2-8.

The foam is used as a crushable impact limiter and a special thermal insulator. The foam exhibits a general increase in compressive strength as temperature decreases. Figure 2.2-4, Figure 2.2-5, and Figure 2.2-6 show the compressive strength for the 10 pound per cubic foot (pcf, 0.16 g/cm^3), 20 pcf (0.32 g/cm^3), and 6 pcf (0.096 g/cm^3) foam as a function of temperature, respectively. Of interest is the area under each temperature curve from 0-60% strain (the recommended energy absorption operation range of the foam). For each foam density, the temperature range considered does not significantly impact the energy absorption characteristics. Also, Figure 2.2-7 shows that the compressive strength difference between -20°F (–29°C) and 75°F (24°C) is relatively similar, indicating at -40°F (-40°C) that the behavior of the foam will not significantly change. Figure 2.2-7 provides the temperature-dependent strength of each foam density at 10% strain from -65°F (-54°C) to 180°F (82°C). The curves show essentially a linear increase in crush strength as temperature decreases. Therefore, the impact properties of the foam are acceptable for use in the temperature range from -40°F (-40°C) to 158°F (70°C).

Table 2.2-3 Crushable Foam Properties

Property	Density	Modulus	Poisson's Ratio
(Unit)	(Mg/mm^3)	(MPa)	(dimensionless)
6 pcf Last-A-Foam	9.61E-11	30.14	0
10 pcf Last-A-Foam	1.60E-10	66.23	0
20 pcf Last-A-Foam	3.20E-10	192.76	0

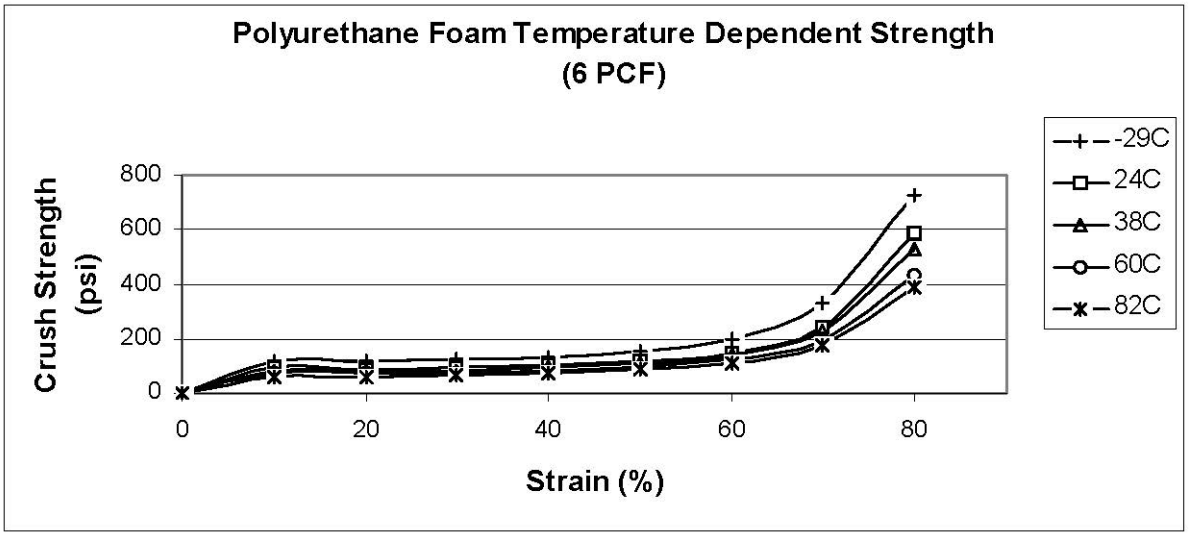

Figure 2.2-4 Temperature Dependent Crush Strength for 6 PCF Polyurethane Foam

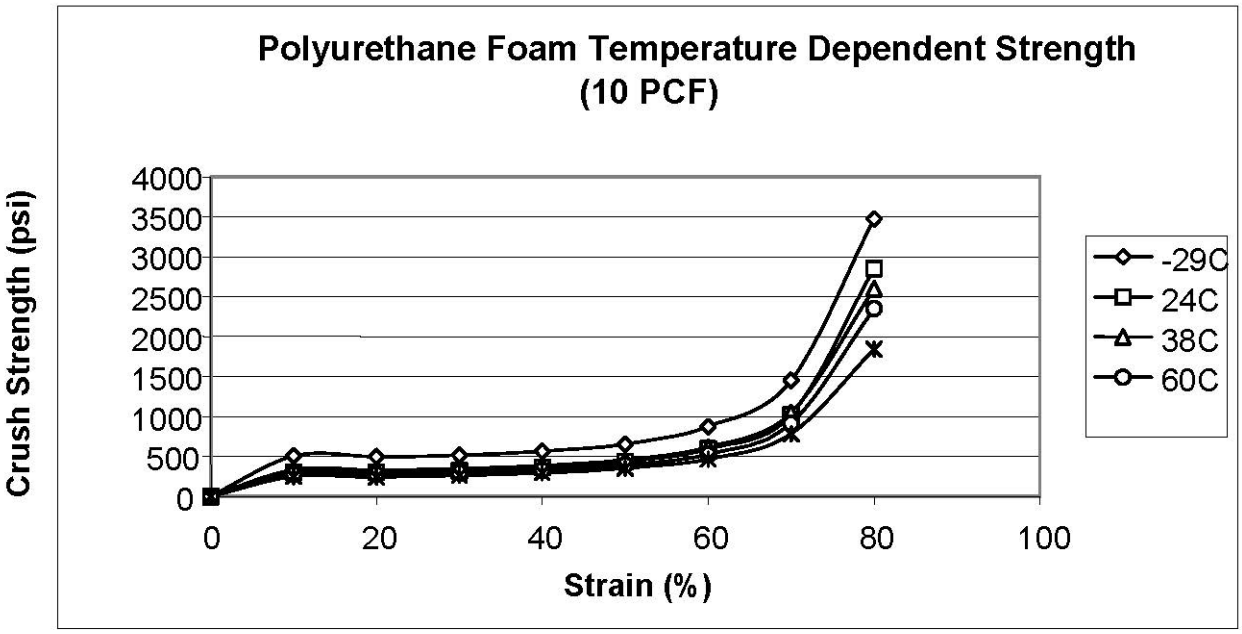

Figure 2.2-5 Temperature Dependent Crush Strength for 10 PCF Polyurethane Foam

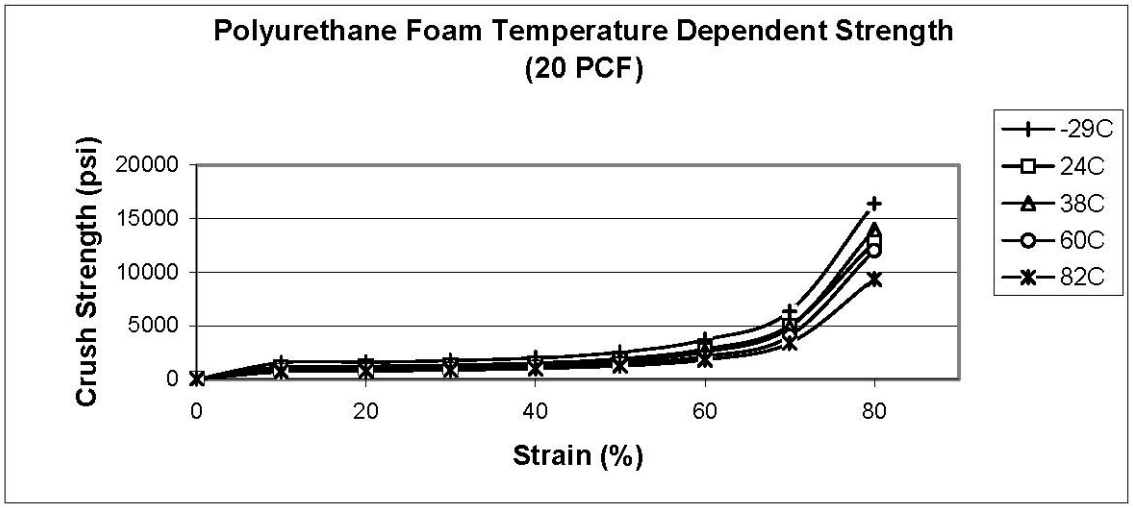

Figure 2.2-6 Temperature Dependent Crush Strength for 20 PCF Polyurethane Foam

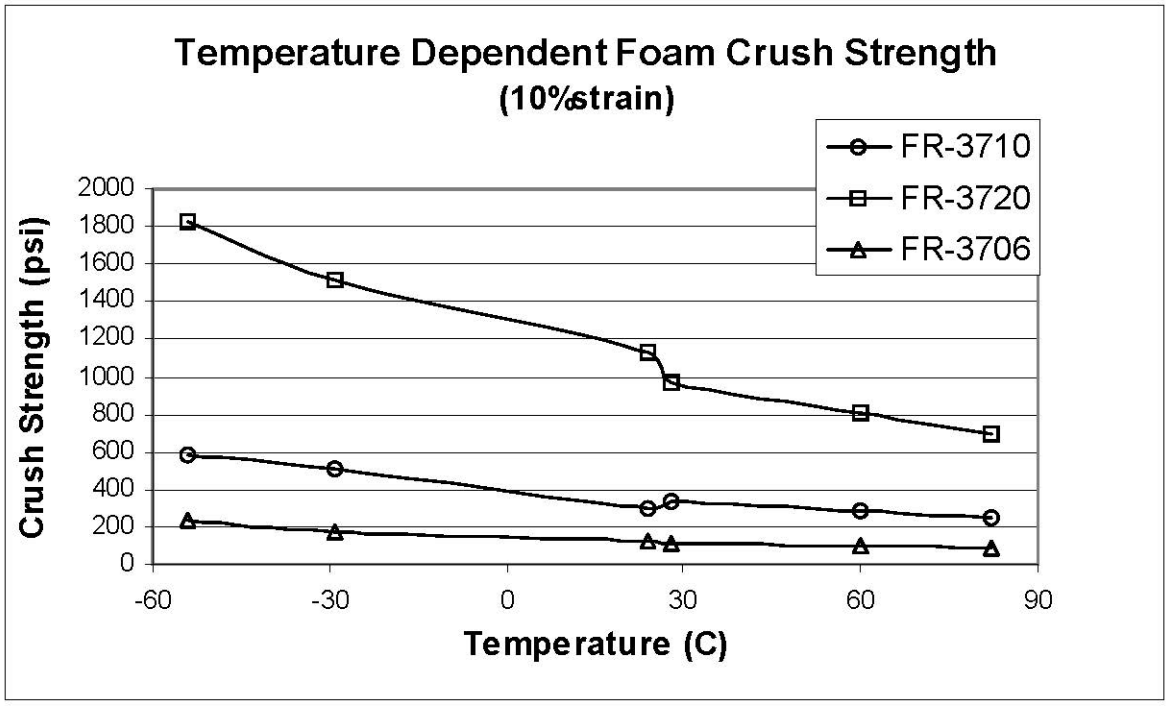

Figure 2.2-7 Temperature Dependent Crush Strength for Traveller Foam at 10% Strain

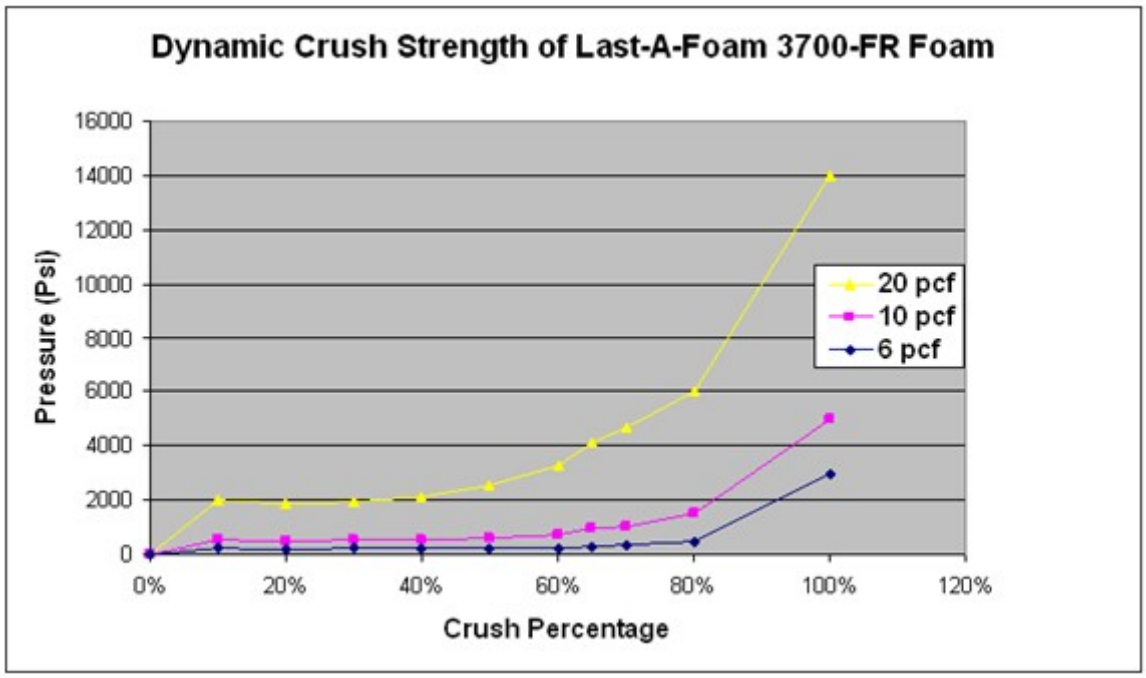

Figure 2.2-8 Dynamic Crush Strengths for Foam Materials Utilized in the Traveller

2.2.1.4 Neoprene

The material properties at 75°F (24°C) assumed for the lateral rubber pad are summarized in Table 2.2-4.

Table 2.2-4 Neoprene (Rubber, 60 durometer) Properties

Property	Symbol	Value (at 75°F)	Units
Density	RO	9.13E-10	Mg/mm^3
Shear Modulus	G	6.21E+00	MPa

2.2.1.5 Ultra-High Molecular Weight Polyethylene

The UHMW polyethylene used for the moderator blocks must have a minimum specific gravity of 0.93 and a molecular weight greater than 3 million. The UHMW polyethylene must be procured per ASTM D4020 [8], and the geometric dimensions are controlled by an engineering drawing.

2.2.1.6 Borated Aluminum Laminate Composite

The neutron absorber plates affixed to the Clamshell are comprised of borated aluminum (BORAL) laminate composite. The BORAL must have a minimum areal density of [ ]^{a,c} and a specified thickness of [ ]^{a,c} per engineering drawings. The effectiveness of the BORAL plates shall be tested per the specifications described in ASTM E748. See Section 8 for the acceptance and maintenance protocols regarding the BORAL neutron poison plates. No structural credit is taken for these plates.

2.2.1.7 Ceramic Insulation (Paper and Felt)

The ceramic insulation used in the Traveller has a maximum use temperature of >1800°F (982°C). Its thermal conductivity is < 1.2 Btu-in/hr-ft2 @ 500°F (0.173 W/m-K @ 260°C). The paper thickness is 0.0625 in (1.59 mm), and the blanket thickness is 0.25 in (6.35 mm).

2.2.1.8 Zirconium and Other Metal Alloy Performance

The choice of Standard Zirconium Alloy used during Traveller drop testing was based upon the energy absorbing capabilities the fuel cladding material used during construction of the fuel assemblies. The stand-alone name Alloy is a generic naming convention because of the proprietary nature of these materials. Cladding may include a chromium coating and/or a Zirconium based liner to enhance in-reactor fuel performance. These cladding features are in addition to the base cladding material. Two non-Zirconium alloys including Aluminum and Stainless Steel alloys are also evaluated for their expected drop test energy absorbing expected performance. The use of common metals does not require a proprietary naming convention and are identified accordingly. Section 2.2.1.8.1 discusses the strain energy absorption capability calculation method.

All Alloys are compared to the Standard Zirconium Alloy when considering their structural performance, specifically the strain energy absorption capability up to failure during a 9-meter drop test. The evaluation

demonstrates Standard Zirconium Alloy bounds all other Alloys. Table 2.2-5 compares all the Alloys and common metals strain energy absorption capability up to failure to the HAC tested Standard Zirconium Alloy, and includes Alloy 1, Alloy 2, Alloy 3, Alloy 4, Alloy 5, chromium-coated Alloy 1, Alloy 1 with liner (Optimized ZIRLO with liner or OZL), chromium-coated Alloy 2, Aluminum Alloy and Stainless Steel Alloy. A combination of chromium-coating and liner cladding configurations will not impact the conclusion, as the base alloys have higher energy absorption capabilities.

As the base cladding defines the required cladding content specification, chemical or galvanic reactions with the existing packaging materials is evaluated and discussed in Section 2.2.2 and includes Aluminum and Stainless Steel.

As Table 2.2-5 shows, Standard Zirconium Alloy is the least ductile of the eleven alloys and metals considered, and failure occurs at a much lower total strain energy compared to the other alloys and metals. Although the specification minimum tensile yield and ultimate stresses, as well as resilience strain energy, are greatest for the Standard Zirconium Alloy, its elongation at fracture is less than the other alloys and metals. By virtue of having less ductility at fracture compared to the other alloys and metals, Standard Zirconium Alloy possesses less total energy absorption capability when compared to all other alloys or metals.

Table 2.2-5 Fuel Rod Strain Energy Absorption Using Minimum Tensile Mechanical Properties

Alloy	Minimum Strain Energy (psi – in/in)		
	Yield Strength	Resilience	Failure
Standard Zirconium Alloy	201	208	**263**
Alloy 1	177	162	**683**
Alloy 2	141	102	**1266**
Alloy 3	126	81	**1159**
Alloy 4	141	102	**1282**
Alloy 5	141	102	**1224**
Alloy 1 with Chrome Coating	177	162	**720**
Alloy 1 with Liner	161	133	**29924**
Alloy 2 with Chrome Coating	141	102	**601**
Aluminum Alloy	95	33	**342**
Stainless Steel Alloy	40	16	**11850**

To bound individual alloy and other metal material properties at elevated temperatures, the specification minimum yield and ultimate strengths were used during the prototype fuel bundle fabrication and during the HAC test sequence. Tables 2.2-6 and 2.2-7 provide the specification minimum yield and ultimate stresses at ambient, 20°C and 70°C temperatures for each of the alloys and metals considered. For all materials, the specification minimum mechanical properties bound or are representative of 20°C and 70°C temperature mechanical properties. When considering specification minimum material properties (and elevated temperatures), including elongation behavior, Standard Zirconium Alloy bounds other alloys and metals with respect to total energy absorption capability. The thin chromium coating remains mechanically stable at

temperatures at or above -40°F (-40°C) when plated onto the base zirconium alloy. In addition, the base zirconium alloy used in all alloy cladding is a hexagonal closed pack (HCP) crystalline structure and those microstructures do not exhibit an apparent nil ductile-brittle transition at temperatures at or above -40°F (-40°C).

As discussed in Section 2.2.1.1, austenitic steels such as 304 stainless steel have a face-centered cubic (FCC) structure and consequently exhibit a ductile-to-brittle transition at cryogenic temperatures near -297°F (-183°C) and brittle fracture of the stainless steel components is not expected. Aluminum alloys, including 5052 and similar aluminum alloys, do not exhibit a ductile-to-brittle temperature transition; consequently, neither ASTM nor ASME specifications require low temperature Charpy or Izod tests of aluminum alloys. Thus, brittle fracture of the aluminum components is not expected.

Table 2.2-6 Fuel Cladding Yield Stress Values vs. Temperature

Alloy	Specification Minimum at Room Temperature (ksi)	Yield Stress at 68°F/20°C (ksi)	Yield Stress at 158°F/70°C (ksi)
Standard Zirconium Alloy	**77**	**87**	**82**
Alloy 1	68	73	69
Alloy 2	54	70	66
Alloy 3	48	56	53
Alloy 4	54	72	69
Alloy 5	54	70	66
Alloy 1 with Chrome Coating	68	74	60
Alloy 1 with Liner	62	73	54
Alloy 2 with Chrome Coating	54	62	54
Aluminum Alloy	18	21	21
Stainless Steel Alloy	29.7	30	25

Table 2.2-7 Fuel Cladding Ultimate Stress Values vs. Temperature

Alloy	Specification Minimum at Room Temperature (ksi)	Ultimate Stress at 68°F/20°C (ksi)	Ultimate Stress at 158°F/70°C (ksi)
Standard Zirconium Alloy	**103**	**116**	**108**
Alloy 1	90	99	94
Alloy 2	80	83	79
Alloy 3	70	70	66
Alloy 4	80	84	80
Alloy 5	80	83	79
Alloy 1 with Chrome Coating	90	102	78

Table 2.2-7 Fuel Cladding Ultimate Stress Values vs. Temperature			
Alloy	**Specification Minimum at Room Temperature (ksi)**	**Ultimate Stress at 68°F/20°C (ksi)**	**Ultimate Stress at 158°F/70°C (ksi)**
Alloy 1 with Liner	80	91	68
Alloy 2 with Chrome Coating	80	85	73
Aluminum Alloy	24	32	32
Stainless Steel Alloy	75	75	68

2.2.1.8.1 Strain Energy Absorption Capability Calculation Method

The total strain energy absorption is the sum of the cladding's moduli of resilience and toughness. Those properties represent the elastic and elastic plus plastic areas under the stress-strain curve, as shown in Figure 2.2-9. The stress-strain curve is obtained from tensile test load-deflection data to permit a direct comparison of all metal alloys.

After the stress-strain curve is plotted from tensile load-deflection test data, the area under the curve is determined by splitting the curve into two basic shapes; a triangle and a rectangle. The triangle is used up to 0.2% strain assuming the curve is still in the elastic region. The second half (plastic region) is estimated using a rectangle by arithmetically averaging the yield stress (S_y) from 0.2% strain with the ultimate stress (S_u) up to the elongation at fracture (failure).

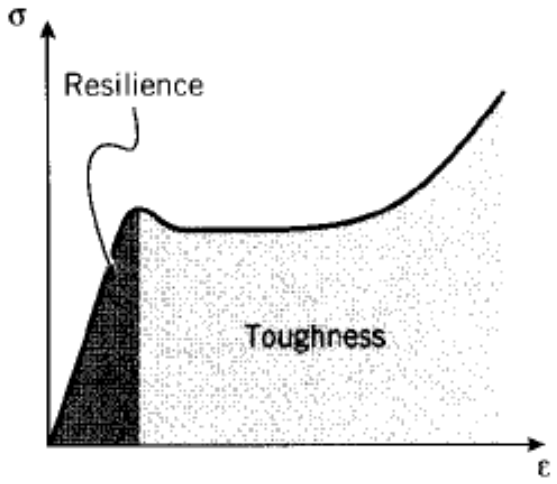

Figure 2.2-9 Resilience and Toughness (Strain Area)

The calculation for Standard Zirconium Alloy (i.e., ZIRLO) is shown below. Figure 2.2-10 provides the ZIRLO cladding stress-strain plot and shows the triangular and rectangular area representations.

Total Strain Energy, K, for Standard ZIRLO is:

$$K_{ZIRLO} = (0.5 \times (\varepsilon_y \times S_{y\text{-}min})) + (S (\varepsilon_{failure} - \varepsilon_y))$$

[

]a,c

Total strain energy absorption calculations demonstrate that Standard Zirconium Alloy has the least total strain energy absorption value of all zirconium alloys and is therefore most susceptible to fracture as compared to other zirconium alloys. It was concluded the drop tested Standard Zirconium Alloy cladding bounds all other zirconium alloys to be transported in the Traveller package with respect to fracture susceptibility.

[ ]a,c

Figure 2.2-10 ZIRLO Cladding Stress-Strain Plot

To compare each Alloys' expected drop test structural performance, each claddings' mechanical tensile properties are compared considering uniaxial loading condition at the moment of impact. The total strain energy evaluation considers both elastic and plastic region which accurately represents cladding mechanical behavior resulting from a drop test as seen in Figure 2.7-17. It is noted from Figure 2.7-19 that 7.5% (20 of 264 rods) were cracked at the end plug location located at the four corners for the Type A testing. This implies that the stresses at the corners was greater compared to the interior cells. Based upon the HAC 30 ft. (9 m) Type A drop test discussed in Section 2.7.1.2 and Figure 2.7-18, the fuel rod failure did not occur at the base cladding. The failure occurred at the bottom end plug weld due to the bending moment applied at this region as the peripheral fuel rods slipped outwards due to the chamfered edge geometry of the bottom nozzle. Bending and buckling of the cladding occurred at the lower span due to the instantaneous axial load without any cladding fracture for the most brittle Standard Zirconium Alloy cladding. Therefore, bending and axial

buckling of the cladding is not considered explicitly as a failure mechanism due to the weld failure mechanism during the 30 ft. (9 m) drop. This is further justified since the base alloys are in the partially or fully-recrystallized annealed condition. Therefore, the strength of the heat affected zone (HAZ) is slightly lower than the base material, and under large dynamic stress, the HAZ quickly hardens to the strength of the base material.

Subsequent Type B configuration HAC 30 ft. (9 m) drop test discussed in Section 2.7.1.4.1 and Figure 2.7-27 demonstred that cladding drop test resposne was load path dependent. By elminating the potential of lower span eccentric loading, the impact load is axially applied to the cladding and its mechanical response is dependent on cladding elastic and plastic strength and ductility. Thus, the alloys and other metals total strain energy absorption is compared, as failure could occur anywhere in the cladding length above the lowest span and was shown to be highly dependent upon loading conditions and load path.

Chromium-coated cladding Alloy 1 or Alloy 2 material, and Alloy 1 with OZL are expected have the same structural response to the 30 ft. (9 m) drop test since: 1) For Alloys with chromium coating, the coating stops prior to the ends of the tube, therefore, the HAZ region is unaffected and 2) the alloys have failed at the base cladding material instead of the HAZ region due to the ductility of the base cladding material. Aluminum and Stainless steel alloys are more ductile compared to the tested Standard Zirconium Alloy cladding and axial impacts loads can be absorbed by plastic deformation without failure. For Stainless steel and aluminum alloy cladding, the end plugs may also be bonded, rather than welded, to the cladding to encapsulate the fuel rods. The bonding methods do not impact the integrity of the base cladding material, nor the expected cladding mechanical performance; therefore, the same energy absorption response is expected for the base cladding.

2.2.1.8.2 Chromium Coated and OZL Liner Cladding Evaluation

Axial tensile testing was conducted on both chromium-coated and OZL cladding to obtain yield and ultimate strength values, as well as elongation at failure. Stress-strain testing up to elongation at failure provides the elastic and plastic mechanical behavior and the data needed to perform the expected cladding behavior after the 30 ft. (9 m) HAC drop test. Axial tensile testing was performed on representative Alloy 1 and Alloy 2 chromium coated cladding samples as well as Lined Alloy 1 for the parametric energy evaluation. Each of the samples underwent room-temperature tensile testing to failure using industry standard methods per controlled procedures.

Testing Results and Total Strain Energy Evaluation

Data from the tensile tests was processed and plotted for both chromium-coated and OZL claddings to calculate the strain energy absorption capability in the same manner as pervious alloys. The stress-strain plot for chromium-coated is shown in Figure 2.2-11, for Alloy 1 cladding with liner in Figure 2.2-12, and chromium-coated Alloy 2 is shown in Figure 2.2-13. Below each figure is the total strain energy calculation result using the methodology shown for Standard Zirconium Alloy in Section 2.2.1.8.1. Chromium-coated Alloy 1 cladding total strain energy absorption capability was calculated to be 720 psi-in/in, Alloy 1 cladding with liner calculated total strain energy absorption capability is 29,924 psi-in/in, and chromium-coated Alloy 2 cladding total strain energy absorption capability was calculated to be 601 psi-in/in. All calculated values are greater than the tested Standard Zirconium Alloy (263 psi-in/in); therefore, both the chromium-coated Alloy 1 cladding and Alloy 1 cladding with liner are less susceptible to mechanical failure after the 9-meter drop test. A combination of chromium-coating and liner cladding configurations will not impact the conclusion, since

the base alloys have higher energy absorption capabilities than the tested Standard ZIRLO.

Based upon this evaluation, there will be no greater fuel assembly damage experienced by any evaluated alloys (i.e., lattice expansion) than what has already been considered in the criticality safety analysis.

[ ]a,c

Figure 2.2-11 Chromium Coated Alloy 1 Cladding Stress-Strain Plot

Total Strain Energy for Chromium-coated Alloy 1 is:

$$K_{ALLOY\ 1\ Cr} = (0.5 \times (\varepsilon_y \times S_{y\text{-}min})) + (S (\varepsilon_{failure} - \varepsilon_y))$$

[

]a,c

[ ]a,c

Figure 2.2-12 OZL Lined Alloy 1 Cladding Stress-Strain Plot

Total Strain Energy for Alloy 1 with liner (OZL) is:

$$K_{ALLOY\ 1\ LINER} = (0.5 \times (\varepsilon_y \times S_{y\text{-}min})) + (S\ (\varepsilon_{failure} - \varepsilon_y))$$

[

]a,c

[ ]a,c

Figure 2.2-13 Chromium Coated Alloy 2 Cladding Stress-Strain Plot

Total Strain Energy for Chromium-coated Alloy 2 is:

$$K_{ALLOY\ 2\ Cr} = (0.5 \text{ x } (\varepsilon_y \text{ x } S_{y\text{-}min})) + (\ S\ (\varepsilon_{failure} - \varepsilon_y))$$

[

]a,c

2.2.1.8.3 Zirconium Based Alloy Material Interactions

All text of Section 2.2.1.8.3 is proprietary marked.
[

]a,c

[

]a,c

2.2.1.8.4 Aluminum Alloy and Stainless Steel Cladding Evaluation

Stress-strain testing up to elongation at failure provides the elastic and plastic mechanical behavior and the data needed to perform the expected cladding behavior after the 30 ft. (9 m) HAC drop test. Axial tensile testing was conducted on Aluminum alloy cladding samples to obtain yield and ultimate strength values, as well as elongation at failure for the parametric energy evaluation. The stainless steel cladding is common Type 304, therefore known published stress-strain curves were used for evaluation. In both cases, samples were subject to room-temperature tensile testing to failure using industry standard methods per controlled procedures.

Total Strain Energy Evaluation

Data from the tensile tests was processed and plotted for both Aluminum alloy and stainless steel claddings to calculate the strain energy absorption capability in the same manner as pervious alloys. The stress-strain plot for Aluminum alloy is shown in Figure 2.2-14 and for stainless steel cladding in Figure 2.2-15. Below each

figure is the total strain energy calculation result using the methodology shown in for Standard Zirconium Alloy in Section 2.2.1.8.1. Aluminum alloy 1 cladding total strain energy absorption capability was calculated to be 601 psi-in/in, and stainless steel cladding total strain energy absorption capability was calculated to be 11,850 psi-in/in. All calculated values are greater than the tested Standard Zirconium Alloy (263 psi-in/in); therefore, both the Aluminum alloy and stainless steel claddings are less susceptible to mechanical failure after the 9-meter drop test.

Based upon this evaluation, there will be no greater fuel assembly damage experienced by the Aluminum alloy or stainless steel cladding (i.e., lattice expansion) than what has already been considered in the criticality safety analysis.

[ ]^{a,c}

Figure 2.2-14 Aluminum Alloy Cladding Stress-Strain Plot

Total Strain Energy for the Aluminum Alloy is:

$$K_{Al} = (0.5 \times (\varepsilon_y \times S_{y\text{-}min})) + (S (\varepsilon_{failure} - \varepsilon_y))$$

[

]^{a,c}

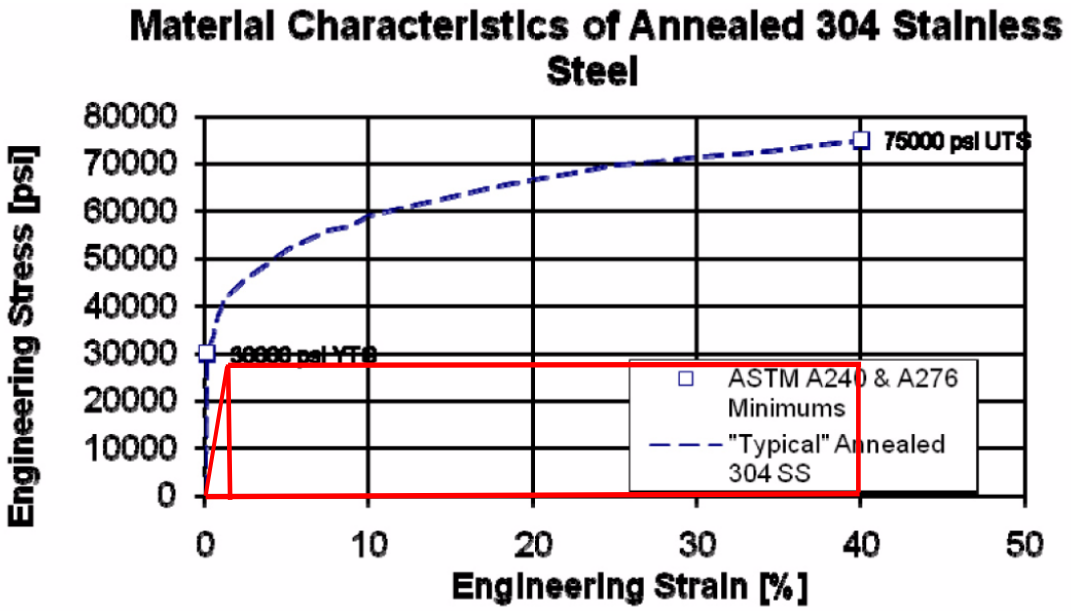

NOTE: The strain energy considered is the area under the drawn red lines include a triangle up to 0.2% strain and a rectangle up to 40% strain.

Figure 2.2-15 Stainless Steel Cladding Stress-Strain Curve

The total strain energy for the stainless steel cladding used a conservative approach from known published data which equate to the specification values in Section 2.2.1.1 as shown below.

The area under the stress-strain curve includes a triangle (at 29.7ksi w/ 0.2% strain) and rectangle (also at 29.7 ksi w/ strain of 40%-0.2%).

Stress at ~.002in/in = 29,732 psi; conservatively assumed 0.2% at minimum yield strength.

Average stress from above ~0.002in/in to ~0.40 in/in = 29,732 psi; conservatively assumed linear strength at minimum yield strength instead of ultimate strength and minimum strain at 40%.

The total strain energy for the stainless steel cladding is therefore:

K_{ss} = (0.5 x .002 x 29,732) + ((29,732) x (.400 - .002)) = 11,850 psi-in/in

2.2.1.8.5 Fuel Rod Endurance Limit Evaluation

All text of Section 2.2.1.8.5 is proprietary marked.
[

]a,c

[

]a,c

Figure 2.2-16 17x17 STD OFA Fuel Assembly, Tube Dimensions and Grid Elevations

[

]a,c

[

]a,c

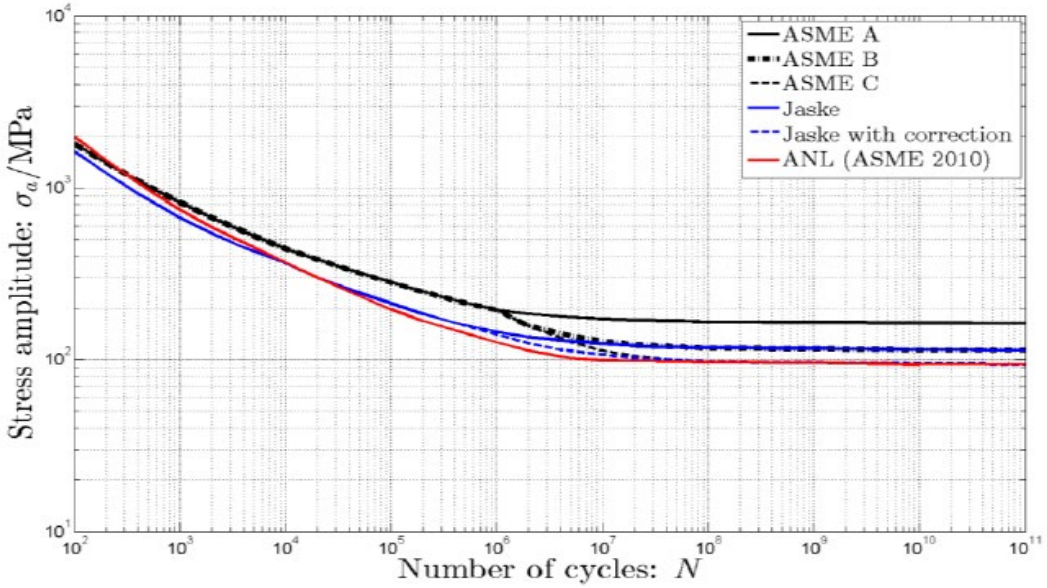

Figure 2.2-18 Design Endurance Limits for Austenitic Stainless Steel

2.2.2 Chemical, Galvanic, or Other Reactions

The Traveller series of packages are fabricated from ASTM A240 Type 304 stainless steel, 6000-series aluminum, borated 1100-series aluminum, polyurethane foam, and polyethylene sheeting. The stainless steel Outerpack does not have significant chemical or galvanic reactions with the interfacing components, air, or water.

The aluminum Clamshell is physically isolated, and environmentally protected, by the Outerpack and therefore will have negligible chemical or galvanic reactions with the interfacing components, air, or water. In addition, the Type 304 stainless steel fasteners that attach various Clamshell components represent a very small area ratio (cathode-to-anode ratio), which renders the reaction insignificant. Therefore, the requirements of 10 CFR 71.43(d) and SSR-6 para. 614 are met.

The Outerpack hinge bolts are zinc plated for the purpose of improving galling resistance, which can be a significant problem when stainless steel fasteners are inserted in stainless steel threaded holes. The plating is not required for chemical or galvanic protection.

2.2.3 Effects of Radiation on Materials

The contents of the package are limited such that the radiation to the packaging material is insignificant. Thus, there are no materials used in the Traveller packages that will be adversely affected by the content radiation under NCT and HAC.

2.3 FABRICATION AND EXAMINATION

2.3.1 Fabrication

The Traveller packages (XL and STD) are manufactured using standard fabrication techniques. No exotic materials or processes are required. Safety-related items needed for criticality safety purposes have specific manufacturing specifications, which clearly delineate all necessary codes, standards, and specifications required to meet design intent. All fabrication specifications are listed on the engineering drawings.

The fabrication processes of the Traveller include basic processes such as cutting, rolling, bending, machining, welding, and bolting. All welding is performed in accordance with ASME Section IX [9].

The manufacturing flow of the Traveller units includes affixing the inner and outer shells of the upper and lower Outerpack assemblies in place. Individual closure components are then aligned and welded in place. Sub-assemblies, such as the forklift pockets, leg structures and stacking brackets, are assembled in a parallel manner and appended to the main assemblies at appropriate times. Upon welding closure of the sub-assemblies, the upper and lower Outerpack assemblies are secured together and poured with polyurethane foam material. Pouring of this material is tightly controlled through the foam manufacturing specification.

When the Traveller is filled with foam, it is ready for final assembly and installation of the Clamshell, which has followed a parallel fabrication process. One difference for the Clamshell is that the faces are manufactured extrusions as opposed to “off-the-shelf” material. The extrusions are fabricated to industry standard specifications. Upon integration of the Clamshell to the Outerpack, final assembly and light grit blasting conclude the manufacturing process.

The containment for the Traveller Type B configuration, the cladding of the fuel rods, is fabricated to standards that exceed the transport requirements due to the service requirements of the fuel in operating nuclear reactors.

2.3.2 Examination

Manufacture of all Traveller packages shall be performed in accordance with strict Quality Assurance (QA) requirements. Included in the manufacture of the packages are examinations to verify that each package is being built to the required specifications. These examinations include the following:

1. Receipt inspections whereby the received components are visually inspected for workmanship, overall part quality, dimensional compliance, and material certification compliance.
2. All welds (which shall be performed by qualified welders/processes) shall be visually examined by a qualified inspector in accordance with AWS D1.6 and ASME Section III, Subsection NF, or engineering-approved equivalents, for stainless steel and aluminum, respectively.
3. Examinations that evaluate form, fit, and function shall be performed on each package to verify its operability and assess its overall quality.

2.4 GENERAL REQUIREMENTS FOR ALL PACKAGES

2.4.1 Minimum Package Size

As shown in Section 1, the smallest overall dimension of the Traveller STD and XL is the width at 27.1 in (68.8 cm). Therefore, the package meets the requirement of 10 CFR 71.43(a) and SSR-6 para. 636 that the smallest overall dimension shall not be less than 4.0 in (10 cm).

2.4.2 Tamper-Indicating Feature

Two (2) tamper indicating seals (wire/lead security seal) are attached between the upper and lower Outerpack halves to provide visual evidence that the closure was not tampered. The tamper indicating seal is not readily breakable and would provide evidence of tampering or opening by an unauthorized person. Thus, the requirements of 10 CFR 71.43(b) and SSR-6 para. 637 are satisfied.

2.4.3 Positive Closure

The Traveller series of packages cannot be opened inadvertently. Positive closure of the Traveller packages is provided by high strength Allen type threaded rods and nuts, which require use of tools and deliberate action to facilitate their removal. There are no other openings in the Outerpack. The number, type, and size of these bolts are provided on the drawings included in Section 1.3.2. Thus, the requirements of 10 CFR 71.43(c) and SSR-6 para. 641 are satisfied.

2.5 LIFTING AND TIE-DOWN STANDARDS FOR ALL PACKAGES

The design loads were determined according to the criteria described in 10 CFR 71 and SSR-6, where appropriate. The Traveller XL package weight bounds the Traveller STD design, as shown in Table 2.1-3. The total weights for each Traveller design include shipping components, where applicable.

2.5.1 Lifting Devices

The lifting criteria is governed by 10 CFR 71.45(a) and SSR-6 para. 608. 10 CFR 71.45(a) states that any lifting attachment that is a structural part of the package must be designed with a minimum safety factor of three against yielding when used to lift the package in its intended manner. In addition, it must be designed so that failure of any lifting device under excessive load would not impair the ability of the package to meet other requirements of 10 CFR 71. The applied loads to the package lifting attachments are:

For the case of Traveller XL:

$$F_{XL} = 3W_{XL} = 3 \times 5{,}230 = 15{,}690 \text{ lbf } (69.79 \text{ kN})$$

For the case of stacked Traveller STDs:

$$F_{STD} = 3W_{2STD} = 3 \times (2 \times 4{,}500) = 27{,}000 \text{ lbf } (120.0 \text{ kN})$$

2.5.1.1 Traveller XL Four Point Lift

The Traveller package is crane lifted using a 4-point lift with attachment points located on the stacking bracket. Figure 2.5-1 shows a sample package with the lifting configurations. The assumed sling angle is 30° and the applied load is F_{XL} = 15,690 lbf (69.79 kN).

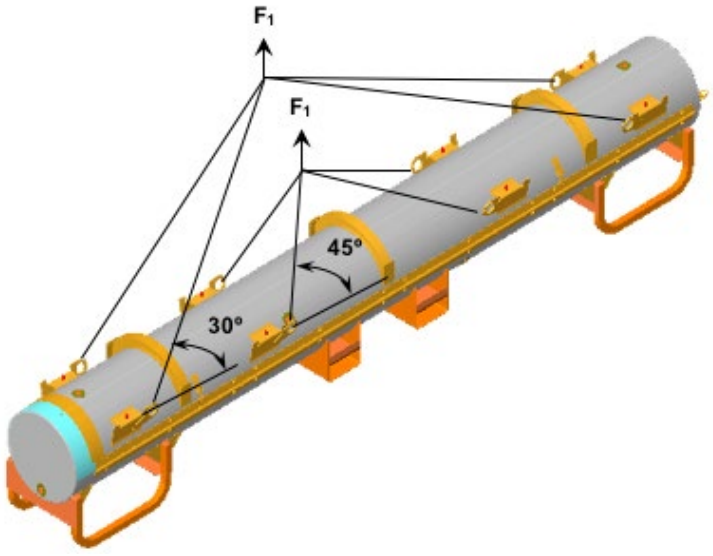

Figure 2.5-1 Traveller XL Lifting Configurations

Based on the lifting configuration, the applied load transferred to each lifting hole, F, is:

$$F = \frac{F_{XL}/4}{\sin 30°} = \frac{15{,}690/4}{\sin 30°} = 7{,}845 \frac{lbf}{hole} \left(34.89 \frac{kg}{hole}\right)$$

The applied forces and resultant components for a single lifting hole are shown in Figure 2.5-2.

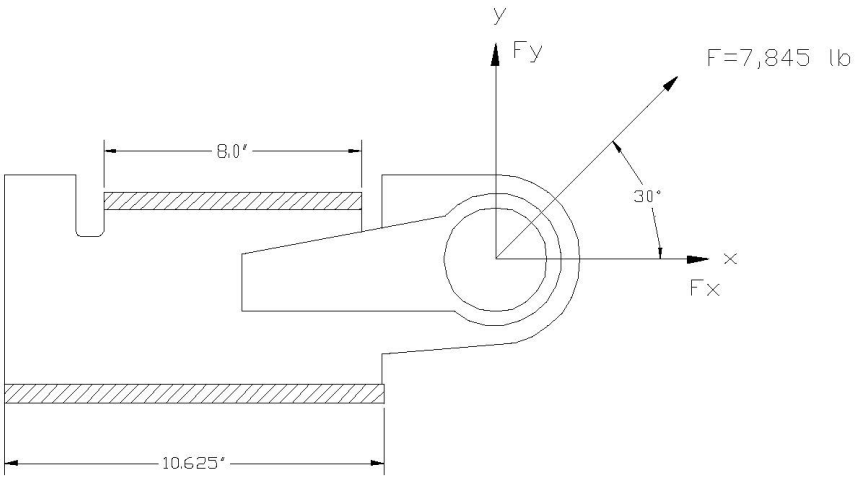

Figure 2.5-2 Lifting Hole Force Detail

The resulting force components, F_x and F_y, are then:

$F_x = F(\cos 30°) = 7{,}845(0.866) = 6{,}794$ lbf (30.2 kN)

and

$F_y = F(\sin 30°) = 7{,}845(0.50) = 3{,}923$ lbf (17.5 kN)

The lifting bracket consists of ASTM A276 SS plate with an attached lifting eye. The lifting eye is 0.25 in (6.35 mm) thick ASTM A276 SS plate and is reinforced with a 0.25 in (6.35 mm) plate doubler. A lifting bracket detail is shown in Figure 2.5-3.

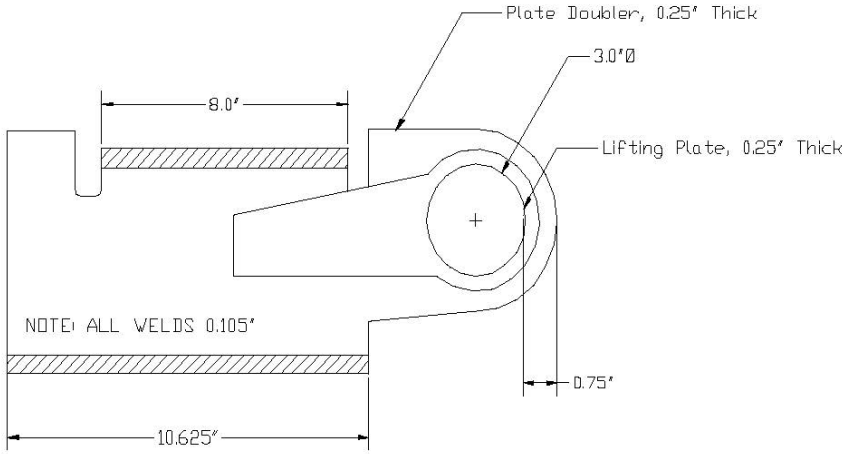

Figure 2.5-3 Lifting Bracket Fabrication Detail

The lifting analysis consists of two calculations: 1) hole tear-out and, 2) weld strength.

The hole tear-out is assumed to occur at the minimum 0.75 in (19.1 mm) section of material in the lifting eye plate. From Section 2.2.1.1, the maximum allowable Shear Yield Stress, τ_y, is 18 ksi (124 MPa). The stressed area is the minimum thickness of 0.5 in (12.7 mm) times the section width of the tear out, 0.75 in (19.1 mm), and double shear is assumed. Thus, the shear area, A, is:

$$A = 2(0.75\ in)(0.5\ in) = 0.75\ in^2\ (484\ mm^2)$$

The elemental volume stress state is described by the Mohr's Circle as shown in Figure 2.5-4. The resulting stress on the element due to the applied load, F, of 7,845 lbf (34.9 kN) is:

$$\sigma_x = {}^{F}/_{A} = \frac{7{,}845\ lbf}{0.75\ in^2} = 10{,}460\ psi\ (72\ MPa)$$

The maximum shear stress on the element is then:

$$\tau_{max} = \sqrt{\left[\frac{(\sigma_{x\prime} - \sigma_{y\prime})}{2}\right]^2 + \tau_{x\prime y\prime}^2} = \sqrt{\left[\frac{(10{,}460 - 0)}{2}\right]^2 + 0} = 5{,}230\ psi\ (36\ MPa)$$

Shear tear-out of the hole is not expected as τ_{max} = 5,230 psi (36 MPa) < τ_{allowx} = 18,000 psi (124 MPa).

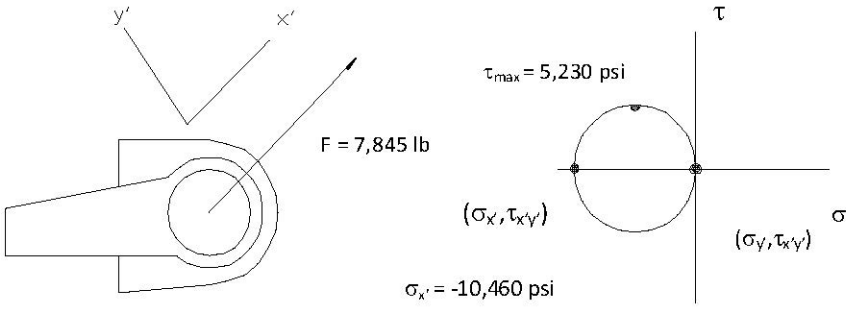

Figure 2.5-4 Hole Tear-out Model and Mohr's Circle Stress State

The weld attaching the lift plates to the Outerpack shell are required to demonstrate that they are adequate to preclude local weld yielding. The analysis assumes that one of the wire ropes is non– functional and three of the four welds bear the lifting load. The weld shear stress is found by τ_{weld} = F/A, where F is the applied vertical or horizontal load and A is the weld area. The assumed weld area is:

$A = h \times l \sin 45°$

Where,

l = (0.75)(10.625 + 8) = 13.97 in from Figure 2.5-2, and

h = 0.105 in, weld thickness

The applied loads are F_x = 6,794 lbf (30.22 kN) in the vertical direction and F_y = 3,923 lbf (17.5 kN) in the horizontal direction. The weld stresses are then:

$$\tau_x = {F_x}/{A} = \frac{6{,}794\ lbf}{0.105\ in \cdot 13.97\ in \cdot cos\ 45°} = 6{,}551\ psi\ (45\ MPa)$$

and,

$$\tau_y = {F_y}/{A} = \frac{3{,}923\ lbf}{0.105\ in \cdot 13.97\ in \cdot sin\ 45°} = 3{,}783\ psi\ (26\ MPa)$$

The stresses τ_x and τ_y are perpendicular to each other, and the resulting weld shear stress, τ_{max}, is:

$$\tau_{max} = \sqrt{(\tau_x^2 + \tau_y^2)} = \sqrt{(6{,}551^2 + 3{,}783^2)} = 7{,}565\ psi\ (52\ MPa)$$

The welds are sufficient to prevent local yielding, as τ_{max} = 7,565 psi (52 MPa) < τ_{allowx} = 12,000 psi (83 MPa).

2.5.1.2 Traveller STD Four-Point Lift

The Traveller STD package may be crane lifted using a 4-point lift with attachment points located on the inner stacking bracket. Figure 2.5-5 shows sample STD packages with the lifting configuration. The assumed sling angle is 45° since the inner lifting brackets are utilized. The applied load is F_{STD} = 27,000 lbf (120.1 kN) from Section 2.5.1.

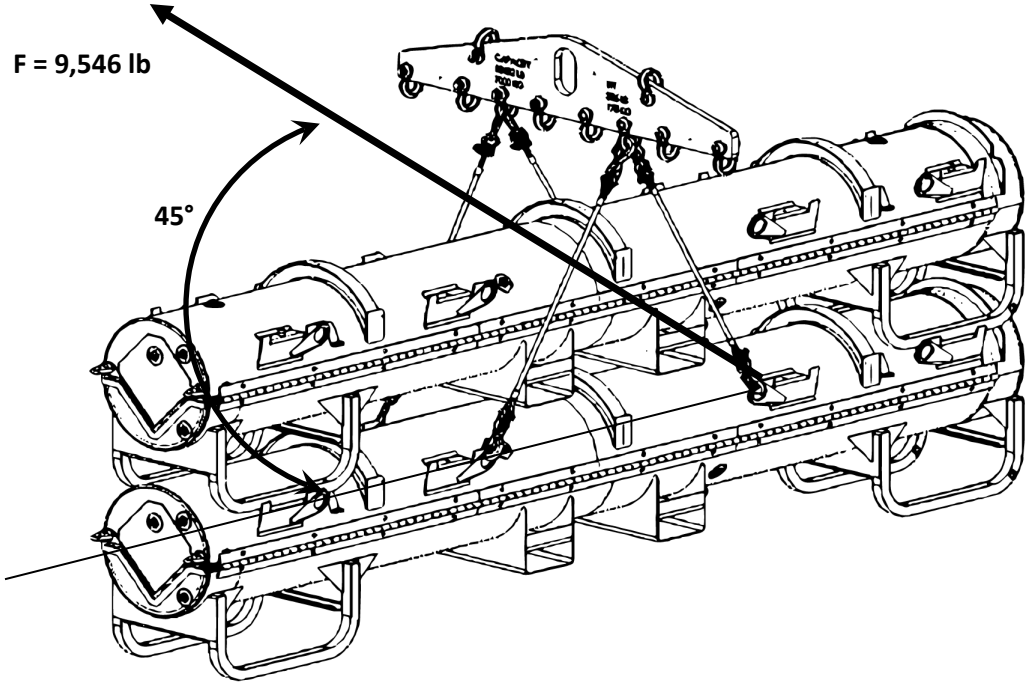

Figure 2.5-5 Traveller STD Stacked Lifting Configuration

The methodology is the same as for the Traveller XL since the load path and structure is assumed nearly

identical. However, the force components are greater:

$$F = \frac{F_{STD}/4}{sin\,45°} = \frac{27{,}000/4}{sin\,45°} = 9{,}546\,\frac{lbf}{hole}\ (42.5\,\frac{kN}{hole})$$

Substituting into the force component geometric relationships:

$F_x = F_y = 6{,}750$ lbf (30.0 kN)

These resultant forces result in the following hole tear-out and weld shear loads using the same equations shown for the Traveller XL and substituting appropriate Traveller STD values:

Hole Tear-Out

$$\tau_{max} = {}^{F}/_{A} = \frac{9{,}546\ lb}{1.5} = 6{,}364 \text{ psi (44 MPa)}$$

Where,

$$A = 4(0.75\ in)(0.5\ in) = 1.5\ in^2\ (968\ mm^2)$$

Shear tear-out of the hole is not expected since τ_{max} = 6,364 psi (44 MPa) < τ_{allowx} = 18,000 psi (124 MPa).

Weld Shear

$$\tau_{max} = {}^{F}/_{A} = \frac{9{,}546\ lbf}{1.04} = 9{,}205 \text{ psi (63 MPa)}$$

Where,

$A = h \times l \sin 45° = 1.04$ in²
l = (0.75)(10.625 + 8) = 13.97 in from Figure 2.5-2, and
h = 0.105 in, weld thickness

Shear tear-out of the hole is not expected since τ_{max} = 9,205 psi (63 MPa) < τ_{allowx} = 12,000 psi (83 MPa).

2.5.1.3 Forklift Analysis

During package lift by a forklift, only the center portion of the package is supported by the forklift extension arms. Consequently, the package is subject to a bending load due to the unsupported weight of the package. The loading conditions include a single Traveller XL and two stacked Traveller STDs.

For the bending evaluation, the Traveller package is conservatively modeled as a cantilever beam with the length equal to half of the overall Traveller length. For the Traveller XL, L_f = 113.1 in (2870 mm) and the design lifting load is distributed over the length of the package, as shown in Figure 2.5-6. The outer shell is the only assumed structure of the package carrying the bending load. This calculation is repeated for Traveller STD with L_f = 98.6 in (2500 mm). The design weights are calculated in Section 2.5.1 as 15,690 lbf (69.79 kN) and 27,000 lbf (120.1 kN) for Traveller XL and two Traveller STD stacked, respectively.

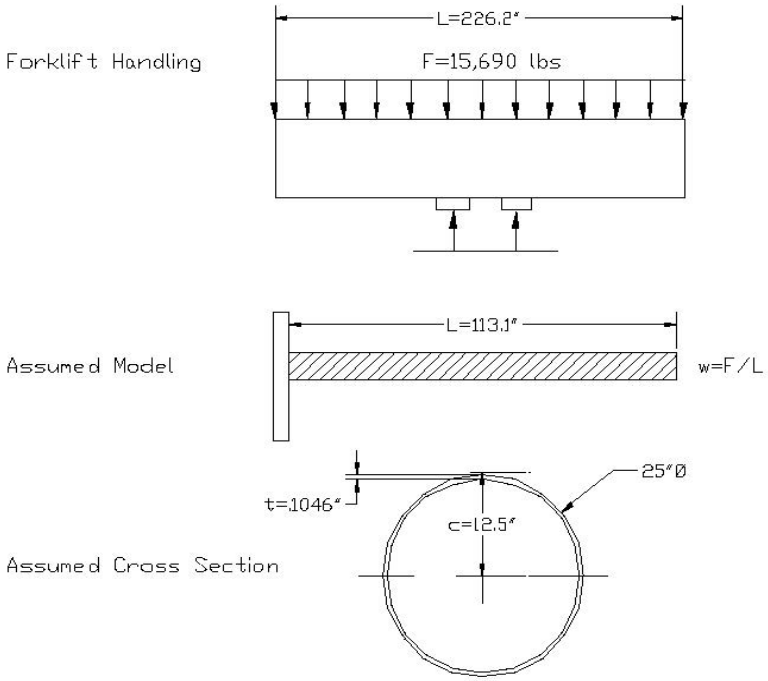

Figure 2.5-6 Forklift Handling XL Model and Assumed Cross Section

The forklift pockets weldments are also subjected to a shear load during lifting as the forks will apply a normal force along the top plate as shown in Figure 2.5-7. Both the single Traveller XL and the Traveller STD doubled stacked conditions are evaluated.

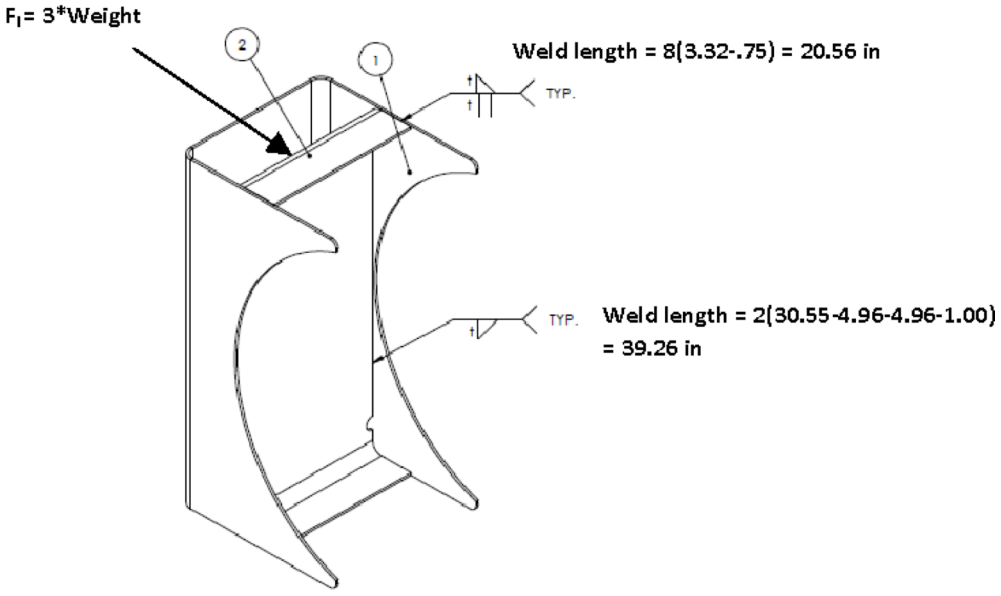

Figure 2.5-7 Forklift Pocket Weld Detail

The bending stress, σ, can be determined from the classic flexure equation:

$$\sigma = \frac{Mc}{I}$$

where c is the distance from the neutral axis to the outer fibers, M is the applied bending moment, and I is the moment of inertia of the section. The applied moment is given by:

$$M = \frac{wL^2}{2}$$

where w equals F/L from Figure 2.5-6. The value for w is:

$$w = \frac{F}{L} = \frac{15{,}690\ lb}{113.1\ in} = 139\frac{lb}{in}$$

Substituting and solving for M:

$$M = \frac{(139)(113.1)^2}{2} = 889{,}017\ in - lb$$

The moment of inertia for the shell, *I*, is calculated as follows:

$$I = \frac{\pi}{4} R_o - R_i$$

where R_o = 12.5 in and R_i = (12.5 – 0.1046) in = 12.395 in.

Therefore,

$$I = \frac{\pi}{4}(12.5^4 - 12.395^4) = 634\ in^4$$

The bending stress, σ_{XL}, is then:

$$\sigma_{XL} = \frac{(889{,}017)(12.5)}{634} = 17{,}528\ psi\ (121\ MPa)$$

Forklift loading is not expected to impact the Traveller XL package by bending since σ_{XL} = 17,528 psi (121 MPa) < σ_{yield} = 30,000 psi (207 MPa). In the case of the Traveller STD stacked, w is:

$$w = \frac{27{,}000\ lb}{98.6\ in} = 274\ lb/in$$

M is thus:

$$M = \frac{(274)(98.6)^2}{2} = 1{,}331{,}909\ in - lb$$

The bending stress, σ_{STD}, is then:

$$\sigma_{STD} = \frac{(1{,}331{,}909)(12.5)}{634} = 26{,}260\ psi\ (181\ MPa)$$

Forklift loading is not expected to impact the Traveller STD packages stacked by bending, as σ_{STD} = 26,260 psi (181 MPa) < σ_{yield} = 30,000 psi (207 MPa).

As previously noted, the model conservatively assumes the outer shell is loaded, and the actual Outerpack structure with foam would provide even greater margin against bending.

2.5.1.4 Weld Shear

The forklift pocket (Item 01 in Figure 2.5-7) weldments are also subjected to a shear load during lifting as the forks will apply a normal force along the top plate (Item 02) bottom surface as shown in Figure 2.5-7. There are two cases to be evaluated: a single Traveller XL and Traveller STD doubled stacked. The applied forces, F_{XL} and F_{STD}, are:

F_{XL} = 15,690 lbf (69.79 kN) for the Traveller XL

F_{STD} = 27,000 lbf (120.1 kN) for the two Traveller STDs stacked

The assumed weld area, A, is:

$A = hl \sin 45°$

Where,

l = (20.56 in + 39.26 in) = 59.82 in, and
h = 0.105 in, weld thickness

The weld stresses, τ_{XL} and τ_{STD}, are then:

$$\tau_{XL} = \frac{F_{XL}}{A}\ and\ \tau_{STD} = \frac{F_{STD}}{A}$$

Substituting values for the Traveller XL,

$$\tau_{XL} = \frac{15{,}690\ lbf}{(0.105\ in)(59.82\ in)\sin 45°} = 3{,}533\ psi\ (24\ MPa)$$

The welds are sufficient to prevent local yielding since τ_{XL} = 3,533 psi (24 MPa) < τ_{allowx} = 12,000 psi (83 MPa).

Substituting values for the Traveller STD,

$$\tau_{STD} = \frac{27{,}000\ lbf}{(0.105\ in)(59.82\ in)\sin 45°} = 6{,}080\ psi\ (42\ MPa)$$

The welds are sufficient to prevent local yielding since τ_{STD} = 6,080 psi (42 MPa) < τ_{allowx} = 12,000 psi (83 MPa).

2.5.1.5 Bolts

During package lift for fuel loading and unloading, the package is hoisted using the two rings attached to the top nozzle end of the Outerpack top. The hoist rings attach to the Outerpack using two 3/8-16 UNC Grade 8 Medium-Carbon socket head cap screws per hoist ring into a welded nut. The screws are fabricated to a minimum proof load of 120,000 psi (827 MPa).

The four screws are subject to shear loading in the most limiting case. The load per bolt is the design lifting load of 15,690 lbf (69.79 kN) distributed by the four bolts. Thus, the load per bolt, F, is 3,923 lbf (17.45 kN). The allowable axial stress is the yield stress of 120,000 psi (827 MPa) and the allowable shear stress is $0.6S_y$, 72,000 psi (496 MPa). The stressed area, A, is 0.0775 in^2 (50 mm^2). The applied stress, τ, is then:

$$\tau = \frac{F}{A} = \frac{3{,}923\ lbf}{0.0775\ in^2} = 50{,}619\ psi\ (349\ MPa)$$

This applied stress is acceptable, as it is less than the allowable shear stress of 72,000 psi (496 MPa) as well as the allowable axial stress of 120,000 psi (827 MPa). Only the Traveller XL is analyzed because it bounds the Traveller STD.

2.5.1.6 Coupling Nut

When the package is vertical, the coupling nut will be subject to a shear load. The nut is 3/8-16 and the material is 304 stainless steel. The allowable shear stress is 18,000 psi (124 MPa). The stressed area of the internal thread, A, is found by:

$$A = 0.7845\left(D - \frac{0.9743}{n}\right)^2 = 0.0775\ in^2$$

Where,

D = 0.375 in, nominal diameter
n = 16 threads per inch.

The shear area, An, is found by:

$$An = \pi\ n\ Le\ Ds_min\left[\frac{1}{2n} + 0.57735(Ds_{min} - En_{max})\right] = 0.222\ in^2$$

Where (per Machinery's Handbook [10]),

n = 16 threads per inch
Le = 0.269 in
Ds_min = 0.364
En_max = 0.340

The shear stress, τ, is then:

$$\tau = \frac{F}{A} = \frac{3{,}923\ lbf}{0.222\ in^2} = 17{,}671\ psi\ (122\ MPa)$$

This is acceptable, as this stress of 17,671 psi (122 MPa) is less than the allowable shear stress of 18,000 psi (124 MPa). Only the Traveller XL is analyzed because it bounds the Traveller STD.

2.5.1.7 Hoist Ring

After the package is in the vertical position, the hoists will be loaded in tension. The applied tensile stress for normal up-ending is found from σ = P/A. The load per 3/8-in (9.53 mm) diameter hoist ring, P, is:

P = 15,690 lbf/2

P = 7,845 lbf

The tensile stress per hoist ring is:

$$\sigma = \frac{7{,}845\ lbf}{2\frac{\pi}{4}(0.375\ in)^2} = 35{,}659\ psi\ (246\ MPa)$$

Since the allowable tensile yield strength, σ_y, is 130 ksi (896 MPa) minimum, the hoist ring satisfies the lifting requirements with a maximum stress, σ, of 35.7 ksi (246 MPa). Only the Traveller XL is analyzed because it bounds the Traveller STD.

2.5.2 Tie-Down Devices

The tie-down requirements are described in 10 CFR 71.45(b)(1,2) and SSR-6 para. 638. 10 CFR 71.45 states that a system of tie-downs that is a structural part of the package must be capable of withstanding, without generating stress in excess of its yield strength, a static force applied to the center of gravity having the following components:

- Vertical: 2 g
- Axial: 10 g
- Transverse: 5 g

Thus, based on the weight of the Traveller XL, the applied tie-down loads for the Traveller are:

- Vertical: 10,460 lbf (46.53 kN)

- Axial: 52,300 lbf (232.6 kN)
- Transverse: 26,150 lbf (116.3 kN)

The Traveller packages are secured to the transport conveyance by means of nylon straps (or chains) across the top of the Outerpack, and by chains that are passed through the leg assembly tray and connected inboard to the conveyance tie-down point. Thus, there are no structural devices designed for tie-down. However, it is possible that the leg assembly or the eight lift eyes could be inadvertently used for tie-downs. According to 10 CFR 71.45, these components require analysis to demonstrate that the inadvertent tie-down locations have either the strength capability required for a tie-down device or be rendered inoperable.

2.5.2.1 Leg Assembly

If the leg assemblies are used as tie-downs and not rendered inoperable for tie-down, the two leg assemblies on the Outerpack base will be loaded. A depiction of this loading configuration is shown in Figure 2.5-8.

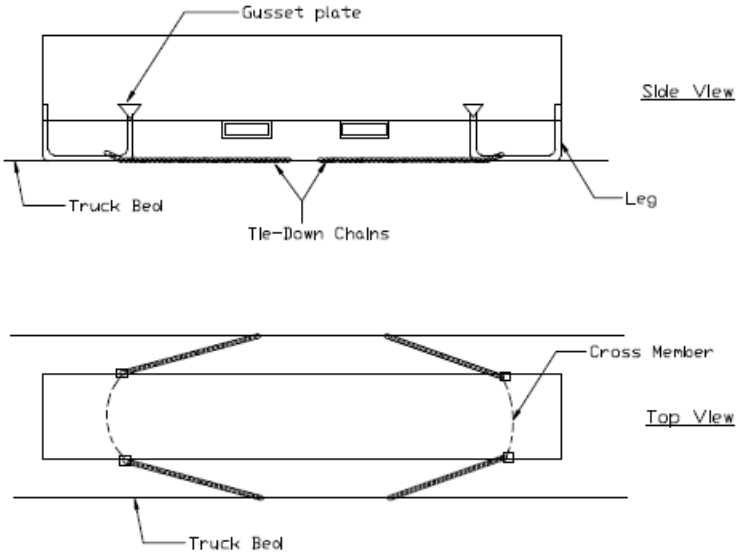

Figure 2.5-8 Leg Assembly Loading Condition During Inadvertent Tie-Down

The chains are assumed to be attached to each leg pair near the truck bed base so that the resulting chain angle (from the side perspective) is small enough to constitute an axially applied resultant load. For this loading condition, both leg pairs are loaded in the axial direction. The resultant applied force is the vector summation of the vertical, axial, and transverse components:

$$F = \sqrt{F_x^2 + F_y^2 + F_z^2}$$

$$F = \sqrt{52{,}300^2 + 26{,}150^2 + 10{,}460^2} = 59{,}401\ lbf\ for\ both\ pairs.$$

Therefore, the applied load for a single leg pair is F/2, or 29,701 lbf (132.1 kN).

The leg assembly is attached to the Outerpack using a gusset plate and an arced cross. Two gusset plates [6 in (152.4 mm) wide each] are welded to the Outerpack base by a continuous 0.10-in (2.54 mm) fillet weld on the outside of the skin. Thus, for single leg pair loading, the total weld length of the cross-member section is 12 in + 12 in, or 24 in (609.6 mm) (Figure 2.5-9).

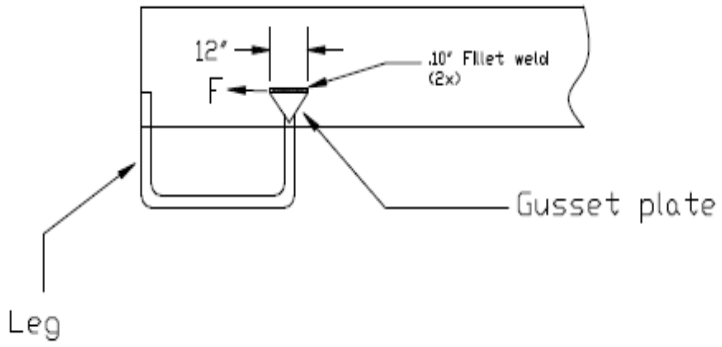

Figure 2.5-9 Welding Depiction at Representative Gusset Plate

The cross members are curved, 7 gage plates welded to the Outerpack base using minimum 0.10 in (2.54 mm) fillet welds, 1 in (25.4 mm) long at 12 places per side as shown in Figure 2.5-10. Thus, the total weld length for each cross member is 12 in (304.8 mm).

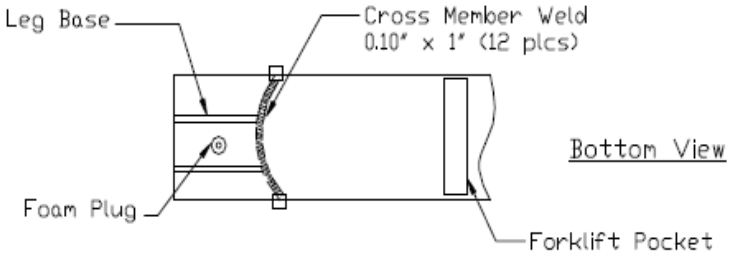

Figure 2.5-10 Welding Depiction at Cross Member

2.5.2.2 Weld Shear Analysis

The leg assembly is attached to the Outerpack shell by both the gusset and cross member welds. These welds are required to demonstrate that they are adequate to preclude local yielding. Axial loading of the resultant force results in a shear load on the welds.

The weld shear stress, τ, is found by:

$$\tau = \frac{F}{A}$$

where F is the applied vector shear load of 29,701 lbf (132.1 kN). The weld area, A, is:

$A = hl \sin 45° = 2.55 \text{ in}^2$

Where,

l = (24 in + 12 in) = 36 in, and
h = 0.10 in, weld thickness

The weld shear stress is then:

$$\tau = \frac{29{,}701\ lbf}{2.55\ in^2} = 11{,}648\ psi\ (80\ MPa)$$

Thus, the welds are sufficient to prevent local yielding since τ_{weld} = 11,648 psi (80 MPa) < τ_{allowx} = 12,000 psi (83 MPa).

2.5.2.3 Lift Eyes

In the event that the lift eyes are used as tie-down, the normal system of tie down would include eight (8) point loads (Figure 2.5-11). The analysis will assume that one of the chains fails per side, so the applied load is for six (6) lift eyes. The chains may be angled at an assumed 30 degrees or vertical as shown in Figure 2.5-11.

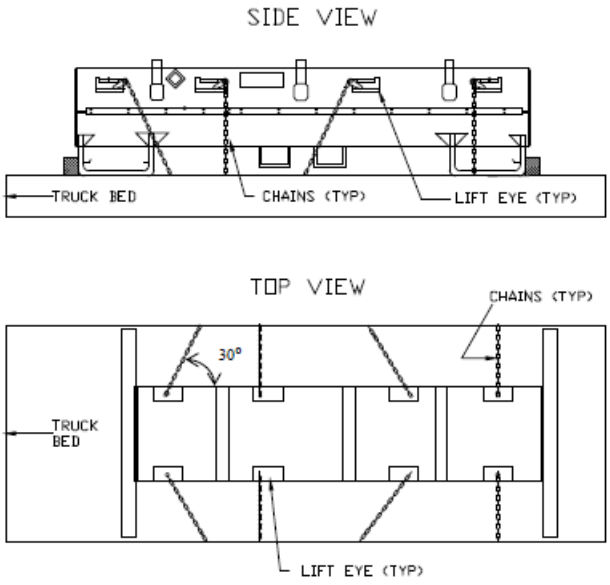

Figure 2.5-11 Lift Eye Loading Assumed Conditions During Inadvertent Tie-Down

The applied load is a combined vector load to the center of gravity of a single package. For this loading condition, each attached lift eye is loaded with 1/6th of the total load. The resultant applied force is the vector summation of the vertical, axial, and transverse components:

$$F = \sqrt{F_x^2 + F_y^2 + F_z^2} = \sqrt{52{,}300^2 + 26{,}150^2 + 10{,}460^2} = 59{,}401 \text{ lbf for both pairs.}$$

Therefore, the applied load for a single life eye is 0.167 F, or 9,900 lbf (44.04 kN).

2.5.2.4 Wind Shear Analysis – Vertical Direction

The lift eye is fillet welded to the Outerpack shell. The top and bottom part of the lift eyes are welded at 8 in (203.2 mm) and 10.63 in (270.0 mm), respectively. Thus, the total weld length for the top and bottom welds subjected to shear is 18.63 in (473.2 mm). A depiction of the loading configuration and lift eye sketch is shown in Figure 2.5-12 for the vertical chain orientation.

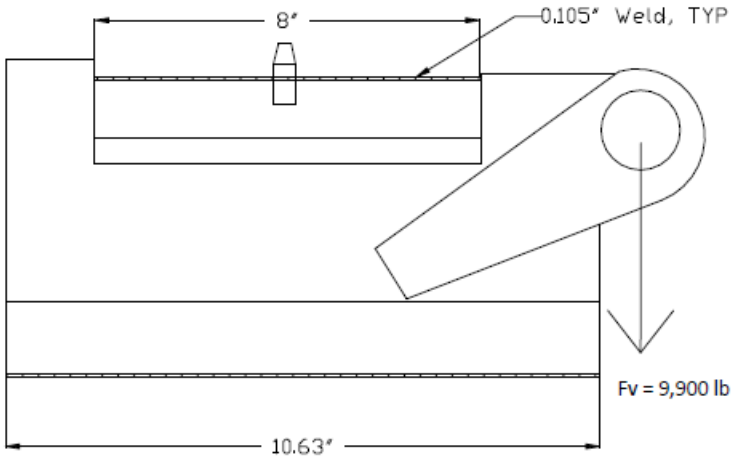

Figure 2.5-12 Vertical Lift Eye Welding Configuration

These welds are required to demonstrate that they are adequate to preclude local yielding for the vertical direction. The weld shear stress, τ_{weld}, is:

$$\tau_{weld} = \frac{F}{A}$$

where F is the applied vector shear load of 9,900 lbf (44.04 kN) and A is the weld area. The weld area, A, is:

$A = hl \sin 45° = 1.38$ in^2

Where,

l = 18.63 in, and
h = 0.105 in, weld thickness

The resulting weld stress, τ_{weld}, is:

$$\tau_{weld} = \frac{9{,}900\ lbf}{1.38\ in^2} = 7{,}158\ psi\ (49\ MPa)$$

Therefore, the welds are sufficient to prevent local yielding since τ_{weld} = 7,158 psi (49 MPa) < τ_{allowx} = 12,000 psi (83 MPa).

2.5.2.5 Weld Shear Analysis – Combined Shear

Figure 2.5-13 shows the lift eye combined shear loading configuration for the angled chain tiedown orientation. Since there are horizontal and axial components, the principal shear force is calculated.

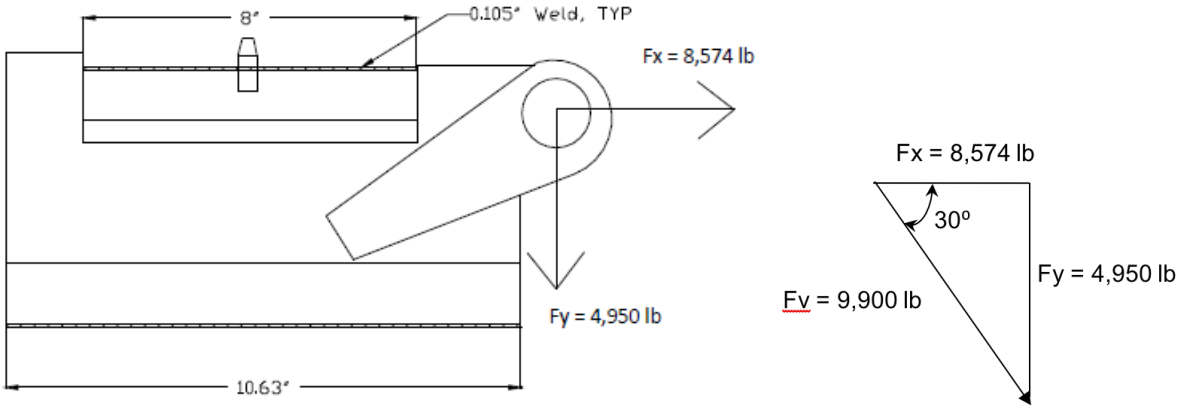

Figure 2.5-13 Combined Shear Lift Eye Welding Configuration

The x-direction weld shear stress, τ_{weldx}, is:

$$\tau_{weldx} = \frac{F_x}{A} = \frac{8{,}574\ lbf}{1.38\ in^2} = 6{,}213\ psi\ (43\ MPa)$$

where F is the applied vector shear load of 9,900 lbf (44.04 kN) and A is the weld area. The weld area is:

$A = hl \sin 45° = 1.38\ in^2$

Where,

l = 18.63 in, and

h = 0.105 in, weld thickness

The y-direction weld shear stress, τ_{weldy}, is:

$$\tau_{weldy} = \frac{F_y}{A} = \frac{4{,}950\ lbf}{1.38\ in^2} = 3{,}586\ psi\ (25\ MPa)$$

where F is the applied vector shear load of 9,900 lbf (44.04 kN) and A is the weld area.

Therefore, the principle shear stress, τ, is:

$$\tau = \sqrt{\tau_x^2 + \tau_y^2} = \sqrt{(6{,}213\ psi)^2 + (3{,}586\ psi)^2} = 7{,}173\ psi\ (49\ MPa)$$

The welds are sufficient to prevent local yielding τ_{max} = 7,173 psi (49 MPa) < τ_{allowx} = 12,000 psi (83 MPa).

2.6 NORMAL CONDITIONS OF TRANSPORT

The package, when subjected to the NCT specified in 10 CFR 71.71, is shown to meet the performance requirements specified in Subpart E of 10 CFR 71. The NCT events were evaluated by analysis and by comparison to testing. Because the NCT pressure and temperatures are well below the design conditions for the fuel cladding, no separate analysis was performed.

2.6.1 Heat

The NCT thermal evaluation for the heat test is described in Section 3.3 of the thermal evaluation. For pre-fire testing, the environment around the package was heated as described in Section 3.3.1. This resulted in a bounding NCT initial temperature of 122°F (50°C) applied to the Traveller package prior to the fire testing.

2.6.1.1 Summary of Pressures and Temperatures

There is no pressure seal in the Traveller series of packagings. Therefore, there is no pressure build up within the package. The fuel rods are defined as the containment boundary. As there is insignificant internal heat generation in the contents, the expected normal condition pressure in the rods will only increase based on the increased temperature from NCT insolation.

Fuel rods are backfilled with helium during fabrication. Type A fuel rods are backfilled to 460 psig (3.17 MPa gauge) at room temperature. Type B fuel rods are backfilled to 275 psig (1.90 MPa gauge). The resulting maximum normal operating pressure (MNOP) for Type A fuel rods is 509 psig (3.51 MPa gauge) and for Type B fuel rods is 305 psig (2.10 MPa gauge) (see Section 3.3.2).

The package must account for temperatures ranging from -40°F (-40°C) to 158°F (70°C) per SSR-6 para. 639 per para. 652 and from -40°F (-40°C) to 100°F (38°C) per 10 CFR 71.71(c)(1,2). Thus, the bounding temperature range to consider for package design is -40°F (-40°C) to 158°F (70°C). The maximum temperature for the following sections was evaluated to 158°F (70°C) and the minimum temperature to -40°F (-40°C).

2.6.1.2 Differential Thermal Expansion

The effects of differential thermal expansion for the Traveller series of packages is negligible due to the design of the package. The most significant differential thermal expansion is between the aluminum Clamshell and the fuel assembly, which is less than 0.25 in (6.35 mm). The differential thermal expansion is accommodated by rubber-cork spacers between the Clamshell and fuel assembly, or by rubber spacers on the axial or lateral spacers.

Differential thermal expansion (DTE) is expected to only impact the fuel assembly and Clamshell interface. The Outerpack is not under physical constraints and can accommodate thermal growth. Differential thermal expansion between the foam and the stainless steel shells of the Outerpack is easily accommodated by the elastic properties (low modulus value) of the foam.

However, the Ultra-High Molecular Weight (UHMW) polyethylene does have a significantly higher coefficient of thermal expansion (CTE) when compared to 304 stainless steel. For this reason, the moderator

panels are segmented along their lengths to accommodate the differential thermal expansion between the polyethylene and the inner stainless steel shells of the Outerpack. Holes in the polyethylene segments are used to attach the panels to the inner Outerpack shells using threaded studs. These studs must not be loaded by the individual panel differential thermal expansion or contraction. For this reason, each hole drilled into the polyethylene panel is significantly large to preclude thermally induced stresses in the bolt studs. The following calculation addresses this case.

The polyethylene moderator blocks are attached by 0.375-in (9.53 mm) diameter weld studs on the inner skin of the on the Outerpack. The weld studs penetrate the moderator blocks through 0.563-in (14.3 mm) diameter holes. The blocks are mounted with a nominal, block-to-block gap of 0.260 in (6.60 mm). The CTEs are:

- 304 stainless steel 9.6 µin/in-°F (5.3 µm/m-°C)
- UHMW polyethylene 72 – 111 µin/in-°F (40 – 61.7 µm/m-°C)

Using the worst difference in expansion coefficients, 100 µin/in-°F (55.6 µm/m-°C), the gaps between the blocks will accommodate heat up from 70°F to 167°F (21°C to 75°C). In addition, there is an additional 0.094 in (2.39 mm) of clearance between the weld studs and each side of the holes in the polyethylene that will allow blocks with less than nominal clearance to slide in a direction to provide uniform clearance along the length of the Traveller.

Because the polyethylene's CTE is much greater than stainless steel, interference between moderator blocks is not an issue when temperature drops. Instead, it is the interference between the blocks and the weld studs. Based on nominal clearances and a maximum distance of 17.0 in (432 mm) from outboard hole-to-outboard hole, the package temperature can drop from 70°F to -41°F (21°C to -41°C) before the polyethylene is stressed. Most of the moderator blocks have significantly smaller distances between the outboard holes [6.5 in to 12.5 in (165 mm to 318 mm)], allowing them to accommodate larger temperature changes.

See the licensing drawings in Section 1 for additional details.

The DTE between the fuel assembly and the Clamshell is evaluated assuming fuel loading is performed at 70°F (21°C) and shipped to a cold environment of -40°F (-40°C) since the aluminum will tend to contract more than the fuel assembly. The thermal expansion, ΔL, is found with the following equation:

$$\Delta L = \alpha(\Delta T)L_o$$

Where,

ΔL = the total growth
L_{o_CS} = the original length of the Clamshell (202 in)
L_{o_FS} = the original length of the fuel assembly (188.86 in – conservative assumed longest length)
ΔT = the temperature change (110°F), and
α = the coefficient of thermal expansion.

For aluminum, α = 13 µin/in-°F (7.2 µm/m-°C). For Zircaloy, α = 2.79 µin/in-°F (1.55 µm/m-°C).

The differential thermal growth between the Clamshell and the fuel assembly, DTE, is then:

$$DTE = \Delta L_{Al} - \Delta L_{Zirlo}$$

$$DTE = \left\{\alpha(\Delta T)L_{o_CS}\right\}_{Al} - \left\{\alpha(\Delta T)L_{o_FA}\right\}_{Zirlo}$$

$$DTE = \left(13\frac{\mu in}{in}\cdot °\text{F}\right)(110°\text{F})(202\ in) - \left(2.79\frac{\mu in}{in}\cdot °\text{F}\right)(110°\text{F})(188.86\ in)$$

$$DTE = 0.29\ in - 0.058\ in = 0.23\ in\ (5.84\ mm)$$

Thus, the fuel assembly grows 0.23 in (5.84 mm) relative to the Clamshell.

The combined thickness of the base cork rubber and axial clamp cork rubber is 0.50 in (12.7 mm) and can accommodate the growth due to differential thermal expansion. Thus, DTE is not a concern. Since the total differential growth associated with the XL Clamshell is greater than the STD Clamshell, it is the bounding calculation.

The cladding of the fuel which serves as containment is not stressed due to differential thermal expansion because a gap remains between the fuel pellet and the cladding at both the cold temperature -40°F (-40°C) and the highest temperature the fuel could see due to the HAC inside the Clamshell were below 219°F (104°C). (see Section 3.4.3.1). DTE stresses in the cladding from transport conditions are negligible as the fuel rods are designed to perform under higher pressures and temperatures of a nuclear reactor.

2.6.1.3 Stress Calculations

The Traveller packages are fabricated from relatively thin sheet metal parts which are not subject to thermal gradients generated from the interior of the package. The packages are also not sealed to the environment; therefore, pressure stress is negated. The most significant stress potential occurs from the differential expansion rates of the bolted polyethylene moderator panels to the inner steel shells of the Outerpack. This potential stress is also negated by design, whereby the panels are made in sections and the bolt clearances and gaps between panels are adequately sized to allow unrestrained growth and contraction.

Successful testing of full scale Traveller XL packages indicates that the stresses associated with differential thermal expansion of the various packaging components are negligible.

Because the temperatures and pressures generated under NCT are well below the design conditions for reactor fuel, no specific calculations were performed for the fuel rod containment.

2.6.1.4 Comparison with Allowable Stresses

As discussed in Section 2.6.1.3, further evaluation of stresses associated with differential thermal expansion for the various Traveller package components is not required. Additionally, the NCT are well below the operating conditions of the fuel. Therefore, no comparison to allowable stresses was performed.

2.6.2 Cold

The package must account for temperatures ranging from -40°F (-40°C) to 158°F (70°C) per SSR-6 para. 639 per para. 652 and from -40°F (-40°C) to 100°F (38°C) per 10 CFR 71.71(c)(1,2). Thus, the bounding temperature range to consider for package design is -40°F (-40°C) to 158°F (70°C).

The materials used in construction of the Traveller packages are not degraded by cold at -40°F (-40°C), as described in Section 2.2.1. Stainless steel and aluminum exhibit no brittle fracture at these temperatures. Therefore, the requirements of 10 CFR 71.71(c)(2) and SSR-6 para. 639 are satisfied.

2.6.3 Reduced External Pressure

The package must account for the effects of external pressure conditions. The effects of reduced external pressure are described in 10 CFR 71.71(c)(3) and SSR-6 para. 616. The reduced external pressure is 3.5 psi (25 kPa) absolute as stated in 10 CFR 71.71(c)(3).

The Traveller packaging utilizes weather gaskets to preclude dust and other contaminants from entering the package. These gaskets are not continuous, and do not form an airtight pressure boundary. The packaging does not maintain a boundary between pressure gradients and is not designed to be pressurized during transport. Thus, internal/external reduced pressure will not impact the structural integrity of the package.

Compared with the internal pressure of the fuel rods, a reduced external pressure of 3.5 psi (25 kPa) would have a negligible effect on the fuel rods.

2.6.4 Increased External Pressure

The package must account for the effects of external pressure conditions. The effects of increased external pressure are described in 10 CFR 71.71(c)(4) and SSR-6 para. 616. The increased external pressure is 20 psi (140 kPa) as stated in 10 CFR 71.71(c)(4).

As the Traveller series of packages are not sealed against pressure, there cannot be any significant differential pressure. See Section 2.6.3.

The fuel rods provide the containment boundary for the Type B configuration, and are designed for the higher pressures experienced in an operating nuclear reactor. Thus, the fuel rods have the capability of withstanding an increased external pressure of 20 psi (140 kPa) for transport conditions, and is further bounded by nuclear reactor operational pressures.

2.6.5 Vibration

The package must be evaluated to consider the effects of normal vibration on the design performance. The package isolation system is designed to dampen normally induced vibrations from transport and is not fundamental to the safe operation of the package. However, the Outerpack must maintain its structural integrity during transport to maintain a safe transport condition, as specified in 10 CFR 71.71(5) and SSR-6 para. 613. Typical attachment to a transport conveyance for the Traveller packages includes nylon straps or chains

mounted both over the package and on the gusset tray connected to the support legs pointed inboard. The loading configuration can be modeled as a simply supported beam. Furthermore, the Outerpack is conservatively modeled considering only the outer shell at the first mode of vibration. The typical natural frequency range for transportation vehicles, f_{nat_TRANS}, is between 3.7 to 8 Hz. The natural frequency of the Outerpack, f_{natOP}, can be determined from the following equation:

$$f_{natOP} = a\sqrt{\frac{EIg/l^3}{m}} = 23\ Hz$$

Where,

a = 1.57 (primary mode coefficient assuming hinge-hinge end conditions for additional conservatism)
E = modulus of elasticity, $29.4 \cdot 10^6$ psi
I = moment of inertia, 634 in^4
g = acceleration due to gravity, 386.4 in/s^2
l = length, 226.2 in
m = mass, 2834 lb

Since the natural frequency of the Outerpack is greater than the natural frequency typical of a transportation vehicle, resonance of the Outerpack is not expected and normally induced vibrations will not preclude the package from performing its design function. The rubber shock mounts effectively isolate and dampen loads and vibrations to the Clamshell and its contents. No resonant vibration conditions, which could fatigue the Clamshell, shall occur during normal conditions of transport.

There are several natural frequencies of the shock mount system depending on direction of movement. The dominant frequency is for vertical movement. Depending on the weight of the fuel assembly being transported, this frequency is between 5.9 and 6.7 Hz for the Traveller XL. The fore and aft pitch frequency is slightly higher (6.9-7.9 Hz) but has a lower amplitude. Road tests have been performed with the suspension system to measure amplitudes during shipping. Figure 2.6-1 is characteristic of the results seen. When the truck travels over a bump, the Clamshell initially sees relatively large accelerations (2-3 g), but this oscillation quickly dampens to accelerations less than 1 g. This 300 mi (483 km) trip involved approximately five and a half hours on the road with $1.4 \cdot 10^5$ total cycles.

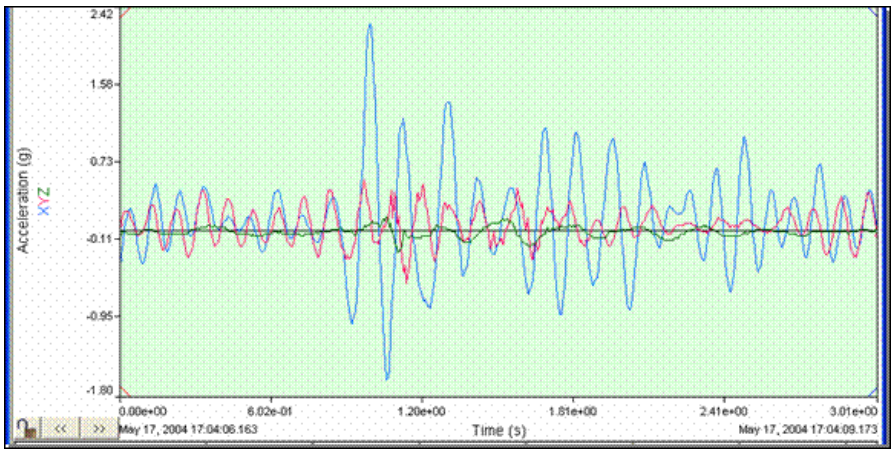

Figure 2.6-1 Sample of Clamshell Accelerations Measured During Road Test (May 11, 2004)

2.6.6 Water Spray

The materials of construction utilized for the Traveller packages are such that the water spray test identified in 10 CFR 71.71(c)(6) and SSR-6 para. 721 will have negligible effect on the package. Further, the Traveller Outerpack is cylindrical, and is specifically shaped to negate water collection. Since the Outerpack shell is fabricated from ASTM A240 Type 304 SS, the water spray will not impact the structural integrity of the package.

2.6.7 Free Drop

Since the gross weight of the bounding Traveller XL package is less than 11,000 lb (5,000 kg), a 4 ft (1.2 m) free drop is conservatively required per 10 CFR 71.71(c)(7) and SSR-6 para. 722. As discussed in Section 2.7.1.2, 4 ft (1.2 m) drops were performed on the Traveller CTU as an initial condition for subsequent HAC tests.

Impact protection of the Traveller package is provided by the Outerpack, which includes a polyurethane foam encapsulated stainless steel structure for side drop protection and impact limiter pillows for end drop protection. Traveller CTU free drop testing and engineering evaluations indicated that NCT free drop events have negligible impact on the integrity of the Traveller package. The NCT free drop testing included a low angle slap-down event, approximately 10 degrees, with the package inverted, which is indicative of a handling accident. The basis for selection of this orientation was that this orientation offered the greatest opportunity to stress the welded joints at the ends of the package. Detailed descriptions of the test results are given in Section 2.7.1.2. Examinations following the CTU testing proved the ability of the Traveller packaging to maintain its structural and criticality control integrity. Therefore, the requirements of 10 CFR 71.71(c)(7) and SSR-6 para. 722 are satisfied.

2.6.8 Corner Drop

The corner drop test does not apply, since the gross weight of the package exceeds 100 lb (50 kg), as specified in 10 CFR 71.71(c)(8) or 221 lb (100 kg) as specified in SSR-6 para. 722.

2.6.9 Compression – Stacking Test

The Traveller package must be subjected to a static compression test per by 10 CFR 71.71(c)(9) and SSR-6 para. 723. Both regulations require that the applied load be the greater of the following: Case 1, an equivalent load of five times the mass of the package or Case 2, the equivalent of 2 psi (13 kPa) multiplied by the vertically projected area of the package. Each case is evaluated with the specifications of the Traveller XL as follows:

Case 1 - the applied stacking force, F_s, for Case 1 is:

$$F_s = 5W_{XL}$$

$$F_s = 5(5{,}230) \text{ lbf}$$

$$F_s = 26{,}150 \text{ lbf } (116.3 \text{ kN})$$

Case 2 - the applied stacking force, F_s, for Case 2 is:

F_s = (Length)(OD)(P)

F_s = (226.2 in)(27.1 in)(2 psi)

F_s = 12,260 lbf (54.54 kN)

Thus, the applied stacking load is F_s = 26,150 lbf (116.3 kN).

The Traveller package must demonstrate elastic stability for a 5 g static load. No credit is taken for the circumferential stiffeners or the forklift support tubes. The analysis assumes the stacking load is uniformly distributed over the four outermost stacking brackets on the Outerpack. Figure 2.6-2 depicts the shell compression/stacking model.

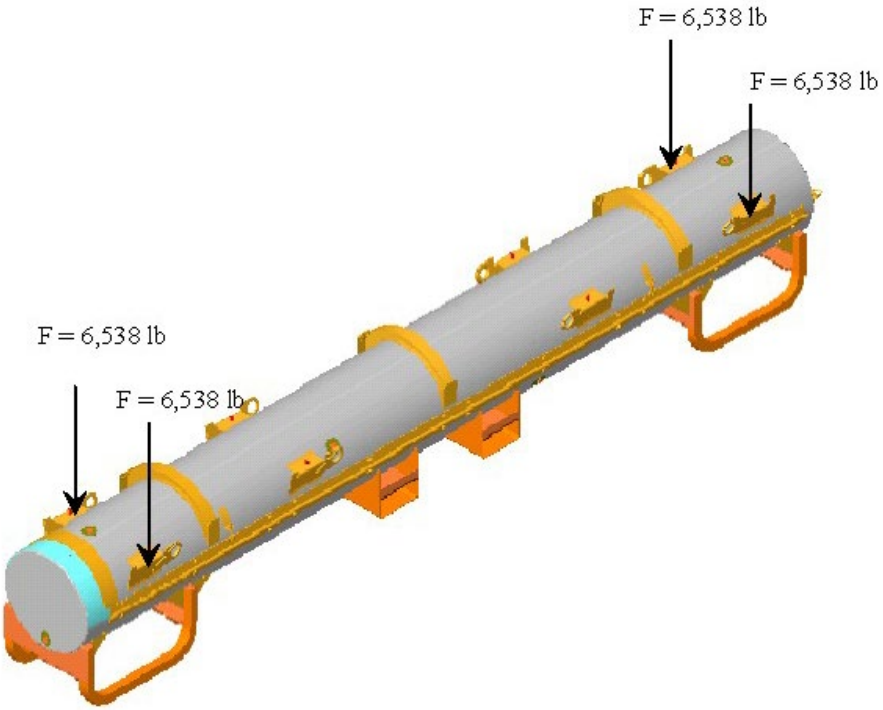

Figure 2.6-2 Compression/Stacking Requirement Analysis Model

The load path is assumed to follow through the welds of the stacking brackets, through the Outerpack side, and then to the leg supports. This assumption is based on the package stacking configuration or the placement of weight on the package top. Each loaded section will be analyzed for its structural integrity.

2.6.9.1 Stacking Bracket

The stacking bracket is expected to experience a shear load on the weld during stacking. The loading configuration for a single bracket is shown in Figure 2.6-3.

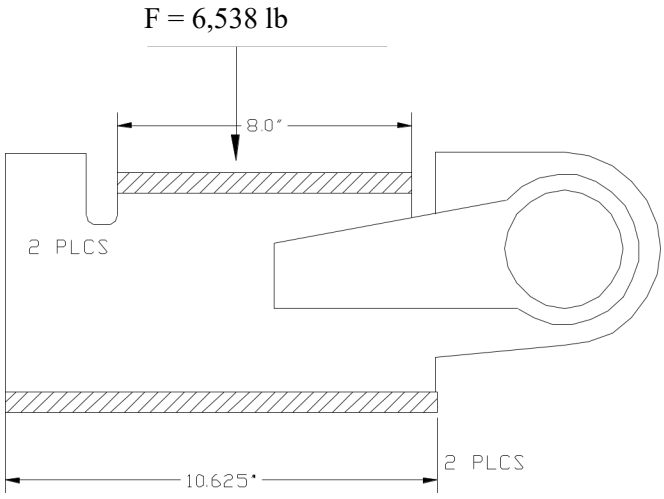

Figure 2.6-3 Stacking Force Model on Stacking Bracket

The load on each stacking bracket is found by dividing the applied load of 26,150 lbf (116.3 kN) by the four brackets that support the load:

F = 26,150 lbf /4

F = 6,538 lbf (29.08 kN)

The weld shear stress is found by τ_{weld} = F/A, where F is the applied vertical or horizontal load and A is the weld area. The assumed weld area is the total weld area of each bracket and is found by:

$A = hl \sin 45° = 1.38$ in^2 (890.3 mm^2)

Where,

l = (10.625 in + 8 in) = 18.625 in from Figure 2.6-3, and
h = 0.105 in, weld thickness

The weld stress, τ, is then:

$$\tau = \frac{F}{A} = \frac{6{,}538\ lbf}{1.38\ in^2} = 4{,}729\ psi\ (32.6\ MPa)$$

Thus, this weld stress is allowable as 4,729 psi (33 MPa) is less than the allowable weld shear stress of 12 ksi (83 MPa).

The welds are the weakest aspect of the stacking plate since the load from the legs is spread over a relatively small, thick plate. However, this needs to be demonstrated by determining the bending stress. Since the load is applied by the 2-in-wide (50.8 mm) leg over the bracket, the assumed model is a uniformly distributed load over a simply supported beam. The bending stress is found by the classic equation: σ = Mc/I, where M is the resultant moment, c is the distance from the neutral axis to the outermost fiber and I is the section moment of inertia. The 304 stainless steel bracket is 8 in (203.2 mm) by 3 in (76.2 mm) and ¼ in (6.35 mm) thick, resulting in the following section properties:

$$c = 0.125\ in$$

$$I = \frac{1}{12} bh^3$$

$$I = \frac{1}{12} \cdot 3\ in \cdot (0.25\ in)^3 = 0.0039\ in^4\ (1625\ mm^4)$$

The bending moment from the well-known simply supported beam:

$$M = \frac{1}{8} wL^2$$

where w is the applied force over the 2 in (50.8 mm) wide and 8 in (203.2 mm) length divided by the total of eight stacking brackets, or [6,538 lbf / (8*2)]/8 in = 51 lbf/in (0.009 kN/mm). Thus, the bending moment is:

$$M = \frac{1}{8} \cdot 51 \frac{lbf}{in} \cdot (3\ in)^2$$

$$M = 57\ in \cdot lbf\ (6.44\ kN \cdot mm)$$

Therefore, the bending stress, σ, is:

$$\sigma = \frac{(57\ in \cdot lb)(0.125\ in)}{0.0039\ in^4} = 1{,}827\ psi\ (13\ MPa)$$

Thus, the bending stress is negligible, even if the effects of stress concentration (at the radial bend) are considered.

2.6.9.2 Outerpack Section

The stacking bracket is expected to experience a compressive load through the package side cross section during stacking as the force follows the projected load path. The loading configuration and model for the Outerpack section is shown in Figure 2.6-4.

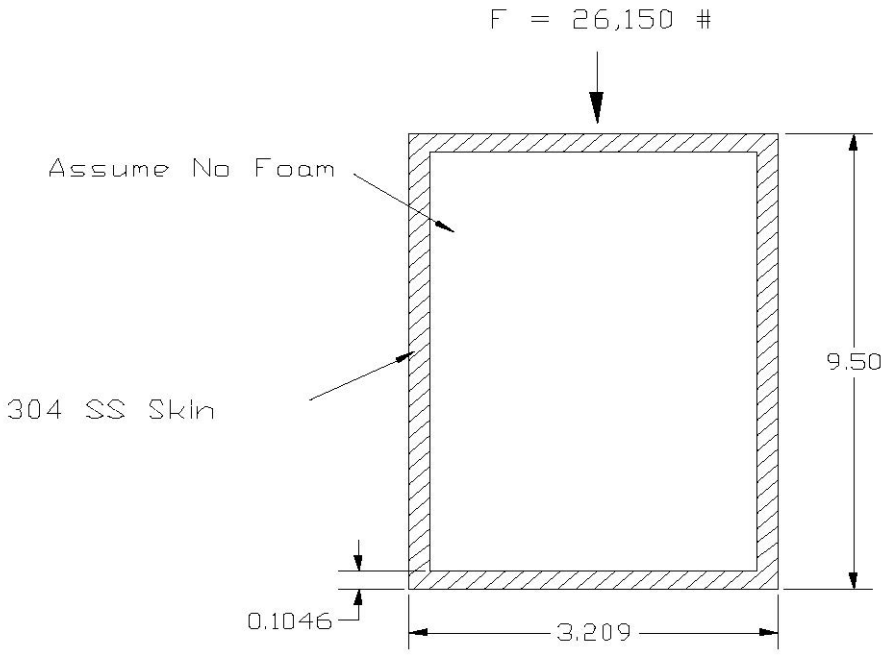

Figure 2.6-4 Outerpack Section Compression Model

The evaluation first examined the slenderness ratio of this section to determine if buckling is applicable. The model conservatively assumed no structural credit for the foam. In addition, the model assumed the force path section is from the base of the stacking bracket to the top of the support leg. The cross section consisted of a rectangular section of dimensions 9.50 in × 3.209 in (241 mm × 81.5 mm) with a wall thickness of 0.1046 in (2.657 mm). The critical buckling load will be calculated and compared to the actual load to determine elastic stability of the Outerpack section.

The slenderness ratio, SR, can be expressed as:

$$SR = {}^{l}/_{k}$$

where l is the effective length of 9.5 in (241 mm), and k is the radius of gyration:

$$k = \sqrt{{}^{I}/_{A}}$$

For the Outerpack section, the moment of inertia, I, and the cross-sectional area, A, are:

$$I = \frac{\left(wl^3 - w_i l_i^3\right)}{12}\ in^4$$

$$I = \frac{(3.209(9.50)^3 - 3.0(9.29)^3)}{12}\ in^4 = 28.8\ in^4\ (1.199 \times 10^7\ mm^4)$$

$$A = wl - w_i l_i$$

$$A = \left(3.209(9.50) - 3.0(9.29)\right) = 2.62\ in^2\ (1690\ mm^2)$$

Thus, the value for k is:

$$k = \sqrt{{28.8\ in^4}/{2.62\ in^2}} = 3.32\ in$$

The corresponding slenderness ratio is then:

$$SR = {9.50\ in}/{3.32\ in} = 2.86$$

The limiting slenderness ratios for columns are as follows:

Long Columns

$$\left({l}/{k}\right)_1 = \sqrt{\frac{2\pi^2\ C\ E}{\sigma_y}}$$

where the end condition, C, is conservatively assumed to be unity, E is Young's Modulus, and σ_y is the yield strength. Substituting values:

$$\left({l}/{k}\right)_1 = \sqrt{\frac{2\pi^2\ (1)\ (29.4E6\ psi)}{30{,}000\ psi}} = 139$$

Short Columns

$$\left({l}/{k}\right)_2 = 0.282\sqrt{\frac{Al^2}{\pi^2\ I}}$$

Substituting values:

$$\left({l}/{k}\right)_2 = 0.282\sqrt{\frac{2.62\ in^2(9.50\ in)^2}{\pi^2\ 28.8\ in^4}} = 0.257$$

Thus, 0.257 < 2.86 (SR) < 139 and the Outerpack section is considered an intermediate column. The critical load for this column is given by:

$$P_{cr} = A\left(\sigma_y - \left\{\frac{\sigma_y\ l}{2\pi\ k}\right\}^2 \frac{1}{CE}\right)$$

$$P_{cr} = 2.62\ in^2 \left(30{,}000\ psi - \left\{ \frac{30{,}000\ psi \cdot 9.50\ in}{2\pi \cdot 3.32\ in} \right\}^2 \frac{1}{1 \cdot 29.4E6\ psi} \right) = 78{,}583\ lbf\ (349.6\ kN)$$

Since the actual load of 26,150 lbf (116.3 kN) is less than the critical buckling load of 78,583 lbf (349.6 kN), the Outerpack section is considered stable during compression from stacking.

2.6.9.3 Leg Support

The leg support is expected to experience a compressive load through the straight top cross section during stacking as the force follows the projected load path. The loading configuration and model for the leg support section is shown in Figure 2.6-5. There are eight (8) leg sections of 2 in × 2 in × 0.120 in (50.8 mm × 50.8 mm × 3.05 mm) 304 SS tubing of approximately 10 in (254 mm) length. The expected load for each leg section is 26,150 lbf / 8 = 3,269 lbf (14.5 kN).

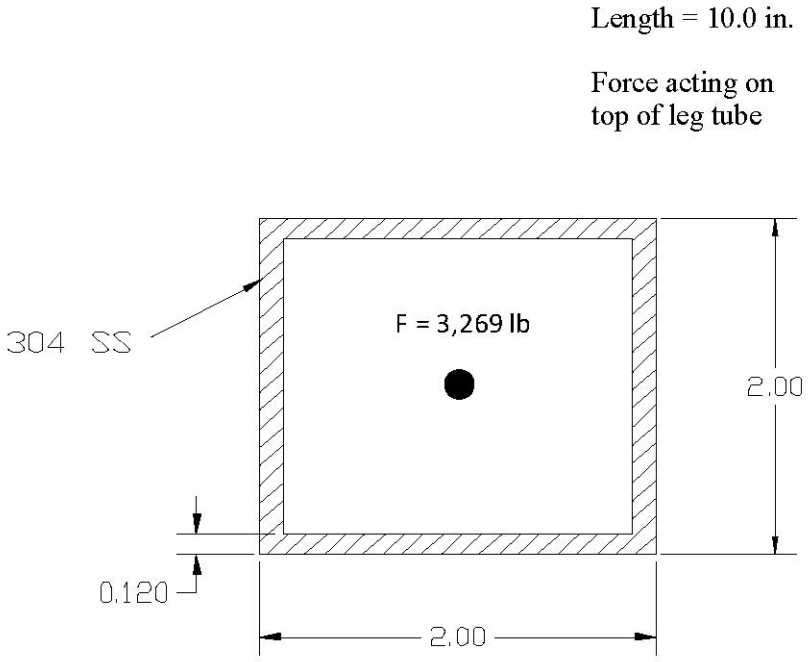

Figure 2.6-5 Leg Support Section Compression Model

The evaluation will first consider the slenderness ratio of this section to determine if buckling is applicable. The critical buckling load will be calculated and compared to the actual load to determine elastic stability of the leg support section. Using the equations presented in Section 2.6.9.2, the moment of inertia, I, is 20 in^4 (8.32 × 10^6 mm^4) and the cross-sectional area, A, is 2.4 in^2 (1548 mm^2), where w = 2.0 in (50.8 mm), l = 10.0 in (254 mm), w_i = 1.76 in (44.7 mm), and l_i = 10.0 in (254 mm). The radius of gyration, k, is then 2.9 in (73.7 mm) and the slenderness ratio, SR, is 3.4.

The limiting slenderness ratios for columns are:

Long Columns

As the limiting slenderness ratio for long columns does not depend on geometry, the long column slenderness ratio here is equal to that presented in Section 2.6.9.2:

$$\left(l/k\right)_1 = 139$$

Short Columns

$$\left(l/k\right)_2 = 0.282\sqrt{\frac{Al^2}{\pi^2 I}}$$

Substituting values:

$$\left(l/k\right)_2 = 0.282\sqrt{\frac{2.4\ in^2(10.0\ in)^2}{\pi^2\ 20\ in^4}} = 0.31$$

Thus, 0.31 < 3.4 (SR) < 139 and the Outerpack section is considered an intermediate column. The critical load for this column is given by:

$$P_{cr} = A\left(\sigma_y - \left\{\frac{\sigma_y\ l}{2\pi\ k}\right\}^2 \frac{1}{CE}\right)$$

$$P_{cr} = 2.4\ in^2\left(30{,}000\ psi - \left\{\frac{30{,}000\ psi \cdot 10.0\ in}{2\pi \cdot 2.9\ in}\right\}^2 \frac{1}{1 \cdot 29.4E6\ psi}\right) = 71{,}978\ lbf\ (320.3\ kN)$$

Since the actual load of 3,269 lbf (14.5 kN) is less than the critical buckling load of 71,978 lbf (320.3 kN), the Outerpack section is considered stable during compression from stacking.

2.6.10 Penetration

The penetration test is an impact test described by 10 CFR 71.71(c)(10) and SSR-6 para. 724. The package must be subject to the impact of the hemispherical end of a vertical steel cylinder of 1.25 in (3.2 cm) diameter and a mass of 13 lb (6 kg) dropped from 40 in (1 m) onto the surface of the package that is expected to be the most vulnerable to puncture.

The penetration test is of negligible consequence to the Traveller series of packages. This conclusion is due to the fact that the Traveller packages are designed to minimize the consequences associated with the much more limiting case of a 40 in (1 m) drop of the entire package onto a puncture rod, as discussed in Section 2.7.3, Puncture. The 12-gauge (2.7 mm) minimum thickness of the outer shell of the Outerpack is not damaged by the puncture event, thus bounding the penetration event. Therefore, the requirements of 10 CFR 71.71(c)(10) and SSR-6 para. 724 are satisfied.

The penetration test can be characterized as a localized impact event on the outer skin of the Outerpack. The energy imparted onto the outer skin is equal to the potential energy of the falling pin:

$$PE = mgh$$

Where, the mass of the pin is 13 lb (6 kg) and the drop height is 40 in (1 m).

To obtain the correct units of energy, the gravitational constant, g_c, must be used in the energy equation:

$$PE_{penetration} = {}^{mgh}/_{g} = mh$$

$$PE_{penetration} = 13\ in \cdot 40\ lb = 520\ in \cdot lb\ (6\ kg \cdot m)$$

By comparison, the energy locally imparted to the outer skin from the pin-puncture drop test is determined from the dropped package mass and the drop height. The mass of the package is 5,230 lb (2,372 kg), and the drop height is 40 in (1 m). Thus,

$$PE_{pin} = 5{,}230\ lb \cdot 40\ in = 209{,}200\ in \cdot lb\ (2{,}410\ kg \cdot m)$$

Pin puncture drop tests have demonstrated that the outer skin was not perforated as a result of impact onto the pin. Since the impact energy of the pin puncture drop test is approximately 400 times greater than that of the pin penetration, the pin puncture drop test bounds the pin penetration. Thus, the pin penetration impact is not expected to result in any significant structural damage to the Outerpack.

2.7 HYPOTHETICAL ACCIDENT CONDITIONS

When subjected to the hypothetical accident conditions as specified in 10 CFR 71.73 and SSR-6 paras. 726-729, the Traveller package meets the performance requirements specified 10 CFR 71 and SSR-6. This conclusion is demonstrated in this section, where the most severe accident condition is addressed, and the package is shown to meet the applicable design criteria. The method of demonstration is through both computer analysis and by testing. The loads specified in 10 CFR 71.73 are applied sequentially, per 10 CFR 71.73(a).

2.7.1 Free Drop

10 CFR 71.73(a)(1) and SSR-6 para. 727 require that a 30 ft (9-meter) free drop be considered for the Traveller series of packages. The free drop is to occur onto a flat, essentially unyielding, horizontal surface, and the package is to strike the surface in an orientation for which the maximum damage is expected. The free drop is addressed by test, in which the most severe orientation is used. The free drop precedes both the puncture and fire tests.

The ability of the Traveller package to adequately withstand this specified drop condition is demonstrated via drop testing of the full-scale Traveller XL. In addition, the ability of the fuel rods to withstand the specified drop condition and maintain a leaktight containment boundary, is demonstrated via drop testing of the Traveller XL Type B configuration. The Traveller XL variant bounds the shorter and lighter Traveller STD design. Simulations using finite element analysis are performed to demonstrate the response of the package to free drop tests with the Clamshell axial spacer (Section 2.12.2) and removable top end plate (Section 2.12.3).

Qualification of the Traveller design consisted of four full-scale test campaigns. The testing programs were designed to challenge the fuel rod integrity, thermal protection and geometric form for criticality control. A total of ten 30 ft (9 m) free drops were performed using full-scale prototypes, Qualification Test Units (QTU), a final Certification Test Unit (CTU) and Type B configuration at a variety of orientations to determine the most severe orientation. These campaigns consisted of prototype design qualification testing [11], QTU testing [12], certification testing with CTU [13], and Type B configuration testing [14]. Table 2.7-1 provides a summary of test specimen, test sequence, and inspection results. Each testing campaign evaluated different aspects of the Traveller design with the Outerpack and Clamshell remaining essentially identical throughout the testing programs with minor design improvements made based on the test results. The following sections, Section 2.7.1.1, Section 2.7.1.2 and Section 2.7.1.4, contain the necessary free drop details for the QTU, CTU and Type B full scale drop testing, respectively, including the bases for the specific drop testing performed.

Table 2.7-1 Traveller Drop Testing Summary	
Test Specimen	**Test Sequence**
Qualification Test Unit I	NCT (1) 50.75-in (1.29m) – Drop onto top nozzle end, Package at low angle 10° drop HAC (2) 33.3-ft (10.15m) CG over top corner – Drop onto top nozzle end, Package at 108° angle (3) 42-in (1.07m) Pin Puncture – Drop onto top nozzle end, Package at 83° angle – Dropped on hinge cumulative damage from (2)
Qualification Test Unit II	NCT (1) 50-in (1.27m) – Drop onto top nozzle end, Package at low angle, 10° drop HAC (2) 33.4-ft (10.18m) – Drop onto bottom nozzle end, Package at 90° angle (3) 42 in (1.07m) Pin Puncture – Impact at Clamshell base (CG), Package at 22° angle
Certification Test Unit	NCT (1) 4 ft (1.2m) Drop – Drop onto top nozzle end, Package at low angle, 9° angle HAC (2) 30 ft (9m) Drop – Bottom nozzle drop, 90° angle (3) 40 in (1m) Pin Puncture – Drop onto side of package, onto hinge, package at 21° angle
Type B Configuration Test	(1) 9m Drop (Clamshell onto bottom end impact limiter) – Bottom nozzle drop – 90° angle

2.7.1.1 QTU Test Sequence

Drop testing of the QTU is divided into two test series: Test series 1 for testing of QTU-1, and Test series 2 for testing QTU-2 [12]. For QTU testing, the Traveller XL package design was used along with a 17×17 XL fuel assembly filled with lead pellets to represent the mass of the UO_2 pellets. QTU testing was to demonstrate package compliance to normal and hypothetical drop test conditions and confirm drop orientations for final testing performed with the certification test unit.

2.7.1.1.1 QTU Test Series 1

QTU test series 1 included a NCT 50.75-in (1.29 m) low angle 10° drop, a HAC 33.3-ft (10.15 m) center of gravity-over- top corner free drop test, and a HAC 42-in (1.07 m) pin-puncture over the top left hinge side. The package test weight was 4,793 lb (2,174 kg). Figure 2.7-1 diagrams the QTU-1 test series drop sequence. Post drop testing a 37-minute pool-fire burn test was performed.

Inspection of the package after the test sequence showed that the Outerpack retained its basic circular pre-test shape except for localized plastic deformation at the top nozzle end accumulated from the drop test series. No bolts failed on the Outerpack after completion of the drop test series. The Outerpack did not separate after any impacts, and the pin did not perforate the inner or outer shell. The most notable Outerpack damage, cumulative of all tests, was the resulting joint tear of approximately 1-1/8 in (28.6 mm) at the Outerpack corner located at the top, left hinge side, as shown in Figure 2.7-2. Individually, the 4-ft (1.2 m) NCT free drop resulted in a local crush zone consisting of approximately 10 in (254 mm) wide, 6 in (152 mm) long axially and no significant depth. The Outerpack damage from the 33.3-ft (10.15 m) drop, after the NCT drop, consisted of local crush approximately 25 in (635 mm) wide (the top nozzle end face), and a maximum crush depth of approximately 3-1/2 in (89 mm). The pin puncture damage included additional tearing of the Outerpack joint, and the indention was approximately 1-1/2 in (38 mm) deep. The Clamshell maintained its shape and positioning in the Outerpack, performing its design function to protect the fuel assembly.

The fuel damage assessment was conducted after the completion of the hypothetical fire condition test conducted a few days later. The fuel assembly of QTU-1 was essentially undamaged. At the top nozzle portion, the fuel assembly locally expanded from 8.375 in (213 mm) nominal to 8.625 in (219 mm) maximum over a length of approximately 2-3 in (50-76 mm). The fuel rod gaps were globally unchanged but local expansion was noted between one rod near Grid 10 with a maximum measured gap of 0.250 in (6.35 mm). The resulting measured maximum local pitch was 0.625 in (15.9 mm) from the 0.496 in (12.6 mm) nominal. Three rods were found to be in contact with each other while the remaining rods were nominally positioned. Intermediate Grids 2-7 were buckled locally, but the fuel rod envelope was unchanged. The bottom nozzle portion of the fuel assembly was slightly compressed from 8.375 (213 mm) nominally to 8.250 in (210 mm) measured. Based on the condition of the fuel assembly, the Clamshell was concluded to have performed successfully. The fuel inspection also indicated that no fuel rods had visibly ruptured, and that the axial position of fuel rods-maintained location between bottom and top nozzle.

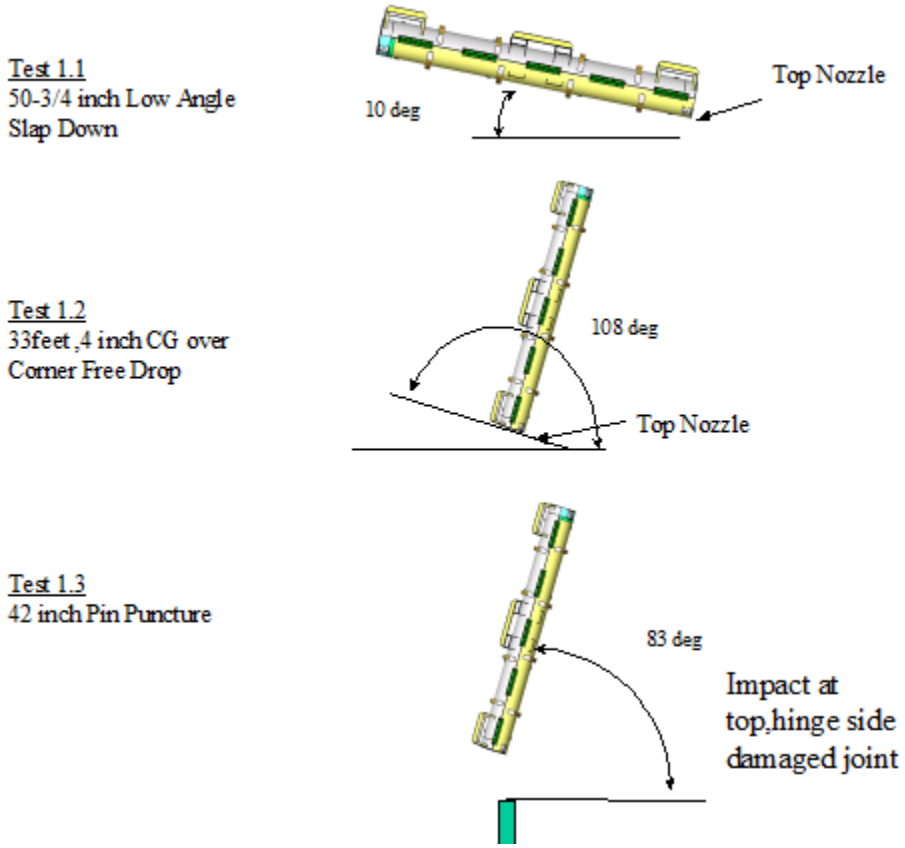

Figure 2.7-1 Traveller QTU-1 Test Series Drop Sequence

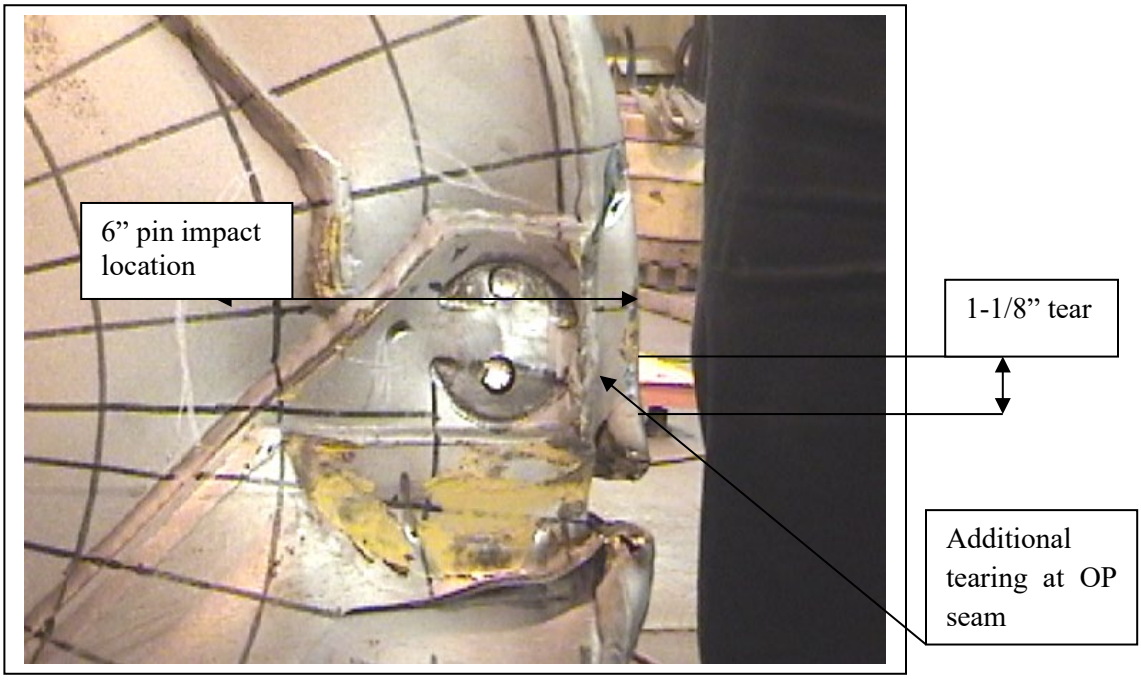

Figure 2.7-2 Traveller QTU-1 Test Series Worst-Case Cumulative Damage

2.7.1.1.2 QTU Test Series 2

QTU test series 2 included a NCT 50-in (1.27 m) low angle 10° top-side drop, a HAC 33.4-ft (10.18 m) bottom end drop test, and a HAC 42-in (1.07 m) pin-puncture over Clamshell base at the CG. The package test weight was 4,778 lb (2,167 kg). Figure 2.7-3 diagrams the QTU-1 test series drop sequence.

Following the test sequence, it was observed that the cumulative external damage to the package was localized to plastic deformation at the top and bottom nozzle end impact zones of the package. The most notable damage zone was a measured 7 in (178 mm) long crumpled area at the bottom nozzle end of the Outerpack, cumulative post-testing. The Outerpack skin was buckled axially but maintained its structural integrity. There were no significant changes in the Outerpack geometry, and no bolt failures were noted. Upon an internal inspection, the pin did not perforate the inner or outer shell. The internal damage was minimal. The Clamshell doors remained closed and the top head and bottom end stayed in position. No change in the Clamshell grid markings were noted, indicating that the Clamshell had not bulged outward (nor compressed). The polyethylene moderator blocks and aluminum neutron "poison plates" maintained position. Individually, the 4-ft (1.2-m) free drop resulted in a local crush zone at the top nozzle end measuring approximately 9-1/2 in (241 mm) wide, 6 in (152 mm) long axially and 7/8 in (22.2 mm) deep. The Outerpack damage from the 33.4-ft (10.18 m) drop, after the NCT drop, consisted of local crumple zone approximately 7 in (178 mm) long maximum as demonstrated by the buckled Outerpack at the bottom nozzle end. A small weld tear was noted on each side of the Outerpack where the leg stand is connected to the end cap. The pin puncture damage was isolated to the impact point located at the package center-of-gravity and was an indented oval of measured dimensions 9 in (229 mm) long by 6 in (152 mm) wide and 2-7/8 in (73.0 mm) deep.

The fuel damage assessment was conducted after the completion of the hypothetical fire condition test conducted a few days later. The fuel assembly of QTU-2 was found to be within the confines of the Clamshell and intact. The impact resulted in a slight ovalizing of the fuel assembly at the bottom nozzle region. Localized expansion from 8.375 in (213 mm) nominal to 8.625 (219 mm) was measured over a length of approximately 12 in (305 mm). The maximum fuel rod gap measured was 0.722 in (18.3 mm) for a single rod resulting in a maximum measured fuel rod pitch of 1.097 in (27.9 mm) from 0.496 in (12.6 mm) nominal. Seven rods were found to be in contact with each other in this section of the fuel assembly, and the remaining rods were nominally positioned. The top nozzle region of the fuel assembly was essentially undamaged. The axial position of fuel rods stayed in position between bottom and top nozzles.

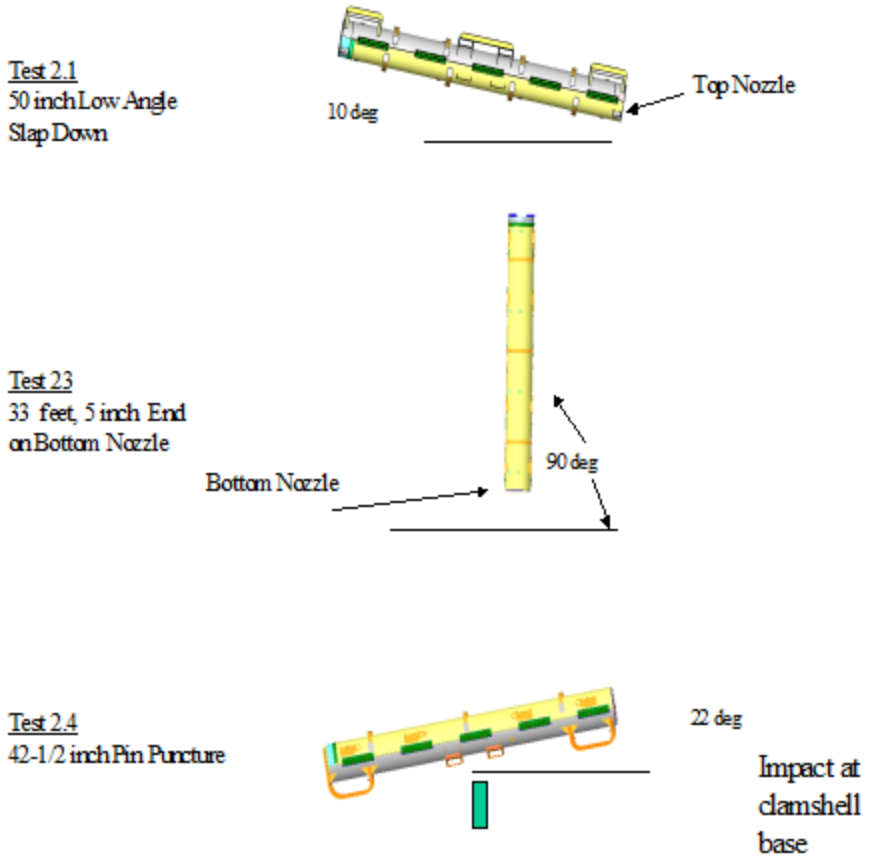

Figure 2.7-3 Traveller QTU-2 Test Series Drop Sequence

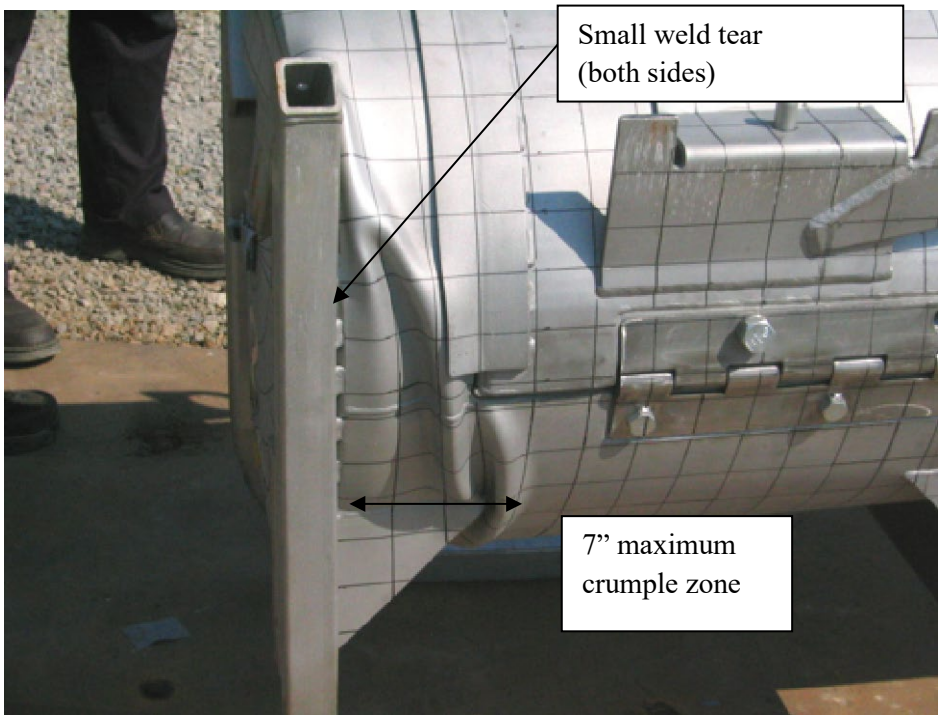

Figure 2.7-4 Traveller QTU-2 Test Series Bottom End Damage

2.7.1.1.3 Summary of QTU Results

Two QTU test series were performed to evaluate the performance of the Traveller XL package. The test series included:

- QTU1 test sequence – NCT 1 m Slap down, HAC 9 m CG over corner, HAC pin puncture
- QTU2 test sequence – Slap down, bottom end drop, pin puncture

Review of the damage to the QTU packages and fuel assemblies showed that damage was minimal and localized. QTU-1 test series concluded localized damage to the top end of the package due to all testing at the top end, an essentially undamaged Clamshell, and essentially undamaged to the fuel assembly with very minor bowing and compaction of the rods. QTU-2 test series concluded damage to the bottom end of the package, an essentially undamaged Clamshell, while the fuel assembly had slight ovalizing with the largest fuel rod bowing near the bottom Grid 1 of the two test series. The QTU tests concluded that QTU-1 test series on the package top end imparted the most damage to the Outerpack, and QTU-2 test series on the bottom end imparted the most damage to the fuel assembly. Since the QTU-1 testing imparted the most damage to the fuel assembly challenging the containment boundary of the fuel rod, the HAC drop testing for the certificate test unit (CTU) was performed for a bottom end drop. Based on the successful testing of the modified QTU test article, minor design changes were incorporated in the manufacturing of the Traveller XL CTU package for final regulatory testing. In summary, testing demonstrated the Traveller package is suitable for compliance to normal and hypothetical mechanical drop test conditions described in 10 CFR 71 and SSR-6.

2.7.1.2 CTU Test Sequence

A Traveller XL package was fabricated to serve as the certification test unit (CTU), shown in Figure 2.7-5 and Figure 2.7-6 and Table 2.7-2. The test included a 50-in (1.27 m) slap down, a 32.8-ft (10.0 m) free drop test impacting the bottom nozzle, and a 42-in (1.07 m) pin-puncture test, shown in Figure 2.7-7 and Table 2.7-3. The test assembly was a lead-filled replica 17×17 XL fuel assembly with fuel rods having an internal helium pressure of 460 psig. The CTU package was thermally saturated for approximately 15 hours prior to testing at a temperature of about 17ºF (-8.3ºC). At the time of testing, the temperature was approximately 24ºF (-4.4ºC). The package's test weight was 4,863 lb (2,206 kg).

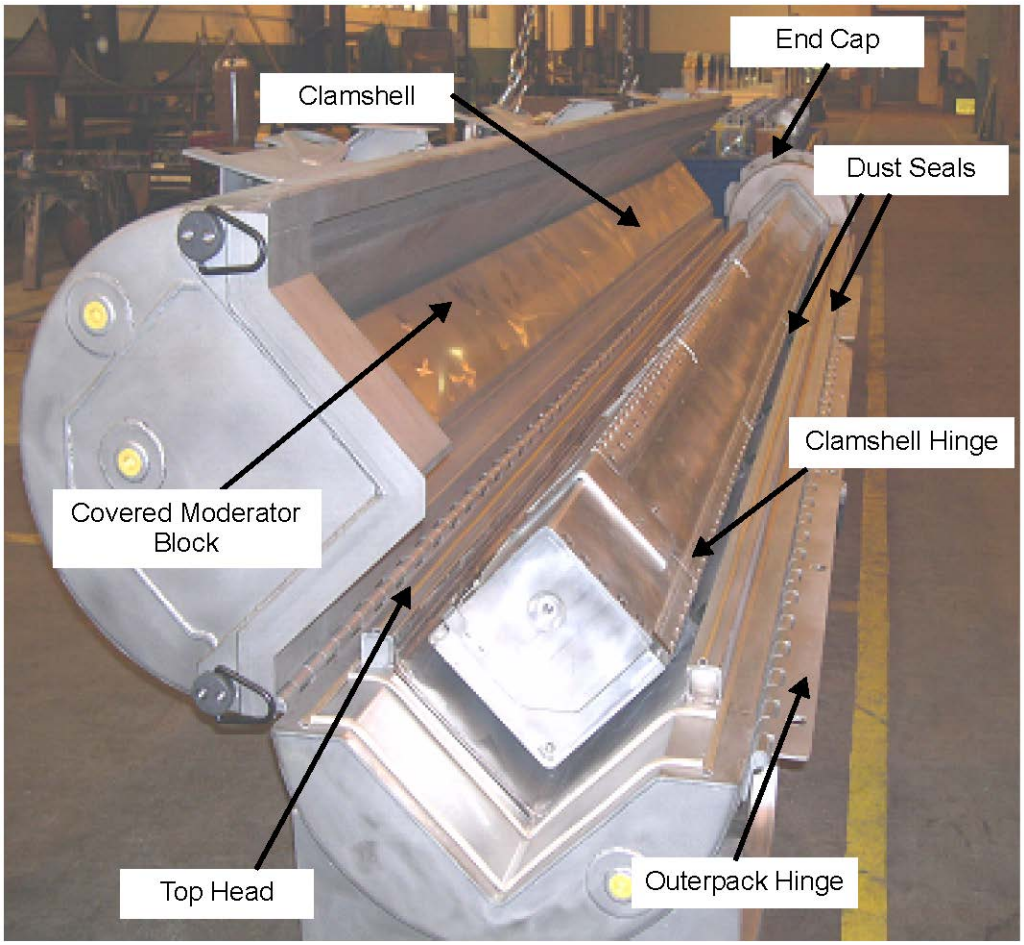

Figure 2.7-5 Traveller CTU Test Article Internal View

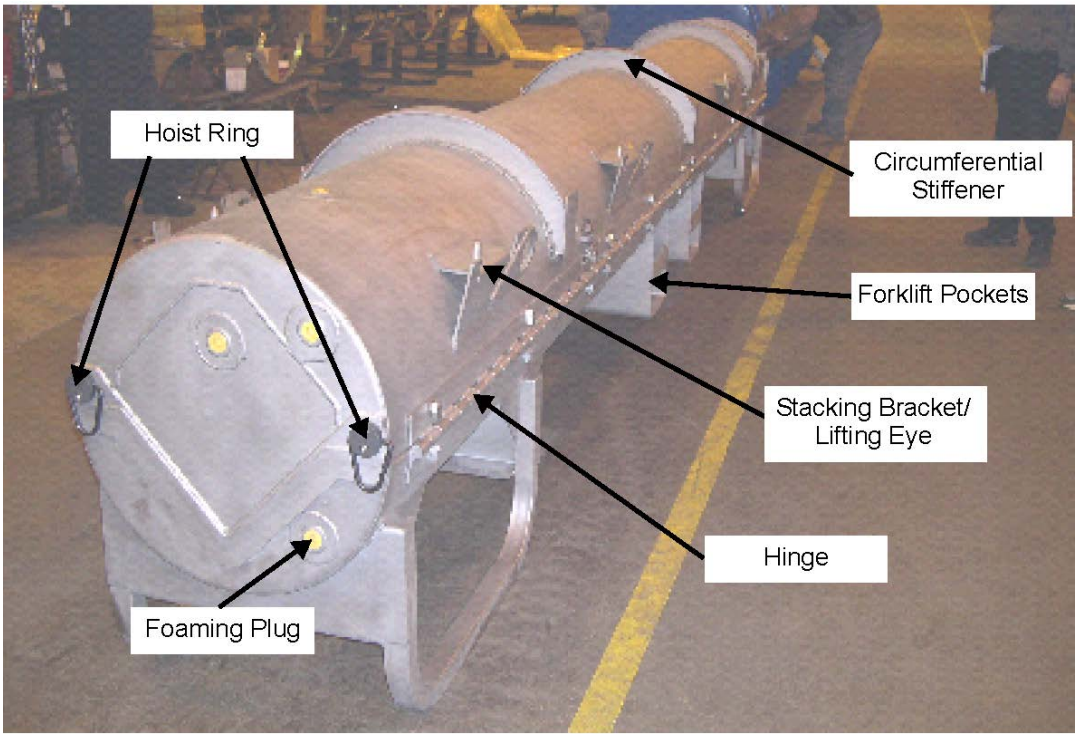

Figure 2.7-6 Traveller CTU External View

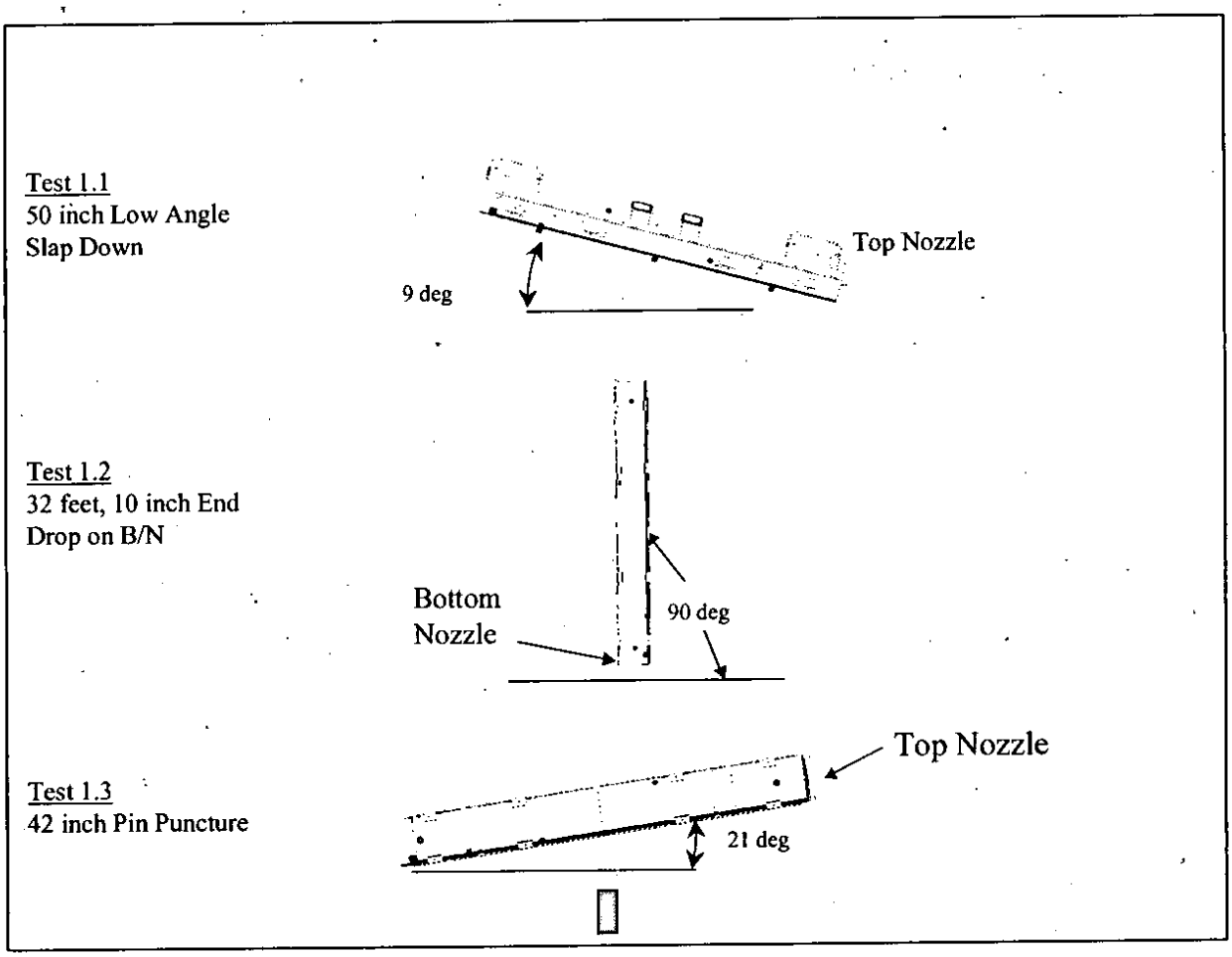

Figure 2.7-7 CTU Drop Test Orientations

Table 2.7-2 Test Weights

	Nominal* Weight	Actual Weight
Weight of Outerpack (Empty):	2633 lb (1194 kg)	2671 lb (1212 kg)
Weight of Clamshell (Empty):	425 lb (193 kg)	440 lb (200 kg)
Weight of packaging (Empty):	3058 lb (1387 kg)	3111 lb (1411 kg)
Total package test weight:	4810 lb (2182 kg)	4863 lb (2206 kg)

Note:
* Nominal total weight includes only Fuel Assembly since drop test was conducted without RCCA. Maximum expected design weight is estimated to be 5071 lb (2300 kg). The top Outerpack section weight is 1063 lb (482 kg) empty and the bottom Outerpack section weight is 1608 lb (729 kg) empty.

Table 2.7-3 CTU Drop Test Orientations

Test Article	F/A Type	Test Sequence	Test Pitch Attitude	Test Roll Attitude	Test Height	Design Feature Tested
CTU	17×17 XL	P1.1) 1.2-m, NCT, Low angle	9°	180°	50 in (1.27m)	Operations of hinges/doors Lattice exp., FR axial position Hinge structural integrity
		P1.2) 9-m Bottom End Drop	90°	0°	32 ft 10 in (10m)	
		P1.3) 1-m Pin-puncture	21°	90°	42 in (1.07m)	

Exterior Inspections After Drop Tests – The exterior of the package was examined after each drop. The inspections found that the Outerpack retained its circular pre-test shape except for localized plastic deformation at the ends. No hinge bolts failed on the Outerpack, the Outerpack did not separate, and neither the inner nor outer shell were perforated in the pin drop test.

Test 1 – The 4-ft (1.2-meter) drop test resulted in a localized dent at the top nozzle end, and near the bottom nozzle end, the stiffener was dented over a length of about 8 in (203 mm). Figure 2.7-8 and Figure 2.7-9 show the damage observed. The normal condition drop produced only local damage to the impact area. The depth of the crush was minimal.

Test 2 – The 32.8-ft (9-m) free drop resulted in localized damage to the bottom nozzle end region. The two bottom nozzle stiffener keeper pins were detached as a result of the impact. The impact created a circumferential ripple located at 9 in (229 mm) (bottom Outerpack) and 12 in (305 mm) (top Outerpack) from the package bottom end. The ripple resulted in a ½ in (12.7 mm) crumple impact, which effectively shortened that section of the package slightly. Two stitch welds located inside the bottom nozzle end stiffener were broken, but this did not compromise the stiffener position. The bottom nozzle end cap stiffener separated to form a 1-3/16 in (30.2 mm) gap, and the gap between the hinge and the cover lip was measured to be approximately 7/16 in (11.1 mm). The hinge at the bottom nozzle end was separated about 1/16 in (1.59 mm) from the Outerpack skin surface after the drop test. Figure 2.7-10 and Figure 2.7-11 shows the damage observed.

Test 3 – The pin puncture test was located on the hinge of the Outerpack at approximately the axial center of gravity. The impact zone locally dented 6 in (152 mm) of hinge length to a maximum measured depth of approximately 1-3/8 in (34.9 mm), Figure 2.7-12. The hinge knuckles were not compromised because of the test. Hinge separation of ½ in (12.7 mm) was noted about 7-1/2 in (191 mm) from the impact point towards the top nozzle end.

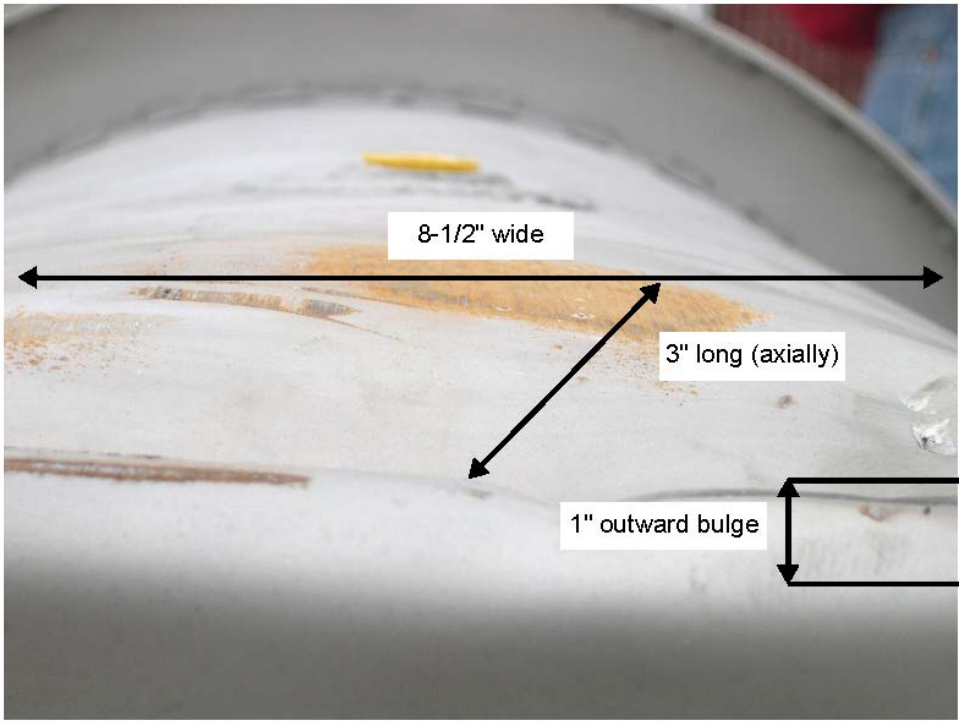

Figure 2.7-8 Top Nozzle End Outerpack Impact Damage

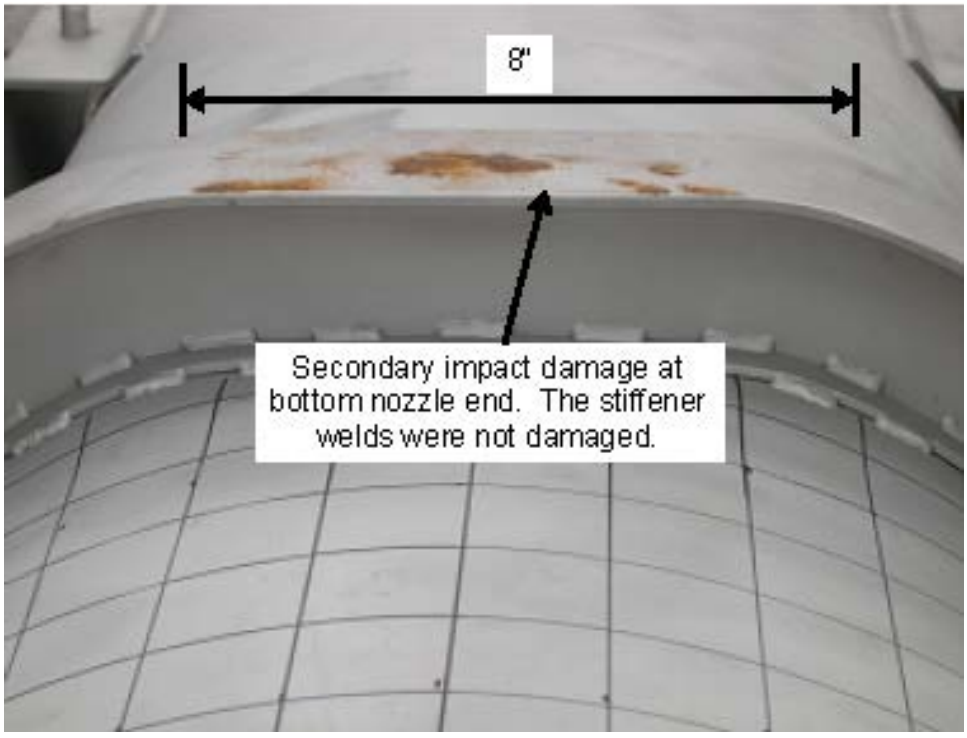

Figure 2.7-9 CTU Outerpack Stiffener After Test 1

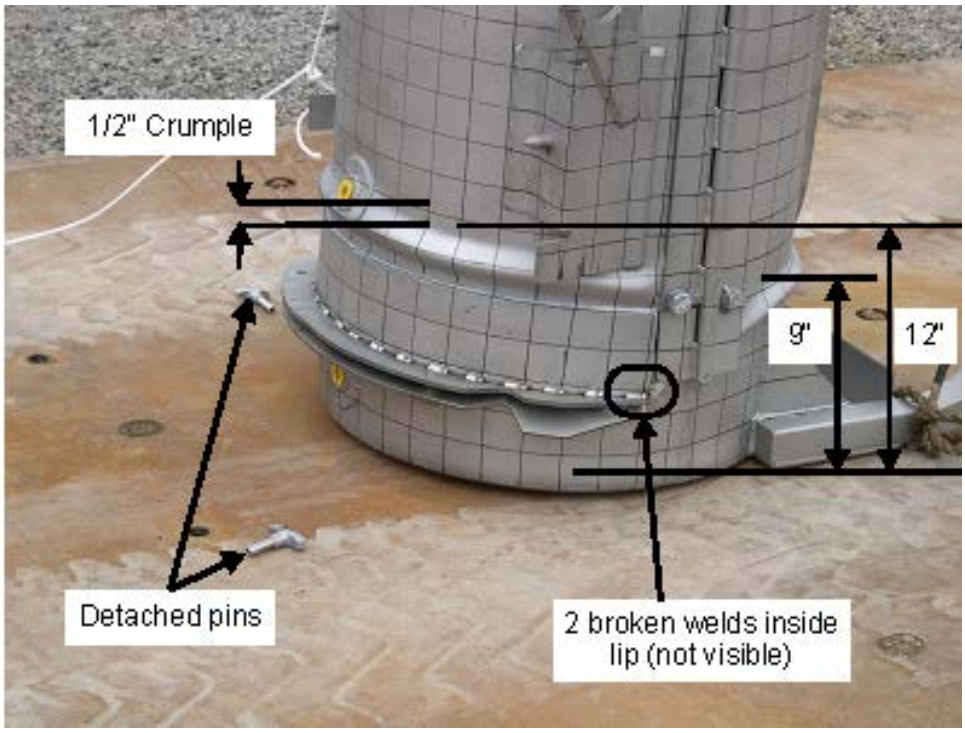

Figure 2.7-10 CTU Outerpack After Test 2

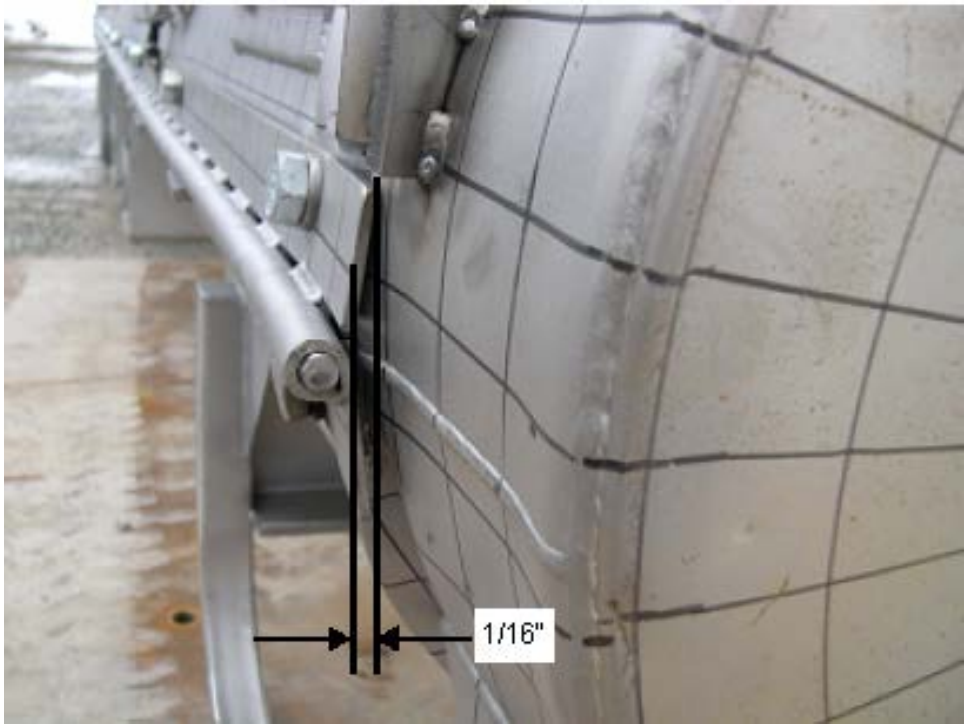

Figure 2.7-11 Hinge Separation at Bottom Nozzle End from Test 2

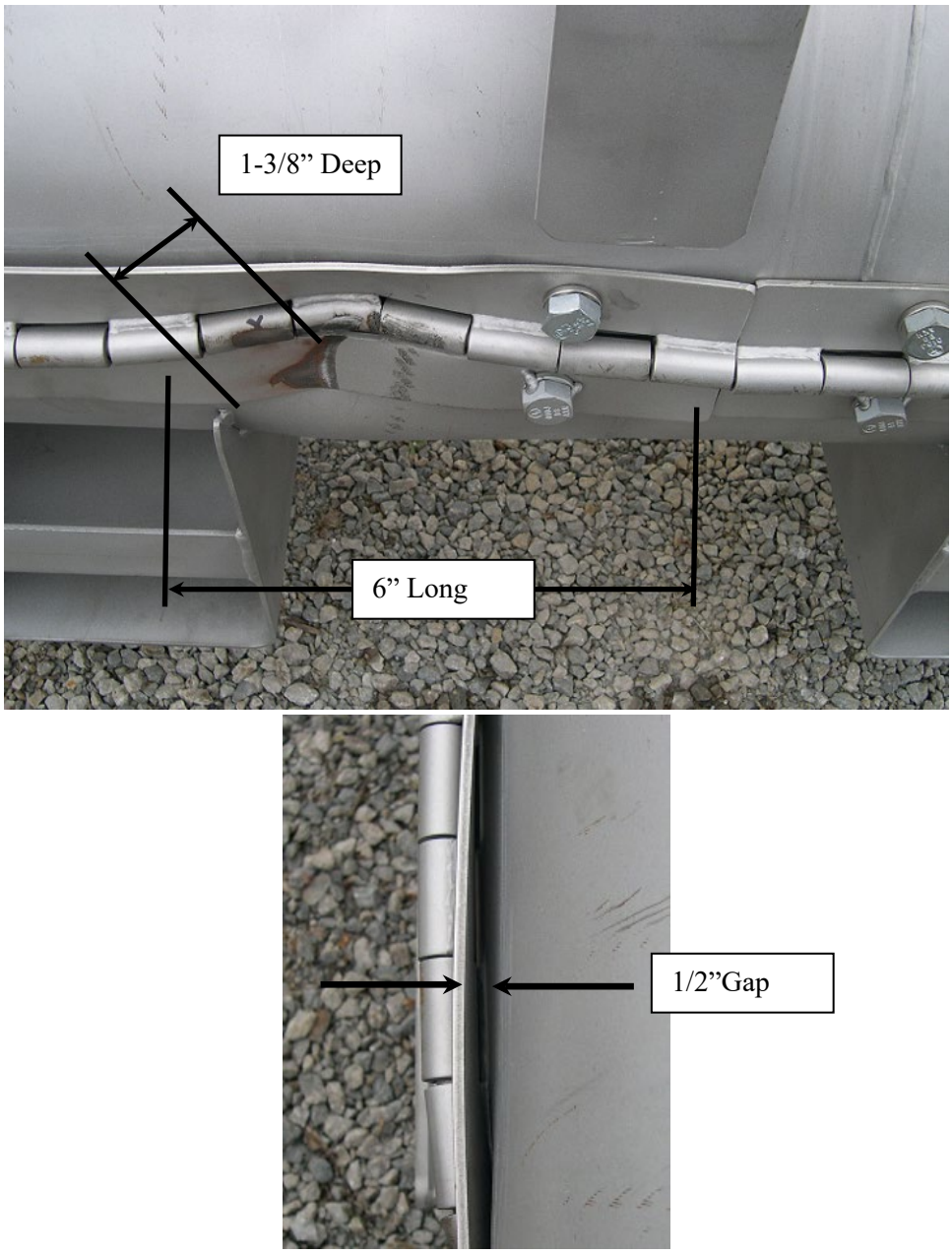

Figure 2.7-12 CTU Outerpack After Test 3

Interior Inspection Results – The CTU was sent to the South Carolina Fire Academy for the burn test immediately after the drop tests were completed. The package was not opened until the following week, approximately five hours after the fire test was completed. In general, the drop test and fire test resulted in minor damage to the Traveller internal structural components. The Clamshell was found intact and closed, Figure 2.7-13, and the simulated poison plates stayed in position. All shock mounts were found to be visibly intact. At the bottom Clamshell plate, a 2-1/2 in (63.5 mm) and a 2-3/4 in (69.9 mm) piece of end lip sheared off. The measured gap was less than 1/16 in (1.59 mm) in the axial direction. The axial location of the fuel rods stayed in position between the bottom and top nozzle. Finally, the moderator blocks were found to be

intact and essentially undamaged after the completion of the drop and fire test. The moderator stud bolts on the top Outerpack were found sheared off, but the moderator cover maintained the moderator position. The stainless steel moderator cover was removed, and the polyethylene moderator was examined. As shown in Figure 2.7-14, the moderator was intact and essentially undamaged.

Figure 2.7-13 CTU Clamshell After Drop and Fire Tests

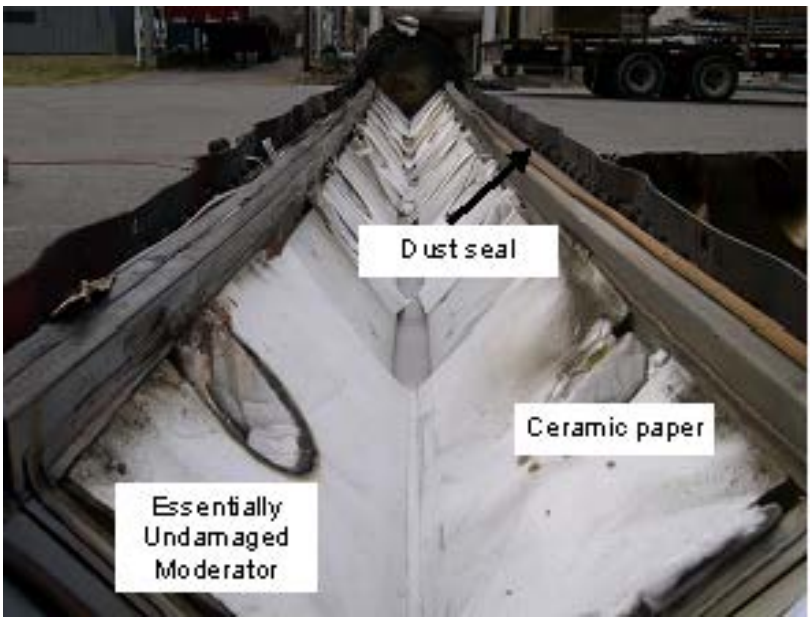

Figure 2.7-14 Outerpack Lid Moderator After Testing

Figure 2.7-15 provides the damage sketch overlaying the pre-tested fuel assembly for comparative purposes. The largest fuel envelope expansion and fuel rod-to-rod gap expansion experienced was between the bottom nozzle and Grid 1. For the 20 in (508 mm) span from the bottom nozzle to Grid 2 of the fuel assembly, the fuel rod envelope expanded from 8-3/8 in (213 mm) average nominal to 9-3/16 in (233 mm). The grid envelope expanded from 8-7/16 in (214 mm) nominal to 8-5/8 in (219 mm) over the same 20 in (508 mm) axial distance. The maximum measured fuel rod pitch in this region increased from 0.496 in (12.6 mm) nominal to 0.990 in (25.1 mm). This was caused by a single bent rod which was bent outward approximately ½ in (12.7 mm). Otherwise, the typical pitch pattern consisted of 2 rod rows touching and the remaining 14 rows at nominal pitch, Figure 2.7-16.

For a length of 10 in (25.4 mm) above Grid 2, the fuel rod envelope compressed from 8-3/8 in (213 mm) nominal to 8-1/4 in (210 mm). This slight compression is due to the single top rod slightly compressed inward. Above this 10 in (254 mm) region, the single rod bent outward about ½ in (12.7 mm) for a length of approximately 25 in (635 mm).

For the 25 in (635 mm) length from between Grids 2 and 3 and up to Grid 4, the single rod resulted in a measured envelope of 8-7/8 in (225 mm), but the remaining envelope of 16 rows was slightly compressed [about 1/16 in (1.59 mm)]. The maximum pitch caused by the single rod was 0.740 in (18.8 mm) compared to 0.496 in (12.6 mm) nominal. Otherwise, the average pitch was nominal.

For the remainder of the fuel assembly from Grid 4 to the top nozzle, the fuel rod envelope compressed about 0.15 in (3.81 mm) and the grid envelope compressed about ¼ in (6.35 mm). The average pitch decreased from 0.496 in (12.6 mm) to 0.459 in (11.7 mm) in this region.

Grid 1 was severely buckled, and the ovality was measured to be 120º for a length of about 20 in (508 mm), Figure 2.7-17. Grids 2 and 3 were broken at the top corner, but otherwise intact. Grids 4-10 were relatively undamaged. The fuel inspection also indicated that 7.5% (20 of 265 rods) were cracked at the end plug locations (Figure 2.7-18). The average crack width measured was approximately 0.030 in (0.762 mm) and the average length was 50% of the rod diameter. The cracked rods were located at the four corners, indicating the vertical impact created symmetrical impact forces to be transmitted through the bottom nozzle and fuel rods (Figure 2.7-19).

The fuel assembly in the CTU was measured before the test and after the burn test at locations shown in Figure 2.7-20 below. Table 2.7-4 provides the pretest dimensions. Table 2.7-5 through Table 2.7-8 provide the post-test dimensions.

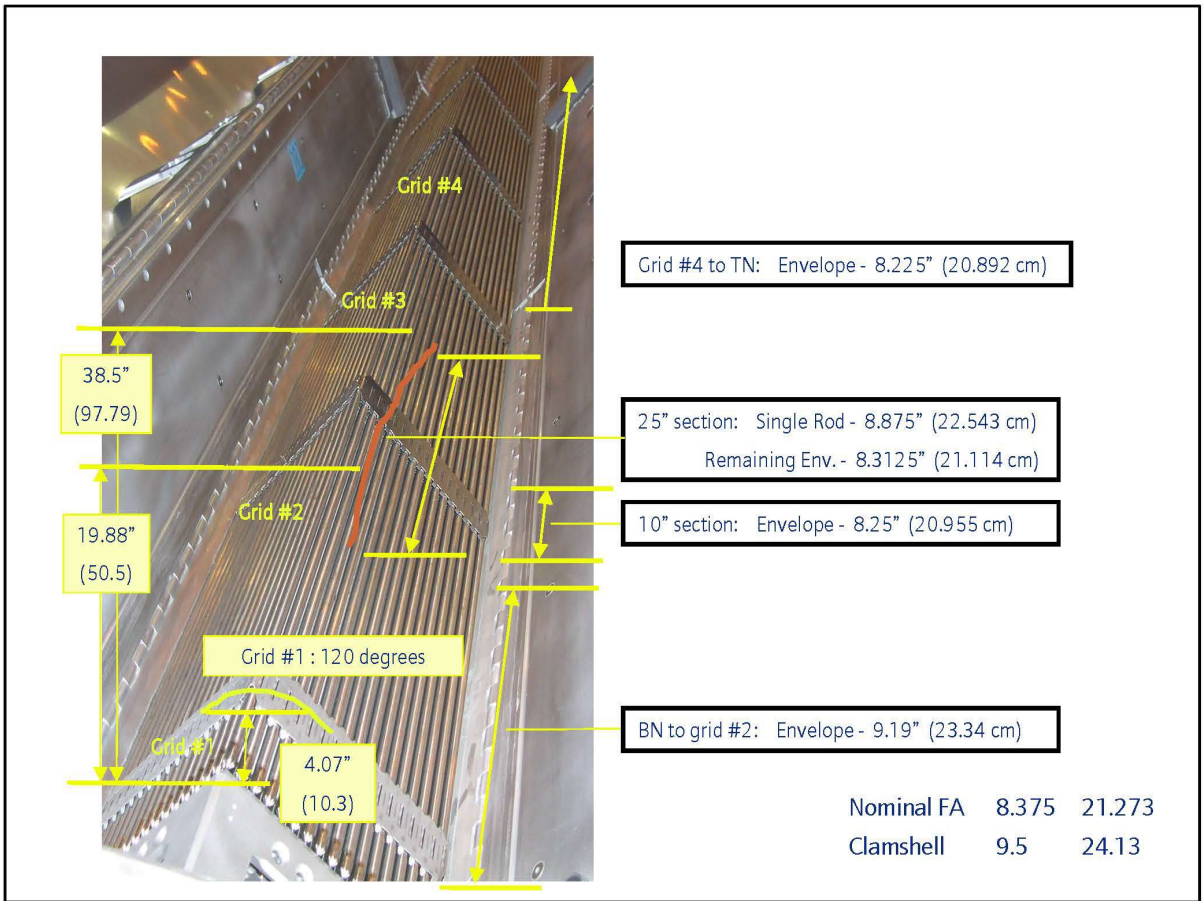

Figure 2.7-15 Fuel Assembly Damage Sketch and Pre-test Assembly

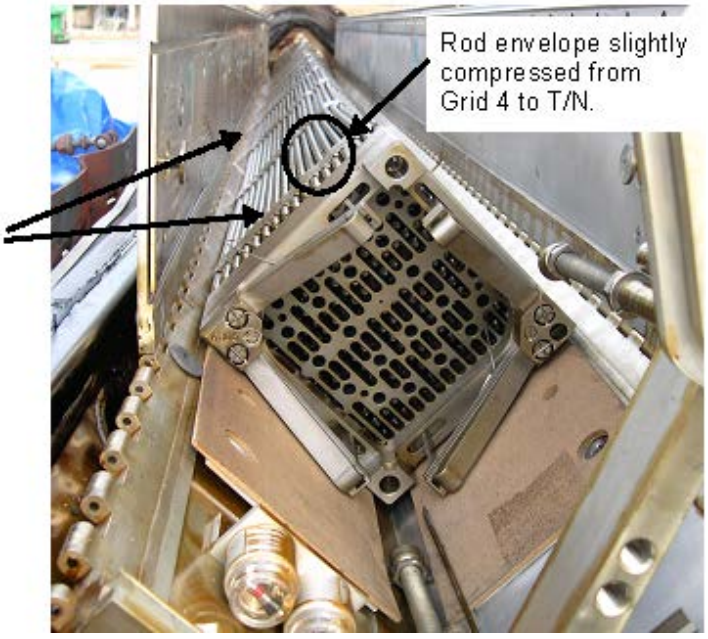

Figure 2.7-16 CTU Fuel Assembly After Testing (top end)

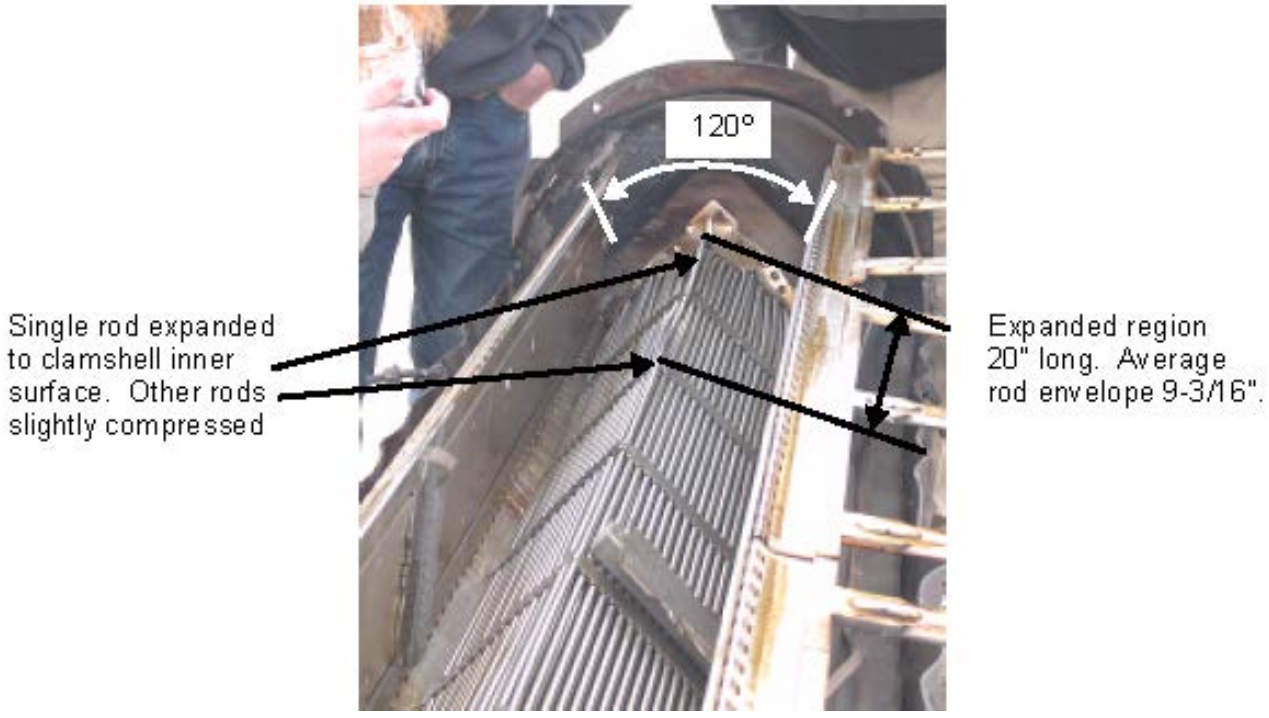

Figure 2.7-17 CTU Fuel Assembly Top End After Testing

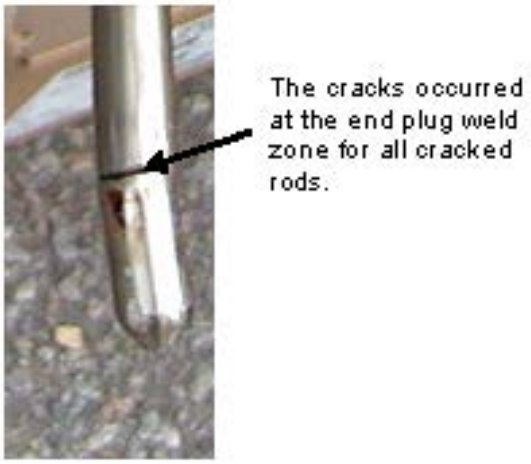

Figure 2.7-18 Cracked Rod from CTU Fuel Assembly

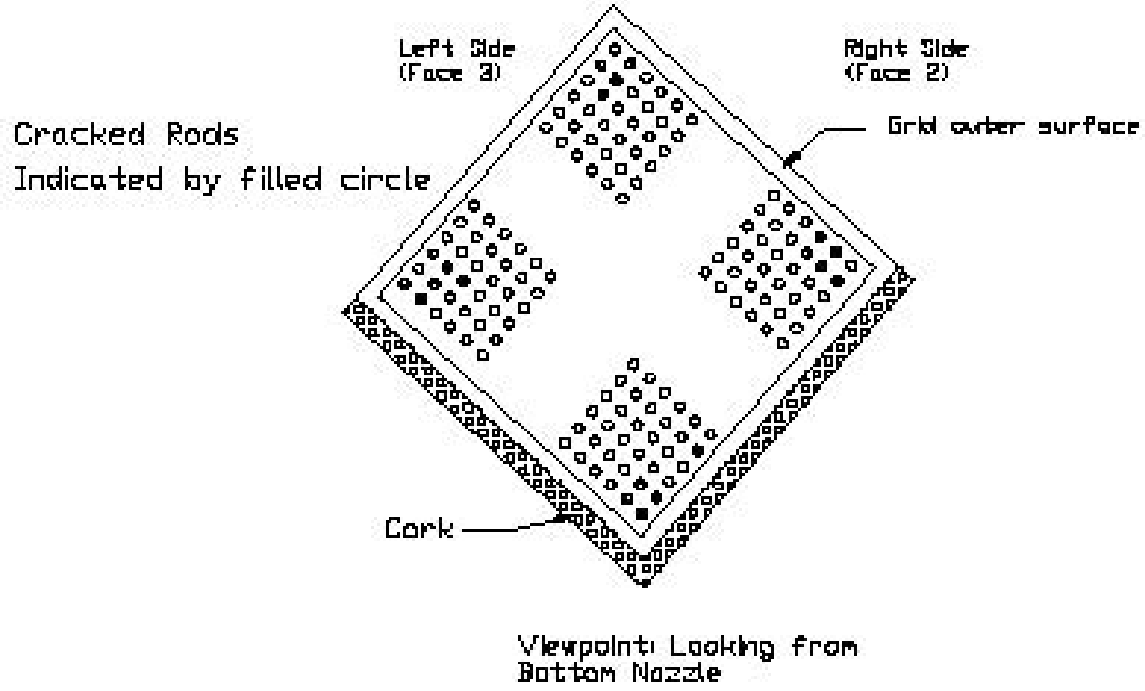

Figure 2.7-19 Cracked Rod Locations on CTU Fuel Assembly

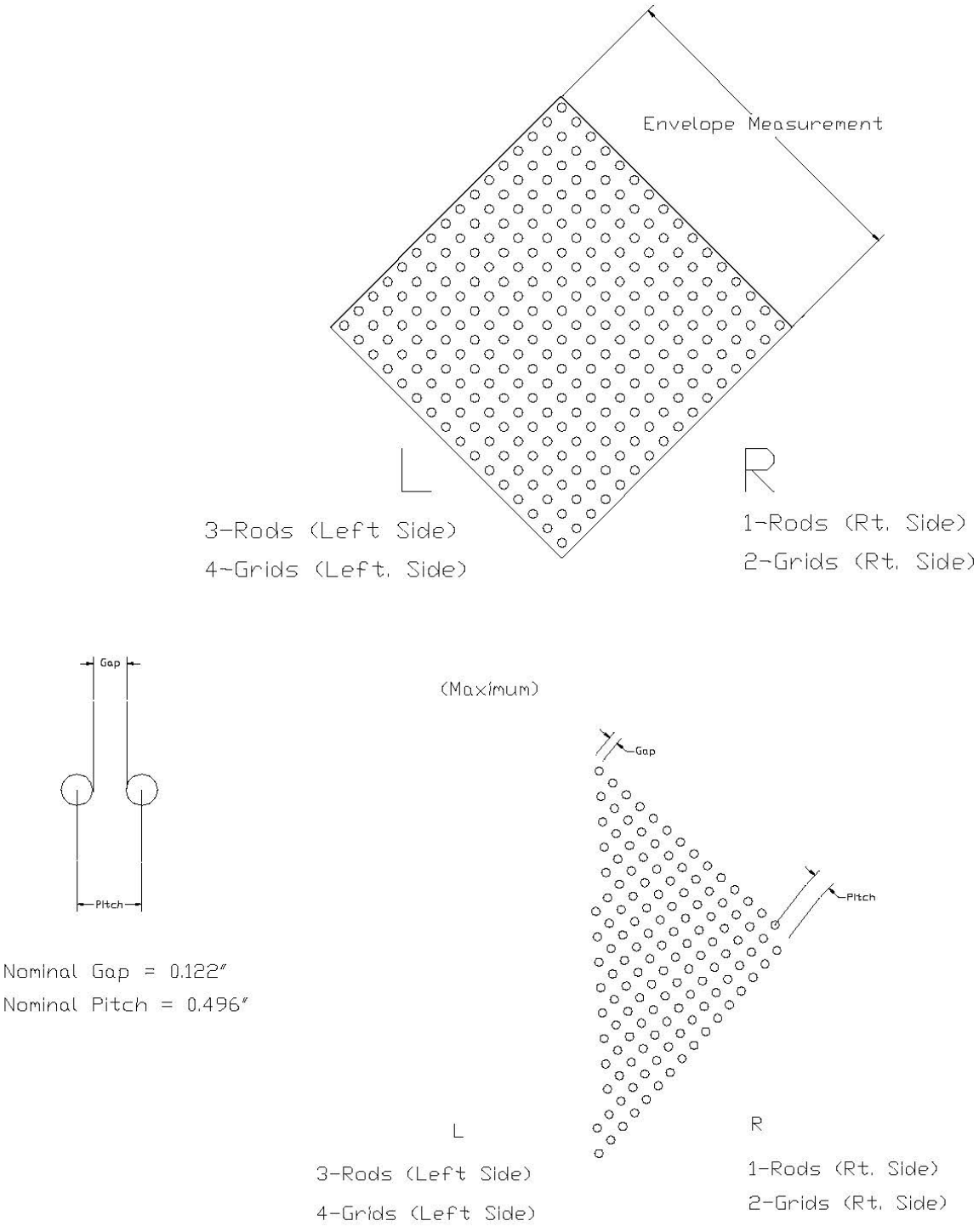

Figure 2.7-20 Measurements Made on CTU Fuel Assembly Before and After Drop Tests

Table 2.7-4 CTU Fuel Assembly Key Dimensions Before Drop Test

Fuel Assembly ID: T/N # LM1F2N

F/A Location	Fuel Envelope (in)	Gap (in)	Pitch (in)
B/N – Grid 1	1: 8-3/8 2: 8-7/16 3: 8-3/8 4: 8-7/16	L – 0.123 R – 0.121	L – 0.498 R – 0.495
Grid 1- Grid 2	1: 8-3/8 2: 8-7/16 3: 8-3/8 4: 8-7/16	L – 0.123 R – 0.124	L – 0.497 R – 0.499
Grid 2- Grid 3	1: 8-3/8 2: 8-7/16 3: 8-3/8 4: 8-7/16	L – 0.121 R – 0.121	L – 0.495 R – 0.495
Grid 3- Grid 4	1: 8-3/8 2: 8-7/16 3: 8-3/8 4: 8-7/16	L – 0.123 R – 0.123	L – 0.497 R – 0.498
Grid 4- Grid 5	Rods: 8-3/8 Grids: 8-7/16	0.121	0.495
Grid 5- Grid 6	Rods: 8-3/8 Grids: 8-7/16	0.123	0.498
Grid 6- Grid 7	Rods: 8-3/8 Grids: 8-7/16	0.122	0.497
Grid 7- Grid 8	Rods: 8-3/8 Grids: 8-7/16	0.123	0.497
Grid 8- Grid 9	Rods: 8-3/8 Grids: 8-7/16	0.123	0.498
Grid 9- Grid 10	Rods: 8-3/8 Grids: 8-7/16	0.121	0.495
Grid 10 – T/N	Rods: 8-3/8 Grids: 8-7/16	0.122	0.497
AVERAGE	Rods: 8-3/8 Grids: 8-7/16	0.122	0.497

Note:
* Measured fractional values were measured to nearest 1/16 in. Measured decimal values were measured to the nearest 0.001 in.

Table 2.7-5 CTU Fuel Assembly Grid Envelope Dimensions After Testing

Location	Measured Grid Envelope Dimension (in)	
	Left Side, LS	Right Side, RS
Grid 1	9-0	8-3/4
Grid 2	8-7/16	8-3/8
Grid 3	9-1/2	9-1/2
Grid 4	8-1/8	8-1/4
Grid 5	8-1/8	8-1/4
Grid 6	8-1/4	8-1/4
Grid 7	8-1/8	8-3/16
Grid 8	8-5/16	8-3/16
Grid 9	8-5/16	7-7/8
Grid 10	8-3/8	8-1/2
MAXIMUM VALUE	9-1/2	9-1/2

Table 2.7-6 CTU Fuel Assembly Rod Envelope Data After Testing

Location	Measured Envelope Dimension (in)		Calculated Maximum Fuel Rod Pitch from Form 1G (in) (Nominal Pitch = 0.496 in)
	Left Side, LS	Right Side, RS	
Between B/N and Grid 1	9-0	8-3/4	0.566
Between Grids 1 and 2	8-5/16 [(1)]	8-5/16 [(1)]	0.990
Between Grids 2 and 3	8-1/2	8-0	0.740
Between Grids 3 and 4	8-7/16	8-1/2	0.715
Between Grids 4 and 5	8-3/16	8-3/16	0.472
Between Grids 5 and 6	8-3/16	8-3/8	0.578
Between Grids 6 and 7	8-1/16	8-1/16	0.550
Between Grids 7 and 8	8-3/8	8-3/16	0.541
Between Grids 8 and 9	8-0	7-13/16	0.483
Between Grids 9 and 10	8-3/8	8-1/2	0.498
Between Grid 10 and T/N	8-3/8	8-0	0.497
MAXIMUM VALUE	9-0	8-3/4	0.990

Note: [(1)] A single rod was measured to the inner Clamshell surface (9-1/2 in). See Figure 2.7-17.

Table 2.7-7 CTU Fuel Assembly Rod Envelope After Testing

Location	Measured Envelope Dimension (in)		Calculated Maximum Fuel Rod Pitch from Form 1G (in) (Nominal Pitch = 0.496 in)
	Left Side, LS	Right Side, RS	
Between B/N and Grid 1	9-0	8-3/4	0.566
Between Grids 1 and 2	8-5/16 (1)	8-5/16 (1)	0.990
Between Grids 2 and 3	8-1/2	8-0	0.740
Between Grids 3 and 4	8-7/16	8-1/2	0.715
Between Grids 4 and 5	8-3/16	8-3/16	0.472
Between Grids 5 and 6	8-3/16	8-3/8	0.578
Between Grids 6 and 7	8-1/16	8-1/16	0.550
Between Grids 7 and 8	8-3/8	8-3/16	0.541
Between Grids 8 and 9	8-0	7-13/16	0.483
Between Grids 9 and 10	8-3/8	8-1/2	0.498
Between Grid 10 and T/N	8-3/8	8-0	0.497
MAXIMUM VALUE	9-0	8-3/4	0.990

Note: (1) A single rod was measured to the inner Clamshell surface (9-1/2 in). See Figure 2.7-17.

Table 2.7-8 CTU Fuel Rod Gap and Pitch Inspection After Testing

Location	Measured Maximum Gap (in)		Calculated Maximum Pitch (in)
	Left Side, LS	Right Side, RS	
Between B/N Grid 1	0.093 (between rows 9 & 10)	0.193 (between rows 6 & 7)	0.566
Between Grids 1 and 2	0.616 (out-lying rod only)	0.563 (out-lying rod only)	0.990
Between Grids 2 and 3	0.207 (one rod) Others touching	0.366 (one rod) Others touching	0.740
Between Grids 3 and 4	0.336	0.340	0.715
Between Grids 4 and 5	0.099	0.050	0.472
Between Grids 5 and 6	0.204	0.084	0.578
Between Grids 6 and 7	0.173 (between rows 2 & 3) Others Nominal	0.176 (between rows 6 & 7) Others Nominal	0.550
Between Grids 7 and 8	0.166	0.064	0.541
Between Grids 8 and 9	0.109	0.060	0.483
Between Grids 9 and 10	0.124	0.090	0.498
Between Grid 10 and T/N	0.123	0.074	0.497
MAXIMUM VALUE	0.616	0.563	0.990

Note: The pitch is calculated by adding the measured gap to the fuel rod diameter.

2.7.1.2.1 Summary of CTU Results

The drop test series included a regulatory normal free drop of 4 ft (1.2 m), a 30-ft (9-m) end drop onto the bottom nozzle, and a 3.3-ft (1-m) pin-puncture test on the hinge. The Traveller XL CTU demonstrated robust structural performance during the drop test. No Outerpack bolts failed and the Outerpack retained its circular pre-test shape. The Outerpack did not separate, and the pin puncture did not perforate the inner or outer shells, nor did it affect the Clamshell in any detrimental way. Minor weld failures on the Outerpack, in the region near the impact, were observed in post-test examinations. These failures had negligible effect on the performance of the CTU. The two quick release pins on the cover lips detached during the drop test, therefore, they could not be used in the burn test as intended. As such, they were not re-installed for the burn testing.

The impact limiter pillows performed as intended, however, they did not sufficiently crush as desired due to the inherent axial flexibility of the 17×17 XL fuel assembly. The moderator sheeting remained completely contained within the sheet metal covering. A small brown spot was observed on the back side of one moderator sheet attached to the Outerpack top half. A very small amount of flow occurred away from the hot spot. This melt spot was small, affecting only a few cubic centimeters of material.

The Clamshell was found intact and closed, and the simulated poison plates maintained their attached position with very little distortion. Minor damage was observed at the location of the impact with the pillow, however, the damage had negligible effect on the performance of the Clamshell. All closure nuts remained intact with no signs of distortion or stress.

The most significant observation from the post-test examinations was 20 cracked fuel rod bottom end plug welds. These cracks occurred in the regions corresponding to the corners of the bottom nozzle. At these corners, the buckled bottom nozzle has steep faces (in excess of 45 degrees), which was exacerbated by the characteristically long legs of the 17×17 XL assembly. The angled faces apply a side force to the local fuel rods as they are decelerated in the impact. The largest crack occurred in a fuel rod located in the outermost row within the assembly. The crack in the rod had a maximum width of approximately 0.075 in (1.91 mm). This width is not sufficiently large enough for loss of fuel from the rod. Further, in all cases of cracked rods, the bottom end plugs did not separate. Therefore, fuel pellets are prevented from exiting any of the cracked rods.

Successful HAC free drop testing of the Traveller XL CTU certification unit indicates that the various structural features are adequately designed to withstand the 30 ft (9 m) free drop event per 10 CFR 71 and SSR-6. The most important result of the testing program was the demonstrated ability of the Traveller XL package, which bounds the Traveller STD, to maintain its criticality safety integrity.

Significant results of the CTU free drop tests are summarized as follows:

1. There was no breach or distortion of the Clamshell aluminum container.
2. There was no evidence of melting or material degradation on the polyethylene sheeting.
3. The Outerpack remained closed and structurally intact.
4. A small number of rods (20) were cracked during drop testing (only seen in bottom-end drops).
5. Rod damage was at the end of the rods only. No damage anywhere else.
6. None of the end plugs separated from the rods.
7. No pellet material was lost from the cracked rods.

2.7.1.3 Summary of QTU and CTU Drop Testing

Test orientations that were the most challenging are a 30-ft (9-m) vertical drop with the bottom end of the package hitting first (CTU test) and a 30-ft (9-m) CG-forward-of-corner drop onto the top end of package with an 18° forward rotation (QTU test). The former has the greatest potential to damage the fuel assembly and the latter is most damaging to the packaging itself. Based on the robust performance of the Traveller XL drop units during testing, orientations that were most severe to the fuel assembly became more significant. From the drop testing and the predictions of the analytic analyses, it was determined that the most severe 30 ft (9 m) free drop orientation was a bottom-end down drop due to: 1) the relatively high deceleration, 2) the greatest opportunity for lattice expansion of the fuel, and 3) the greatest opportunity for fire damage as a result of the subsequent pool-fire thermal testing.

The top-down end drop produces significantly lower deceleration due to buckling of the axial clamp mechanism bolts. Additional free drop oblique angles were tested for QTU and CTU units, including low angle orientations, which resulted in the least amount of packaging damage. The bottom-down end drop caused the greatest damage to the axial impact limiters or "pillows" and the fuel assembly contents. CTU testing confirmed that the test fuel assembly experienced large lattice expansion and cracked fuel rods in the bottom nozzle region of the fuel assembly, however, maintained the Type A, fissile package configuration critical safe geometry. The resolution of the cracked fuel rods for the Type B configuration is discussed in Section 2.7.1.4.

2.7.1.4 Type B Full Scale Drop Testing

In order to license the Traveller as a Type B fissile package, design changes and subsequent 30-ft (9-m) HAC testing were required to demonstrate that all fuel rods meet the leaktight criterion defined in Section 4.2. A 30-ft (9-m) drop test of a lead-filled replica 17×17 XL fuel assembly with an XL RTP Clamshell and XL impact limiter was performed to demonstrate the fuel assembly and fuel rod response in the Traveller (Type B) Clamshell when subject to the 30-ft (9-m) HAC testing. This testing did not include the full Outerpack, only the end impact limiter required to absorb the energy of the falling Clamshell and fuel assembly. The Type B configuration Clamshell is the same as the Clamshell used in the CTU testing, described in Section 2.7.1.2, with the addition of a top axial restraint and a bottom support spacer for both functional and drop testing evaluation. For this test, only the Outerpack bottom end impact limiter under the bottom nozzle of the fuel assembly was used. However, the Type B configuration Outerpack to be manufactured is structurally identical to the Outerpack used in the CTU testing described in Section 2.7.1.2.

As described in Section 2.7.1.2.1, the basis for the bottom-end CTU free drop was that orientation, when paired with a 17×17 XL fuel assembly, produced the most damage in the fuel assembly. This was because the 17×17 XL featured very long bottom nozzle support legs, allowing considerable strain of the bottom nozzle and the greatest potential for failed fuel rods. Therefore, to determine if the addition to the Clamshell of the bottom support spacer prevents failed fuel rods, as happened in the CTU drop testing, the same bottom-end free drop orientation was tested. As no other drop orientation resulted in a failure of fuel rod integrity, the conclusion made from the CTU bottom-end drop results is that the deformation of the bottom nozzle caused the fuel rods to bend and, as a result, the rods cracked at the bottom end cap weld. Thus, the failure of the fuel rods was solely due to the deformation of the bottom nozzle because of the relatively weak bottom nozzle support legs.

It was determined that this failure mode of the fuel rods can be mitigated by properly supporting the bottom nozzle with a rigid structure. If the bottom nozzle is properly supported, the Outerpack bottom pillow provides sufficient impact protection to preclude failure of the fuel rods in a bottom-end drop. For a bottom nozzle design with corner support legs, this is accomplished with the bottom support spacer that sits inside of the legs, supporting the bottom nozzle. For a bottom nozzle design without corner support legs, there is less of a concern for this sort of nozzle deformation, however, to ensure rigid support of the bottom nozzle, the fuel assembly rests on a solid plate.

The full-scale drop test utilized a 17×17 XL lead-filled, production quality fuel assembly with fuel rods helium backfilled and pressurized internally to 275 psig (1,896 kPa gauge). Although the MNOP of the fuel rods is ~10% greater than this pressure, as discussed above, the failure of the rods in prior CTU testing was solely from the bending of the fuel rods due to the deformation of the bottom nozzle corner support legs. A small increase in fuel rod pressure is insignificant, as long as the deformation of the bottom nozzle and resulting bending of the fuel rods is avoided. To ensure the bounding fuel design including transport mass was drop tested, each fuel type's maximum design weight and their corresponding core component maximum design weights were evaluated. The results of this evaluation are provided in Table 2.7-9. It can be seen that the heaviest potential transport mass is the 17x17 XL fuel type hosting a core component assembly. In addition, of all the fuel types, the 17x17 XL possesses the longest corner legs which when buckled result in the greatest fuel rod cracking potential. Therefore, Type B full scale testing was based upon on 17x17 XL fuel assembly design which is the maximum fuel assembly and core component combined weight of all fuel array types transported in the Traveller package. The replica fuel assembly was loaded into a production quality Traveller XL Clamshell that was modified by adding a top axial restraint and a bottom support spacer. The modified XL Clamshell was dropped onto the current Traveller XL impact limiter. It is noted that this test resulted in a secondary slap-down after the Clamshell with loaded replica fuel assembly impacted the rigid engineered drop test pad, the Clamshell rotated and impacted the surrounding asphalt parking lot.

The entire Type B Outerpack was not included in the drop test since the Clamshell is de-coupled from the Outerpack by the shock mounts during a free-fall impact event. The Outerpack independently impacts the ground target and the Clamshell then continues to fall and eventually impacts the impact limiter. The result of the inelastic collision between the Outerpack and the ground demonstrates that all loads associated with the Outerpack are zero (i.e. insignificant kinetic energy) when the Clamshell impacts the Outerpack, which shows the system is uncoupled. The only coupling between Clamshell and Outerpack is the area under the end Clamshell, referred to as the end limiter, which is un-deformed and at rest on the ground when the Clamshell impacts it. The remainder of the Outerpack is not affected during the Clamshell impact. The Type B testing without an Outerpack is slightly more conservative than a full package drop test, since the energy absorbed by the shock mounts is not considered. In addition, drop tests with a full package were shown to have a single impact event, whereas for Type B testing, the Clamshell and test fuel assembly underwent a secondary impact, or slap-down, because of the configuration.

Table 2.7-9 Traveller Maximum Fuel Assembly and Core Component Weights			
Fuel Array Type/Length	**Max Fuel Assembly Weight (lb)**	**Max Core Component Weight (lb)**	**Max Total Weight (lb)**
14x14 STD	1274	130	1404
15x15 STD	1476	165	1641
16x16 STD	1336	126	1462
17x17 STD	1496	180	1676
17x17 XL	1753	218	1971
17x17 XL (AP1000)	1770	176	1944

2.7.1.4.1 Type B Full Scale Drop Test Sequence

A fuel assembly is positioned on top of a reusable 6000 Series aluminum bottom support spacer. The bottom support spacer rests on top of the Clamshell bottom plate and fits under the fuel assembly bottom nozzle structure, shown in Figure 2.7-21. The bottom support spacer is a stiff structure with full length sides, void center, and sufficient top thickness to ensure the fuel assembly bottom nozzle flow plate is supported during all transport conditions. A rubber pad is glued to the top of the support spacer to avoid surface scratching. The overall bottom support spacer geometry and length will vary based on fuel assembly type to ensure there is a conforming fit between the fuel assembly bottom nozzle and the support spacer.

The bottom support spacer, as tested for the 17×17 XL fuel Type B configuration, is a stiff structure with a nominal 0.56-in (14.2 mm) web top thickness. During the hypothetical accident conditions, its stiffness ensures that it transfers the package's kinetic energy into the Clamshell structure and then to the Outerpack impact limiter, thus assuring the fuel rods remain leaktight.

Clamping mechanisms that interface with the contents provide axial and lateral restraint during all transport conditions. An adjustable, threaded rod-clamping device provides axial restraint at the top of the fuel assembly. The design of the top axial restraint components, as shown in Figure 2.7-22, includes a fuel restraint and two (2) fuel assembly axial studs, threaded through the RTP. The length and configuration of the top axial restraint components depends on the fuel assembly type.

As tested for the 17×17 XL fuel Type B configuration, the 300 Series stainless steel top axial restraint along with the two (2) 300 Series stainless steel fuel assembly axial studs, is threaded through the removable top plate to contact the upper side of the top nozzle flow plate or the core component assembly upper surface, as shown in Figure 2.7-22. The top axial restraint provides positive axial hold-down during normal transport conditions. For a top-down hypothetical accident condition impact, the top axial restraint absorbs impact energy via buckling due to its slender geometry.

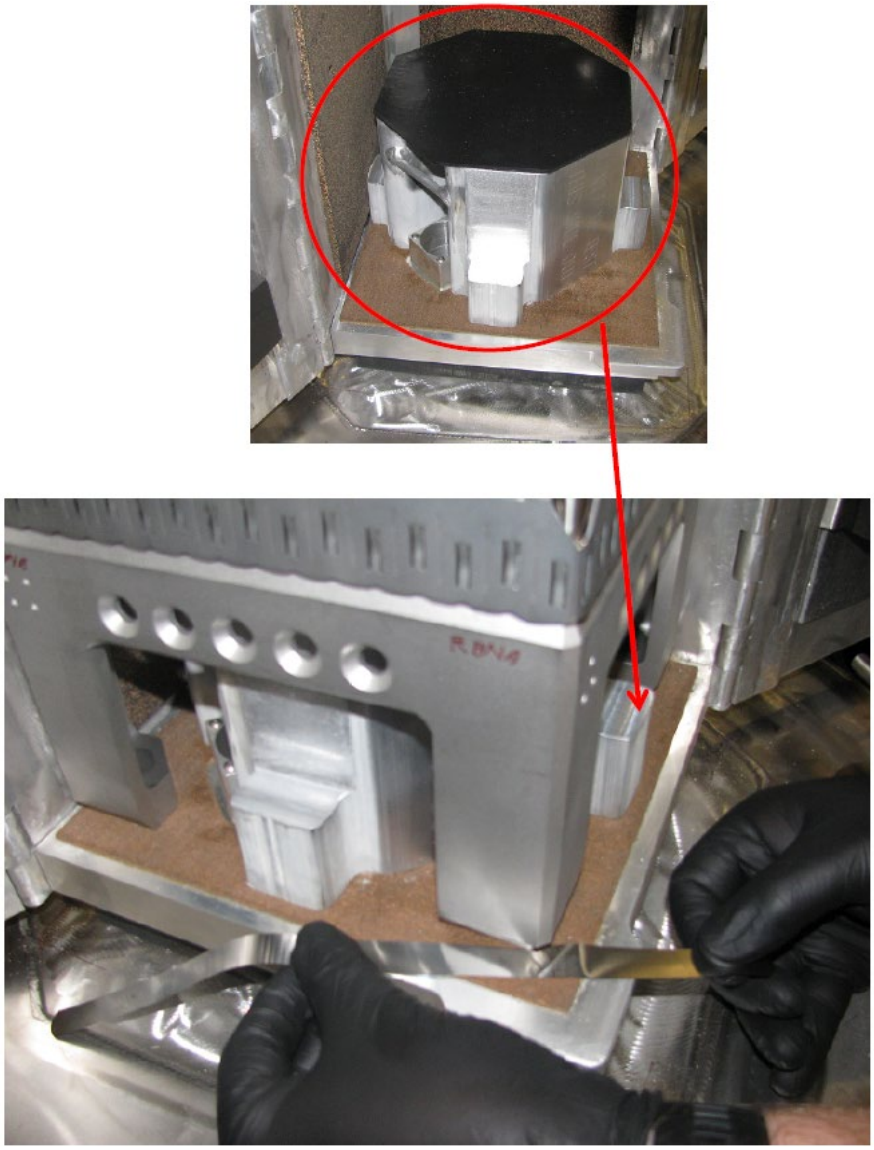

Figure 2.7-21 Type B Bottom Support Spacer/Fuel Assembly Interface Pre-test

Figure 2.7-22 Type B Center RTP Fit-up Pre-test

The verified, measured weights were compared to the expected licensed maximum weights. Based upon the test article's measured values, a final drop height was adjusted to 34.08 ft (10.4 m) to obtain the correct equivalent bounding kinetic energy. Figure 2.7-23 shows the test article prior to the drop test. The test temperature was measured to be 71.6°F (22°C).

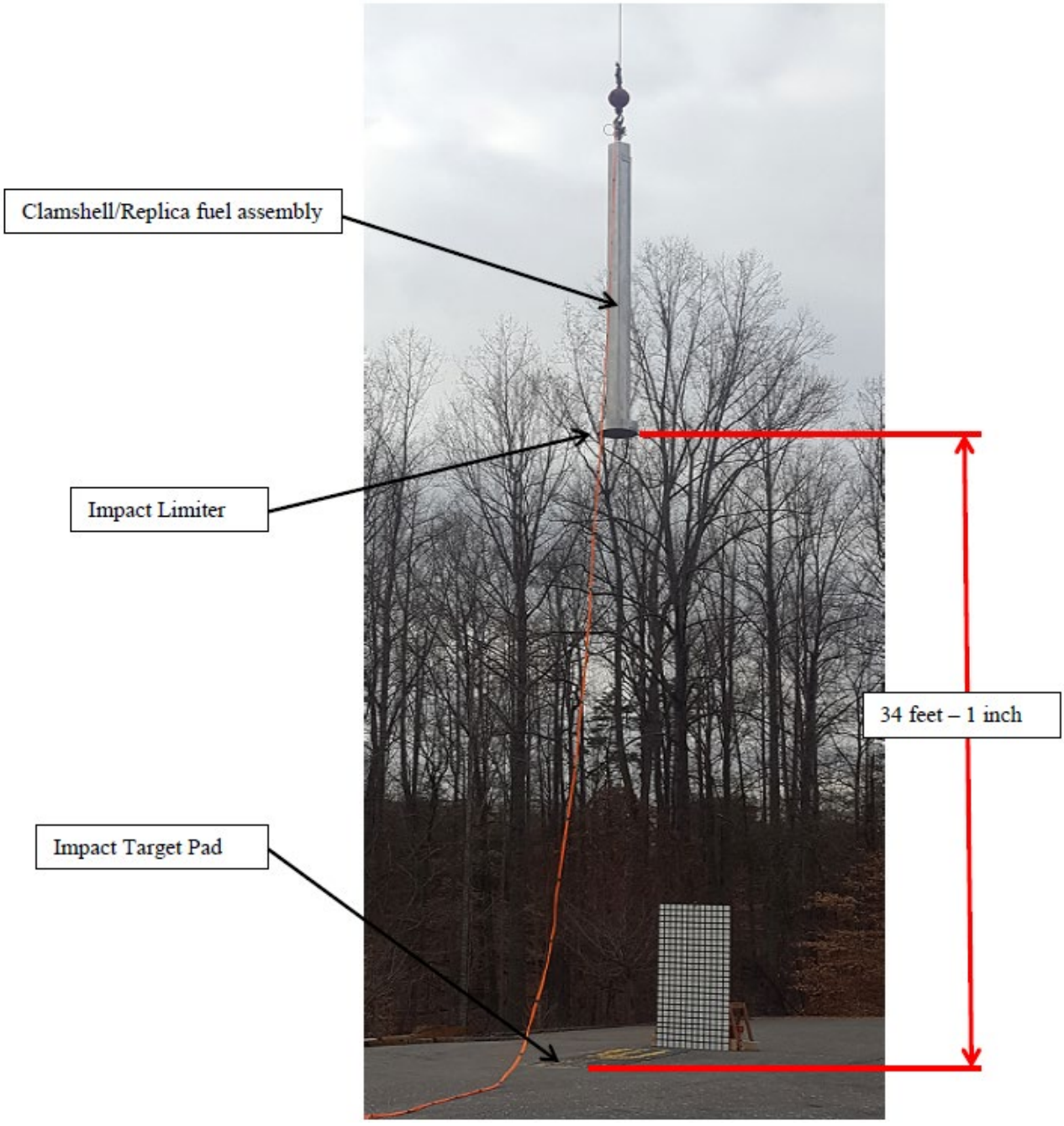

Figure 2.7-23 Type B Drop Test Final Set-up

The Clamshell nominal weight for the Type B configuration is the same as the Type A configuration Clamshell plus the required bottom support spacer and the top axial restraint. Table 2.7-10 provides the actual test weights and recommendations for design maximum weight, then the recommended nominal Clamshell weight (Bottom Support Spacer + Top Axial Restraint + 467 lb). The 17×17 XL fuel assembly has the largest free space between the base of the bottom nozzle legs and the underside of the bottom nozzle flow plate of all fuel types and thus bounds all other spacer designs.

Table 2.7-10 Type B Drop Test Licensing Weight Summary		
Package Feature	**Test Weight, lb**	**Recommended Design Maximum Weight, lb**
Bottom Support Spacer	8.8	10
Top Axial Restraint	2.6	3
Additional Weight TOTAL	11.4	13
Clamshell (Type A) Weight	-	467
Nominal Clamshell Weight, Type B	-	480

Traveller Type B design weight summaries to be used for design and licensing evaluations are presented in Table 2.7-11. The design and licensing basis gross weight is calculated from the nominal weight plus 2% manufacturing uncertainty. The maximum tare weight is the design and licensing basis gross weight less the maximum fuel assembly weight. Design values are rounded up to the nearest ten after the maximum tare weight is determined.

Table 2.7-11 demonstrates that the total package design and licensing weight for the Type B configuration is bounded by the maximum design and licensing weight for the Traveller Type A configuration and all calculations applicable to the Type A configuration will be applicable to the Type B configuration. In addition, all structural Upender evaluations for the Type A configuration are applicable to the Type B configuration, as the maximum design weight is unchanged at 5,230 lb (2,372 kg). The vibration characteristics are also not impacted since the Clamshell modification is added components, and thus are considered insignificant, and there are no changes to the shock mitigation systems from the Type A configuration to the Type B configuration.

Table 2.7-11 Type B Design Weight Summary		
	Traveller STD	**Traveller XL**
Nominal Outerpack Weight, lb (kg)	2368 (1074)	2670 (1211)
Max. Fuel Assembly Weight, lb (kg)	1650 (748)	1971 (894)
Nominal Clamshell Weight, lb (kg)	385 (175)	480 (217)
Nominal Total Weight, lb (kg)	4403 (1997)	5121 (2323)
Design and Licensing Basis Gross Weight, lb (kg)	4500 (2041)	5230 (2372)
Design Tare Weight, lb (kg)	2850 (1293)	3260 (1479)

After completion of the drop test, the impact limiter was characterized for crater depth. The four-corner measured crush depth was 3.375 in (85.7 mm). Slow-motion video analysis of the background grid pattern indicates approximately 4 in (102 mm) of Clamshell vertical displacement during the deceleration event.

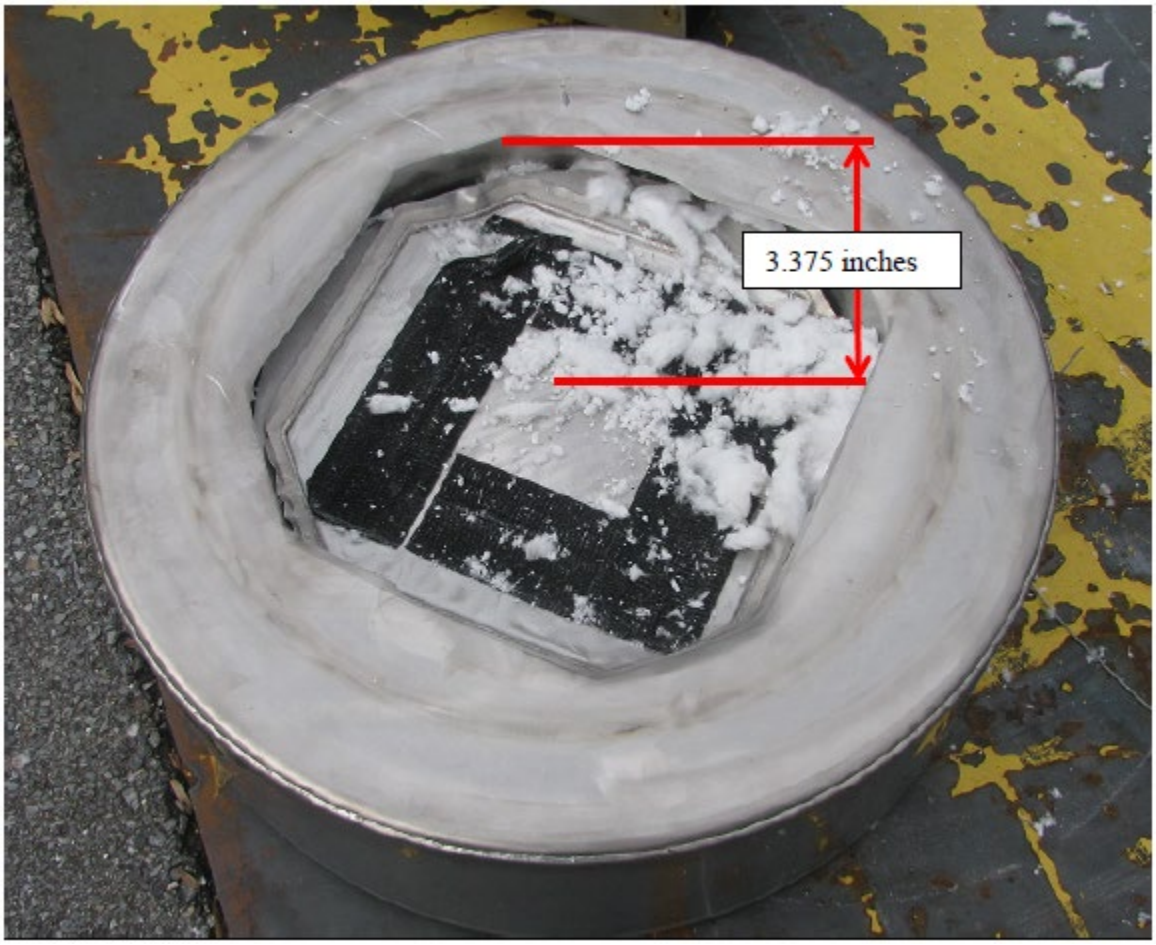

Figure 2.7-24 Impact Limiter Post-test Condition

The Clamshell underwent two impacts: a primary bottom-end impact, then a secondary impact onto its side. Although 8 of the 11 Clamshell latch welds were fractured, the Clamshell remained closed by the remaining 3 latches and the tongue-in-groove joint between the left and right main doors. The overall Clamshell geometry was unchanged with only localized deformed corners at the secondary impact locations (Figure 2.7-25, adjacent to point "A" circled on the hinge left end). Figure 2.7-25 also shows a typical broken weld latch. The Removable Top Plate (RTP) and the top axial restraint were all found secure and intact (Figure 2.7-26). There was a slight, visual bend to the components, but it was not measurable and is considered negligible. An interior Clamshell inspection demonstrated that the BORAL plates were bolted secure, although locally buckled most likely from the secondary impact. Otherwise, the interior of the Clamshell was intact and not structurally compromised.

Figure 2.7-25 Clamshell Exterior Post-test Condition (Bottom End)

Figure 2.7-26 Clamshell RTP Post-test Condition

The fuel assembly was visually and mechanically inspected, and post-test measurements taken, to characterize the impact load effects. Globally, the damage was minimal; see Figure 2.7-27 below. The fuel assembly essentially maintained its pre-test envelope geometry. No grids were broken; only buckled locally. From Table 2.7-12, both top and bottom nozzle expansion and compression were negligible as the changes were measured less than 0.006 in (0.152 mm). Also from Table 2.7-12, grid expansion was negligible as the expansion measured was less than 0.004 in (0.102 mm).

Figure 2.7-27 Global Fuel Assembly Post-test Condition

A detailed image of the Grid 8 area is shown in Figure 2.7-28 to demonstrate localized fuel rod expansion and compression behavior. The expansion occurred on the outer "upper" rows and reacted with compression at the outer "lower" rows. Also, of note is the grid's mechanical "accordion" response to the secondary impact as it buckled. There were no observed broken grids.

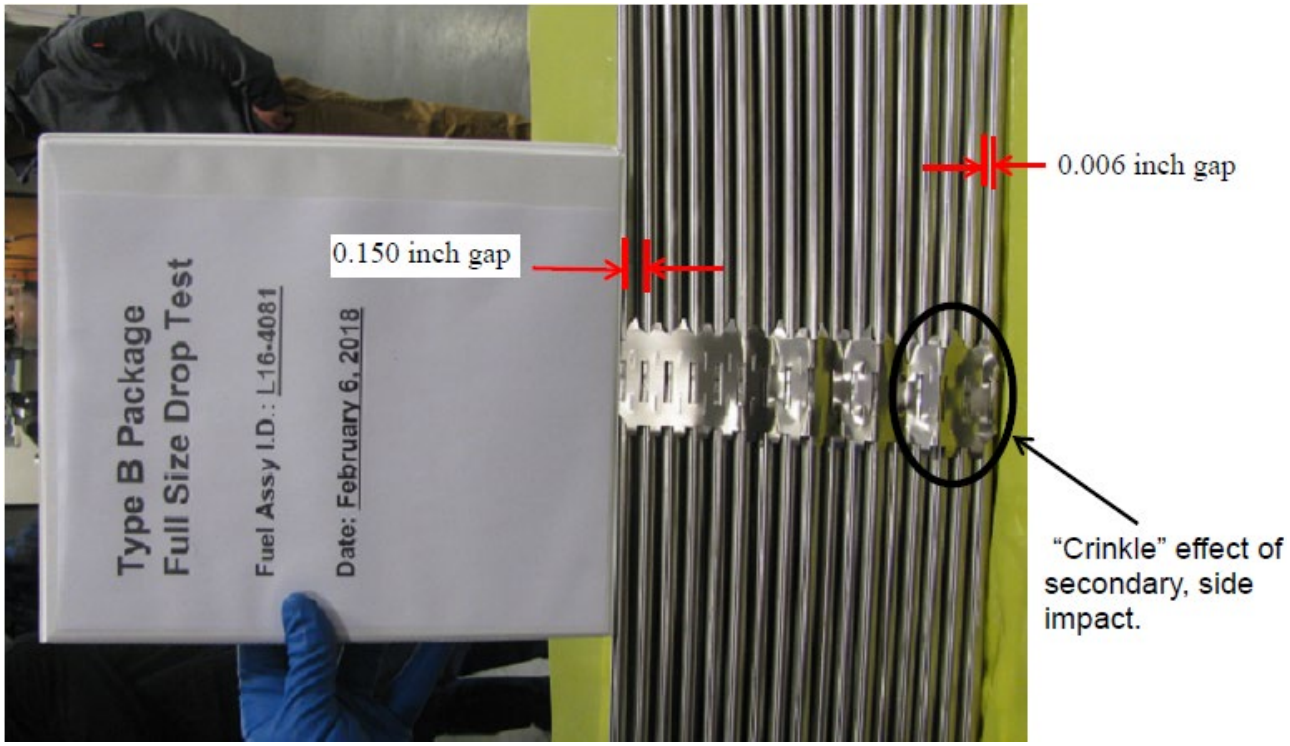

Figure 2.7-28 Localized Fuel Rod Expansion and Grid Buckling Post-test

After the drop testing, each of the 264 replica fuel rods was verified for leaktightness [$1x10^{-7}$ ref. air·cm^3/s ($2x10^{-7}$ std He·cm^3/s) for at least 1 atm_{abs} upstream pressure and 0.01 atm_{abs} or less downstream pressure] using an evacuated envelope gas detector (ANSI N14.5, style A.5.4 [15]). The rods were loaded into the chamber in batches to reduce the pump-down time; a total of 8 batches were needed. Chamber leak testing was performed from 20 hours until 48 hours after the drop test was complete. All rods were found leaktight. To address the event a non-visible crack resulted in all of the helium leaking out prior to chamber leak testing (which theoretically would test as leaktight using the chamber test equipment), two additional measures were taken. First, the detector-probe technique (i.e. a "sniff" test) accurate to $1x10^{-4}$ ref. air·cm^3/s was executed along the entire length of the fuel assembly and in between fuel rods. The probe test was performed approximately 30 minutes after the drop test occurred. No leaks were detected. Secondly, a control fuel rod was pierced with an approximate 0.24-in-long × 0.04-in-deep (6.10 mm × 1.02 mm) hole (pierced until audible pressure release) approximately 18 hours before the first chamber leak test. It was placed in the leak chamber after the completion of Batch 8 chamber testing, and helium was detected. This verified that any visible or non-visible crack would have resulted in a detectable leak.

2.7.1.4.2 Summary of Type B Full Scale Drop Testing

Detailed post-test fuel assembly envelope measurements are provided in Table 2.7-12, and detailed post-test fuel rod and fuel gap measurements are provided in Table 2.7-13. All dimensions are reported in inches, and the temperature during the inspections was measured to be 72.0°F (22.2°C).

Significant results of the Type B full scale drop testing are as follows:

1. All 264 fuel rods remained leaktight, as defined in ANSI N14.5, Section 6.3.2,
2. There was no measurable change to the individual fuel rod outside diameters,
3. The top and bottom nozzles did not expand or compress a significant amount considering measuring precision [dimensional change less than 0.006 in (0.152 mm)],
4. The maximum grid envelope expansion occurred at Grid 3 and was measured to be 0.004 in (0.102 mm), which is considered negligible considering measuring precision,
5. The maximum grid envelope compression occurred at Grid 8 and was measured to be 0.519 in (13.2 mm),
6. The maximum fuel rod gap was measured to be 0.150 in (3.81 mm) between Grids 5-8 (at three places along these spans) as a result of the measured gap expansion of 0.025 in (0.635 mm),
7. The resulting maximum fuel rod pitch, based upon nominal 0.374 in (9.50 mm) fuel rod outside diameter and maximum measured 0.150-in (3.81 mm) gap, is 0.524 in (13.3 mm) between Grids 5-8,
8. The maximum fuel rod gap compression was measured to be 0.124 in (3.15 mm) between Grid 9 and the Top Nozzle as a result of the measured 0.003-in (0.076 mm) gap,
9. The Clamshell remained closed and structurally intact, confining the fuel assembly,
10. Clamshell damage was limited to 8 of 11 local latch weld breaks,
11. The BORAL plates were intact and secured by all screws, with local buckling,
12. The impact limiter average measured crush depth was 3.375 in (85.7 mm).

Table 2.7-12 Post-test Fuel Assembly Measured Maximum and Minimum Envelope Characterization Dimensions (in)

Feature/Area of Interest	Pre-test Max/Min	Post-test Max/Min	Maximum Expansion	Maximum Compression
Bottom Nozzle (B/N)	8.425/8.422	8.430/8.425	0.008	0.00
Grid 1 (P-grid)	8.421/8.414	8.424/8.416	0.01	0.005
Grid 2	8.410/8.408	8.405/8.345	None	0.065
Grid 3	8.409/8.408	8.412/8.334	0.004	0.075
Grid 4	8.410/8.404	None /8.275*	None	0.135
Grid 5	8.412/8.410	None /8.220*	None	0.192
Grid 6	8.411/8.409	None /8.086*	None	0.325
Grid 7	8.413/8.409	None /7.973*	None	0.440
Grid 8	8.411/8.408	NA/7.892*	None	0.519
Grid 9	8.412/8.409	8.377/7.912	None	0.500
Grid 10	8.419/8.417	8.419/8.274	0.002	0.145
Top Nozzle (T/N)	8.406/8.404	8.410/8.407	0.006	None

Note: * Only minimum was measured to obtain the maximum compression value at these locations.

Table 2.7-13 Post-test Fuel Assembly Measured Maximum and Minimum Gap Characterization Dimensions (in)

Feature/Area of Interest	Pre-test Max/Min	Post-test Max/Min	Maximum Expansion	Maximum Compression
B/N-Grid 1 Span (includes P-grid)	0.121/0.120	0.121/0.100	None	0.021
Grid 1-Grid 2 Span	0.126/0.124	0.124/0.100	None	0.026
Grid 2-Grid 3 Span	0.126/0.124	0.123/0.080	None	0.046
Grid 3-Grid 4 Span	0.125/0.123	0.122/0.067	None	0.058
Grid 4-Grid 5 Span	0.126/0.123	0.121/0.045	None	0.081
Grid 5-Grid 6 Span	0.127/0.125	0.150/0.006	0.025	0.121
Grid 6-Grid 7 Span	0.126/0.125	0.150/0.006	0.025	0.120
Grid 7-Grid 8 Span	0.127/0.125	0.150/0.006	0.025	0.121
Grid 8-Grid 9 Span	0.127/0.124	0.129/0.029	0.005	0.098
Grid 9-T/N Span	0.127/0.125	0.129/0.003	0.004	0.124

2.7.2 Crush

The crush test specified in 10 CFR 71.73(c)(2) and SSR-6 para. 727 is required only when the specimen has mass not greater than 1,100 lb (500 kg), an overall density not greater than 62.4 lb/ft^3 (1,000 kg/m^3), and radioactive contents greater than 1,000 A_2, not as special form. The gross weights of the Traveller packages are greater than 1,100 lb (500 kg). Therefore, the dynamic crush test of 10 CFR 71.73(c)(2) and SSR-6 para. 727 is not applicable to the Traveller series of packages.

2.7.3 Puncture

10 CFR 71 requires performing a puncture test in accordance with the requirements of 10 CFR 71.73(c)(3) and SSR-6 para. 727. The puncture test involves a 40 in (1 m) drop onto the upper end of a solid, vertical, cylindrical, mild steel bar mounted on an essentially unyielding, horizontal surface. The bar must be 6 in (15 cm) in diameter, with the top surface horizontal and its edge rounded to a radius of not more than 1/4 in (6 mm). The minimum length of the bar is to be 8 in (20 cm). The ability of the bounding Traveller XL packages to adequately withstand this specified drop condition is demonstrated via testing of the Certification Test Unit (CTU).

2.7.3.1 Technical Basis for the Puncture Drop Tests

To properly select the worst-case package orientation for the puncture drop test, items that could compromise criticality integrity of the Traveller package must be clearly identified. For the Traveller XL package design, the foremost item to be addressed is the integrity of the Clamshell and the neutron moderation and absorption materials (i.e. neutron absorber plate and polyethylene sheeting). The integrity of the Clamshell and the criticality control features may be compromised by two methods:

1. Breach of the Clamshell boundary, and/or
2. Degradation of the neutron moderation/control materials due to fire.

For the above reasons, testing must consider orientations that attack the Outerpack closure assembly, which may result in an excessive opening into the interior for subsequent fire event, and/or the Clamshell, which contains the fuel assembly. Based on prototype testing and computer simulations of the pin puncture event, the pin puncture has insufficient energy to cause significant damage to the Outerpack hinge closure system or to the Clamshell (including components within the Clamshell).

The greatest possibility of cumulative damage to the package occurs when the pin puncture is located within the area of impact of the 30 ft (9 m) drop. These locations further challenge the welded joints adjacent to the crushed area between the Outerpack outer shell and the end cap. Two pin puncture locations were tested in QTU testing, and both had insignificant impact on the structural and thermal performance of the package (See Section 2.7.1.1).

Based on the above discussion, the Traveller XL CTU was evaluated with the pin puncture located such that the pin impacted directly on an Outerpack hinge at a low impact angle. This test was chosen to challenge the hinge's ability to take a pin impact and still perform its important function of thermally protecting the seam between Outerpack bottom and top assemblies. The thermal protection offered by the hinge is described in more detail in Section 3.

2.7.3.2 Summary of Results from the Puncture Drop Test

Successful HAC puncture drop testing of the CTU indicates that the various Traveller XL packaging features are adequately designed to withstand the HAC puncture drop event. The most important result of the testing program was the demonstrated ability of the bounding Traveller XL to maintain its structural integrity. Significant results of the puncture drop testing are as follows:

1. Minor damage to the Outerpack and Outerpack hinge.
2. No effect on the structural or thermal performance of the package.
3. There was no evidence of separation of the Outerpack seam, which would allow hot gases to enter the Outerpack.
4. No evidence of movement occurred that would have significantly affected the geometry or structural integrity of the Clamshell.
5. There was no evidence of loss of contents from the Clamshell due to the puncture events.
6. There was no evidence of deterioration of the polyethylene sheeting in the subsequent fire event.
7. There was no evidence of deterioration of the borated-aluminum sheeting (simulated) in the subsequent fire event.

Further details of the puncture drop test results are provided in Section 2.7.1.2.

2.7.4 Thermal

Subpart F of 10 CFR 71 and SSR-6 require performing a thermal test in accordance with the requirements of

10 CFR 71.71(c)(4) and SSR-6 para. 728. To demonstrate the performance capabilities of the Traveller packaging when subjected to the HAC thermal test specified in 10 CFR 71.71(c)(4) and SSR-6 para. 728, a full-scale CTU was burned in a fully engulfing pool fire. The test unit was subjected to a 30 ft (9 m) free drop, and a 4 ft (1.2 m) puncture drop, prior to being burned, as discussed above. Further details of the thermal performance of the Traveller XL CTU are provided in Section 3, Thermal Evaluation.

The CTU was exposed to a minimum 1,475ºF (800ºC), 30-minute pool fire, as discussed in Section 3. Following the minimum 30-minute fire, the CTU was cooled naturally in air, without any active cooling systems.

2.7.4.1 Summary of Pressures and Temperatures

During HAC the packaging pressure is assumed to be 0 psig since the Outerpack and Clamshell are not sealed. For the Type A configuration, the maximum pressure of the fuel rods is 596 psig (4.11 MPa). For the Type B configuration, where the containment boundary is the cladding of the fuel rods, the maximum HAC pressure is 358 psig (2.47 MPa gauge), as calculated in Section 4.3. Peak temperatures for the Clamshell, as recorded by five (5) temperature indicating strips, were 219ºF (104ºC). No loss of material was observed in the polyethylene material (See Section 3.4.3).

2.7.4.2 Differential Thermal Expansion

Due to the construction of the Traveller Outerpack, light sheet metal constructed primarily of the same material, 304 SS, there are no significant thermal stresses. The Clamshell is constructed so that there is no significant constraint on any component as it heats up and cools down. The fuel cladding which provides containment is likewise designed for thermal transients, greater than what is found in the normal conditions of transport and the fuel rod can expand in the package without binding.

2.7.4.3 Stress Calculations

The Traveller package was qualified by CTU test. No stress calculations were performed.

2.7.4.4 Comparison with Allowable Stresses

The Traveller package was qualified by CTU test. No stress calculations were performed.

2.7.5 Immersion – Fissile Material

Subpart F of 10 CFR 71 requires performing an immersion test for fissile material packages in accordance with the requirements of 10 CFR 71.73(c)(6) and SSR-6 para. 733. As water leakage to the most reactive credible extent has been assumed for the criticality analysis, detailed in Section 6, it is not necessary to evaluate the package for the immersion – fissile material requirement.

2.7.6 Immersion – All Packages

The immersion test is a hypothetical accident condition test that evaluates the effects of static water pressure

head on the structural integrity of the package. The test condition is described by 10 CFR 71.73(c)(6) and SSR-6 para. 729. The regulations state that the package must be immersed under a head of water of at least 50 ft (15 m) for at least 8 hours in the most damaging orientation. For demonstration purposes, an external gauge pressure of 21.7 psi (150 kPa) is considered to meet the test conditions.

Subpart F of 10 CFR 71 requires performing an immersion test for fissile material packages in accordance with the requirements of 10 CFR 71.73(c)(6) and SSR-6 para. 729. Because of the seal configuration (see Section 1), the Traveller STD and Traveller XL series of packages are not leak-tight under external overpressure. In the event of water submersion, the inner portion of the package will fill with water creating equal hydrostatic pressure on the Outerpack and Clamshell surfaces. This condition would not result in a stress gradient through the Outerpack or Clamshell. Therefore, immersion will not impact the structural integrity of the package.

The pressure associated with water immersion will not damage the rods or challenge the fuel rods ability to maintain a leak tight containment boundary for the Type B configuration. During routine conditions the fuel rods are back filled with helium to an internal pressure up to 460 psig (3.17 MPa gauge) in the Type A configuration and 275 psig (1.90 MPa gauge) in the Type B configuration. Increasing the external pressure during immersion counteracts the internal pressure reducing the stresses generated in the cladding material. Therefore, the fuel rods maintain leak tight conditions during immersion.

2.7.7 Deep Water Immersion Test (for Type B Packages Containing More than 10^5 A_2)

The contents of the Traveller are not authorized to contain more than 10^5 A_2. Therefore, the Traveller is exempt from this testing.

2.7.8 Summary of Damage

As discussed in the previous sections, the cumulative damaging effects of the free drops, puncture drop, and thermal tests were satisfactorily withstood by the Traveller XL CTU. Subsequent examinations of the CTU confirmed that integrity of the criticality control components was maintained throughout the test series. The geometry of the Clamshell remained essentially unchanged from the pretest condition. In addition, the Fuel Assembly was well protected and experienced damage that was within acceptance criteria. Therefore, the requirements of 10 CFR 71.73 and SSR-6 paras. 726-729 have been adequately satisfied.

2.8 ACCIDENT CONDITIONS FOR AIR TRANSPORT OF PLUTONIUM

The Traveller is not presently authorized for air transport of plutonium.

2.9 ACCIDENT CONDITIONS FOR FISSILE MATERIAL FOR AIR TRANSPORT

The Traveller is not presently authorized for air transport.

2.10 SPECIAL FORM

The contents of the Traveller series of packages do not classify as a special form material.

2.11 FUEL RODS

In the Traveller XL and STD packages, the fuel rods within the package provide containment for the nuclear fuel. This containment was successfully demonstrated in 2 full-scale test campaigns, comprising a total of two (2) 30-ft (9 m) free drops. The first campaign (Type A Configuration), which involved dropping a complete Traveller package, also included 4 ft (1.2 m) free-drops and pin puncture tests. The second campaign (Type B Configuration) was only for a Clamshell, end impact limiter, and dummy fuel assembly, and was only for the 30-ft (9-m) free drop. The first campaign resulted in cracked rods, however, no pellets were released from the fuel rods. The second campaign included the use of an additional aluminum block placed in the bottom stand region of the fuel assembly. This block kept the bottom region of the fuel assembly from splaying out during the end drop. As a result, the rods remained leaktight after the 30-ft (9-m) drop.

2.11.1 Type A Configuration

One (1) full-scale Traveller XL package (CTU) was tested in a bottom-down end drop orientation for Type A contents. This fuel assembly (dummy Westinghouse 17×17 XL) experienced a small percentage of rods with cracked welds in the location of the bottom end plug. Post-test inspection of the fuel assembly indicated that approximately 7.5% of the fuel rods were visibly cracked at the end plug weld zone. The average magnitude of the crack widths measured approximately 0.030 in (0.76 mm), encompassing about one-half of a rod diameter. This minor cracking is considered insignificant since fuel pellets of diameter 0.374 in (9.50 mm) are approximately 12.5 times larger than the average visible crack widths. A crack width of 0.075 in (1.91 mm) was the largest observed, and this width is not sufficient for fuel pellets to escape. Therefore, the containment system satisfies its requirement of containing loss of fuel for Type A contents.

Due to the nature of the bottom-down end impact, the fuel rod array is tightly packed and forced into the bottom nozzle. As the bottom nozzle buckles, the rods located nearest the corners of the adapter plate experience a side loading due to the deformed shape of the plate. This moment is sufficient to crack the weld. Further details can be found in Section 2.7.1.2.

2.11.2 Type B Configuration

For the Type B configuration, the results of the Type A testing were not satisfactory due to resultant cracked rods. Therefore, another test was done for the Type B configuration with the bottom support spacer as described in Section 2.1.1. The Type B test campaign resulted in 100% containment of the fuel pellets within each rod of the fuel assembly, as verified by post-drop leak testing, proving the basis for the Type B configuration.

The entire Outerpack was not included in the drop test since the Clamshell is de-coupled from the Outerpack by the shock mounts during a free-fall impact event. The Outerpack independently impacts the ground target and the Clamshell then continues to fall and eventually impacts the impact limiter. The Type B testing without an Outerpack is slightly more conservative than a full package drop test since the energy absorbed by the shock mounts is not considered. In addition, drop tests with a full package were shown to have a single impact event, whereas the Clamshell and test fuel assembly underwent a secondary impact, or slap-down, as a result of this drop test. Detailed post-test fuel assembly envelope measurements are provided in Table 2.7-12, and detailed post-test fuel rod and fuel gap measurements are provided in Table 2.7-13. All dimensions are reported in inches, and the temperature during the inspections was measured to be 72.0°F (22.2°C).

Significant results of the Type B full scale drop testing are as follows:

1. All 264 fuel rods tested leaktight as defined in ANSI N14.5, Section 6.3.2,
2. There was no measurable change to the individual fuel rod outside diameters,
3. The top and bottom nozzles did not expand or compress a significant amount considering measuring precision [dimensional change less than 0.006 in (0.152 mm)],
4. The maximum grid envelope expansion occurred at Grid 3 and was measured to be 0.004 in (0.102 mm), which is considered negligible considering measuring precision,
5. The maximum grid envelope compression occurred at Grid 8 and was measured to be 0.519 in (13.2 mm),
6. The maximum fuel rod gap was measured to be 0.150 in (3.81 mm) between Grids 5-8 (at three places along these spans) as a result of the measured gap expansion of 0.025 in (0.635 mm),
7. The resulting maximum fuel rod pitch, based upon nominal 0.374 in (9.50 mm) fuel rod outside diameter and maximum measured 0.150-in (3.81 mm) gap, is 0.524 in (13.3 mm) in between Grids 5-8,
8. The maximum fuel rod gap compression was measured to be 0.124 in (3.15 mm) between Grid 9 and the Top Nozzle as a result of the measured 0.003-in (0.076 mm) gap,
9. The Clamshell remained closed and structurally intact, confining the fuel assembly,
10. Clamshell damage was limited to 8 of 11 local latch weld breaks,
11. The BORAL plates were intact and secured by all screws, with local buckling,
12. The impact limiter average measured crush depth was 3.375 in (85.7 mm).

Further details of the Type B full scale drop test results are provided in Section 2.7.1.4.1.

2.11.3 Rod Pipe

The Traveller Clamshell is primarily designed to transport PWR fuel assemblies. To accommodate Type A loose fuel rods, a Rod Pipe is provided. It is a 304 stainless steel Rod Pipe with a maximum diameter of 6.625 in (168.3 mm) (6" Schedule 40 pipe), a maximum length of 200 in (5,080 mm), and a maximum loaded weight of 1,650 lb (748 kg).

The response of the Traveller to the 30-ft (9-m) HAC drop test resulted in the kinetic energy being absorbed by the Outerpack impact limiter, due to the combined mass of the fuel assembly and Clamshell, and minor fuel assembly buckling. As a result, the strain damage to the fuel assembly was minimal, and the Clamshell retained its pre-test geometry and structural integrity, even though the full stroke of the impact limiter was not utilized. The Rod Pipe design is qualified through drop testing. When subject to the 30-ft (9-m) impact test described in 10 CFR 71.73, the Rod Pipe is expected to utilize the full stroke of the impact limiter due to its rigidity with impact forces less than that imparted to the fuel assembly. This is due to the fact the loaded Rod Pipe maximum mass of 1,650 lb (748 kg) is less than the maximum fuel assembly mass used for the 30-ft (9-m) impact test. The testing is described in detail in the following sub-sections.

2.11.3.1 Drop Test Basis

To demonstrate the Rod Pipe's structural integrity for HAC and NCT, a 30.5 ft (9.3 m) vertical end drop test onto an engineered drop test pad was performed using a full-length Rod Pipe filled with 1,650 lb (748 kg)

ballast and attached lower impact pillow with rubber spacer. The impact pillow was secured to the rod pipe with wire to simulate the spacing/gap that exists between the Rod Pipe and Clamshell. The pipe assembly was dropped from a height of 30.5 ft (9.3 m) to accommodate manufacturing tolerances. The ballast simulating the loose rods was comprised of a combination of chain and solid bar stock. Solid bar stock has a greater axial rigidity than the actual thin-walled cladding associated with the loose rods. Assumptions used during the drop test include:

- No credit was taken for the energy absorbing properties of the Outerpack outer shell primary structure and the rubber shock mounts.
- No structural credit was taken for the Clamshell strength and energy absorption.
- The drop height was 9.3 meters compared to 9.0 meters required by the regulation.
- The solid ballast resulted in a greater shear load imparted to the flange end as compared to standard loose rods.

2.11.3.2 Drop Test Results

The pre and post-test characterization consisted of critical rod pipe measurements (Figure 2.11-1) as well other visual inspections of joints (i.e. welds, fasteners). In addition, post drop test inspections included measurements of the rubber spacer and lower impact limiter to quantify their impact response. Figure 2.11-2 and Figure 2.11-3 show the localized flange damage. Table 2.11-1 presents the pre- and post- test characterization of the Rod Pipe.

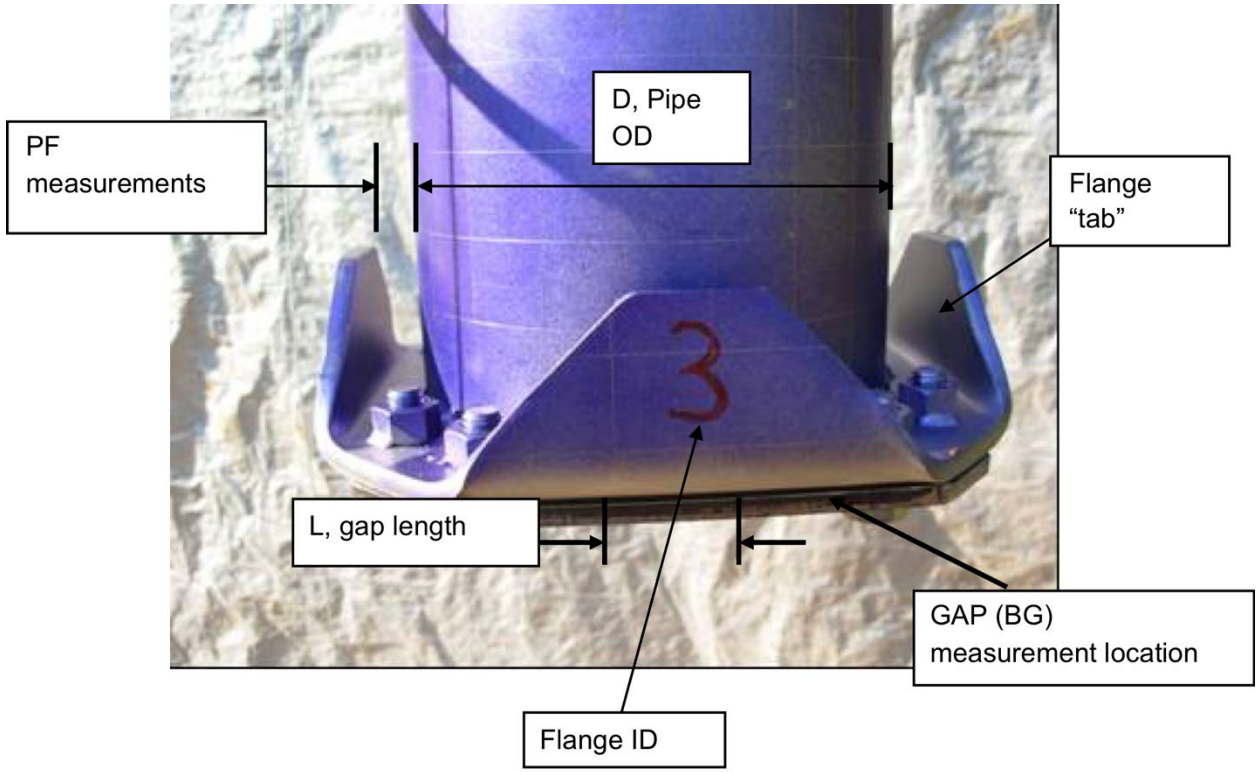

D = Pipe OD, BG = Bottom Flange gap, PF = Pipe-Flange gap, L = Gap Length (post-test only)

Figure 2.11-1 Rod Pipe Characteristics for Evaluation

The drop test did not result in unacceptable damage to the Rod Pipe. There were no measurable changes in the pipe dimensions and no welds were found compromised. Furthermore, testing indicated the following:

- The Rod Pipe outside diameter was unchanged (no buckling).
- All bolts were intact (top and bottom end) and the end flanges were secure.
- The end plate damage was localized to the flange-pipe interface with the largest measured gap of 0.24 in (0.61cm) of flange side 3 (Table 2.11-1).
- The flange damage was localized to the "tabs", which were bent in slightly.
- All welds (flange nut welds, lifting welds) were intact.

Table 2.11-1 Rod Pipe Evaluations for Vertical End Drop Test

Flange Side	Characteristic			
	D [1] in (cm)	**BG in (cm)**	**L in (cm)**	**PF in (cm)**
1, Pre-test	6.614 (16.79)	<.002 (<.005)	N/A	.76 (1.93)
1, Post-test	6.616 (16.80)	.16 (.41)	3.0 (7.6)	.07 (.18)
Change	**.002 (.005)**	**.16 (.41)**	**3.0 (7.6)**	**.69 (1.75)**
2, Pre-test	N/A	<.002 (<.005)	N/A	.75 (1.91)
2, Post-test	N/A	.05 (.13)	2.5 (6.4)	.27 (.69)
Change	N/A	**.05 (.13)**	**2.5 (6.4)**	**.48 (1.22)**
3, Pre-test	N/A	<.002 (<.005)	N/A	.75 (1.91)
3, Post-test	N/A	.24 (.61)	3.0 (7.6)	.58 (1.47)
Change	N/A	**.24 (.61)**	**3.0 (7.6)**	**.17 (.43)**
4, Pre-test	N/A	<.002 (<.005)	N/A	.73 (1.85)
4, Post-test	N/A	.08 (.20)	2.25 (5.7)	.65 (1.65)
Change	N/A	**.08 (.20)**	**2.25 (5.7)**	**.08 (.20)**

[1] Maximum pipe OD = 6.668 in (16.99 cm) and Minimum pipe OD = 6.594 in (16.75 cm) per ASTM A999. Pipe OD measurement is average of 10 measurements at 5 locations above and below the middle flange.

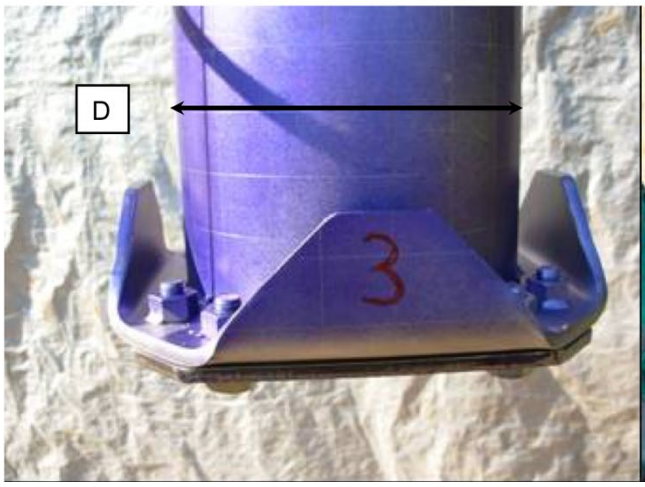

Figure 2.11-2 Flange 3 Pre-test

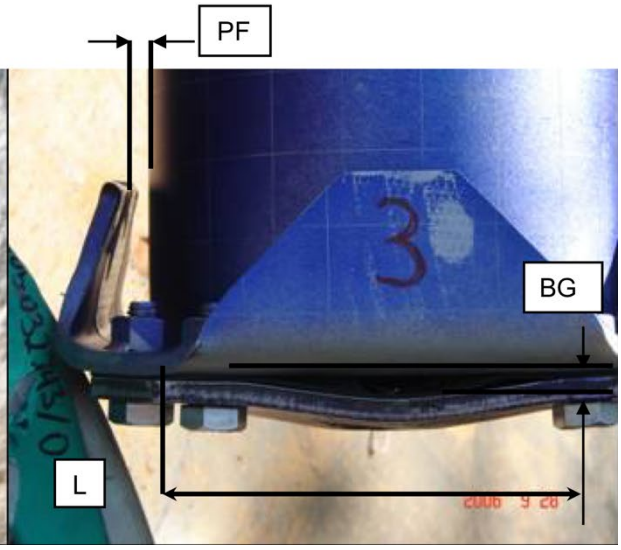

Figure 2.11-3 Flange 3 Post-test

Post-test inspection of the rubber spacer and lower impact pillow indicated damage as expected (Figure 2.11-4). The rubber spacer was torn at the pre-cut square holes. The lower impact pillow thickness was reduced by approximately 29% and was crushed from 4.32 inches (11 cm) per Figure 2.11-4 to 3.00 in (7.6 cm). Where the Rod Pipe impacted the lower impact pillow, the structural weld cracked approximately 3/4 of its original circumference (Figure 2.11-4), which was anticipated. Both components provided adequate protection of the Rod Pipe.

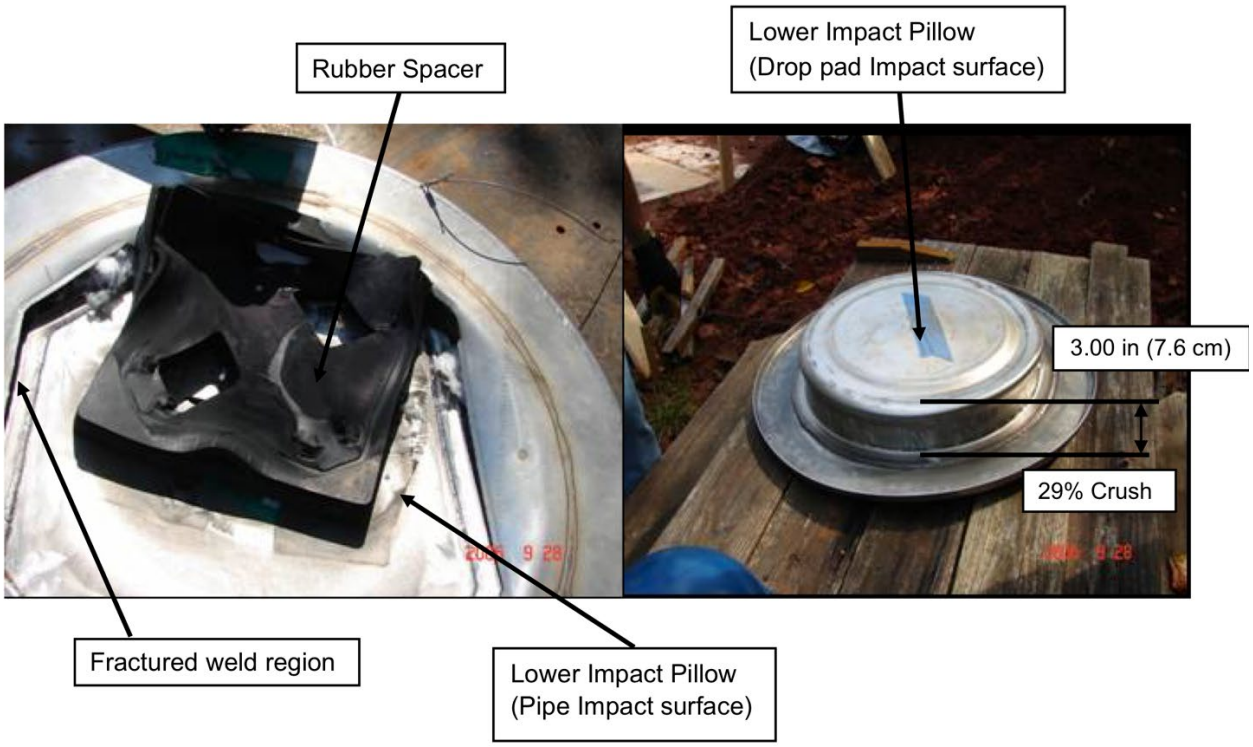

Figure 2.11-4 Rubber Spacer and Impact Limiter Post-test Conditions

2.12 APPENDICES

The following appendices are included with Section 2:

2.12.1 References
2.12.2 Clamshell Axial Bottom Spacer Structural Evaluation
2.12.3 Clamshell Removable Top Plate Structural Evaluation

2.12.1 References

[1] U.S. Nuclear Regulatory Commission Code of Federal Regulations, Title 10 Part 71, "Packaging and Transport of Radioactive Material," 10 CFR 71, 2018.

[2] International Atomic Energy Agency, "Regulations for the Safe Transport of Radioactive Material," Specific Safety Requirements No. SSR-6, 2012.

[3] American Welding Society (AWS), "Structural Welding Code - Stainless Steel," AWS D1.6.

[4] American Society of Mechanical Engineers (ASME), "Boiler & Pressure Vessel Code Section III, Rules for Construction of Nuclear Facility Components, Division 1 - Subsection NF, Supports," 2001 with 2003 Addenda.

[5] American Society of Mechanical Engineers (ASME), "Boiler & Pressure Vessel Code, Section II Materials, Part D - Properties," 2001 with 2003 Addenda.

[6] ANSYS Inc., "ANSYS Workbench," SAS, Inc..

[7] Livermore Software Technology Corporation, "LS-DYNA".

[8] ASTM International, "Standard Specification for Ultra-High-Molecular-Weight Polyethylene Molding and Extrustion Materials," ASTM D4020.

[9] American Society of Mechanical Engineers (ASME), "Boiler & Pressure Vessel Code, Section IX - Welding, Brazing and Fusing Qualifications," 2001 with 2003 Addenda.

[10] E. Oberg, F. D. Jones, H. L. Horton and H. H. Ryffel, "Machinery's Handbook 26th Edition," Industrial Press Inc., New York, 2000.

[11] Westinghouse Electric Co., "Traveller Package Verification Test Report," PD-03-45, 2003.

[12] Westinghouse Electric Co., "Traveller Package Regulatory Verification Drop Test Report," MD1-03-66, 2003.

[13] Westinghouse Electric Co., "Traveller Package Final Regulatory Verification Drop Test Report," MD1-04-45, 2004.

[14] Westinghouse Electric Co., "Traveller Type B Full Scale Regulatory Drop Test Final Verification Test Report," SFDT-18-15 Rev. 0, 2018.

[15] American National Standards Institute (ANSI), "American National Standard for Radioactive Materials - Leakage Tests on Packages for Shipment," ANSI N14.5-2014, 2014.

[16] J. E. Shigley, Mechanical Engineering Design, McGraw-Hill, 1977.

2.12.2 Clamshell Axial Bottom Spacer Structural Evaluation

2.12.2.1 Background

The XL Clamshell may be configured to include an aluminum axial bottom spacer assembly to ship fuel types that normally would ship inside a Traveller STD package, as shown in Figure 2.12-1. The structural performance of the axial bottom spacer assembly in a bottom-down 30 ft (9 m) hypothetical drop is evaluated to determine if there is any buckling of the spacer [a 6-inch (152 mm) Schedule 40 aluminum pipe] that could then damage or deform the Clamshell.

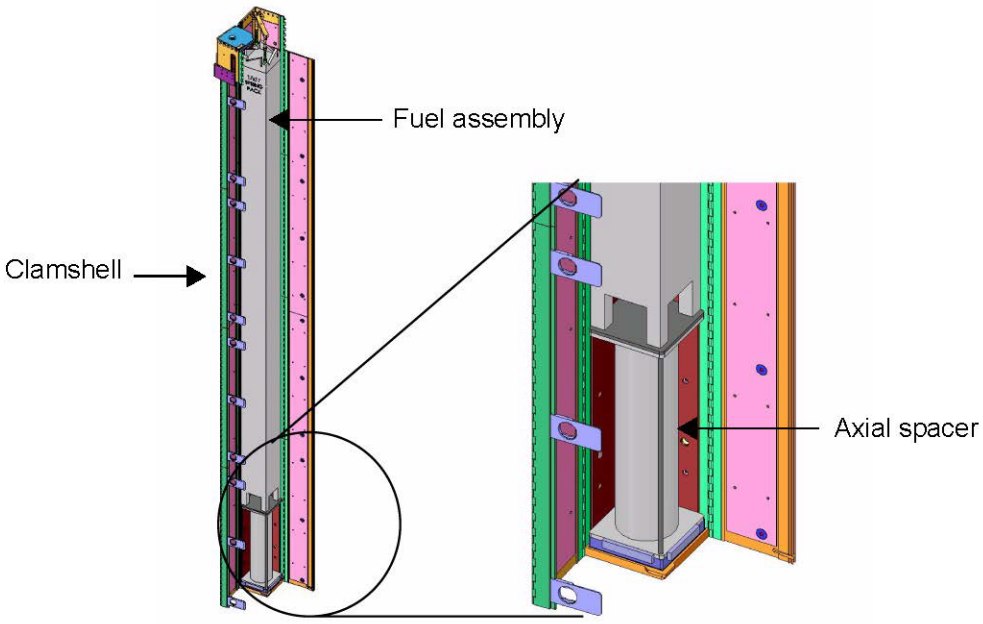

Figure 2.12-1 Axial Bottom Spacer Below Fuel Assembly in Traveller XL Clamshell

The fuel assembly is assumed to be restrained in the Clamshell to prevent any secondary impact within the Clamshell. The axial bottom spacer below the fuel assembly, when needed, and a top axial restraint restrain the contents to the Clamshell, and as such the Clamshell and contents decelerate as a coupled mass. The top axial restraint, fuel assembly structure, or spacer may absorb kinetic energy during the deceleration that results from an end drop impact.

Any structural deformation of the axial bottom spacer assembly shall not change the shape of the Clamshell or compromise the ability of the Clamshell to confine the fuel assembly. The Clamshell panel doors shall remain securely closed, end plates shall remain securely in place, hinges attaching the panel doors and multi-point cammed latch shall remain intact, and dimensions of the Clamshell shall not be altered.

The primary impact with the unyielding surface occurs on the Outerpack end impact limiter. The Outerpack decelerates quickly within a few milliseconds of the primary impact because the contact area of the end surface is large and stiff, and there is no significant rebound. The Outerpack is completely decelerated by the time a secondary impact occurs inside the package as the Clamshell, suspended in the lower Outerpack on rubber

mounts, continues to fall and contact the inside surface of the end impact limiter.

A crushable foam "pillow" is integrated into the end impact limiter to absorb kinetic energy from the secondary impact between the Clamshell and inside surface of the lower Outerpack end impact limiter. This pillow is a solid disk made from 6 pcf (0.096 g/cm^3) polyurethane foam. It has a nominal diameter of 12.00 in (305 mm) and a nominal height of 3.60 in (91 mm). The stiffer foam in the Outerpack end impact limiter, 20 pcf (0.32 g/cm^3) density, is located below and around the soft pillow. This stiffer component end impact limiter functions to decelerate the Outerpack at all high drop angle orientations.

2.12.2.2 Conclusions

Results of the simulated bottom-down 32.8 ft (10 m) impact predict that there is no significant risk of damage to the Clamshell due to buckling of the axial bottom spacer assembly. The 28.94-in (735.1 mm) long spacer assembly is too short to fail in a classic Euler buckling manner. Instead, the axial bottom spacer may locally crumple near its bottom and top ends during the impact. This local crumpling does not result in large column bowing displacements that could impart forces on the Clamshell panel doors or base.

2.12.2.3 Detailed Calculations and Evaluations

A Traveller XL finite element (FE) model of the entire package was originally used to simulate the impact testing. A new LS-DYNA Traveller model was created to simulate features of the XL package affected by the end impact orientation. The new model is more efficient and was used to evaluate the structural performance of the axial bottom spacer in the vertical end impact.

2.12.2.3.1 Assumptions

Specific assumptions used in the FEA simulation are as follows:

1. The assumed mass of the FA was 1,676 lb (760 kg).
2. The FA is modeled with distributed point-element masses and is therefore not elastic. This is very conservative since actual drop testing revealed the weak axial stiffness of a FA (it vibrates and bows during end impacts).
3. The drop height was conservatively increased from 30 ft to 32.8 ft (9 m to 10 m).
4. The FA bottom nozzle and axial bottom spacer assembly were modeled without any restraints and they are therefore free to rotate/tilt. In actuality, the FA itself would keep the bottom nozzle relatively horizontal and the Clamshell walls will further restrain both items.
5. The majority of the mass of the Outerpack has not been included in this analysis because it does not significantly affect the Clamshell impact. More specifically, the Outerpack impact event is finished within only a few milliseconds, therefore the bottom limiter is simply waiting for the Clamshell impact into it. This assumption based on CTU testing has been validated in a separate FEA run which did include the remaining Outerpack mass.
6. The foam crush characteristics include extrapolation from 80% crush to 100% crush for model stability purposes. As mentioned earlier, actual pillow crushing was measured to be only about 50%. This is because the FA is not a rigid "hammer" that has no axial elasticity. This effect has been proven to be quite significant. However, in these simulations, the severe impact of the rigid-mass modeling of the fuel assembly was used. In some cases, this forces the crush curves to be extrapolated to 100%.

7. The longest axial bottom spacer assembly is considered the bounding FA/Spacer combination.
8. LS-DYNA incorporates strain capability into the plastic regions of metallic material properties, therefore the "strain hardening" effects for aluminum were included in the model. These values are difficult to obtain, and therefore engineering judgement was used to assume the modulus after the yield. This was assumed to be a very low, linear value of 38.87 ksi (268 MPa). This represents almost no strain hardening from yield to failure.

2.12.2.3.2 Method

The Lawrence Livermore finite element code, LS-DYNA®, was used to determine the loads, displacements, accelerations, and strains of a Traveller XL shipping package containing a 17×17 STD fuel assembly with RCCA when dropped onto a flat unyielding surface from a height of 10 m. LS-DYNA 970, Revision 5434a [7], is a general-purpose finite element code for analyzing the large deformation dynamic response of structures. This software was selected because it allows the analysis to include the effects of large deformation, large strain, material non-linearity, contact, and failure of materials.

Only the bottom end of the FA is modeled, the remainder of the assembly mass is simulated through point-mass elements. The weight of the remainder of the Clamshell is also modeled with point-mass elements. The Clamshell is an aluminum box with a solid 1-in (25.4-mm) thick bottom plate. The axial bottom spacer assembly is modeled with the 1.25-in (31.8-mm) thick bottom rubber pad included, however, the 3/8-in (9.5-mm) thick rubber pad on the top surface was not modeled.

Figure 2.12-2 shows components, materials, and meshing for the FEA simulation. The material properties assumed for the aluminum, stainless steel, crushable foams, and rubber pad are summarized in Section 2.2.1. The compressive strength difference between the crushable foams is shown in Figure 2.2-8. Figure 2.2-2 shows the stress-strain curve of the 304 stainless steel properties used in the LS-DYNA simulation. The dimensions for the analysis and relevant material properties are summarized in Table 2.12-1.

The appropriate properties of neoprene rubber (rubber pad) for this simulation are difficult to determine exactly. Further, neoprene rubber does not obey Hooke's Law because it exhibits non-linear behavior. For this simulation, a value of 0.9 ksi (6.21 MPa) was used for the shear modulus (G) of the 1.18-in (30-mm) thick lower rubber pad.

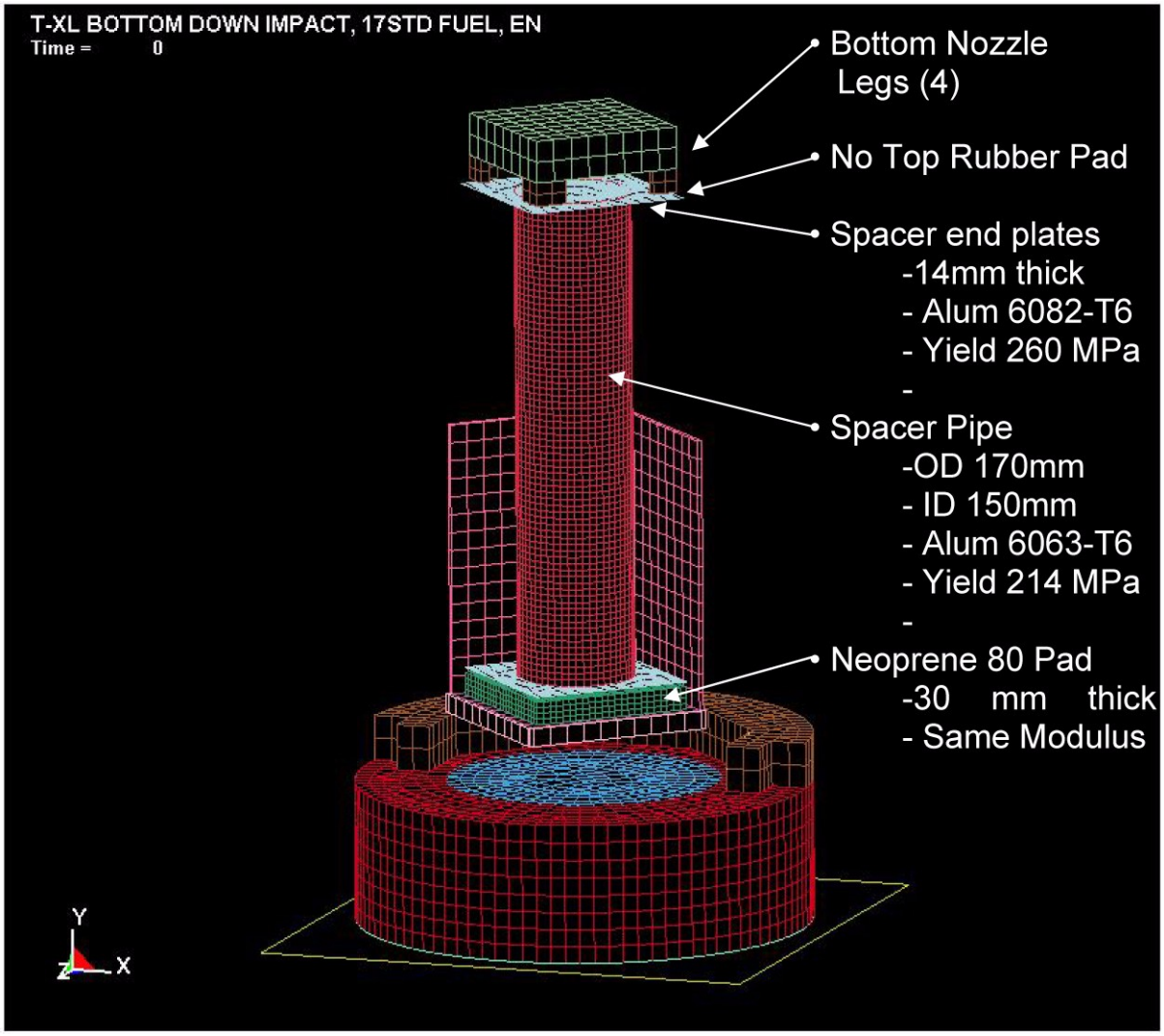

Figure 2.12-2 FEA Model – Axial Spacer

Table 2.12-1 Dimension and Material Properties of Axial Bottom Spacer	
Support Pipe:	
Exterior Diameter - mm (in):	170 (6.69)
Interior Diameter - mm (in):	150 (5.91)
Length - mm (in):	671.1 (26.42)
Wall Thickness - mm (in):	10 (0.39)
Material	6063-T6
Yield Strength - MPa (ksi)	214 (31.0)
Base Plates:	
Thickness - mm (in)	14 (.55)
Length - mm (in):	228.6 (9.00)
Material	6082-T6
Yield Strength - MPa (ksi)	262 (38.0)
Top Rubber Pad:	
Length - mm (in):	228.6 (9.00)
Thickness - mm (in)	10 (0.39)
Material	Neoprene 80
Bottom Rubber Pad:	
Length - mm (in):	228.6 (9.00)
Thickness - mm (in)	30 (1.18)
Material	Neoprene 80
Rod Handle:	No
Side Rubber Pad:	No
Total Assembly Length - mm (in):	735.1 (28.94)

2.12.2.3.3 Calculation Results

The 32.8 ft (10 m) initial drop height of the Traveller simulation yields an impact velocity of 45.93 ft/s (14.00 m/s). The FEA simulation shown in Figure 2.12-3 predicts deformation of the top spacer end plate, but no buckling or plastic deformation of the spacer pipe. From the displacement history of the top surface of the pillow shown in Figure 2.12-4, the total crush distance into the end impact limiter is approximately 3.70 in (94 mm). Figure 2.12-5 shows the kinetic energy history (MJ) of the axial spacer model.

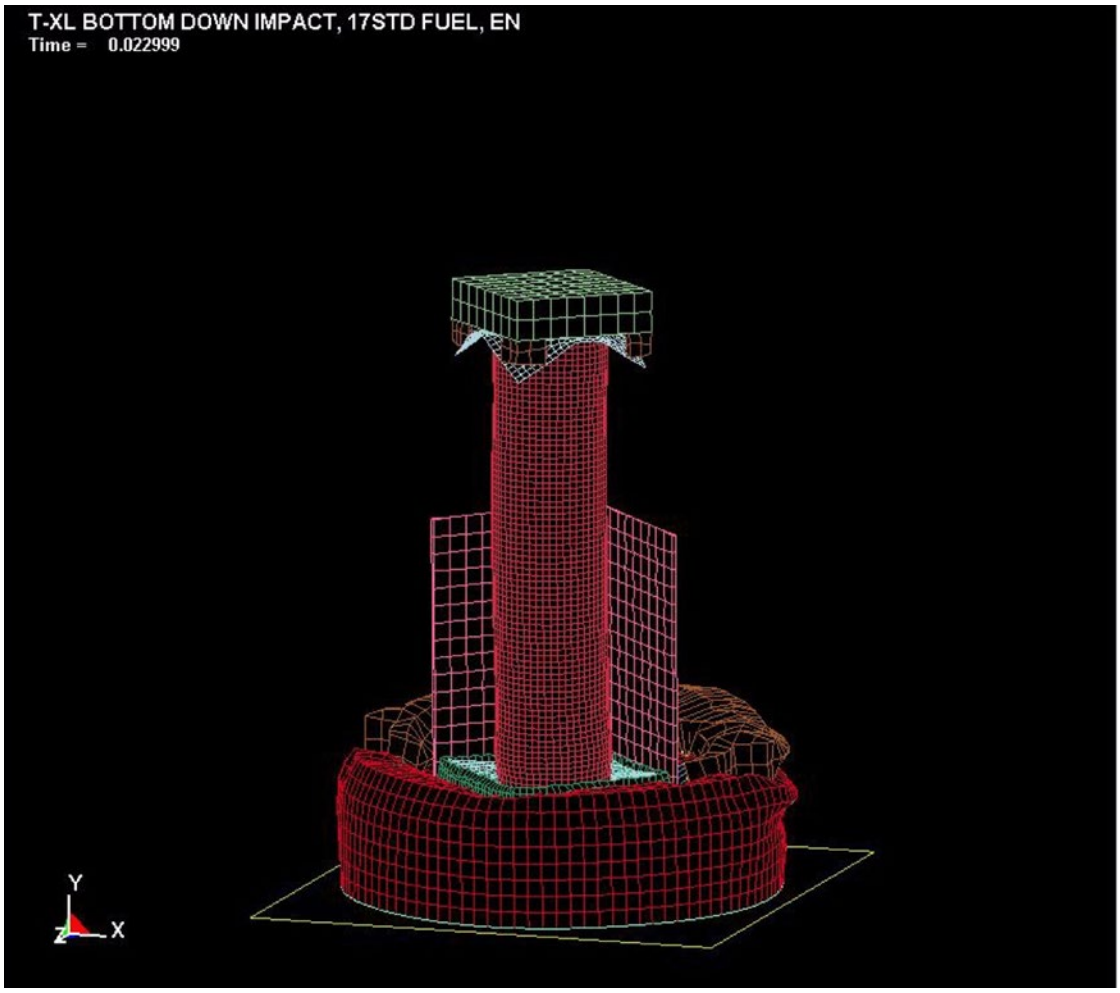

Figure 2.12-3 Deformed Model with Axial Spacer at 23 ms (the end of the impact)

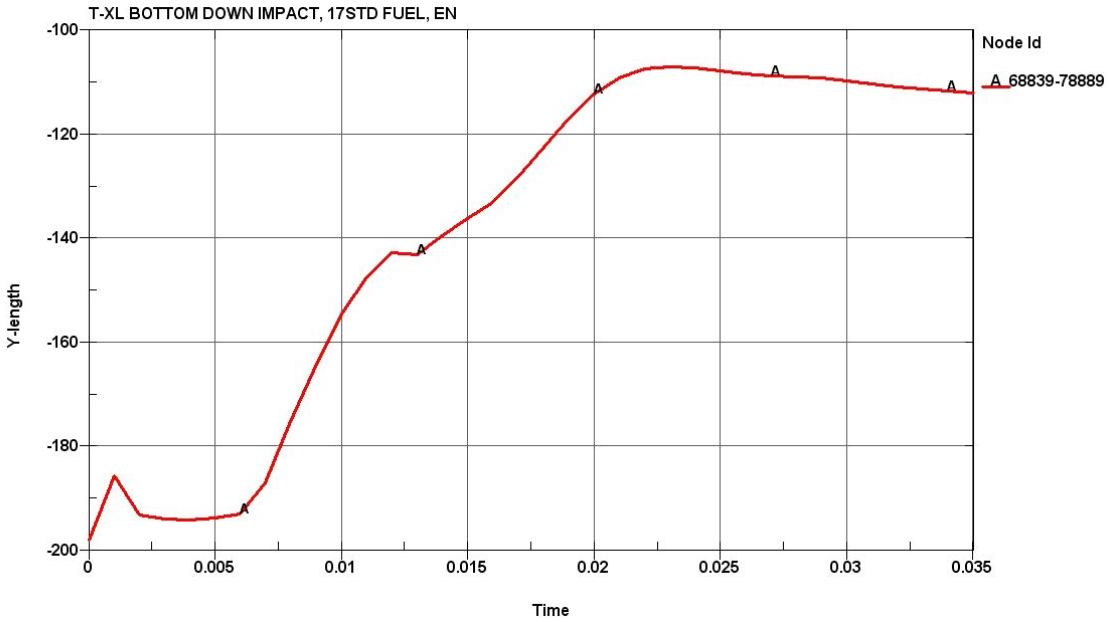

Figure 2.12-4 Predicted Total End Crushing (mm) with Axial Spacer

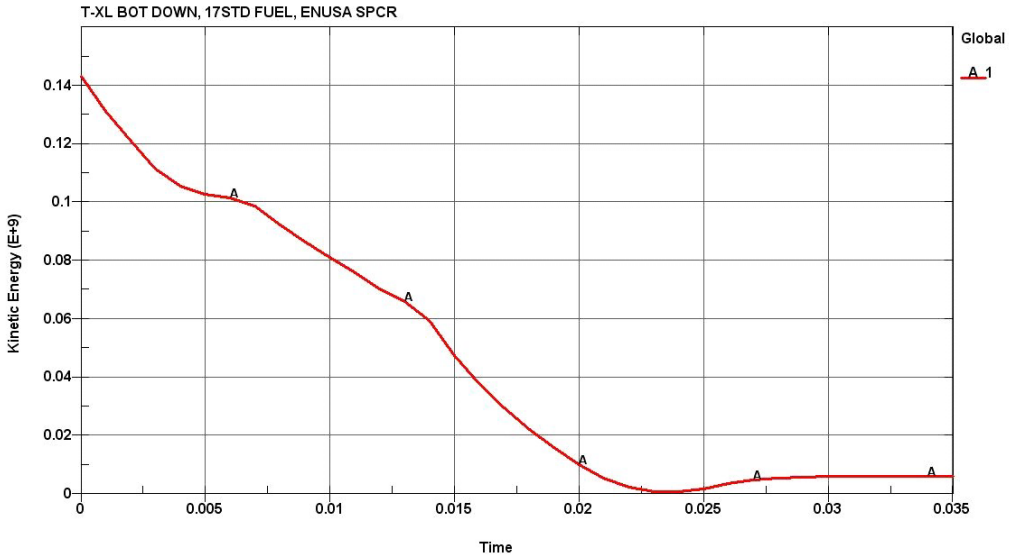

Figure 2.12-5 Kinetic Energy History (MJ) of the Axial Spacer Model

2.12.2.3.4 Validation

The many assumptions used to develop the LS-DYNA non-linear finite element stress code, including those needed to model the materials and impact, are validated by comparing the simulation results to the actual drop tests for the Traveller XL. Comparisons between certification test unit results and FEA simulation demonstrates that physical phenomenon governing shipping package impacts are simulated with adequate fidelity using the LS-DYNA model.

In a 32.2 ft (10.0 m) free drop impacting the bottom end of the package, CTU Test 1.2, the pillow was observed to crush approximately 1.8 in (45 mm). The simulation with axial bottom spacer predicted the end limiter assembly (Pillow and high-density end limiter) is crushed 3.62 in (92 mm). The simulation predicts more absorption of the kinetic energy in the end impact limiter than observed in the actual drop test. This is due primarily to the assumption in the simulation that the fuel assembly is a rigid mass. For the actual drop test, there was significant energy absorbed in the deformation of the fuel assembly bottom nozzle and fuel rods during the deceleration.

In addition to the comparison of the energy absorbed by the end impact limiter, the axial force required to cause buckling of the axial bottom spacer pipe, P_{cr}, can be estimated using the Euler buckling equation assuming that neither end is fixed (page 115, [16]):

$$P_{cr} = \pi^2 \cdot E \cdot \frac{I}{L^2}$$

where,

E = Modulus of elasticity, 1.00E+07 psi
I = Moment of inertia
L = Length of the column

Using the dimensions from Table 2.12-1, the critical axial force is calculated as follows:

$$I = \frac{\pi}{64}(D^4 - d^4)$$

$$I = \frac{\pi}{64}((6.69\ in)^4 - (5.91\ in)^4) = 38.44\ in^4\ (1.60 \cdot 10^7\ mm^4)$$

where,

D = outer diameter
d = inner diameter

thus,

$$P_{cr} = \pi^2 \cdot 1.00 \cdot 10^7 psi \cdot \frac{38.44\ in^4}{(26.42\ in)^2} = 5.44 \cdot 10^6\ lbf\ (24.2\ kN)$$

Assuming a conservative fuel assembly gross weight of 2,000 lb (907 kg) and a deceleration of 200 g, the maximum load on the spacer would be approximately 400,000 lbf (1,779 kN). This is significantly lower than the critical Euler value calculated for the axial spacer pipe and consistent with the FEA simulation that predicted no buckling of the axial spacer.

2.12.3 Clamshell Removable Top Plate Structural Evaluation

2.12.3.1 Background

The fuel assembly is assumed to be restrained in the Clamshell to prevent any secondary impact within the Clamshell. The spacer below the fuel assembly, when needed, and an axial restraint clamping mechanism restrain the contents to the Clamshell, and as such the Clamshell and contents decelerate as a coupled mass. The top end axial restraint, fuel assembly structure, and/or bottom spacer components may absorb kinetic energy during the deceleration that results from an end drop impact.

Operational experience with the Traveller package revealed that some fuel types could not be loaded or unloaded vertically with existing customer handling tools. In particular, the 17×17 XL fuel with guide pins could not be vertically loaded/unloaded into the Traveller due to an interference between the handling tool and the Clamshell Shear Lip. Figure 2.12-6 shows the 17×17 XL top nozzle with the handling tool attached and fully seated. Figure 2.12-7 shows the potential interference. The tool cannot be installed or removed without tilting the fuel handling tool and potentially damaging the fuel assembly.

Additional evaluation revealed similar interference issues when handling fuel assemblies that included Core Component Assemblies (CCA). A new Clamshell top head configuration was designed to eliminate the interference from the Shear Lip. Both the original Fixed Top Plate (FTP) configuration and an alternate configuration called the Removable Top Plate (RTP) are described in Section 1.

The primary impact with the unyielding surface occurs on the Outerpack end impact limiter. The Outerpack decelerates quickly within a few milliseconds of the primary impact because contact area of the end surface is large and stiff, and there is no significant rebound. The Outerpack is completely decelerated by the time a secondary impact occurs inside the package as the Clamshell, suspended on rubber mounts, continues to fall and contact the inside surface of the end impact limiter.

A crushable foam "pillow" is integrated into the end impact limiter to absorb kinetic energy from the secondary impact between the Clamshell and inside surface of the Outerpack end impact limiter. This pillow is a solid disk made from 6 pcf (0.096 g/cm^3) polyurethane foam. It has a diameter of 12.00 in (305 mm) and a height of 3.60 in (91 mm). The stiffer foam in the Outerpack end impact limiter, with 20 pcf (0.32 g/cm^3) density, is located below and around the soft pillow. This stiffer component end impact limiter functions to decelerate the Outerpack at all high drop angle orientations.

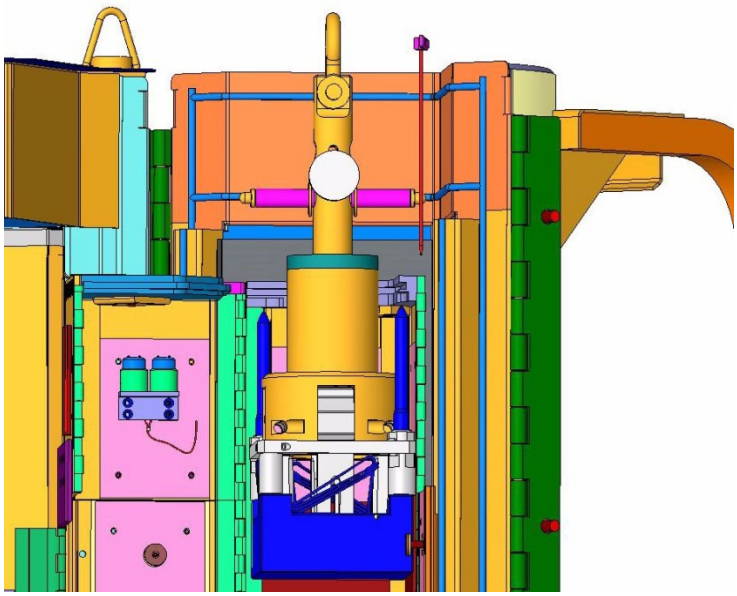

Figure 2.12-6 Fuel Handling Tool Grappled to a 17×17 Top Nozzle (in blue) within the Opened Outerpack and Clamshell

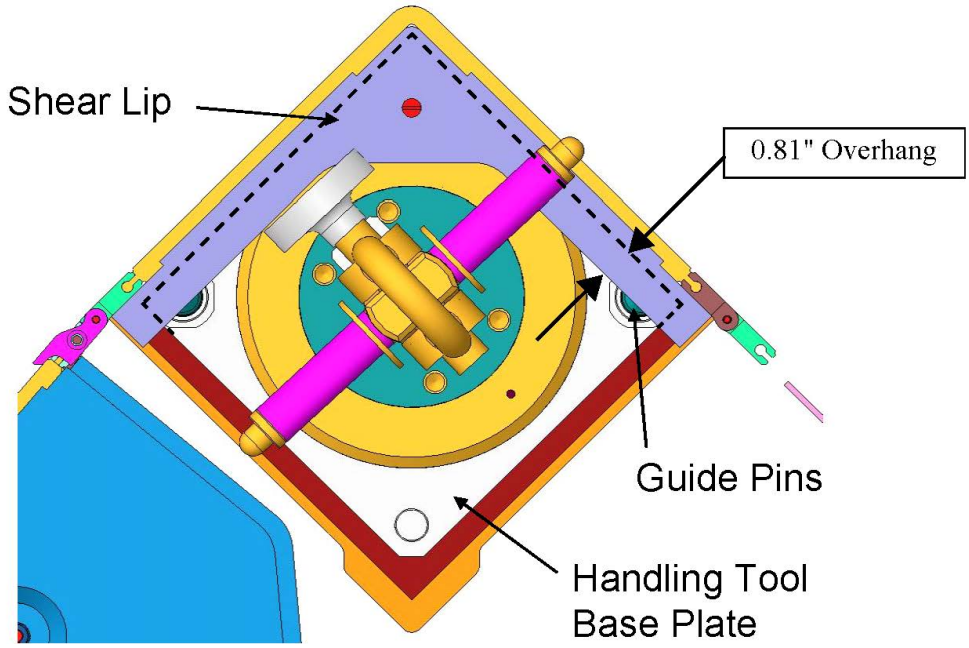

Figure 2.12-7 Fuel Handling Tool Shown Attached to a 17×17 Fuel Assembly and Behind the Overhanging Shear Lip

2.12.3.2 Conclusions

One of the most damaging orientations for the Clamshell and contents during impact is the end over center of gravity. The top-down impact challenges the integrity of the Clamshell's top end plate. End over center of gravity drop testing was performed using a certification test unit (CTU) and simulated using a finite element

(FE) model. Both the actual drop tests and the FE model showed that the FTP design was acceptable. Simulation of the drop test with the RTP shows that this alternate end top plate design is also acceptable.

The screw fasteners that secure the top end plate components to the top access door and Clamshell base are the weakest structure in either the FTP or RTP. These screws resist shear forces resulting from the secondary impact of the fuel assembly or fuel rod box on the top end plate during an end drop. Each screw is a stainless steel flat head cap screw, ½ in (12.7 mm) diameter - 13 threads per inch (1/2-13). These screw fasteners are not subject to large shear forces because the fuel assembly or fuel rod box is restrained in the Clamshell to prevent secondary impact on the end plate.

2.12.3.3 Detailed Calculations and Evaluations

A Traveller XL finite element (FE) model of the entire package was originally used to simulate the impact testing. A new LS-DYNA Traveller model was created to simulate features of the XL package affected by the end impact orientation. The new model is more efficient and was used to evaluate the structural performance of the axial space in the vertical end impact.

2.12.3.4 Method

The Lawrence Livermore, finite element code LS-DYNA® was used to determine the loads, displacements, accelerations, and strains of a Traveller XL shipping package containing a 17×17 XL fuel assembly with RCCA when dropped onto a flat unyielding surface from a height of 32.8 ft (10 m). LS-DYNA 970, Revision 5434a [7], is a general-purpose, finite element code for analyzing the large deformation dynamic response of structures. This software was selected because it allows the analysis to include the effects of large deformation, large strain, material non-linearity, contact, and failure of materials.

Only the top end of the FA is modeled, the remainder of the assembly mass is simulated through point-mass elements. The weight of the remainder of the Clamshell is also modeled with point-mass elements. The Clamshell is an aluminum box with a solid 1-in (25.4 mm) thick top plate. Figure 2.12-8 shows components and meshing for the FEA simulation.

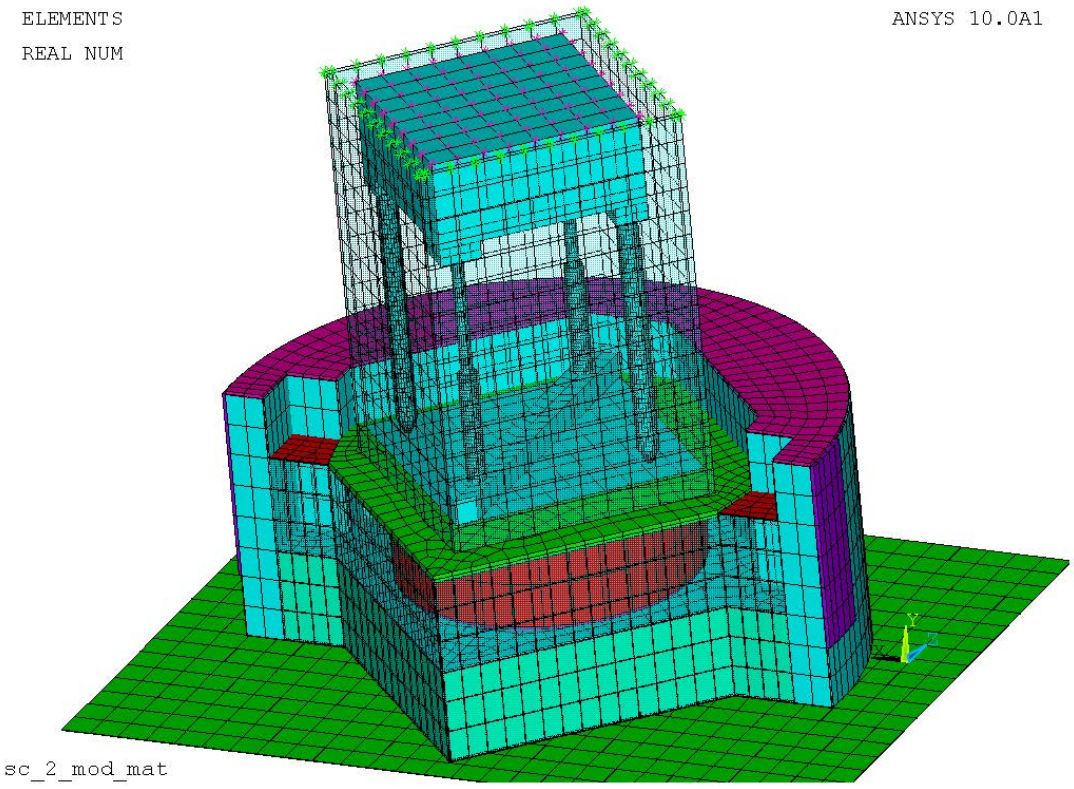

Figure 2.12-8 Traveller Top End Plate FEA Model

2.12.3.5 Calculation Results

The LS-DYNA model was also used to evaluate the maximum shear forces in the shear bar screws (simulated as the shear forces at the interfaces between the top plate and the extrusion walls). The peak shear force of the worst wall (i.e. across 5 screws) still showed a factor of safety of approximately 2.02 using conservative assumptions (i.e. ignoring friction between the wall and the plate for example).

The complete impact event for the RTP design without guide pins is shown in Figure 2.12-9 at various times; a snapshot of the initial impact and impact end events. Figure 2.12-10 shows the rigid wall impact force history of RTP model and Figure 2.12-11 shows the kinetic energy history (MJ) of the axial spacer model.

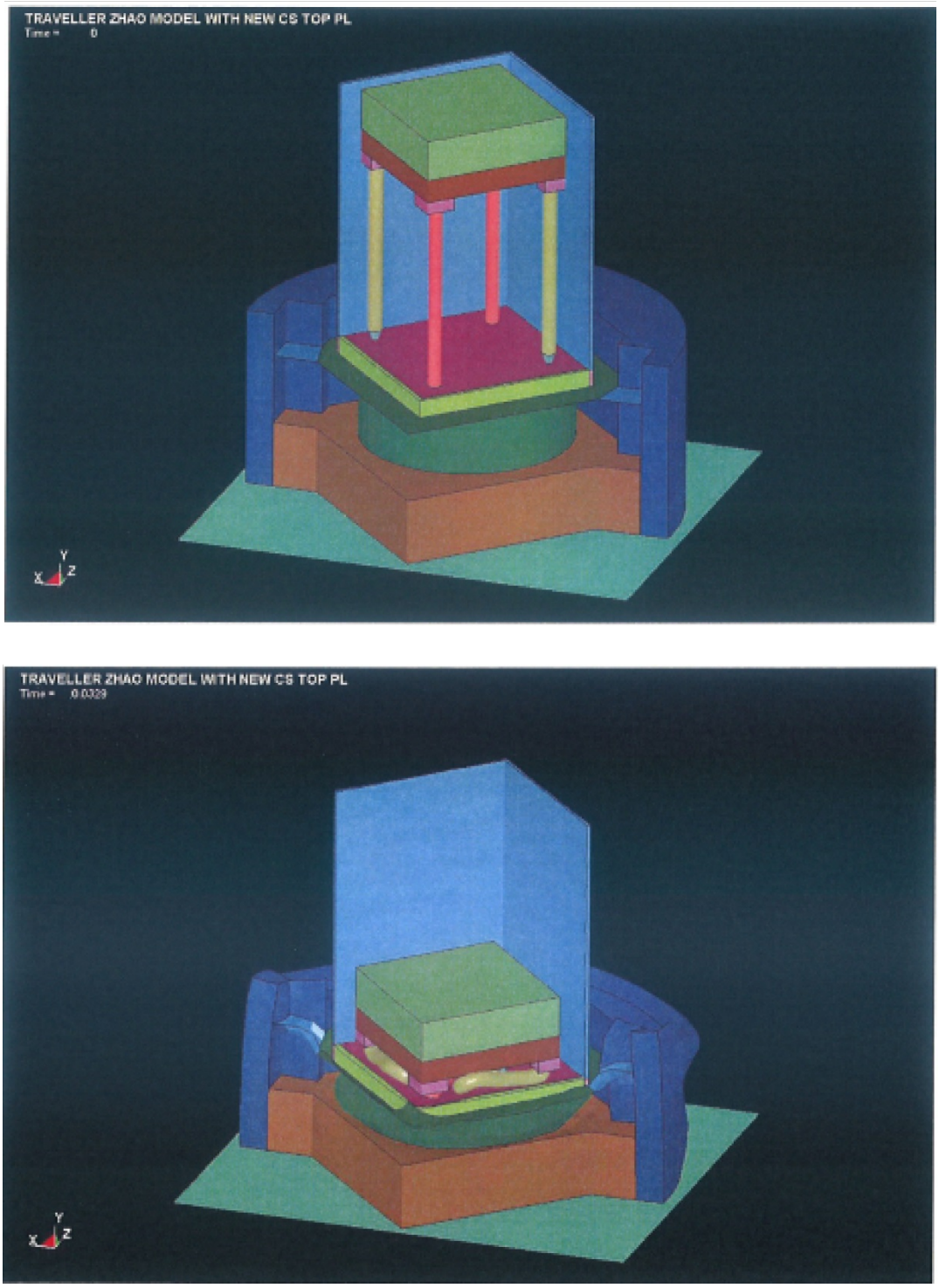

Figure 2.12-9 RTP Model at Beginning of Impact (0 ms) and End of Impact (33 ms)

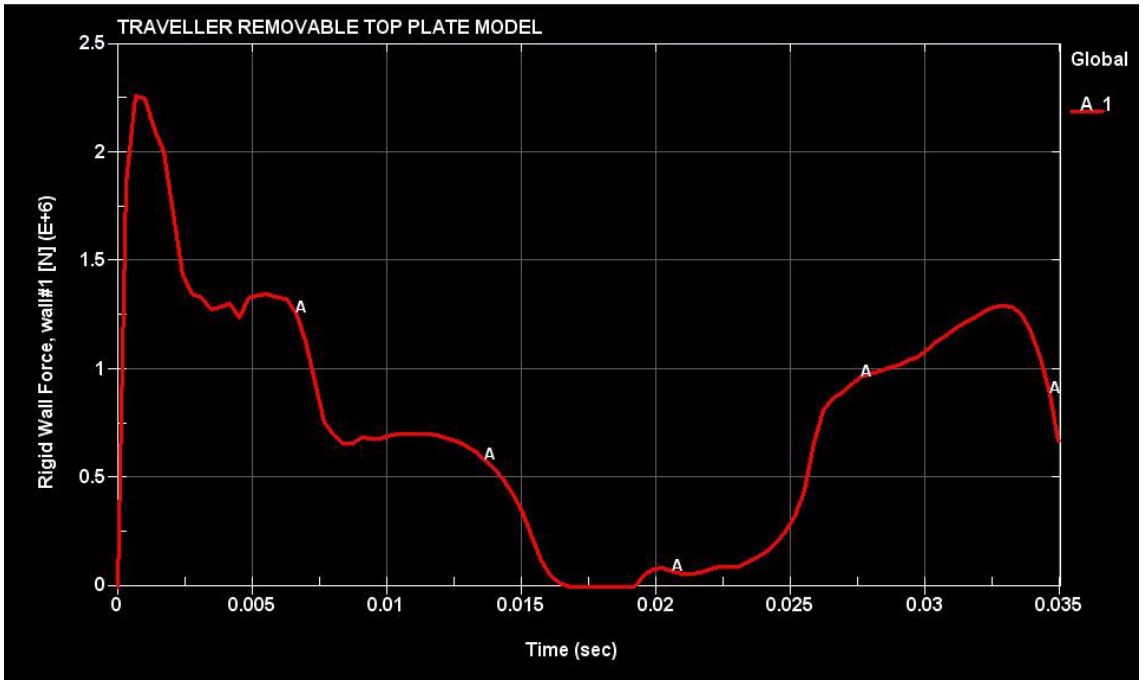

Figure 2.12-10 Rigid Wall Impact Force History of RTP Model

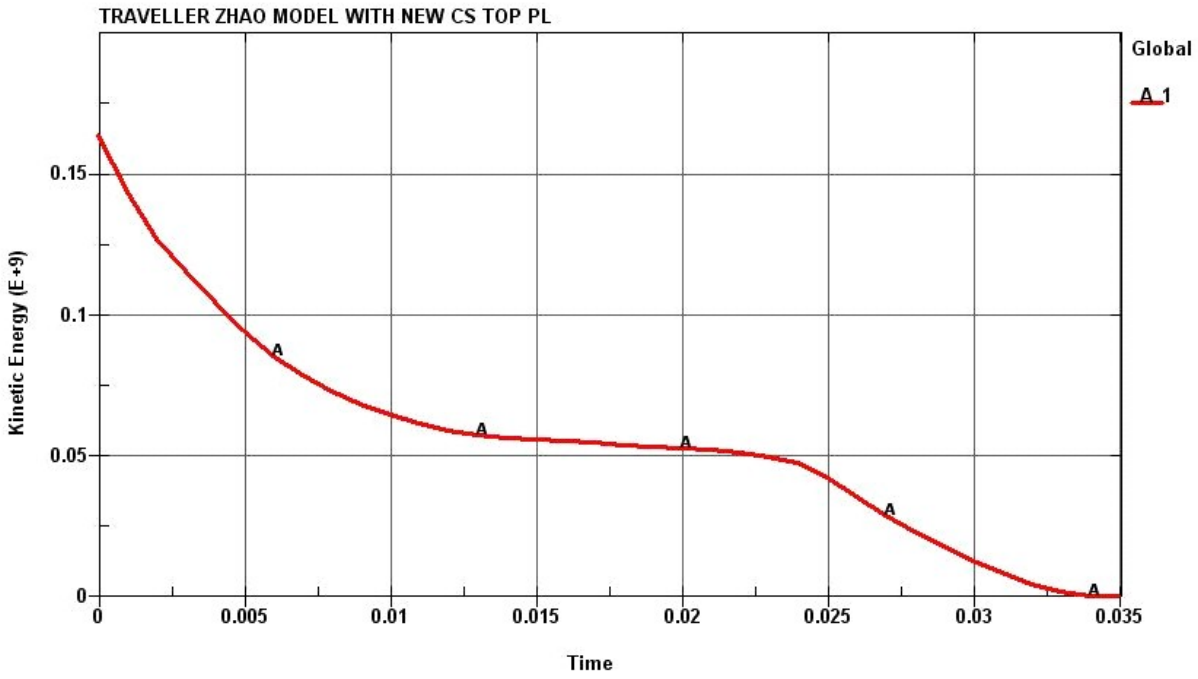

Figure 2.12-11 Kinetic Energy History of RTP Model (MJ vs. s)

2.12.3.6 Validation

The many assumptions used to develop the LS-DYNA non-linear finite element stress code, including those needed to model the materials and impact, are validated by comparing the simulation results to the actual drop tests for the Traveller XL. Comparisons between CTU results and the FEA simulation demonstrate that the physical phenomenon governing shipping package impacts is simulated with adequate fidelity using the LS-DYNA model.

The buckling of the axial clamp studs and the pillow are very similar to the previous drop tests done with the qualification test unit (QTU). Figure 2.12-12 shows good agreement of the computer simulated post-drop deformed shape of the top nozzle compared to the actual dropped nozzle.

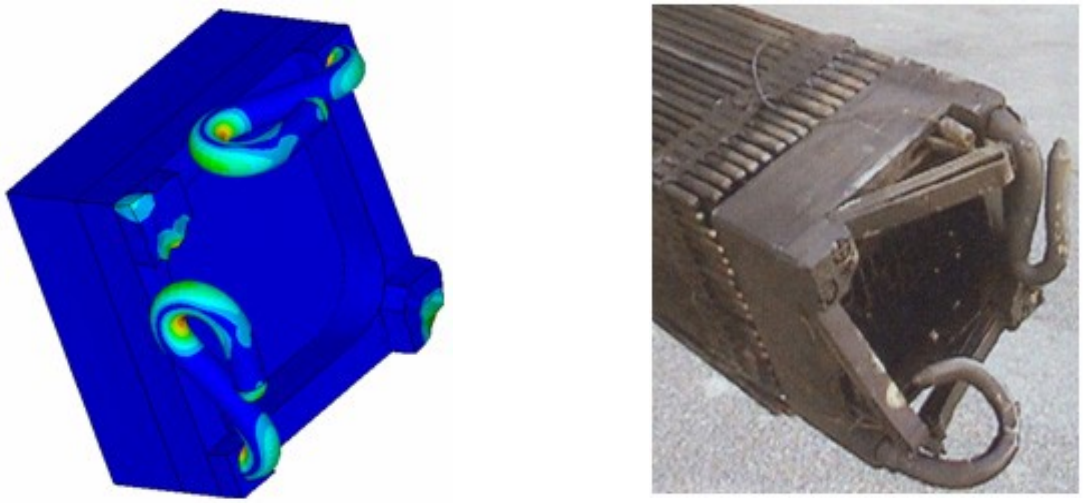

Figure 2.12-12 Comparison of Simulated Top Nozzle Damage (left) to Drop Test (right)

2.12.4 Side Skirted/Four Legged Bottom Nozzle Support Spacer Structural Evaluation

2.12.4.1 Background

Some four legged bottom nozzles are fabricated with side skirts to mitigate debris ingress during reactor operation. The skirt structure is comprised of a flat outer section with an internal pocket. The Type B configuration for side skirted bottom nozzles with four legs is very similar to those four legged bottom nozzles requiring a bottom support spacer and axial clamping mechanisms for the top nozzle. This bottom spacer is a reusable 6000 Series aluminum stiff structure comprised of two-tiers with a solid upper portion and a stiff, voided, lower portion (Figure 2.12-13). The lower tier provides structural support for the four corner legs, and the upper tier provides clearance for the side skirts as well as sufficient thickness to ensure the fuel assembly bottom nozzle flow plate is supported during all transport conditions. A rubber pad is glued to the top of the support spacer to avoid surface scratching, and to ensure the 3/32 inch gap between the bottom nozzle flow plate and rigid support spacer upper surface is occupied. The overall bottom support spacer geometry and length will vary based on fuel assembly type to ensure there is a conforming fit between the fuel assembly bottom nozzle and the support spacer.

A fuel assembly is positioned on top of the bottom support spacer which is placed on top of the Clamshell bottom plate. The fuel assembly bottom nozzle inner structure passes over the top tier, and then the four legs contact the bottom tier as shown in Figure 2.7-21. The top tier is not visible once the fuel assembly is fully seated in the Clamshell. During the hypothetical accident conditions, the bottom support spacer's stiffness ensures that it transfers the package's kinetic energy into the Clamshell structure and then to the Outerpack impact limiter, thus assuring the fuel rods remain leaktight.

Clamping mechanisms that interface with the contents provide axial and lateral restraint during all transport conditions. An adjustable, threaded rod-clamping device provides axial restraint at the top of the fuel assembly. The design of the top axial restraint components, as shown in Figure 2.7-22, includes a fuel restraint and two (2) fuel assembly axial studs, threaded through the RTP. The length and configuration of the top axial restraint components depends on the fuel assembly type.

Physical Type B drop testing (for a bottom nozzle design with four corner support legs) demonstrated that fuel rod failure from eccentric loading can be mitigated by properly supporting the bottom nozzle with a rigid structure. If the bottom nozzle is properly supported, the Outerpack bottom pillow provides sufficient impact protection to preclude failure of the fuel rods in a bottom-end drop. The purpose of this analysis is to present finite element (FE) evaluations of a Type B package configuration with a side-skirted four legged bottom nozzle.

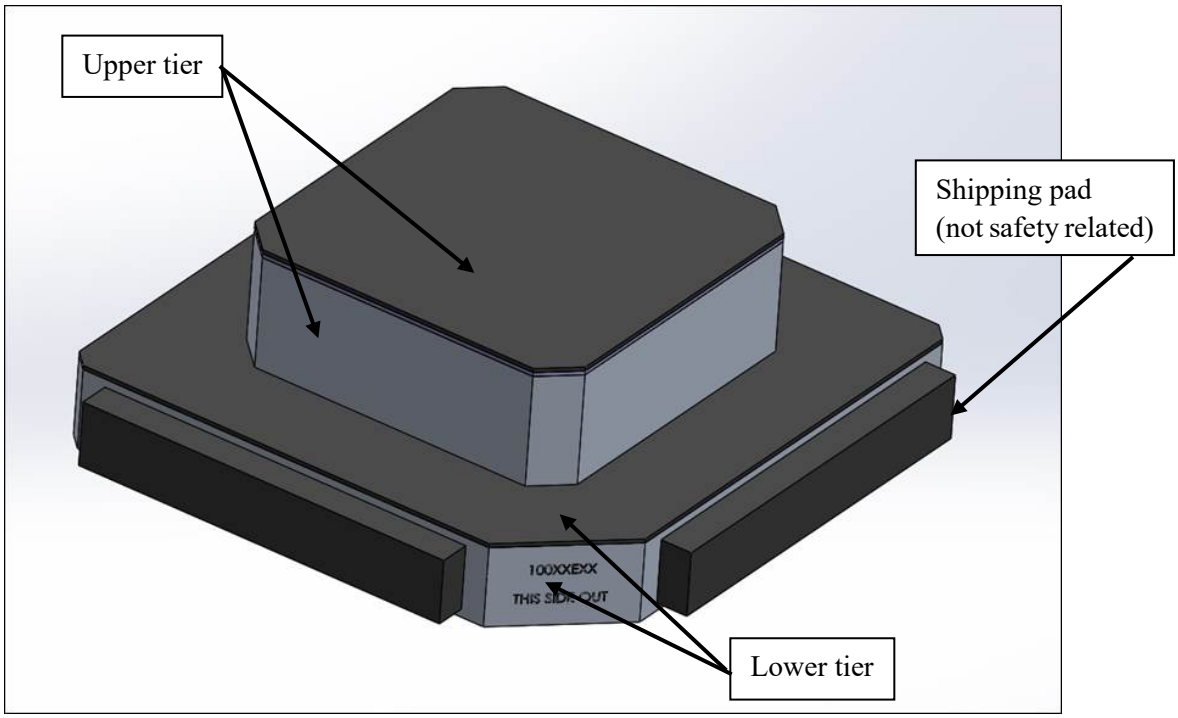

Figure 2.12-13 Bottom Support Spacer for Side Skirted/Four Legged Bottom Nozzles

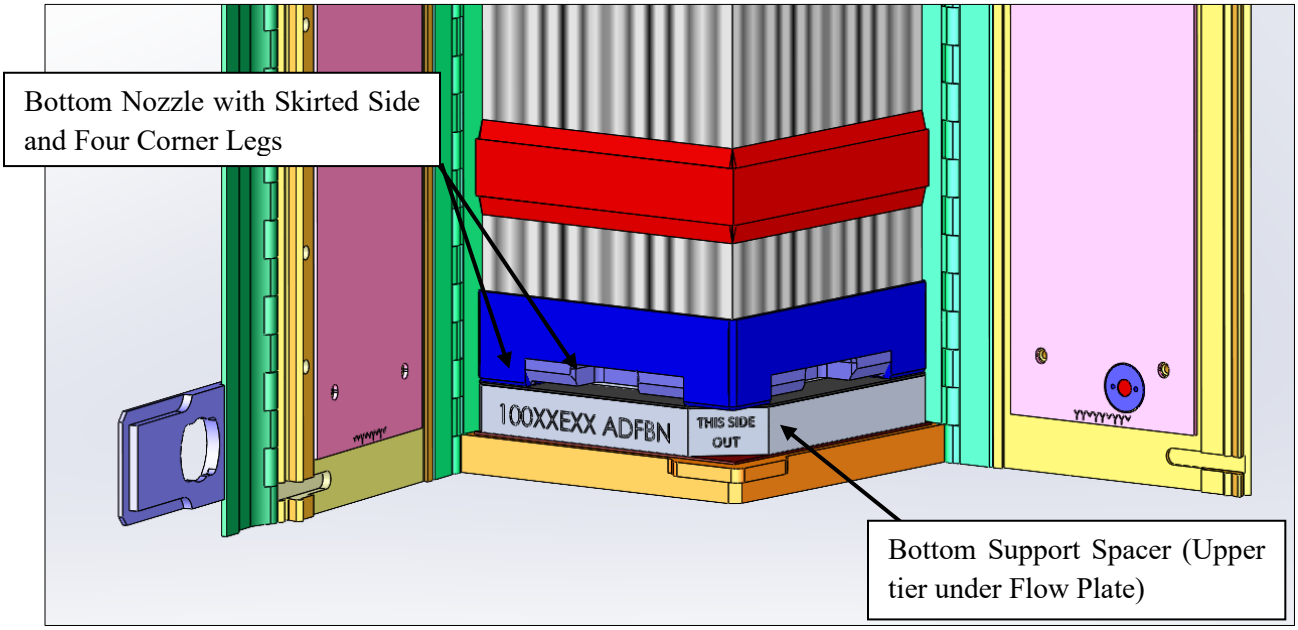

Figure 2.12-14 Fuel Assembly Fully Seated on Two-Tiered Bottom Support Spacer

2.12.4.2 Conclusions

Finite element simulations, using LS-DYNA, showed no buckling nor significant deformation of the four legged, side skirted bottom nozzle, bottom support spacer, nor fuel rods. The bottom-down impact is shown in Figure 2.12-15 at its peak loading (~12 ms) with the Clamshell walls removed for clarity. The figure shows the bottom Clamshell plate crushing into the central portion of the impact limiter. The crush depth in these simulations matches the crush depth of the Type B physical drop test and its original FEA simulation almost exactly. The physical Type B test and subsequent FEA simulation showed a crush of ~92.5 mm (~3.64") as discussed in Section 2.12.4.6. The Type B simulation with the two-tiered bottom support spacer and side skirted, four legged bottom nozzle showed a crush depth of -92.7 mm (~3.65"). These similar results were expected since the same finite element model was used in both simulations, with the only changes being an XL bottom nozzle and XL bottom support spacer were replaced with a side skirted (four legged) bottom nozzle and the two-tiered bottom support spacer.

The results also show the stability of the fuel rods with no buckling for both bottom support spacer designs. The side skirted/four legged bottom nozzle flow plate post simulation geometry indicated no significant deformation or plastic strain since the bottom support spacer essentially acts as rigid members during the impact event.

It is concluded that the strength of this bottom support spacer is adequate to stabilize and support the side skirted, four legged bottom nozzle during a bottom-down impact. As a result, the fuel assembly rods are stable and do not buckle or fail during impact.

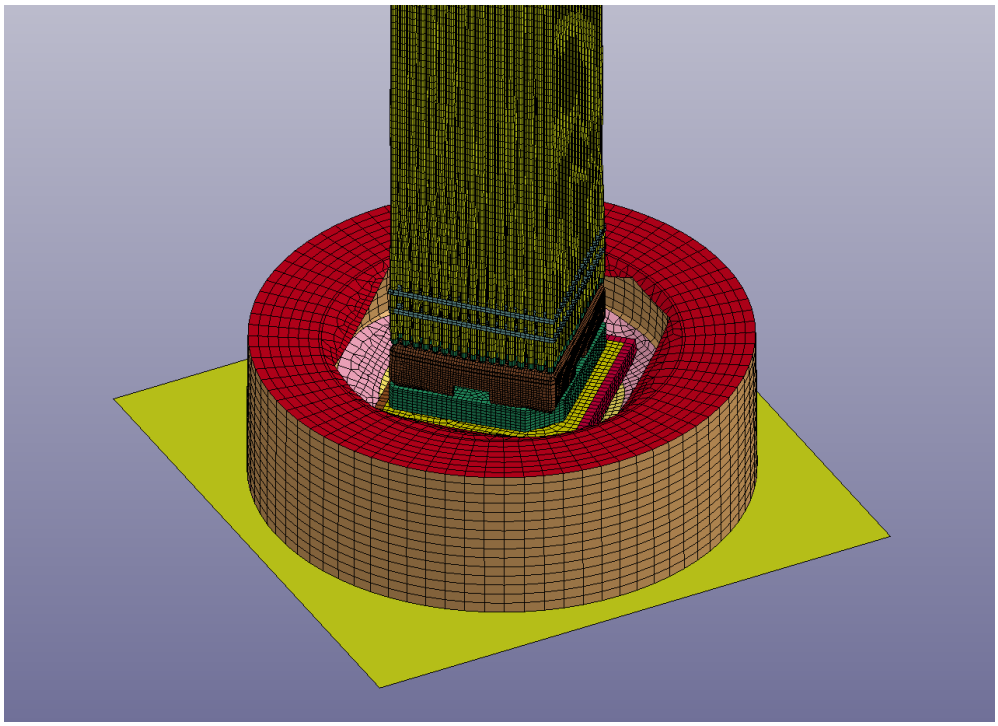

Figure 2.12-15 FEA 9-meter Drop Simulation at Peak Load for Side Skirted/Four Legged Bottom Nozzle with Two-Tiered Bottom Support Spacer (~12 ms)

2.12.4.3 Detailed Calculations and Evaluations

The successful testing and subsequent simulation of the Type B configuration were made possible primarily through the use of the bottom support spacer which prevented the bottom nozzle from distorting during a bottom-down end drop. The rigid aluminum spacer prevents the bottom nozzle flow plate (or adapter plate) from bowing, then completely buckling under the impact load of the fuel rods. This same solution is applied to the Type B variant with a side skirted/four corner legged bottom nozzle. The spacer is made of 6061 aluminum (per ASTM B209), machined from 3.5" plate stock. The base is machined to an 8.50" square, and the upper portion is machined to 5.50" square. Holes are machined into the bottom face to avoid contact with the trip accelerometers and to reduce mass for easier handling, but do not reduce the structural integrity. Upon installation, a nominal intended interference of 3/32" exists between the fuel assembly flow plate (bottom surface) and the bottom support spacer upper metal surface. This gap is taken up by the compression of the 1/8 inch thick foam rubber attached to the top tier metal surface. The four legs contact the lower tier 1/16 inch thin rubber pad for a conformal fit onto the bottom support spacer lower tier portion.

2.12.4.4 Method

In order to simulate a Type B package, it was first necessary to create a benchmarked finite element model that replicated the results of the original CTU drop test (that resulted in fuel rod failure) as well as the Type B testing (that resulted in no fuel rod failure). This was accomplished using LS-DYNA software. With good agreement between the actual CTU drop test and the FEA, that simulation was re-run to compare with the Type B drop results. Since there was excellent agreement between the Type B drop tests and the computer simulation, the FEA model was then updated to include the Type B two-tiered bottom support spacer and the side skirted/four legged bottom nozzle for an XL fuel assembly. This validation process is discussed in Section 2.12.4.6.

These finite element simulations assume that the mass of the fuel pellets is included in the mass of the fuel clad. Additionally, pressure stiffening of the clad is not included in the models. The simulated bottom grid which was included near the bottom of the fuel assembly to more accurately represent the actual grid stiffness was not utilized in this model to optimize computational run time. The agreement between the physical test and FEA results showed the additional support was not needed to stabilize the fuel rods.

The fuel clad density was adjusted to account for the mass of the entire fuel rod, as shown in the FEA models. Only the lowest 40 inches (1,016 mm) was explicitly modeled. The assumption is that elastic and plastic deformations were only observed in the first meter of fuel rod length for the actual drop test fuel assembly, so the remainder of the clad was not explicitly needed in simulations. Furthermore, only the bottom 15 inches (380 mm) of the Clamshells walls were explicitly modeled since those walls do not absorb significant amounts of kinetic energy. The balance of the Clamshell mass was included at the top of these Clamshell walls using mass nodes. The Clamshell walls are known to remain stable based on actual drop testing. Only the bottom of the Outerpack was modeled in the simulations because the impact forces and displacements of the fuel & Clamshell are only affected by the portion of the Outerpack that is in the impact load path. This region of the Outerpack is referred to as the "bottom impact limiter."

The material properties assumed for the aluminum and stainless steel can be seen in Tables 2.12-2 and 2.12-3, respectively. Figure 2.12-16 shows the true stress-strain curve for the Annealed 304SS components, and Figure 2.12-17 shows the bi-linear stress strain curve for the ZIRLO Clad material with failure strain of only 12%. All material properties correspond to ambient temperature. The 6 PCF and 20 PCF foam dynamic crushing characteristics are shown in Figure 2.12-18. Note that the dynamic correction factor of 5.45 is included in these curves.

Table 2.12-2 Aluminum 6005-T5 and 6061-T6 Aluminum at 75 degrees F Properties

Property	Symbol	Value	Units
Density	RO	2.70E-09 (0.10)	Mg/mm^3 (lb/in^3)
Modulus of Elasticity	E	69 (10.2)	kN/mm^2 (MSI)
Poisson's Ratio	PR	0.33	dimensionless
Yield Strength	SIGY	0.24 (34.8)	kN/mm^2 (ksi)
Hardening Modulus	ETAN	0.27 (39.2)	kN/mm^2 (ksi)

Table 2.12-3 Annealed Type 304 Stainless Steel Properties

Property	Symbol	Value	Units
Density	RO	8.00E-09 (2.89E-01)	Mg/mm^3 (lb/in^3)
Modulus of Elasticity	E	195 (28.3)	kN/mm^2 (MSI)
Poisson's Ratio	PR	0.31	dimensionless
Yield Strength	SIGY	0.207 (30)	kN/mm^2 (ksi)

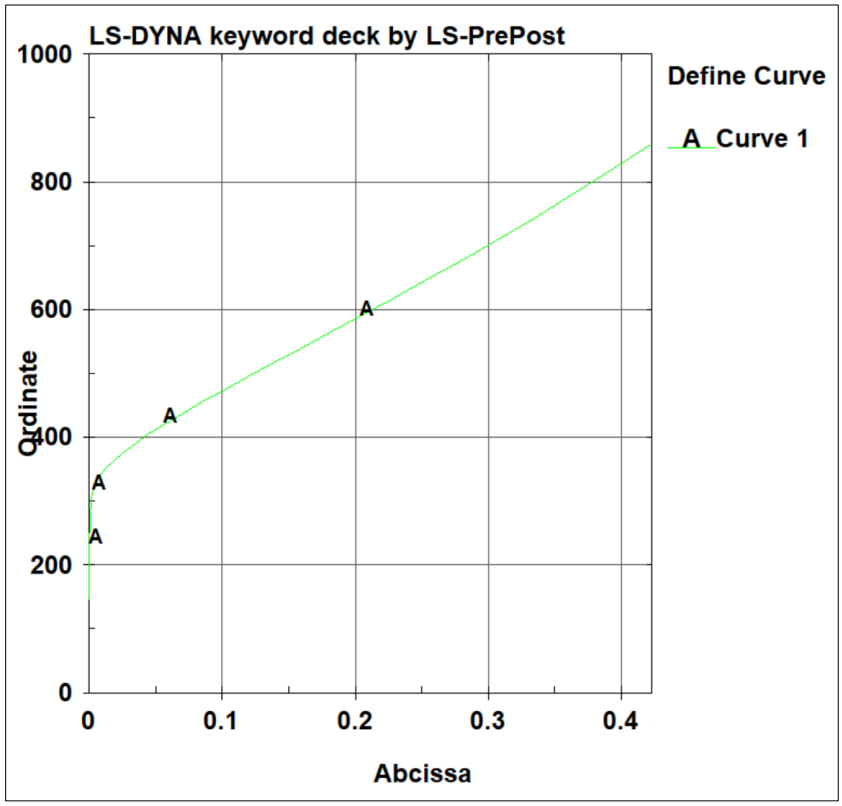

Figure 2.12-16 True Stress-Strain Curve for Traveller 304 Stainless Steel Components (MPa)

[ ]^{a,c}

Figure 2.12-17 Bi-linear Stress-Strain Curve for ZIRLO Fuel Clad (MPa)

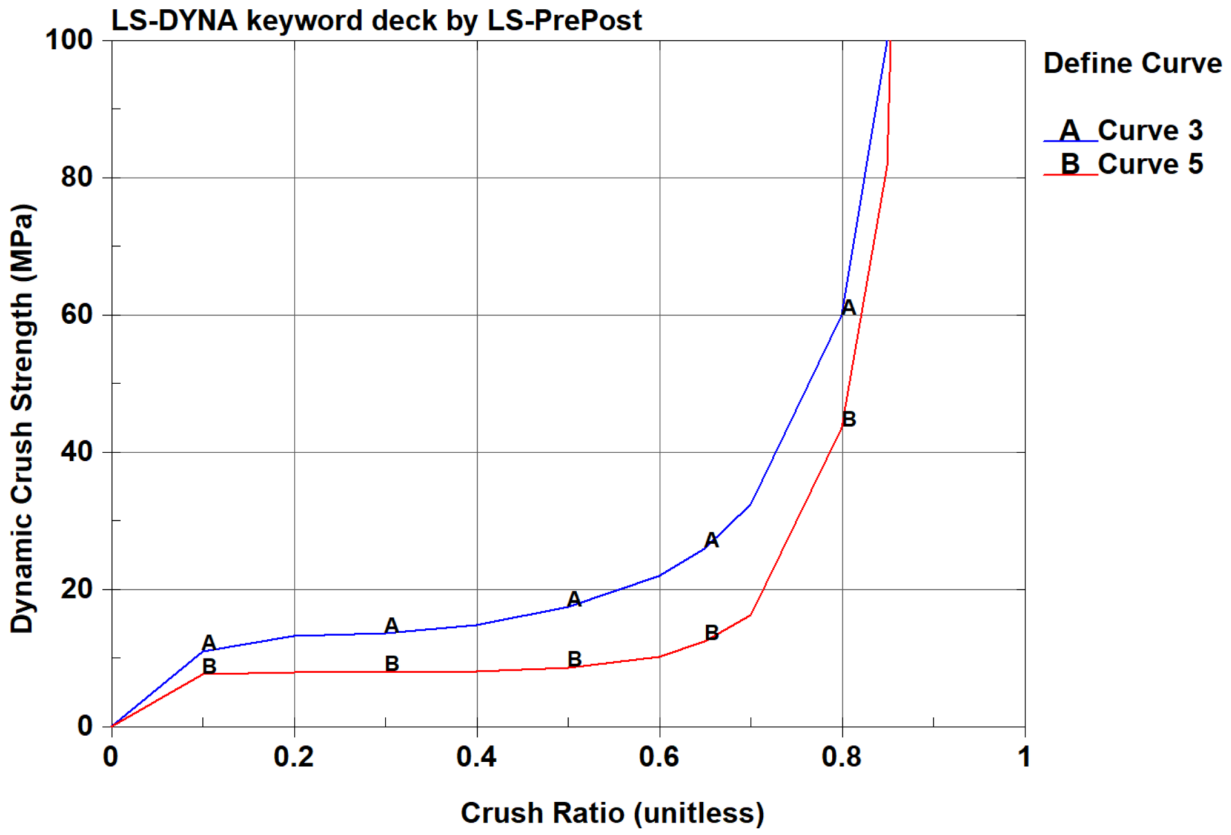

Figure 2.12-18 6 PCF Pillow (Curve B) & 20 PCF Limiter (Curve A) Dynamic Crush Strength

2.12.4.5 Calculation Results

For this evaluation, the Type B finite element model was modified by simply replacing the 17 XL bottom nozzle and single piece bottom support spacer with a side skirted, four legged bottom nozzle and its corresponding bottom aluminum two-tiered support spacer. The results were not expected to change in any significant way since a fitted rigid support spacer prevents buckling of the bottom nozzle and therefore eliminates fuel rods to buckling since the bottom nozzle flow plate does not deform. This new simulation results match the original Type B (for four legged bottom nozzles without side skirts) results very closely as demonstrated by the pillow crush plate depth and no fuel rod buckling from Figures 2.12-15 and 2.12-28.

The kinetic, internal, and total energy plot (Joules vs seconds) for the side skirted, four legged bottom nozzles is shown in Figure 2.12-19. Minimum energy occurs at approximately 12 milli-seconds. Note that all hourglass and sliding energy losses are minimal in the total energy curve. This kinetic energy plot is virtually identical with the Type B simulation (for the four legged bottom nozzle) when Figure 2.12-15 is compared to Figure 2.12-28.

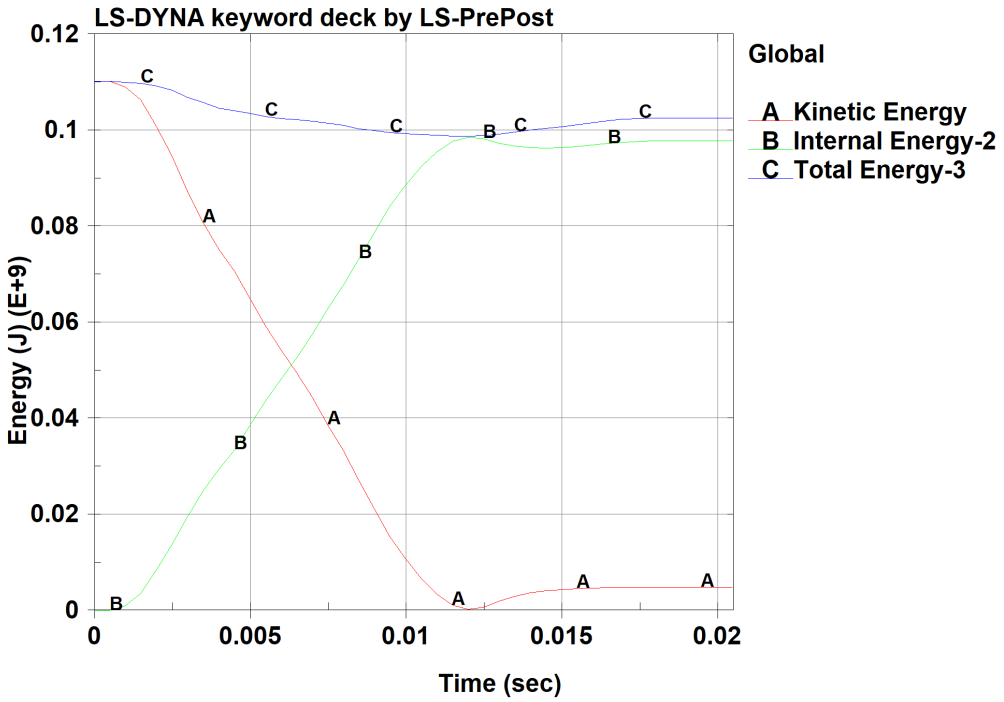

Figure 2.12-19 Kinetic Energy Plot of Type B Simulated Impact for Side Skirted/Four Legged Bottom Support Spacer

Figure 2.12-20 shows the resultant pillow crush plate displacement of this bottom support spacer. The figure details four nodes' (42, 59, 472275, and 472504; randomly picked) displacement on the Pillow crush plate which are displaced toward the ground in the impact. The approximate average Y-displacement of these nodes is -92.7 mm (~3.65 inches). Therefore, the stopping distance, d, is 3.65 inches or 0.304 feet. When comparing with the physical Type B drop test and the subsequent simulation, there is excellent agreement; the original Type B simulation crush depth is 3.64 inches as presented in Section 2.12.4.6.2.

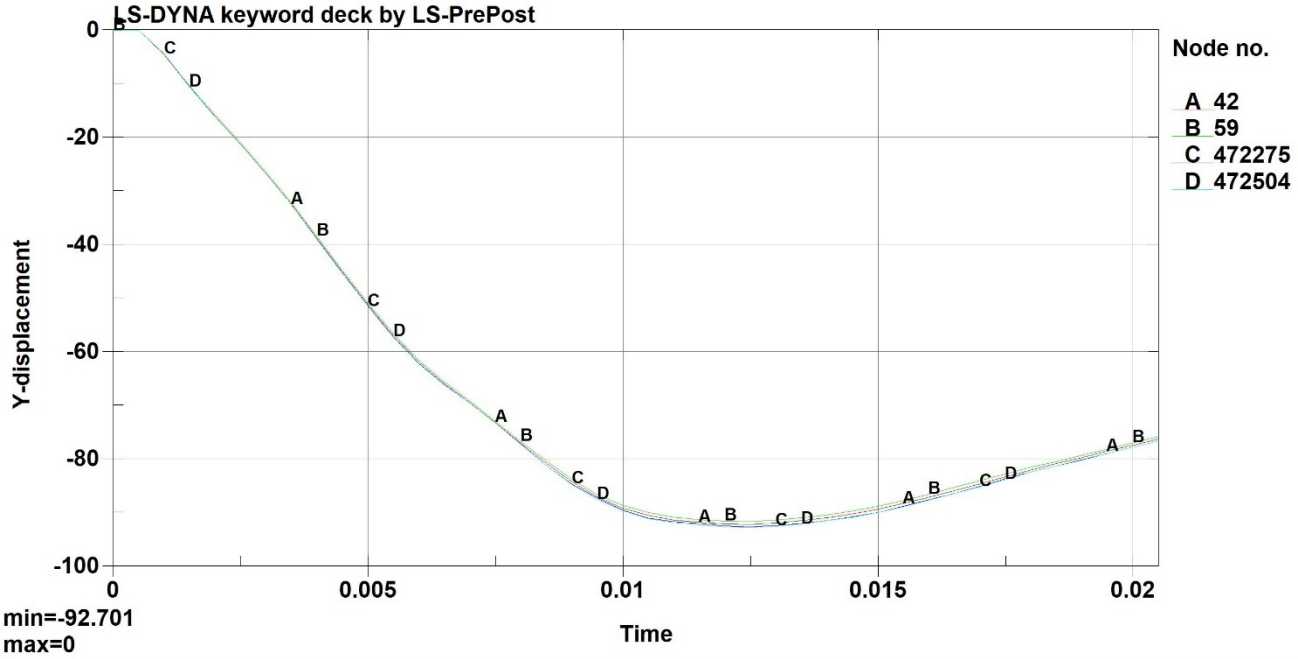

Figure 2.12-20 Y-Displacement of Pillow Crush Plate (mm vs sec)

The average impact deceleration, or impact g's, is also of great significance, as this quantifies the expected impact deceleration force and also allows for comparison against previous physical tests and their computer simulations. The bottom support spacer prevents the bottom nozzle from buckling and in turn it prevents fuel rods from buckling as was shown by Type B testing with a replica fuel assembly and a bottom support spacer. The energy that was absorbed in these fuel assembly components during the CTU impact (and resulted in cracked fuel rods at the bottom end plug heat affected weld zone) is now forced into the Pillow crushing and the limiter foam crushing. This increased energy into the Pillow translates into increased crush depth and therefore longer deceleration distance to stop. This means the average impact g's are significantly lower than CTU results as demonstrated by the physical Type B drop test results, and also by subsequent computer simulations that benchmarked the actual drop tests.

The impact velocity of this Type B model was set to correspond to a 10.06 m (33.1 ft) free drop, resulting in a final velocity value of 14.05 m/s, or 46.1 ft/s. The average impact g's on the Clamshell and fuel are calculated using the equation:

$Vf^2 = Vi^2 - 2ad$
where:
Vf = final velocity or 0 ft/s
Vi = initial velocity or 46.1 ft/sec
a = average deceleration in ft/sec^2
d = stopping distance or Pillow crush depth (ignores limiter crush)

Solving the equation above for "a" gives:
$a = - (Vf^2 – Vi^2) / 2d$
$a = - (0^2 – 46.1^2) / (2 \times 0.3035)$
$a = - 3501\ ft/sec^2$

If we divide by 32.2, we can see the equivalent impact "g's."

Average Impact g's = 108 g's

This value is the same as the first Type B simulation described below in Section 2.12.4.6.2. The agreement with the validated and benchmarked Type B fuel assembly with four legged bottom nozzle and its associated bottom support spacer with respect to pillow crush depth, calculated deceleration force, and also the fuel assembly and fuel rod structural stability (no deformation or buckling), demonstrates that the bottom support spacer used in conjunction with the side skirted, four legged bottom nozzle provides structural adequacy during transport conditions.

2.12.4.6 Validation

Prior to performing the finite element analysis for the side skirted, four legged bottom nozzle with a Traveller XL fuel assembly (maximum mass) and its associated bottom support spacer, a benchmarked FE model was developed for the Type B physical drop test based upon the CTU physical drop test.

2.12.4.6.1 Type B FEA Model Development

The most critical aspect of the CTU simulation was that it be able to replicate the fuel rod failures that were observed in the actual CTU bottom-down 9-meter hypothetical drop. A total of 20 fuel rods were broken at the weld interface between the fuel rod clad and bottom end plug (BEP). The bottom nozzle was severely plastically deformed and several fuel rods were buckled near the corners. As a result of cracked rods, this orientation was determined to be the most challenging to the fuel. The root cause of the cracked rods was determined to be side forces generated by a buckling bottom nozzle flow plate. Upon further investigation it was found that the impact limiter pillow had only crushed approximately 1.8 inches, or about one-half of the available crush stroke length. The subsequent time reduction to decelerate coupled with buckled bottom nozzle legs resulted in eccentric loading at the BEP and mechanical failure.

A finite element model of the CTU was developed to benchmark the drop test parameters so that structural solutions could be evaluated that would eliminate fuel rod cracking and bottom nozzle buckling. Figure 2.12-21 shows the FE model developed and includes fuel rods, the bottom nozzle and the required XL fuel assembly mass. For additional conservatism, only two lower grids are included in the computer simulation. The drop velocity of the computer model was set to 10.06 m which results in a free drop impact velocity of 14.05 m/s, or 46.1 ft/s.

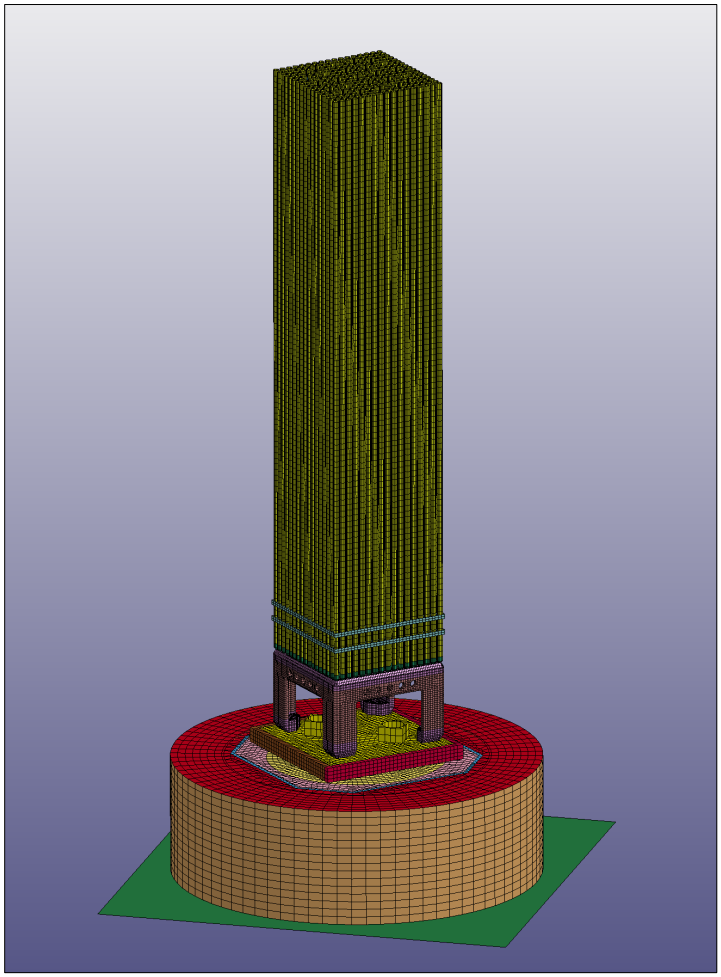

Figure 2.12-21 Traveller CTU Model Developed for FEA (Clamshell Walls Removed for Clarity)

The results of the computer simulation were in excellent agreement with the physical drop tests. Figure 2.12-22 shows the computer simulation on the left and the physical test results on the right. Furthermore, the bottom nozzle flow plate deformed geometry compared well with the actual post-test deformed bottom nozzle flow plate as shown in Figure 2.12-23.

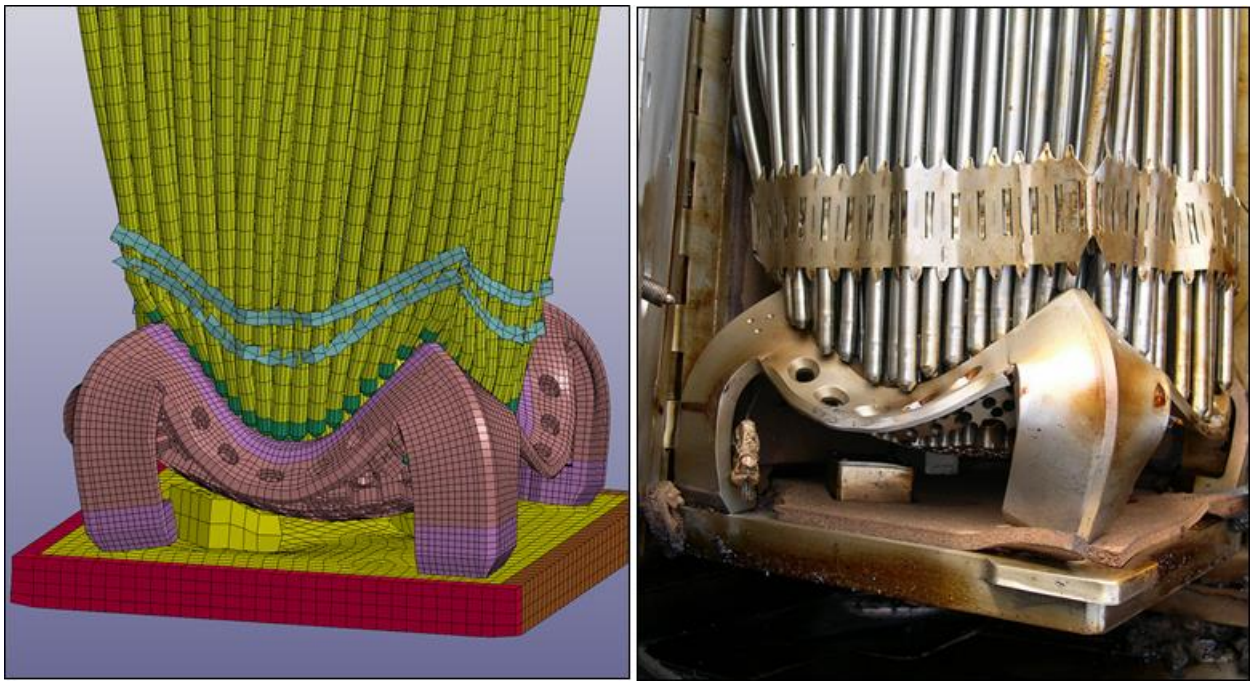

Figure 2.12-22 CTU Model and Actual Bottom Nozzle Deformed Shape After Impact

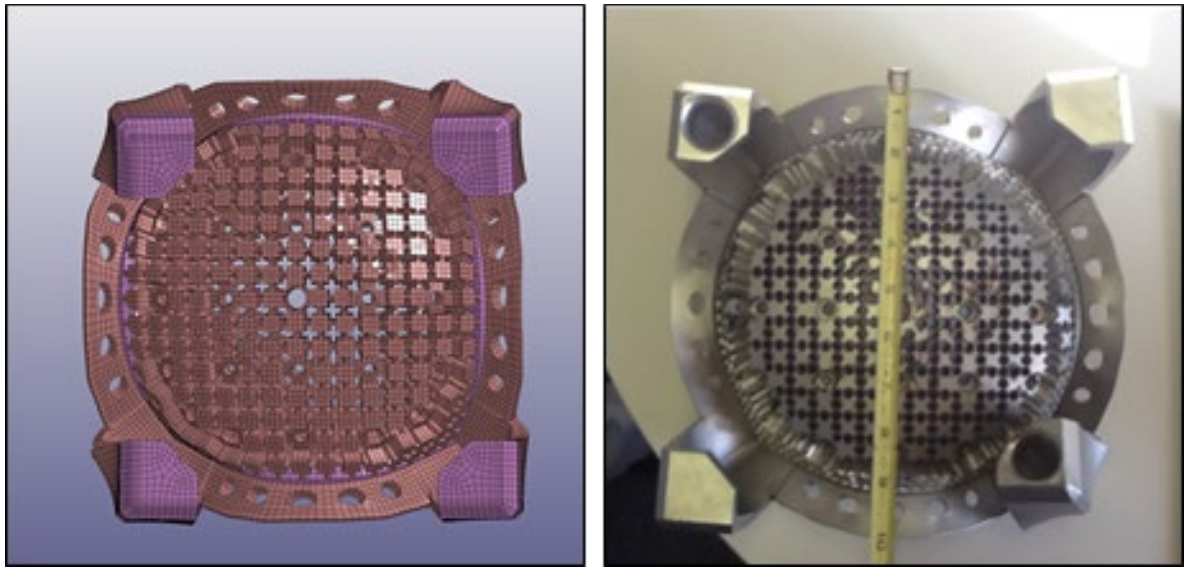

Figure 2.12-23 CTU Model and Actual Bottom Nozzle Deformed Shape After Impact (Bottom View)

The impact deceleration of the fuel assembly/Clamshell are also key factors in benchmarking the FE model simulation because the fuel rods can buckle and plastically deform if the deceleration g's are excessive. The weakest component in the load path at impact is the impact pillow that readily crushes during the event. The foam is manufactured by General Plastic and has carefully controlled material and thermal properties. At 6 lb/ft^3, the Pillow foam crushes approximately half of its original thickness during the drop, or 1.8 inches.

The CTU FE model results in a 1.61 inch Pillow foam crush, which is excellent agreement.

If the deceleration is assumed to be constant, then the average impact g's experienced by the fuel/Clamshell is ~195-220 g's (corresponding to 1.8" and 1.61" impact depth, respectively). The fact that the Pillow crushes approximately the same amount for both the actual test and the simulation demonstrates that the computer model simulation is benchmarked against the physical tests.

With good agreement between the actual CTU drop results and the computer simulation, the FEA model was then updated to include the bottom support spacer component and then re-run to simulate how a Type B model would perform. Figure 2-12.24 shows the bottom support spacer (in green) under the fuel assembly and the XL four legged bottom nozzle. The final step was to perform the physical drop test with the Type B Clamshell containing 17x17 XL fuel assembly and bottom nozzle, and then compare results to the FEA simulation.

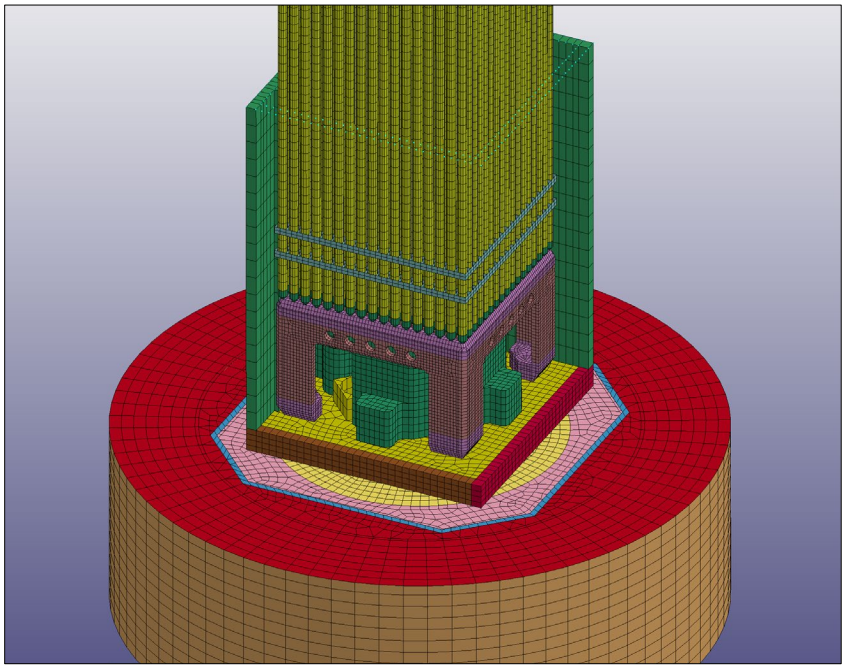

Figure 2.12-24 Type B Model for XL Fuel Assembly with Four Legged Bottom Nozzle Including Bottom Support Spacer

2.12.4.6.2 Type B FEA Model Validation

After successful Type B drop test (all fuel rods tested leak free), the Type B drop test computer simulation was completed. The simulation results were compared against physical test results for the fuel assembly bottom nozzle and fuel rods, as well as the impact limiter pillow crush depth to calculated resultant deceleration force. The Type B finite element model (shown without the support spacer) with its constituents is in Figure 2.12-25. Solid element types utilize both the default "constant stress solid element" for the Clamshell walls and foam components, and the fully integrated solid element type for the bottom nozzle.

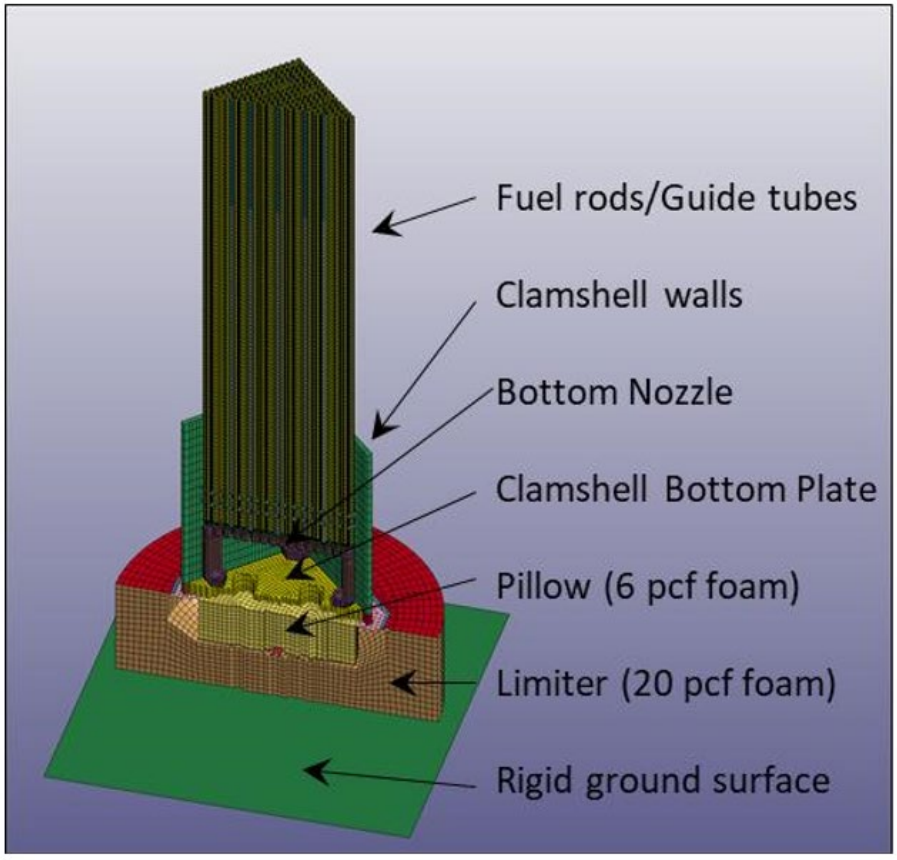

Figure 2.12-25 Type B Model for Drop Simulation (Support Spacer not Shown)

The drop height of the Type B model was set to 10.06 m which results in a free drop impact velocity of 14.05 m/s, or 46.1 ft/s. Figure 2.12-26 shows the kinetic, internal, and total energy plot (Joules vs seconds) of the Type B finite element simulation. Minimum energy occurs at approximately 12 milli-seconds. Note that all hourglass and sliding energy losses are minimal in the total energy curve. Figure 2.12-27 shows four nodes on the Pillow crush plate which are displaced toward the ground in the impact (i.e. nodes: 42, 59, 472275, and 472504). The approximate average Y-displacement of these nodes is -92.5 mm (~3.64 inches). Therefore, the stopping distance, d, is 3.64 inches or 0.3035 feet.

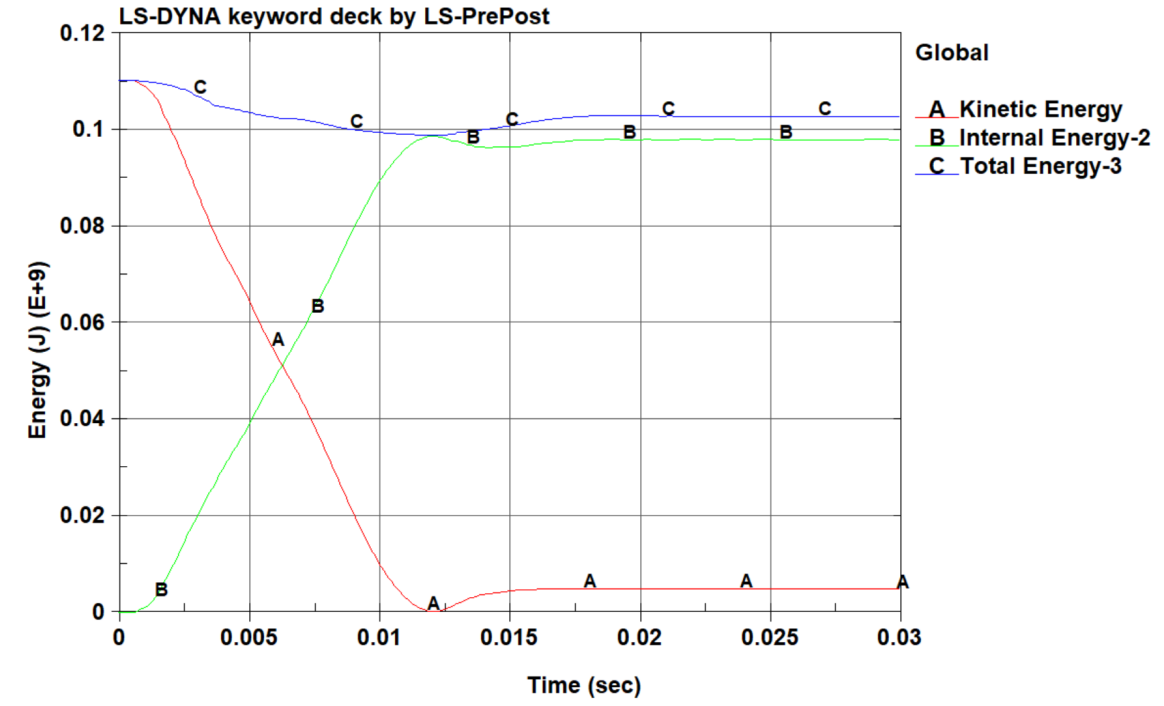

Figure 2.12-26 Kinetic Energy Plot of Type B Simulated Impact (J vs sec)

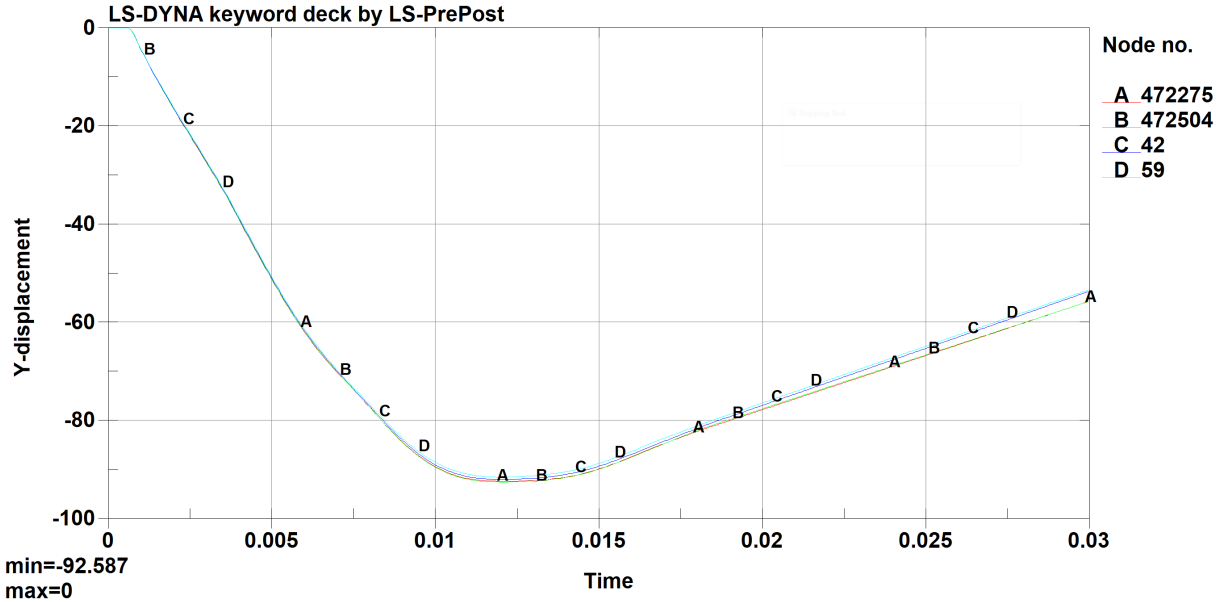

Figure 2.12-27 Y Displacement of Nodes on Pillow Crush Plate (mm vs sec)

The average impact g's on the Clamshell and fuel are calculated using the equation:

$Vf^2 = Vi^2 - 2ad$
where:
Vf = final velocity or 0 ft/s
Vi = initial velocity or 46.1 ft/sec
a = average deceleration in ft/sec^2
d = stopping distance or Pillow crush depth (ignores limiter crush)

Solving the equation above for "a" gives:
$a = - (Vf^2 – Vi^2) / 2d$
$a = - (0^2 – 46.1^2) / (2 \times 0.3035)$
$a = - 3501\ ft/sec^2$

If we divide by 32.2, we can see the equivalent impact "g's."

Average Impact g's = 108 g's

This value is quite low and is about half of the average g's experienced by the CTU impact. The Pillow crushing of the actual Type B Full Scale Regulatory drop test measured approximately 3.4 inches; therefore, the model simulation is in good agreement with actual testing.

The post drop actual 17x17 XL fuel assembly is shown below in Figure 2.12-28 (see left side image). The Clamshell doors have been opened and the bottom limiter assembly is not included. The right half of Figure 2.12-28 shows the corresponding post drop simulation of the Type B LS-DYNA model. The spacer is shown by green elements. The Clamshell walls have been removed for clarity. No fuel rods buckled nor did the bottom nozzle experience any significant buckling and are fuel rods were tested to be leak-free.

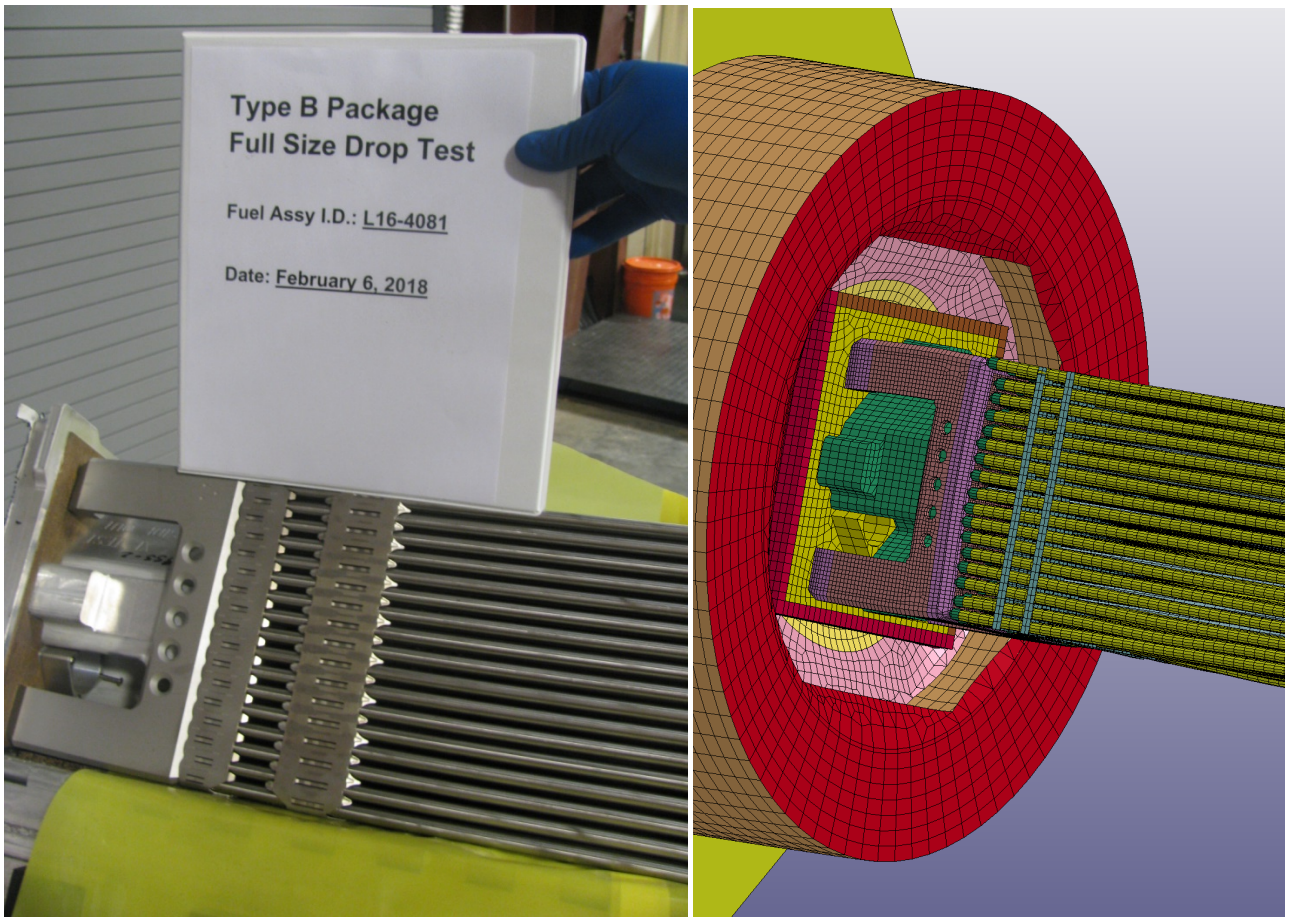

Figure 2.12-28 Fuel Assembly After Drop (Left) and Type B Model After Simulated Drop

TABLE OF CONTENTS

3.0 THERMAL EVALUATION 3-1
3.1 DESCRIPTION OF THERMAL DESIGN 3-1
3.1.1 Design Features 3-1
3.1.2 Contents Decay Heat 3-2
3.1.3 Summary Table of Temperatures 3-2
3.1.4 Summary Maximum Pressures 3-2
3.2 MATERIAL PROPERTIES AND COMPONENT SPECIFICATIONS 3-3
3.2.1 Material Properties 3-3
3.2.1.1 Cladding Materials 3-4
3.2.2 Component Specifications 3-6
3.3 THERMAL EVALUATION UNDER NORMAL CONDITIONS OF TRANSPORT 3-7
3.3.1 Heat and Cold 3-7
3.3.2 Maximum Normal Operating Pressure 3-7
3.4 THERMAL EVALUATION UNDER HYPOTHETICAL ACCIDENT CONDITIONS 3-9
3.4.1 Initial Conditions 3-9
3.4.2 Fire Test Conditions 3-9
3.4.2.1 Fire Test Setup 3-9
3.4.2.2 Fire Testing 3-11
3.4.2.3 Post-Fire Analysis 3-12
3.4.2.4 Moderator Block Examination 3-18
3.4.2.5 Summary of Results 3-21
3.4.3 Maximum Temperatures and Pressures 3-21
3.4.3.1 Maximum Temperatures 3-21
3.4.3.2 Maximum Pressures 3-21
3.4.4 Maximum Thermal Stresses 3-23
3.4.5 Accident Conditions for Fissile Material Packages for Air Transport 3-23
3.5 APPENDICES 3-24
3.5.1 References 3-25
3.5.2 Traveller Thermal Evaluation by Analysis 3-26

LIST OF TABLES

Table 3.1-1 Summary Table of Temperatures for Traveller Materials 3-2
Table 3.2-1 Thermal Properties of Key Traveller Materials 3-3
Table 3.2-2 Thermal Properties of Key Fuel Assembly Materials 3-4
Table 3.4-1 Summary of Recorded Temperatures During Burn Test 3-14
Table 3.4-2 Optical Thermometer Data Sheet (West Side, °C) 3-18
Table 3.4-3 Optical Thermometer Data Sheet (East Side, °C) 3-18
Table 3.4-4 Moderator Block Weights 3-19
Table 3.5-1 Temperature-Dependent Thermal Conductivity Used to Model Polyurethane Foam 3-27

LIST OF FIGURES

Figure 3.2-1 Burst Temperature Versus Internal Pressure for Chromium-Coated Optimized ZIRLO, STD ZIRLO and Optimized ZIRLO 3-6
Figure 3.4-1 Thermocouple Locations Measuring Fire Temperature During CTU Burn Test 3-10
Figure 3.4-2 Pool Fire Test Setup 3-10
Figure 3.4-3 Orientation of CTU for Thermal Test 3-11
Figure 3.4-4 Traveller CTU During Pool Fire Test 3-11
Figure 3.4-5 Fire Suppression System Engaged 3-12
Figure 3.4-6 Polyurethane Char in Outerpack Seam After Burn Test 3-13
Figure 3.4-7 Brown Polyurethane Residue Inside Outerpack After Burn Test 3-13
Figure 3.4-8 Location and Indicated Temperatures of Temperature Strip Sets 3-14
Figure 3.4-9 Fire Temperatures Measured at the Corners of the Pool 3-15
Figure 3.4-10 Data from Direction Flame Thermometers (DFTs) 3-16
Figure 3.4-11 Skin Temperature Data from East Side of CTU 3-16
Figure 3.4-12 Skin Temperature Data from West Side of CTU 3-17
Figure 3.4-13 Fire Temperature Data from East Side of CTU 3-17
Figure 3.4-14 Fire Temperature Data from West Side of CTU 3-17
Figure 3.4-15 Location of Possible Combustion of Moderator 3-20
Figure 3.4-16 Localized Melt Spot in Lid Moderator Block 3-20
Figure 3.4-17 Burst Temperature versus Internal Pressure for Zircalloy Cladding 3-22
Figure 3.5-1 Approach Used to Generate Analytical Model Geometry 3-26
Figure 3.5-2 Calculated Radial Temperature Distribution for 30 Minute Fire (800°C) 3-28
Figure 3.5-3 Calculated Radial Temperature Distribution for 30 Minute Fire (1000°C) 3-29

3.0 THERMAL EVALUATION

This section evaluates the thermal performance of the Traveller package for the normal conditions of transport (NCT) and hypothetical accident conditions (HAC). The Traveller package is designed transport low-enriched uranium, nuclear reactor fuel assemblies, which do not generate heat.

3.1 DESCRIPTION OF THERMAL DESIGN

3.1.1 Design Features

The Traveller package utilizes an aluminum Clamshell with BORAL neutron poison plates to hold a single fuel assembly. The Clamshell is mounted within a cylindrical Outerpack fabricated from 304 stainless steel and flame-retardant polyurethane foam. The stainless steel/foam composite provides thermal insulation during the NCT and HAC. Most of the heat capacity is within the Outerpack, provided by the polyethylene moderator, the aluminum Clamshell and the fuel assembly itself, reducing the peak temperatures within the package.

The fuel rods, which contain the radioactive material, are designed to withstand temperatures of 1,204°C (2,200°F) without substantial damage. The primary packaging temperature limitation is the ultra-high molecular weight (UHMW) polyethylene moderator located on the inside surface of the Outerpack. UHMW Polyethylene was selected for use as a moderator because it retains its chemical composition and therefore its hydrogen content past the melting temperature. Because of its very high viscosity, it will not flow significantly and will not change chemical composition unless subject to a high temperature oxygen atmosphere.

Predictive NCT thermal analysis results show that heat transfer due to conduction and radiation is sufficiently low enough where temperatures within the Outerpack are below the temperature at which materials degrade. Therefore, the Traveller package meets the NCT thermal requirements. The NCT discussion is provided in Section 3.3.

To qualify the Traveller package for the HAC, two Qualification Tests Units (QTU) of the Traveller were built subjected to drop testing and subjected to multiple tests. The information obtained from these tests was incorporated into the Traveller Certification Test Unit (CTU) testing program. The CTU was subjected to drop testing, as described in Section 2.7 and burned in accordance with 10 CFR 71.73(c)(4) [1] and SSR-6 para. 728(a) [2]. The package survived the test with maximum internal temperatures less than 180°C (356°F). Therefore, the Traveller package meets the HAC performance requirements. The results of this test are described in Section 3.4.

3.1.2 Contents Decay Heat

The content is a fresh fuel assembly or fuel rods, and thus the decay heat is insignificant (< 1 Watt) and not applicable for the Traveller package.

3.1.3 Summary Table of Temperatures

The maximum temperatures that affect structural integrity, containment, and criticality for the NCT and HAC are provided in Table 3.1-1. For NCT, a conservative steady-state thermal analysis was performed. The uniform package NCT temperature is 48°C (118°F). HAC fire temperatures of the package components are from the CTU testing program. All measured temperatures are within the limits specified in Section 3.2.

Table 3.1-1 Summary Table of Temperatures for Traveller Materials

Material	NCT Maximum (°C)	HAC Fire Test (°C)
Fuel Assembly	48	104
Clamshell Interior / Aluminum / BORAL	48	104
Stainless steel	48	177
UHMW Polyethylene	48	177
Polyurethane Foam	48	177

3.1.4 Summary Maximum Pressures

For Type B contents, the fuel rods represent the containment boundary of the Traveller package. The maximum pressure within the containment, the fuel rods, during NCT is 305 psig (2,100 kPa gauge). The maximum pressure during HAC is 358 psig (2,468 kPa gauge).

The Outerpack is fitted with weather gaskets to prevent rain, dirt, dust and water spray from entering the package. The gaskets are not continuous, and thus do not provide an airtight seal. Acetate plugs are utilized to alleviate pressure build up within the double walled Outerpack during temperature extremes. Additionally, the Clamshell is not air tight and cannot retain pressure. Therefore, the Traveller package maintains equilibrium with external air pressure.

3.2 MATERIAL PROPERTIES AND COMPONENT SPECIFICATIONS

3.2.1 Material Properties

The Traveller package series is fabricated primarily from four materials: stainless steel, aluminum, Ultra-High Molecular Weight (UHMW) polyethylene, and flame-retardant polyurethane foam. The Outerpack is fabricated from stainless steel and polyurethane foam. The interior Clamshell holding the fuel assembly is fabricated from aluminum with BORAL neutron poison plates attached. The UMHW polyethylene is used as a neutron moderator and is located on the inside walls of the Outerpack, between the Outerpack and Clamshell. The important room temperature material properties are provided in Table 3.2-1.

The melt temperature of the polyurethane foam is not provided because it is a thermoset material that decomposes before melting. The polyurethane foam is a fire-retardant foam that, when heated above 204°C (399°F), produces an intumescent char that seals voids and continues to provide insulation.

The fuel assembly significantly affects the response of the overall package during a hypothetical fire. Because the fuel assembly may account for as much as 40% of the total package weight, the thermal capacity of the fuel assembly has a significant effect on the interior temperature of the package. Key materials for the fuel assembly are shown in Table 3.2-2. As discussed in Section 3.4.3.1, temperatures inside the Clamshell were measured below 104°C (219°F). All key fuel assembly materials have melt temperatures well below the internal Clamshell maximum temperature; therefore, all key fuel assembly materials will remain thermo-mechanically stable after the fire test.

Table 3.2-1 Thermal Properties of Key Traveller Materials

Material	Density	Service Temperature Range	Melting Temperature	Thermal Conductivity	Specific Heat
304 Stainless Steel(1)	8.3 g/cc (0.29 lb/in^3)	-40–538°C (-40–1000°F)	1400–1455°C (2550–2650°F)	14.2 W/m-K (8.2 BTU/hr-ft-°F)	0.5 J/g-°C (0.12 BTU/lb-°F)
6005 Aluminum(2)	2.8 g/cc (0.098 lb/in^3)	-40–538°C (-40–1000°F)	582–652°C (1080–1210°F)	167 W/m-K (96.1 BTU/hr-ft-°F)	0.88 J/g-°C (0.21 BTU/lb-°F)
UHMW Polyethylene(3)	0.932 - 0.945 g/cc (0.0337 - 0.0341 lb/in^3)	-150–82°C (-240–180°F)	125–138°C (257–280°F)	0.42 W/m-K (0.24 BTU/hr-ft-°F)	2.2 J/g-°C (0.526 BTU/lb-°F)
Polyurethane Foam(4)	0.166 g/cc (0.0058 lb/in^3)	-195–121°C (-320–250°F)	N/A	0.041 W/m-K (0.023 BTU/hr-ft-°F)	1.15 J/g-°C (0.275 BTU/lb-°F)

Notes:
(1) [3] Chapter 3, "Type 304 and 304L Stainless Steel", Sections 3.5 and 3.6.
(2) [4] 6005 Aluminum, Page 701.
(3) [5] UHMW Polyethylene, Page 169.
(4) [6] Polyurethane foam

Table 3.2-2 Thermal Properties of Key Fuel Assembly Materials

Material	Mass in FA(5)	Melt Temperature	Thermal Conductivity	Specific Heat
304 Stainless Steel	22 kg (49 lb) See Note 7	1400-1455°C (2550-2650°F)	14.2 W/m-K (8.2 BTU/hr-ft-°F)	0.5 J/g-°C (0.12 BTU/lb-°F)
Inconel(1)	2.7 kg (6 lb) See Note 7	1354-1413°C (2470-2580°F)	14.9 W/m-K (8.6 BTU/hr-ft-°F)	0.44 J/g-°C (0.106 BTU/lb-°F)
Zircalloy 4(2)	150 kg (330 lb)	1850°C (3360°F)	21.5 W/m-K (12.4 BTU/hr-ft-°F)	0.285 J/g-°C (0.0681 BTU/lb-°F)
Uranium Dioxide(3)	608.3 kg (1341 lb)	2750°C (4982°F)	5.86 W/m-K (3.39 BTU/hr-ft-°F)	0.237 J/g-°C (0.0565 BTU/lb-°F)
Uranium Silicide(4)	724.3 kg 1596 lb	1665°C (3029°F)	8.46 W/m-K (4.89 BTU/hr-ft-°F)	0.192 J/g-°C (0.0458 BTU/lb-°F)
Aluminum Alloy(6)	See Note 7	649°C (1200°F)	138 W/m-K (79.8 BTU/hr-ft-°F)	0.90 J/g-°C (0.22 BTU/lb-°F)

Notes:
(1) [3] Chapter 5, "Alloy 718", Sections 5.5 and 5.6.
(2) [7] Pages 323, 351.
(3) [7] Pages 164-165.
(4) [3] Chapter 18, "Uranium Silicide (U_3Si_2)"
(5) Calculated based on drop tested 17x17 XL fuel assembly
(6) [8] Pages 90-91
(7) Mass may vary for Type A quantities in a Rod Pipe.

3.2.1.1 Cladding Materials

Zircalloy cladding in-reactor performance can be enhanced by an external chromium coating or an internal zirconium-tin alloy lining, known as Optimized ZIRLO Liner (OZL). In both cases, the fuel rod base cladding is fabricated of zirconium (Zircalloy 4), with base cladding thermal properties described in Table 3.2-2. As discussed in Section 2.2.1.8, there are variants of zirconium alloys which require performance evaluation for specific conditions. The HAC thermal tested fuel cladding is the Standard Zirconium Alloy.

Chromium-Coated Optimized ZIRLO

[

]^{a,c}

[

]a,c

Optimized ZIRLO Liner

[

]a,c

Thermo-Mechanical Stability

[

]a,c

[ ]^{a,c}

Figure 3.2-1 Burst Temperature Versus Internal Pressure for Chromium-Coated Optimized ZIRLO, STD ZIRLO and Optimized ZIRLO

Stainless Steel and Aluminum Cladding

Both stainless steel and aluminum were shown to be more ductile than the tested Standard ZIRLO cladding as discussed in Section 2.2.1.8.4, and those cladding material also have greater total strain energy absorption capability than Standard ZIRLO. During a fire test, those cladding will be exposed to the maximum measured internal Clamshell temperature of 104°C (219°F) as presented in Section 3.4.3.1. Ductile alloy cladding burst behavior in Figure 3.2.1 demonstrated that there is an approximate order of magnitude difference between the burst temperature and the maximum measured test temperature in the Clamshell. Since both stainless steel and aluminum are more ductile than Standard ZIRLO and the Clamshell internal maximum fire test temperature is at least 500°C (932°F) less than the cladding melt temperature, both claddings are concluded to be thermo-mechanically stable after the fire test.

3.2.2 Component Specifications

The materials used in the construction of Traveller package, such as series 300 stainless steel and aluminum, are not sensitive to temperatures within the range of -40ºC to 800ºC (-40°F to 1,475ºF) that spans the NCT and HAC environment. As shown in Table 3.2-1 and Table 3.2-2, stainless steel has a melting point above 1,400°C (2,550°F), and maximum service temperature of 538°C (1,000°F). Similarly, aluminum has a maximum service temperature of 538°C (1,000°F). Thermoplastic components operate within their respective specified temperature limits. For the UHMW polyethylene the maximum service temperature is 82°C (180°F). Detailed technical specifications are provided on the licensing drawings (See Appendix 1.3)

3.3 THERMAL EVALUATION UNDER NORMAL CONDITIONS OF TRANSPORT

This section presents the results of the thermal analysis of the package for the NCT specified in 10 CFR 71.71.

3.3.1 Heat and Cold

To evaluate the performance of the Traveller package when subjected to the heat requirements specified in 10 CFR 71.71(c)(1), a steady-state thermal analysis was performed (see Appendix 3.5.2). Boundary conditions include an ambient temperature of 38°C (100°F) and solar insolation of 400 W/m² (400 g cal/cm²). No internal heat generation is assumed since the contents contain insignificant heat-generating radioactive material. Results of the calculation indicate a uniform package temperature of approximately 48°C (118°F). Therefore, the accessible surfaces of the package do not exceed 50°C (122°F) for nonexclusive use shipments as specified in 10 CFR 71.43(g).

For cold conditions, the minimum environmental temperature that the package will be subjected to is -40°C (-40°F), per 10 CFR 71.71(c)(2). Given zero decay heat load of the contents, the minimum temperature of the Traveller package is -40°C (-40°F). All materials used in the Traveller package are capable of sustained use at -40°C (-40°F).

Packaging components sensitive to ambient temperatures include the UHMW polyethylene moderator blocks and polyurethane foam. UHMW polyethylene can maintain continuous operation in temperatures from -150°C (-240°F) to 82°C (180°F) [8] [9]. The polyurethane foam is stable from -195°C (-320°F) to 121°C (250°F) [6]. Since these temperature sensitive materials and all structural materials are within the NCT temperature limits, the package is expected to meet all performance requirements specified in 10 CFR 71.71(c).

3.3.2 Maximum Normal Operating Pressure

The packaging is not hermetically sealed, allowing interior pressure of the Clamshell and Outerpack to adjust with changes in elevation and allowing expansion/contraction of internal air during temperature changes.

For the Type A configuration, fuel rods are pressurized with helium, while containment is not required, the fuel rods are considered for the confinement boundary. The typical internal pressure for the rods, P_1, can be up to 460 psig (474.7 psia or 3.27 MPa). Since there is insignificant heat generation by the contents, the expected normal condition pressure in the rods will only increase based on the increased temperature from NCT insolation. The initial temperature applied to the Traveller package prior to the fire testing to bound NCT conditions was 50°C (see Section 3.5.1). The increase in temperature from room temperature, T_1 (20°C = 293.15 K), to this NCT temperature, T_2 (50°C = 323.15 K), results in a maximum NCT pressure, P_2, of 509 psig (3.51 MPa gauge) based on the ideal gas law, calculated as:

$$P_2 = P_1 \cdot \left(\frac{T_2}{T_1}\right) = 474.7 \text{ psia} \cdot \left(\frac{323.15 \text{ K}}{293.15 \text{ K}}\right) = 523.28 \text{ psia} = 508.60 \text{ psig (3.51 MPa gauge)}$$

For the Type B configuration, fuel rods are defined as the containment boundary, and are pressurized with helium. The typical internal pressure for the rods, P_1, can be up to 275 psig (289.7 psia or 1.90 MPa). Since there is insignificant heat generation by the contents, the expected normal condition pressure in the rods will only increase based on the increased temperature from NCT insolation. The initial temperature applied to the

Traveller package prior to the fire testing to bound NCT conditions was 50°C (see Section 3.5.1). The increase in temperature from room temperature, T_1 (20°C = 293.15 K), to this NCT temperature, T_2 (50°C = 323.15 K), results in a maximum NCT pressure, P_2, of 305 psig (2.10 MPa gauge) based on the ideal gas law, calculated as:

$$P_2 = P_1 \cdot \left(\frac{T_2}{T_1}\right) = 289.7 \text{ psia} \cdot \left(\frac{323.15 \text{ K}}{293.15 \text{ K}}\right) = 319.35 \text{ psia} = 304.6 \text{ psig (2.10 MPa gauge)}$$

3.4 THERMAL EVALUATION UNDER HYPOTHETICAL ACCIDENT CONDITIONS

The primary verification of the package performance under HAC was demonstrated in the fire test of a full-scale Traveller XL package loaded with a simulated fuel assembly. The test package was identified as the certification test unit (CTU). The fire test was performed with the following objectives:

- Test the Traveller package in a manner that meets or exceeds regulatory requirements of SSR-6 and 10 CFR 71.
- Demonstrate that the fuel assembly survives intact, without potential release of radioactivity.
- Demonstrate that the UHMW polyethylene moderator survives essentially intact retaining at least 90% of the hydrogen within the UHMW polyethylene.
- Demonstrate that the fuel assembly survives without cladding rupture caused by excessive temperatures inside the Clamshell.

3.4.1 Initial Conditions

Prior to fire testing the CTU followed the impact test sequence presented in Section 2.7. Although the Outerpack and fuel assembly suffered minor damage during the test sequence, the Clamshell including BORAL neutron poison plates and UHMW polyethylene moderator were essentially undamaged. In preparation for fire testing, the CTU was pre-heated by covering the package with a canvas tent; approximately 16 hours before the fire test, air temperatures around the package prior to testing averaged 50°C (122°F). The air temperature and outside surface temperature dropped to approximately 5°C (41°F). However, the interior of the package remained above 38°C (100°F).

3.4.2 Fire Test Conditions

The fire test was performed in accordance with 10 CFR 71.73 and SSR-6 para. 728. Following free drop testing, puncture testing and pre-heating, the CTU was installed in the burn pool. To record the temperature of the package during the fire, twenty-two (22) thermocouples were used that measured flame temperatures immediately around the Traveller and the Outerpack outer skin, as shown in Figure 3.4-1. Before and during the pool fire, temperature measurements were made of the package at sixteen (16) locations. During the test, temperatures were measured at six (6) locations on the package skin, at twelve (12) locations inside the pool fire, at four (4) locations using directional flame thermometers (DFTs) facing away from the package, and from outside the fire using two optical thermometers.

3.4.2.1 Fire Test Setup

The CTU was positioned on a stand in a water pool as shown in Figure 3.4-2. As shown in Figure 3.4-3, the bottom of the package was positioned approximately 1 m (37 in) from the top of the fire pool surface. The distance of the outer facility walls beyond the edge of the package were 1.7 m (67 in) at the ends and 1.82 m (71.5 in) at the sides.

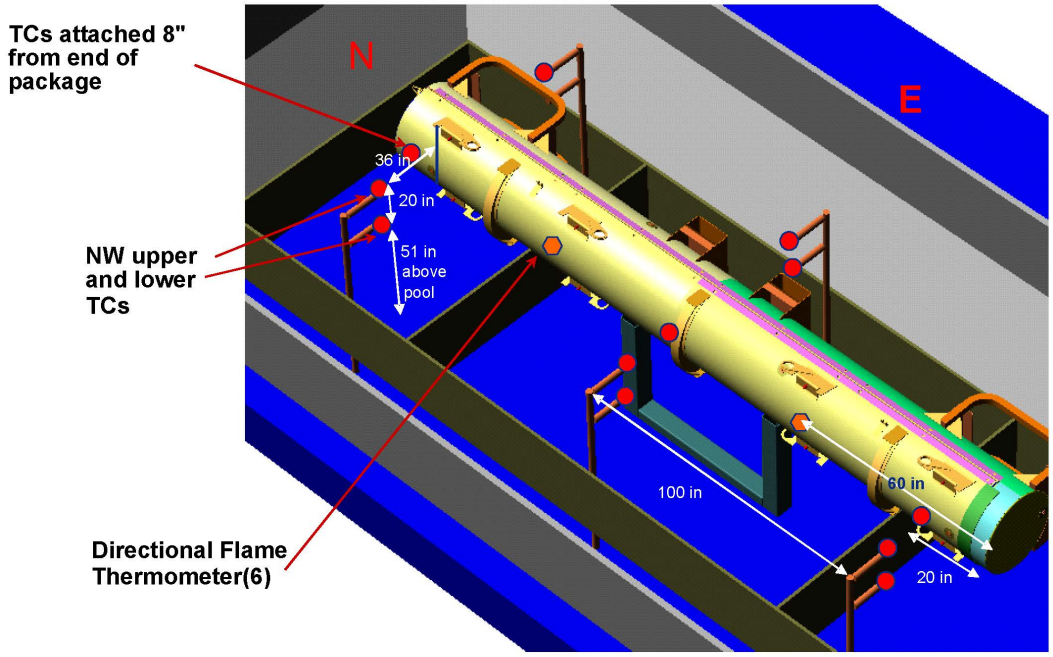

Figure 3.4-1 Thermocouple Locations Measuring Fire Temperature During CTU Burn Test

Figure 3.4-2 Pool Fire Test Setup

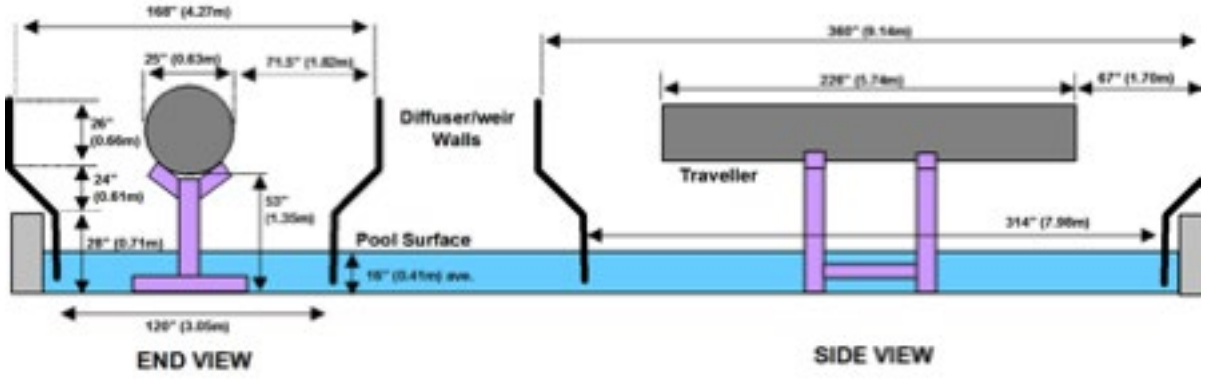

Figure 3.4-3 Orientation of CTU for Thermal Test

3.4.2.2 Fire Testing

Once positioning and instrumenting the CTU was complete, fuel was pumped into manifolds under the surface of the pool to provide an even distribution of fuel for the pool fire. Approximately one minute after the fuel on the surface of the pool was ignited, the test article was completely engulfed in flames. The fuel system continued to pump fuel into the fire until 32 minutes after the pool was ignited. The pool fire was extinguished approximately one minute later. Figure 3.4-4 shows the CTU full engulfed in flames. From the onset of the fire, temperatures were measured continuously. The 30-minute average temperatures were 904°C (1,659°F) on the package skin, 859°C (1,578°F) within the flame, 833°C (1,531°F) as measured by the DFTs, and 958°C (1,757°F) as measured by the optical thermometers.

Figure 3.4-4 Traveller CTU During Pool Fire Test

As shown in Figure 3.4-5, the pool fire was extinguished within 60 seconds using a foam fire suppression system. This system did not cool the test article, which naturally cooled after the test. It was noted that the polyurethane foam at the Outerpack vent ports continued to burn many minutes after the fire was terminated.

Figure 3.4-5 Fire Suppression System Engaged

3.4.2.3 Post-Fire Analysis

After the pool fire was extinguished, the package was removed from the pool and allowed to naturally cool. Small amounts of smoke were observed to be coming from the package seams. The package was opened, and the interior was examined. Significant amounts of intumescent polyurethane residue were observed along the Outerpack seam, Figure 3.4-6, and brown resin from the polyurethane was observed inside the package, Figure 3.4-7. As shown in Figure 3.4-8, internal temperature strips recorded peak temperatures. The peak indicated temperature was 177°C (351°F). Examination of the fuel assembly and the moderator blocks showed no significant heat damage.

Figure 3.4-6 Polyurethane Char in Outerpack Seam After Burn Test

Figure 3.4-7 Brown Polyurethane Residue Inside Outerpack After Burn Test

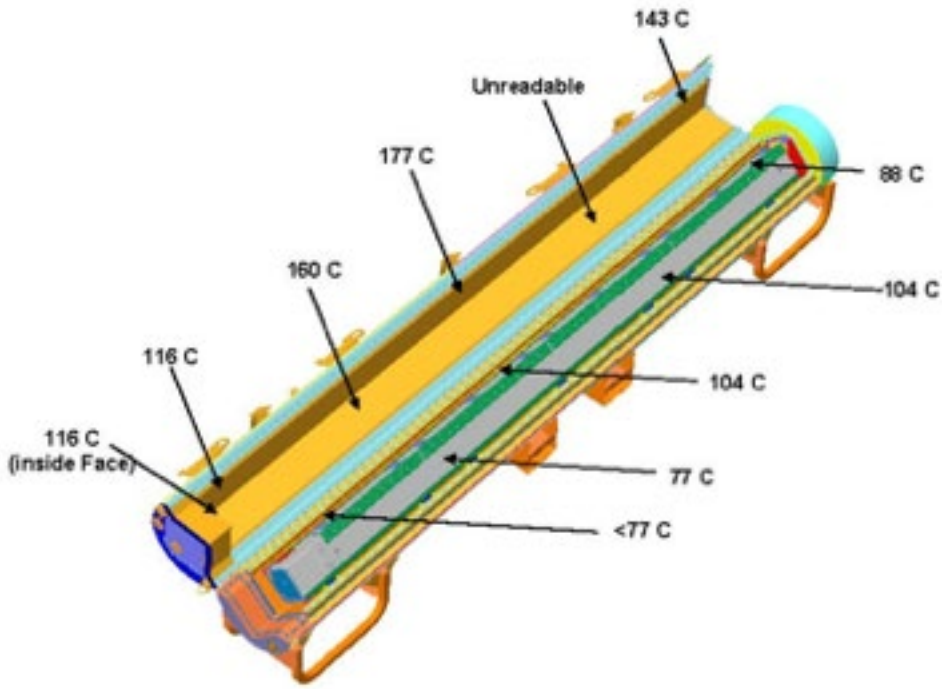

Figure 3.4-8 Location and Indicated Temperatures of Temperature Strip Sets

Table 3.4-1 summarizes the thermocouple data for the test. Some of the thermocouples had average temperatures under 800°C (1,475°F) but all experienced temperatures above 900°C (1,652°F) during the test, demonstrating that the fire covered the complete pool area. Some of the minimum temperatures recorded are due to the time selected for the 30-minute average, i.e. at the initiation or termination of the fire. As a result, the 30-minute period selected for averaging data includes data when some thermocouples were heating-up at the initiation of the fire and when some were cooling-off after the termination of the fire. The data shows that the average skin temperature, the average DFT temperature and the average temperature of thermocouples in the flame were all above 800°C (1,475°F) for the 30-minute period selected.

Table 3.4-1 Summary of Recorded Temperatures During Burn Test

TC Location	30 Minute Ave (°C)	Max Temp (°C)	Min Temp (°C)
NE Lower Flame	727	959	275
NE Upper Flame	925	1245	493
E Lower Flame	926	1155	489
E Upper Flame	904	1163	532
SE Lower Flame	714	962	291
SE Upper Flame	924	1245	484
NW Lower Flame	630	906	329
NW Upper Flame	748	1059	458
W Lower Flame	997	1162	640
W Upper Flame	1027	1173	661
SW Lower Flame	827	1032	230
SW Upper Flame	1000	1213	598
NE DFT	804	907	454

Table 3.4-1 Summary of Recorded Temperatures During Burn Test			
TC Location	**30 Minute Ave (°C)**	**Max Temp (°C)**	**Min Temp (°C)**
SE DFT	801	964	338
NW DFT	854	1016	541
SW DFT	876	1003	594
NE Skin	878	1058	610
E Skin	917	1073	699
SE Skin	903	1088	542
NW Skin	725	990	492
W Skin	974	1080	682
SW Skin	1028	1143	719

As shown in Figure 3.4-9, thermocouples in the corners of the pool were not engulfed for as long as the package itself, the 30-minute average temperature for the corners is lower than in the center of the pool. The total average for all the thermocouples in the flame was 862°C (1,584°F) versus 812°C (1,494°F) for the corner thermocouples in the flame.

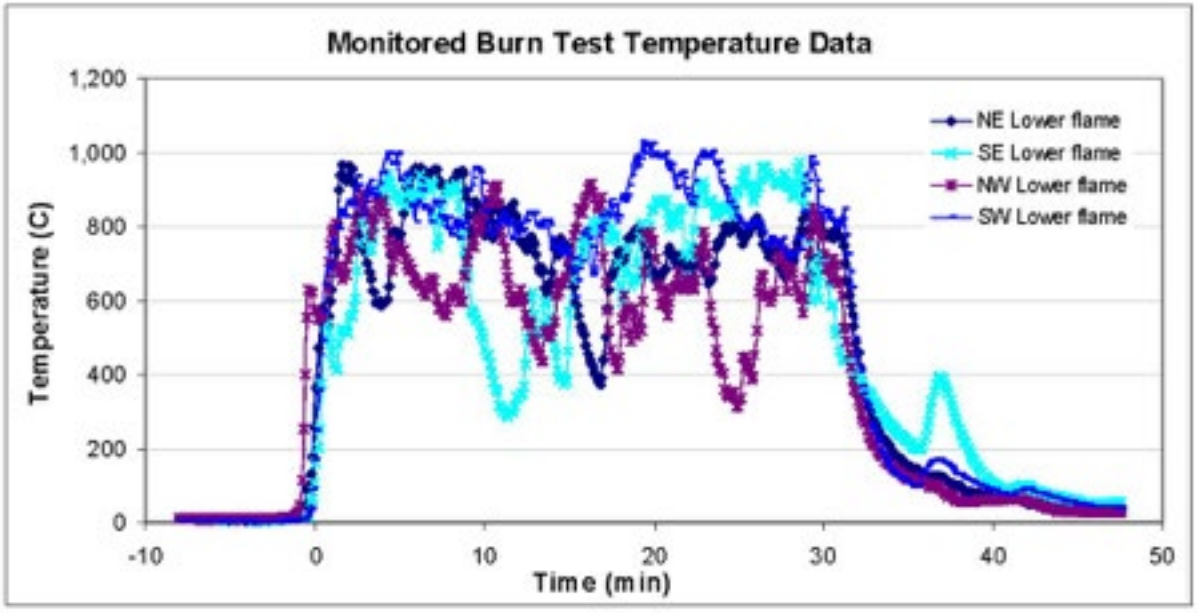

Figure 3.4-9 Fire Temperatures Measured at the Corners of the Pool

As shown in Figure 3.4-10, the DFT average readings are also lower for similar reasons. The DFTs insulated the thermocouple and attached face plate from convective heat transfer. Radiative heat transfer was dominant by design. Because these devices faced away from the package, they recorded equilibrium temperature based on radiation from the fire and reradiation to cold surfaces outside the fire, without contribution from convection.

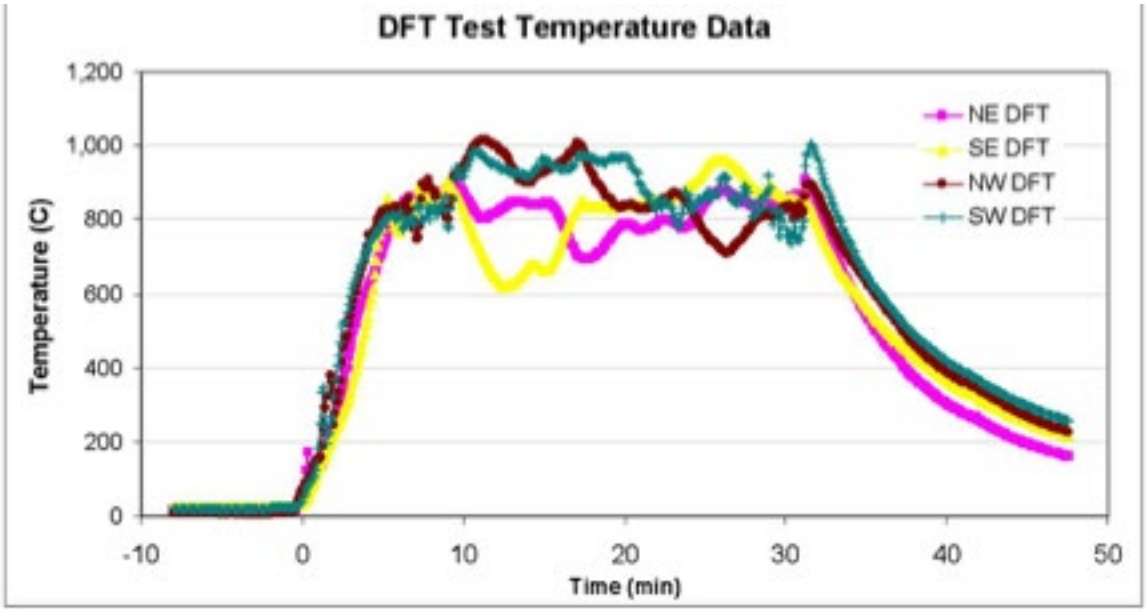

Figure 3.4-10 Data from Direction Flame Thermometers (DFTs)

As shown in Figure 3.4-11 through Figure 3.4-14, the skin temperature is an equilibrium temperature that includes convective heat transfer from hot combustion gases. As a result, its temperatures are higher.

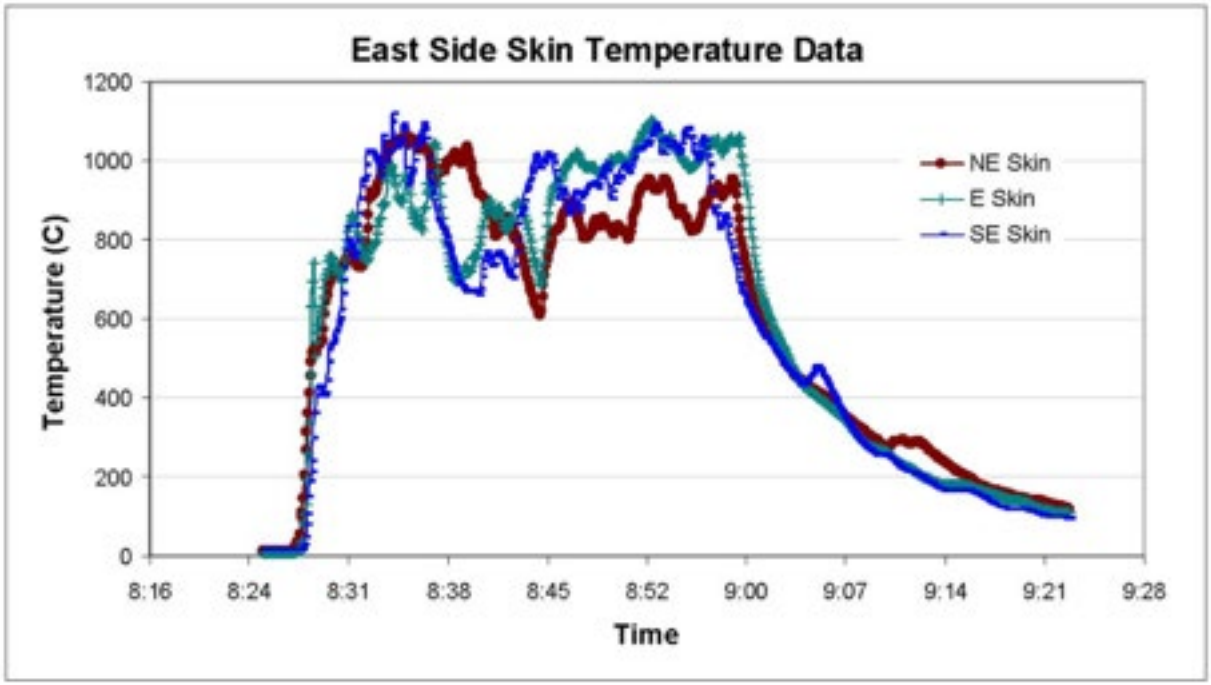

Figure 3.4-11 Skin Temperature Data from East Side of CTU

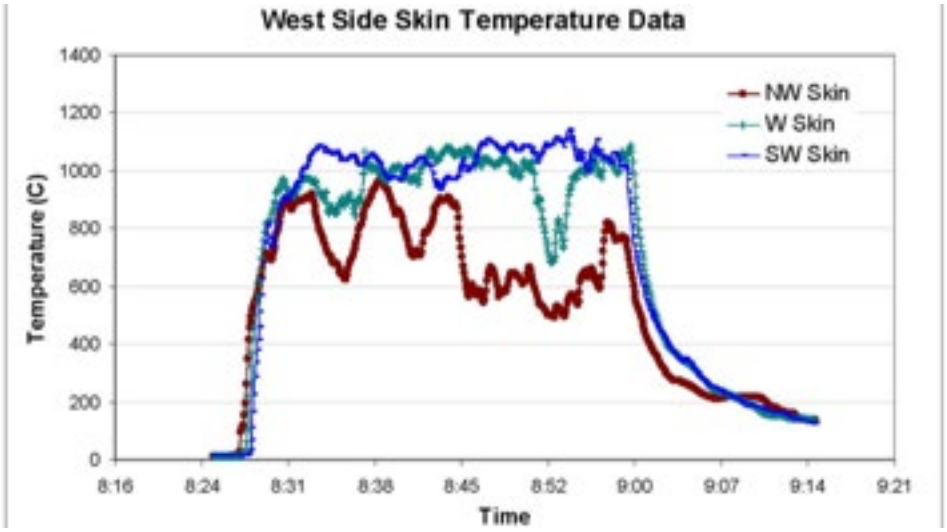

Figure 3.4-12 Skin Temperature Data from West Side of CTU

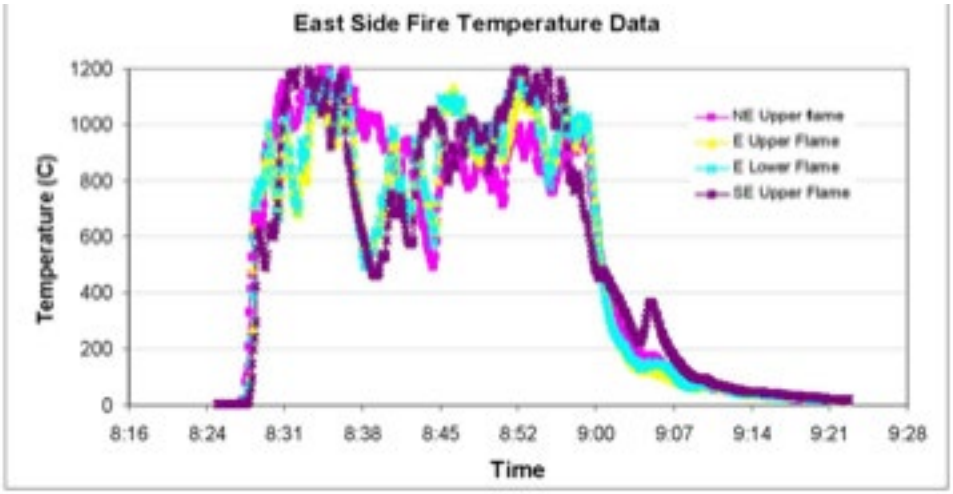

Figure 3.4-13 Fire Temperature Data from East Side of CTU

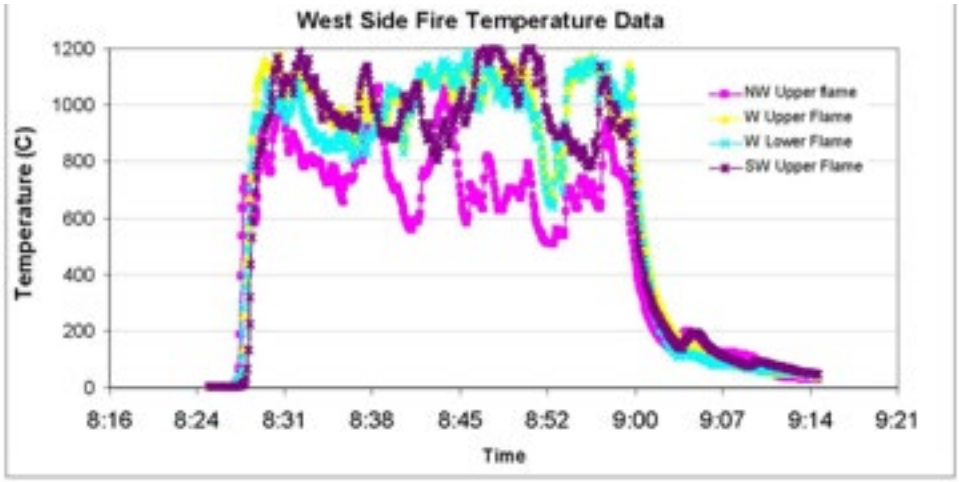

Figure 3.4-14 Fire Temperature Data from West Side of CTU

Temperature data was also collected using two portable, single wavelength optical thermometers. One was located on a raised platform on the west side of the package. The second was located on the east side of the package. Temperature data was recorded by hand. This data is shown in Table 3.4-2 and Table 3.4-3.

Table 3.4-2 Optical Thermometer Data Sheet (West Side, °C)

Time After Pool Fire Ignition	Temperature (North End)	Temperature (Middle)	Temperature (South End)
0 minutes	922	944	874
5 minutes	1047	973	1025
10 minutes	1002	1092	993
15 minutes	937	847	987
20 minutes	1177	982	942
25 minutes	1062	1073	1058
30 minutes	898	1162	968
35 minutes	525	460	484
40 minutes	318	362	294

Table 3.4-3 Optical Thermometer Data Sheet (East Side, °C)

Time After Pool Fire Ignition	Temperature (North End)	Temperature (Middle)	Temperature (South End)
0 minutes	800	1000	936
5 minutes	978	1062	837
10 minutes	1037	948	932
15 minutes	842	996	835
20 minutes	590	1120	978
25 minutes	552	969	1048
30 minutes	1098	740	980
35 minutes	No Data	No Data	No Data
40 minutes	No Data	No Data	No Data

3.4.2.4 Moderator Block Examination

An examination of the moderator blocks after the burn test revealed no significant damage. One small portion of moderator at the bottom end of the package showed signs of combustion, Figure 3.4-15. The very localized nature of the burn marks (on both the moderator and the refractory fiber felt insulation that covered the moderator) indicates that this was probably caused during the fabrication process. The stainless-steel cover sheets are welded into place after the moderator blocks are bolted in and covered with insulation. It appears that the welding torch was applied to the moderator, causing a small amount of damage. A brown spot was observed on the back side of one moderator block attached to the Outerpack lid. The polyethylene at this location appears to have been heated to melt temperature, Figure 3.4-16. A very small amount of flow occurred away from the hot spot. This melt spot was small, affecting only a few cubic centimeters of material. The twelve polyethylene moderator blocks were weighed before installation into the package, after the fire test, and subsequent disassembly. Table 3.4-4 compares the weight measurements before and after the fire test. Those measurements show that there was no significant weight loss within the accuracy of the measurements for all

the blocks and therefore all blocks retained sufficient hydrogen content.

In addition to the polyethylene block post-test inspections, a visual examination of the shock mounts indicated that they were all intact relative to their pre-test locations.

Table 3.4-4 Moderator Block Weights

Position	**Weight Before Test (lb)**	**Weight After Test (lb)**
Base top left	47.1	47.1
Base top right	47.2	47.2
Base lower left	44.6	44.8
Base lower right	46.3	46.2
Lid top left	40.4	40.7
Lid top right	40.4	40.1
Lid lower left	40.4	40.6
Lid lower right	40.4	40.3
Total	346.8	347.0

Ultra-high molecular weight (UHMW) polyethylene was selected as the neutron moderator for the Traveller package because of its high hydrogen content, its ductility at very low temperatures and its high viscosity at temperatures well above its melt point due to the long molecular chains (MW=3,000,000 to 6,000,000). The relative solution viscosity as measured by ASTM D4020 must be greater than 1.44 [1] and is typically found to be 2.3 to 3.5 dl/g (at 135°C, 275°F) [2]. As a result, UHMW polyethylene does not liquefy above its melt temperature. Also, molded UHMW polyethylene parts are typically made at relatively high temperatures (~200°C, ~400°F) and very high pressures (~100 bar). Its excellent stability allows it to be used in some applications at temperatures as high as 450°C (842°F) [3].

Experience in the Traveller test program has shown that the material will soften but not run, even when heated to near vaporization temperature (349°C, 660°F). However, the Traveller design encapsulates the moderator with stainless steel. This is primarily done to prevent oxygen from reaching the moderator, should it reach vaporization temperature, but it does serve a secondary function of ensuring that the moderator does not significantly distort or flow at high temperatures.

The highest measured temperature inside the package was 177°C (351°F), which is lower than the typical process temperature used to create the UHMW sheets installed in the Traveller. Its unchanged appearance and, more importantly, its unchanged weight indicate that the plastic did not lose a significant amount of its hydrogen during the test.

[1] Section 1.5, minimum relative viscosity of 1.44 [11]
[2] Rel. Solution Viscosity of UHMWPE (Appendix 3.6.3) [8]
[3] Ultra-High Molecular Weight Polyethylene (UHMWPE) [5]

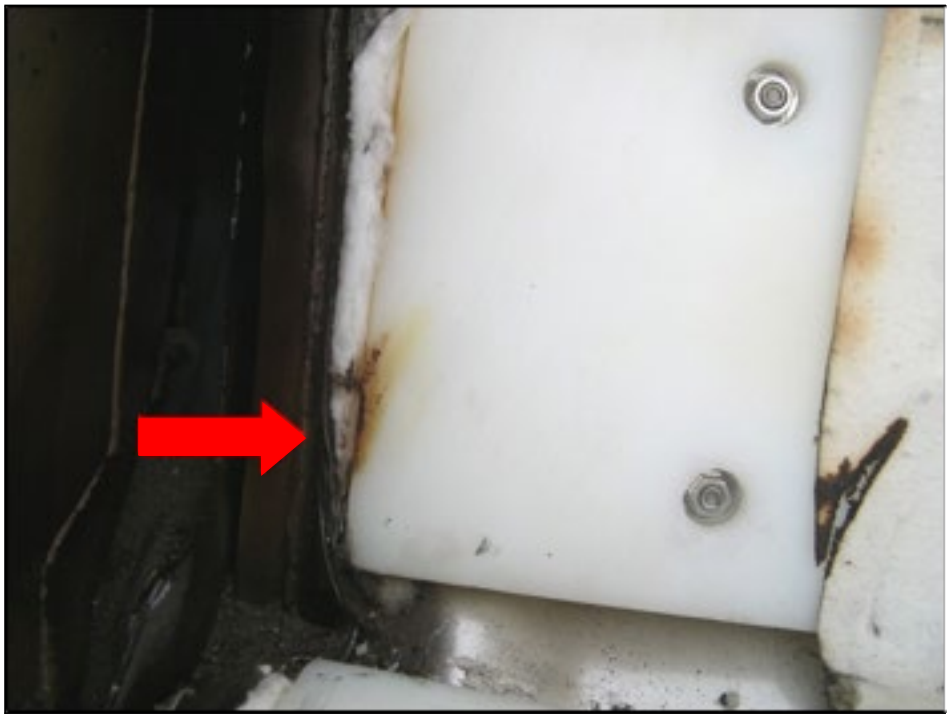

Figure 3.4-15 Location of Possible Combustion of Moderator

Figure 3.4-16 Localized Melt Spot in Lid Moderator Block

3.4.2.5 Summary of Results

Fire testing of the Traveller CTU was performed to show the packaging meets the performance requirements specified for hypothetical accident conditions as specified in 10 CFR 71.73 (c) and SSR-6 para. 728. The testing demonstrated that the Traveller packaging successfully protects its contents with a polyurethane insulated, double walled, stainless steel Outerpack that provides sufficient insulation to prevent significant heat conduction and maintain low interior temperatures during a hypothetical fire accident. The test results of full-scale package in a fully engulfing pool fire shows the design exceeds regulatory requirements for hypothetical accident conditions.

3.4.3 Maximum Temperatures and Pressures

3.4.3.1 Maximum Temperatures

Review of the fire testing data shows that the 30-minute average temperature on the CTU Outerpack outer skin was 904°C (1,659°F). Temperatures inside the CTU Outerpack were measured using temperature indicating strips. Review of the strip data on the Outerpack lid recorded temperatures of 177°C (351°F) or below. Temperatures on the inside surface of the top and bottom impact limiters were 116°C (241°F) and 149°C (300°F), respectively. Temperatures inside the Clamshell were below 104°C (219°F).

The Traveller design surrounds the fuel assembly and polyethylene moderator with an insulated outer package. As a result, the outer surface of the package quickly reaches equilibrium with the fire while the interior remains cool. This is indicated by analysis and by the burn tests described above. All temperatures remained below 177°C (351°F) and most locations remained below 100°C (212°F). No significant thermal damage was observed in the fuel assembly, Clamshell including BORAL neutron poison plates or moderator blocks after the fire test. The moderator blocks were weighed before and after the fire test and no measurable reduction in mass was found.

3.4.3.2 Maximum Pressures

The maximum pressure for a fuel rod is a function of the initial helium fill pressure. As the fuel rod is heated, the pressure within the cladding increases. The fuel is conservatively evaluated at the maximum temperature of the inside of the Clamshell during the HAC thermal event of 104°C (219°F). The maximum pressure of the containment cladding is determined by applying the ideal gas law. For the Type A configuration, the maximum internal rod pressure, P_1, is 460 psig (474.7 psia or 3.27 MPa). For HAC, the increase in internal pressure due to the increase in temperature from room temperature, T_1 (20°C = 293.15 K), to the maximum HAC temperature, T_2 (104°C = 377.15 K), based on the ideal gas law would result in a maximum HAC pressure, P_2, of 596 psig (4.11 MPa gauge), calculated as:

$$P_2 = P_1 \cdot \left(\frac{T_2}{T_1}\right) = 474.7 \text{ psia} \cdot \left(\frac{377.15 \text{ K}}{293.15 \text{ K}}\right) = 610.7 \text{ psia} = 596.0 \text{ psig (4.11 MPa)}$$

For the Type B configuration, the maximum internal rod pressure, P_1, is 275 psig (289.7 psia or 1.90 MPa). For HAC, the increase in internal pressure due to the increase in temperature from room temperature, T_1 (20°C = 293.15 K), to the maximum HAC temperature, T_2 (104°C = 377.15 K), based on the ideal gas law would result in a maximum HAC pressure, P_2, of 358 psig (2.47 MPa gauge), calculated as:

$$P_2 = P_1 \cdot \left(\frac{T_2}{T_1}\right) = 289.7 \text{ psia} \cdot \left(\frac{377.15 \text{ K}}{293.15 \text{ K}}\right) = 372.7 \text{ psia} = 358 \text{ psig (2.47 MPa)}$$

The Traveller packaging design is non-pressurized and cannot retain internal pressure. Weather gaskets are discontinuous, and thus prevent internal pressurization during the hypothetical fire and during normal variations in temperature and atmospheric pressure. The polyurethane foam space between the inner and outer shells of the Outerpack is protected from pressurization using vent plugs. Every internal foam compartment within the Outerpack is protected by at least one acetate plug that will melt in the event of a fire and allow the internal spaces to vent. As a result, no significant increase in pressure was observed during the testing, nor is anticipated in any hypothetical accident condition.

To evaluate the performance of the Type B rods during HAC fire conditions, data from burst tests at elevated temperatures performed on a large sampling of production quality rods is used. It is important to note, the fuel rods are designed for a reactor environment where significantly higher temperatures and pressures would be experienced. Figure 3.4-17 shows the temperature and pressure relationship for the burst tested rods. For quantitative comparison, from Figure 3.4-17, a pressure of approximately 400 psig is equivalent to a burst temperature of approximately 1800°F (982°C). The maximum recorded fire test Clamshell interior test temperature from Section 3.1.3, Table 3.1-1 is 219°F (104°C) which is used as the fuel assembly temperature value. Therefore, it is concluded that the expected maximum internal rod pressure of 358 psig will not result in fuel rod leakage during HAC fire conditions.

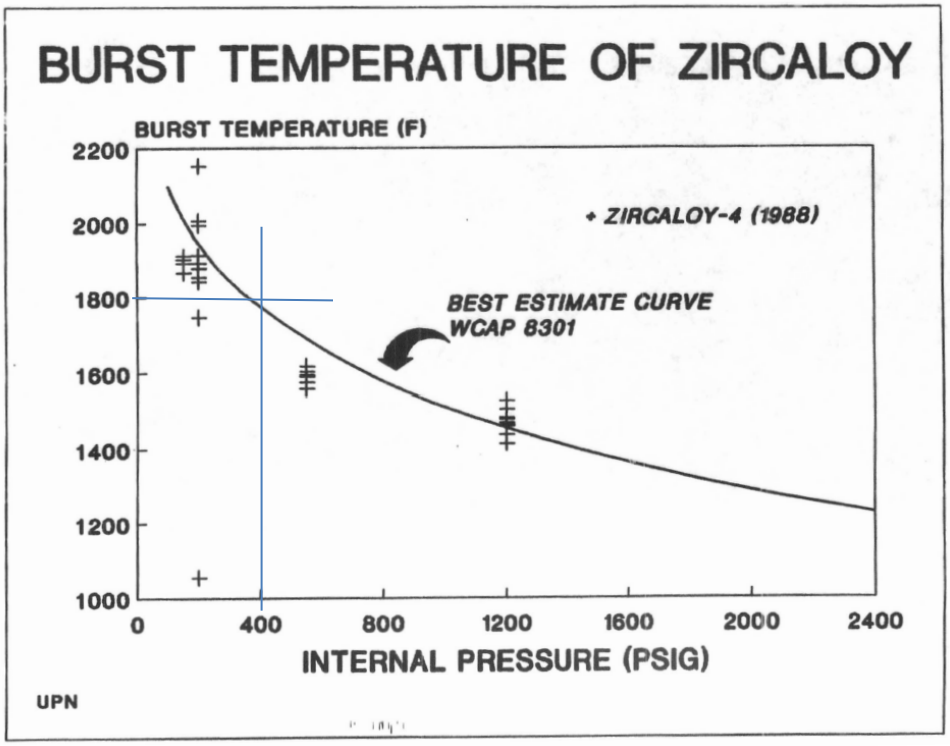

Figure 3.4-17 Burst Temperature versus Internal Pressure for Zircalloy Cladding

3.4.4 Maximum Thermal Stresses

Due to the construction of the Traveller Outerpack, light sheet metal constructed primarily of the same material, 304 SS, there are no significant thermal stresses. The Clamshell is constructed so that there is no significant constraint on any component as it heats up and cools down. The fuel cladding which provides containment is likewise designed for thermal transients, greater than what is found in the normal conditions of transport and the fuel rod can expand in the package without binding.

3.4.5 Accident Conditions for Fissile Material Packages for Air Transport

Approval for air transport is not requested for the Traveller package.

3.5 APPENDICES

The following appendices are included to provide amplifying information on material contained elsewhere in Section 3.

- 3.5.1: References
- 3.5.2: Traveller Thermal Evaluation by Analysis

3.5.1 References

[1] U.S. Nuclear Regulatory Commission, "Code of Federal Regulations Title 10 Part 71 - Packaging and Transportation of Radioactive Material," 2018.

[2] International Atomic Energy Agency, "Regulations for the Safe Transport of Radioactive Material," Specific Safety Requirements No. SSR-6, 2012 Edition.

[3] G. Pan, "Product Engineering Materials Property Manual," Rev. 7, Westinghouse Electric Company, LLC, 2008.

[4] F. Kreith and J. F. Kreider, "Principles of Solar Engineering," Hemisphere Publishing Co., 1978.

[5] ASM International, "Engineered Materials Handbook Volume 2: Engineering Plastics," 1988.

[6] General Plastics Manufacturing Company, "General Plastics LAST-A-FOAM® FR-3700 for Crash and Fire Protection of Nuclear Material Shipping Containers," 1991.

[7] A. B. McIntosh and T. J. Heal, "Materials for Nuclear Engineers," Interscience Publishers, 1960.

[8] ASM Handbook Volume 2, "Properties and Selection: Nonferrous Alloys and Special-Purpose Materials, Properties of Wrought Aluminum Alloys (page 90-91)," ASM International, 1990.

[9] Sterling Plastics Inc., "Material Information," [Online]. Available: http://sterlingplasticsinc.com/materials/uhmw-ultra-high-molecular-weight-polyethylene/. [Accessed May 2018].

[10] M. Lewin and J. Preston, Handbook of Fiber Science and Technology: Vollume III, High Technology Fibers Part D, New Yord: Marcel Dekker, Inc., 1983.

[11] Oak Ridge National Laboratory, "SCALE Version 4.4: A Modular Code System for Performing Standardized Computer Analyses for Licensing Evaluation," 2000.

[12] ASTM International, "Standard Specification for Ultra-High Molecular-Weight Polyethylene Molding and Extrusion Materials," ASTM D4020 - 11, 2011.

3.5.2 Traveller Thermal Evaluation by Analysis

To evaluate the NCT and HAC performance of the Traveller package, a simplified computer model was developed using the HEATING7.2 code distributed by Oak Ridge National Laboratory as a part of SCALE 4.4 [10]. The model was built in cylindrical coordinates using the simplified geometry shown in Figure 3.5-1. This simplification was possible because:

- Primary temperature variations occur in the Outerpack foam that is cylindrical on the outside
- Simplifying interior foam surface by making it cylindrical is conservative
- The large length to diameter ratio (8.9:1) minimizes end effects
- The ends have twice the thickness of polyurethane foam as the sides, further reducing end effects

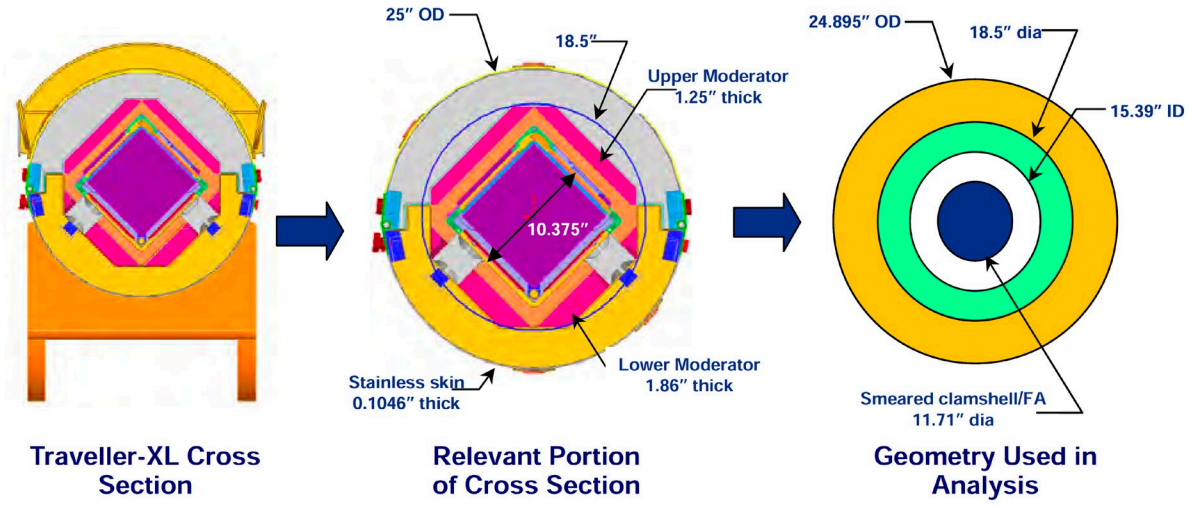

Figure 3.5-1 Approach Used to Generate Analytical Model Geometry

Three material regions were used in the analysis: Polyurethane foam with an average density of 10 pcf (0.16 g/cm^3), Polyethylene, and a smeared mixture representing the mid-section of the Clamshell and fuel assembly.

The Clamshell and fuel assembly region were modeled as a heat sink representing a 17×17 XL fuel assembly within the 9.50 inch (24.13 cm) inside dimension aluminum Clamshell. Because the end effects were to be ignored in this model, the fuel assembly nozzles and the Clamshell end plates were not included in this calculation. This resulted in the following material ratios:

- Aluminum Clamshell – 359.7 lb (163.2 kg) with a specific heat of 0.23 BTU/lb-°F (0.96 J/g-°C)
- Uranium Dioxide – 1,341 lb (608.3 kg) with a specific heat of 0.0565 BTU/lb-°F (0.237 J/g-°C)
- Zircalloy 4 – 330 lb (149.7 kg) with a specific heat of 0.0681 BTU/lb-°F (0.285 J/g-°C)

The Traveller XL Clamshell is 202.0 inches (513.1 cm) long. The heat sink region weighs 2,031 lb (921.2 kg), has an average specific heat of 0.891 BTU/lb-°F (3.730 J/g-°C) and a smeared density of 0.0934 lb/in^3 (2.58 g/cm^3).

A volumetric average conductivity was generated for the Clamshell and fuel assembly region by calculating a volume-smeared conductivity by using the ratio of conductivity to volume for each material.

- Aluminum Clamshell – 3,560 in^3 (58,300 cc) with a conductivity of 104 BTU/hr-ft-°F (180 W/m-K)
- Uranium Dioxide – 3,380 in^3 (55,400 cc) with a conductivity of 3.39 BTU/hr-ft-°F (5.86 W/m-K)
- Zircaloy 4 – 1,400 in^3 (23,000 cc) with a conductivity of 12.4 BTU/hr-ft-°F (21.4 W/m-K)

Total volume used in the Clamshell/fuel assembly region is 21,700 in^3 (356,000 cc). This results in a smeared conductivity of 18.3 BTU/hr-ft-°F (31.7 W/m-K). This approximation is valid only because the heat input rate is very low, allowing the region to be almost isothermal, even with low conductivities.

The Traveller XL Outerpack contains approximately 426 lb (193 kg) of UHMW polyethylene with specific heat of 0.526 BTU/lb-°F (2.2 J/g-°C) and a conductivity of 24 BTU/hr-ft-°F (41.5 W/m-°C). The total length of the moderator within the Outerpack is approximately 206 inches (523 cm). For the geometry defined for the model, this results in a smeared polyethylene density of 0.0249 lb/in^3 (0.689 g/cc), which is 74% of the predicted minimum density. The polyethylene acts as a heat sink and also as insulation of the primary heat sink.

The polyurethane foam room-temperature properties are given in Table 3.5-1. The properties change significantly, however, as the foam temperature increases, resulting in pyrolization that occurs between 316 and 343°C (600 and 650°F). After charring, the material has the general appearance of very low-density carbon foam. For the analytical model, the room temperature specific heat and conductivity were used up to 316°C (600°F). Above 343°C (650°F), the temperature-dependent conductivity of air was used instead. Between 316 and 343°C (600 and 650°F)., the foam's specific heat is assumed to drop to zero.

Table 3.5-1 Temperature-Dependent Thermal Conductivity Used to Model Polyurethane Foam

Temperature (°F)	Conductivity (BTU/hr-ft-°F)	Conductivity (W/m-K)
100	0.0230	0.0398
600	0.0230	0.0398
650	0.0249	0.0431
700	0.0268	0.0464
800	0.0286	0.0495
1000	0.0319	0.0552
1500	0.0400	0.0692
2000	0.0502	0.0869

This analysis was performed to bound the anticipated response and was done by analyzing the response of the package at 800°C (1,475°F) external conditions with a fire emissivity of 0.9 and a package emissivity of 0.8, as defined by 10 CFR 71.73. The NCT steady state analysis is the precondition for the fire. The package reached a uniform temperature of 48°C (118°F) prior to the application of the fire boundary conditions. The first analysis performed modeled a 30-minute fire with flame temperature of 800°C (1,475°F). The analysis showed

significant temperature variation through the thickness of the polyurethane foam. Peak temperatures on the inside surface of the foam reached 100°C (212°F) approximately 80 minutes after the beginning of the fire (50 minutes after the end of the fire). Results of the 800°C (1,475°F) analysis are presented in Figure 3.5-2

In anticipation of higher temperature during the pool fire, the analysis was repeated assuming a 1000°C (1,832°F) fire temperature. The peak temperature within the UHMW polyethylene (at the interface between the polyurethane foam and the UHMW polyethylene) was calculated to reach 106°C (223°F). This is below the 125 – 138°C (257 – 280°F) melt temperature of the polyethylene and well below the temperature at which the melted polyethylene viscosity is low enough to flow easily. Results of the 1000°C (1,832°F) analysis are presented in Figure 3.5-3.

The thermal analysis performed demonstrated several important features/characteristics of the design. Because of the urethane foam insulating the Outerpack, exterior skin temperatures quickly rise to near equilibrium with the fire outside the package. The Clamshell and fuel assembly temperature rise very slowly due to the insulation and the specific heat of the aluminum Clamshell, polyethylene moderator, and the fuel assembly. The primary mechanisms that can result in significantly higher internal temperatures are hot gas infiltration during the fire and internal combustion during and after the fire test. It is not believed that these mechanisms can be accurately predicted by analysis. As a result, regulatory compliance of the package's thermal performance is demonstrated using pool fire tests, culminating with a full-scale fire test.

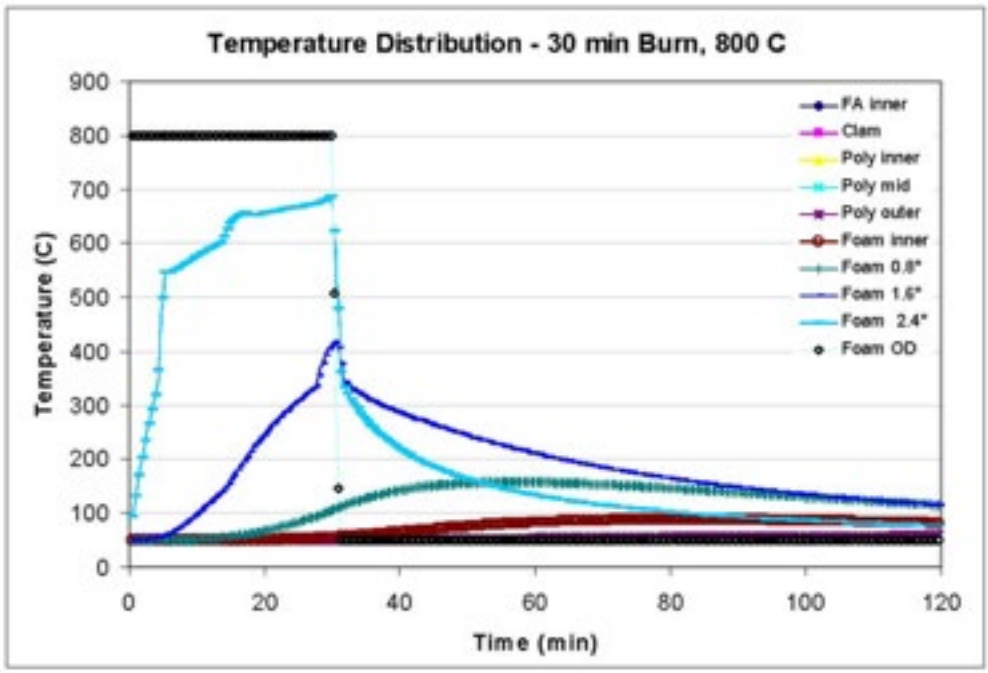

Figure 3.5-2 Calculated Radial Temperature Distribution for 30 Minute Fire (800°C)

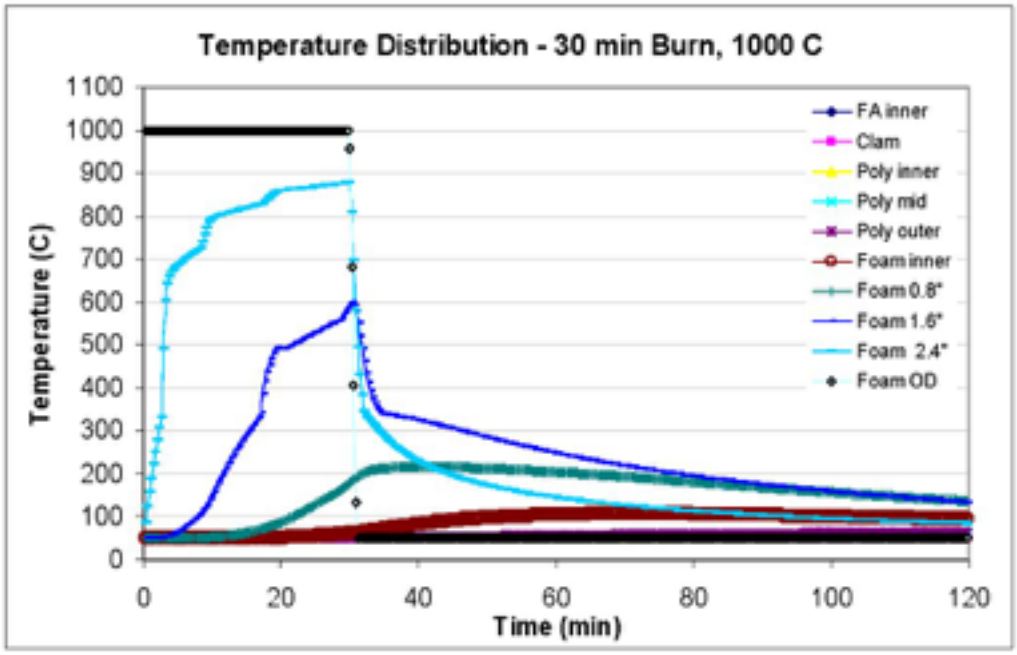

Figure 3.5-3 Calculated Radial Temperature Distribution for 30 Minute Fire (1000°C)

TABLE OF CONTENTS

4.0 CONTAINMENT EVALUATION 4-1
4.1 DESCRIPTION OF THE CONTAINMENT SYSTEM 4-1
4.2 CONTAINMENT UNDER NORMAL CONDITIONS OF TRANSPORT 4-2
4.3 CONTAINMENT UNDER HYPOTHETICAL ACCIDENT CONDITIONS 4-2
4.4 LEAKAGE RATES FOR PACKAGE TYPE B CONFIGURATION 4-3
4.5 APPENDICES 4-4
4.5.1 References 4-4

4.0 CONTAINMENT EVALUATION

The contents for the Traveller packaging allow for quantities of material that exceed a Type A quantity, denoted as Type B quantity. Thus, this section provides guidance for and demonstrates compliance with the containment requirements established 10 CFR 71 [1] and SSR-6 [2]. The requirements outlined in this section only apply to contents that exceed a Type A quantity. As discussed in Section 1.2.2.2, if the contents are established to be suitable for the Type A configuration of the Traveller package, they are exempt from the requirements of this section. A summary of the containment requirements for the Type B configuration of the Traveller is provided below:

1. **Fuel Rod Weld Inspection –** 100% visual and radiographic or ultrasonic inspections on the top and bottom end plug welds on all fuel rods

   (Type A contents may only require weld inspections on an approved sampling of rods)

2. **Fuel Rod Leakage Rate Testing –** 100% fabrication leak testing of all fuel rods to the leak tight criterion: $1x10^{-7}$ ref·cm^3/s, with a sensitivity of $5x10^{-8}$ ref·cm^3/s or less.

   (Type A contents may only require leak testing on an approved sampling of rods and may allow greater leakage rates)

3. **Shoring Devices –** For all shipments of the Type B configuration of the Traveller package, the axial restraints required include a bottom support (i.e., spacer or plate) along with the top axial clamping mechanism, as described in Section 1.2.1.5.3. The lengths of these components are specific to the fuel design being transported, but each specific design ensures a conformal fit between the Clamshell, fuel assembly, and shoring components.

   (Type A configuration uses spacers and axial restraints for shoring, as necessary)

4.1 DESCRIPTION OF THE CONTAINMENT SYSTEM

For the Type B configuration, the containment boundary of the package is established as the sealed zirconium alloy cladding of the fuel rods being shipped. The three components that comprise the containment boundary are the cladding tube and the top and bottom end plugs. For every fuel rod, the radioactive material being transported may be up to the contaminated uranium specification per the content limits defined in Table 1-2, as outlined in Section 1.2.2.2. All uranium pellets are encapsulated by cylindrical zirconium alloy cladding that is seal welded after the pellets are stacked inside the rod. Thus, there are no openings in the containment boundary, and a rod cannot be opened unintentionally. The only components that make up the containment boundary are the base material of the cladding (tube and end plugs) and the welds on each end of the tube that attach the end plugs. The cladding and end plugs of all fuel rods are zirconium alloys (physical properties described in Section 2.2.1.8).

The fuel rods shipped in the Traveller package are fabricated in a facility with a quality assurance program, which satisfies the provisions of subpart H of 10CFR71 and/or equivalent. The welds of the end plugs to the rod tube are visually inspected and checked using non-destructive methods, such as radiographic or ultrasonic testing, for integrity.

4.2 CONTAINMENT UNDER NORMAL CONDITIONS OF TRANSPORT

The containment criterion of the Traveller Type B configuration is set at the leaktight criterion, as defined in ANS N14.5-2014 [3]. Based on this ANSI standard, a package is "leaktight" when the leakage rate is less than or equal to $1x10^{-7}$ ref·cm^3/s, which is defined as "the degree of package containment that, in a practical sense, precludes any significant release of radioactive materials." In other words, regardless of the activities in the contents, if the package is demonstrated to be leaktight during all NCT, the containment requirement of 10 CFR 71.51(a)(1) is met.

After each rod is seal welded, all fuel rods in the Type B configuration are inspected and tested to ensure that they meet the leaktight criterion. Rods may be tested individually or in batches, so long as the cumulative leakage rate from all rods in a single test is less than the $1x10^{-7}$ ref·cm^3/s criterion.

As discussed in Section 3.3.2, the Type B fuel rods are pressurized with helium up to a maximum pressure of 275 psig (1.90 MPa gauge). Based on the increased temperature from NCT insolation, the MNOP of the fuel rod containment boundary is 305 psig (2.1 MPa gauge).

This equates to an increase in internal rod pressure of approximately 10%. An increase in internal rod pressure of this magnitude will not affect the structural integrity of the fuel rod cladding, as the fuel rods are designed for the higher operating pressures of a nuclear reactor.

Because the allowable leakage rate for NCT and HAC is the same, the Type B configuration free drop testing results summarized in Section 2.7.1.4 bound any potential NCT effects, and the structural effects of NCT are covered by this testing.

4.3 CONTAINMENT UNDER HYPOTHETICAL ACCIDENT CONDITIONS

Compliance with the containment requirements of 10 CFR 71.51(a)(2) is demonstrated through drop testing and subsequent leak testing of the tested fuel assembly. The acceptance criterion for the leak testing of the dropped assembly is based on leaktightness, as defined in ANSI N14.5-2014. As discussed in Section 2.7.1.4, worst case drop testing was conducted for the Traveller Type B configuration utilizing the bottom support spacer and top axial restraint components to help protect the fuel from a free drop. Based on this testing, there is minimal deformation to the rod cladding from a free drop in the Type B configuration (with the bottom support spacer and top axial restraint). All rods meet the leaktight criterion post drop, thus the HAC release rate requirement of 10 CFR 71.51(a)(2) is met and it is acceptable to transport contaminated uranium with trace amounts of materials, as defined in Table 1-2, in the Traveller Type B configuration.

As stated in Section 3.4.3, the maximum temperatures inside the Clamshell were below 104°C (219°F) during the HAC fire accident. For a rod pressure of 275 psig (1.90 MPa gauge), the increase in internal pressure due to the increase in temperature from room temperature (20°C, 293.15 K) to the maximum HAC temperature (104°C, 377.15 K) results in a maximum HAC fuel rod pressure of 358 psig (2.47 MPa gauge), as calculated in Section 3.4.3.2

These fuel rods are designed to survive a reactor environment where significantly higher temperatures and pressures would be experienced. The fuel rod cladding is designed to survive internal pressures in the range of >600 psig (4.14 MPa gauge) at temperatures much higher than the 104°C (219°F) experienced by the rods during a transport HAC fire accident. Thus, the internal pressure from a fire accident would not compromise the integrity of the containment boundary.

4.4 LEAKAGE RATES FOR PACKAGE TYPE B CONFIGURATION

Table 1 in ANSI N14.5-2014 provides the testing requirements for leakage testing of the containment boundary of a package. The leakage tests listed include: Design, Fabrication, Maintenance, Periodic, and Pre-shipment. However, not all of these tests are applicable to the Traveller Type B configuration. The typical packaging containment boundary that these tests are intended to cover are containment vessels that are used multiple times over the life of the packaging. However, from the perspective of the Traveller Type B configuration, the containment boundary of the radioactive material is the zirconium alloy cladding of each fuel rod. Thus, the number of uses for the containment boundary of the package is only once, as the fuel is only intended to be transported from the fabrication facility to the power plant at which it is used. As such, the Design, Maintenance, and Periodic leak tests are not applicable to the Traveller Type B configuration.

For each Type B shipment, the basic process is: (1) fuel rods are fabricated, (2) 100% of all fuel rods are tested for helium leakage, (3) a fuel assembly is built with rods that pass the helium leakage rate test, and (4) the fuel assembly is loaded into the Traveller package in the Type B configuration and shipped to the plant for use. Based on this process, the Fabrication and Pre-shipment leakage tests are completed as a single test during the fabrication process. Thus, the leakage rate tests for the containment boundary of each fuel rod is a single test during the fuel assembly fabrication process to the leaktight criterion of 1×10^{-7} ref·cm^3/s. The maximum allowable sensitivity of the test is one half of the allowable leakage rate (i.e. $\leq 5 \times 10^{-8}$ ref·cm^3/s).

The test method used for leak testing the fuel rods is the Evacuated Envelope – Gas Detector method per Section A.5.4 of ANSI N14.5-2014. This test takes advantage of the fact that all fuel rods are pressurized with helium. All rods are loaded into a test chamber that is evacuated and the helium leakage rate from the rods is measured to ensure compliance with the leaktight criterion for the Traveller Type B configuration. Fuel rods may be tested all at once or in batches, as long as 100% of fuel rods are tested.

4.5 APPENDICES

4.5.1 References

[1] U.S. Nuclear Regulatory Commission Code of Federal Regulations, Title 10 Part 71, "Packaging and Transport of Radioactive Material," 2016.

[2] International Atomic Energy Agency, "Regulations for the Safe Transport of Radioactive Material," 2012.

[3] American National Standards Institute, Inc., "American National Standard For Radioactive Materials - Leakage Tests on Packages for Shipment," ANSI N14.5-2014, 2014.

[4] ASTM International, "Standard Specification for Uranium Hexafluoride to Less than 5% 235U," ASTM C996-15, 2015.

TABLE OF CONTENTS

5.0 SHIELDING EVALUATION 5-1
5.1 DESCRIPTION OF SHIELDING DESIGN 5-1
5.1.1 Design Features 5-1
5.1.2 Summary Table of Maximum Radiation Levels 5-2
5.2 SOURCE SPECIFICATION 5-3
5.2.1 Gamma Source 5-4
5.2.2 Neutron Source 5-5
5.3 SHIELDING MODEL 5-6
5.3.1 Configuration of Source and Shielding 5-6
5.3.2 Material Properties 5-6
5.4 SHIELDING EVALUATION 5-7
5.4.1 Methods 5-7
5.4.2 Computer Codes – MCNP6 5-7
5.4.3 MCNP6 Model Tallies 5-7
5.4.4 Dose Rate Calculations 5-8
5.4.5 Input and Output Data 5-9
5.4.6 Flux-to-Dose-Rate Conversion 5-10
5.4.7 External Radiation Levels 5-11
5.5 APPENDICES 5-12
5.5.1 References 5-12

LIST OF TABLES

Table 5.1-1 Maximum Radiation Levels for Normal Conditions of Transport 5-2
Table 5.1-2 Maximum Radiation Levels for Hypothetical Accident Conditions 5-2
Table 5.2-1 Maximum Radionuclide Concentration for Contaminated Uranium 5-3
Table 5.2-2 ORIGEN Radionuclide Inventory Input 5-3
Table 5.2-3 Grouped Photon Spectrum 5-4
Table 5.2-4 Grouped Neutron Spectrum 5-5
Table 5.4-1 ANSI/ANS-6.1.1 1977 Flux-to-Dose Conversion Factors 5-10
Table 5.4-2 MCNP Dose Rate Calculation Results 5-11

LIST OF FIGURES

Figure 5.1-1 Traveller STD Clamshell and Outerpack Packaging Dimensions 5-1
Figure 5.3-1 Dose Rate Analysis Source Configuration 5-6
Figure 5.4-1 Dose Rate Model Tallies 5-8

5.0 SHIELDING EVALUATION

The contents for the Traveller packaging allow for quantities of material that exceed a Type A quantity. Thus, it is demonstrated herein that the maximum allowable quantity of radioactive material in the Traveller will not result in exterior dose rates exceeding the established 10 CFR 71 [1] and SSR-6 [2] limits. More specifically, compliance is demonstrated for the dose rate limits in 10 CFR 71.47(a) (SSR-6 paras. 527-528) and 10 CFR 71.51(a)(2) (SSR-6 para. 659).

5.1 DESCRIPTION OF SHIELDING DESIGN

5.1.1 Design Features

The purpose of the Traveller packaging is to protect the fuel assembly contents during transport and isolate the fissile contents of separate packagings from each other. The design features of the Traveller packaging are solely for structural, thermal, and criticality safety purposes. Although there are metal and foam components in the packaging that would shield some radiation, this is not their design purpose. As such, no materials of the Traveller packaging are credited for the shielding analysis. Only the spacing offset from the Clamshell to the outer surface of the Outerpack is credited for dose rate calculations. The Traveller STD Clamshell cavity has dimensions of 9.31 in × 9.31 in × 171 in (23.65 cm × 23.65 cm × 434.34 cm) and the Outerpack outer shell has a diameter of 25 in (63.5 cm) and a height of 195.87 in (497.51 cm). The dimensions of these regions and this model geometry is shown in Figure 5.1-1. During the HAC drop-test series, there was minimal concentrated deformation to the Outerpack, therefore packaging dimensions are considered the same for NCT and HAC.

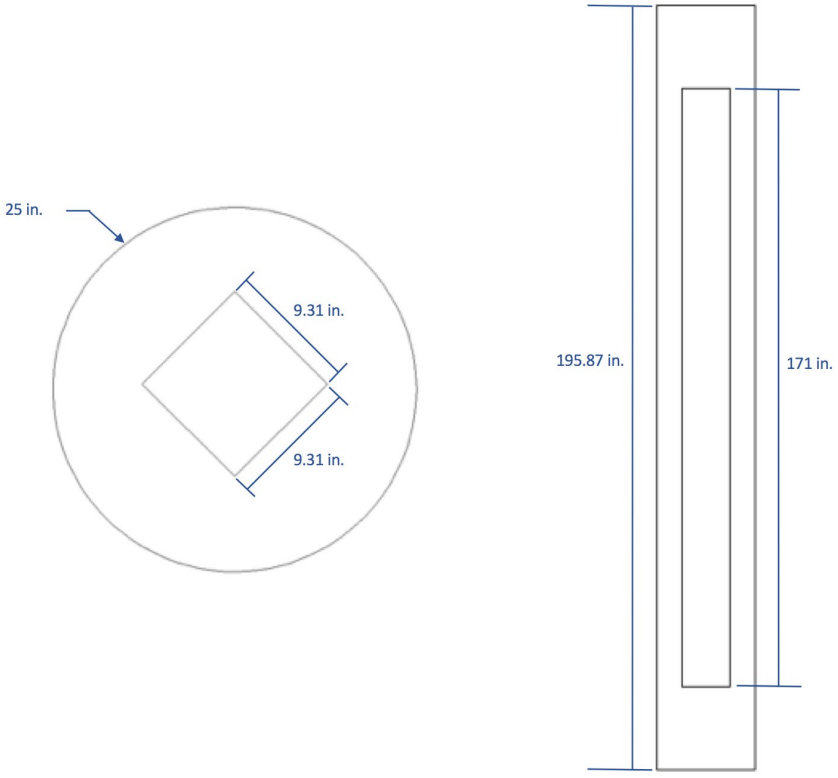

Figure 5.1-1 Traveller STD Clamshell and Outerpack Packaging Dimensions

5.1.2 Summary Table of Maximum Radiation Levels

The results of the NCT and HAC dose rate analyses are summarized below in Table 5.1-1 and Table 5.1-2, respectively. These reported dose rates are based on a bounding source term for 5.0 wt.% ^{235}U contaminated uranium with trace amounts of materials, as defined by the isotopic content specification in Table 1-2. Based on the results of this dose rate analysis, compliance with the respective dose rate limits of 10 CFR 71 and SSR-6 is demonstrated for the Traveller package transporting contaminated UO_2 fuel with trace amounts of materials, as defined in Table 1-2.

Although the source term and resulting calculated maximum dose rates are based on the original licensing basis enrichment of 5.0 wt.% ^{235}U, a small increase in enrichment to 6.0 wt.% ^{235}U does not significantly affect the calculated dose rates and would not result in any regulatory dose rate limits being exceeded. The content radionuclide limits of the radioactive material are based on the total mass of uranium (in gU), so a change in enrichment only varies the maximum permissible quantities of ^{235}U and ^{238}U in the contents. Variations in only these two radionuclides does not significantly affect the external dose rates of the package, thus variations in enrichment do not result in external dose rate limits exceeding the regulatory dose rate limits.

Table 5.1-1 Maximum Radiation Levels for Normal Conditions of Transport

Normal Conditions of Transport	External Surface (mrem/hr)		1m from External Surface (mrem/hr)	
Radiation	**Radial**	**Axial**	**Radial**	**Axial**
Gamma	1.325	0.190	0.2276	0.0128
Neutron	0.031	0.003	0.0053	0.0002
Total	1.356	0.194	0.2329	0.0130
10 CFR 71.47(a) Limit	200	200	10 [1]	10 [1]

Notes: [1] Transport index may not exceed 10.

Table 5.1-2 Maximum Radiation Levels for Hypothetical Accident Conditions

Hypothetical Accident Conditions of Transport	1m from External Surface (mrem/hr)	
Radiation	**Radial**	**Axial**
Gamma	0.2276	0.0128
Neutron	0.0053	0.0002
Total	0.2329	0.0130
10 CFR 71.51(a)(2) Limit	1,000	1,000

5.2 SOURCE SPECIFICATION

Based on the maximum quantity of 32 kg of ^{235}U, as specified in Section 1.2.2.2, and an enrichment of 5.0 wt.% ^{235}U, the resultant maximum quantity of uranium in the Traveller package is 640 kg. The maximum radionuclide activity is determined based on this uranium mass and the contaminated uranium content limit, as defined in Table 1-2, and shown in Table 5.2-1, column 'Content Limits'. The maximum radionuclide activity calculation is provided in Table 5.2-1, for the bounding mass of 640 kgU.

Table 5.2-1 Maximum Radionuclide Concentration for Contaminated Uranium

Content	Content Limits	Max Quantity	Specific Activity (Ci/g) [4]	Activity (Ci)
^{232}U	0.05 µg/gU [1]	3.20E-02 g	2.20E+01	7.04E-01
^{234}U	2000 µg/gU [1]	1.28E+03 g	6.20E-03	7.94E+00
^{235}U	50,000 µg/gU	3.20E+04 g	2.20E-06	7.04E-02
^{236}U	25,000 µg/gU [2]	1.60E+04 g	6.50E-05	1.04E+00
^{238}U	Remainder	5.91E+05 g	3.40E-07	2.01E-01
^{99}Tc	5 µg/gU [1]	3.20E+00 g	1.70E-02	5.44E-02
Alpha Activity from Np and Pu	3300 Bq/kgU [1]	2.11E+06 Bq	-	5.71E-05
Total Gamma Activity	$4.4x10^5$ MeV Bq/ kgU [1]	3.68E+08 Bq [3]	-	9.94E-03

Note: [1] Based on contaminated uranium limits, as defined in Table 1-2.
[2] Established limit for WEC fuels.
[3] Calculated using the largest mean gamma energy from ASTM C1295-15 (0.766 MeV).
[4] Values from 10 CFR 71 Appendix A.

The Oak Ridge Isotope Generation code (ORIGEN) of the SCALE 6.1.2 code package [3] is used to calculate the neutron and photon source spectra to be used in the dose rate analysis. The maximum isotope activities are used as inputs to ORIGEN, which calculates the resultant neutron and photon source spectra. The ORIGEN neutron and photon source calculations consider decay of each isotope as well as neutrons generated from α-n interactions and bremsstrahlung gammas in a UO_2 matrix. As the calculated source spectra are based on the maximum possible activities, they are considered bounding of any slightly contaminated uranium fuel contents of the Traveller, as limited by Table 1-2. Based on the results of Table 5.2-1, the radionuclide inventory used in ORIGEN to determine the maximum Traveller source term is listed in Table 5.2-2. Regarding the activity for "Alpha Activity from Np and Pu," all activity is contributed to ^{242}Pu because of its spontaneous fission neutron emissions. However, the contribution to the neutron source from any Np or Pu isotope is insignificant to the total neutron source.

Table 5.2-2 ORIGEN Radionuclide Inventory Input

Isotope	Activity (Ci)
^{232}U	7.04E-01
^{234}U	7.94E+00
^{235}U	7.04E-02
^{236}U	1.04E+00
^{238}U	2.01E-01
^{99}Tc	5.44E-02
^{242}Pu	5.71E-05

Based on the radionuclide inventory listed in Table 5.2-2, the grouped photon and neutron source spectra in Section 5.2.1 and Section 5.2.2, respectively, were calculated. The "Total Gamma Activity" is added into the resulting photon source spectra from the ORIGEN calculation (See Table 5.2-3). The source spectra provided in Table 5.2-3 and Table 5.2-4 are bounding photon and neutron sources, respectively, for the bounding contaminated uranium contents. For each neutron or gamma energy listed, ORIGEN groups the emissions from all isotopes that are within an energy in the group. Each group is defined as the band between two listed energies. For example, under the gamma energy (E) of 0.8 MeV in Table 5.2-3 all gammas emitted between the lower energy, in this case 0.7 MeV and 0.8 MeV are grouped. To make the neutron and photon spectra bounding for dose rate calculations, it is considered that all neutrons or gammas in a group are emitted at the maximum energy of the group. For example, in the 0.7 MeV – 0.8 MeV energy gamma group, it is considered that all gammas are emitted at 0.8 MeV. As stated in Note 2 of Table 1-2, the content limits are applicable at the time of shipment. This precludes the significant buildup of any daughter products (specifically, Tl-208 from the decay of U-232) that could increase the source term and result in higher dose rates than calculated.

As the UO_2 source material is modeled in the MCNP dose rate calculation, the code explicitly simulates fissions and n,γ interactions in the fuel. Thus, the additional sources of radiation from subcritical multiplication and n,γ interactions are considered in the dose rate calculations.

5.2.1 Gamma Source

Table 5.2-3 Grouped Photon Spectrum

E (MeV)	ORIGEN Source (γ/s)	Total Gamma Activity (γ/s)	Total (γ/s)	I(E)
12.0	3.4570E-01	0	3.4570E-01	1.1427E-10
10.0	6.7150E+00	0	6.7150E+00	2.2196E-09
8.00	5.9350E+01	0	5.9350E+01	1.9618E-08
6.00	5.2380E+02	0	5.2380E+02	1.7314E-07
4.00	1.2410E+03	0	1.2410E+03	4.1020E-07
3.00	1.3970E+03	0	1.3970E+03	4.6177E-07
2.50	2.5470E+03	0	2.5470E+03	8.4189E-07
1.80	4.7320E+03	0	4.7320E+03	1.5641E-06
1.34	9.8530E+03	0	9.8530E+03	3.2568E-06
0.90	1.9450E+02	0	1.9450E+02	6.4290E-08
0.80	2.1690E+04	3.6762E+08	3.6765E+08	1.2152E-01
0.70	2.8440E+03	0	2.8440E+03	9.4006E-07
0.67	1.3500E+04	0	1.3500E+04	4.4623E-06
0.60	8.2700E+04	0	8.2700E+04	2.7336E-05
0.50	1.9550E+05	0	1.9550E+05	6.4621E-05
0.40	3.1850E+06	0	3.1850E+06	1.0528E-03
0.30	1.3120E+08	0	1.3120E+08	4.3367E-02
0.20	2.5230E+09	0	2.5230E+09	8.3395E-01
		Total	3.0253E+09	1.00E+00

5.2.2 Neutron Source

Table 5.2-4 Grouped Neutron Spectrum

E (MeV)	ORIGEN Source (n/s)	I(E)
12.0	7.0830E-01	5.4927E-05
10.0	6.5830E+00	5.1050E-04
8.00	5.5380E+01	4.2946E-03
6.00	4.2420E+02	3.2896E-02
4.00	1.2670E+03	9.8253E-02
3.00	1.7950E+03	1.3920E-01
2.48	2.1980E+03	1.7045E-01
2.00	2.1110E+03	1.6370E-01
1.50	7.7940E+02	6.0441E-02
1.30	3.8870E+02	3.0143E-02
1.20	3.8650E+02	2.9972E-02
1.10	3.8530E+02	2.9879E-02
1.00	3.8340E+02	2.9732E-02
0.90	3.7770E+02	2.9290E-02
0.80	3.7000E+02	2.8693E-02
0.70	3.6010E+02	2.7925E-02
0.60	3.5590E+02	2.7599E-02
0.50	3.4940E+02	2.7095E-02
0.40	3.3080E+02	2.5653E-02
0.30	3.0790E+02	2.3877E-02
0.20	2.6230E+02	2.0341E-02
Total	1.2895E+04	1.00E+00

5.3 SHIELDING MODEL

5.3.1 Configuration of Source and Shielding

For the model geometry, the dimensions are based on the Traveller STD packaging. For this variant, the Clamshell cavity has dimensions of 9.31 in × 9.31 in × 171 in (23.65 cm × 23.65 cm × 434.34 cm) and the Outerpack outer shell has a diameter of 25 in (63.5 cm) and a height of 197 in (500.38 cm). The dimensions of these regions and this model geometry are shown in Figure 5.1-1. During the HAC drop-test series, there was minimal concentrated deformation to the Outerpack (see Section 2.7.1), therefore no changes to the Outerpack dimensions are modeled for HAC. Note that all space in this model, except the uranium source material, is void as no credit is taken for attenuation/scattering provided by the packaging or fuel assembly structure (cladding and grid structure materials).

The contents are modeled as a single cylindrical cell that is 136.7 in (347.218 cm) long, corresponding to the shortest current fuel design, to minimize the distribution of the source. The lumped UO_2 fuel volume is equivalent to the 640 kgU maximum mass used for the source term calculation and a UO_2 density of 10.96 g/cm^3. The lumped UO_2 content mass is 5 wt% ^{235}U enriched uranium pushed into the top corner of the Clamshell cavity to minimize spacing between the source and dose rate locations (See Figure 5.3-1). Because the neutron and photon source spectra are based on slightly contaminated uranium contents and the activities are determined on a per kgU basis, the activity can be considered to be uniformly distributed throughout the fuel. Thus, the distribution of activity throughout the UO_2 region is uniform. The source location is shown in Figure 5.3-1, and the photon and neutron spectra and total source strengths are listed in Table 5.2-3 and Table 5.2-4, respectively.

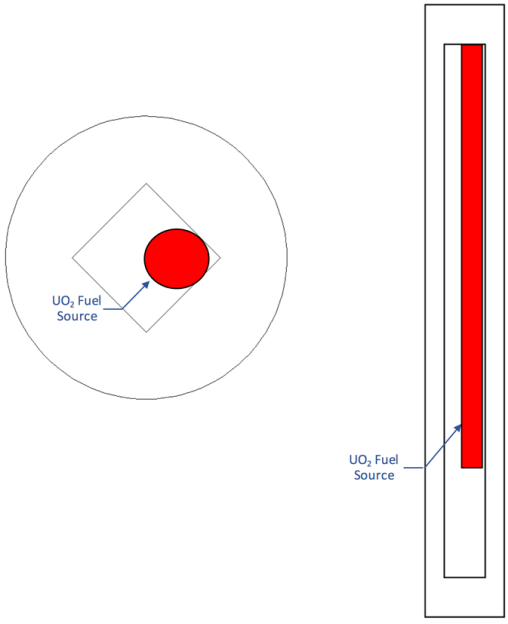

Figure 5.3-1 Dose Rate Analysis Source Configuration

5.3.2 Material Properties

As no materials are modeled in the dose rate calculations, there are no material properties input for the packaging. The fuel material is modeled as 5 wt% ^{235}U enriched UO_2 at a density of 10.96 g/cm^3.

5.4 SHIELDING EVALUATION

5.4.1 Methods

For this dose rate analysis, the MCNP6 particle transport code is used to calculate external dose rates for the package, to demonstrate compliance with the regulatory dose rate limits in 10 CFR 71. The bounding source terms calculated using the ORIGEN code, as described in Section 5.2, are used as input in the MCNP dose rate calculations.

5.4.2 Computer Codes – MCNP6

Dose rate calculations for this analysis are performed using MCNP6 [4]. MCNP is a Monte Carlo radiation-transport code that tracks multiple particle types. For the dose rate calculations in this report, MCNP is used to tally neutron and photon fluxes in specific regions of interest, to calculate the resulting dose rates at each regulatory dose rate location. The dose rate calculations use the photon transport library MCPLIB84, which compiles data from the ENDF/B-VI.8 library, and the neutron transport library ENDF71x, which compiles data from the ENDF/V-VII.1 library [5].

5.4.3 MCNP6 Model Tallies

The dose rate calculations use cell tallies that determine the particle flux at the location of interest. Using the ANSI/ANS-6.1.1 1977 Flux-to-Dose-Rate conversion factors [6] (See Section 5.4.6), the calculated neutron and photon fluxes are converted to dose rates. The cell tallies are small volumes, such that the flux is not averaged over too large of an area. The axial tallies are directly above the center of the source and the radial tallies are at the axial center of the source. The tally locations and relative sizes are shown in Figure 5.4-1.

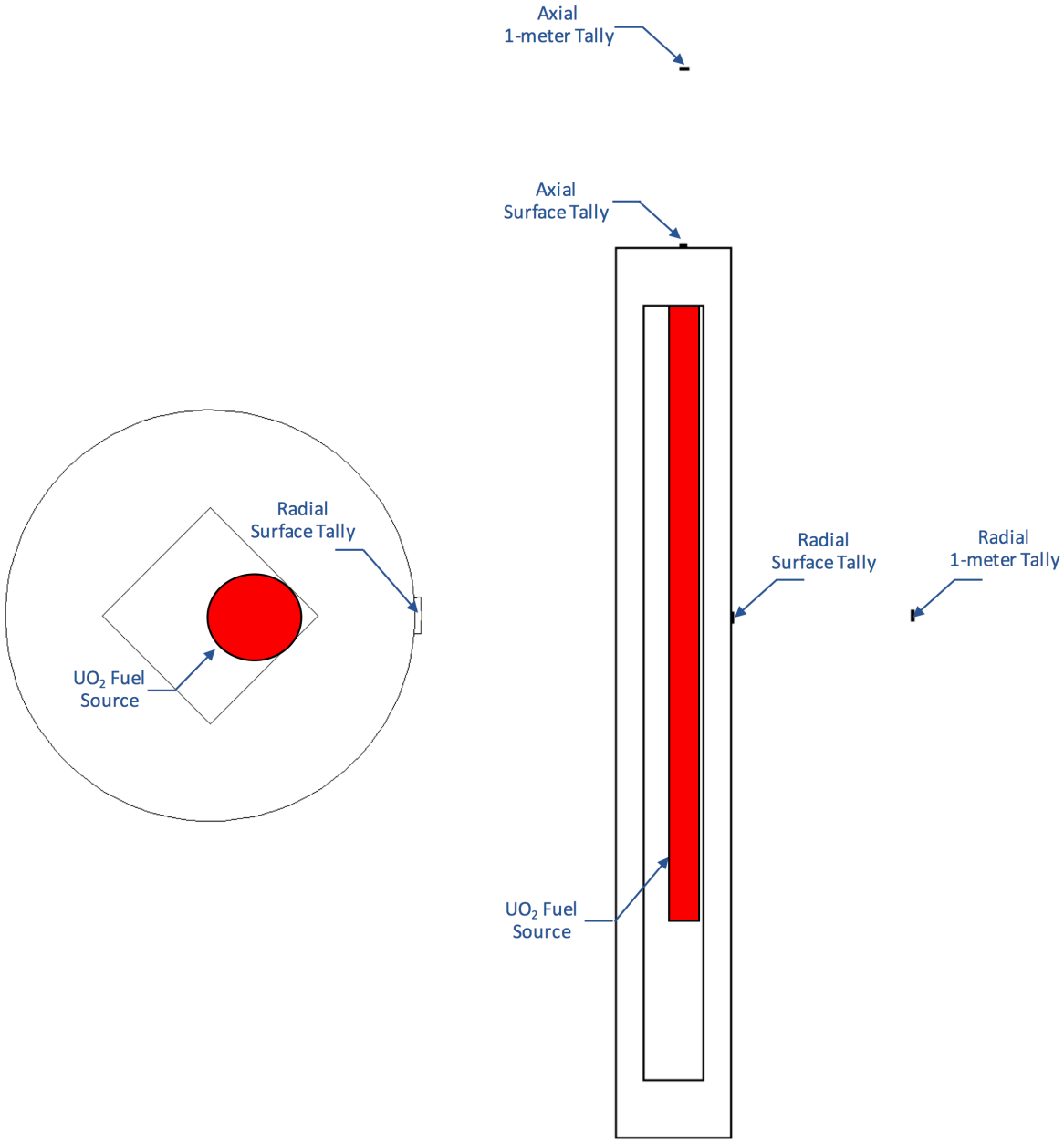

Figure 5.4-1 Dose Rate Model Tallies

5.4.4 Dose Rate Calculations

The dose rate, normalized per emitted particle, is calculated in MCNP by tallying the particle flux at each dose rate location and applying flux-to-dose rate conversion factors (see Table 5.4-1). For the neutron and photon dose rate calculation, a tally multiplier equal to the total neutron or total photon source strength is applied to each tally, such that the output dose rate is based on the total neutron or photon source.

$$D_{X,p}\left[\frac{\text{mrem}}{\text{hr}}\right] = \phi_{X,E,p}\left[\frac{\frac{\text{Particles}}{\text{cm}^2}}{\text{Emitted Particle}}\right] \cdot DF_{p,E}\left[\frac{\frac{\text{mrem}}{\text{hr}}}{\frac{\text{particle}}{\text{cm}^2 \cdot \text{s}}}\right] \cdot S_p\left[\frac{\text{Emitted Particle}}{\text{s}}\right] \quad \text{[EQN. 1]}$$

Where,

$D_{X,G,p}$ = MCNP Output Dose Rate at regulatory location X, for particle type p (n or γ)

$\phi_{X,E,p}$ = MCNP Calculated Flux at regulatory location X, for particle type p tallied at energy E

$DF_{p,E}$ = Flux-to-Dose Rate Conversion Factor for particle type p at energy E

S_p = Total Source Strength for particle type p (1.2895E+04 for n and 3.0253E+09 for γ)

To account for the uncertainty in the result of the statistical MCNP calculation, the calculated dose rate is increased by 2σ.

$$D^{\sigma}_{X,p}\left[\frac{\text{mrem}}{\text{hr}}\right] = D_{X,p} + 2 \cdot D_{X,p} \cdot \sigma_{X,p} \quad \text{[EQN. 2]}$$

Where,

$D^{\sigma}_{X,p}$ = Dose Rate at location X, for particle type p (n or γ) including uncertainty

$D_{X,p}$ = MCNP Output Dose Rate at location X, for particle type p

$\sigma_{X,p}$ = Fractional standard deviation at location X, for particle type p

The total dose rate at each regulatory dose rate location is calculated by summing the total neutron and gamma dose rates with uncertainty included, as calculated in EQN 2.

$$D_X\left[\frac{\text{mrem}}{\text{hr}}\right] = D_{X,n} + D_{X,\gamma} \quad \text{[EQN. 3]}$$

Where,

D_X = Total Dose Rate at location X from both neutrons and gammas

5.4.5 Input and Output Data

Input and output data for the ORIGEN source term calculation and the MCNP dose rate analysis of the package will be submitted separately. The tally fluctuation chart and probability density function plot were studied for each MCNP tally to ensure proper tally bin convergence. This, along with a check of the reported fsd for each tally bin and the additional statistical information reported for MCNP tallies, ensures the reliability of all MCNP calculated dose rate results.

5.4.6 Flux-to-Dose-Rate Conversion

Consistent with NUREG-1617, Section 5.5.4.3 [7], the ANSI/ANS-6.1.1 1977 gamma and neutron flux-to-dose rate conversion factors are used. The specific values are listed in Table 5.4-1.

Table 5.4-1 ANSI/ANS-6.1.1 1977 Flux-to-Dose Conversion Factors

Gamma Conversion Factors		Neutron Conversion Factors	
Gamma Energy (MeV)	**Conversion Factor (mrem/hr)/(γ/cm^2-s)**	**Neutron Energy (MeV)**	**Conversion Factor (mrem/hr)/(n/cm^2-s)**
0.01	3.96E-03	2.50E-08	3.67E-03
0.03	5.82E-04	1.00E-07	3.67E-03
0.05	2.90E-04	1.00E-06	4.46E-03
0.07	2.58E-04	1.00E-05	4.54E-03
0.10	2.83E-04	1.00E-04	4.18E-03
0.15	3.79E-04	1.00E-03	3.76E-03
0.20	5.01E-04	1.00E-02	3.56E-03
0.25	6.31E-04	1.00E-01	2.17E-02
0.30	7.59E-04	5.00E-01	9.26E-02
0.35	8.78E-04	1.00E+00	1.32E-01
0.40	9.85E-04	2.50E+00	1.25E-01
0.45	1.08E-03	5.00E+00	1.56E-01
0.50	1.17E-03	7.00E+00	1.47E-01
0.55	1.27E-03	1.00E+01	1.47E-01
0.60	1.36E-03	1.40E+01	2.08E-01
0.65	1.44E-03	2.00E+01	2.27E-01
0.70	1.52E-03		
0.80	1.68E-03		
1.00	1.98E-03		
1.40	2.51E-03		
1.80	2.99E-03		
2.20	3.42E-03		
2.60	3.82E-03		
2.80	4.01E-03		
3.25	4.41E-03		
3.75	4.83E-03		
4.25	5.23E-03		
4.75	5.60E-03		
5.00	5.80E-03		
5.25	6.01E-03		
5.75	6.37E-03		
6.25	6.74E-03		
6.75	7.11E-03		
7.50	7.66E-03		
9.00	8.77E-03		
11.0	1.03E-02		
13.0	1.18E-02		
15.0	1.33E-02		

5.4.7 External Radiation Levels

The results of the MCNP dose rate calculations for the Traveller package shipping a maximum load of contaminated uranium, as defined by Table 1-2, are presented in Table 5.4-2. It has been determined that sufficient convergence of all MCNP tallies has been achieved through a check of the statistical information in the MCNP outputs. The results in this table demonstrate compliance of the Traveller package with a maximum activity content with all 10 CFR 71 dose rate requirements for a non-exclusive use package transport. All package surface dose rates are well below the 10 CFR 71.47(a) requirement of 200 mrem/hr. As the NCT and HAC geometry and source are identical, the calculated 1-meter dose rates demonstrate compliance with both the 10 CFR 71.47(a) NCT requirement of a TI of 10 (10 mrem/hr) and the 10 CFR 71.51(a)(2) HAC requirement of 1000 mrem/hr at 1 meter. The small increase in the HAC dose rate from accounting for the localized deformations from a free drop or pin puncture would not be sufficient to increase the 1-meter dose rate enough to result in the HAC dose rate exceeding the regulatory limit. Additionally, the lack of deformation of the packaging and contents from NCT and HAC demonstrates compliance with the IAEA SSR-6 para. 648 requirement that there would be no increase of more than 20% in the maximum radiation level on the exterior surface of the package due to NCT. As there is no significant deformation of the packaging or contents from NCT, there will be no significant change in the package surface dose rate.

Table 5.4-2 MCNP Dose Rate Calculation Results

Dose Rate Location		Neutron Dose Rate (mrem/hr) [1,2]	Gamma Dose Rate (mrem/hr) [1]	Total (mrem/hr) [1,2]
Package Surface	Radial	0.0308	1.3252	1.3559
	Axial	0.0034	0.1901	0.1935
1 Meter	Radial	0.0053	0.2276	0.2329
	Axial	0.0002	0.0128	0.0130

Note: [1] Listed dose rates include 2σ uncertainty on top of calculated value.
[2] Includes dose rate contribution from secondary particles (subcritical multiplication and n,γ)

5.5 APPENDICES

5.5.1 References

[1] U.S. Nuclear Regulatory Commission Code of Federal Regulations, Title 10 Part 71, "Packaging and Transport of Radioactive Material," 2016.

[2] International Atomic Energy Agency, "Regulations for the Safe Transport of Radioactive Material," 2012.

[3] Oak Ridge National Laboratory, "Scale: A Comprehensive Modeling and Simulation Suite for Nuclear Safety Analysis an Design," ORNL/TM-2005/39, Version 6.1, 2011.

[4] Los Alamos National Laboratory, "Initial MCNP 6 Release Overview - MCNP6 Version 1.0," LA-UR-13-22934, Rev.0, 2013.

[5] Los Alamos National Laboratory, "Listing of Available ACE Data Tables," LA-UR-13-21822, Rev.2, 2014.

[6] American Nuclear Society, "Neutron and Gamma Flux-To-Dose Conversion Factors," ANSI/ANS 6.1.1-1977, 1977.

[7] U.S. Nuclear Regulatory Commission, "Standard Review Plan for Transportation Packages for Spent Nuclear Fuel," NUREG-1617, 2000.

TABLE OF CONTENTS

6.0 CRITICALITY EVALUATION 6-1
6.1 DESCRIPTION OF CRITICALITY DESIGN 6-1
6.1.1 Design Features 6-1
6.1.1.1 Confinement System 6-1
6.1.1.2 Flux Traps 6-1
6.1.2 Summary Table of Criticality Evaluation 6-2
6.1.2.1 Contents Grouping 6-3
6.1.3 Criticality Safety Index 6-4
6.2 FISSILE MATERIAL CONTENTS 6-5
6.2.1 Group 1 6-6
6.2.2 Group 2 6-9
6.2.3 Group 4 6-10
6.2.4 Rod Pipe 6-13
6.3 GENERAL CONSIDERATIONS 6-14
6.3.1 Model Configuration 6-14
6.3.1.1 Rod Pipe 6-17
6.3.1.2 Conditions of Transport 6-18
6.3.2 Material Properties 6-19
6.3.2.1 Non-Fissile, Non-Radioactive Reactor Core Components 6-19
6.3.2.2 UO_2 6-19
6.3.2.3 U_3Si_2 6-19
6.3.2.4 Zircaloy Cladding 6-20
6.3.2.5 Guide Tubes/Instrument Tubes 6-20
6.3.2.6 Flooding and Reflecting Water 6-20
6.3.2.7 Fuel Assembly Structural Materials 6-20
6.3.2.8 Aluminum 6-20
6.3.2.9 304 Stainless Steel 6-21
6.3.2.10 Ultra-High Molecular Weight Polyethylene 6-21
6.3.2.11 BORAL Neutron Absorber Plates 6-21
6.3.2.12 Hydrogenous Packaging Materials 6-21
6.3.2.13 Hydrogenous Packing Materials 6-22
6.3.2.14 Extreme Cold Case (-40°C) Effects 6-22
6.3.2.15 Summary of SCALE Material Compositions 6-22
6.3.3 Computer Codes and Cross-Section Libraries 6-25
6.3.3.1 SCALE 6.1.2 6-25
6.3.3.2 SCALE 6.1.3 6-25
6.3.3.3 Convergence Criteria 6-26
6.3.4 Demonstration of Maximum Reactivity 6-27
6.3.4.1 Categorized Fuel Assembly Determination 6-28
6.3.4.2 Baseline Case 6-28
6.3.4.3 Sensitivity Studies 6-35
6.4 SINGLE PACKAGE EVALUATION 6-48
6.4.1 Configuration 6-48
6.4.1.1 Baseline Configurations 6-48
6.4.1.2 Sensitivity Study Configurations 6-50
6.4.2 Results 6-51
6.4.2.1 Single Package – Maximum Reactivity Results Summary 6-51
6.4.2.2 Sensitivity Study Results 6-52
6.5 EVALUATION OF PACKAGE ARRAYS UNDER NORMAL CONDITIONS OF TRANSPORT 6-71
6.5.1 Configuration 6-71
6.5.1.1 Baseline Configurations 6-71
6.5.1.2 Sensitivity Study Configurations 6-74
6.5.2 Results 6-75

6.5.2.1 NCT Package Array – Maximum Reactivity Results Summary 6-75
6.5.2.2 Sensitivity Study Results 6-75
6.6 PACKAGE ARRAYS UNDER HYPOTHETICAL ACCIDENT CONDITIONS 6-87
6.6.1 Configuration 6-87
6.6.1.1 Baseline Configuration 6-87
6.6.1.2 Sensitivity Study Configurations 6-90
6.6.2 Results 6-91
6.6.2.1 HAC Package Array – Maximum Reactivity Results Summary 6-91
6.6.2.2 Sensitivity Study Results 6-92
6.7 FISSILE MATERIAL PACKAGES FOR AIR TRANSPORT 6-110
6.7.1 Configuration 6-110
6.7.2 Results 6-110
6.8 BENCHMARK EVALUATIONS 6-111
6.8.1 Applicability of Benchmark Experiments 6-111
6.8.2 Bias Determination 6-112
6.9 APPENDIX 6-114
6.9.1 References 6-115
6.9.2 Categorized Fuel Assembly Analysis 6-116
6.9.2.1 CFA Results 6-116
6.9.2.2 Organizing Fuel Assemblies into Bins 6-117
6.9.2.3 Determination of Categorized Fuel Assemblies 6-118
6.9.2.4 Determination of Most Reactive Secondary Parameters 6-120
6.9.2.5 Bin Permutation Model 6-120
6.9.2.6 CFA Most Reactive Secondary Parameters 6-121
6.9.3 Baseline Detailed Results 6-146
6.9.3.1 Single Package, Fuel Assembly 6-146
6.9.3.2 Single Package, Rod Pipe 6-150
6.9.3.3 Package Array, NCT, Fuel Assembly 6-155
6.9.3.4 Package Array, NCT, Rod Pipe 6-157
6.9.3.5 Package Array, HAC, Fuel Assembly 6-158
6.9.3.6 Package Array, HAC, Rod Pipe 6-165
6.9.4 Combined Cases 6-168

LIST OF TABLES

Table 6-1 Summary Table of Upper Subcritical Limits 6-3
Table 6-2 Summary Table of Criticality Evaluation 6-4
Table 6-3 Criticality Safety Index Summary 6-4
Table 6-4 Bin Listing for Each Fuel Assembly Group 6-5
Table 6-5 Group 1 Fuel Assembly Bins 6-6
Table 6-6 Group 1 Fuel Assembly Bins 6-7
Table 6-7 Group 1 Fuel Assembly Bins 6-7
Table 6-8 Group 2 Fuel Assembly Bins 6-9
Table 6-8A Group 4 Fuel Assembly Bins 6-11
Table 6-8B Group 4 Fuel Assembly Bins 6-11
Table 6-9 Major Dimensions of Each Traveller Variant Model 6-15
Table 6-10 Major Dimensions of Rod Pipe Model 6-17
Table 6-11 Summary of Compound Material Compositions 6-23
Table 6-12 Summary of Alloy/Mixture Material Compositions 6-24
Table 6-13 Summary of BORAL Plate Core Material Composition 6-25
Table 6-14 Bin Listing for Each Fuel Assembly Group 6-28
Table 6-15 Rod Pipe UO_2 Baseline Evaluation - Fuel Rod and Pitch Values 6-33
Table 6-16 Rod Pipe U_3Si_2 Baseline Evaluation - Fuel Rod and Pitch Values 6-34
Table 6-17 Baseline and Sensitivity Studies Configurations for Each Package Arrangement 6-36
Table 6-17A Baseline and Sensitivity Study Configurations for Group 4 6-37
Table 6-18 Cladding Diameter Tolerances Examined 6-44
Table 6-19 Fuel Pellet Diameter Tolerances Examined 6-44
Table 6-20 Fuel Rod Pitch Tolerances Examined 6-45
Table 6-21 Summary of Groups 1 and 2 Single Package Baseline Configurations 6-48
Table 6-22 Summary of Rod Pipe Single Package Baseline Configurations 6-49
Table 6-23 Single Package Sensitivity Study Bounding Configurations – PWR Fuel Assembly Groups 6-50
Table 6-24 Rod Pipe Single Package Sensitivity Studies Bounding Configurations 6-51
Table 6-25 Single Package – Maximum Reactivity Results Summary 6-51
Table 6-26 Single Package Assessed Penalties, Δk_u, PWR Fuel Assembly Groups 6-52
Table 6-27 Annular Blanket Sensitivity Results – Single Package, NCT, PWR Fuel Assembly Groups 6-53
Table 6-28 Fuel Assembly Position Sensitivity Results – Single Package, NCT, PWR Fuel Assembly Groups 6-53
Table 6-29 Polyethylene Packing Sensitivity Results – Single Package, NCT, PWR Fuel Assembly Groups 6-54
Table 6-30 SS Rod Replacement Sensitivity Results – Single Package, NCT, PWR Fuel Assembly Groups 6-54
Table 6-31 Tolerance Sensitivity Results – Single Package, NCT, PWR Fuel Assembly Groups 6-54
Table 6-31A ADOPT Fuel Results – Single Package, NCT, PWR Fuel Assembly Groups 6-55
Table 6-32 Annular Blanket Sensitivity Results – Single Package, HAC, PWR Fuel Assembly Groups 6-55
Table 6-33 Moderator Block Density Results – Single Package, HAC, PWR Fuel Assembly Groups 6-56
Table 6-34 Fuel Assembly Position Sensitivity Results – Single Package, HAC, PWR Fuel Assembly Groups 6-57
Table 6-35 Polyethylene Sensitivity Results – Single Package, HAC, PWR Fuel Assembly Groups 6-57
Table 6-36 Axial Rod Displacement Sensitivity Results – Single Package, HAC, PWR Fuel Assembly Groups 6-59
Table 6-37 SS Rod Replacement Sensitivity Results – Single Package, HAC, PWR Fuel Assembly Groups 6-59
Table 6-38 Tolerance Sensitivity Results – Single Package, HAC, PWR Fuel Assembly Groups 6-60
Table 6-38A ADOPT Fuel Results – Single Package, HAC, PWR Fuel Assembly Groups 6-60
Table 6-39 Single Package Assessed Penalties, Δk_u, Rod Pipe 6-61
Table 6-40 Annular Blanket Sensitivity Results – Single Package, NCT, Rod Pipe 6-61
Table 6-41 Rod Pipe Position Sensitivity Results – Single Package, NCT, Rod Pipe 6-63
Table 6-42 Polyethylene Packing Sensitivity Results – Single Package, NCT, Rod Pipe 6-63
Table 6-43 Tolerance Sensitivity Results – Single Package, NCT, Rod Pipe 6-65
Table 6-43A ADOPT Fuel Results – Single Package, NCT, Rod Pipe 6-65
Table 6-44 Annular Blanket Sensitivity Results – Single Package, HAC, Rod Pipe 6-65
Table 6-45 Rod Pipe Position Sensitivity Results – Single Package, HAC, Rod Pipe 6-67
Table 6-46 Moderator Block Density Results – Single Package, HAC, Rod Pipe 6-67
Table 6-47 Polyethylene Sensitivity Results – Single Package, HAC, Rod Pipe 6-68
Table 6-48 Tolerance Sensitivity Results – Single Package, HAC, Rod Pipe 6-70

Table 6-48A ADOPT Fuel Results – Single Package, HAC, Rod Pipe 6-70
Table 6-49 Summary of NCT Package Array Baseline Configuration 6-71
Table 6-50 Summary of Rod Pipe NCT Package Array Configurations 6-73
Table 6-51 NCT Package Array Sensitivity Study Bounding Configurations – PWR Fuel Assembly Groups 6-74
Table 6-52 NCT Package Array Sensitivity Study Bounding Configurations – Rod Pipe 6-74
Table 6-53 NCT Package Array – Maximum Reactivity Results Summary 6-75
Table 6-54 NCT Package Array Assessed Penalties, Δk_u 6-75
Table 6-55 Annular Blanket Sensitivity Results – Package Array, NCT, PWR Fuel Assembly Groups 6-76
Table 6-56 Fuel Assembly Position Sensitivity Results – Package Array, NCT, PWR Fuel Assembly Groups 6-78
Table 6-57 Package OD Tolerance Results – Package Array, NCT, PWR Fuel Assembly Groups 6-78
Table 6-58 Polyethylene Packing Sensitivity Results – Package Array, NCT, PWR Fuel Assembly Groups 6-79
Table 6-59 SS Rod Replacement Sensitivity Results – Package Array, NCT, PWR Fuel Assembly Groups 6-79
Table 6-60 Tolerance Sensitivity Results – Package Array, NCT, PWR Fuel Assembly Groups 6-80
Table 6-61 Steel Nozzle Reflector Sensitivity Results – Package Array, NCT, PWR Fuel Assembly Groups 6-81
Table 6-61A ADOPT Fuel Results – Package Array, NCT, PWR Fuel Assembly Groups 6-81
Table 6-62 Rod Pipe NCT Package Array Assessed Penalties, Δk_u 6-82
Table 6-63 Annular Blanket Sensitivity Results – Package Array, NCT, Rod Pipe 6-83
Table 6-64 Rod Pipe Position Sensitivity Results – Package Array, NCT, Rod Pipe 6-84
Table 6-65 Package OD Tolerance Sensitivity Results – Package Array, NCT, Rod Pipe 6-84
Table 6-66 Polyethylene Packing Sensitivity Results – Package Array, NCT, Rod Pipe 6-85
Table 6-67 Tolerance Sensitivity Results – Package Array, NCT, Rod Pipe 6-86
Table 6-67A ADOPT Fuel Results – Package Array, NCT, Rod Pipe 6-86
Table 6-68 Summary of PWR Fuel Assembly Groups HAC Package Array Configurations 6-87
Table 6-69 Summary of Rod Pipe HAC Package Array Configurations 6-89
Table 6-70 HAC Package Array Sensitivity Study Bounding Configurations – PWR Fuel Assembly Groups 6-90
Table 6-71 HAC Package Array Sensitivity Study Bounding Configurations – Rod Pipe 6-91
Table 6-72 HAC Package Array – Maximum Reactivity Results Summary 6-91
Table 6-73 HAC Package Array Assessed Penalties, Δk_u, PWR Fuel Assembly Groups 6-92
Table 6-74 Annular Blanket Sensitivity Results – HAC Package Array, PWR Fuel Assembly Groups 6-93
Table 6-75 Clamshell/Fuel Assembly Position Results – HAC Package Array, PWR Fuel Assembly Groups 6-95
Table 6-76 Moderator Block Density Results – HAC Package Array, PWR Fuel Assembly Groups 6-95
Table 6-77 Package Outer Diameter Tolerance Results – HAC Package Array, PWR Fuel Assembly Groups 6-96
Table 6-78 Polyethylene Sensitivity Results – HAC Package Array, PWR Fuel Assembly Groups 6-96
Table 6-79 Axial Rod Displacement Sensitivity Results – Single Package, HAC, PWR Fuel Assembly Groups 6-99
Table 6-80 SS Rod Replacement Sensitivity Results – Single Package, HAC, PWR Fuel Assembly Groups 6-100
Table 6-81 Tolerance Sensitivity Results – HAC Package Array, PWR Fuel Assembly Groups 6-101
Table 6-82 Steel Nozzle Reflector Sensitivity Results – HAC Package Array, PWR Fuel Assembly Groups 6-102
Table 6-82A ADOPT Fuel Results – HAC Package Array, PWR Fuel Assembly Groups 6-102
Table 6-83 HAC Package Array Assessed Penalties, Δk_u, Rod Pipe 6-103
Table 6-84 Annular Blanket Sensitivity Results – HAC Package Array, Rod Pipe 6-103
Table 6-85 Rod Pipe Position Sensitivity Results – HAC Package Array, Rod Pipe 6-105
Table 6-86 Moderator Block Density Results – HAC Package Array, Rod Pipe 6-105
Table 6-87 Package Outer Diameter Tolerance Sensitivity Results – HAC Package Array, Rod Pipe 6-105
Table 6-88 Polyethylene Sensitivity Results – HAC Package Array, Rod Pipe 6-106
Table 6-89 Tolerance Sensitivity Results – HAC Package Array, Rod Pipe 6-107
Table 6-90 Flooding Configuration Results – HAC Package Array, Rod Pipe 6-108
Table 6-90A ADOPT Fuel Results – HAC Package Array, Rod Pipe 6-109
Table 6-91 Benchmark Experiment Summary 6-112
Table 6-92 Parameter Correlation Coefficient Results 6-112
Table 6-93 Categorized Fuel Assemblies for Input into Package Assessment – Groups 1 and 2 6-116
Table 6-94 Categorized Fuel Assemblies for Input into Package Assessment – Groups 1 and 2 6-117
Table 6-94A Categorized Fuel Assemblies for Input into Package Assessment – Group 4 6-117
Table 6-95 Bin Organization Example 6-118
Table 6-96 Fuel Pellet Radius Range Determination 6-119
Table 6-97 Secondary Fuel Assembly Parameter Ranges – Groups 1 and 2 6-121
Table 6-97A Secondary Fuel Assembly Parameter Ranges – Group 4 6-122

Table 6-98 Effect of Secondary Parameters on k-inf - 14 Bin 1 6-123
Table 6-99 Effect of Secondary Parameters on 14 Bin 2..... 6-124
Table 6-100 Effect of Secondary Parameters on 15 Bin 1..... 6-125
Table 6-101 Effect of Secondary Parameters on 15 Bin 2..... 6-126
Table 6-102 Effect of Secondary Parameters on 16 Bin 1..... 6-127
Table 6-103 Effect of Secondary Parameters on 16 Bin 2..... 6-128
Table 6-104 Effect of Secondary Parameters on 16 Bin 3..... 6-129
Table 6-105 Effect of Secondary Parameters on 17 Bin 1..... 6-130
Table 6-106 Effect of Secondary Parameters on 17 Bin 2..... 6-131
Table 6-107 Effect of Secondary Parameters on 18 Bin 1..... 6-132
Table 6-107A Effect of Secondary Parameters on k-inf - 14 Bin 1, Group 4 6-134
Table 6-107B Effect of GT/IT Secondary Parameters on k-inf – 14 Bin 1, Group 4..... 6-135
Table 6-107C Effect of Secondary Parameters on k-inf – 14 Bin 2, Group 4..... 6-136
Table 6-107D Effect of GT/IT Secondary Parameters on k-inf – 14 Bin 2, Group 4..... 6-137
Table 6-107E Effect of Secondary Parameters on on k-inf – 15 Bin 3, Group 4..... 6-138
Table 6-107F Effect of GT/IT Secondary Parameters on k-inf – 15 Bin 3, Group 4..... 6-139
Table 6-107G Effect of Secondary Parameters on k-inf – 16 Bin 2, Group 4..... 6-140
Table 6-107H Effect of GT/IT Secondary Parameters on k-inf – 16 Bin 2, Group 4..... 6-141
Table 6-107I Effect of Secondary Parameters on k-inf – 16 Bin 3, Group 4..... 6-142
Table 6-107J Effect of GT/IT Secondary Parameters on k-inf – 16 Bin 3, Group 4..... 6-143
Table 6-107K Effect of Secondary Parameters on k-inf – 17 Bin 1, Group 4..... 6-144
Table 6-107L Effect of GT/IT Secondary Parameters on k-inf – 17 Bin 1, Group 4..... 6-145
Table 6-108 Single Package, CFA-Package Variant Comparison Results..... 6-146
Table 6-109 Axial Position Baseline Results – Single Package, NCT, PWR Fuel Assembly Groups..... 6-147
Table 6-110 Axial Position Baseline Results – Single Package, HAC, PWR Fuel Assembly Groups 6-148
Table 6-111 Single Package, NCT, Rod Pipe Package Variant Results..... 6-150
Table 6-112 Single Package, HAC, Rod Pipe Fuel OR-Pitch Combination – Maximum Results 6-152
Table 6-113 UO_2 Single Package, HAC, Rod Pipe Fuel OR-Pitch Combination – Pitch Variation 6-152
Table 6-114 U_3Si_2 Single Package, HAC, Rod Pipe Fuel OR-Pitch Combination – Pitch Variation..... 6-153
Table 6-115 UO_2 Single Package, HAC, Rod Pipe Fuel OR-Pitch Combination – Refined Parameter Study 6-154
Table 6-116 Package Array, NCT, CFA Package Variant Results..... 6-155
Table 6-117 Axial Position Baseline Results –Package Array, NCT, PWR Fuel Assembly Groups..... 6-156
Table 6-118 Package Array, NCT, Rod Pipe-Package Variant Comparison Results..... 6-157
Table 6-119 Package Array, HAC, CFA Package Variant Results 6-158
Table 6-120 Axial Position Baseline Results –Package Array, HAC, PWR Fuel Assembly Groups 6-159
Table 6-121 Partial Flooding Baseline Results – Package Array, HAC, PWR Fuel Assembly Groups 6-160
Table 6-122 Preferential Flooding Baseline Results – Package Array, HAC, PWR Fuel Assembly Groups 6-162
Table 6-123 Package Array, HAC, Rod Pipe Fuel OR-Pitch Combination – Maximum Results..... 6-165
Table 6-124 UO_2 Package Array, HAC, Rod Pipe Fuel OR-Pitch Combination – Pitch Variation..... 6-166
Table 6-125 U_3Si_2 Package Array, HAC, Rod Pipe Fuel OR-Pitch Combination – Pitch Variation 6-166
Table 6-126 UO_2 Package Array, HAC, Rod Pipe Fuel OR-Pitch Combination – Refined Parameter Study 6-167
Table 6-127 *Maximum* k_{eff} vs. Combined Case Results..... 6-168

LIST OF FIGURES

Figure 6-1 Cross Section of the Flux Trap System for STD/XL ... 6-2
Figure 6-2 Group 1 Fuel Rod Patterns. Not to Scale. ... 6-8
Figure 6-3 Group 1 Fuel Rod Patterns. Not to Scale. ... 6-8
Figure 6-4 Group 1 Fuel Rod Patterns. Not to Scale. ... 6-8
Figure 6-5 Group 2 Fuel Rod Patterns. Not to Scale. ... 6-9
Figure 6-5A Group 4 Fuel Rod Patterns. Not to Scale. ... 6-12
Figure 6-5B Group 4 Fuel Rod Patterns. Not to Scale. ... 6-12
Figure 6-6 Front Cross-Sections of the Traveller STD/XL ... 6-16
Figure 6-7 Top to bottom: Side Cross-Sections of the Traveller STD and XL ... 6-16
Figure 6-8 Top to bottom: Top Moderator Block Cross-Sections of the Traveller STD and XL ... 6-17
Figure 6-9 Side Cross Section of the Traveller Showing PWR Group 1/2 Fuel Assembly Axial Position Study ... 6-30
Figure 6-10 Cutaway of Traveller XL with 17 Bin 2 Showing the Lattice Pitch Expansion Section ... 6-31
Figure 6-11 The Six Flooding Configurations for PWR Fuel Assembly Groups ... 6-32
Figure 6-12 Rod Pipe, UO_2 Fuel Array Modeling in Rod Pipe ... 6-34
Figure 6-13 Rod Pipe, U_3Si_2 NCT Case (left) and Two HAC Cases (right) ... 6-35
Figure 6-14 NCT Single Package Baseline Case vs. Fuel Assembly Shift ... 6-38
Figure 6-15 HAC Package Array Baseline Case vs. Clamshell and Fuel Assembly Shift ... 6-38
Figure 6-16 PWR Fuel Assembly Polyethylene Outer Wrap NCT Configuration ... 6-40
Figure 6-17 PWR Fuel Assembly Polyethylene Outer Wrap HAC Configurations ... 6-40
Figure 6-18 Uniform Polyethylene Melt HAC Configuration – PWR Fuel Assemblies ... 6-41
Figure 6-19 Uniform Polyethylene Wrap NCT/HAC Configuration – Rod Pipe ... 6-41
Figure 6-20 PWR Fuel Assembly Collected Polyethylene Melt Configuration ... 6-42
Figure 6-21 Rod Pipe Collected Polyethylene Melt Configuration ... 6-42
Figure 6-22 Corner Rod Displacement Configurations – 17 Bin 1 ... 6-43
Figure 6-23 Random Rod Displacement Configurations – 17 Bin 1 ... 6-43
Figure 6-24 SS Replacement Rod Configurations – 17 Bin 1 ... 6-44
Figure 6-25 Example of NCT Stainless Steel Nozzle Configuration, Shown in Green ... 6-46
Figure 6-26 Example of HAC Stainless Steel Nozzle Configuration, Shown in Green ... 6-46
Figure 6-27 Rod Pipe HAC Package Array Flooding Configurations ... 6-47
Figure 6-28 Cross-section of Groups 1 and 2 NCT and Group 4 Single Package Baseline Case ... 6-48
Figure 6-29 Cross-section Groups 1 and 2 HAC Single Package Baseline Case ... 6-49
Figure 6-30 Annular Blanket Sensitivity – Single Package, NCT (Groups 1 & 2) ... 6-53
Figure 6-31 Annular Blanket Sensitivity Results – Single Package, HAC (Groups 1 & 2) ... 6-56
Figure 6-31A Annular Blanket Sensitivity Results – Single Package, HAC (Group 4) ... 6-56
Figure 6-32 Polyethylene Sensitivity Results – Single Package, HAC (Groups 1 & 2) ... 6-58
Figure 6-32A Polyethylene Sensitivity Results – Single Package, HAC (Group 4) ... 6-58
Figure 6-33 Axial Rod Displacement Sensitivity Results – Single Package, HAC (Groups 1 & 2) ... 6-59
Figure 6-34 Annular Blanket Sensitivity – Single Package, NCT (Rod Pipe UO_2 Fuel Rods) ... 6-62
Figure 6-35 Annular Blanket Sensitivity – Single Package, NCT (Rod Pipe U_3Si_2 Fuel Rods) ... 6-62
Figure 6-36 Polyethylene Packing Sensitivity – Single Package, NCT (Rod Pipe UO_2 Fuel Rods) ... 6-64
Figure 6-37 Polyethylene Packing Sensitivity – Single Package, NCT (Rod Pipe U_3Si_2 Fuel Rods) ... 6-64
Figure 6-38 Annular Blanket Sensitivity Results – Single Package, HAC (Rod Pipe UO_2 Fuel Rods) ... 6-66
Figure 6-39 Annular Blanket Sensitivity Results – Single Package, HAC (Rod Pipe U_3Si_2 Fuel Rods) ... 6-66
Figure 6-40 Polyethylene Sensitivity Results – Single Package, HAC (Rod Pipe UO_2 Fuel Rods) ... 6-69
Figure 6-41 Polyethylene Sensitivity Results – Single Package, HAC (Rod Pipe U_3Si_2 Fuel Rods) ... 6-69
Figure 6-42 Group 1, NCT 250-package Array with Height of Two Packages ... 6-72
Figure 6-43 Group 2 NCT 60-package Array with Height of One Package ... 6-72
Figure 6-43A Group 4 NCT 100-package Array with Height of One Package ... 6-72
Figure 6-44 Rod Pipe NCT 379-package Array with Height of One Package ... 6-73
Figure 6-45 Annular Blanket Sensitivity – Package Array, NCT (Group 1) ... 6-77
Figure 6-46 Annular Blanket Sensitivity – Package Array, NCT (Group 2) ... 6-77
Figure 6-46A Annular Blanket Sensitivity – Package Array, NCT (Group 4) ... 6-77
Figure 6-47 Annular Blanket Sensitivity – Package Array, NCT (Rod Pipe UO_2 Fuel Rods) ... 6-83
Figure 6-48 Annular Blanket Sensitivity – Package Array, NCT (Rod Pipe U_3Si_2 Fuel Rods) ... 6-84

Figure 6-49 Polyethylene Packing Sensitivity – Package Array, NCT (Rod Pipe UO_2 Fuel Rods) 6-85
Figure 6-50 Polyethylene Packing Sensitivity – Package Array, NCT (Rod Pipe U_3Si_2 Fuel Rods) 6-86
Figure 6-51 Group 1, HAC 100-package Array 6-88
Figure 6-52 Group 2, HAC 24-package Array 6-88
Figure 6-52A Group 4, HAC 40-package Array 6-88
Figure 6-53 Rod Pipe, HAC 150-package Array 6-89
Figure 6-54 Annular Blanket Sensitivity – HAC Package Array (Group 1) 6-94
Figure 6-55 Annular Blanket Sensitivity – HAC Package Array (Group 2) 6-94
Figure 6-55A Annular Blanket Sensitivity – HAC Package Array (Group 4) 6-94
Figure 6-56 Polyethylene Sensitivity Results – HAC Package Array (Group 1) 6-97
Figure 6-57 Polyethylene Sensitivity Results – HAC Package Array (Group 2) 6-98
Figure 6-57A Polyethylene Sensitivity Results – HAC Package Array (Group 4) 6-98
Figure 6-58 Axial Rod Displacement Sensitivity Results – HAC Package Array (Group 1) 6-99
Figure 6-59 Axial Rod Displacement Sensitivity Results – HAC Package Array (Group 2) 6-100
Figure 6-60 Annular Blanket Sensitivity – HAC Package Array (Rod Pipe UO_2 Fuel Rods) 6-104
Figure 6-61 Annular Blanket Sensitivity – HAC Package Array (Rod Pipe U_3Si_2 Fuel Rods) 6-104
Figure 6-62 Polyethylene Sensitivity Results – HAC Package Array (Rod Pipe UO_2 Fuel Rods) 6-107
Figure 6-63 Polyethylene Sensitivity Results – HAC Package Array (Rod Pipe U_3Si_2 Fuel Rods) 6-107
Figure 6-64 Flooding Configuration Sensitivity Results – HAC Package Array (Rod Pipe UO_2 Rods) 6-109
Figure 6-65 Flooding Configuration Sensitivity Results – HAC Package Array (Rod Pipe U_3Si_2 Rods) 6-109
Figure 6-66 EALF USLSTATS Plot 6-113
Figure 6-67 Fuel Rod Patterns of 16 Bin 1 (left) and 16 Bin 2 (right) – Not to Scale 6-118
Figure 6-68 x-y (left) and x-z (right) Cross Sections of a Fuel Assembly Permutation. Not to Scale. 6-120
Figure 6-69 Trend Plot of Effect of Secondary Parameters on k-inf – 14 Bin 1 6-124
Figure 6-70 Trend Plot of Effect of Secondary Parameters on k-inf – 14 Bin 2 6-125
Figure 6-71 Trend Plot of Effect of Secondary Parameters on k-inf – 15 Bin 1 6-126
Figure 6-72 Trend Plot of Effect of Secondary Parameters on k-inf – 15 Bin 2 6-127
Figure 6-73 Trend Plot of Effect of Secondary Parameters on k-inf – 16 Bin 1 6-128
Figure 6-74 Trend Plot of Effect of Secondary Parameters on k-inf – 16 Bin 2 6-129
Figure 6-75 Trend Plot of Effect of Secondary Parameters on k-inf – 16 Bin 3 6-130
Figure 6-76 Trend Plot of Effect of Secondary Parameters on k-inf – 17 Bin 1 6-131
Figure 6-77 Trend Plot of Effect of Secondary Parameters on k-inf – 17 Bin 2 6-132
Figure 6-78 Trend Plot of Effect of Secondary Parameters on k-inf – 18 Bin 1 6-133
Figure 6-78A Trend Plot of Effect of Secondary Parameters on k-inf – 14 Bin 1, Group 4 6-134
Figure 6-78B Trend Plot of Effect of GT/IT Secondary Parameters on k-inf – 14 Bin 1, Group 4 6-135
Figure 6-78C Trend Plot of Effect of Secondary Parameters on k-inf – 14 Bin 2, Group 4 6-136
Figure 6-78D Trend Plot of Effect of GT/IT Secondary Parameters on k-inf – 14 Bin 2, Group 4 6-137
Figure 6-78E Trend Plot of Effect of Secondary Parameters on k-inf – 15 Bin 3, Group 4 6-138
Figure 6-78F Trend Plot of Effect of GT/IT Secondary Parameters on k-inf – 15 Bin 3, Group 4 6-139
Figure 6-78G Trend Plot of Effect of Secondary Parameters on k-inf – 16 Bin 2, Group 4 6-140
Figure 6-78H Trend Plot of Effect of GT/IT Secondary Parameters on k-inf – 16 Bin 2, Group 4 6-141
Figure 6-78I Trend Plot of Effect of Secondary Parameters on k-inf – 16 Bin 3, Group 4 6-142
Figure 6-78J Trend Plot of Effect of GT/IT Secondary Parameters on k-inf – 16 Bin 3, Group 4 6-143
Figure 6-78K Trend Plot of Effect of Secondary Parameters on k-inf – 17 Bin 1, Group 4 6-144
Figure 6-78L Trend Plot of Effect of GT/IT Secondary Parameters on k-inf – 17 Bin 1, Group 4 6-145
Figure 6-79 Axial Position Baseline Results – Single Package, NCT, Groups 1 and 2 6-149
Figure 6-80 Axial Position Baseline Results – Single Package, HAC, Groups 1 and 2 6-149
Figure 6-80A Axial Position Baseline Results – Single Package, HAC, Group 4 6-150
Figure 6-81 Effect of Preferential Flooding Configuration on k_{eff} (Group 1) 6-163
Figure 6-82 Effect of Preferential Flooding Configuration on k_{eff} (Group 2) 6-163
Figure 6-82A Effect of Preferential Flooding Configuration on k_{eff} (Group 4) 6-164

6.0 CRITICALITY EVALUATION

6.1 DESCRIPTION OF CRITICALITY DESIGN

A comprehensive description of the Traveller packaging is provided in Section 1. This section provides a description of the package (i.e. packaging and contents) that is sufficient for understanding the features of the Traveller that maintain criticality safety.

6.1.1 Design Features

The Traveller shipping package carries a single pressurized water reactor (PWR) fuel assembly or a single Rod Pipe that holds PWR and/or boiling water reactor (BWR) fuel rods. The Traveller is made up of two basic components: 1) an Outerpack and 2) a Clamshell, which is a separate inner shell designed to support the contents. The Outerpack is a long cylindrical design consisting of a top and bottom half hinged together. Each half consists of a stainless steel (SS) outer shell, a layer of rigid polyurethane foam, and an inner SS shell. The inside of the Outerpack is lined with polyethylene moderator blocks. The neutron-moderating ultra-high molecular weight (UHMW) polyethylene moderator blocks are affixed to the upper and lower halves of the Outerpack. See Section 1.2 for additional features of the Traveller beyond criticality safety.

The Clamshell structural components consist of an aluminum base, two aluminum panel doors hinged to the base, a small top access door, and bottom and top end plates. BORAL® neutron absorber plates are located in each axial side of the Clamshell. The Clamshell is a rectangular aluminum box that completely encloses the contents and is mounted in the Outerpack with rubber shock mounts. The Clamshell configuration is designed such that it retains its original dimensions when subjected to the HAC tests. Figure 6-1 displays a cross-section view of the package criticality model.

The criticality model configurations are defined in Section 6.3. Details include conditions of transport and properties of materials of construction and moderating materials.

6.1.1.1 Confinement System

The *confinement system* for the Traveller consists of the fuel rods, the fuel assembly or Rod Pipe, the Clamshell assembly including the neutron absorber plates, and the Outerpack. These structural components are intended to maintain criticality safety of the package. The Clamshell assembly for all transport scenarios maintains confinement of the contents.

6.1.1.2 Flux Traps

The Traveller package features a unique flux trap system that does not require an accident condition (i.e. flooding) in order to function. The flux trap system reduces neutron communication between packages in an array. This system features BORAL® neutron absorber plates located in each axial side of the Clamshell that act in conjunction with UHMW polyethylene moderator blocks, which are affixed to the walls of the Outerpack inner cavity. The BORAL plates have a minimum ^{10}B areal density of [ ]^{a,c}. Neutrons leaving one package must past through two regions of moderator blocks and then BORAL neutron absorber plates before reaching the contents of another package. In addition, the structural materials of the Traveller for which credit

is taken in the criticality safety analysis provide additional neutron absorption. Any flooding enhances the performance of the flux trap in a package array. Figure 6-1 shows the flux trap in a single Traveller XL package. The Traveller STD has a smaller Clamshell configuration than the Traveller XL.

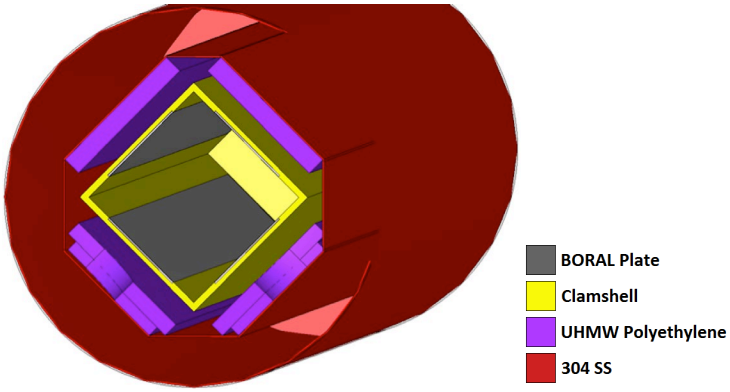

Figure 6-1 Cross Section of the Flux Trap System for STD/XL

6.1.2 Summary Table of Criticality Evaluation

The following analyses demonstrate that the Traveller complies fully with the requirements of 10 CFR 71 [1] and SSR-6 [2]. The nuclear criticality safety requirements for fissile material packages are satisfied for single package and array configurations under normal conditions of transport (NCT) and hypothetical accident conditions (HAC). A criticality safety evaluation was completed for the four package transport arrangements, including the Traveller STD and XL packaging variants, and the contents consisting of two separate PWR fuel assembly Groups and loose rod contents in the Rod Pipe.

The Traveller Type B configuration for Groups 1 and 2 fuel assembly contents is identical to the Type A configuration, with regard to the criticality safety analysis method. This is because the Type B testing (summarized in Section 2.7.1.4) resulted in significantly less damage to the fuel assembly than was experienced in the Type A testing (summarized by Certificate Test Unit results in Section 2.7.1.3). Thus, no credit is taken in the criticality modeling or method for the resultant configuration of the fuel assembly after Type B testing, as the Type A testing resulted in more damage to the package and fuel assembly content. For Group 4 fuel assembly contents at an increased enrichment of 6 wt.% ^{235}U, credit is taken in the criticality safety analysis for the resultant Type B testing documented in Section 2.7.1.4. Principally, this results in the removal of the expanded lattice section of the fuel assembly in the Group 4 criticality safety analysis. See Section 6.3.1 for the full discussion of the changes to the modeling for Group 4 fuel assembly contents.

Allowance for sensitivity studies includes the following: material and fabrication tolerances and geometric or material representations of transport conditions, such as package testing conclusions. The parameter variation is quantified by direct perturbation methodology: evaluation by varying a parameter from the baseline case.

The sensitivity studies examine parameters independently of one another, i.e. each sensitivity study uses the baseline case as the starting or comparison point. A sensitivity study case is determined to have a more reactive result (i.e. penalizing) only if the case's increase in $k_{eff} + 2\sigma$ is greater than or equal to 2σ (i.e. statistically

significant) from the baseline case ($k_{eff} + 2\sigma$) analyzed. The difference in $k_{eff} + 2\sigma$ from the baseline case value is tallied and summed for all parameters with a positive impact on neutron multiplication (Δk_u). No action is taken for sensitivity studies or parameter variations that result in a reduction in k_{eff} or statistically insignificant result (i.e. less than 2σ).

The maximum multiplication factor (*Maximum* k_{eff}) is used to summarize the limiting value for the contents and transport condition and used to demonstrate that criteria to establish subcriticality are satisfied. *Maximum* k_{eff} is the calculated multiplication factor k_{eff} (k_p) of the configuration plus the statistical uncertainty for k_p as two times the standard deviation (σ_p) for the calculation method plus the total summation of the parametric variations (Δk_u), as shown in the following equation:

$$Maximum\ k_{eff} = k_p + 2\sigma_p + \Delta k_u$$

Using the upper subcritical limit 1 (USL1) function presented in Section 6.8.2, the following USLs presented in Table 6-1 were calculated for each package arrangement using the energy of average lethargy causing fission (EALF) of each Group's baseline case and an administrative margin (Δk_m) of 0.05. The *Maximum* k_{eff} for each package arrangement is listed in Table 6-2, Summary Table of the Criticality Evaluation.

Table 6-1 Summary Table of Upper Subcritical Limits

Contents	wt% ^{235}U	Limiting EALF (eV)	Bias and Uncertainty ($\beta - \Delta\beta$)	USL ($1 - \Delta k_m + \beta - \Delta\beta$)
Groups 1 and 2 (Single)	5 wt.%	0.294655	-0.00933	0.94067
Group 1 (Array)	5 wt.%	0.195762	-0.00838	0.94162
Group 2 (Array)	5 wt.%	0.270923	-0.00910	0.94090
Group 4 (Single and Array)	6 wt.%	0.279004	-0.00918	0.94082
Rod Pipe UO_2 Fuel Rods (Single and Array)	7 wt.%	0.319064	-0.00956	0.94044
Rod Pipe U_3Si_2 Fuel Rods (Single and Array)	5 wt.%	0.310042	-0.00947	0.94053

6.1.2.1 Contents Grouping

PWR fuel assemblies are organized with similar fuel assemblies into defined bins. PWR fuel assembly Groups define the allowable fuel assembly contents, with each Group containing like bins. The bounding parameters of the fuel assembly contents in a bin are represented by categorized fuel assemblies (CFA), for the criticality analyses. The Group 1 configuration is applicable to the Traveller STD and XL variants with square-pitch PWR fuel assemblies enriched up to 5-wt.% ^{235}U. The Group 2 configuration is applicable to only the Traveller XL variant with square-pitch PWR fuel assemblies enriched up to 5-wt.% ^{235}U. The Group 4 configuration is applicable to the Traveller STD and XL variants with square-pitch PWR fuel assemblies enriched up to 6 wt.% ^{235}U. The Rod Pipe configuration is applicable to the Traveller STD and/or XL variants, as defined by fuel rod content. This configuration allows for the shipment of loose PWR or BWR fuel rods in a Rod Pipe located inside the Clamshell. These restrictions are detailed in Section 6.2. For all contents listed in Table 6-2, *Maximum* k_{eff} is less than its respective USL.

Table 6-2 Summary Table of Criticality Evaluation

Enrichment	Content	Limiting CFA / Fuel Parameters	Condition of Transport	Array Size	*Maximum* k_{eff}	Reference
5 wt% ^{235}U	**Groups 1 and 2 (Single)**	18 Bin 1	NCT	--	0.92151	Table 6-25
		17 Bin 1	HAC		0.92087	
	Group 1 (Array)	17 Bin 2	NCT	5N = 250	0.30942	Table 6-53
		17 Bin 1	HAC	2N = 100	0.93783	Table 6-72
	Group 2 (Array)	16 Bin 1	NCT	5N = 60	0.31379	Table 6-53
		18 Bin 1	HAC	2N = 24	0.93945	Table 6-72
6 wt% ^{235}U	**Group 4 (Single)**	17 Bin 1	HAC	--	0.90692	Table 6-25
	Group 4 (Array)	15 Bin 3	NCT	5N = 100	0.31609	Table 6-53
		17 Bin 1	HAC	2N = 40	0.93943	Table 6-72
7 wt% ^{235}U	**Rod Pipe UO_2 Fuel Rods (Single)**	Fuel OR = 3.5 cm Fuel Half-Pitch = 3.5 cm	NCT	--	0.63579	Table 6-25
		Fuel OR = 0.55 cm Fuel Half-Pitch = 1.0 cm	HAC		0.79577	
	Rod Pipe UO_2 Fuel Rods (Array)	Fuel OR = 3.5 cm Fuel Half-Pitch = 3.5 cm	NCT	5N = 379	0.59478	Table 6-53
		Fuel OR = 0.50 cm Fuel Half-Pitch = 1.0 cm	HAC	2N = 150	0.81588	Table 6-72
5 wt% ^{235}U	**Rod Pipe U_3Si_2 Fuel Rods (Single)**	Fuel OR = 0.4851 cm Fuel Half-Pitch = 0.4851 cm	NCT	--	0.72879	Table 6-25
		Fuel OR = 0.4851 cm Fuel Half-Pitch = 1.0101 cm	HAC		0.73961	
	Rod Pipe U_3Si_2 Fuel Rods (Array)	Fuel OR = 0.4851 cm Fuel Half-Pitch = 0.4851 cm	NCT	5N = 379	0.69571	Table 6-53
		Fuel OR = 0.4851 cm Fuel Half-Pitch = 0.9851 cm	HAC	2N = 150	0.76836	Table 6-72

6.1.3 Criticality Safety Index

The CSI is equivalent to 50/N, rounded up to the nearest tenth. As described in Section 6.2, the contents are distinguished by which contents types are applicable to which variant(s) of the Traveller. The CSI for each package arrangement is listed in Table 6-3.

Table 6-3 Criticality Safety Index Summary

Content	5N	2N	N	CSI
Group 1	250	100	50	1.0
Group 2	60	24	12	4.2
Group 4	100	40	20	2.5
Rod Pipe	379	150	75	0.7

6.2 FISSILE MATERIAL CONTENTS

The contents consist of either a single PWR fuel assembly or loose fuel rods, as defined in Section 1.2.2, Contents. The UO_2 or U_3Si_2 fuel is modeled as a continuous rod, with no credit taken for dishing or chamfering on pellets, and with a maximum active fuel length defined by the respective bin. The organization of similar fuel assemblies into defined bins is described in Section 6.3.4. The UO_2 is modeled at theoretical density (10.96 g/cm^3) with the uranium modeled at the maximum permissible enrichment for the respective content (i.e. 5 wt.%, 6 wt.%, or 7 wt.% ^{235}U) and the remaining uranium modeled as ^{238}U. For UO_2 contents, PWR Group 1 and 2 fuel assemblies are limited to an enrichment of 5 wt.% ^{235}U and PWR Group 4 fuel assemblies are limited to an enrichment of 6 wt.% ^{235}U. For UO_2 loose rods, enrichment is limited to 7 wt.% ^{235}U. UO_2 contents may be doped with up to 700 ppm Cr_2O_3 and up to 200 ppm Al_2O_3 (i.e. ADOPT rods). The U_3Si_2 is modeled at theoretical density (12.2 g/cm^3) with the uranium modeled as 5 wt.% ^{235}U and the remaining uranium modeled as ^{238}U. For further material properties, see Section 6.3.2. Non-fissile, non-radioactive core components can be shipped with a PWR fuel assembly. For PWR Groups 1 and 2, there are no restrictions on guide tubes and instrument tubes (GT/IT) within a PWR fuel assembly. For PWR Group 4, GT/IT are credited and have the restrictions listed in Section 6.2.3.

Three Groups define the allowable fuel assembly contents, with each Group containing like bins. Table 6-4 shows the breakdown of the bins in the Groups. The fourth content defines the loose fuel rods. English units are the design requirement for the content dimensions; hence, the conversion to SI units, which is required for modeling, is rounded.

Table 6-4 Bin Listing for Each Fuel Assembly Group

Group 1		Group 2	Group 4	
• 14 Bin 1	• 16 Bin 2	• 16 Bin 1	• 14 Bin 1	• 16 Bin 2
• 14 Bin 2	• 16 Bin 3	• 18 Bin 1	• 14 Bin 2	• 16 Bin 3
• 15 Bin 1	• 17 Bin 1		• 15 Bin 3	• 17 Bin 1
• 15 Bin 2	• 17 Bin 2			

6.2.1 Group 1

The applicable parameters and fuel rod patterns for each bin in Group 1 are specified in Table 6-5 through Table 6-7 and Figure 6-2 through Figure 6-4. For any fuel assembly that meets the specification of a given bin, the most limiting configuration has been analyzed, as demonstrated in Section 6.3.4.

The following restrictions apply to all Group 1 bins:

(1) All fuel must consist of only UO_2. ^{235}U enrichment is limited to a maximum of 5 wt.%. Fuel rods in any location of the assembly may include UO_2 pellets that are doped with up to 700 ppm Cr_2O_3 and up to 200 ppm Al_2O_3 (i.e. ADOPT rods).

(2) For each parameter, the listed tolerance limit applies to all bins included in the table. For maximum parameters, only the positive tolerance is limited and for minimum parameters, only the negative tolerance is limited.

(3) All rod cladding must be composed of a zirconium alloy. Cladding may include a chromium coating of 25 μm thick, nominally and/or include an Optimized ZIRLO Liner (OZL).

(4) There is no restriction on the length of top and bottom annular blankets. The annular fuel pellet inner diameter in the blanket region must be ≥0.155 in. and ≤0.183 in. (≥0.3937 cm and ≤0.4648 cm).

(5) Any quantity of stainless steel replacement rods is allowed in the fuel assembly.

(6) Polyethylene packing materials are limited to 2.00 kg in the Clamshell and shall not have a hydrogen density greater than 0.1325 g/cm^3.

Table 6-5 Group 1 Fuel Assembly Bins

Description	Tolerance Limit	14 Bin 1	14 Bin 2	15 Bin 1
Array Size	-	14x14	14x14	15x15
Fuel Rods	-	176	179	204
Non-Fuel Holes	-	20	17	21
Nominal Pitch (in./cm)	+0.0050 (+0.0127)	0.580 (1.4732)	0.556 (1.4122)	0.563 (1.4300)
Minimum Fuel Pellet Outer Diameter (in./cm)	-0.0007 (-0.0018)	0.3805 (0.9665)	0.3439 (0.8735)	0.3582 (0.9098)
Minimum Cladding Inner Diameter (in./cm)	-0.0020 (-0.0051)	0.3855 (0.9792)	0.3489 (0.8862)	0.3636 (0.9235)
Minimum Cladding Thickness (in./cm)	-0.0020 (-0.0051)	0.0245 (0.0622)	0.0228 (0.0579)	0.0228 (0.0579)
Maximum Active Fuel Length (in./cm)	+0.50 (+1.27)	136.70 (347.22)	144.00 (365.76)	144.00 (365.76)

Table 6-6 Group 1 Fuel Assembly Bins

Description	Tolerance Limit	15 Bin 2
Array Size	-	15x15
Fuel Rods	-	205
Non-Fuel Holes	-	20
Nominal Pitch (in./cm)	+0.0118 (+0.03)	0.5630 (1.4300)
Minimum Fuel Pellet OD (in./cm)	-0.0007 (-0.0018)	0.3580 (0.9092)
Minimum Cladding ID (in./cm)	-0.002 (-0.0051)	0.3627 (0.9214)
Minimum Cladding Thickness (in./cm)	-0.002 (-0.0051)	0.0265 (0.0674)
Maximum Active Fuel Length (in./cm)	+0.50 (+1.27)	139.76 (355.00)

Table 6-7 Group 1 Fuel Assembly Bins

Description	Tolerance Limit	16 Bin 2	16 Bin 3	17 Bin 1	17 Bin 2
Array Size	-	16x16	16x16	17x17	17x17
Fuel Rods	-	236	235	264	264
Non-Fuel Holes	-	20	21	25	25
Nominal Pitch (in./cm)	+0.0050 (+0.0127)	0.506 (1.2852)	0.485 (1.2319)	0.496 (1.2598)	0.502 (1.2751)
Minimum Fuel Pellet OD (in./cm)	-0.0007 (-0.0018)	0.3220 (0.8179)	0.3083 (0.7831)	0.3083 (0.7831)	0.3238 (0.8225)
Minimum Cladding ID (in./cm)	-0.002 (-0.0051)	0.3265 (0.8293)	0.3125 (0.7938)	0.3125 (0.7938)	0.3276 (0.8321)
Minimum Cladding Thickness (in./cm)	-0.002 (-0.0051)	0.0210 (0.0533)	0.0210 (0.0533)	0.0210 (0.0533)	0.0220 (0.0559)
Maximum Active Fuel Length (in./cm)	+0.50 (+1.27)	150.00 (381.00)	144.00 (365.76)	168.00 (426.72)	144.00 (365.76)

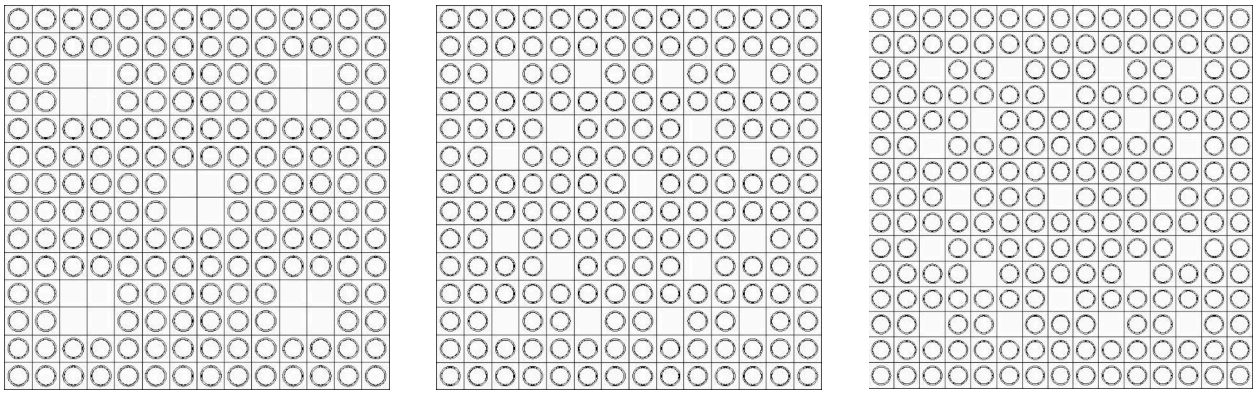

14 Bin 1 **14 Bin 2** **15 Bin 1**

Figure 6-2 Group 1 Fuel Rod Patterns. Not to Scale.

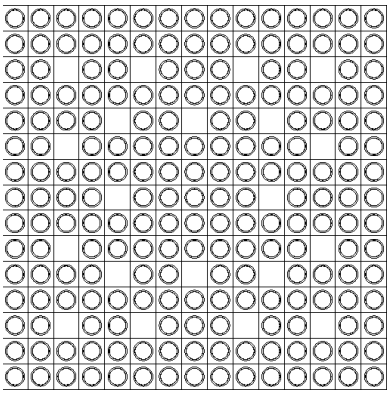

15 Bin 2

Figure 6-3 Group 1 Fuel Rod Patterns. Not to Scale.

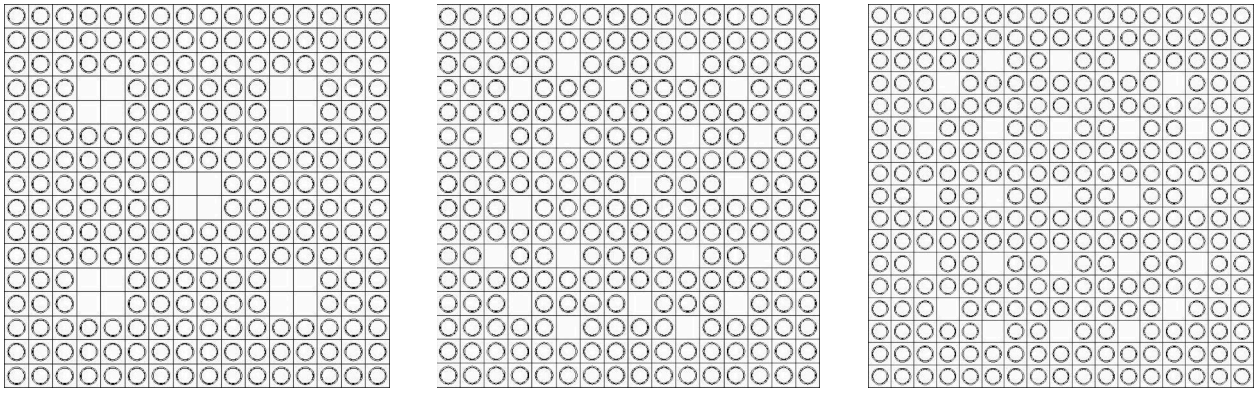

16 Bin 2 **16 Bin 3** **17 Bin 1 / Bin 2**

Figure 6-4 Group 1 Fuel Rod Patterns. Not to Scale.

6.2.2 Group 2

The applicable parameters and fuel rod patterns for each bin in Group 2 are specified in Table 6-8 and Figure 6-5. For any fuel assembly that meets the specification of a given bin, the most limiting configuration has been analyzed, as demonstrated in Section 6.3.4.

The following restrictions apply to all Group 2 bins:

(1) All fuel must consist of only UO_2. ^{235}U enrichment is limited to a maximum of 5 wt.%. Fuel rods in any location of the assembly may include UO_2 pellets that are doped with up to 700 ppm Cr_2O_3 and up to 200 ppm Al_2O_3 (i.e. ADOPT rods).

(2) For each parameter, the listed tolerance limit applies to all bins included in the table. For maximum parameters, only the positive tolerance is limited and for minimum parameters, only the negative tolerance is limited.

(3) All rod cladding must be composed of a zirconium alloy. Cladding may include a chromium coating of 25 μm thick, nominally and/or include an Optimized ZIRLO Liner (OZL).

(4) The length of top and bottom annular blankets is limited to 20.0 in. (50.8 cm). The annular fuel pellet inner diameter in the blanket region must be ≥0.155 in. and ≤0.183 in. (≥0.3937 cm and ≤0.4648 cm).

(5) Any quantity of stainless steel replacement rods is allowed in the fuel assembly.

(6) Polyethylene packing materials are limited to 2.00 kg in the Clamshell and shall not have a hydrogen density greater than 0.1325 g/cm^3.

Table 6-8 Group 2 Fuel Assembly Bins

Description	Tolerance Limit	16 Bin 1	18 Bin 1
Array Size	-	16x16	18x18
Fuel Rods	-	236	300
Non-Fuel Holes	-	20	24
Nominal Pitch (in./cm)	+0.0118 (+0.03)	0.563 (1.430)	0.500 (1.270)
Minimum Fuel Pellet OD (in./cm)	-0.0007 (-0.0018)	0.3581 (0.9097)	0.3165 (0.8039)
Minimum Cladding ID (in./cm)	-0.002 (-0.0051)	0.3665 (0.9310)	0.3236 (0.8220)
Minimum Cladding Thickness (in./cm)	-0.002 (-0.0051)	0.0283 (0.0720)	0.0252 (0.0640)
Maximum Active Fuel Length (in./cm)	+0.50 (+1.27)	153.54 (390.00)	153.54 (390.00)

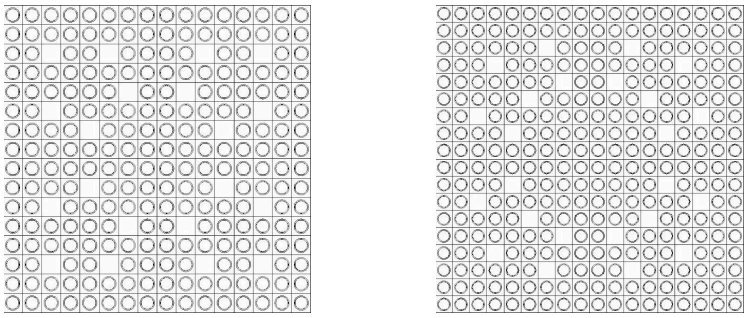

16 Bin 1 **18 Bin 1**

Figure 6-5 Group 2 Fuel Rod Patterns. Not to Scale.

6.2.3 Group 4

The applicable parameters and fuel rod patterns for each bin in Group 4 are specified in Table 6-8A through Table 6-8B and Figure 6-5A through Figure 6-5B. For any fuel assembly that meets the specification of a given bin, the most limiting configuration has been analyzed, as demonstrated in Section 6.3.4.

The following restrictions apply to all Group 4 bins:

(1) All fuel must consist of only UO_2. ^{235}U enrichment is limited to a maximum of 6 wt.%. Fuel rods in any location of the assembly may include UO_2 pellets that are doped with up to 700 ppm Cr_2O_3 and up to 200 ppm Al_2O_3 (i.e. ADOPT rods).

(2) For each parameter, the listed tolerance limit applies to all bins included in the table. For maximum parameters, only the positive tolerance is limited and for minimum parameters, only the negative tolerance is limited.

(3) All rod cladding must be composed of a zirconium alloy. Cladding may include a chromium coating of 25 μm thick, nominally and/or include an Optimized ZIRLO Liner (OZL).

(4) The length of top and bottom annular fuel pellet blankets is limited to 20.0 in. (50.8 cm) at each end. The annular fuel pellet inner diameter in the blanket region must be ≥0.155 in. and ≤0.183 in. (≥0.3937 cm and ≤0.4648 cm).

(5) Any quantity of stainless steel replacement rods is allowed in the fuel assembly.

(6) Polyethylene packing materials are limited to 2.00 kg in the Clamshell and shall not have a hydrogen density greater than 0.1325 g/cm^3.

Table 6-8A Group 4 Fuel Assembly Bins

Description	Tolerance Limit	14 Bin 1	16 Bin 2
Array Size	-	14x14	16x16
Fuel Rods	-	176	236
Non-Fuel Holes	-	20	20
Guide Tubes/Instrument Tubes	-	5[a]	5[a]
Nominal Pitch (in./cm)	+0.0050 (+0.0127)	0.580 (1.4732)	0.506 (1.2852)
Minimum Fuel Pellet Outer Diameter (in./cm)	-	0.3805 (0.9665)	0.3220 (0.8179)
Minimum Cladding Inner Diameter (in./cm)	-	0.3855 (0.9792)	0.3265 (0.8293)
Minimum Cladding Thickness (in./cm)	-	0.0245 (0.0622)	0.0210 (0.0533)
Minimum GT/IT Inner Diameter (in./cm)	-	0.9630 (2.4460)	0.5450 (1.3843)
Minimum GT/IT Thickness (in./cm)	-	0.0360 (0.0914)	0.0360 (0.0914)
Maximum Active Fuel Length (in./cm)	+0.50 (+1.27)	136.70 (347.22)	150.00 (381.00)

Note: [a] Each GT/IT occupies four non-fuel holes that constitute a 2x2 lattice section.

Table 6-8B Group 4 Fuel Assembly Bins

Description	Tolerance Limit	14 Bin 2	15 Bin 3	16 Bin 3	17 Bin 1
Array Size	-	14x14	15x15	16x16	17x17
Fuel Rods	-	179	204	235	264
Non-Fuel Holes	-	17	21	21	25
Guide Tubes/Instrument Tubes	-	17	21	21	25
Nominal Pitch (in./cm)	+0.0010 (+0.0025)	0.556 (1.4122)	0.563 (1.4300)	0.485 (1.2319)	0.496 (1.2598)
Minimum Fuel Pellet OD (in./cm)	-	0.3439 (0.8735)	0.3654 (0.9281)	0.3083 (0.7831)	0.3083 (0.7831)
Minimum Cladding ID (in./cm)	-	0.3489 (0.8862)	0.3709 (0.9421)	0.3125 (0.7938)	0.3125 (0.7938)
Minimum Cladding Thickness (in./cm)	-	0.0228 (0.0579)	0.0228 (0.0579)	0.0210 (0.0533)	0.0210 (0.0533)
Minimum GT/IT Inner Diameter (in./cm)	-	0.3720 (0.9449)	0.4970 (1.2624)	0.3810 (0.9677)	0.3950 (1.0033)
Minimum GT/IT Thickness (in./cm)	-	0.0147 (0.0373)	0.0147 (0.0373)	0.0157 (0.0399)	0.0137 (0.0348)
Maximum Active Fuel Length (in./cm)	+0.50 (+1.27)	144.00 (365.76)	144.00 (365.76)	144.00 (365.76)	168.00 (426.72)

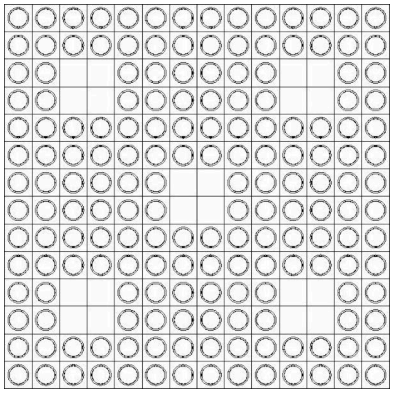

14 Bin 1

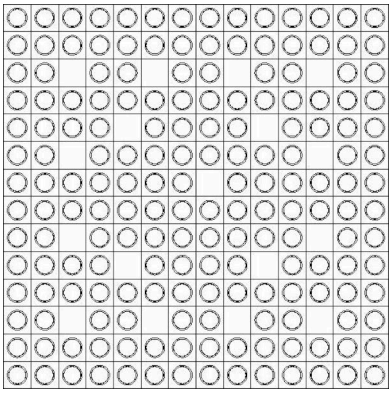

14 Bin 2

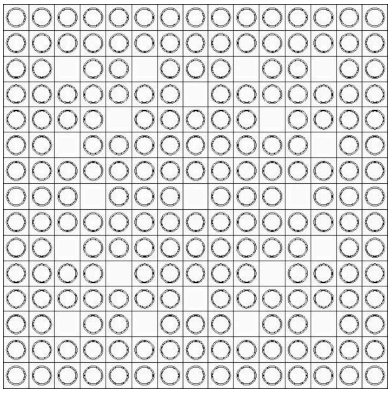

15 Bin 3

Figure 6-5A Group 4 Fuel Rod Patterns. Not to Scale.

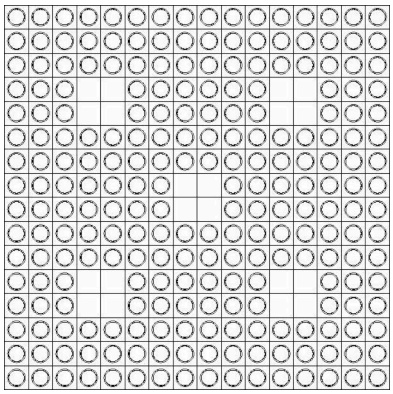

16 Bin 2

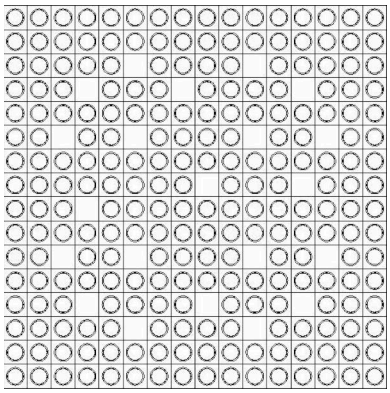

16 Bin 3

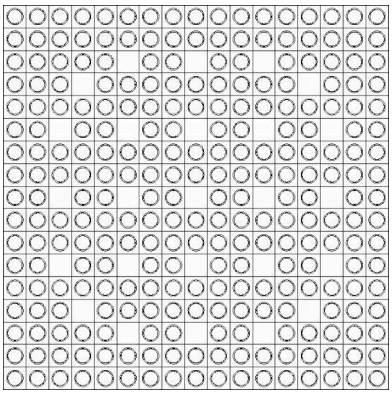

17 Bin 1

Figure 6-5B Group 4 Fuel Rod Patterns. Not to Scale.

6.2.4 Rod Pipe

The Rod Pipe contents category is only applicable to loose PWR or BWR fuel rod contents in the Rod Pipe. This category has the following restrictions for either UO_2 or U_3Si_2 fuel rods:

(1) For UO_2 Fuel Rods,
   a. Loose fuel rods may include UO_2 pellets that are doped with up to 700 ppm Cr_2O_3 and up to 200 ppm Al_2O_3 (i.e. ADOPT rods).
   b. Can only be shipped in the Traveller STD or XL Rod Pipe configuration.
   c. Maximum uranium enrichment of 7.0 wt.% ^{235}U.
   d. Maximum activity: limited to Type A configuration
   e. Fuel pellet diameter must be ≥0.308 in. (≥0.7823 cm).
   f. Maximum stack length equivalent to the Rod Pipe inner length.
   g. Maximum number of rods per Rod Pipe: up to Rod Pipe capacity.
   h. All cladding material may be either aluminum, stainless steel, or zirconium alloy. Zirconium alloy may include a chromium coating of 25 μm thick, nominally and/or include an Optimized ZIRLO Liner (OZL) per Section 2.2.1.8.
   i. Allowable integral absorbers: gadolinia, erbia, boron, and hafnium.
   j. No limit on annular fuel pellet blanket length. The annular fuel pellet inner diameter in the blanket region must be ≥0.155 in. and ≤0.183 in. (≥0.3937 cm and ≤0.4648 cm). For annular IDs >0.183 in. (0.4648 cm), the annular ID must be equivalent to no more than 44% of the fuel pellet OD. Wrapping, sleeving, or packing materials inside the Rod Pipe shall not have a hydrogen density greater than 0.1325 g/cm^3. There is no limit on the mass of packing materials in the Rod Pipe.

(2) For U_3Si_2 Fuel Rods,
   a. Can only be shipped in the Traveller STD Rod Pipe configuration.
   b. Maximum uranium enrichment: 5.0 wt.% ^{235}U.
   c. Maximum activity: limited to Type A configuration
   d. Maximum number of rods in the Rod Pipe: 60 rods.
   e. Fuel pellet diameter must be ≥0.3078 in. and ≤0.3820 in. (≥0.7818 cm and ≤0.9703 cm).
   f. Maximum stack length equivalent to the Rod Pipe inner length.
   g. All cladding material may be either aluminum, stainless steel, zirconium alloy. Zirconium alloy may include a chromium coating of 25 μm thick, nominally and/or include an Optimized ZIRLO Liner (OZL) per Section 2.2.1.8.
   h. Allowable integral absorbers: gadolinia, erbia, boron, and hafnium.
   i. No limit on annular fuel pellet blanket length. The annular fuel pellet inner diameter in the blanket region must be ≥0.155 in. and ≤0.183 in. (≥0.3937 cm and ≤0.4648 cm).
   j. Wrapping, sleeving, or packing materials inside the Rod Pipe shall not have a hydrogen density greater than 0.1325 g/cm^3. There is no limit on the mass of packing materials in the Rod Pipe.

6.3 GENERAL CONSIDERATIONS

6.3.1 Model Configuration

The Traveller is a long, cylindrical packaging that can carry one PWR fuel assembly or loose PWR and/or BWR fuel rods in a Rod Pipe. The Outerpack of the Traveller is modeled as a single, cylindrical shell made of 12-gauge Type 304 Stainless Steel (SS304) sheet metal. No stacking or handling features are modeled, which reduces the effective spacing between packages in an array. The Outerpack inner shell is also modeled as 12-gauge SS304 sheet metal. These two Outerpack halves modeled are the only steel components for which credit is taken in the two Traveller variant models. Minor package components, including fastening fixtures, bolts, content skeletal materials, etc., are not modeled. Thus, no credit is taken for the absorption and reflection provided by these components in the criticality evaluation.

For the two Traveller variant models, the Outerpack inner cavity contains the UHMW moderator blocks and the Clamshell, which houses the fuel assembly or Rod Pipe. The Clamshell has grooves along the length of the inner walls that contain the BORAL neutron absorber plates. The positioning of the Clamshell in the inner cavity with respect to the moderator blocks is shown in Figure 6-6. As shown in Figure 6-7, the UHMW moderator blocks are modeled as the same length as the Clamshell even though they are physically longer than the Clamshell. This assumption is bounding by restricting the effective length of the flux trap. Moderator blocks have cutouts for the shock mounts, which provide shock absorption for the Clamshell in order to prevent damage to the contents during routine transport. The shock mount materials are not modeled in this analysis, however modeling the cutouts removes UHMW polyethylene and allows for increased neutron cross talk between packages in an array. The shock mount cutout configurations, as specified by the licensing drawing, are modeled as shown in Figure 6-8. In addition, the centering of the Clamshell in the Outerpack inner cavity provided by the shock mounts is credited. The major dimensions of both packaging variant's model are listed in Table 6-9. English units are the design requirement for the Traveller variant dimensions; hence the conversion to SI units, which is required for modeling, is rounded.

The Traveller STD and XL Type B configuration is identical to the Type A configuration with regard to the criticality safety analysis models. The Type B configuration shoring components, described in Section 1.2.1.5.3, are removable and do not provide a criticality safety function. Thus, no differences in the Type A and Type B packaging configuration exists for the criticality modeling.

Table 6-9 Major Dimensions of Each Traveller Variant Model

Component	Dimension	Traveller Variant	
		STD in. (cm)	**XL in. (cm)**
Outerpack	Overall Length	195.87 (497.5098)	224.87 (571.1698)
	Diameter	25.0 (63.50)	25.0 (63.50)
	Outer Shell Thickness	0.1046 (0.2657)	0.1046 (0.2657)
	Inner Shell Thickness	0.1046 (0.2657)	0.1406 (0.2657)
	Top Pillow Length	8.21 (20.8534)	8.21 (20.8534)
	Bottom Pillow Length	8.21 (20.8534)	8.21 (20.8534)
	Cavity Height	18.28 (46.4312)	18.26 (46.3804)
	Cavity Width	17.0 (43.18)	17.0 (43.18)
	Cavity Length	179.45 (455.803)	208.45 (529.463)
Moderator Blocks	Upper Block Width	9.48 (24.0792)	9.48 (24.0792)
	Upper Block Thickness	1.25 (3.175)	1.25 (3.175)
	Large Lower Block Width	9.34 (23.7236)	9.34 (23.7236)
	Large Lower Block Thickness	1.00 (2.54)	1.00 (2.54)
	Small Lower Block Width	7.85 (19.939)	7.85 (19.939)
	Small Lower Block Thickness	0.75 (1.905)	0.75 (1.905)
Clamshell	Clamshell Length	173.0 (439.42)	202.0 (513.08)
	Inner width/height [1]	9.12 (23.1648)	9.62 (24.4348)
	Wall Thickness	0.288 (0.7135)	0.288 (0.7315)
	Top Plate Thickness	1.00 (2.54)	1.00 (2.54)
	Bottom Plate Thickness	1.00 (2.54)	1.00 (2.54)
BORAL Plates	Active Poison Length	168.0 (426.72)	197.0 (500.38)
	Width	6.00 (15.24)	6.00 (15.24)
	Thickness	[	]a,c

Note: Dimensions defined by licensing drawings and verified to SolidWorks model; [1] Dimension modeled includes +1 tolerance

The following model components are shown in Figure 6-6:

(1) Outerpack shell (SS304)
(2) Outerpack inner cavity shell (SS304)
(3) UHMW moderator blocks (polyethylene)
(4) Clamshell (aluminum)
(5) BORAL plates

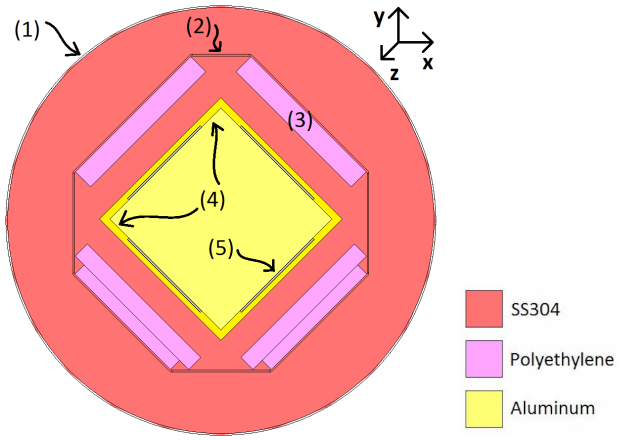

Figure 6-6 Front Cross-Sections of the Traveller STD/XL

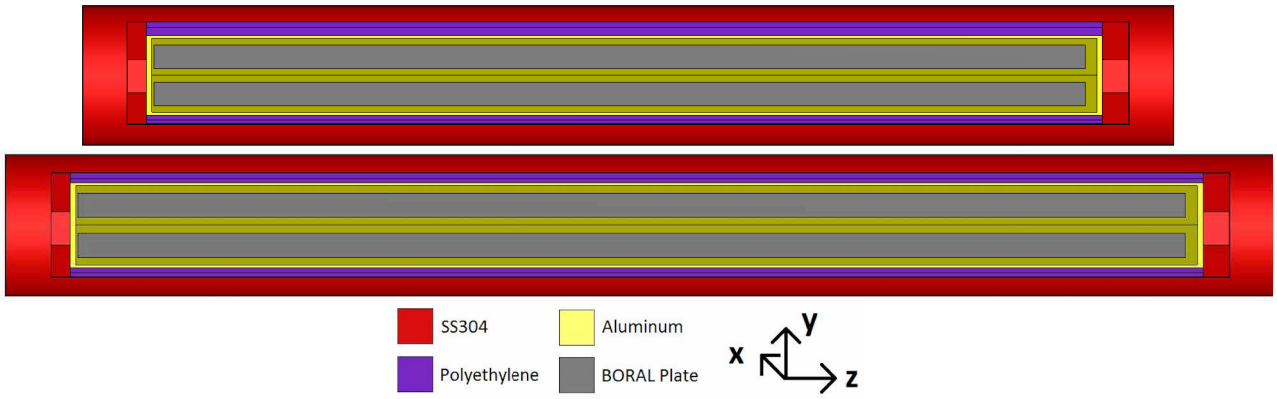

Figure 6-7 Top to bottom: Side Cross-Sections of the Traveller STD and XL

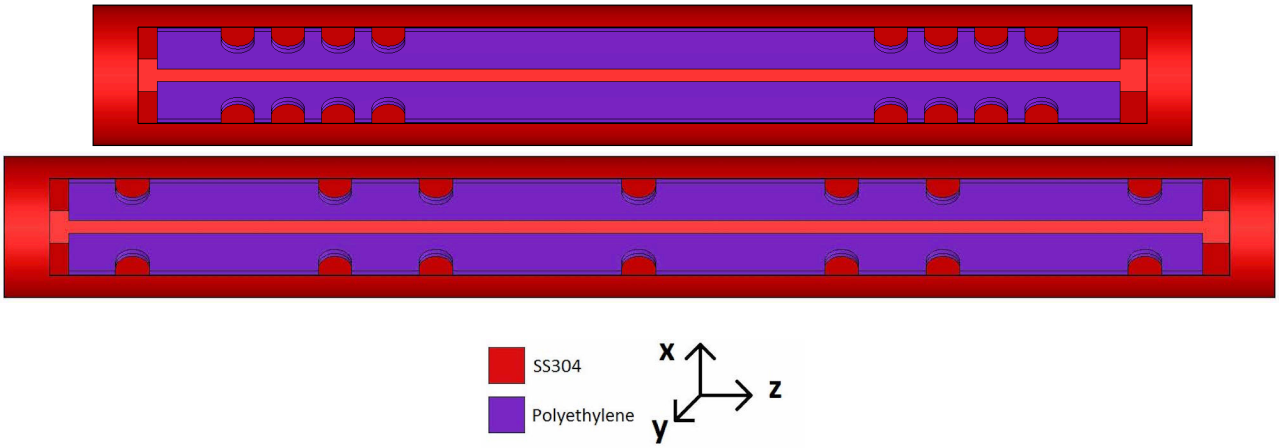

Figure 6-8 Top to bottom: Top Moderator Block Cross-Sections of the Traveller STD and XL

6.3.1.1 Rod Pipe

The Rod Pipe is a 6-in. diameter, Schedule 40 SS304 pipe with end caps. The Rod Pipe licensing drawing specifies a maximum pipe length (pipe + end cap + end bolts) of 200 in. (508 cm), which is utilized for the Traveller XL model. The length is shortened to the Clamshell inner cavity length (pipe + end cap + end bolts) of 171 in. (434.3 cm) for the Traveller STD model. The pipe is modeled as a simple, hollow cylindrical shell. As a result, the pipe end bolts are not represented in the models, thus the pipe exterior length is 198 in. for the Traveller XL and 169 in. for the Traveller STD. The Rod Pipe end caps are flanged and square; however, the excess material outside the pipe OD is insignificant to the neutron activity and thus is neglected in the model. The major dimensions of each variant's Rod Pipe model are listed in Table 6-10.

Table 6-10 Major Dimensions of Rod Pipe Model

Dimension	Traveller Variant			
	STD		XL	
	in.	cm	in.	cm
Pipe OD	6.63	16.8402	6.63	16.8402
Pipe ID	6.065	15.4051	6.065	15.4051
Pipe end plate	0.25	0.635	0.25	0.635
Pipe exterior length [1]	169	429.26	198	502.92
Pipe interior length [2]	168.5	427.99	197.5	501.65
Pipe end bolts	1.0	2.54	1.0	2.54

Note: [1] XL exterior length is pipe + end caps (no bolts), STD exterior length is Clamshell inner cavity length; [2] Pipe interior length = exterior length – 2x end plates

6.3.1.2 Conditions of Transport

Before commencing the NCT and HAC sensitivity studies, a baseline case for NCT and a baseline case for HAC are established. These baseline cases are the most reactive NCT and HAC single package and package array configurations possible, based on the effects, as applicable, of axial positioning of the fuel assembly within the Clamshell, lattice pitch expansion length, and flooding configuration. Three studies are performed to determine which cases define the baseline cases. First, the Categorized Fuel Assembly (CFA) established for each bin (See Section 6.9.2) is modeled in the applicable Traveller variant(s) under both conditions of transport to determine the most reactive CFA-package variant for the baseline cases. Using these baseline cases, sensitivity studies are then evaluated for both NCT and HAC to determine the most reactive configuration for each.

For NCT, no Outerpack deformation is modeled and the moderator blocks are modeled at full density. For the fuel assembly contents, no lattice expansion is modeled, and the CFA is modeled against the bottom inner surface of the Clamshell. Each fuel pin is modeled with its full nominal pitch, thus fuel rods closest to the Clamshell are spaced from the Clamshell by the nominal pitch distance. For the Rod Pipe contents, fuel rods are modeled close-packed with no lattice expansion. For a single package, the package is fully flooded including the fuel-clad gap. For a package array, no flooding is modeled, except for the Rod Pipe where the Rod Pipe is always flooded for package array evaluations. Under NCT, the model boundary has a 20 cm-thick water reflector.

There was minimal damage to the UHMW polyethylene moderator blocks of the packaging from the fire test. The effect of the loss of moderator block material was examined as a sensitivity study, as discussed in Section 6.3.4.3.3. The CFAs are modeled against the bottom inner surface of their respective Clamshell. The fuel-clad gap is modeled with full water flooding. Each fuel pin in the non-expanded lattice section of the CFA is modeled with its full nominal pitch, thus the fuel rods closest to the Clamshell are spaced from the Clamshell by the nominal pitch distance. For the Rod Pipe contents, fuel rods are modeled at the peak water-to-fuel ratio. In a single package, the entire package is flooded. For a package array, flooding to the most reactive credible extent in the Traveller is modeled, as discussed in Sections 6.3.4.2.1.4 and 6.3.4.3.12. Under HAC, the model boundary has a 20 cm-thick water reflector.

6.3.1.2.1 Groups 1 and 2 PWR Fuel Assembly Contents HAC Modeling

For Group 1 and Group 2 contents with a maximum enrichment of 5 wt.% ^{235}U, the Traveller Type B configuration is identical to the Type A configuration with regard to the criticality safety analysis model and method. This is because the Type B testing (summarized in Section 2.7.1.4) resulted in significantly less damage to the fuel assembly than was experienced in the Type A testing (summarized in Section 2.7.1.4). Thus, no credit is taken in the criticality modeling or method for the resultant configuration of the fuel assembly after Type B testing, as the Type A testing resulted in more damage to the package and fuel assembly content.

During the Type A HAC drop-test series, there was minimal concentrated deformation to the Outerpack. Therefore, no changes to Outerpack dimensions are modeled. However, the test fuel assembly did experience damage and lattice expansion in some of the drop tests. As discussed in Section 6.3.4.2.1.3, lattice pitch expansion was modeled as 20.0 in. long (50.8 cm) to bound the results of the worst-case drop testing.

6.3.1.2.2 Group 4 PWR Fuel Assembly Contents HAC Modeling

For Group 4 contents with a maximum enrichment of 6 wt.% ^{235}U, credit is taken for the significantly lesser amount of damage to the test fuel assembly that occurred in the Type B testing, summarized in Section 2.7.1.4. To allow for the increased enrichment effect on increasing k_{eff}, the minimal damage to the Type B test fuel assembly, including no lattice expansion and no axial rod displacement, is modeled in the Group 4 fuel assembly contents criticality safety analysis. Otherwise, the modeling and method of the Group 4 contents is identical to the Group 1 and Group 2 contents.

6.3.2 Material Properties

6.3.2.1 Non-Fissile, Non-Radioactive Reactor Core Components

Reactor core components that may be shipped with the radioactive/fissile contents of the Traveller are non-fissile, non-radioactive components that have specific functions within a reactor core but have no primary function in a transport scenario. The core component may function as a flux suppressant or as a neutron absorber during reactor operation and does not alter the design of the fuel assembly. As such, it is not evaluated in the package criticality safety analysis because its function as a neutron absorber decreases the reactivity of the system. In addition, for the transport evaluation, core components in a fuel assembly would displace water in a flooding condition of the criticality safety transport model and decrease moderation, and therefore decrease reactivity. Therefore, the non-fissile, non-radioactive reactor core components are not credited or modeled in the criticality safety analysis. These reactor core components are described further in Section 1.2.2.1.3.

6.3.2.2 UO_2

The UO_2 is modeled as the SCALE Standard Composition Library built-in compound "uo2." The uranium consists of ^{235}U at the maximum permissible enrichment for the respective case (see Table 6-11) and the remainder of the uranium is modeled as ^{238}U. The UO_2 is modeled at its theoretical density of 10.96 g/cm^3. Other uranium isotopes are assumed to be ^{238}U because these other isotopes (1) are not fissile, (2) only exist in small amounts, and (3) have thermal neutron absorption cross sections that are greater than ^{238}U. This material is summarized in Table 6-11. ADOPT UO_2 rods may include up to 700 ppm Cr_2O_3 and up to 200 ppm Al_2O_3. This material is added to the SCALE model with the elemental SCALE materials for chromium, aluminum and oxygen. The material composition for the ADOPT fuel is provided in Table 6-12. The enrichment modeled for the ADOPT fuel matches the enrichment of the non-ADOPT fuel modeled for a given enrichment.

6.3.2.3 U_3Si_2

The alternative loose rod fuel material U_3Si_2 is modeled as a compound composition of three atoms U and two atoms Si. The uranium consists of 5 wt.% ^{235}U and 95 wt.% ^{238}U, and the composition is modeled at its theoretical density of 12.2 g/cm^3. Other uranium isotopes are assumed to be ^{238}U because these other isotopes (1) are not fissile, (2) only exist in small amounts, and (3) have thermal neutron absorption cross sections that are greater than ^{238}U. This material is summarized in Table 6-11.

6.3.2.4 Zircaloy Cladding

All cladding modeled is specified as the SCALE Standard Composition Library built-in alloy "zirc4," which represents the alloy Zircaloy-4. This material is modeled at its theoretical density of 6.56 g/cm^3 and it has the alloy composition listed in Table 6-12. As discussed in Section 2.2.1.8, the base zircaloy cladding may include features of chromium-coating and/or have an Optimized ZIRLO Liner (OZL). The addition of clad coatings and liners are neglected from the criticality analysis as they will have a negligible effect on the system reactivity through removal of moderation and presence of neutron absorbing materials. Additionally, the advanced cladding features are in addition to the base cladding and may not be credited in the minimum clad thickness requirement.

6.3.2.5 Guide Tubes/Instrument Tubes

For Group 1 and 2 content, Guide tubes/instrument tubes (GT/IT) are replaced with void under dry conditions and with light water under flooding conditions. Modeling the GT/IT as void under dry conditions allows for more neutron communication in an assembly and between packages in an array. Modeling the GT/IT as light water under flooding conditions promotes more neutron moderation and reflection in the fuel assembly envelope than the materials of construction of any GT/IT configuration. No credit is taken for the presence of GT/IT, thus there are no restrictions on guide tubes and instrument tubes.

For Group 4 content, the GT/IT modeled are specified as the SCALE Standard Composition Library built-in alloy "zirc4," which represents the alloy Zircaloy-4. This material is modeled at its theoretical density of 6.56 g/cm^3 and it has the alloy composition listed in Table 6-12.

6.3.2.6 Flooding and Reflecting Water

All water is modeled as the SCALE Standard Composition Library built-in compound "h2o," and is summarized in Table 6-11. This water consists of only ^{1}H and ^{16}O with a S(α,β) thermal kernel. The water is modeled with SCALE's nominal water density, 0.9982 g/cm^3. In situations where a variation in water density is examined, the volume fraction of the material is altered.

6.3.2.7 Fuel Assembly Structural Materials

No credit is taken for fuel assembly structural materials (including rod end caps, top and bottom nozzles, and grid spacers) in this analysis. These materials are modeled as void in dry conditions and as full density light water in flooding conditions, as full density light water promotes more neutron moderation and reflection in the fuel assembly envelope than the structural materials of the fuel assembly and bounds any structural material configuration.

6.3.2.8 Aluminum

All structural aluminum of the packaging is modeled as elemental aluminum at its theoretical density of 2.702 g/cm^3. This was determined to be bounding of the aluminum alloys of construction in the model (6061-T6 and 6005-T5/6005A-T5 aluminum alloys) as elemental aluminum has a lower density than these alloys and a reduced neutron cross-section compared to the alloy elements. This does not include the Type 1100 aluminum alloy cladding of the BORAL plates, which is discussed in Section 6.3.2.11.

6.3.2.9 304 Stainless Steel

The 304 stainless steel of the packaging is modeled as the 304 stainless steel composition presented in PNNL-15870 [3]. Its density is modeled as 8.0 g/cm^3 and has the alloy composition listed in Table 6-12.

6.3.2.10 Ultra-High Molecular Weight Polyethylene

The moderator blocks of the Traveller are made of UHMW polyethylene, which is modeled as the SCALE Standard Composition Library built-in compound "polyethylene" with the chemical formula CH_2, which utilizes the hydrogen-in-polyethylene S(α,β) thermal kernel. Its density is modeled as 0.92 g/cm^3 for both NCT and HAC. This material is summarized in Table 6-11.

6.3.2.11 BORAL Neutron Absorber Plates

BORAL is a clad composite of Type 1100 aluminum alloy and boron carbide (B_4C) that consists of three distinct layers: the two outer layers of cladding (solid, Type 1100 aluminum alloy) and the central layer (referred to as the "core"), consisting of a uniform aggregate of fine, B_4C particles held within a Type 1100 aluminum alloy matrix. See Table 6-12 for the composition of Type 1100 aluminum alloy.

6.3.2.11.1 BORAL Core Atom Number Density

The Traveller licensing drawings require a minimum ^{10}B areal density of [ ]^{a,c} in the BORAL core. However, credit is only taken for 75% of the ^{10}B, as recommended in NUREG/CR-5661 [4]. This results in a modeled ^{10}B areal density of [ ]^{a,c}. The number densities presented in Table 6-13 are calculated for a nominal BORAL core thickness of [ ]^{a,c} and void fraction of [ ]^{a,c}.

The number densities for each of the constituents of the BORAL core are calculated using the following process:

1. The ^{10}B number density is calculated based on the minimum areal density ([ ]^{a,c}), core thickness ([ ]^{a,c}), and atomic mass of ^{10}B
2. The ^{11}B number density is then calculated based on the natural abundances of ^{10}B and ^{11}B in Boron
3. The Carbon in the B_4C portion of the BORAL Core is calculated using the total number density of Boron in the core, and the stoichiometric ratio of Boron to Carbon (4:1)
4. The number densities of the elements in the Type 1100 aluminum alloy portion of the core are determined by first calculating the volume fraction of the alloy in the core. This is calculated as the remainder of volume in the core, accounting for the B_4C and void (i.e. $V_{Al} = 1 - V_{B4C} - [\ ]^{a,c}$). With this volume fraction and the nominal density of the alloy, the effective density of the alloy in the core is calculated. The number density of each element can then be calculated using this effective density and the weight fraction and atomic mass of the respective element in the alloy.

6.3.2.12 Hydrogenous Packaging Materials

The remaining materials specified in licensing drawings (rubber shock mounts, ceramic fiber blanket, polyurethane foam insulation, and acetate plugs) have all been determined to have lower hydrogen densities than water. Therefore, in flooding situations, these materials are replaced with water. In dry conditions, these

materials are replaced with void. In the applicable transport condition models, both of these configurations have been determined to be bounding.

6.3.2.13 Hydrogenous Packing Materials

For routine conditions of transport, fuel assemblies and fuel rods are wrapped in sheets of polyethylene to protect the contents from foreign material such as dust and debris. Various types of hydrogenous materials may be used for packing. A bounding polyethylene density of 0.922 g/cm^3 is modeled, as it is a hydrogen-rich material. This material is used as the basis to define a hydrogen density limit for hydrogenous packing materials. Using polyethylene with a chemical formula of CH_2, a density of 0.922 g/cm^3, and the atomic weight of carbon (12.0107) and hydrogen (1.00794), a bounding hydrogen density of 0.1325 g/cm^3 is calculated. This material is summarized in Table 6-11.

6.3.2.14 Extreme Cold Case (-40°C) Effects

Any reactivity effect on a low-enriched uranium (LEU) fuel package due to an extreme cold case (-40°C) would be minimal. Reactivity effects would be due to the temperature effects on neutron cross-sections and changes in the density of the packaging and moderating materials.

A reduction in the temperature of LEU fuel would cause the ^{238}U thermal absorption resonances to become taller and thinner, narrowing the energy range of resonance peaks and decreasing the range of neutron energies absorbed in the resonance. As described in Section 6.3.3, the 293 K (20°C) cross sections were used. For a total temperature difference of 60°C (from 20°C to -40°C), this difference in resonance peaks is insignificant.

A change in the temperature of water from 20°C to -40°C would result in a phase change from liquid water to solid ice. As water freezes, it expands, reducing its density from ~1 g/cm^3 to ~0.92 g/cm^3. A reduction in water density results in a reduction in hydrogen density, effectively reducing neutron moderation in the system. Thus, any change in material densities due to a temperature change from 20°C to -40°C would not result in an increase in k_{eff} as there are no resulting changes to packaging components; there is only the potential for a reduction in moderation due to the expansion of water as a result of freezing.

6.3.2.15 Integral Absorbers

Integral absorbers are allowable contents within the fuel assembly or loose fuel rods, including, but not limited to, gadolinia, erbia, boron, chromium and hafnium. Integral absorber materials have specific functions within the fuel but have no primary function in a transport scenario. The integral absorber may function as a flux suppressant or as a neutron absorber during reactor operation and does not alter the design of the fuel assembly. As such, it is not evaluated in the package criticality safety analysis because its function as a neutron absorber decreases the reactivity of the system. Therefore, the integral absorbers are not credited or modeled in the criticality safety analysis.

6.3.2.16 Summary of SCALE Material Compositions

When elements are listed in Table 6-11, Table 6-12, or Table 6-13, the isotopic abundances of naturally occurring elements in the SCALE Standard Composition Library are used.

Table 6-11 Summary of Compound Material Compositions

Material	Density (g/cm^3)	Constituent	Number of Atoms per Molecule
UO_2 (5 wt.% ^{235}U, 95 wt.% ^{238}U 6 wt.% ^{235}U, 94 wt.% ^{238}U 7 wt.% ^{235}U, 93 wt.% ^{238}U)	10.96	U	1
		O	2
U_3Si_2 (5 wt.% ^{235}U, 95 wt.% ^{238}U)	12.2	U	3
		Si	2
Light Water	0.9986	H	2
		O	1
UHMW Polyethylene (Moderator blocks)	0.92	C	1
		H	2
Polyethylene Packing Materials	0.922	C	1
		H	2

Table 6-12 Summary of Alloy/Mixture Material Compositions

Material	Density (g/cm^3)	Constituent	Weight Fraction
Zircaloy-4	6.56	Zr	0.98230
		Sn	0.01450
		Fe	0.00210
		Cr	0.00100
		Hf	0.00010
304 Stainless Steel	8.00	C	0.00040
		Si	0.00500
		P	0.00023
		S	0.00015
		Cr	0.19000
		Mn	0.01000
		Fe	0.70173
		Ni	0.09250
Type 1100 Aluminum Alloy	2.71	Al	0.99500
		Si	0.00162
		Mn	0.00017
		Fe	0.00162
		Cu	0.00125
		Zn	0.00034
ADOPT UO_2 Fuel (700 ppm Cr_2O_3, 200 ppm Al_2O_3)	10.96	UO_2	0.999179
		Cr	0.000478
		Al	0.000106
		O	0.000315

Table 6-13 Summary of BORAL Plate Core Material Composition

Material	Density (g/cm^3)	Constituent	Atom Number Density (atoms/barn-cm)
BORAL Core (B_4C and Type 1100 Aluminum Alloy aggregate)	[ ]^{a,c}	^{10}B	[ ]^{a,c}
		^{11}B	[ ]^{a,c}
		C	[ ]^{a,c}
		Al	[ ]^{a,c}
		Si	[ ]^{a,c}
		Mn	[ ]^{a,c}
		Fe	[ ]^{a,c}
		Cu	[ ]^{a,c}
		Zn	[ ]^{a,c}

6.3.3 Computer Codes and Cross-Section Libraries

6.3.3.1 SCALE 6.1.2

SCALE 6.1.2 was used for all Group 1, Group 2, and loose rod contents criticality safety analyses.

The Criticality Safety Analysis Sequence with KENO-VI (CSAS6) of the SCALE 6.1.2 code package was used to calculate values of k_{eff} for this analysis [5]. KENO-VI is a Monte Carlo criticality program used to calculate the k_{eff} of three-dimensional (3-D) systems. The ENDF/B-VII.0 continuous energy neutron cross-section data were used for all cases in this analysis. Each case analyzed used the default room temperature (293 K) cross sections. SCALE is a categorized modeling and simulation suite for nuclear safety analysis and design developed and maintained by Oak Ridge National Laboratory under contract with the U.S. Nuclear Regulatory Commission, U.S. Department of Energy, and the National Nuclear Security Administration to perform reactor physics, criticality safety, radiation shielding, and spent fuel characterization for nuclear facilities and transportation/storage package designs.

6.3.3.2 SCALE 6.1.3

SCALE 6.1.3 was used for all Group 4 contents criticality safety analyses. The update from version 6.1.2 to version 6.1.3 of SCALE involved no changes to the SCALE code (i.e. CSAS6) or cross-section data (i.e., ENDF/B-VII.0) that are relevant to the calculation of k_{eff} for criticality safety between the two code versions.

The Criticality Safety Analysis Sequence with KENO-VI (CSAS6) of the SCALE 6.1.3 code package was used to calculate values of k_{eff} for this analysis [6]. KENO-VI is a Monte Carlo criticality program used to calculate the k_{eff} of three-dimensional (3-D) systems. The ENDF/B-VII.0 continuous energy neutron cross-section data were used for all cases in this analysis. Each case analyzed used the default room temperature (293 K) cross sections. SCALE is a categorized modeling and simulation suite for nuclear safety analysis and design developed and maintained by Oak Ridge National Laboratory under contract with the U.S. Nuclear

Regulatory Commission, U.S. Department of Energy, and the National Nuclear Security Administration to perform reactor physics, criticality safety, radiation shielding, and spent fuel characterization for nuclear facilities and transportation/storage package designs.

6.3.3.3 Convergence Criteria

For each package arrangement examined, different neutron history configurations were utilized to obtain proper source convergence. For all analyses, a minimum of 450 total generations with a minimum of 10,000 neutrons per generation and a minimum of 150 skipped generations were analyzed for a minimum of 3,000,000 active neutron histories. The number of histories analyzed was increased as needed in order to achieve adequate source convergence. In addition, output files were examined to verify source convergence by examining the "average k-effective by generation" plot run, the "average k-effective by generation skipped" plot, and the "frequency for generations" plot.

6.3.4 Demonstration of Maximum Reactivity

The most reactive cases for each package variant, content Group, and condition of transport were determined through three sequential analyses:

(1) Modeling CFAs that represent the most reactive configuration of a bin.
(2) Determination of NCT and HAC baseline cases for each package arrangement.
(3) Sensitivity studies analyzed for both baseline cases to demonstrate maximum reactivity for NCT and HAC safety case configurations and each package arrangement.

The first analysis determined the bounding CFA of each bin. A bin is a grouping of fuel assemblies that have in common three primary parameters: array size (e.g. 17x17), number and location of non-fueled holes, and as-designed nominal fuel rod pitch. Organizing fuel assemblies into bins reduces the quantity of fuel assemblies that need to be specified. The CFA of each bin for Group 1 and 2 is a bounding combination of three secondary fuel assembly design parameters: fuel pellet diameter, fuel-clad gap, and cladding thickness. Group 4 includes these parameters and credits bounding guide tube/instrument tube (GT/IT) inner diameters and thicknesses. The secondary parameter range of each bin is determined by the fuel assembly designs that constitute the bin. Every combination of these secondary parameters is evaluated to ensure that the fuel assembly permutations span the breadth of each secondary parameter range. By comparing all fuel assembly permutations, the effect of each secondary parameter on k_{eff} is determined. The in-depth CFA analysis is presented in Section 6.9.2, and the results of the CFA analysis are summarized in Section 6.3.4.1.

The second and third analyses modeled the CFAs with the Traveller packaging to demonstrate compliance with the regulatory requirements of 10 CFR 71 and SSR-6 for single packages and package arrays. The second analysis determines the baseline cases, which are bounding CFA-package variant combinations for each Group for both NCT and HAC. The baseline case evaluation models the CFAs for each Group in each applicable package variant to determine both the most reactive CFAs and package variant, as applicable. A similar method is applied to the Rod Pipe contents. The baseline case evaluation also determined which axial position of the content in the Clamshell is most reactive and the most reactive flooding configuration, as applicable to the transport condition. See Section 6.3.4.2 for the full baseline case explanation.

Upon determining the baseline cases, the third analysis evaluates sensitivity studies, independently of one another, to determine the reactivity effect of the baseline cases due to parametric variation studies. Parameters such as annular fuel pellet blankets, SS replacement rods, polyethylene packing material configurations, fuel tolerances, and various HAC testing resultant damage configurations were analyzed. If a sensitivity study resulted in a statistically significant more reactive configuration than the baseline case, the increase in $k_{eff} + 2\sigma$ (Δk_u) was summed for each sensitivity study and added to the baseline case ($k_p + 2\sigma_p$) in order to produce the final safety case value of k_{eff} (*Maximum* k_{eff}). See Section 6.3.4.3 for the full sensitivity study explanation. For PWR Groups 1 and 2, a combined case study is provided in Appendix 6.9.4 to compare the individual penalty method for each sensitivity study, utilized in the body of this section, to a single case combining all worst-case configurations determined from each sensitivity study. The combined study is not completed for PWR Group 4, because Group 4 contents have relatively small penalties compared to Groups 1 and 2.

6.3.4.1 Categorized Fuel Assembly Determination

The CFA analysis, presented in Section 6.9.2, determined the bounding parameters for each bin. Each CFA represents the most reactive configuration of secondary parameters of a bin, all of which model the minimum fuel pellet diameter, cladding ID, and cladding thickness for Groups 1 and 2 as the most reactive configuration. For Group 4, the minimized secondary parameters and the minimum GT/IT inner diameter and GT/IT thickness are bounding. Because fuel assemblies are designed to be under-moderated for reactor operation, reducing the secondary parameters to the evaluated minimum values increases neutron moderation in a transport evaluation by allowing for increased water presence within the fuel envelope. Presented in Table 6-14 are the bins applicable to the fuel assembly Groups. A CFA is generated for each bin.

Table 6-14 Bin Listing for Each Fuel Assembly Group

Group 1		Group 2	Group 4	
• 14 Bin 1	• 16 Bin 2	• 16 Bin 1	• 14 Bin 1	• 16 Bin 2
• 14 Bin 2	• 16 Bin 3	• 18 Bin 1	• 14 Bin 2	• 16 Bin 3
• 15 Bin 1	• 17 Bin 1		• 15 Bin 3	• 17 Bin 1
• 15 Bin 2	• 17 Bin 2			

6.3.4.2 Baseline Case

For each content and package variant combination, one baseline NCT case and one baseline HAC case were determined for single package and package array. Each baseline case is a bounding combination of the content and package variant for each condition of transport. The baseline configuration is based on the effects of modeling a CFA (or the Rod Pipe) in the packaging, axial positioning of the content within the Clamshell, and flooding configuration, as applicable to each condition of transport. The following outline shows the method used in selecting the NCT and HAC baseline cases for the CFA Package Array evaluation. The baseline case method for the Rod Pipe is described in Section 6.3.4.2.2.
Method Outline Application Example:

Group 1 Package Array NCT and HAC Baseline Case Determination

1. NCT Baseline Case
    a. CFA-Package Variant Comparison
        i. Compare Traveller variants by modeling equivalent CFAs in both the STD and XL
        ii. Compare CFAs in most reactive Traveller variant (Traveller XL)
    b. Baseline Case Determination
        i. Compare axial positions of limiting CFA in most reactive Traveller variant
2. HAC Baseline Case
    a. CFA-Package Variant Comparison
        i. Compare Traveller variants by modeling equivalent CFAs in both the STD and XL
        ii. Compare CFAs in most reactive Traveller variant (Traveller XL)
    b. Baseline Case Determination
        i. Compare axial positions of limiting CFA in most reactive Traveller variant
        ii. Compare different flooding configurations for limiting flooding configuration

6.3.4.2.1 Fuel Assemblies

6.3.4.2.1.1 CFA-Package Variant Comparison

The first part of the baseline case determination is the CFA-package variant comparison. This examines the CFAs as presented in Section 6.9.2.1 in each applicable package variant for NCT and HAC with the following configuration:

- Active fuel lengths plus one fabrication tolerance.
- No lattice pitch expansion length considered for NCT and 20 in. (50.8 cm) of lattice pitch expansion length for HAC Group 1 and Group 2. Per Section 6.3.1.2.2, no lattice expansion is considered for HAC Group 4.
- Nominal fuel assembly lattice rests against the bottom of the Clamshell in the radial, x-y plane for Group 1 and 2 and is centered in Group 4.
- All regions flooded for single package analyses. All floodable regions are modeled as void for NCT package array cases. For HAC package array cases, the fuel-clad gap, fuel assembly envelope, and Clamshell inner cavity modeled as fully flooded with all other floodable regions modeled as dry. For Group 4, the fuel-clad gap and fuel assembly envelope are initially flooded while the Clamshell is dry.
- Close, full water reflection (20+ cm thick) surrounding the single package and package arrays.

These comparisons result in one bounding CFA-package variant combination for each fuel assembly Group, for each NCT and HAC package arrangement. For Group 1, shorter fuel assemblies that are capable of being shipped in the STD were also modeled in the XL in order to perform a reactivity comparison between Traveller variants. It was determined in this analysis that the Traveller XL bounds all Traveller STD configurations in the Group 1 package arrangement. As stated in Section 6.2.2, the Traveller XL is the only applicable packaging variant in the Group 2 package arrangement. Based on the Group 1 conclusion that the Traveller XL is bounding of the Traveller STD, only the Traveller XL was modeled for Group 4 contents.

6.3.4.2.1.2 Axial Position of Fuel Assembly in Clamshell

As a part of the baseline evaluation, the axial position of the fuel assembly in the Clamshell is examined to determine the bounding position. Figure 6-9 shows three different cases from the axial position study. The axial position of the fuel assembly has an impact on k_{eff} for several reasons:

(1) Small gaps exist between the BORAL plates and the axial ends of the Clamshell.
(2) The shock mount cutouts (see Figure 6-8) in the moderator blocks can increase neutron communication between packages.
(3) The centering of the fuel assembly affects axial reflection in the package due to the flooded Clamshell under HAC.

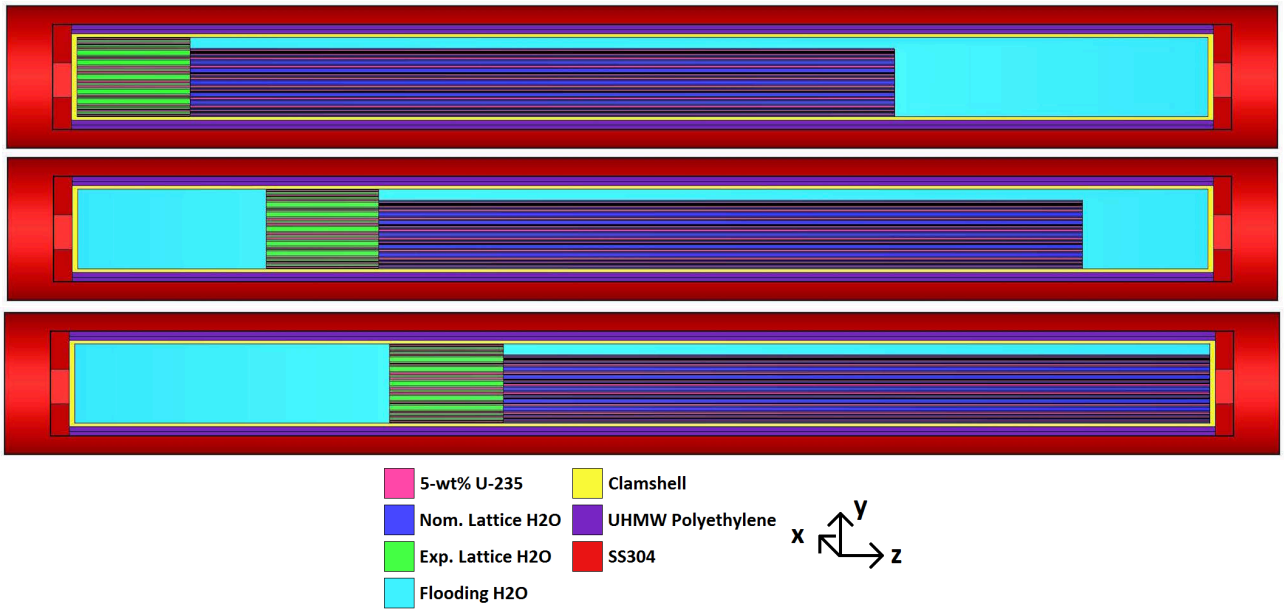

Figure 6-9 Side Cross Section of the Traveller Showing PWR Group 1/2 Fuel Assembly Axial Position Study

6.3.4.2.1.3 HAC Lattice Pitch Expansion Length

Under HAC for Group 1 and Group 2, the lattice pitch expansion length is modeled as 20.0 in. long (50.8 cm) with the lattice pitch expanded fully and uniformly to the inner boundary of the Clamshell. Some of the testing resulted in the fuel assembly experiencing some kind of lattice modification. In the worst case, for the 20-in. span from the bottom nozzle to Grid 2, the fuel rod envelope expanded from 8-3/8 in. (21.27 cm) average nominal to 9-3/16 in. (23.34 cm) with a single rod bent outward approximately ½ in. (1.27 cm). Otherwise, the typical pitch pattern consisted of 2 rod rows touching and the remaining 14 rows at nominal pitch. See Section 2.7.1.2 for details. To bound the worst-case drop test results, the lattice pitch expansion length is modeled at 20 in. (50.8 cm) with the lattice fully and uniformly expanded to the Clamshell boundary. This is a conservative modeling decision because only one fuel rod bowed during the drop test and no fuel rod expanded to the Clamshell boundary. Explicitly modeling the expanded lattice region results in a water-to-fuel ratio that is closer to the optimal value than the nominal fuel region. Lattice expansion is modeled for single package and package array configurations under HAC. A cross-section of the lattice pitch expansion as modeled in SCALE is shown in Figure 6-10.

Under HAC for Group 4, no lattice pitch expansion is modeled as the additional Type B drop testing documented in Section 2.7.1.4 showed that no significant damage occurred to the test fuel assembly.

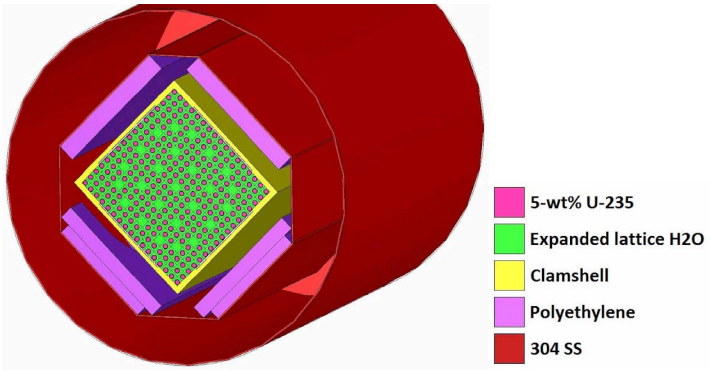

Figure 6-10 Cutaway of Traveller XL with 17 Bin 2 Showing the Lattice Pitch Expansion Section

6.3.4.2.1.4 HAC Package Array Flooding Configuration

Six different flooding configurations were examined for all fuel assembly Groups and HAC package array cases in order to determine which flooding configuration is bounding. The first configuration, also known as the partial flooding scenario, is a more realistic scenario with a full-density water level that rises throughout the Outerpack inner cavity, Clamshell, and fuel assembly simultaneously. The five other configurations, known as the preferential flooding (also called differential or sequential flooding) scenarios, instead model the fuel assembly envelope and fuel-clad gap as always fully flooded and then vary the water density in one or more selected flooded regions of the Traveller packaging, while holding the remaining packaging regions as void. The five preferential flooding configurations are:

(1) Outerpack inner cavity outside of the Clamshell,
(2) The Clamshell cavity,
(3) The Outerpack outer cavity,
(4) The entire Traveller,
(5) The region between packages (interspersed moderation).

These configurations are shown in Figure 6-11 for square Clamshell configurations. The most reactive flooding configuration for each fuel assembly package array arrangement consists of a fully flooded Clamshell cavity, including the fuel envelope and fuel-clad gap, with all other floodable regions of the package array as void (preferential flooding configuration 2). The optimum interspersed moderation configuration is void between packages in an array.

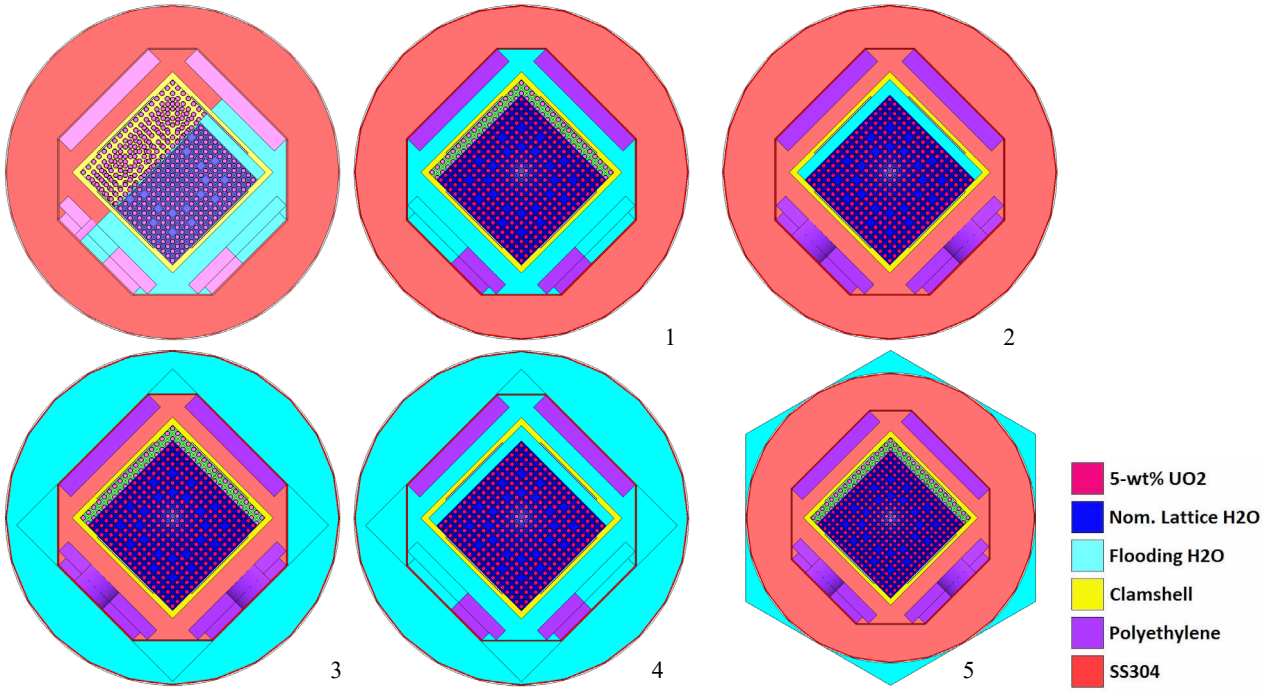

Figure 6-11 The Six Flooding Configurations for PWR Fuel Assembly Groups

6.3.4.2.2 Rod Pipe

For the UO_2 baseline evaluation, the range of fuel pellet outer radii (OR) evaluated is from 0.154 in. (0.3912 cm) to 2.756 in. (7.0002 cm), as shown in Table 6-15 for NCT, and from 0.154 in. (0.3912 cm) to 0.256 in. (0.650 cm) for HAC. The range of pellet OR only represents a variation in water-to-fuel ratio, to ensure peak reactivity is evaluated. The pitch is close-packed for all NCT examinations; thus the pitch is equivalent to the fuel pellet diameter. For HAC, the pitch is increased through a peak water-to-fuel ratio. Both square and hexagonal pitch types are modeled for each condition of transport. A baseline case is determined for the single package and package array and for NCT and HAC each. Comparison of results for the varying fuel pellet OR and half-pitch sets a bounding combination as the baseline for each transport condition for use in the sensitivity study analyses. No cladding material is modeled; thus no inner/outer radius or thickness is specified. The loose fuel rods are modeled as long cylindrical fuel stacks, thus the presence of cladding is required for geometric confinement.

Table 6-15 Rod Pipe UO_2 Baseline Evaluation - Fuel Rod and Pitch Values

NCT [1]		HAC	
Fuel OR in. (cm)	**Fuel OR continued in. (cm)**	**Fuel OR in. (cm)**	**Half-Pitch [2] cm**
0.154 (0.391)	0.394 (1.000)	0.154 (0.391)	Fuel OR
0.167 (0.425)	0.591 (1.500)	0.167 (0.425)	Fuel OR +0.10
0.177 (0.450)	0.787 (2.0)	0.177 (0.450)	Fuel OR +0.25
0.187 (0.475)	0.984 (2.5)	0.187 (0.475)	Fuel OR +0.50
0.197 (0.500)	1.181 (3.0)	0.197 (0.500)	Fuel OR +0.75
0.217 (0.550)	1.378 (3.5)	0.217 (0.550)	--
0.236 (0.600)	1.575 (4.0)	0.236 (0.600)	--
0.256 (0.650)	1.772 (4.5)	0.256 (0.650)	--
0.276 (0.700)	1.969 (5.0)	--	--
0.295 (0.750)	2.165 (5.5)	--	--
0.315 (0.800)	2.362 (6.0)	--	--
0.335 (0.850)	2.559 (6.5)	--	--
0.354 (0.900)	2.756 (7.0)	--	--
0.394 (1.000)	--	--	--

Note: [1] Half-pitch = Fuel OR for NCT. [2] All five half-pitch values are modeled for each fuel OR.

The number of pitch cells in the Rod Pipe defines the number of rods modeled, which is estimated by calculating the area of a single pitch cell and dividing the area of the Rod Pipe cavity by the single pitch cell area, as shown in Figure 6-12. With this method, the Rod Pipe inner radial boundary will cut through the pitch cells against the Rod Pipe inner boundary. The total number of rods includes these cut cells. The quantity of fuel rods that can be physically inserted into the Rod Pipe is less than the value evaluated due to the addition of packing materials that protect the fuel rods during transport.

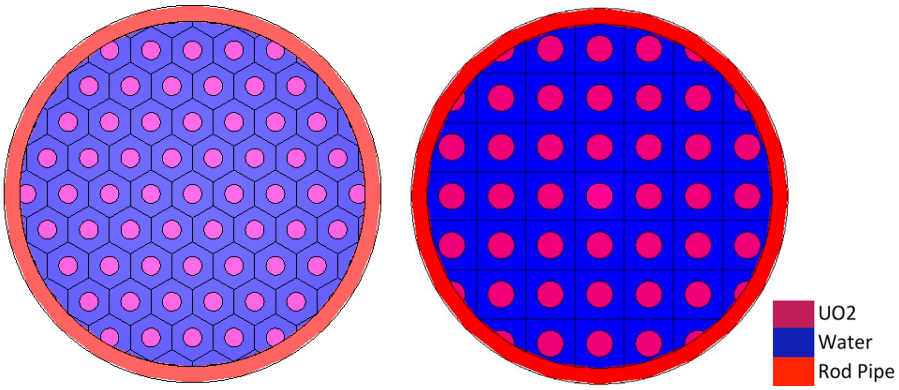

Figure 6-12 Rod Pipe, UO_2 Fuel Array Modeling in Rod Pipe

For the U_3Si_2 evaluation, the range of fuel pellet OR evaluated is from 0.154 in. (0.3909 cm) to 0.191 in. (0.4851 cm) for NCT and HAC, as shown in Table 6-16. The pitch is close-packed for all NCT examinations, thus the pitch is equivalent to the fuel pellet diameter, and the contents are centered in the Rod Pipe. For HAC, the pitch is increased to values that result in fewer than 60 fuel rods being modeled in the Rod Pipe in order to consider partial loadings and ensure the peak water-to-fuel ratio had been achieved. These configurations are shown in Figure 6-13.

Table 6-16 Rod Pipe U_3Si_2 Baseline Evaluation - Fuel Rod and Pitch Values

NCT [a]	HAC	
Fuel OR in. (cm)	**Fuel OR in. (cm)**	**Half-Pitch [b] cm**
0.154 (0.391)	0.154 (0.391)	Fuel OR +0.15
0.163 (0.415)	0.163 (0.415)	Fuel OR +0.20
0.172 (0.438)	0.172 (0.438)	Fuel OR +0.25
0.182 (0.462)	0.182 (0.462)	Fuel OR +0.30
0.191 (0.485)	0.191 (0.485)	Fuel OR +0.35
--	--	Fuel OR +0.40
--	--	Fuel OR +0.425 [c]
--	--	Fuel OR +0.45
--	--	Fuel OR +0.475
--	--	Fuel OR +0.50
--	--	Fuel OR +0.525 [d]
--	--	Fuel OR +0.55
--	--	Fuel OR +0.60
--	--	Fuel OR +0.65
--	--	Fuel OR +0.70
--	--	Fuel OR +0.75
--	--	Fuel OR +0.80
--	--	Fuel OR +0.85

Note: [a] Half-pitch = Fuel OR for NCT. [b] All 17 half-pitch values are modeled for each fuel OR.
[c] half-pitch only modeled for hexagonal pitch cases. [d] half-pitch only modeled for square pitch cases

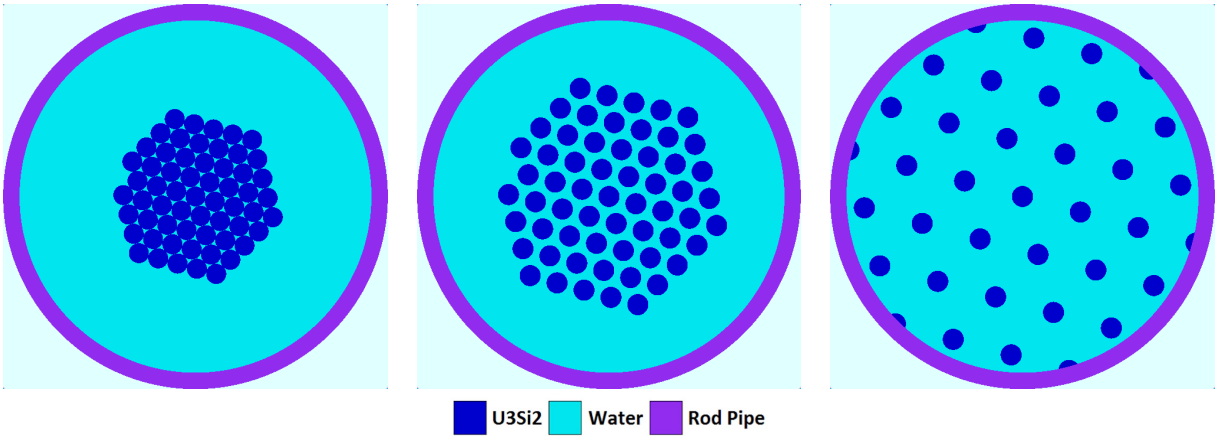

Figure 6-13 Rod Pipe, U_3Si_2 NCT Case (left) and Two HAC Cases (right)

For both loose rod contents, the lattice expansion study is not applicable, as the entire active fuel length is expanded through the optimum water-to-fuel ratio of the Rod Pipe. The axial position of the fuel inside the Rod Pipe is also not applicable because the fuel is modeled as the full inner length of the Rod Pipe.

6.3.4.3 Sensitivity Studies

The baseline cases, one each for NCT and HAC for each package arrangement, are subjected to several sensitivity studies, which are detailed in Table 6-17 and the following subsections. Note that Groups 1 and 2 are grouped together in this table. Both Groups are analyzed separately, but since they both contain PWR fuel assembly contents and modeling techniques, the same sensitivity studies are evaluated. The sensitivity studies for Group 4 are detailed in Table 6-17A. A sensitivity study case is determined to have a more reactive result (i.e. penalizing) only if the case's increase in $k_{eff} + 2\sigma$ is greater than or equal to 2σ (i.e. statistically significant) from the baseline case ($k_{eff} + 2\sigma$) analyzed. No action is taken for sensitivity studies or parameter variations that result in a reduction in k_{eff} or statistically insignificant result (i.e. less than 2σ difference). The summed increase in $k_{eff} + 2\sigma$ (Δk_u) is added to the baseline case ($k_p + 2\sigma_p$), producing a final value of k_{eff} (*Maximum* k_{eff}), as stated in Section 6.1.2. This process is repeated for all applicable package arrangements to demonstrate maximum reactivity for NCT and HAC of each package arrangement.

Table 6-17 Baseline and Sensitivity Studies Configurations for Each Package Arrangement

Case	Description	Groups 1 and 2 (Single)		Groups 1 and 2 (Arrays)		Rod Pipe (Single)		Rod Pipe (Arrays)	
		NCT	HAC	NCT	HAC	NCT	HAC	NCT	HAC
Lattice expansion	Expanded lattice pitch region.	--	X	--	X	--	--	--	--
Axial fuel position	Determination of the worst-case axial position of the fuel assembly in the Clamshell.	X	X	X	X	--	--	--	--
Flooding configuration	Assessment of several flooding configurations' effect on the behavior of k_{eff}.	--	--	--	X	--	--	--	X
Annular fuel pellet blanket study	Assessment of the behavior of k_{eff} with annular fuel pellet blankets in the fuel assembly.	X	X	X	X	X	X	X	X
Clamshell/fuel assembly/Rod Pipe shift study	Assessment of the behavior of k_{eff} by shifting the position of the Clamshell and/or fuel assembly in the inner cavity, or Rod Pipe in the Clamshell	X	X	X	X	X	X	X	X
Moderator block density study	Assessment of the behavior of k_{eff} with a 1% reduction in the density of the UHMW moderator blocks.	--	X	--	X	--	X	--	X
Package outer diameter tolerance study	Assessment of the behavior of k_{eff} upon examining the tolerance of the Outerpack outer diameter.	--	--	X	X	--	--	X	X
Polyethylene packing materials study	Assessment of the behavior of k_{eff} with polyethylene packing materials in the fuel assembly/Rod Pipe.	X	X	X	X	X	X	X	X
Axial rod displacement study	Assessment of the behavior of k_{eff} with rods shifted up axially in the fuel assembly as the result of an end drop.	--	X	--	X	--	--	--	--
Stainless Steel replacement rod study	Assessment of the behavior of k_{eff} with stainless steel rods replacing fuel rods in the fuel assembly.	X	X	X	X	--	--	--	--
Cladding diameter tolerance study	Assessment of the behavior of k_{eff} modeling fuel rod cladding diameter tolerances.	X	X	X	X	--	--	--	--
Fuel pellet diameter tolerance study	Assessment of the behavior of k_{eff} modeling fuel pellet diameter tolerances.	X	X	X	X	X	X	X	X
Fuel rod pitch tolerance study	Assessment of the behavior of k_{eff} modeling fuel rod pitch tolerances.	X	X	X	X	--	--	--	--
Steel nozzle reflector study	Assessment of the behavior of k_{eff} modeling two nozzle reflector configurations at both ends of a fuel assembly.	--	--	X	X	--	--	--	--

Table 6-17A Baseline and Sensitivity Study Configurations for Group 4

Case	Description	Group 4 (Single)	Group 4 (Arrays)	
			NCT	HAC
Flooding configuration	Assessment of several flooding configurations' effect on the behavior of k_{eff}.	--	--	X
Axial fuel position	Determination of the worst-case axial position of the fuel assembly in the Clamshell.	X	X	X
Annular fuel pellet blanket study	Assessment of the behavior of k_{eff} with annular fuel pellet blankets in the fuel assembly.	X	X	X
Clamshell/fuel assembly shift study	Assessment of the behavior of k_{eff} by shifting the position of the Clamshell and fuel assembly in the inner cavity.	X	X	X
Moderator block density study	Assessment of the behavior of k_{eff} with a 1% reduction in the density of the UHMW moderator blocks.	X	--	X
Package outer diameter tolerance study	Assessment of the behavior of k_{eff} upon examining the tolerance of the Outerpack outer diameter.	--	X	X
Polyethylene packing materials study	Assessment of the behavior of k_{eff} with polyethylene packing materials in the fuel assembly	X	X	X
Stainless Steel replacement rod study	Assessment of the behavior of k_{eff} with stainless steel rods replacing fuel rods in the fuel assembly.	X	X	X
Fuel rod pitch tolerance study	Assessment of the behavior of k_{eff} modeling fuel rod pitch tolerances.	X	X	X
Steel nozzle reflector study	Assessment of the behavior of k_{eff} modeling two nozzle reflector configurations at both ends of a fuel assembly.	--	X	X
ADOPT study	Assessment of the behavior of k_{eff} modeling ADOPT fuel instead of UO_2.	X	X	X

6.3.4.3.1 Annular Fuel Pellet Blanket Study

This study examined the addition of varying lengths of annular fuel pellet blanket lengths equally to the top and bottom of every rod in an assembly or Rod Pipe. The annulus ID was analyzed between 0.155 in. (0.3937 cm) and 0.183 in. (0.4648 cm). The fuel void resulting from the addition of an annulus to the fuel rod was modeled as flooded for all single package arrangements, void for NCT package array arrangements, and flooded for HAC package array arrangements.

For the Rod Pipe NCT assessments, proportionally larger-sized annular IDs were examined, as the limiting case for NCT involved large-diameter fuel rods with a pellet OR of 1.3780 in. (3.5 cm). As a result, modeling the nominal annular fuel pellet inner diameters typical of PWR fuel rods results in no meaningful effect to k_{eff}. Instead, for the loose rod contents, a proportional annular ID was modeled in order to better capture the effect of modeling annular fuel pellet blankets. The nominal annular fuel pellet IDs of PWR fuel assemblies are approximately 44% of their respective fuel pellet ODs. Therefore, for the 1.3780 in. (3.5 cm) fuel pellet ORs of the NCT single package and package array cases, a 0.6063 in. (1.54 cm) annular fuel pellet IR was modeled to capture this proportional effect.

6.3.4.3.2 Clamshell, Fuel Assembly, or Rod Pipe Shift Study

For the fuel assembly contents, two Clamshell and/or fuel assembly-shifting configurations were examined. In the baseline cases for all arrangements, the fuel assembly rests against the bottom of the Clamshell in the x-y plane, as shown in Figure 6-14.

For single package and package array NCT evaluations, the fuel assembly was modeled centered in the Clamshell, as the nozzles, grid structures, and packing would result in the fuel assembly being approximately centered in the Clamshell, as shown in Figure 6-14.

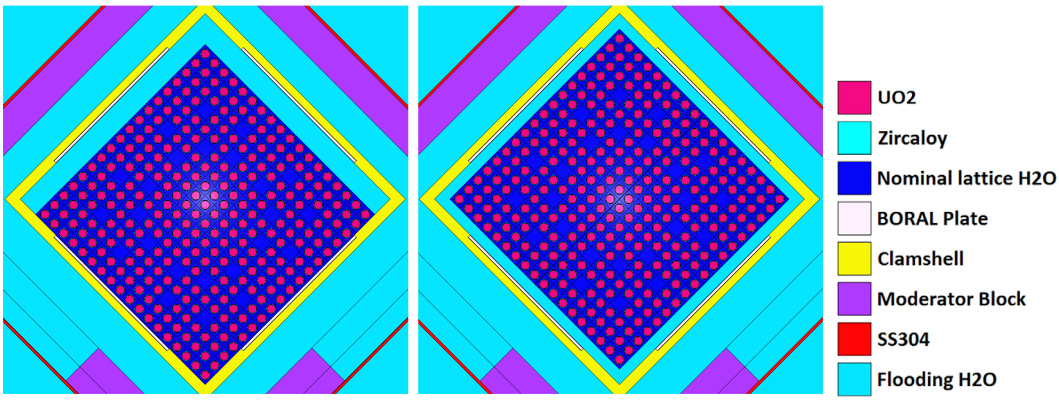

Figure 6-14 NCT Single Package Baseline Case vs. Fuel Assembly Shift

For the single package and package array HAC evaluations, the Clamshell and fuel assembly were both shifted to the top of the inner cavity in order to simulate the package array flipping over in an accident condition. Refer to Figure 6-15. This scenario assumes the Clamshell separates from the shock mounts and rests nearly against the upper moderator blocks.

For Group 4 contents, the fuel assembly is modeled centered nominally, like the centered case shown in Figure 6-14. For all Group 4 content evaluations, the two shifted positions examined are shown in Figure 6-15.

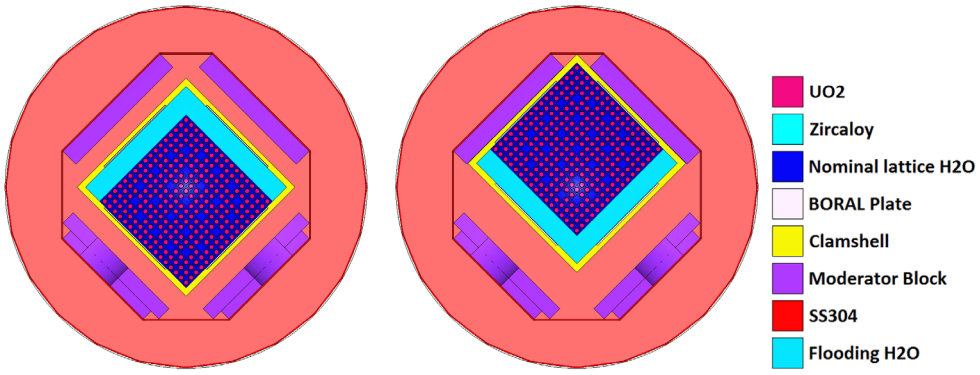

Figure 6-15 HAC Package Array Baseline Case vs. Clamshell and Fuel Assembly Shift

In the Rod Pipe single package and package array arrangements under NCT, the Rod Pipe was examined as both centered in the Clamshell and shifted down in the Clamshell. For HAC, the Rod Pipe was examined shifted up, centered, and shifted down in the Clamshell in order to determine the bounding positioning of the Rod Pipe.

6.3.4.3.3 Moderator Block Density Reduction Study

As described in detail in Section 6.1.1.2, the moderator blocks are designed to work in conjunction with the BORAL plates as part of the flux trap system, which reduces neutron communication between packages in an array. Therefore, a reduction in moderator block density results in more neutron communication between packages in an array. The density reduction of the polyethylene moderator blocks is examined for all HAC package arrangements in order to determine the effect on k_{eff}. The polyethylene density is examined at nominal density (0.92 g/cm^3) and a 1% density reduction (0.9108 g/cm^3).

An objective of the fire test presented in Section 3.4.2.4 was to show that greater than 90% of the hydrogen content of the moderator block was retained post-fire. The largest mass reduction experienced of any individual moderator block was -0.7%. As a result, a 1% reduction in all moderator block density was evaluated to bound the largest individual moderator block mass reduction.

6.3.4.3.4 Package Outer Diameter Sensitivity Study

The package outer diameter sensitivity study was only examined for the package arrays of each arrangement, as adjusting the spacing between packages in an array directly affects the effective fissile density. Licensing Drawings list the tolerance of the packaging's OD as ±0.20 in. (±0.508 cm). The package OD was examined at plus and minus one tolerance in order to determine the effect on k_{eff}.

6.3.4.3.5 Polyethylene Packing Materials Study

For routine conditions of transport, fuel assemblies and loose fuel rods in the Traveller are wrapped in sheets of polyethylene in order to protect the contents from foreign material, such as dust and debris. Various types of polyethylene are used with a density of 0.922 g/cm^3 modeled in this analysis. The mass of polyethylene present is varied to determine a packing material limit. The NCT cases are modeled as dry and the addition of polyethylene may increase reactivity of the system during NCT. Therefore, the addition of polyethylene is evaluated to determine its effect on k_{eff}. Since polyethylene has a higher hydrogen density than light water, the addition of polyethylene wrap under HAC can result in an increased reactivity. Additionally, during a HAC fire event under extreme temperatures, the polyethylene wrap could potentially melt and redistribute in the contents, producing a more reactive system; therefore, three different configurations are examined for the polyethylene packing material HAC sensitivity study. However, it is important to note that none of the currently used polyethylene materials are likely to melt in an accident situation. During the package HAC testing, as described in Section 3.4, the highest temperature measured on the outside of the Clamshell during this process was below material melt temperatures.

For PWR Groups 1 and 2 and the Rod Pipe analyses, the thermal evaluation and the criticality safety analyses were originally developed in parallel. The thermal fire testing had not been completed when the original criticality safety analyses were developed. Therefore, bounding HAC criticality methods, not based on fire test

results, were assumed with respect to the polyethylene packing materials, such that the polyethylene would melt. Thus, the uniform melt and collected melt studies were analyzed in addition to the outer wrap study. The PWR Group 4 criticality safety analysis was developed after the thermal fire testing was completed, and thus these studies are not analyzed for PWR Group 4. As shown in Section 3.1.3, fire testing determined that the maximum temperature inside the Clamshell was 104°C (219°F). This maximum temperature is below the lowest melting temperature of polyethylene of 111°C (232°F) to 190°C (374°F) for induced viscous melt. Because the uniform melt and collected melt polyethylene studies are representative of bounding, assumed worst-case HAC and not the physical package thermal performance as demonstrated via fire testing, these studies are not analyzed for PWR Group 4.

6.3.4.3.5.1 Outer Wrap Configuration for All PWR Fuel Assembly Groups

The outer wrap configuration represents a routine condition for fuel assemblies. The polyethylene is modeled as wrapped around the fuel assembly under NCT and HAC. The polyethylene extends halfway from the fuel rod outer radius to the edge of the lattice cell. The NCT outer wrap configuration is modeled as shown in Figure 6-16. Under HAC, three different configurations of polyethylene wrap are examined to represent the movement of the wrap into the fuel assembly envelope due to melting and redistribution. The first configuration simulates the polyethylene as utilized in routine conditions of transport with it wrapped around the fuel assembly. As mass is added to the polyethylene, the additional polyethylene fills in towards the centerline of the fuel assembly such that the outer fuel rods become partially encapsulated in polyethylene, as shown in Figure 6-17.

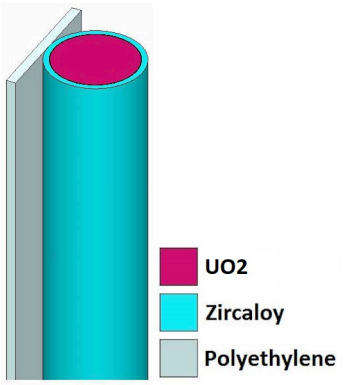

Figure 6-16 PWR Fuel Assembly Polyethylene Outer Wrap NCT Configuration

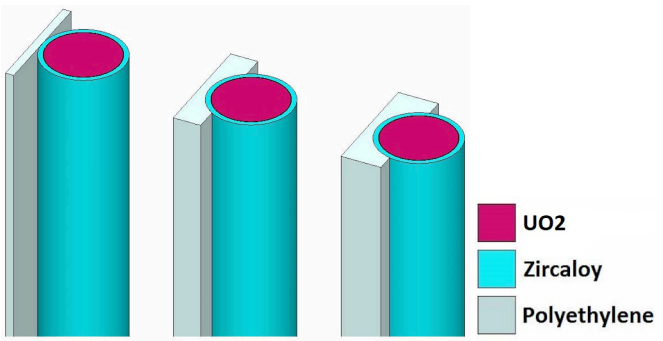

Figure 6-17 PWR Fuel Assembly Polyethylene Outer Wrap HAC Configurations

6.3.4.3.5.2 Uniform Melt Configuration for HAC Package Arrangements

The second configuration simulates the polyethylene melting from its outer wrap position and fully and uniformly encapsulating each fuel rod of the assembly in the radial direction, as shown in Figure 6-18. To model different masses of polyethylene, the thickness is adjusted. As mentioned earlier in Section 6.3.4.3.5, this study is only evaluated for PWR Group 1 and 2, and Rod Pipe.

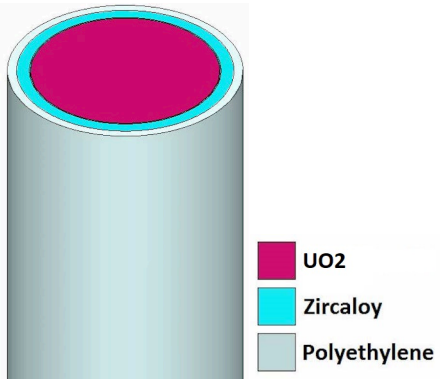

Figure 6-18 Uniform Polyethylene Melt HAC Configuration – PWR Fuel Assemblies

For both routine and normal conditions of transport of loose fuel rods, the rods are wrapped individually in sheets of polyethylene prior to being inserted into the Rod Pipe, which protects the fuel rods from rubbing against each other and foreign material. This configuration is examined for both NCT and HAC with the polyethylene fully and uniformly encapsulating each fuel rod in the radial direction, as shown in Figure 6-19. To model different masses of polyethylene, the thickness is adjusted.

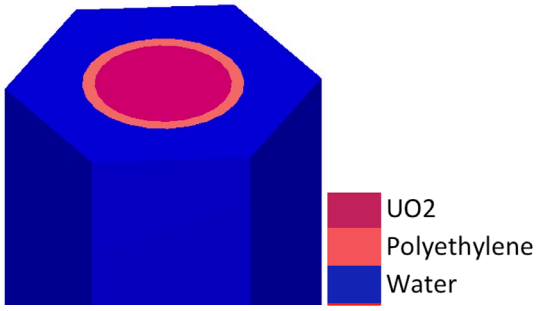

Figure 6-19 Uniform Polyethylene Wrap NCT/HAC Configuration – Rod Pipe

6.3.4.3.5.3 Collected Polyethylene Melt Configuration for HAC Package Arrangements

The third and final configuration simulates the polyethylene melting from its outer wrap position and collecting in the expanded lattice region, where the mass of polyethylene is modified by increasing the height of the modeled polyethylene. As mentioned earlier in Section 6.3.4.3.5, this study is only evaluated for PWR Group 1 and 2, and Rod Pipe.

An example fuel assembly collected melt model is shown in Figure 6-20 and a Rod Pipe collected melt model is shown in Figure 6-21. Collected melt is typically the bounding configuration due to (1) the increased moderation capability of polyethylene in comparison with water and (2) polyethylene collecting in the expanded lattice region, which is more reactive than the nominal lattice region.

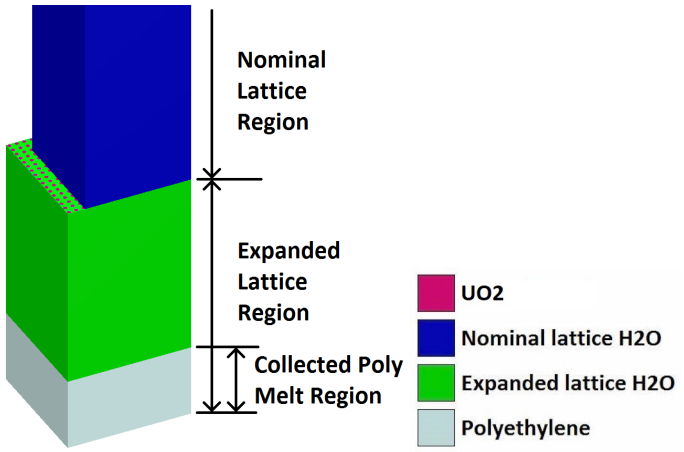

Figure 6-20 PWR Fuel Assembly Collected Polyethylene Melt Configuration

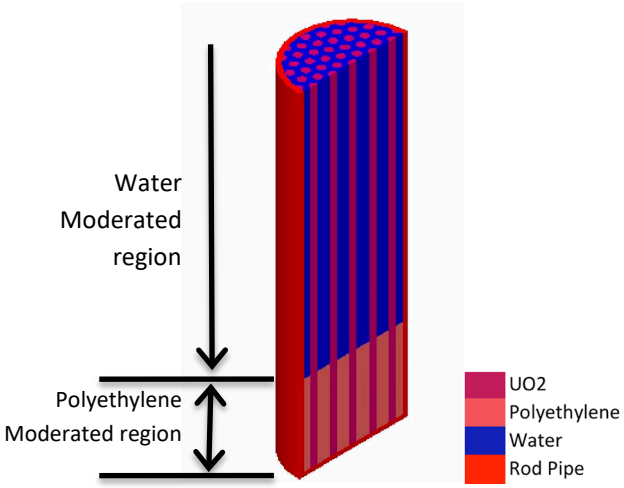

Figure 6-21 Rod Pipe Collected Polyethylene Melt Configuration

6.3.4.3.6 PWR Fuel Assembly Axial Rod Displacement Study

The axial displacement of individual fuel rods to the top of the Clamshell is a result of a package vertical drop during HAC. In Type A prototype testing of the package, the guide pins buckled and four (4) fuel rods were displaced axially through the assembly but did not extend beyond the neutron poison plates. This study was done to conservatively bound the fuel rod axial displacement encountered by fully displacing fuel rods to the opposite end of the Clamshell. This displacement is modeled in two configurations: a corner displacement, where two adjacent edge rows are displaced in unison, or a random displacement, where random rods throughout the fuel assembly are all displaced to the axial top of the Clamshell. The random rods are selected

in a symmetrical pattern, dispersed throughout the fuel assembly grid. 20, 40, and 64 (or 68, depending on the Group) displaced rods are evaluated. The largest number of displaced rods is equivalent to two adjacent rows of fuel rods on two adjacent sides of the lattice, as shown in Figure 6-22. The three random rod displacement cases model the same number of displaced rods as the three corner rod displacement configurations. This study is only applicable to Groups 1 and 2. Examples of these two displaced fuel rod layouts are shown in Figure 6-22 and Figure 6-23.

As the Type B testing documented in Section 2.7.1.4, no rods experienced axial displacement, thus axial fuel rod displacement is not evaluated for PWR Group 4 fuel assembly contents.

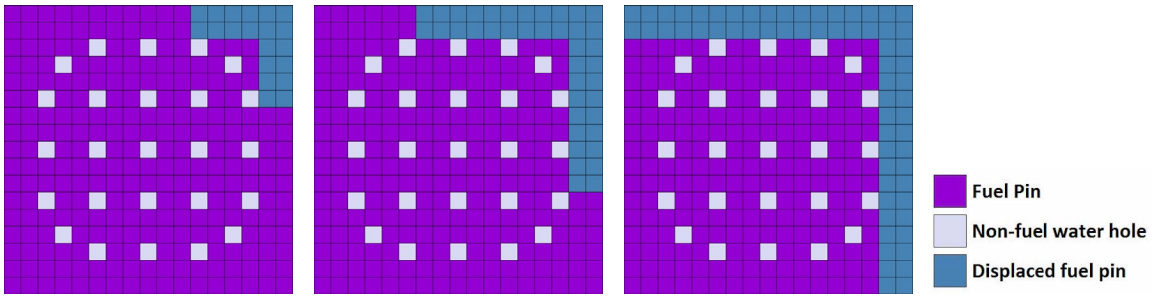

Figure 6-22 Corner Rod Displacement Configurations – 17 Bin 1

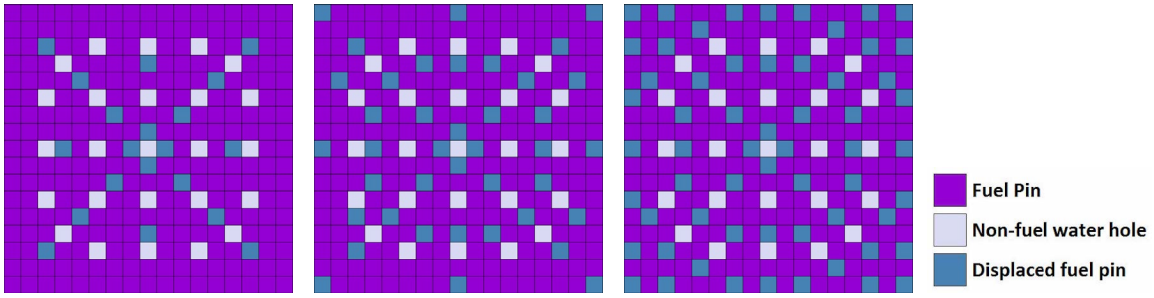

Figure 6-23 Random Rod Displacement Configurations – 17 Bin 1

6.3.4.3.7 PWR Fuel Assembly Stainless Steel Replacement Rod Study

Replacement of fuel rods in the fuel assembly with SS rods may be necessary for core performance. This study is only applicable to Groups 1 and 2 and examines the effect on k_{eff}. These rods are added in two configurations: the first configuration replaces two outer edge rows; the second configuration replaces fuel rods with SS rods in "random" locations throughout the fuel assembly. An example of both configurations is shown in Figure 6-24. The random rods are selected in a symmetrical pattern, but are dispersed throughout the fuel assembly grid. The SS rods are modeled with the same OD as their respective fuel rods. The random rod displacement configuration models the same number of displaced rods as the corner rod displacement configuration, while ensuring symmetry is maintained.

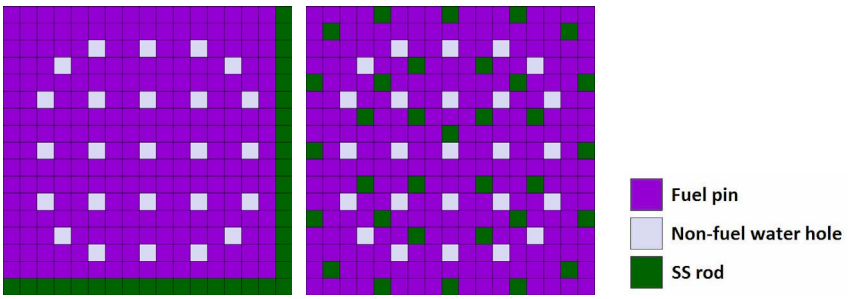

Figure 6-24 SS Replacement Rod Configurations – 17 Bin 1

6.3.4.3.8 Cladding Diameter Tolerance Study

The fuel rod cladding of each fuel assembly has a specified fabrication tolerance. Therefore, tolerance in cladding radial dimensions ID and OD and its effect on k_{eff} was examined. The tolerance ranges examined for each package arrangement are listed in Table 6-18 and are created based on the fuel assemblies of each bin. The tolerance is applied to the cladding ID and OD independently. Cladding tolerance was not examined for the Rod Pipe arrangement because no cladding was modeled in the Rod Pipe analysis. The nominal cladding dimensions including tolerance of any fuel assembly to be shipped as Group 4 contents must meet the minimum cladding dimensions specified for Group 4 contents in Section 6.2. Therefore, this study is not analyzed for Group 4 contents.

Table 6-18 Cladding Diameter Tolerances Examined

Contents	Cladding Diameter Tolerance	
	in.	cm
Group 1	±0.002	±0.0051
Group 2	±0.002	±0.0051
Rod Pipe	--	--

6.3.4.3.9 Fuel Pellet Diameter Tolerance Study

The fuel pellet diameter of each fuel assembly has a specified fabrication tolerance. Therefore, the tolerance variation in the fuel pellet radial dimension and its effect on k_{eff} was examined. The tolerance ranges examined for each package arrangement are listed in Table 6-19 and are created based on the fuel assemblies of each bin. The largest tolerance of the Groups is applied to the Rod Pipe content. The nominal fuel pellet dimensions including tolerance of any fuel assembly to be shipped as Group 4 contents must meet the minimum fuel pellet dimensions specified for Group 4 contents in Section 6.2. Therefore, this study is not analyzed for Group 4 contents.

Table 6-19 Fuel Pellet Diameter Tolerances Examined

Contents	Fuel Pellet Diameter Tolerance	
	in.	cm
Group 1	±0.0005, ±0.0007	±0.0013, ±0.0018
Group 2	±0.0005, ±0.0007	±0.0013, ±0.0018
Rod Pipe	±0.0010, ±0.0014	±0.0025, ±0.0036

6.3.4.3.10 Fuel Rod Pitch Tolerance Study

The fuel rod pitch of each fuel assembly has a specified fabrication tolerance. Therefore, its effect on k_{eff} was examined. The tolerance ranges examined are listed in Table 6-20 and are created based on the fuel assemblies of each bin. This study was not done for the Rod Pipe package arrangement, as the loose rods are not restricted to a design lattice configuration. The Group 1 single package fuel rod pitch tolerance range includes Group 1 and 2 tolerance values because they were analyzed together in the single package evaluation. Therefore, Group 1 and 2 single package tolerance range is larger than the Group 1 package array fuel rod pitch tolerance. For HAC, only the pitch of the nominal lattice region is changed because the maximum possible pitch is already modeled in the expanded lattice region. For Group 4, 14 Bin 1 and 16 Bin 2 have a larger fuel rod pitch tolerance of ±0.005 in. (±0.0127 cm). This pitch is not evaluated in this study as 14 Bin 1 and 16 Bin 2 are well bounded by the respective bounding bins for the Group 4 single package, NCT package array, and HAC package array baseline evaluations in Sections 6.9.3.1, 6.9.3.3, and 6.9.3.5.

Table 6-20 Fuel Rod Pitch Tolerances Examined

Contents	Evaluation	Condition	Fuel Rod Pitch Tolerance	
			in.	cm
Groups 1 and 2	Single Package	NCT	-0.0685, -0.0343, +0.0059, +0.0118	-0.174, -0.087, +0.015, +0.03
		HAC	-0.0785, -0.0393, +0.0059, +0.0118	-0.1994, -0.0997, +0.015, +0.03
Group 1	Package Array	NCT and HAC	±0.001, ±0.005	±0.0025, ±0.0127
Group 2	Package Array	NCT	-0.0335, -0.0167, +0.0059, +0.0118	-0.085, -0.0425, +0.015, +0.03
		HAC	-0.0630, -0.0315, +0.0059, +0.0118	-0.16, -0.08, +0.015, +0.03
Group 4	All	All	±0.001	±0.0025
Rod Pipe	--	--	--	--

6.3.4.3.11 Steel Nozzle Reflector Study

This study is included to determine if modeling the top and bottom nozzles as their materials of construction, instead of replacing them with full-density light water, could result in an increase in reactivity for a package array under NCT or HAC. In the baseline cases, the top and bottom nozzles are modeled as void for NCT and the top and bottom nozzles are modeled as full-density light water for HAC. For this study, three configurations, one NCT and two HAC cases, are examined with a 66 lb (30 kg) SS304 top nozzle and a 33 lb (15 kg) SS304 bottom nozzle. The nozzles are modeled as blocks, equivalent in the x- and y-dimensions to the fuel envelope of each assembly, with the height of the blocks being adjusted to accommodate the full mass of stainless steel.

For NCT, solid blocks that model 50% density SS304 are added to the top and bottom of the fuel assemblies. This configuration is shown in Figure 6-25 with the nozzle regions colored green. For the first HAC configuration, solid blocks are modeled as 50% density SS304 with the remaining volume of the blocks as full density water. The other HAC configuration models the top and bottom nozzles as 100% density SS304. An example of the HAC configuration is shown in Figure 6-26 with the nozzle regions colored green.

For Group 4 NCT package array, the baseline case models the fuel assembly against the top of the Clamshell. Adding the steel nozzle reflector shifts the fuel assembly away from the end, as shown in Figure 6-25. As evidenced in the axial position study in Section 6.9.3.3.2, the axial shift away from the against the top of the Clamshell reduces k_{eff}. Therefore, an adjusted baseline case that models the fuel assembly at the same axial position as the nozzle case is added to determine the effect of adding the nozzle alone without the effect of shifting the assembly.

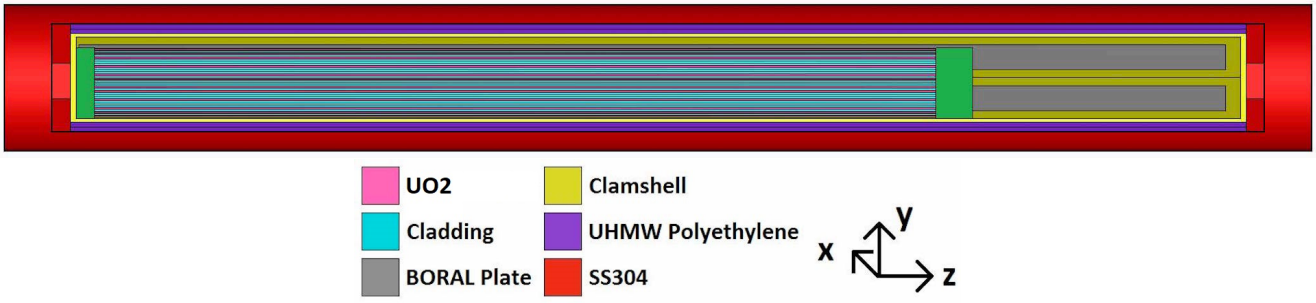

Figure 6-25 Example of NCT Stainless Steel Nozzle Configuration, Shown in Green

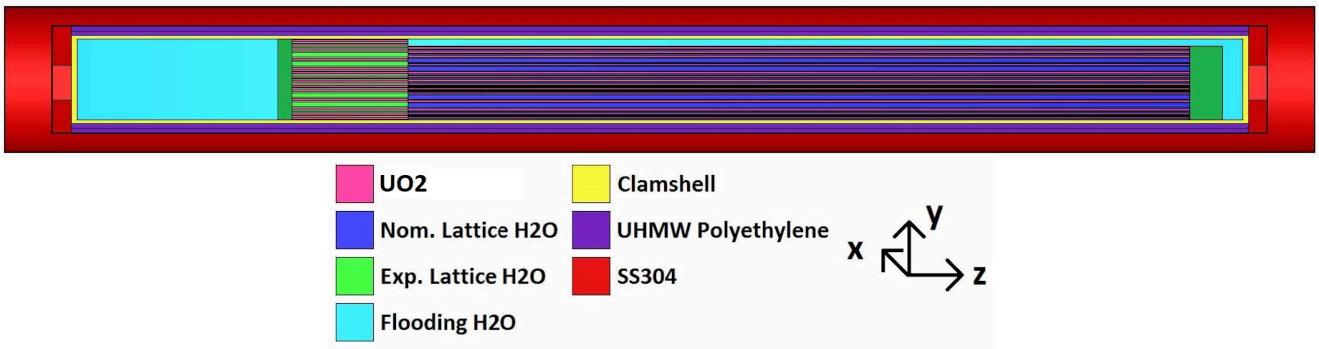

Figure 6-26 Example of HAC Stainless Steel Nozzle Configuration, Shown in Green

6.3.4.3.12 HAC Rod Pipe Package Array Flooding Configuration Study

Preferential flooding is evaluated for package array HAC by holding one packaging cavity as flooded with full density water or void, while one or more of the other packaging cavities varies the water density. The first configuration floods the regions outside of the Clamshell, but not the Clamshell cavity. The second configuration floods only the Clamshell cavity. Figure 6-27 shows the regions that are moderated for each case.

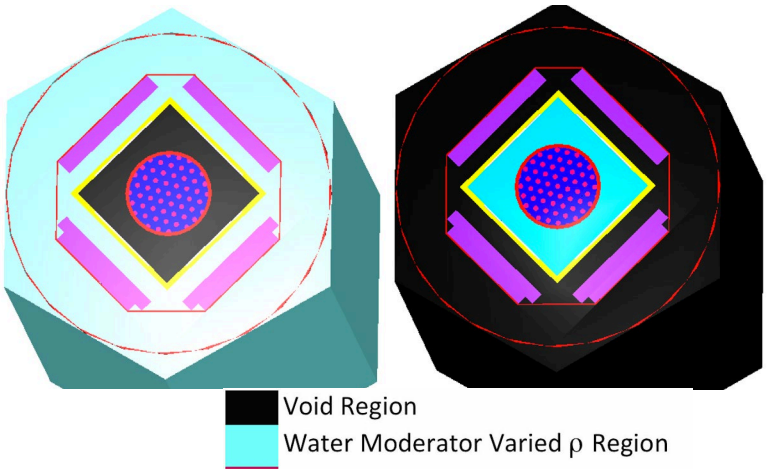

Figure 6-27 Rod Pipe HAC Package Array Flooding Configurations

6.3.4.3.13 ADOPT Fuel Study

This study evaluates the effect of UO_2 fuel with ADOPT fuel instead of standard UO_2 fuel. Because the additives in ADOPT rods are limited to very small quantities (700 ppm Cr_2O_3 and up to 200 ppm Al_2O_3), the reactivity effect is expected to be minimal. While fuel assemblies or the loose fuel rod contents may contain any number of ADOPT fuel rods in any location, this study models every rod in the fuel assembly or rod pipe with ADOPT fuel. This study is only applied to PWR Groups 1, 2, and 4 and UO_2 loose rods. ADOPT fuel is not a permissible content in U_3Si_2 loose rods.

6.4 SINGLE PACKAGE EVALUATION

6.4.1 Configuration

For all single package arrangements and conditions of transport, all inner spaces of the package are modeled as flooded with full-density water, including the fuel-clad gap where applicable. Additional material modeling is specified in Section 6.3.2. Several materials, including fuel structural components and packaging components (e.g. Outerpack foam regions, ceramic fiber blankets, and shock mounts, etc.), are replaced with full-density water. The single package is reflected with 20 cm of full-density water.

6.4.1.1 Baseline Configurations

As described in Section 6.3.4.2, a baseline case is evaluated for both content Groups and Rod Pipe configurations under NCT and HAC. Baseline configurations represent a bounding model that is carried forward to the sensitivity studies to demonstrate maximum reactivity.

6.4.1.1.1 PWR Fuel Assembly Groups

For the baseline case determination, as defined in Section 6.3.4.2.1, first the bounding CFA-package variant combination is determined. For the Groups 1 and 2 single package assessment, the Traveller XL is consistently more reactive than the Traveller STD under NCT and HAC. This conclusion is applied to Group 4. As discussed in Section 6.3.4.2.1.2, the positioning of the fuel assembly is examined because of the physical properties of the packaging. Detailed results of the baseline case determination are shown in Section 6.9.3.1. The NCT baseline configuration is shown in Figure 6-28 and the HAC baseline configuration is shown in Figure 6-29. The baseline cases are summarized in Table 6-21. Note that for PWR Group 4, a single baseline case is modeled that bounds both NCT and HAC.

Table 6-21 Summary of Groups 1 and 2 Single Package Baseline Configurations

Condition of Transport	Traveller Variant	Contents (Group)	Lattice Expansion Length (cm)	Axial Position (cm)	Flooding Configuration	$k_{eff} \pm \sigma$
NCT	XL	18 Bin 1 (1 & 2)	0.0	72.583	All Regions	0.88499 ± 0.00059
HAC	XL	17 Bin 1 (1 & 2)	50.8	87.122	All Regions	0.90209 ± 0.00049
HAC	XL	17 Bin 1 (4)	--	42.545	All Regions	0.90483 ± 0.00026

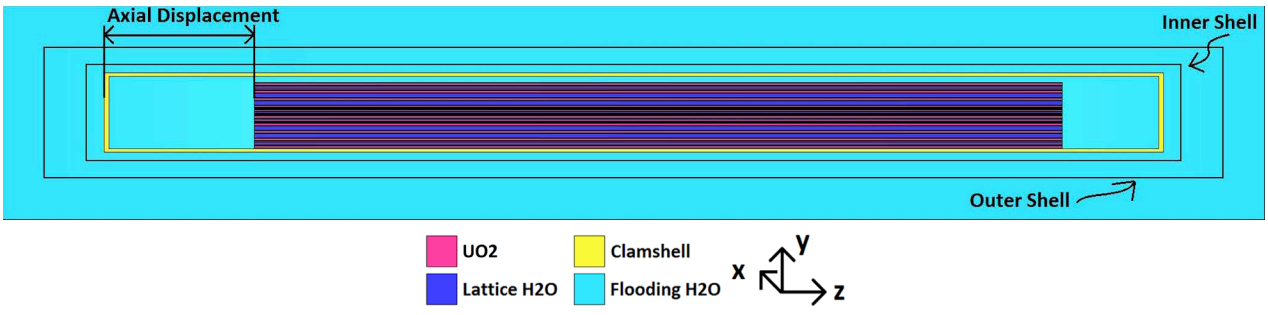

Figure 6-28 Cross-section of Groups 1 and 2 NCT and Group 4 Single Package Baseline Case

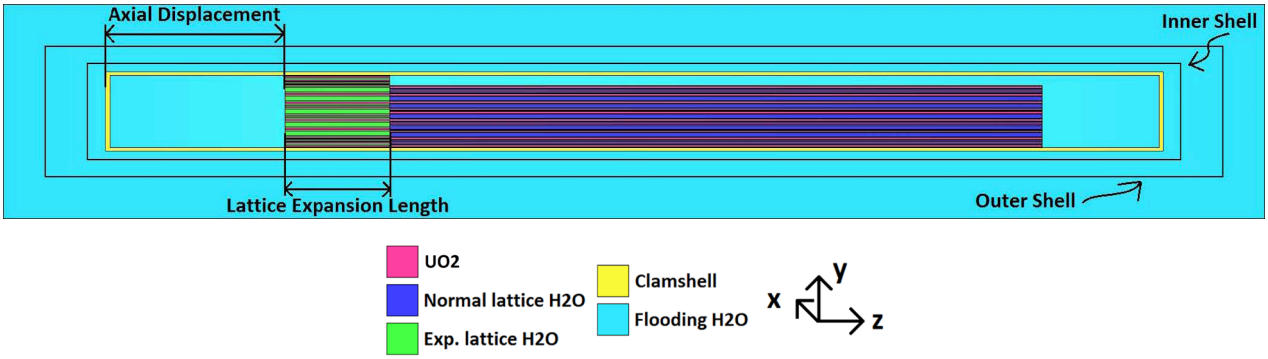

Figure 6-29 Cross-section Groups 1 and 2 HAC Single Package Baseline Case

6.4.1.1.2 Rod Pipe

For the baseline case determination, as defined in Section 6.3.4.2.2, loose rods are modeled in the Rod Pipe. The pitch is expanded starting with a close pack configuration for NCT expanding through a peak water-to-fuel ratio by increasing the pitch for HAC. The pitch type is modeled as both square and hexagonal as the small variation of geometry varies the water-to-fuel ratio slightly. The Traveller STD and Traveller XL packages are evaluated with the Rod Pipe as the only loose rod shipment configuration. The single package is fully flooded to increase moderation of the single package fissile content. Detailed results of the Rod Pipe contents analysis are shown in Section 6.9.3.2. Comparison of the Traveller STD to Traveller XL baseline results show that the Traveller XL is consistently more reactive than the Traveller STD. There are two Rod Pipe baseline cases for UO_2 fuel rods, which are bounding of all UO_2 Rod Pipe configurations under NCT and HAC for the Traveller STD and XL variants. There are two Rod Pipe baseline cases for U_3Si_2 fuel rods, which are bounding of all U_3Si_2 Rod Pipe configurations under NCT and HAC for the Traveller STD variant. The baseline cases are summarized in Table 6-22.

Table 6-22 Summary of Rod Pipe Single Package Baseline Configurations

Contents	Condition of Transport	Traveller Variant	Fuel OR (cm)	Pitch-Type	Fuel Rod Half-Pitch (cm)	Flooding Configuration	$k_{eff} \pm \sigma$
UO_2 Fuel Rods	NCT	XL	3.5	Square	3.5	All regions	0.56435 ± 0.00086
UO_2 Fuel Rods	HAC	XL	0.55	Hexagonal	1.00	All regions	0.72106 ± 0.00047
U_3Si_2 Fuel Rods	NCT	STD	0.4851	Square	0.4851	All regions	0.42948 ± 0.00037
U_3Si_2 Fuel Rods	HAC	STD	0.4851	Hexagonal	1.0101	All regions	0.67492 ± 0.00049

6.4.1.2 Sensitivity Study Configurations

Several sensitivity studies are completed for the NCT and HAC single package evaluation. The following summary tables list the as-penalized configurations of each sensitivity study. An entry of "None" signifies that the study resulted in no penalty and an entry of "--" signifies that the study did not require analyzing based on transport condition. The baseline case with the sum of penalties from sensitivity studies defines the most reactive configuration for demonstration of maximum reactivity.

6.4.1.2.1 PWR Fuel Assembly Groups

Listed in Table 6-23 are the bounding, as-penalized configurations of each sensitivity study for PWR Fuel Assembly Groups.

Table 6-23 Single Package Sensitivity Study Bounding Configurations – PWR Fuel Assembly Groups

Sensitivity Study	Groups 1 and 2		Group 4
	NCT	HAC	NCT/ HAC
Annular Fuel Pellet Blanket	Full-length	Full-length	20.0 in. (50.8 cm)
Fuel Assembly Shift	Centered	Centered	None
Moderator Block Density	--	1% density reduction	None
Polyethylene Packing Materials	5.54 kg of polyethylene	2 kg of polyethylene	None
Axial Rod Displacement	--	None	--
Stainless Steel Rods	None	None	None
Cladding Tolerance	Minimum cladding thickness	Minimum cladding thickness	--
Fuel Pellet Diameter Tolerance	None	None	--
Fuel Rod Pitch Tolerance	+ Tolerance	+ Tolerance	+ Tolerance
ADOPT Fuel	None	ADOPT rods	None

Note: '--' signifies the study was not applicable to the condition of transport analyzed. 'None' signifies that the sensitivity study did not result in a statistically significant increase in reactivity over the baseline case.

6.4.1.2.2 Rod Pipe

Listed in Table 6-24 are the bounding, as-penalized configurations of each sensitivity study for Rod Pipe content.

Table 6-24 Rod Pipe Single Package Sensitivity Studies Bounding Configurations

Sensitivity Study	Bounding Configuration UO_2 Fuel Rods		Bounding Configuration U_3Si_2 Fuel Rods	
	NCT	HAC	NCT	HAC
Annular Fuel Pellet Blanket	Full-length with proportional ID	Full-length	Full-length	None
Rod Pipe Position in Clamshell	None	None	None	None
Moderator Block Density	--	None	--	None
Polyethylene Packing Materials	18.32 kg polyethylene wrap	Rod Pipe full of polyethylene	36.30 kg polyethylene wrap	Rod Pipe full of polyethylene
Fuel Pellet Diameter Tolerance	None	None	+Tolerance	None
ADOPT Fuel	None	None	--	--

Note: '--' signifies the study was not applicable to the condition of transport analyzed. 'None' signifies that the sensitivity study did not result in a statistically significant increase in reactivity over the baseline case.

6.4.2 Results

6.4.2.1 Single Package – Maximum Reactivity Results Summary

The maximum reactivity, *Maximum* k_{eff}, is defined by the bounding baseline $k_p + 2\sigma_p$ plus the sum of penalties assessed for each sensitivity study (Δk_u). See Table 6-25 for a summary of the *Maximum* k_{eff} results. Final values of maximum reactivity fall under the USL, as calculated per Section 6.8.

Table 6-25 Single Package – Maximum Reactivity Results Summary

Condition of Transport	Traveller Variant	Bounding Content	$k_{eff} \pm \sigma$	$k_p + 2\sigma_p$	Δk_u	*Maximum* k_{eff}	USL
NCT	XL	18 Bin 1 (Group 1 & 2)	0.88499 ± 0.00059	0.88617	0.03534	0.92151	0.94067
HAC	XL	17 Bin 1 (Group 1 & 2)	0.90209 ± 0.00049	0.90307	0.01780	0.92087	0.94067
HAC	XL	17 Bin 1 (Group 4)	0.90483 ± 0.00026	0.90535	0.00157	0.90692	0.94082
NCT	XL	Rod Pipe UO_2 Fuel Rods	0.56435 ± 0.00086	0.56607	0.06972	0.63579	0.94044
HAC	XL	Rod Pipe UO_2 Fuel Rods	0.72106 ± 0.00047	0.72200	0.07377	0.79577	0.94044
NCT	STD	Rod Pipe U_3Si_2 Fuel Rods	0.42948 ± 0.00037	0.43022	0.29857	0.72879	0.94053
HAC	STD	Rod Pipe U_3Si_2 Fuel Rods	0.67492 ± 0.00049	0.67590	0.06371	0.73961	0.94053

6.4.2.2 Sensitivity Study Results

As discussed in Section 6.3.4.3, the NCT and HAC baseline cases, for each package arrangement, are subjected to several sensitivity studies, which are detailed in Table 6-17. Each sensitivity study is compared to the baseline case. The most reactive configuration resulting in the largest positive difference in $k_{eff} + 2\sigma$ from the baseline case value that is also greater than or equal to two times the baseline σ is tallied and summed to define the total penalty assessed (Δk_u).

6.4.2.2.1 PWR Fuel Assembly Groups Results Summary

Table 6-26 shows the summary of the penalty assessed for the sensitivity studies evaluated for the Groups 1, 2, and 4 contents. Note that only HAC is analyzed for Group 4 because the only difference between NCT and HAC is the moderator block density study, the presence of which under HAC bounds NCT. An entry of "0.0" signifies that the study resulted in no positive penalty on reactivity and an entry of "--" signifies that the study did not require analyzing based on transport condition.

Table 6-26 Single Package Assessed Penalties, Δk_u, PWR Fuel Assembly Groups

Sensitivity Study	Groups 1 and 2		Group 4
	NCT	HAC	HAC
Annular Fuel Pellet Blanket	0.01273	0.0	0.00077
Centered Fuel Assembly	0.00202	0.00266	0.0
Moderator Block Density	--	0.00157	0.0
Polyethylene Packing Materials	0.00168	0.00284	0.0
Axial Rod Displacement	--	0.0	--
Stainless Steel Rods	0.0	0.0	0.0
Cladding Tolerance	0.00529	0.00495	--
Fuel Pellet Diameter Tolerance	0.0	0.0	--
Fuel Rod Pitch Tolerance	0.01362	0.00457	0.00080
ADOPT Fuel Rods	0.0	0.00121	0.0
Total Penalty (Δk_u)	**0.03534**	**0.01780**	**0.00157**

6.4.2.2.2 PWR Fuel Assembly Groups 1 and 2 NCT Detailed Results

The annular blanket sensitivity study, as defined in Section 6.3.4.3.1, examined the addition of varying annular fuel pellet ID and lengths of annular fuel pellet blanket lengths equally to the top and bottom of an assembly. Table 6-27 defines the parameters evaluated and the results. Figure 6-30 displays the result trends for Groups 1 and 2. The most reactive case is highlighted.

Note that for Group 4 single package, only HAC is analyzed because the only difference between NCT and HAC is the moderator block density study, the presence of which under HAC bounds NCT.

Table 6-27 Annular Blanket Sensitivity Results – Single Package, NCT, Groups 1 and 2							
Contents (Group)	**Traveller Variant**	**Annulus Diameter**	**Annulus Length (cm)**	**k_{eff}**	**σ**	**$k_{eff} + 2\sigma$**	**$\Delta(k_{eff} + 2\sigma)$**
18 Bin 1 (1 & 2)	XL	**Baseline Case**		0.88499	0.00059	0.88617	--
		0.155 in. (0.3937 cm)	48.9	0.88628	0.00057	0.88742	0.00125
			97.8	0.8897	0.00055	0.89080	0.00463
			146.7	0.894	0.00048	0.89496	0.00879
			195.6	0.89784	0.00053	0.89890	0.01273
		0.183 in. (0.4648 cm)	48.9	0.88528	0.00053	0.88634	0.00017
			97.8	0.88915	0.00058	0.89031	0.00414
			146.7	0.89277	0.00048	0.89373	0.00756
			195.6	0.89604	0.00053	0.89710	0.01093

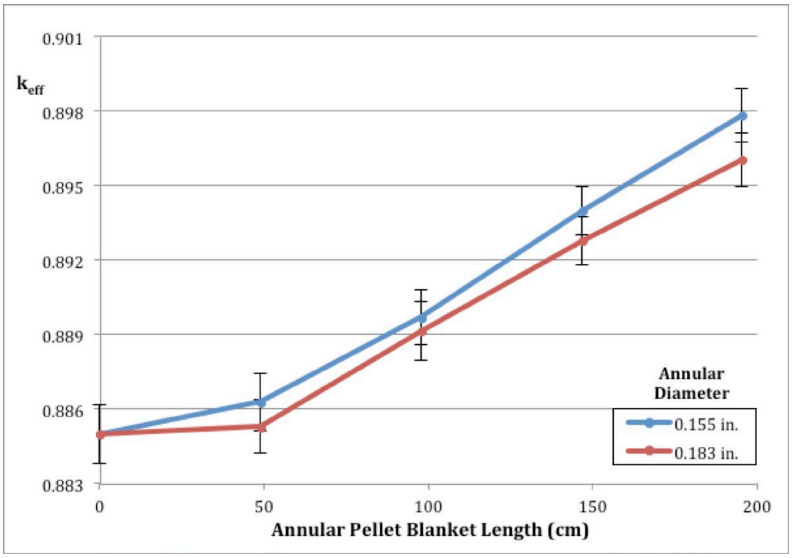

Figure 6-30 Annular Blanket Sensitivity – Single Package, NCT (Groups 1 & 2)

The fuel assembly position sensitivity study, as defined in Section 6.3.4.3.2, examined the centering of the fuel assembly in the Clamshell. Table 6-28 defines the parameter evaluated and the results. The most reactive case is highlighted.

Table 6-28 Fuel Assembly Position Sensitivity Results – Single Package, NCT, Groups 1 and 2						
Contents (Group)	**Traveller Variant**	**Fuel Assembly Position**	**k_{eff}**	**σ**	**$k_{eff} + 2\sigma$**	**$\Delta(k_{eff} + 2\sigma)$**
18 Bin 1 (1 & 2)	XL	**Baseline Case**	0.88499	0.00059	0.88617	--
		Centered	0.88715	0.00052	0.88819	0.00202

The polyethylene packing materials sensitivity study, as defined in Section 6.3.4.3.5, examined the presence of an outer wrap around the fuel assembly. Table 6-29 defines the parameter evaluated and the results. The most reactive case is highlighted.

Table 6-29 Polyethylene Packing Sensitivity Results – Single Package, NCT, Groups 1 and 2

Contents (Group)	Traveller Variant	Poly Model	Poly Mass (kg)	k_{eff}	σ	$k_{eff} + 2\sigma$	$\Delta(k_{eff} + 2\sigma)$
18 Bin 1 (1 & 2)	XL	**Baseline Case**	0	0.88499	0.00059	0.88617	--
		Outer Wrap	5.54	0.88691	0.00047	0.88785	0.00168

The SS replacement rod sensitivity study, as defined in Section 6.3.4.3.7, examined replacement of fuel rods with SS rod within the fuel assembly. Table 6-30 defines the parameters evaluated and the results. The most reactive case is highlighted.

Table 6-30 SS Rod Replacement Sensitivity Results – Single Package, NCT, Groups 1 and 2

Contents (Group)	Traveller Variant	SS Rod Configuration	k_{eff}	σ	$k_{eff} + 2\sigma$	$\Delta(k_{eff} + 2\sigma)$
18 Bin 1 (1 & 2)	XL	**Baseline Case**	0.88499	0.00059	0.88617	--
		Corner	0.85862	0.00051	0.85964	-0.02653
		Random	0.8353	0.00058	0.83646	-0.04971

The tolerance sensitivity studies evaluate cladding dimensions, fuel pellet diameter, and fuel rod pitch, as defined in Sections 6.3.4.3.8, 6.3.4.3.9, and 6.3.4.3.10, respectively. Table 6-31 defines the parameter dimensions evaluated and the results. The most reactive case is highlighted for each tolerance parameter.

Table 6-31 Tolerance Sensitivity Results – Single Package, NCT, Groups 1 and 2

Content (Group)	Traveller Variant	Tolerance Parameter		k_{eff}	σ	$k_{eff} + 2\sigma$	$\Delta(k_{eff} + 2\sigma)$
18 Bin 1 (1 & 2)	XL	**Baseline Case**		0.88499	0.00059	0.88617	--
Cladding Tolerance		**ID Tolerance (in.)**	**OD Tolerance (in.)**	k_{eff}	σ	$k_{eff} + 2\sigma$	$\Delta(k_{eff} + 2\sigma)$
18 Bin 1 (1 & 2)	XL	-0.002	-0.002	0.88547	0.00048	0.88643	0.00026
			nominal	0.88296	0.00049	0.88394	-0.00223
			+0.002	0.87955	0.00052	0.88059	-0.00558
		nominal	-0.002	0.88832	0.00061	0.88954	0.00337
			nominal	0.88499	0.00059	0.88617	--
			+0.002	0.88320	0.00052	0.88424	-0.00193
		+0.002	-0.002	0.89042	0.00052	0.89146	0.00529
			nominal	0.88805	0.00045	0.88895	0.00278
			+0.002	0.88548	0.00055	0.88658	0.00041
Pellet Diameter Tolerance		**Pellet OD Tolerance (in.)**		k_{eff}	σ	$k_{eff} + 2\sigma$	$\Delta(k_{eff} + 2\sigma)$
18 Bin 1 (1 & 2)	XL	-0.0007		0.88553	0.00035	0.88623	0.00006
		-0.0005		0.88562	0.00038	0.88638	0.00021
		+0.0005		0.8852	0.00038	0.88596	-0.00021
		+0.0007		0.88443	0.00036	0.88515	-0.00102
Pitch Tolerance		**Pitch Tolerance (in.)**		k_{eff}	σ	$k_{eff} + 2\sigma$	$\Delta(k_{eff} + 2\sigma)$
18 Bin 1 (1 & 2)	XL	-0.0685		0.76608	0.00056	0.76720	-0.11897
		-0.0343		0.83591	0.00048	0.83687	-0.04930
		+0.0059		0.89201	0.00055	0.89311	0.00694
		+0.0118		0.89863	0.00058	0.89979	0.01362

The ADOPT fuel sensitivity study, as defined in Section 6.3.4.3.13, examined the effect of replacing standard UO_2 fuel with ADOPT fuel. Table 6-33A lists the results of the study. The most reactive case is highlighted.

Table 6-31A ADOPT Fuel Results – Single Package, NCT, PWR Fuel Assembly Groups

Contents (Group)	Traveller Variant	Fuel Material	k_{eff}	σ	$k_{eff} + 2\sigma$	$\Delta(k_{eff} + 2\sigma)$
18 Bin 1 (1 & 2)	XL	UO_2	0.88499	0.00059	0.88617	--
		ADOPT	0.88470	0.00060	0.88590	-0.00027

6.4.2.2.3 PWR Fuel Assembly Groups HAC Detailed Results

The annular blanket sensitivity study, as defined in Section 6.3.4.3.1, examined the addition of varying annular fuel pellet ID and lengths of annular fuel pellet blanket lengths equally to the top and bottom of an assembly. Table 6-32 defines the parameters evaluated and the results. Figure 6-31 displays the result trends for Groups 1 and 2, and Figure 6-31A displays the result trend for Group 4. The most reactive case is highlighted.

Table 6-32 Annular Blanket Sensitivity Results – Single Package, HAC, PWR Fuel Assembly Groups

Content (Group)	Traveller Variant	Annulus Diameter	Annulus Length (cm)	k_{eff}	σ	$k_{eff} + 2\sigma$	$\Delta(k_{eff} + 2\sigma)$
17 Bin 1 (1 & 2)	XL	**Baseline Case**		0.90209	0.00049	0.90307	--
		0.155 in. (0.3937 cm)	13	0.90189	0.0006	0.90309	0.00002
			26	0.89915	0.00048	0.90011	-0.00296
			39	0.89378	0.00049	0.89476	-0.00831
			50.8	0.88971	0.00058	0.89087	-0.01220
			95.038	0.89038	0.00050	0.89138	-0.01169
			139.277	0.89054	0.00048	0.89150	-0.01157
			183.515	0.89123	0.00059	0.89241	-0.01066
		0.183 in. (0.4648 cm)	13	0.90188	0.00054	0.90296	-0.00011
			26	0.89602	0.00054	0.89710	-0.00597
			39	0.88734	0.00058	0.8885	-0.01457
			50.8	0.87900	0.00052	0.88004	-0.02303
			95.038	0.88073	0.00055	0.88183	-0.02124
			139.277	0.88022	0.00061	0.88144	-0.02163
			183.515	0.88055	0.00052	0.88159	-0.02148
17 Bin 1 (4)	XL	**Baseline Case**		0.90483	0.00026	0.90535	--
		0.155 in. (0.3937 cm)	13.0	0.90499	0.00026	0.90551	0.00016
			26.0	0.90495	0.00025	0.90545	0.00010
			39.0	0.90444	0.00029	0.90502	-0.00033
			50.8	0.90558	0.00027	0.90612	0.00077
		0.183 in. (0.4648 cm)	13.0	0.90486	0.00026	0.90538	0.00003
			26.0	0.90490	0.00023	0.90536	0.00001
			39.0	0.90520	0.00025	0.90570	0.00035
			50.8	0.90554	0.00024	0.90602	0.00067

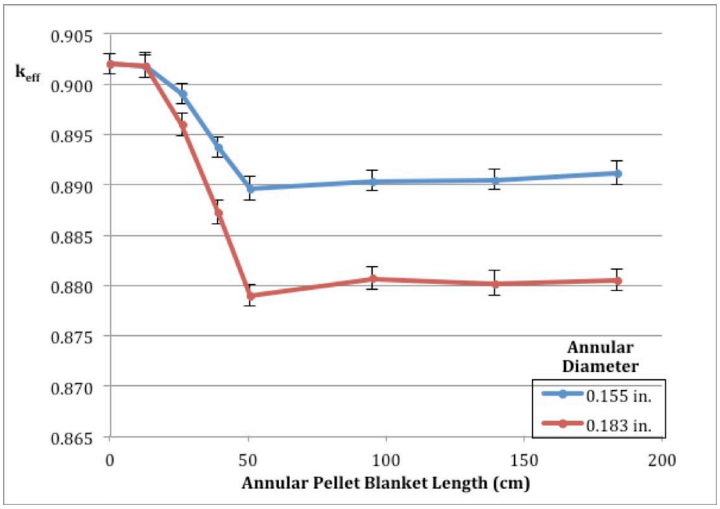

Figure 6-31 Annular Blanket Sensitivity Results – Single Package, HAC (Groups 1 & 2)

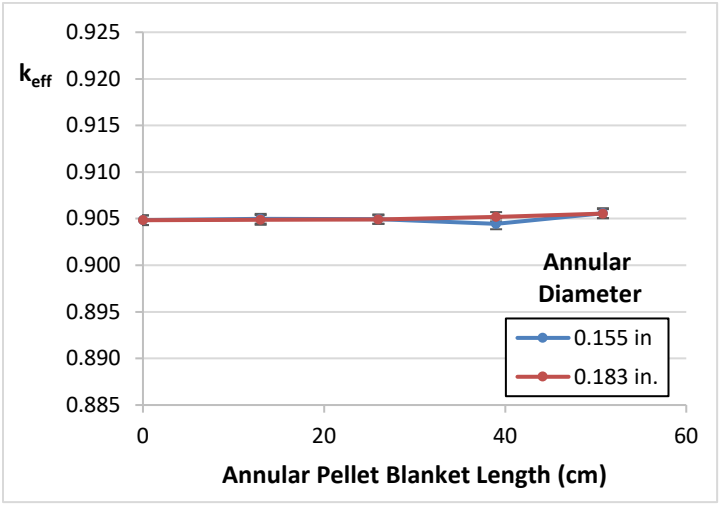

Figure 6-31A Annular Blanket Sensitivity Results – Single Package, HAC (Group 4)

The moderator block density reduction sensitivity study, as defined in Section 6.3.4.3.3, examined the post-fire condition of the moderator block. Table 6-33 defines the parameter evaluated and the results. The most reactive case is highlighted.

Table 6-33 Moderator Block Density Results – Single Package, HAC, PWR Fuel Assembly Groups

Content (Group)	Traveller Variant	Moderator Block Density (g/cm^3)	k_{eff}	σ	$k_{eff} + 2\sigma$	$\Delta(k_{eff} + 2\sigma)$
17 Bin 1 (1 & 2)	XL	**Baseline Case**	0.90209	0.00049	0.90307	--
		0.9108	0.90358	0.00053	0.90464	0.00157
17 Bin 1 (4)	XL	**Baseline Case**	0.90483	0.00026	0.90535	--
		0.9108	0.90495	0.00032	0.90559	0.00024

The fuel assembly position sensitivity study, as defined in Section 6.3.4.3.2, examined the centering and upward positioning of the fuel assembly in the Clamshell. Table 6-34 presents the parameters evaluated and the results. The most reactive case is highlighted.

Table 6-34 Fuel Assembly Position Sensitivity Results – Single Package, HAC, PWR Fuel Assembly Groups

Contents (Group)	Traveller Variant	Fuel Assembly Position	k_{eff}	σ	$k_{eff} + 2\sigma$	$\Delta(k_{eff} + 2\sigma)$
17 Bin 1 (1 & 2)	XL	**Baseline Case**	0.90209	0.00049	0.90307	--
		Centered	0.90457	0.00058	0.90573	0.00266
		Up	0.90258	0.00053	0.90364	0.00057
17 Bin 1 (4)	XL	Down	0.89579	0.00026	0.89631	-0.00904
		Baseline Case	0.90483	0.00026	0.90535	--
		Up	0.89641	0.00028	0.89697	-0.00838

The polyethylene packing materials sensitivity study, as defined in Section 6.3.4.3.5, examined a conservative representation of polyethylene packing materials through HAC. For the Traveller, 2.0 kg of polyethylene packing materials is the limit for the package. Table 6-35 defines the parameters evaluated and the results. Figure 6-32 displays the result trends for Groups 1 and 2 and Figure 6-32A displays the result trend for Group 4. The most reactive case is highlighted.

Table 6-35 Polyethylene Sensitivity Results – Single Package, HAC, PWR Fuel Assembly Groups

Content (Group)	Traveller Variant	Poly Model	Poly Mass (kg)	k_{eff}	σ	$k_{eff} + 2\sigma$	$\Delta(k_{eff} + 2\sigma)$
17 Bin 1 (1 & 2)	XL	**Baseline Case**	0.0	0.90209	0.00049	0.90307	--
		Outer Wrap	2.27	0.90310	0.00048	0.90406	0.00099
			3.74	0.90267	0.00060	0.90387	0.00080
			4.83	0.90376	0.00064	0.90504	0.00197
			5.71	0.90499	0.00051	0.90601	0.00294
			6.46	0.90610	0.00077	0.90764	0.00457
			7.12	0.90562	0.00050	0.90662	0.00355
		Uniform Wrap	2.0	0.90402	0.00053	0.90508	0.00201
			4.0	0.90551	0.00058	0.90667	0.00360
			6.0	0.90546	0.00059	0.90664	0.00357
			8.0	0.90688	0.00064	0.90816	0.00509
			10.0	0.90865	0.00058	0.90981	0.00674
		Collected Melt	2.0	0.90473	0.00059	0.90591	0.00284
			4.0	0.90734	0.00055	0.90844	0.00537
			6.0	0.91456	0.00050	0.91556	0.01249
			8.0	0.92283	0.00046	0.92375	0.02068
			10.0	0.93141	0.00061	0.93263	0.02956
17 Bin 1 (4)	XL	**Baseline Case**	0.0	0.90483	0.00026	0.90535	--
		Outer Wrap	1.0	0.90503	0.00027	0.90557	0.00022
			2.0	0.90468	0.00026	0.90520	-0.00015
			3.0	0.90521	0.00025	0.90571	0.00036

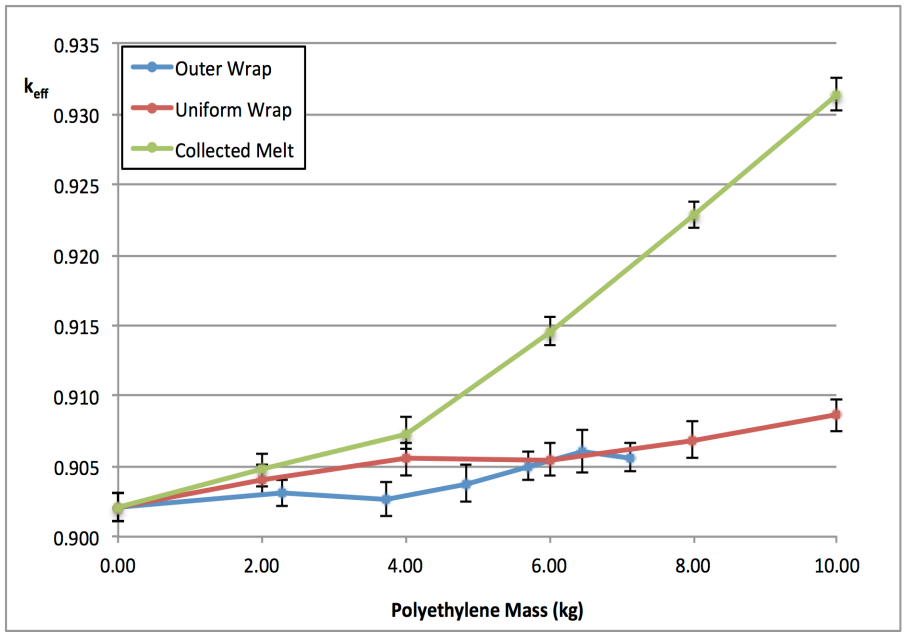

Figure 6-32 Polyethylene Sensitivity Results – Single Package, HAC (Groups 1 & 2)

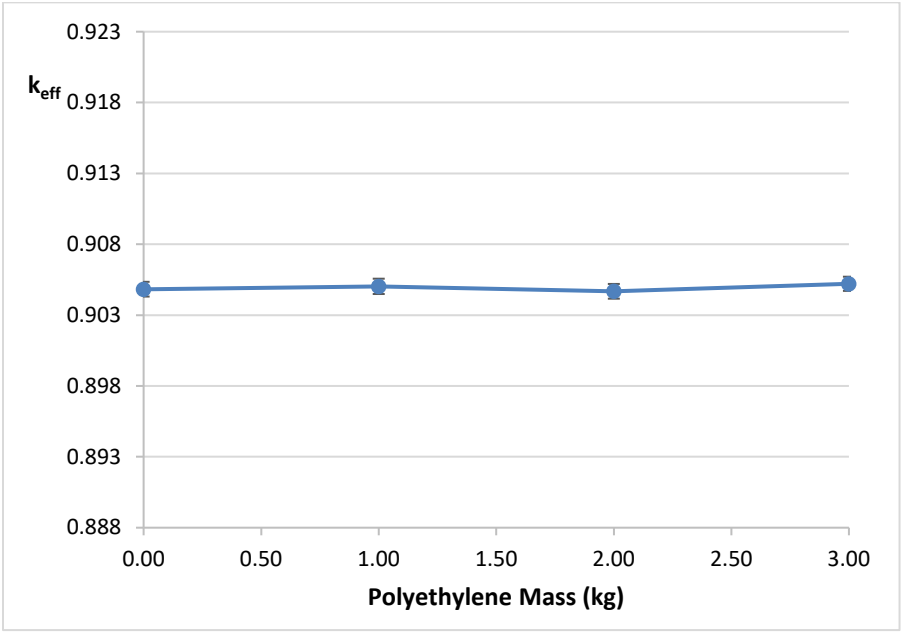

Figure 6-32A Polyethylene Sensitivity Results – Single Package, HAC (Group 4)

The axial rod displacement sensitivity study, as defined in Section 6.3.4.3.6, examined the movement of fuel rods out of the lattice because of drop testing. Table 6-36 defines the parameters evaluated and the results. Figure 6-33 displays the result trends for Groups 1 and 2. The most reactive case is highlighted.

Table 6-36 Axial Rod Displacement Sensitivity Results – Single Package, HAC, PWR Fuel Assembly Groups							
Content (Group)	**Traveller Variant**	**Rod Configuration**	**Number of Rods**	**k_{eff}**	**σ**	**$k_{eff} + 2\sigma$**	**$\Delta(k_{eff} + 2\sigma)$**
17 Bin 1 (1 & 2)	XL	**Baseline Case**	0	0.90209	0.00049	0.90307	--
		Corner	20	0.89365	0.0005	0.89465	-0.00842
			40	0.88297	0.00068	0.88433	-0.01874
			64	0.87615	0.00049	0.87713	-0.02594
		Random	20	0.89533	0.00048	0.89629	-0.00678
			40	0.89038	0.00059	0.89156	-0.01151
			64	0.88085	0.00054	0.88193	-0.02114

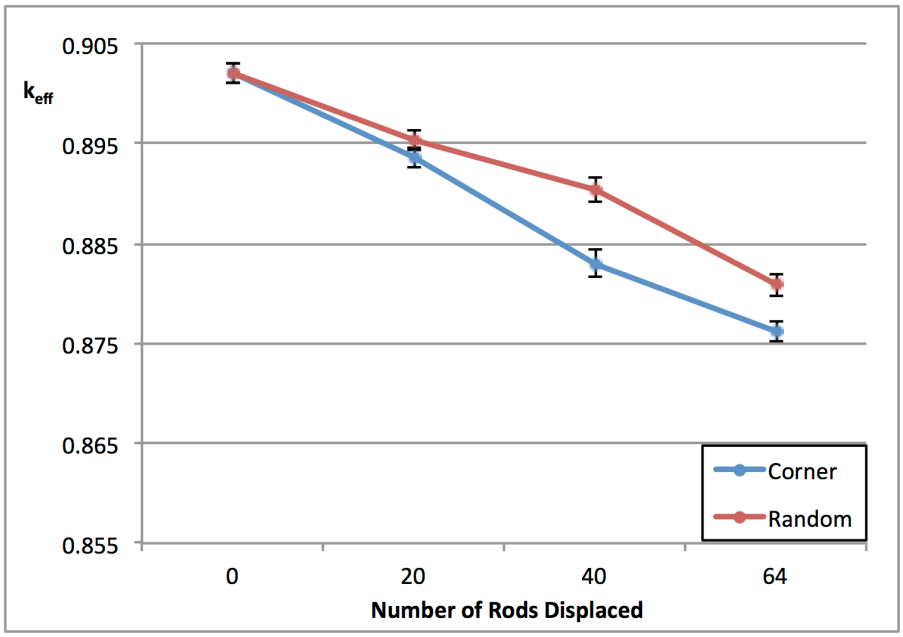

Figure 6-33 Axial Rod Displacement Sensitivity Results – Single Package, HAC (Groups 1 & 2)

The SS replacement rod sensitivity study, as defined in Section 6.3.4.3.7, examined replacement of fuel rods with SS rod within the fuel assembly. Table 6-37 defines the parameters evaluated and the results. The most reactive case is highlighted.

Table 6-37 SS Rod Replacement Sensitivity Results – Single Package, HAC, PWR Fuel Assembly Groups						
Content (Group)	**Traveller Variant**	**SS Rod Configuration**	**k_{eff}**	**σ**	**$k_{eff} + 2\sigma$**	**$\Delta(k_{eff} + 2\sigma)$**
17 Bin 1 (1 & 2)	XL	**Baseline Case**	0.90209	0.00049	0.90307	--
		Corner	0.88409	0.0006	0.88529	-0.01778
		Random	0.84703	0.00056	0.84815	-0.05492
17 Bin 1 (4)	XL	**Baseline Case**	0.90483	0.00026	0.90535	--
		Corner	0.87048	0.00027	0.87102	-0.03433
		Random	0.85720	0.00024	0.85768	-0.04767

The tolerance sensitivity studies evaluate cladding dimensions, fuel pellet diameter, and fuel rod pitch, as defined in Sections 6.3.4.3.8, 6.3.4.3.9, and 6.3.4.3.10, respectively. Table 6-38 defines the parameter dimensions evaluated and the results. The most reactive case is highlighted for each package variant and tolerance parameter.

Table 6-38 Tolerance Sensitivity Results – Single Package, HAC, PWR Fuel Assembly Groups

Content (Group)	Traveller Variant	Tolerance Parameter		k_{eff}	σ	$k_{eff} + 2\sigma$	$\Delta(k_{eff} + 2\sigma)$
17 Bin 1 (1 & 2)	XL	**Baseline Case**		0.90209	0.00049	0.90307	--
17 Bin 1 (4)	XL	**Baseline Case**		0.90483	0.00026	0.90535	--
Cladding Tolerance		**ID Tolerance (in.)**	**OD Tolerance (in.)**	k_{eff}	σ	$k_{eff} + 2\sigma$	$\Delta(k_{eff} + 2\sigma)$
17 Bin 1 (1 & 2)	XL	-0.002	-0.002	0.90225	0.00052	0.90329	0.00022
			nominal	0.90131	0.00065	0.90261	-0.00046
			+0.002	0.90113	0.00061	0.90235	-0.00072
		nominal	-0.002	0.90490	0.00050	0.90590	0.00283
			nominal	0.90209	0.00049	0.90307	--
			+0.002	0.90076	0.00054	0.90184	-0.00123
		+0.002	-0.002	0.90662	0.0007	0.90802	0.00495
			nominal	0.90484	0.0005	0.90584	0.00277
			+0.002	0.90206	0.00072	0.90350	0.00043
Pellet Diameter Tolerance		**Pellet OD Tolerance (in.)**		k_{eff}	σ	$k_{eff} + 2\sigma$	$\Delta(k_{eff} + 2\sigma)$
17 Bin 1 (1 & 2)	XL	-0.0007		0.90314	0.00038	0.90390	0.00083
		-0.0005		0.90278	0.00040	0.90358	0.00051
		+0.0005		0.90235	0.00040	0.90315	0.00008
		+0.0007		0.90321	0.00036	0.90393	0.00086
Pitch Tolerance		**Pitch Tolerance (in.)**		k_{eff}	σ	$k_{eff} + 2\sigma$	$\Delta(k_{eff} + 2\sigma)$
17 Bin 1 (1 & 2)	XL	-0.0785		0.89208	0.00048	0.89304	-0.01003
		-0.0393		0.89594	0.00049	0.89692	-0.00615
		+0.0059		0.90504	0.00057	0.90618	0.00311
		+0.0118		0.9066	0.00052	0.90764	0.00457
17 Bin 1 (4)	XL	-0.001		0.90358	0.00025	0.90408	-0.00127
		+0.001		0.90563	0.00026	0.90615	0.00080

The ADOPT Fuel sensitivity study, as defined in Section 6.3.4.3.13, examined the effect of replacing standard UO_2 fuel with ADOPT fuel. Table 6-38A lists the results of the study. The most reactive case is highlighted.

Table 6-38A ADOPT Fuel Results – Single Package, HAC, PWR Fuel Assembly Groups

Contents (Group)	Traveller Variant	Fuel Material	k_{eff}	σ	$k_{eff} + 2\sigma$	$\Delta(k_{eff} + 2\sigma)$
17 Bin 1 (1 & 2)	XL	**Baseline (UO_2)**	0.90209	0.00049	0.90307	--
		ADOPT	0.90310	0.00059	0.90428	0.00121
17 Bin 1 (4)	XL	**Baseline (UO_2)**	0.90483	0.00026	0.90535	--
		ADOPT	0.90444	0.00026	0.90496	-0.00039

6.4.2.2.4 Rod Pipe

Table 6-39 shows the summary of the penalty assessed for the sensitivity studies evaluated for the Rod Pipe contents. An entry of "0.0" signifies that the study resulted in no positive penalty on reactivity and an entry of "--" signifies that the study did not require analyzing based on transport condition.

Table 6-39 Single Package Assessed Penalties, Δk_u, Rod Pipe

Sensitivity Study	Penalty Assessed			
	Rod Pipe UO_2 Fuel Rods		Rod Pipe U_3Si_2 Fuel Rods	
	NCT	HAC	NCT	HAC
Annular Blanket Length	0.04278	0.00427	0.02104	0.0
Rod Pipe Position in Clamshell	0.0	0.0	0.0	0.0
Moderator Block Density Reduction	--	0.0	--	0.0
Polyethylene Packing Materials	0.02694	0.06950	0.27573	0.06371
Fuel Pellet Tolerance	0.0	0.0	0.00180	0.0
ADOPT Fuel	0.0	0.0	--	--
Total Penalty (Δk_u)	0.06972	0.07377	0.29857	0.06371

6.4.2.2.4.1 Single Package, Rod Pipe, NCT Sensitivity Studies

The annular blanket sensitivity study, as defined in Section 6.3.4.3.1, examined the addition of varying annular fuel pellet ID and lengths of annular fuel pellet blanket lengths equally to the top and bottom of a fuel rod. Table 6-40 shows the parameters evaluated and the results, and Figure 6-34 and Figure 6-35 display the result trends. The most reactive case is highlighted for each package variant.

Table 6-40 Annular Blanket Sensitivity Results – Single Package, NCT, Rod Pipe

Contents	Traveller Variant	Annulus Diameter	Annulus Length (cm)	k_{eff}	σ	$k_{eff} + 2\sigma$	$\Delta(k_{eff} + 2\sigma)$
Rod Pipe UO_2 Fuel Rods	XL	**Baseline Case**		0.56435	0.00086	0.56607	--
		0.155 in. (0.3937 cm)	13	0.56459	0.00037	0.56533	-0.00074
			26	0.56514	0.00039	0.56592	-0.00015
			39	0.5652	0.00047	0.56614	0.00007
			78	0.56576	0.0004	0.56656	0.00049
			250.825	0.56688	0.00051	0.56790	0.00183
		0.183 in. (0.4648 cm)	13	0.56569	0.00041	0.56651	0.00044
			26	0.56492	0.00044	0.5658	-0.00027
			39	0.56532	0.00038	0.56608	0.00001
			78	0.56567	0.00039	0.56645	0.00038
			250.825	0.56645	0.00036	0.56717	0.00110
		1.213 in. (3.0810 cm)	13	0.56525	0.00046	0.56617	0.00010
			26	0.56758	0.00039	0.56836	0.00229
			39	0.5776	0.0005	0.5786	0.01253
			78	0.59614	0.0005	0.59714	0.03107
			250.825	0.60801	0.00042	0.60885	0.04278

Table 6-40 Annular Blanket Sensitivity Results – Single Package, NCT, Rod Pipe

Contents	Traveller Variant	Annulus Diameter	Annulus Length (cm)	k_{eff}	σ	$k_{eff} + 2\sigma$	$\Delta(k_{eff} + 2\sigma)$
Rod Pipe U_3Si_2 Fuel Rods	STD	Baseline Case		0.42948	0.00037	0.43022	--
		0.155 in. (0.3937 cm)	13	0.42961	0.00043	0.43047	0.00025
			26	0.43025	0.00040	0.43105	0.00083
			39	0.43036	0.00045	0.43126	0.00104
			78	0.43733	0.00037	0.43807	0.00785
			213.995	0.44356	0.00041	0.44438	0.01416
		0.183 in. (0.4648 cm)	13	0.4298	0.00036	0.43052	0.00030
			26	0.43079	0.00039	0.43157	0.00135
			39	0.43225	0.00052	0.43329	0.00307
			78	0.44193	0.00039	0.44271	0.01249
			213.995	0.45020	0.00053	0.45126	0.02104

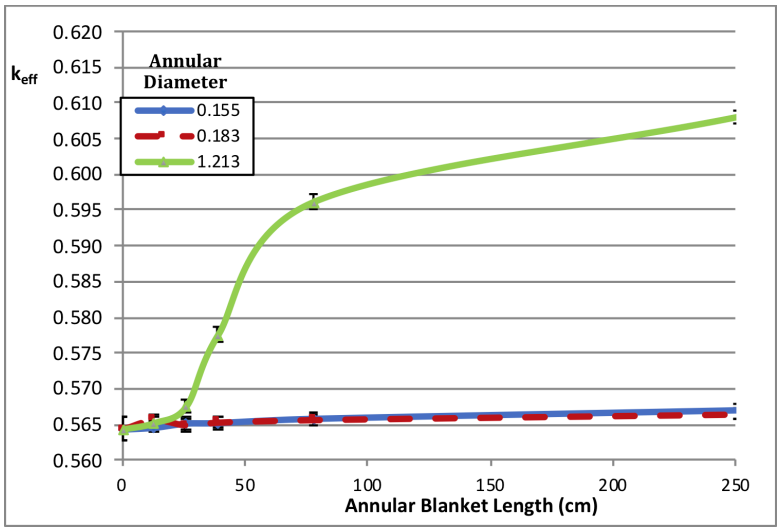

Figure 6-34 Annular Blanket Sensitivity – Single Package, NCT (Rod Pipe UO_2 Fuel Rods)

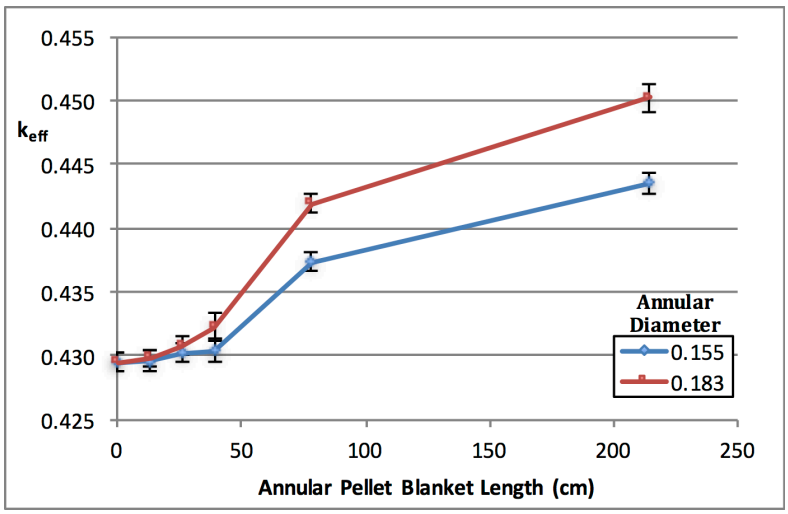

Figure 6-35 Annular Blanket Sensitivity – Single Package, NCT (Rod Pipe U_3Si_2 Fuel Rods)

The Rod Pipe position sensitivity study, as defined in Section 6.3.4.3.2, examined the shifting of the Rod Pipe in the Clamshell. Table 6-41 defines the parameter evaluated and the results. The most reactive case is highlighted for each package variant.

Table 6-41 Rod Pipe Position Sensitivity Results – Single Package, NCT, Rod Pipe

Contents	Traveller Variant	Rod Pipe Position	k_{eff}	σ	$k_{eff} + 2\sigma$	$\Delta(k_{eff} + 2\sigma)$
Rod Pipe UO_2 Fuel Rods	XL	**Baseline Case**	0.56435	0.00086	0.56607	--
		Down	0.53002	0.00069	0.53140	-0.03467
Rod Pipe U_3Si_2 Fuel Rods	STD	**Baseline Case**	0.42948	0.00037	0.43022	--
		Down	0.42161	0.00037	0.42235	-0.00787

The polyethylene packing materials sensitivity study, as defined in Section 6.3.4.3.5, examined the presence of an outer wrap around each fuel rod. Table 6-42 defines the parameter evaluated and the results and Figure 6-36 and Figure 6-37 display the result trends. The most reactive case is highlighted for each package variant. The peak k_{eff} due to polyethylene wrap addition encompasses the largest polyethylene addition modeled, however the highest value of $k_{eff} + 2\sigma$ is far below the USL of 0.94044. Therefore, based on single package NCT, no limitation of polyethylene packing materials is imposed on the Traveller packaging with Rod Pipe.

Table 6-42 Polyethylene Packing Sensitivity Results – Single Package, NCT, Rod Pipe

Contents	Traveller Variant	Poly Model	Poly Mass (kg)	k_{eff}	σ	$k_{eff} + 2\sigma$	$\Delta(k_{eff} + 2\sigma)$
Rod Pipe UO_2 Fuel Rods	XL	**Baseline Case**	0.0	0.56435	0.00086	0.56607	--
		Outer Wrap	1.67	0.57444	0.00045	0.57534	0.00927
			2.19	0.57812	0.00039	0.5789	0.01283
			4.28	0.59052	0.0004	0.59132	0.02525
			18.32	0.59219	0.00041	0.59301	0.02694
			30.89	0.5825	0.00049	0.58348	0.01741
Rod Pipe U_3Si_2 Fuel Rods	STD	**Baseline Case**	0.0	0.42948	0.00037	0.43022	--
		Outer Wrap	1.85	0.44955	0.00037	0.45029	0.02007
			3.79	0.47114	0.00042	0.47198	0.04176
			7.96	0.51601	0.00045	0.51691	0.08669
			17.41	0.60257	0.00048	0.60353	0.17331
			36.30	0.70497	0.00049	0.70595	0.27573

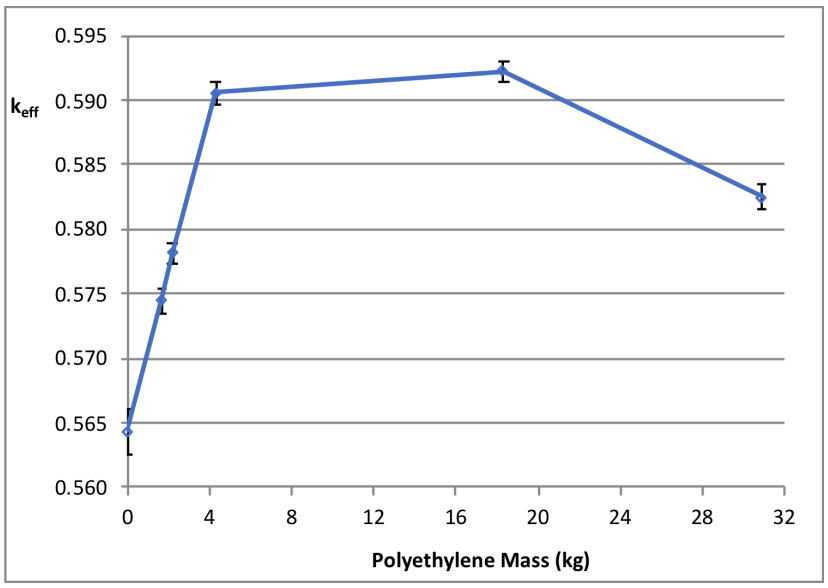

Figure 6-36 Polyethylene Packing Sensitivity – Single Package, NCT (Rod Pipe UO_2 Fuel Rods)

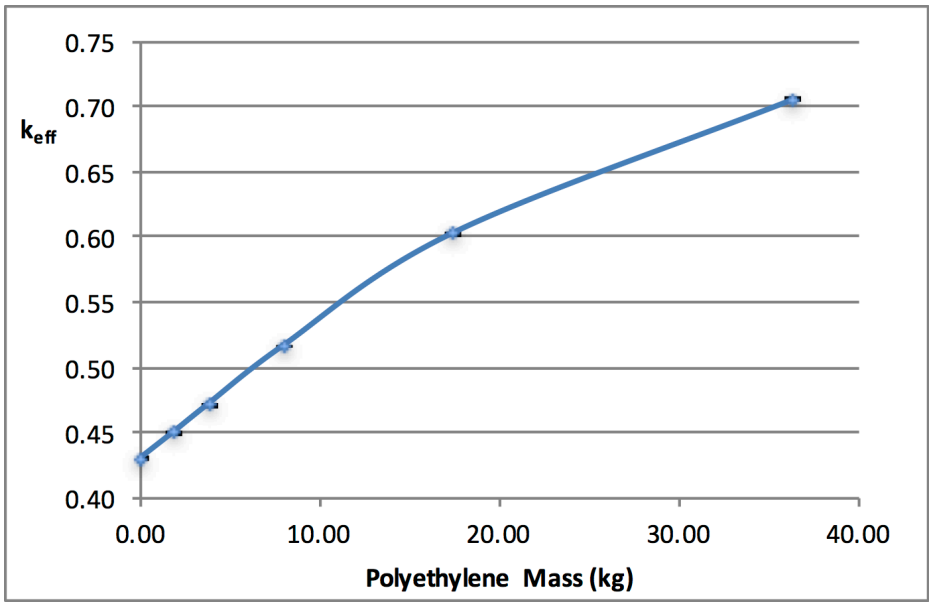

Figure 6-37 Polyethylene Packing Sensitivity – Single Package, NCT (Rod Pipe U_3Si_2 Fuel Rods)

The tolerance sensitivity study evaluates fuel pellet diameter only, as defined in Section 6.3.4.3.9. The Rod Pipe contents are not defined by cladding and pitch parameters, thus there is no tolerance evaluation as explained in Section 6.3.4.3.8 and 6.3.4.3.10, respectively. Table 6-43 defines the parameter dimensions evaluated and the results. The most reactive case is highlighted for each package variant and tolerance parameter.

Table 6-43 Tolerance Sensitivity Results – Single Package, NCT, Rod Pipe						
Contents	**Traveller Variant**	**Pellet OD Tolerance (in.)**	**k_{eff}**	**σ**	**$k_{eff} + 2\sigma$**	**$\Delta(k_{eff} + 2\sigma)$**
Rod Pipe UO_2 Fuel Rods	XL	-0.0014	0.56586	0.00038	0.56662	0.00055
		-0.0010	0.56534	0.00041	0.56616	0.00009
		Baseline Case	0.56435	0.00086	0.56607	--
		+0.0010	0.56500	0.00041	0.56582	-0.00025
		+0.0014	0.56506	0.00038	0.56582	-0.00025
Rod Pipe U_3Si_2 Fuel Rods	STD	-0.0014	0.42895	0.00037	0.42969	-0.00053
		-0.0010	0.42891	0.00034	0.42959	-0.00063
		Baseline Case	0.42948	0.00037	0.43022	--
		+0.0010	0.42995	0.00037	0.43069	0.00047
		+0.0014	0.43130	0.00036	0.43202	0.00180

The ADOPT Fuel sensitivity study, as defined in Section 6.3.4.3.13, examined the effect of replacing standard UO_2 fuel with ADOPT fuel. Table 6-43A lists the results of the study. The most reactive case is highlighted.

Table 6-43A ADOPT Fuel Results – Single Package, NCT, Rod Pipe						
Content	**Traveller Variant**	**Fuel**	**k_{eff}**	**σ**	**$k_{eff} + 2\sigma$**	**$\Delta(k_{eff} + 2\sigma)$**
Rod Pipe UO_2 Fuel Rods	XL	**Baseline (UO_2)**	0.56435	0.00086	0.56607	--
		ADOPT	0.56616	0.00079	0.56774	0.00137

6.4.2.2.4.2 Single Package, Rod Pipe, HAC Sensitivity Studies

The annular blanket sensitivity study, as defined in Section 6.3.4.3.1, examined the addition of varying annular fuel pellet ID and lengths of annular fuel pellet blanket lengths equally to the top and bottom of a fuel rod. Table 6-44 defines the parameters evaluated and the results, and Figure 6-38 and Figure 6-39 display the result trends. The most reactive case is highlighted for each package variant.

Table 6-44 Annular Blanket Sensitivity Results – Single Package, HAC, Rod Pipe							
Contents	**Traveller Variant**	**Annulus Diameter**	**Annulus Length (cm)**	**k_{eff}**	**σ**	**$k_{eff} + 2\sigma$**	**$\Delta(k_{eff} + 2\sigma)$**
Rod Pipe UO_2 Fuel Rods	XL	**Baseline Case**		0.72106	0.00047	0.72200	--
		0.155 in. (0.3937 cm)	13.0	0.71982	0.00053	0.72088	-0.00112
			26.0	0.71937	0.00051	0.72039	-0.00161
			39.0	0.72075	0.00045	0.72165	-0.00035
			78.0	0.72039	0.00055	0.72149	-0.00051
			250.825	0.72362	0.00048	0.72458	0.00258
		0.183 in. (0.4648 cm)	13.0	0.71964	0.00048	0.72060	-0.00140
			26.0	0.72117	0.00054	0.72225	0.00025
			39.0	0.72079	0.00051	0.72181	-0.00019
			78.0	0.72103	0.00049	0.72201	0.00001
			250.825	0.72515	0.00056	0.72627	0.00427

Table 6-44 Annular Blanket Sensitivity Results – Single Package, HAC, Rod Pipe

Contents	Traveller Variant	Annulus Diameter	Annulus Length (cm)	k_{eff}	σ	$k_{eff} + 2\sigma$	$\Delta(k_{eff} + 2\sigma)$
Rod Pipe U_3Si_2 Fuel Rods	STD	**Baseline Case**		0.67492	0.00049	0.67590	--
		0.155 in. (0.3937 cm)	13.0	0.67441	0.00053	0.67547	-0.00043
			26.0	0.67528	0.00049	0.67626	0.00036
			39.0	0.67498	0.0005	0.67598	0.00008
			78.0	0.67390	0.00051	0.67492	-0.00098
			213.995	0.66959	0.00043	0.67045	-0.00545
		0.183 in. (0.4648 cm)	13.0	0.67466	0.00049	0.67564	-0.00026
			26.0	0.67508	0.00046	0.67600	0.00010
			39.0	0.67542	0.00051	0.67644	0.00054
			78.0	0.67460	0.00055	0.67570	-0.00020
			213.995	0.66599	0.0005	0.66699	-0.00891

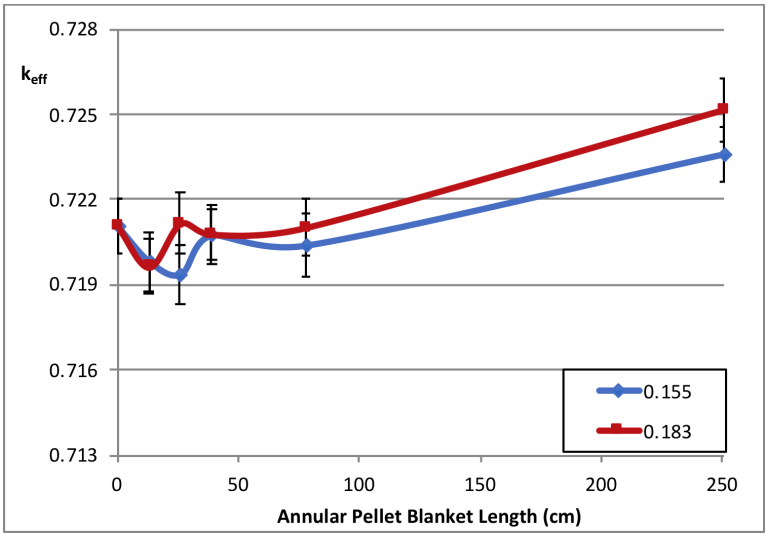

Figure 6-38 Annular Blanket Sensitivity Results – Single Package, HAC (Rod Pipe UO_2 Fuel Rods)

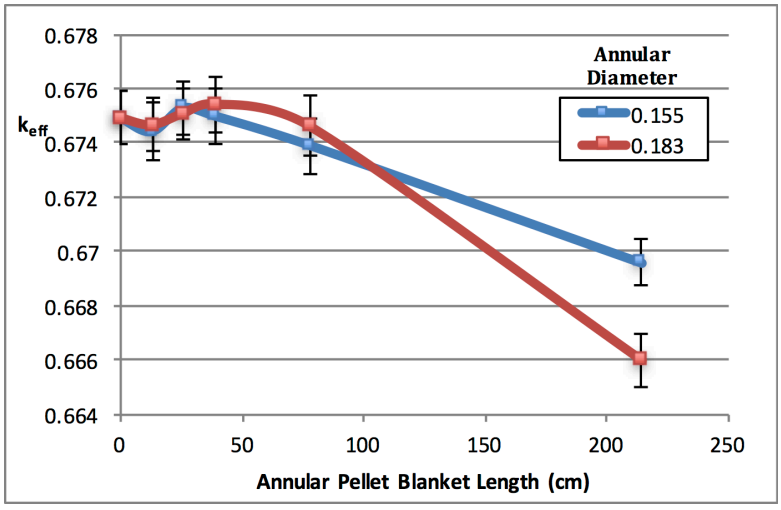

Figure 6-39 Annular Blanket Sensitivity Results – Single Package, HAC (Rod Pipe U_3Si_2 Fuel Rods)

The Rod Pipe position sensitivity study, as defined in Section 6.3.4.3.2, examined the shifting of the Rod Pipe in the Clamshell from the centerline, baseline position. Table 6-45 defines the parameter evaluated and the results. The most reactive case is highlighted for each package variant.

Table 6-45 Rod Pipe Position Sensitivity Results – Single Package, HAC, Rod Pipe

Contents	Traveller Variant	Fuel Assembly Position	k_{eff}	σ	$k_{eff} + 2\sigma$	$\Delta(k_{eff} + 2\sigma)$
Rod Pipe UO_2 Fuel Rods	XL	**Baseline Case**	0.72106	0.00047	0.72200	--
		Up	0.69442	0.00053	0.69548	-0.02652
		Down	0.69464	0.00057	0.69578	-0.02622
Rod Pipe U_3Si_2 Fuel Rods	STD	**Baseline Case**	0.67492	0.00049	0.67590	--
		Up	0.65502	0.00046	0.65594	-0.01996
		Down	0.65424	0.00045	0.65514	-0.02076

The moderator block density reduction sensitivity study, as defined in Section 6.3.4.3.3, examined the post-fire condition of the moderator block. Table 6-46 defines the parameter evaluated and the results. The most reactive case is highlighted for each package variant.

Table 6-46 Moderator Block Density Results – Single Package, HAC, Rod Pipe

Content	Traveller Variant	Moderator Block Density (g/cm^3)	k_{eff}	σ	$k_{eff} + 2\sigma$	$\Delta(k_{eff} + 2\sigma)$
Rod Pipe UO_2 Fuel Rods	XL	**Baseline Case**	0.72106	0.00047	0.72200	--
		0.9108	0.72012	0.00058	0.72128	-0.00072
Rod Pipe U_3Si_2 Fuel Rods	STD	**Baseline Case**	0.67492	0.00049	0.67590	--
		0.9108	0.67526	0.00047	0.67620	0.00030

The polyethylene packing materials sensitivity study, as defined in Section 6.3.4.3.5, examined a conservative representation of polyethylene packing materials through HAC. Table 6-47 defines the parameters evaluated and the results, and Figure 6-40 and Figure 6-41 display the result trends. The most reactive case is highlighted for each package variant. As the full height melt is limiting, therefore, no limit on polyethylene packing materials is imposed on the Traveller packaging with the loose Rod Pipe as a result of the single package polyethylene evaluation under HAC.

Table 6-47 Polyethylene Sensitivity Results – Single Package, HAC, Rod Pipe

Content	Traveller Variant	Poly Model	Poly Mass (kg)	k_{eff}	σ	$k_{eff} + 2\sigma$	$\Delta(k_{eff} + 2\sigma)$
Rod Pipe UO_2 Fuel Rods	XL	**Baseline Case**	0	0.72106	0.00047	0.72200	--
		Uniform Wrap	3.39	0.72304	0.00047	0.72398	0.00198
			4.50	0.72385	0.00046	0.72477	0.00277
			9.38	0.72977	0.00053	0.73083	0.00883
			20.33	0.74164	0.00056	0.74276	0.02076
			46.91	0.77311	0.00047	0.77405	0.05205
		Collected Melt	0.62	0.72065	0.00048	0.72161	-0.00039
			1.87	0.72025	0.0005	0.72125	-0.00075
			2.49	0.72307	0.00058	0.72423	0.00223
			3.12	0.73063	0.00052	0.73167	0.00967
			4.36	0.74779	0.0005	0.74879	0.02679
			6.24	0.76478	0.00059	0.76596	0.04396
			9.35	0.77659	0.00052	0.77763	0.05563
			12.47	0.78369	0.00058	0.78485	0.06285
			62.56	0.79048	0.00051	0.79150	0.06950
Rod Pipe U_3Si_2 Fuel Rods	STD	**Baseline Case**	0	0.67492	0.00049	0.67590	--
		Uniform Wrap	2.51	0.67631	0.00052	0.67735	0.00145
			3.33	0.67744	0.00048	0.67840	0.00250
			7.00	0.68013	0.00045	0.68103	0.00513
			15.30	0.68898	0.00044	0.68986	0.01396
			32.42	0.70946	0.00045	0.71036	0.03446
			51.32	0.73184	0.00049	0.73282	0.05692
		Collected Melt	0.68	0.67501	0.00045	0.67591	0.00001
			2.04	0.67508	0.00049	0.67606	0.00016
			2.72	0.67696	0.00047	0.67790	0.00200
			3.40	0.68373	0.00048	0.68469	0.00879
			4.76	0.69969	0.00049	0.70067	0.02477
			6.80	0.71436	0.00049	0.71534	0.03944
			10.19	0.72531	0.00051	0.72633	0.05043
			13.59	0.73053	0.00046	0.73145	0.05555
			58.17	0.73847	0.00057	0.73961	0.06371

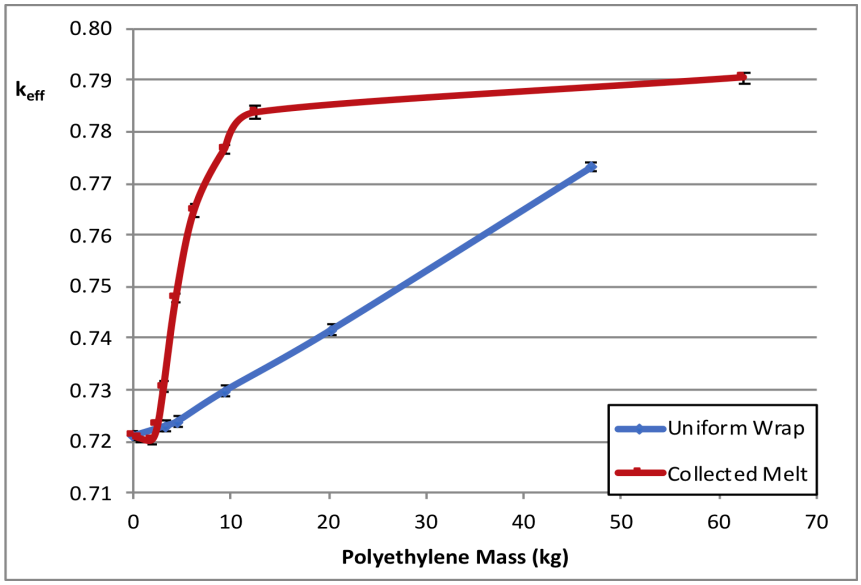

Figure 6-40 Polyethylene Sensitivity Results – Single Package, HAC (Rod Pipe UO_2 Fuel Rods)

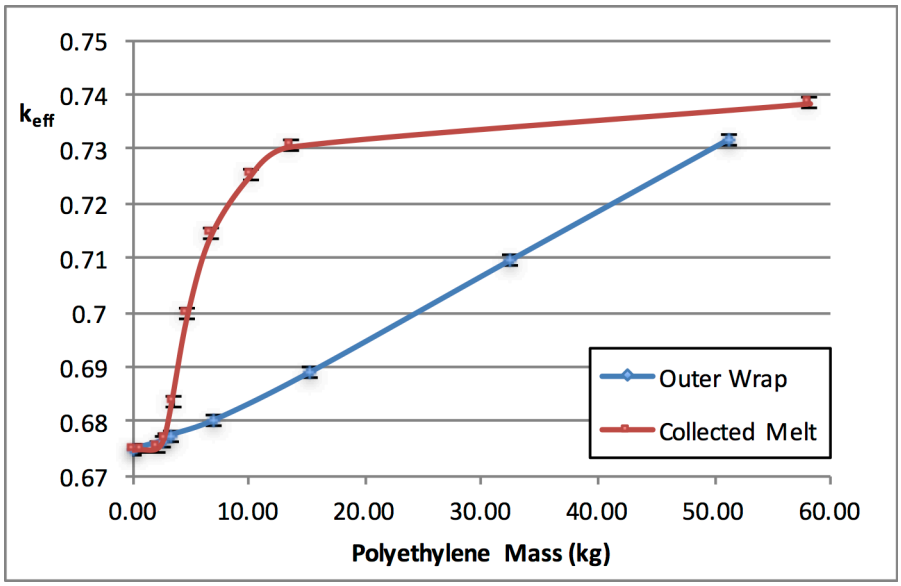

Figure 6-41 Polyethylene Sensitivity Results – Single Package, HAC (Rod Pipe U_3Si_2 Fuel Rods)

The tolerance sensitivity study evaluates fuel pellet diameter only, as defined in Section 6.3.4.3.9. The Rod Pipe contents are not defined by cladding and pitch parameters, thus there is no tolerance evaluation as explained in Section 6.3.4.3.8 and 6.3.4.3.10, respectively. Table 6-48 defines the parameter dimensions evaluated and the results. The most reactive case is highlighted.

Table 6-48 Tolerance Sensitivity Results – Single Package, HAC, Rod Pipe

Content	Traveller Variant	Pellet OD Tolerance (in.)	k_{eff}	σ	$k_{eff} + 2\sigma$	$\Delta(k_{eff} + 2\sigma)$
Rod Pipe UO_2 Fuel Rods	XL	-0.0014	0.72049	0.00047	0.72143	-0.00057
		-0.0010	0.72083	0.00049	0.72181	-0.00019
		Baseline Case	0.72106	0.00047	0.72200	--
		+0.0010	0.72009	0.00044	0.72097	-0.00103
		+0.0014	0.72012	0.00050	0.72112	-0.00088
Rod Pipe U_3Si_2 Fuel Rods	STD	-0.0014	0.67439	0.00059	0.67557	-0.00033
		-0.0010	0.67513	0.00049	0.67611	0.00021
		Baseline Case	0.67492	0.00049	0.67590	--
		+0.0010	0.67487	0.00050	0.67587	-0.00003
		+0.0014	0.67481	0.00051	0.67583	-0.00007

The ADOPT Fuel sensitivity study, as defined in Section 6.3.4.3.13, examined the effect of replacing standard UO_2 fuel with ADOPT fuel. Table 6-48A lists the results of the study. The most reactive case is highlighted.

Table 6-48A ADOPT Fuel Results – Single Package, HAC, Rod Pipe

Content	Traveller Variant	Fuel	k_{eff}	σ	$k_{eff} + 2\sigma$	$\Delta(k_{eff} + 2\sigma)$
Rod Pipe UO_2 Fuel Rods	XL	**Baseline (UO_2)**	0.72106	0.00047	0.72200	--
		ADOPT	0.71964	0.00053	0.72070	-0.00130

6.5 EVALUATION OF PACKAGE ARRAYS UNDER NORMAL CONDITIONS OF TRANSPORT

6.5.1 Configuration

For the evaluation of package arrays under NCT, all inner spaces of the package are modeled as void, including the fuel-clad gap. Additional material modeling is specified in Section 6.3.2. Several materials, including fuel assembly structural components and packaging components (e.g. Outerpack foam regions, ceramic fiber blankets, and shock mounts, etc.), are replaced with void. The package array is reflected with 20 cm of full-density water.

6.5.1.1 Baseline Configurations

As described in Section 6.3.4.2, a baseline case is evaluated for both content Groups and Rod Pipe configurations under NCT. Baseline configurations represent a bounding model that is carried forward to the sensitivity studies to demonstrate maximum reactivity.

6.5.1.1.1 PWR Fuel Assembly Groups

For the baseline case determination, as defined in Section 6.3.4.2.1, first the bounding CFA-package variant combination is determined. For both Groups 1 and 2, the Traveller XL is consistently more reactive than the Traveller STD for an array under NCT. This conclusion is applied to Group 4. As discussed in Section 6.3.4.2.1.2, the axial positioning of the fuel assembly is examined due to the physical geometry of the packaging. Detailed results of the baseline case determination are shown in Section 6.9.3.3.2. The NCT baseline configurations are summarized in Table 6-49. The array configurations are shown in Figure 6-42, Figure 6-43, and Figure 6-43A.

Table 6-49 Summary of NCT Package Array Baseline Configuration

Traveller Variant	Contents (Group)	Array Size (5N)	Array Height	Axial Position (cm)	Flooding Configuration	$k_{eff} \pm \sigma$
XL	17 Bin 2 (1)	250	2	Top: 2.54 Bottom: 119.27	None	0.30888 ± 0.00027
XL	16 Bin 1 (2)	60	1	119.27	None	0.30950 ± 0.00026
XL	15 Bin 3 (4)	100	1	143.51	None	0.30731 ± 0.00020

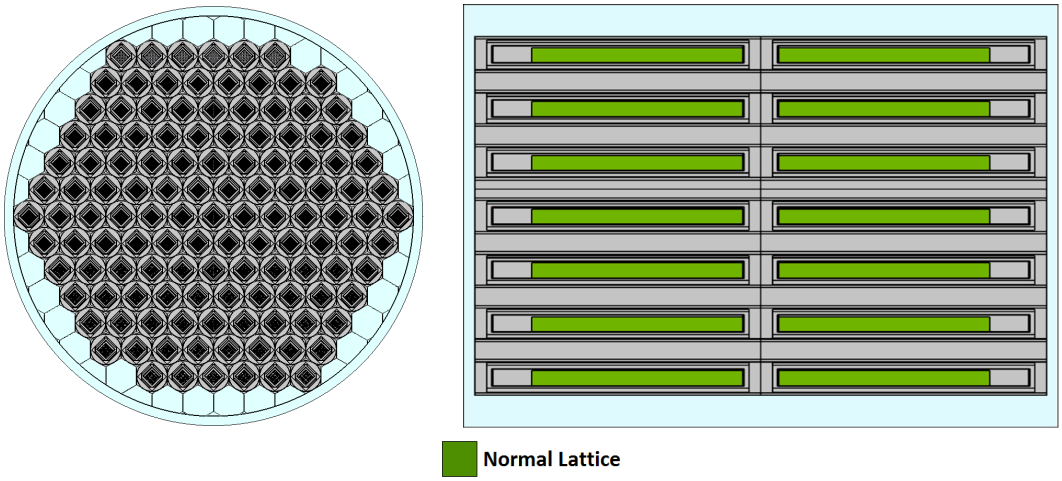

Figure 6-42 Group 1 NCT 250-package Array with Height of Two Packages

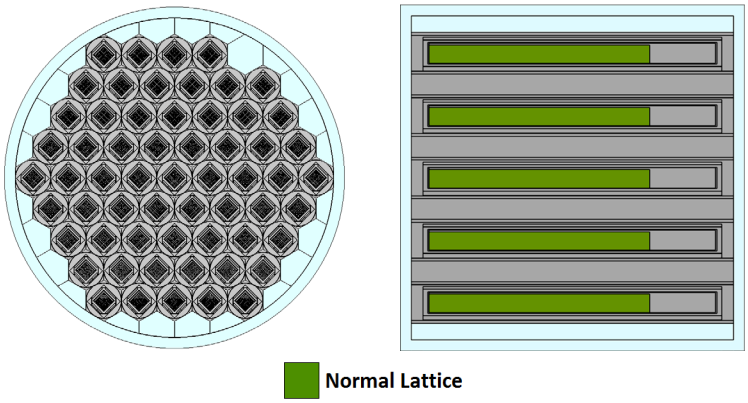

Figure 6-43 Group 2 NCT 60-package Array with Height of One Package

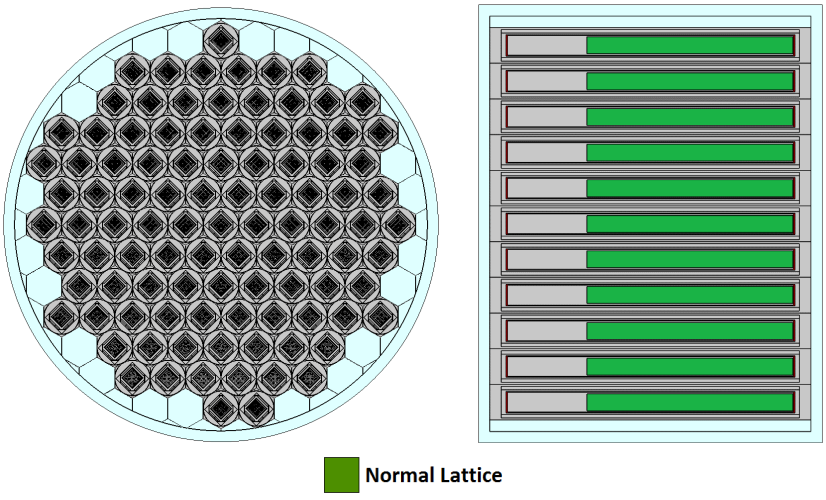

Figure 6-43A Group 4 NCT 100-package Array with Height of One Package

6.5.1.1.2 Rod Pipe

For the Rod Pipe, NCT package array baseline case determination, as defined in Section 6.3.4.2.2, loose rods are modeled in the Rod Pipe with a close-packed pitch equivalent to the fuel pellet OD. The pitch type is modeled as both square and hexagonal as the small variation of geometry varies the water-to-fuel ratio slightly. The Rod Pipe is flooded with full-density water with all remaining floodable regions void. Detailed results of the Rod Pipe NCT package array baseline case determination are shown in Section 6.9.3.4. For UO_2 fuel rods, comparison of the Traveller STD to Traveller XL baseline results show that, for the limiting fuel rod/pitch combination, the Traveller XL is consistently more reactive than the Traveller STD. The NCT package array baseline configurations for the Rod Pipe with UO_2 fuel rods and U_3Si_2 fuel rods is summarized in Table 6-50 and shown in Figure 6-44.

Table 6-50 Summary of Rod Pipe NCT Package Array Configurations

Contents	Traveller Variant	Array Size (5N)	Array Height	Fuel OR (cm)	Pitch-Type	Fuel Half-Pitch (cm)	Flooding Configuration	$k_{eff} \pm \sigma$
UO_2 Fuel Rods	XL	379	1	3.5	Square	3.5	Inside Rod Pipe	0.46657 ± 0.00067
U_3Si_2 Fuel Rods	STD	379	1	0.4851	Square	0.4851	Inside Rod Pipe	0.41633 ± 0.00035

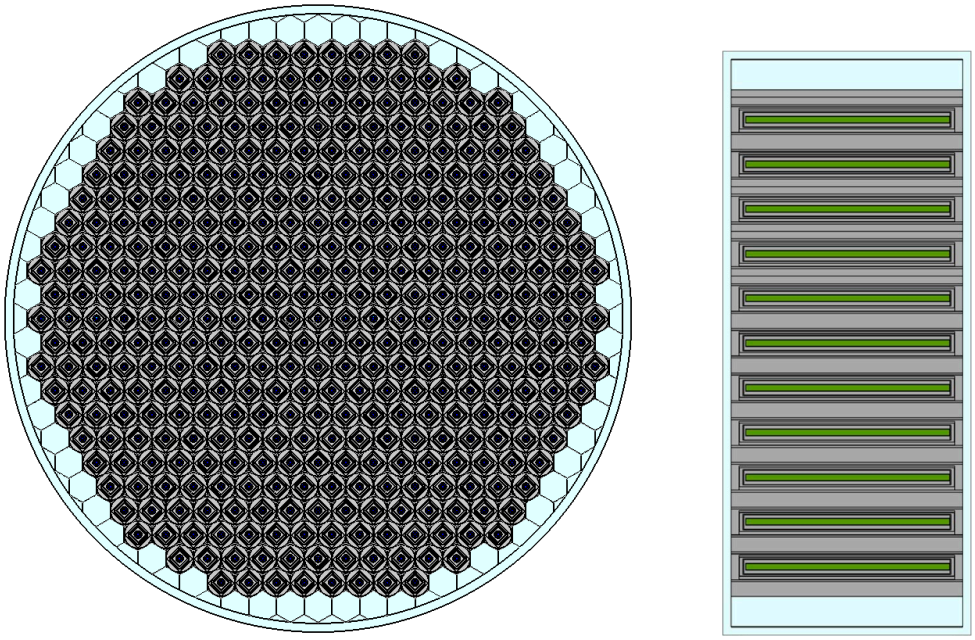

Figure 6-44 Rod Pipe NCT 379-package Array with Height of One Package

6.5.1.2 Sensitivity Study Configurations

Several sensitivity studies are completed for the NCT package array evaluation. The following summary tables list the bounding, as-penalized configurations of each sensitivity study. An entry of "None" signifies that the study resulted in no penalty and an entry of "--" signifies that the study did not require analyzing based on transport condition. The baseline case with the sum of penalties from sensitivity studies defines the most reactive configuration for demonstration of maximum reactivity.

6.5.1.2.1 PWR Fuel Assembly Groups

Listed in Table 6-51 are the bounding, as-penalized configurations of each sensitivity study for Groups 1, 2, and 4.

Table 6-51 NCT Package Array Sensitivity Study Bounding Configurations – PWR Fuel Assembly Groups

Sensitivity Study	Group 1	Group 2	Group 4
Annular Fuel Pellet Blanket	None	None	None
Clamshell/Fuel Assembly Shift	None	None	Up
Package OD Tolerance	None	None	None
Polyethylene Packing Materials	None	None	None
SS Rods	None	None	None
Cladding Tolerance	None	Minimum cladding thickness	--
Fuel Pellet Diameter Tolerance	None	None	--
Fuel Rod Pitch Tolerance	+ Tolerance	+ Tolerance	None
Steel Reflector	None	None	None
ADOPT Fuel	None	None	None

Note: 'None' signifies that the sensitivity study did not result in a statistically significant increase in reactivity over the baseline case.

6.5.1.2.2 Rod Pipe

Listed in Table 6-52 are the bounding, as-penalized configurations of each sensitivity study for Rod Pipe content.

Table 6-52 NCT Package Array Sensitivity Study Bounding Configurations – Rod Pipe

Sensitivity Study	Bounding Configuration UO_2 Fuel Rods	Bounding Configuration U_3Si_2 Fuel Rods
Annular Fuel Pellet Blanket	Full-length with proportional ID	Full-length
Rod Pipe Position in Clamshell	Down	None
Package OD Tolerance	None	None
Fuel Pellet Diameter Tolerance	+ Tolerance	None
Polyethylene Packing Materials	1.0 cm-thick polyethylene wrap	0.3654 cm-thick polyethylene wrap
ADOPT Fuel	ADOPT rods	--

Note: 'None' signifies that the sensitivity study did not result in a statistically significant increase in reactivity over the baseline case.

6.5.2 Results

6.5.2.1 NCT Package Array – Maximum Reactivity Results Summary

The maximum reactivity, *Maximum* k_{eff}, is defined by the bounding baseline $k_p + 2\sigma_p$ plus the sum of penalties assessed for each sensitivity study (Δk_u). See Table 6-53 for a summary of the *Maximum* k_{eff} results. All final values of maximum reactivity fall under the USL, as calculated per Section 6.8.

Table 6-53 NCT Package Array – Maximum Reactivity Results Summary

Traveller Variant	Bounding Content	$k_{eff} \pm \sigma$	$k_p + 2\sigma_p$	Δk_u	*Maximum* k_{eff}	USL
XL	17 Bin 2 (Group 1)	0.30888 ± 0.00027	0.30942	0.0	0.30942	0.94162
XL	16 Bin 1 (Group 2)	0.30950 ± 0.00026	0.31002	0.00377	0.31379	0.94090
XL	15 Bin 3 (Group 4)	0.30731 ± 0.00020	0.30771	0.00838	0.31609	0.94082
XL	Rod Pipe UO_2 Fuel Rods	0.46675 ± 0.00067	0.46809	0.12669	0.59478	0.94044
STD	Rod Pipe U_3Si_2 Fuel Rods	0.41633 ± 0.00035	0.41703	0.27868	0.69571	0.94053

6.5.2.2 Sensitivity Study Results

As discussed in Section 6.3.4.3, the NCT package array baseline cases, for each package variant, are subjected to several sensitivity studies. Each sensitivity study is compared to the baseline case. The most reactive configuration resulting in the largest positive difference in $k_{eff} + 2\sigma$ from the baseline case ($k_{eff} + 2\sigma$) value that is also greater than or equal to two times the baseline σ is tallied and summed to define the total penalty assessed (Δk_u).

6.5.2.2.1 PWR Fuel Assembly Groups Results Summary

Table 6-54 shows the summary of the penalty assessed for the sensitivity studies evaluated for all Group contents. An entry of "0.0" signifies that the study resulted in no positive penalty on reactivity.

Table 6-54 NCT Package Array Assessed Penalties, Δk_u

Sensitivity Study	Group 1	Group 2	Group 4
Annular Fuel Pellet Blanket	0.0	0.0	0.0
Fuel Assembly Shift	0.0	0.0	0.00838
Package OD Tolerance	0.0	0.0	0.0
Polyethylene Packing Materials	0.0	0.0	0.0
SS Rods	0.0	0.0	0.0
Cladding Tolerance	0.0	0.00084	--
Fuel Pellet Diameter Tolerance	0.0	0.0	--
Fuel Rod Pitch Tolerance	0.00053	0.00293	0.0
Steel Reflector	0.0	0.0	0.0
ADOPT Fuel	0.0	0.0	0.0
Total Penalty (Δk_u)	**0.00053**	**0.00377**	**0.00838**

6.5.2.2.2 PWR Fuel Assembly Groups Detailed Results

The annular blanket sensitivity study, as defined in Section 6.3.4.3.1, examined the addition of annular fuel pellet blankets and varying the annular inner ID and blanket length. Annular fuel pellet blankets are added symmetrically to the top and bottom of an assembly. Table 6-55 defines the parameters evaluated and the results. Figure 6-45, Figure 6-46, and Figure 6-46A display the result trends for Groups 1, 2 and 4, respectively. The most reactive case is highlighted for each Group.

Table 6-55 Annular Blanket Sensitivity Results – Package Array, NCT, PWR Fuel Assembly Groups

Contents (Group)	Traveller Variant	Annulus Diameter	Annulus Length (cm)	k_{eff}	σ	$k_{eff} + 2\sigma$	$\Delta(k_{eff} + 2\sigma)$
17 Bin 2 (1)	XL	**Baseline Case**		0.30888	0.00027	0.30942	--
		0.155 in. (0.3937 cm)	45.9	0.30217	0.00029	0.30275	-0.0067
			91.8	0.29643	0.00026	0.29695	-0.0125
			137.6	0.28650	0.00025	0.28700	-0.0224
			183.5	0.27587	0.00025	0.27637	-0.0331
		0.183 in. (0.4648 cm)	45.9	0.30054	0.00026	0.30106	-0.0084
			91.8	0.29203	0.00023	0.29249	-0.0169
			137.6	0.27831	0.00028	0.27887	-0.0306
			183.5	0.25951	0.00026	0.26003	-0.0494
16 Bin 1 (2)	XL	**Baseline Case**		0.30950	0.00026	0.31002	--
		0.155 in. (0.3937 cm)	48.9	0.30691	0.00027	0.30745	-0.0026
			97.8	0.30246	0.00026	0.30298	-0.0070
			146.7	0.29423	0.00024	0.29471	-0.0153
			195.6	0.28265	0.00024	0.28313	-0.0269
		0.183 in. (0.4648 cm)	48.9	0.30619	0.00025	0.30669	-0.0033
			97.8	0.29968	0.00023	0.30014	-0.0099
			146.7	0.28801	0.00026	0.28853	-0.0215
			195.6	0.27082	0.00025	0.27132	-0.0387
15 Bin 3 (4)	XL	**Baseline Case**		0.30731	0.00020	0.30771	--
		0.155 in. (0.3937 cm)	13.0	0.30667	0.00022	0.30711	-0.00060
			26.0	0.30553	0.00020	0.30593	-0.00178
			39.0	0.30497	0.00021	0.30539	-0.00232
			50.8	0.30387	0.00029	0.30445	-0.00326
		0.183 in. (0.4648 cm)	13.0	0.30657	0.00024	0.30705	-0.00066
			26.0	0.30500	0.00021	0.30542	-0.00229
			39.0	0.30440	0.00025	0.30490	-0.00281
			50.8	0.30324	0.00022	0.30368	-0.00403

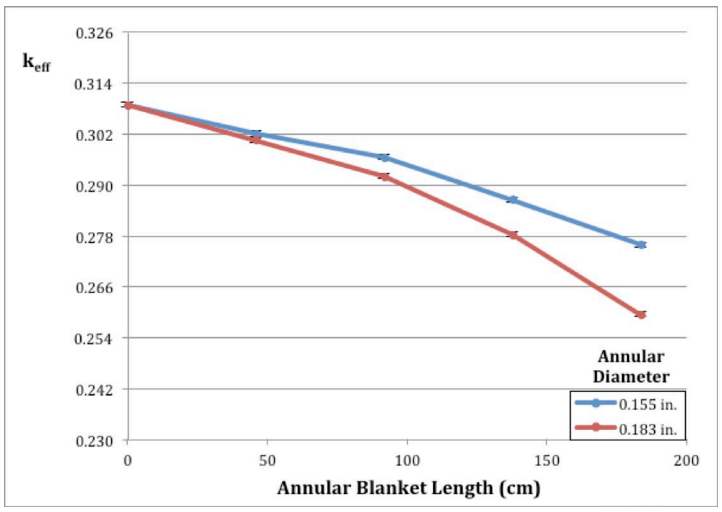

Figure 6-45 Annular Blanket Sensitivity – Package Array, NCT (Group 1)

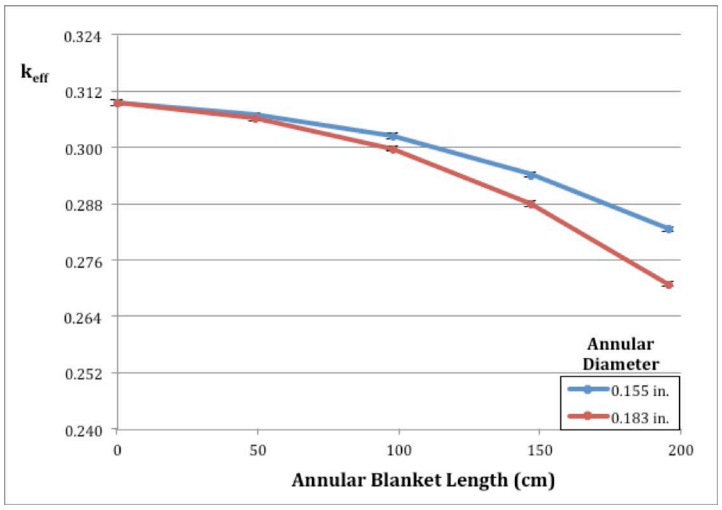

Figure 6-46 Annular Blanket Sensitivity – Package Array, NCT (Group 2)

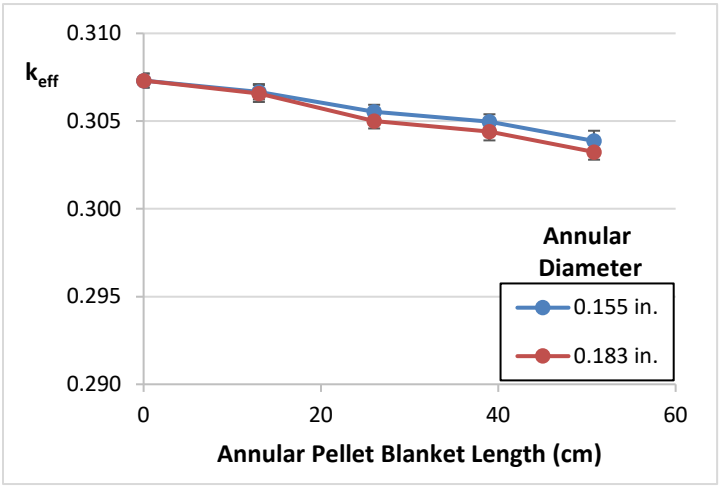

Figure 6-46A Annular Blanket Sensitivity – Package Array, NCT (Group 4)

The fuel assembly position sensitivity study, as defined in Section 6.3.4.3.2, examined the shifting of the fuel assembly in the Clamshell. Table 6-56 defines the parameter evaluated and the results. The most reactive case is highlighted for each Group.

Table 6-56 Fuel Assembly Position Sensitivity Results – Package Array, NCT, PWR Fuel Assembly Groups

Contents (Group)	Traveller Variant	Fuel Assembly Position	k_{eff}	σ	$k_{eff} + 2\sigma$	$\Delta(k_{eff} + 2\sigma)$
17 Bin 2 (1)	XL	**Baseline Case**	0.30888	0.00027	0.30942	--
		Centered	0.30321	0.00023	0.30367	-0.00575
16 Bin 1 (2)	XL	**Baseline Case**	0.30950	0.00026	0.31002	--
		Centered	0.30755	0.00025	0.30805	-0.00197
15 Bin 3 (4)	XL	Down	0.31383	0.00022	0.31427	0.00656
		Baseline Case	0.30731	0.00020	0.30771	--
		Up	0.31567	0.00021	0.31609	0.00838

The package outer diameter tolerance directly affects the spacing of the packages, thus the tolerance is evaluated, as defined in Section 6.3.4.3.4. Table 6-57 defines the parameter evaluated and the results. The most reactive case is highlighted for each Group, and there is no statistically significant (i.e. greater than 2σ) effect in adjusting the outer diameter of the packages in an NCT array.

Table 6-57 Package OD Tolerance Results – Package Array, NCT, PWR Fuel Assembly Groups

Contents (Group)	Traveller Variant	Package Outer Diameter Tolerance (in.)	k_{eff}	σ	$k_{eff} + 2\sigma$	$\Delta(k_{eff} + 2\sigma)$
17 Bin 2 (1)	XL	-0.2	0.30884	0.00031	0.30946	0.00004
		Nominal	0.30888	0.00027	0.30942	--
		+0.2	0.30811	0.00025	0.30861	-0.00081
16 Bin 1 (2)	XL	-0.2	0.31000	0.00024	0.31048	0.00046
		Nominal	0.30950	0.00026	0.31002	--
		+0.2	0.30930	0.00025	0.30980	-0.00022
15 Bin 3 (4)	XL	-0.2	0.30727	0.00020	0.30767	-0.00004
		Nominal	0.30731	0.00020	0.30771	--
		+0.2	0.30701	0.00022	0.30745	-0.00026

The polyethylene packing materials sensitivity study, as defined in Section 6.3.4.3.5, examined the presence of an outer wrap around the fuel assembly for NCT configuration. Table 6-58 defines the parameter evaluated and the results. The most reactive case is highlighted for each Group.

Table 6-58 Polyethylene Packing Sensitivity Results – Package Array, NCT, PWR Fuel Assembly Groups							
Contents (Group)	**Traveller Variant**	**Poly Model**	**Poly Mass (kg)**	**k_{eff}**	**σ**	**$k_{eff} + 2\sigma$**	**$\Delta(k_{eff} + 2\sigma)$**
17 Bin 2 (1)	XL	**Baseline Case**	0.00	0.30888	0.00027	0.30942	--
		Outer Wrap	4.89	0.29270	0.00027	0.29324	-0.01618
16 Bin 1 (2)	XL	**Baseline Case**	0.00	0.30950	0.00026	0.31002	--
		Outer Wrap	5.90	0.29545	0.00024	0.29593	-0.01409
15 Bin 3 (4)	XL	**Baseline Case**	0.0	0.30731	0.00020	0.30771	--
		Outer Wrap	1.0	0.30119	0.00020	0.30159	-0.00612
			2.0	0.29768	0.00019	0.29806	-0.00965
			3.0	0.29516	0.00022	0.29560	-0.01211

The SS replacement rod sensitivity study, as defined in Section 6.3.4.3.7, examined the replacement of fuel rods with SS rods in the fuel assembly. Table 6-59 defines the parameters evaluated and the results. The most reactive case is highlighted for each Group.

Table 6-59 SS Rod Replacement Sensitivity Results – Package Array, NCT, PWR Fuel Assembly Groups						
Bounding Content	**Traveller Variant**	**SS Rod Configuration**	**k_{eff}**	**σ**	**$k_{eff} + 2\sigma$**	**$\Delta(k_{eff} + 2\sigma)$**
17 Bin 2 (1)	XL	**Baseline Case**	0.30888	0.00027	0.30942	--
		Corner	0.26461	0.00028	0.26517	-0.04425
		Random	0.27926	0.00023	0.27972	-0.0297
16 Bin 1 (2)	XL	**Baseline Case**	0.30950	0.00026	0.31002	--
		Corner	0.26204	0.00024	0.26252	-0.0475
		Random	0.27269	0.00023	0.27315	-0.03687
15 Bin 3 (4)	XL	**Baseline Case**	0.30731	0.00020	0.30771	--
		Corner	0.25869	0.00021	0.25911	-0.04860
		Random	0.26857	0.00021	0.26899	-0.03872

The tolerance sensitivity studies evaluate cladding dimensions, fuel pellet diameter, and fuel rod pitch, as defined in Section 6.3.4.3.8, 6.3.4.3.9, and 6.3.4.3.10, respectively. Table 6-60 defines the parameter dimensions evaluated and the results. The most reactive case is highlighted for each Group and tolerance parameter.

Table 6-60 Tolerance Sensitivity Results – Package Array, NCT, PWR Fuel Assembly Groups

Content (Group)	Traveller Variant	Tolerance Parameter (in.)		k_{eff}	σ	$k_{eff} + 2\sigma$	$\Delta(k_{eff} + 2\sigma)$
17 Bin 2 (1)	XL	**Baseline Case**		0.30888	0.00027	0.30942	--
16 Bin 1 (2)	XL	**Baseline Case**		0.30950	0.00026	0.31002	--
15 Bin 3 (4)	XL	**Baseline Case**		0.30731	0.00020	0.30771	--
Cladding Tolerance		**ID Tolerance (in.)**	**OD Tolerance (in.)**	k_{eff}	σ	$k_{eff} + 2\sigma$	$\Delta(k_{eff} + 2\sigma)$
17 Bin 2 (1)	XL	-0.002	-0.002	0.30850	0.00025	0.30900	-0.00042
			nominal	0.30849	0.00029	0.30907	-0.00035
			+0.002	0.30775	0.00026	0.30827	-0.00115
		nominal	-0.002	0.30909	0.00026	0.30961	0.00019
			nominal	0.30888	0.00027	0.30942	0.00000
			+0.002	0.30810	0.00028	0.30866	-0.00076
		+0.002	-0.002	0.30903	0.00024	0.30951	0.00009
			nominal	0.30878	0.00028	0.30934	-0.00008
			+0.002	0.30816	0.00025	0.30866	-0.00076
16 Bin 1 (2)	XL	-0.002	-0.002	0.30950	0.00024	0.30998	-0.00004
			nominal	0.30893	0.00029	0.30951	-0.00051
			+0.002	0.30919	0.00027	0.30973	-0.00029
		nominal	-0.002	0.31024	0.00025	0.31074	0.00072
			nominal	0.30950	0.00026	0.31002	0.00000
			+0.002	0.30953	0.00023	0.30999	-0.00003
		+0.002	-0.002	0.31036	0.00025	0.31086	0.00084
			nominal	0.31030	0.00027	0.31084	0.00082
			+0.002	0.30950	0.00025	0.31000	-0.00002
Pellet Diameter Tolerance		**Pellet OD Tolerance (in.)**		k_{eff}	σ	$k_{eff} + 2\sigma$	$\Delta(k_{eff} + 2\sigma)$
17 Bin 2 (1)	XL	-0.0007		0.30801	0.00029	0.30859	-0.00083
		-0.0005		0.30773	0.00026	0.30825	-0.00117
		+0.0005		0.30903	0.00024	0.30951	0.00009
		+0.0007		0.30918	0.00031	0.30980	0.00038
16 Bin 1 (2)	XL	-0.0007		0.30922	0.00025	0.30972	-0.00030
		-0.0005		0.30951	0.00027	0.31005	0.00003
		+0.0005		0.30963	0.00027	0.31017	0.00015
		+0.0007		0.30992	0.00024	0.31040	0.00038
Pitch Tolerance		**Pitch Tolerance (in.)**		k_{eff}	σ	$k_{eff} + 2\sigma$	$\Delta(k_{eff} + 2\sigma)$
17 Bin 2 (1)	XL	-0.005		0.30744	0.00025	0.30794	-0.00148
		-0.001		0.30833	0.00024	0.30881	-0.00061
		+0.001		0.30868	0.00026	0.30920	-0.00022
		+0.005		0.30947	0.00024	0.30995	0.00053
16 Bin 1 (2)	XL	-0.0335		0.30154	0.00026	0.30206	-0.00796
		-0.0167		0.30487	0.00035	0.30557	-0.00445
		+0.0059		0.31090	0.00024	0.31138	0.00136
		+0.0118		0.31241	0.00027	0.31295	0.00293
15 Bin 3 (4)	XL	-0.001		0.30697	0.00019	0.30735	-0.00036
		+0.001		0.30759	0.00021	0.30801	0.00030

The steel nozzle reflector sensitivity study, as defined in Section 6.3.4.3.11, examined the addition of two 50% density SS blocks at the top and bottom of the fuel assembly, simulating the top and bottom nozzles and their respective masses of steel. Table 6-61 defines the parameter evaluated and the results. The most reactive case is highlighted for each Group. As stated in Section 6.3.4.3.11, an adjusted baseline case is added for Group 4 to separate the effect of the steel nozzle shifting the axial position of the fuel assembly from adding the steel nozzle. The adjusted baseline case shows that the steel nozzle has little to no effect on k_{eff} and the decrease in k_{eff} is driven by the shifting of the fuel assembly axially to accommodate the steel nozzle.

Table 6-61 Steel Nozzle Reflector Sensitivity Results – Package Array, NCT, PWR Fuel Assembly Groups

Contents (Group)	Traveller Variant	Stainless Steel Nozzle Configuration	k_{eff}	σ	$k_{eff} + 2\sigma$	$\Delta(k_{eff} + 2\sigma)$
17 Bin 2 (1)	XL	**Baseline Case**	0.30888	0.00027	0.30942	--
		50% density SS304	0.29967	0.00038	0.30043	-0.00899
16 Bin 1 (2)	XL	**Baseline Case**	0.30950	0.00026	0.31002	--
		50% density SS304	0.30718	0.00026	0.30770	-0.00232
15 Bin 3 (4)	XL	**Baseline Case**	0.30731	0.00020	0.30771	--
		Adjusted Baseline Case	0.30391	0.00020	0.30431	-0.00340
		50% density SS304	0.30371	0.00018	0.30407	-0.00364 (Δ-0.00024)

The ADOPT fuel sensitivity study, as defined in Section 6.3.4.3.13, examined the effect of replacing standard UO_2 fuel with ADOPT fuel. Table 6-61A lists the results of the study. The most reactive case is highlighted.

Table 6-61A ADOPT Fuel Results – Package Array, NCT, PWR Fuel Assembly Groups

Contents (Group)	Traveller Variant	Fuel	k_{eff}	σ	$k_{eff} + 2\sigma$	$\Delta(k_{eff} + 2\sigma)$
17 Bin 2 (1)	XL	**Baseline (UO_2)**	0.30888	0.00027	0.30942	--
		ADOPT	0.30845	0.00027	0.30899	-0.00043
16 Bin 1 (2)	XL	**Baseline (UO_2)**	0.30950	0.00026	0.31002	--
		ADOPT	0.30939	0.00024	0.30987	-0.00015
15 Bin 3 (4)	XL	**Baseline (UO_2)**	0.30731	0.00020	0.30771	--
		ADOPT	0.30737	0.00028	0.30793	0.00022

6.5.2.2.3 Rod Pipe Results Summary

Table 6-62 shows the summary of the penalties assessed for the sensitivity studies analyzed for Rod Pipe NCT package array evaluation. An entry of "0.0" signifies that the study resulted in no positive penalty on reactivity.

Table 6-62 Rod Pipe NCT Package Array Assessed Penalties, Δk_u

Sensitivity Study	Penalty Assessed	
	Rod Pipe UO_2 Fuel Rods	**Rod Pipe U_3Si_2 Fuel Rods**
Annular Fuel Pellet Blanket	0.05967	0.02234
Rod Pipe Position in Clamshell	0.00263	0.0
Package OD Tolerance	0.0	0.0
Polyethylene Packing Materials	0.06112	0.25634
Fuel Pellet Diameter Tolerance	0.00181	0.0
ADOPT Fuel	0.00146	--
Total Penalty (Δk_u)	**0.12669**	**0.27868**

6.5.2.2.4 Rod Pipe Detailed Results

The annular blanket sensitivity study, as defined in Section 6.3.4.3.1, examined the addition of varying annular fuel pellet ID and lengths of annular fuel pellet blanket lengths equally to the top and bottom of a fuel rod. Table 6-63 defines the parameters evaluated and the results, and Figure 6-47 and Figure 6-48 display the result trends. The most reactive case is highlighted for each package variant.

Table 6-63 Annular Blanket Sensitivity Results – Package Array, NCT, Rod Pipe

Contents	Traveller Variant	Annulus Diameter	Annulus Length (cm)	k_{eff}	σ	$k_{eff} + 2\sigma$	$\Delta(k_{eff} + 2\sigma)$
Rod Pipe UO_2 Fuel Rods	XL	**Baseline Case**		0.46675	0.00067	0.46809	--
		0.155 in. (0.3937 cm)	13	0.46788	0.00037	0.46862	0.00053
			26	0.46815	0.00036	0.46887	0.00078
			39	0.4684	0.00036	0.46912	0.00103
			78	0.46799	0.00036	0.46871	0.00062
			250.825	0.46954	0.00037	0.47028	0.00219
		0.183 in. (0.4648 cm)	13	0.46853	0.00043	0.46939	0.0013
			26	0.46872	0.00041	0.46954	0.00145
			39	0.46814	0.00039	0.46892	0.00083
			78	0.4683	0.00035	0.469	0.00091
			250.825	0.46947	0.00039	0.47025	0.00216
		1.213 in. (3.0810 cm)	13	0.46853	0.0004	0.46933	0.00124
			26	0.47043	0.00045	0.47133	0.00324
			39	0.4727	0.00041	0.47352	0.00543
			78	0.48777	0.00039	0.48855	0.02046
			250.825	0.52692	0.00042	0.52776	0.05967
Rod Pipe U_3Si_2 Fuel Rods	STD	**Baseline Case**		0.41633	0.00035	0.41703	--
		0.155 in. (0.3937 cm)	13	0.41548	0.00040	0.41628	-0.00075
			26	0.41637	0.00037	0.41711	0.00008
			39	0.41653	0.00039	0.41731	0.00028
			78	0.42092	0.00038	0.42168	0.00465
			213.995	0.43094	0.00039	0.43172	0.01469
		0.183 in. (0.4648 cm)	13	0.41625	0.00040	0.41705	0.00002
			26	0.41679	0.00037	0.41753	0.00050
			39	0.41799	0.00038	0.41875	0.00172
			78	0.42454	0.00042	0.42538	0.00835
			213.995	0.43849	0.00044	0.43937	0.02234

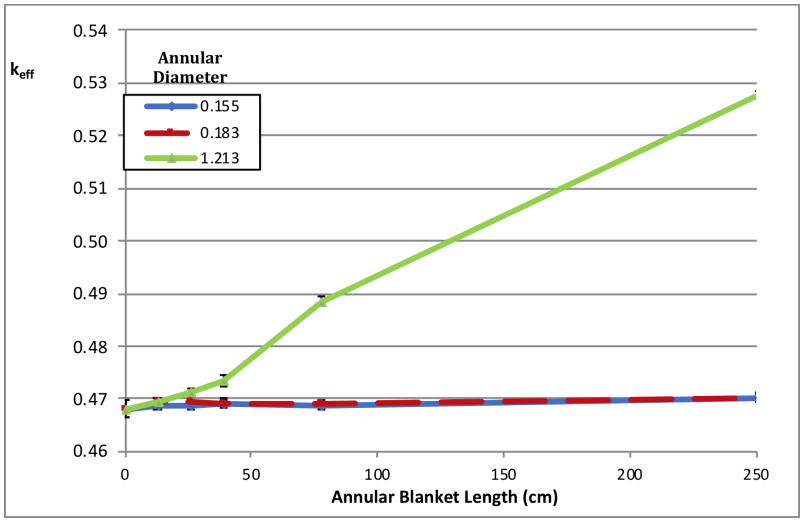

Figure 6-47 Annular Blanket Sensitivity – Package Array, NCT (Rod Pipe UO_2 Fuel Rods)

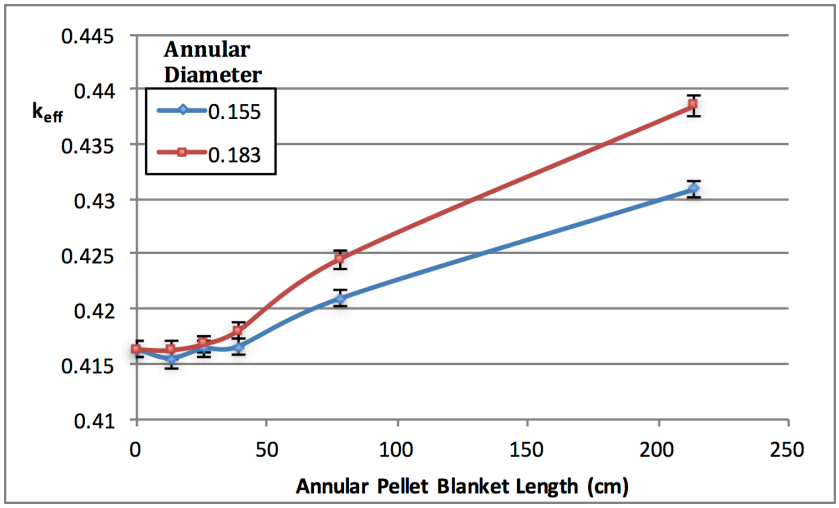

Figure 6-48 Annular Blanket Sensitivity – Package Array, NCT (Rod Pipe U_3Si_2 Fuel Rods)

The Rod Pipe position sensitivity study, as defined in Section 6.3.4.3.2, examined the shifting of the Rod Pipe in the Clamshell from the centered, baseline position. Table 6-64 defines the parameter evaluated and the results. The most reactive case is highlighted for each package variant.

Table 6-64 Rod Pipe Position Sensitivity Results – Package Array, NCT, Rod Pipe

Contents	Traveller Variant	Fuel Assembly Position	k_{eff}	σ	$k_{eff} + 2\sigma$	$\Delta(k_{eff} + 2\sigma)$
Rod Pipe UO_2 Fuel Rods	XL	**Baseline Case**	0.46675	0.00067	0.46809	--
		Down	0.46982	0.00045	0.47072	0.00263
Rod Pipe U_3Si_2 Fuel Rods	STD	**Baseline Case**	0.41633	0.00035	0.41703	--
		Down	0.41477	0.00039	0.41555	-0.00148

The package outer diameter tolerance directly affects the spacing of the packages in an array, thus the tolerance is evaluated, as defined in Section 6.3.4.3.4. Table 6-65 defines the parameter evaluated and the results. The most reactive case is highlighted for each package variant, and there is no statistically significant (i.e. greater than 2σ) effect in adjusting the outer diameter of the packages in an NCT array.

Table 6-65 Package OD Tolerance Sensitivity Results – Package Array, NCT, Rod Pipe

Contents	Traveller Variant	Package Outer Diameter (in.)	k_{eff}	σ	$k_{eff} + 2\sigma$	$\Delta(k_{eff} + 2\sigma)$
Rod Pipe UO_2 Fuel Rods	XL	-0.2	0.46817	0.00041	0.46899	0.00090
		Nominal	0.46675	0.00067	0.46809	--
		+0.2	0.46721	0.00041	0.46803	-0.00006
Rod Pipe U_3Si_2 Fuel Rods	STD	-0.2	0.41638	0.00038	0.41714	0.00011
		Nominal	0.41633	0.00035	0.41703	--
		+0.2	0.41571	0.00039	0.41649	-0.00054

The polyethylene packing materials sensitivity study for the Rod Pipe NCT package array evaluation, as defined in Section 6.3.4.3.5, examined the presence of an outer wrap around each fuel rod. Table 6-66 defines the parameter evaluated and the results, and Figure 6-49 and Figure 6-50 display the trend. The most reactive case is highlighted for each package variant. Based on package array NCT, no limitation of polyethylene packing materials is imposed on the Traveller packaging with Rod Pipe

Table 6-66 Polyethylene Packing Sensitivity Results – Package Array, NCT, Rod Pipe

Contents	Traveller Variant	Poly Model	Poly Mass (kg)	k_{eff}	σ	$k_{eff} + 2\sigma$	$\Delta(k_{eff} + 2\sigma)$
Rod Pipe UO_2 Fuel Rods	XL	**Baseline Case**	0.00	0.46675	0.00067	0.46809	--
		Outer Wrap	1.67	0.47942	0.00039	0.48020	0.01211
			2.19	0.48287	0.00036	0.48359	0.01550
			4.28	0.49650	0.00045	0.49740	0.02931
			18.32	0.52692	0.00039	0.52770	0.05961
			30.89	0.52825	0.00048	0.52921	0.06112
Rod Pipe U_3Si_2 Fuel Rods	STD	**Baseline Case**	0.00	0.41633	0.00035	0.41703	--
		Outer Wrap	1.85	0.4342	0.00042	0.43504	0.01801
			3.79	0.45568	0.00039	0.45646	0.03943
			7.96	0.49859	0.00039	0.49937	0.08234
			17.41	0.58134	0.00044	0.58222	0.16519
			36.30	0.67249	0.00044	0.67337	0.25634

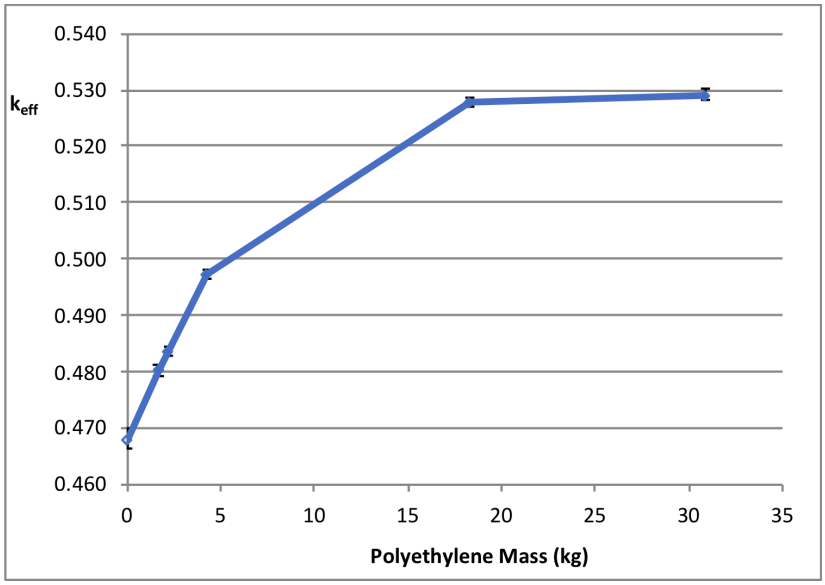

Figure 6-49 Polyethylene Packing Sensitivity – Package Array, NCT (Rod Pipe UO_2 Fuel Rods)

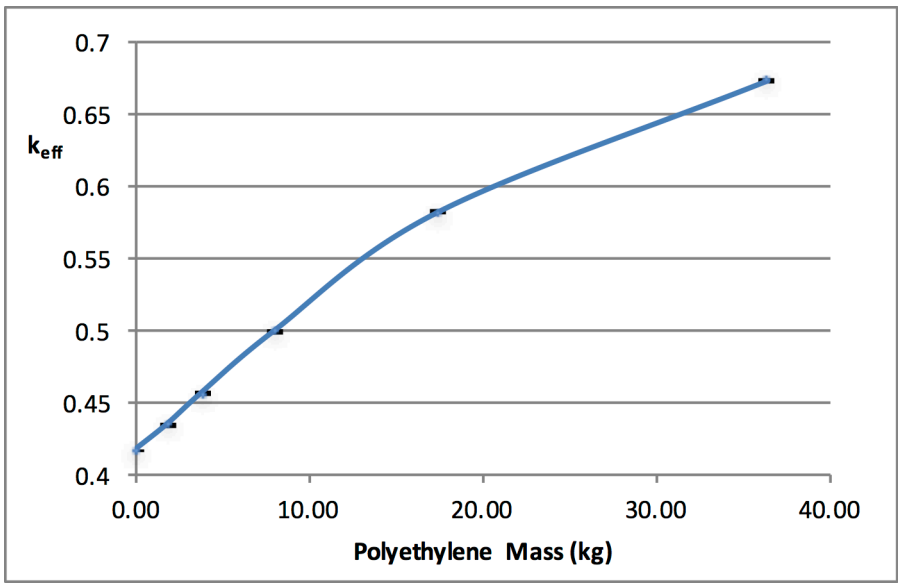

Figure 6-50 Polyethylene Packing Sensitivity – Package Array, NCT (Rod Pipe U_3Si_2 Fuel Rods)

The tolerance sensitivity study evaluates fuel pellet diameter only, as defined in Section 6.3.4.3.9. The Rod Pipe contents are not defined by cladding and pitch parameters, thus there is tolerance evaluation as explained in Section 6.3.4.3.8 and 6.3.4.3.10, respectively. Table 6-67 defines the parameter dimensions evaluated and the results. The most reactive case is highlighted for each package variant and tolerance parameter.

Table 6-67 Tolerance Sensitivity Results – Package Array, NCT, Rod Pipe

Content	Traveller Variant	Pellet Diameter Tolerance (in.)	k_{eff}	σ	$k_{eff} + 2\sigma$	$\Delta(k_{eff} + 2\sigma)$
Rod Pipe UO_2 Fuel Rods	XL	-0.0014	0.46806	0.00037	0.46880	0.00071
		-0.0010	0.46828	0.00040	0.46908	0.00099
		Nominal	0.46675	0.00067	0.46809	--
		+0.0010	0.46906	0.00042	0.46990	0.00181
		+0.0014	0.46768	0.00034	0.46836	0.00027
Rod Pipe U_3Si_2 Fuel Rods	STD	-0.0014	0.41511	0.00037	0.41585	-0.00118
		-0.0010	0.41508	0.00036	0.41580	-0.00123
		Nominal	0.41633	0.00035	0.41703	--
		+0.0010	0.41664	0.00041	0.41746	0.00043
		+0.0014	0.41641	0.00037	0.41715	0.00012

The ADOPT Fuel sensitivity study, as defined in Section 6.3.4.3.13, examined the effect of replacing standard UO_2 fuel with ADOPT fuel. Table 6-67A lists the results of the study. The most reactive case is highlighted.

Table 6-67A ADOPT Fuel Results – Package Array, NCT, Rod Pipe

Content	Traveller Variant	Fuel	k_{eff}	σ	$k_{eff} + 2\sigma$	$\Delta(k_{eff} + 2\sigma)$
Rod Pipe UO_2 Fuel Rods	XL	**Baseline (UO_2)**	0.46675	0.00067	0.46809	--
		ADOPT	0.46823	0.00066	0.46955	0.00146

6.6 PACKAGE ARRAYS UNDER HYPOTHETICAL ACCIDENT CONDITIONS

6.6.1 Configuration

For all package array arrangements under hypothetical accident conditions, the Clamshell interior and fuel assembly envelope are modeled as flooded with full-density water, including the fuel-clad gap where applicable. Additional material modeling is specified in Section 6.3.2. Several materials, including fuel structural components and packaging components (e.g. Outerpack foam regions, ceramic fiber blankets, and shock mounts, etc.), are replaced with void, as this promotes the most neutron cross-talk between packages in an array. The package array is reflected with at least 20 cm of full-density water.

6.6.1.1 Baseline Configuration

As described in Section 6.3.4.2, a baseline case is evaluated for all content Groups and Rod Pipe configurations under HAC. Baseline configurations represent a bounding model that is carried forward to the sensitivity studies to demonstrate maximum reactivity.

6.6.1.1.1 PWR Fuel Assembly Groups

Detailed results of the CFA-package variant comparison for the HAC package array assessment are shown in Section 6.9.3.5. The Traveller XL is consistently more reactive than the Traveller STD under HAC in a package array. In addition, an array with a height of one package is more reactive than a height of two packages. Therefore, the Traveller STD and packages arrays with a height of two packages are not further analyzed for the package array under HAC evaluation.

6.6.1.1.1.1 Baseline Case Determination

For the baseline case determination, as defined in Section 6.3.4.2.1, first the bounding CFAs-package variant combination is determined. For both Groups 1 and 2, the Traveller XL is consistently more reactive than the Traveller STD for an array under HAC. This conclusion is applied to Group 4. As discussed in Section 6.3.4.2.1.2, the positioning of the fuel assembly is examined because of the physical properties of the packaging. Flooding configuration is examined in order to determine moderation by water to the most reactive, credible extent. Detailed results of the baseline case determination are shown in Section 6.9.3.5. The HAC baseline configurations are summarized in Table 6-68. Each of the array configurations are shown in Figure 6-51, Figure 6-52, and Figure 6-52A.

Table 6-68 Summary of PWR Fuel Assembly Groups HAC Package Array Configurations

Traveller Variant	Contents (Group)	Array Size (2N)	Array Height	Lattice Expansion Length (cm)	Axial Position (cm)	Flooding Configuration	$k_{eff} \pm \sigma$
XL	17 Bin 1 (1)	100	1	50.8	87.122	Fuel Assembly and Clamshell	0.92688 ± 0.00031
XL	18 Bin 1 (2)	24	1	50.8	72.583	Fuel Assembly and Clamshell	0.91690 ± 0.00025
XL	17 Bin 1 (4)	40	1	--	42.545	Fuel Assembly and Clamshell	0.93810 ± 0.00023

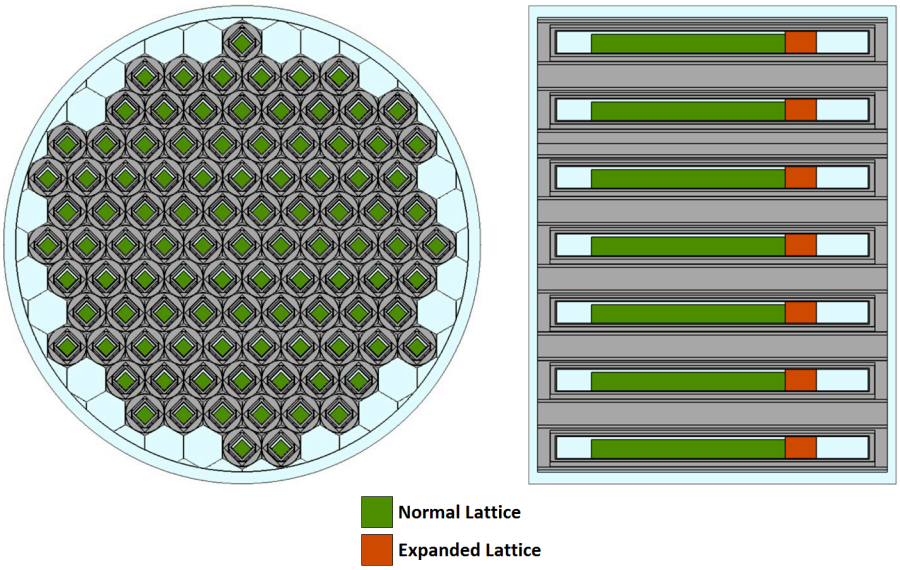

Figure 6-51 Group 1, HAC 100-package Array

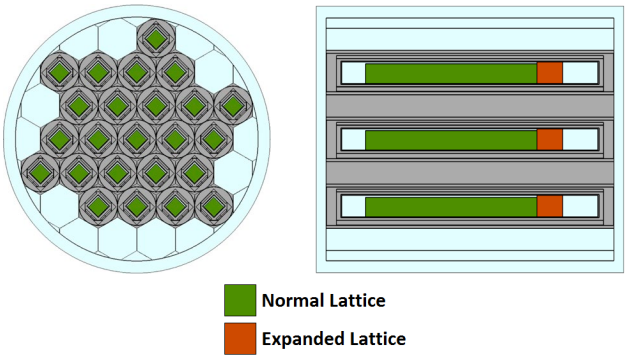

Figure 6-52 Group 2, HAC 24-package Array

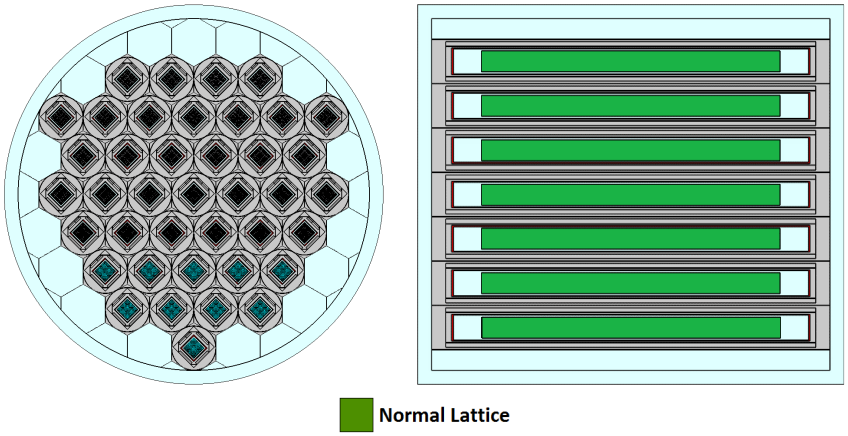

Figure 6-52A Group 4, HAC 40-package Array

6.6.1.1.2 Rod Pipe

For the Rod Pipe, HAC package array baseline case determination, as defined in Section 6.3.4.2.2, loose rods are modeled in the Rod Pipe and the pitch is expanded through a peak water-to-fuel ratio by changing the pitch for various fuel radii. The pitch type is modeled as both square and hexagonal, as this small variation in geometry varies the water-to-fuel ratio slightly. For the package array under HAC, the Clamshell and Rod Pipe interior regions are fully flooded with all other package interior and exterior regions modeled as void. Detailed results of the Rod Pipe HAC package array baseline case determination are shown in Section 6.9.3.6. For UO_2 fuel rods, comparison of the Traveller STD to Traveller XL baseline results show that, for the limiting fuel rod/pitch combination, the Traveller XL is consistently more reactive than the Traveller STD. The HAC package array baseline configurations for the Rod Pipe with UO_2 fuel rods and U_3Si_2 fuel rods are summarized in Table 6-69 and shown in Figure 6-53.

Table 6-69 Summary of Rod Pipe HAC Package Array Configurations

Contents	Traveller Variant	Array Size (2N)	Array Height	Fuel OR (cm)	Pitch-Type	Fuel Rod Half-Pitch (cm)	Flooding Configuration	$k_{eff} \pm \sigma$
UO_2 Fuel Rods	XL	150	1	0.50	Hexagonal	1.0	Rod Pipe and Clamshell	0.66385 ± 0.00050
U_3Si_2 Fuel Rods	STD	150	1	0.4851	Hexagonal	0.9851	Rod Pipe and Clamshell	0.62316 ± 0.00048

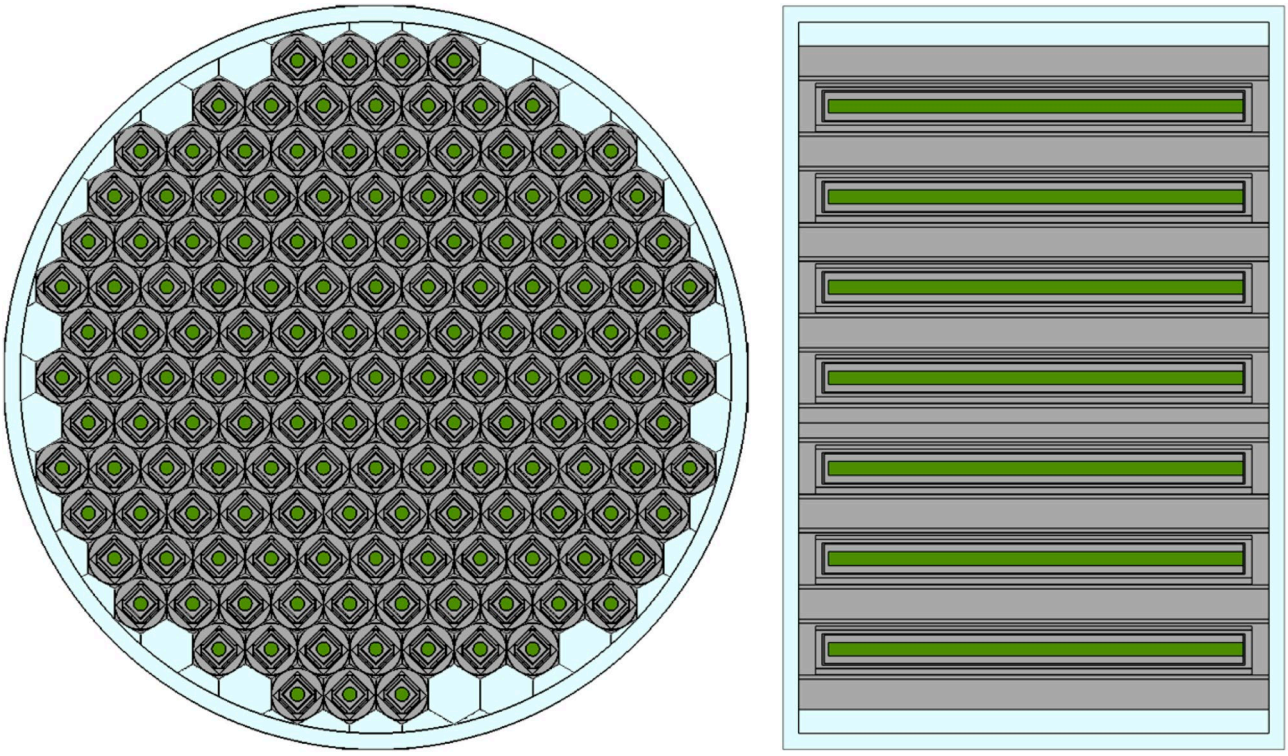

Figure 6-53 Rod Pipe, HAC 150-package Array

6.6.1.2 Sensitivity Study Configurations

Several sensitivity studies are analyzed for the HAC package array evaluation. The following summary tables list the bounding, as-penalized configurations of each sensitivity study. An entry of "None" signifies that the study resulted in no penalty and an entry of "--" signifies that the study did not require analyzing based on transport condition. The baseline case ($k_p + 2\sigma_p$) with the sum of penalties from the sensitivity studies (Δk_u) defines the most reactive configuration (*Maximum* $k_{eff} = k_p + 2\sigma_p + \Delta k_u$) and demonstrates the maximum reactivity for HAC package arrays.

6.6.1.2.1 PWR Fuel Assembly Groups

Listed in Table 6-70 are the bounding, as-penalized configurations of each sensitivity study for the Groups 1 and 2 HAC package array evaluations.

Table 6-70 HAC Package Array Sensitivity Study Bounding Configurations – PWR Fuel Assembly Groups

Sensitivity Study	Group 1	Group 2	Group 4
Annular Fuel Pellet Blanket	None	None	None
Clamshell/Fuel Assembly Shift	Clamshell/fuel assembly shifted up	Clamshell/fuel assembly shifted up	None
Moderator Density	None	None	None
Package OD Tolerance	None	- Tolerance	None
Polyethylene Packing Materials	2.00 kg of uniform melt	2.00 kg of collected melt	None
Axial Rod Displacement	None	None	--
Stainless Steel Rods	None	None	None
Cladding Tolerance	Minimum cladding thickness	Minimum cladding thickness	--
Fuel Pellet Diameter Tolerance	None	- Tolerance	--
Fuel Rod Pitch Tolerance	+ Tolerance	+ Tolerance	+ Tolerance
Steel Nozzle Reflector	None	None	None
ADOPT Fuel	None	None	None

Note: 'None' signifies that the sensitivity study did not result in a statistically significant increase in reactivity over the baseline case and '--' signifies the study was not done.

6.6.1.2.2 Rod Pipe

Listed in Table 6-71 are the bounding, as-penalized configurations of each sensitivity study for the Rod Pipe HAC package array evaluation.

Table 6-71 HAC Package Array Sensitivity Study Bounding Configurations – Rod Pipe

Sensitivity Study	Bounding Configuration UO_2 Fuel Rods	Bounding Configuration U_3Si_2 Fuel Rods
Annular Fuel Pellet Blanket	Full length	None
Rod Pipe Position in Clamshell	Centered	Centered
Moderator Density	None	1% density reduction
Package OD Tolerance	- Tolerance	- Tolerance
Fuel Pellet Diameter Tolerance	None	None
Polyethylene Packing Materials	Rod Pipe full of polyethylene	Rod Pipe full of polyethylene
Moderation Variation	Clamshell and Rod Pipe fully flooded	Clamshell and Rod Pipe fully flooded
ADOPT Fuel	None	--

Note: 'None' signifies that the sensitivity study did not result in a statistically significant increase in reactivity over the baseline case.

6.6.2 Results

6.6.2.1 HAC Package Array – Maximum Reactivity Results Summary

The maximum reactivity, *Maximum* k_{eff}, is defined by the bounding baseline ($k_p + 2\sigma_p$) plus the sum of penalties assessed for each sensitivity study (Δk_u). See Table 6-72 for a summary of the *Maximum* k_{eff} results. Final values of maximum reactivity fall under the USL, as calculated per Section 6.8.

Table 6-72 HAC Package Array – Maximum Reactivity Results Summary

Contents	Traveller Variant	Array Size (2N)	Array Height	Bin	$k_{eff} \pm \sigma$	$k_p + 2\sigma_p$	Δk_u	*Maximum* k_{eff}	USL
Group 1	XL	100	1	17 Bin 1	0.92688 ± 0.00031	0.92750	0.01033	0.93783	0.94162
Group 2	XL	24	1	18 Bin 1	0.91690 ± 0.00025	0.91740	0.02205	0.93945	0.94090
Group 4	XL	40	1	17 Bin 1	0.93810 ± 0.00023	0.93856	0.00087	0.93943	0.94082
Rod Pipe UO_2 Fuel Rods	XL	150	1	--	0.66385 ± 0.00050	0.66485	0.15103	0.81588	0.94044
Rod Pipe U_3Si_2 Fuel Rods	STD	150	1	--	0.62316 ± 0.00048	0.62412	0.14424	0.76836	0.94053

6.6.2.2 Sensitivity Study Results

As discussed in Section 6.3.4.3, for each package arrangement, the HAC package array baseline cases are subjected to several sensitivity studies. Each sensitivity study is compared to the baseline case. The most reactive configuration resulting in the largest positive difference in $k_{eff} + 2\sigma$ from the baseline case value that is also greater than or equal to two times the baseline σ is tallied and summed to define the total penalty assessed (Δk_u).

6.6.2.2.1 PWR Fuel Assembly Groups Results Summary

Table 6-73 shows the summary of the penalty assessed for the sensitivity studies evaluated for the PWR Fuel Assembly Group contents. An entry of "0.0" signifies that the study resulted in no positive penalty on reactivity and an entry of "--" signifies that the study was not done.

Table 6-73 HAC Package Array Assessed Penalties, Δk_u, PWR Fuel Assembly Groups

Sensitivity Study	Group 1	Group 2	Group 4
Annular Fuel Pellet Blanket	0.0	0.0	0.0
Clamshell/Fuel Assembly Shift	0.00353	0.00351	0.0
Moderator Density	0.0	0.0	0.0
Package OD Tolerance	0.0	0.00101	0.0
Polyethylene Packing Materials	0.00079	0.00154	0.0
Axial Rod Displacement	0.0	0.0	--
Stainless Steel Rods	0.0	0.0	0.0
Cladding Tolerance	0.00310	0.00451	--
Fuel Pellet Diameter Tolerance	0.0	0.00050	--
Fuel Rod Pitch Tolerance	0.00291	0.01098	0.00087
Steel Nozzle Reflector	0.0	0.0	0.0
ADOPT Fuel	0.0	0.0	0.0
Total Penalty (Δk_u)	**0.01033**	**0.02205**	**0.00087**

6.6.2.2.2 PWR Fuel Assembly Groups Detailed Results

The annular blanket sensitivity study, as defined in Section 6.3.4.3.1, examined the addition of varying annular fuel pellet ID and lengths of annular fuel pellet blanket lengths equally to the top and bottom of an assembly. Table 6-74 defines the parameters evaluated and the results. Figure 6-54, Figure 6-55, and Figure 6-55A display the result trends for each PWR fuel assembly Group. The most reactive case is highlighted for each Group.

Table 6-74 Annular Blanket Sensitivity Results – HAC Package Array, PWR Fuel Assembly Groups

Contents (Group)	Traveller Variant	Annulus Diameter	Annulus Length (cm)	k_{eff}	σ	$k_{eff} + 2\sigma$	$\Delta(k_{eff} + 2\sigma)$
17 Bin 1 (1)	XL	**Baseline Case**		0.92688	0.00031	0.92750	--
		0.155 in. (0.3937 cm)	13.0	0.92561	0.00030	0.92621	-0.00129
			26.0	0.92288	0.00025	0.92338	-0.00412
			39.0	0.91941	0.00027	0.91995	-0.00755
			50.8	0.91674	0.00026	0.91726	-0.01024
			95.0383	0.91693	0.00025	0.91743	-0.01007
			139.2767	0.91789	0.00026	0.91841	-0.00909
			183.5150	0.91828	0.00025	0.91878	-0.00872
		0.183 in. (0.4648 cm)	13.0	0.92413	0.00025	0.92463	-0.00287
			26.0	0.92016	0.00024	0.92064	-0.00686
			39.0	0.91504	0.00024	0.91552	-0.01198
			50.8	0.91111	0.00024	0.91159	-0.01591
			95.0383	0.91117	0.00029	0.91175	-0.01575
			139.2767	0.91067	0.00026	0.91119	-0.01631
			183.5150	0.91016	0.00025	0.91066	-0.01684
18 Bin 1 (2)	XL	**Baseline Case**		0.91690	0.00025	0.91740	--
		0.155 in. (0.3937 cm)	13.0	0.91685	0.00024	0.91733	-0.00007
			26.0	0.91648	0.00026	0.91700	-0.00040
			39.0	0.91544	0.00027	0.91598	-0.00142
			50.8	0.91547	0.00028	0.91603	-0.00137
		0.183 in. (0.4648 cm)	13.0	0.91650	0.00025	0.91700	-0.00040
			26.0	0.91544	0.00024	0.91592	-0.00148
			39.0	0.91436	0.00025	0.91486	-0.00254
			50.8	0.91340	0.00024	0.91388	-0.00352
17 Bin 1 (4)	XL	**Baseline Case**		0.93810	0.00023	0.93856	--
		0.155 in. (0.3937 cm)	13.0	0.93787	0.00028	0.93843	-0.00013
			26.0	0.93817	0.00028	0.93873	0.00017
			39.0	0.93827	0.00027	0.93881	0.00025
			50.8	0.93834	0.00024	0.93882	0.00026
		0.183 in. (0.4648 cm)	13.0	0.93756	0.00024	0.93804	-0.00052
			26.0	0.93799	0.00026	0.93851	-0.00005
			39.0	0.93839	0.00023	0.93885	0.00029
			50.8	0.93811	0.00029	0.93869	0.00013

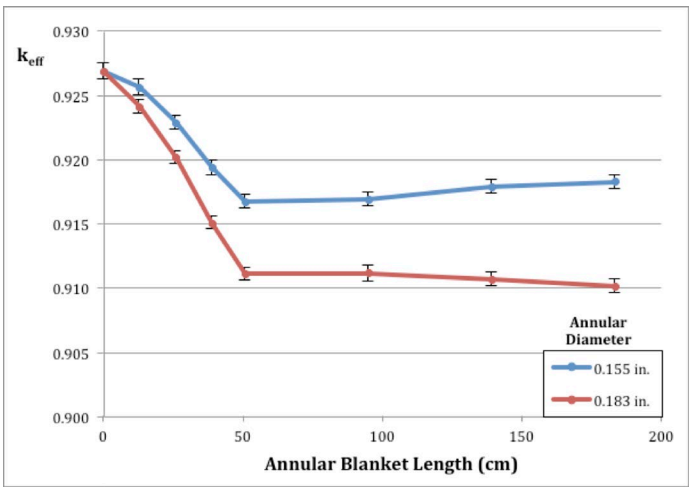

Figure 6-54 Annular Blanket Sensitivity – HAC Package Array (Group 1)

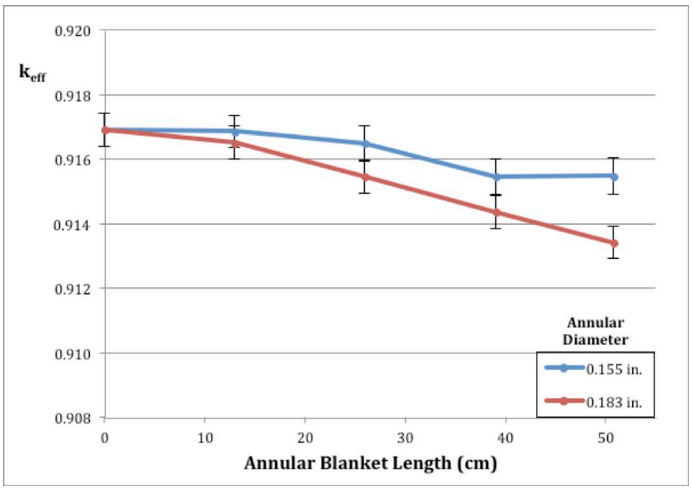

Figure 6-55 Annular Blanket Sensitivity – HAC Package Array (Group 2)

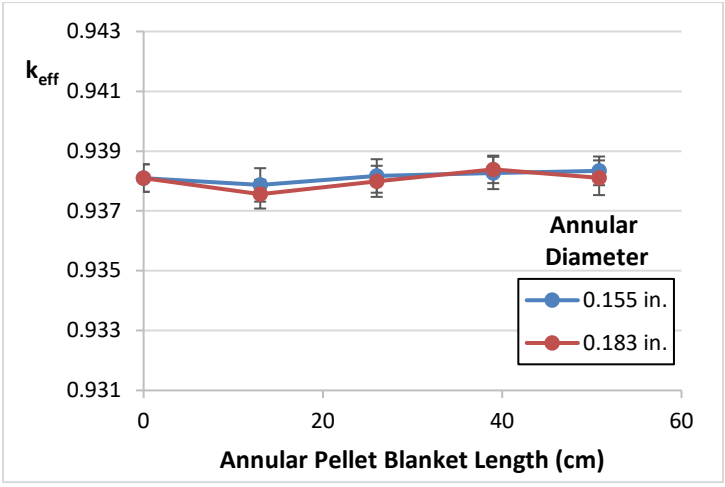

Figure 6-55A Annular Blanket Sensitivity – HAC Package Array (Group 4)

The Clamshell/fuel assembly position sensitivity study, as defined in Section 6.3.4.3.2, examined the shifting of the Clamshell to the top of the inner cavity and the fuel assembly to the top of the Clamshell in the x-y plane. Table 6-75 defines the parameter evaluated and the results. The most reactive case is highlighted for each Group.

Table 6-75 Clamshell/Fuel Assembly Position Results – HAC Package Array, PWR Fuel Assembly Groups

Contents (Group)	Traveller Variant	Clamshell Position	Fuel Assembly Position	k_{eff}	σ	$k_{eff} + 2\sigma$	$\Delta(k_{eff} + 2\sigma)$
17 Bin 1 (1)	XL	**Baseline Case**		0.92688	0.00031	0.92750	--
		Up	Up	0.93047	0.00028	0.93103	0.00353
18 Bin 1 (2)	XL	**Baseline Case**		0.91690	0.00025	0.91740	--
		Up	Up	0.92043	0.00024	0.92091	0.00351
17 Bin 1 (4)	XL	Center	Down	0.92579	0.00032	0.92643	-0.01213
		Baseline Case		0.93810	0.00023	0.93856	--
		Up	Up	0.92975	0.00023	0.93021	-0.00835

The moderator block density reduction sensitivity study, as defined in Section 6.3.4.3.3, examined the post-fire condition of the moderator block. Table 6-76 defines the parameter evaluated and the results. The most reactive case is highlighted for each Group.

Table 6-76 Moderator Block Density Results – HAC Package Array, PWR Fuel Assembly Groups

Content (Group)	Traveller Variant	Moderator Block Density (g/cm^3)	k_{eff}	σ	$k_{eff} + 2\sigma$	$\Delta(k_{eff} + 2\sigma)$
17 Bin 1 (1)	XL	**Baseline Case**	0.92688	0.00031	0.92750	--
		0.9108	0.92735	0.00028	0.92791	0.00041
18 Bin 1 (2)	XL	**Baseline Case**	0.91690	0.00025	0.91740	--
		0.9108	0.91721	0.00028	0.91777	0.00037
17 Bin 1 (4)	XL	**Baseline Case**	0.93810	0.00023	0.93856	--
		0.9108	0.93844	0.00026	0.93896	0.00040

The package outer diameter tolerance sensitivity study, as defined in Section 6.3.4.3.4, examined the effect of the Traveller outer diameter tolerance on k_{eff} by altering the package spacing in an array. Table 6-77 defines the parameter evaluated and the results. The most reactive case is highlighted for each Group.

Table 6-77 Package Outer Diameter Tolerance Results – HAC Package Array, PWR Fuel Assembly Groups						
Content (Group)	**Traveller Variant**	**Package Outer Diameter (in.)**	**k_{eff}**	**σ**	**$k_{eff} + 2\sigma$**	**$\Delta(k_{eff} + 2\sigma)$**
17 Bin 1 (1)	XL	-0.2	0.92720	0.00026	0.92772	0.00022
		Nominal	0.92688	0.00031	0.92750	--
		+0.2	0.92617	0.00027	0.92671	-0.00079
18 Bin 1 (2)	XL	-0.2	0.91791	0.00025	0.91841	0.00101
		Nominal	0.91690	0.00025	0.91740	--
		+0.2	0.91729	0.00027	0.91783	0.00043
17 Bin 1 (4)	XL	-0.2	0.93773	0.00027	0.93827	-0.00029
		Nominal	0.93810	0.00023	0.93856	--
		+0.2	0.93775	0.00023	0.93821	-0.00035

The polyethylene packing materials sensitivity study, as defined in Section 6.3.4.3.5, examined a conservative representation of polyethylene packing materials through HAC. Table 6-78 defines the parameters evaluated and the results. Figure 6-56, Figure 6-57, and Figure 6-57A display the result trends for Group 1, Group 2, and Group 4. A limit of 2.00 kg of polyethylene packing materials is imposed on the Traveller, and the bounding case corresponding to the polyethylene limit set is highlighted for each Group.

Table 6-78 Polyethylene Sensitivity Results – HAC Package Array, PWR Fuel Assembly Groups							
Content (Group)	**Traveller Variant**	**Poly Model**	**Poly Mass (kg)**	**k_{eff}**	**σ**	**$k_{eff} + 2\sigma$**	**$\Delta(k_{eff} + 2\sigma)$**
17 Bin 1 (1)	XL	**Baseline Case**	0.0	0.92688	0.00031	0.92750	--
		Outer Wrap	2.27	0.92619	0.00025	0.92669	-0.00081
			3.56	0.92758	0.00027	0.92812	0.00062
			4.69	0.92771	0.00024	0.92819	0.00069
			5.83	0.92797	0.00025	0.92847	0.00097
			7.03	0.92810	0.00026	0.92862	0.00112
			8.16	0.92879	0.00025	0.92929	0.00179
		Uniform Wrap	2.00	0.92775	0.00027	0.92829	0.00079
			4.00	0.92881	0.00024	0.92929	0.00179
			6.00	0.92974	0.00024	0.93022	0.00272
			8.00	0.93068	0.00024	0.93116	0.00366
			10.00	0.93152	0.00026	0.93204	0.00454
		Collected Melt	2.00	0.92744	0.00029	0.92802	0.00052
			4.00	0.92961	0.00028	0.93017	0.00267
			6.00	0.93429	0.00033	0.93495	0.00745
			8.00	0.94120	0.00027	0.94174	0.01424
			10.00	0.94802	0.00027	0.94856	0.02106

Table 6-78 Polyethylene Sensitivity Results – HAC Package Array, PWR Fuel Assembly Groups							
Content (Group)	**Traveller Variant**	**Poly Model**	**Poly Mass (kg)**	**k_{eff}**	**σ**	**$k_{eff} + 2\sigma$**	**$\Delta(k_{eff} + 2\sigma)$**
18 Bin 1 (2)	XL	**Baseline Case**	0.00	0.91690	0.00025	0.91740	--
		Outer Wrap	2.34	0.91693	0.00025	0.91743	0.00003
			3.80	0.91718	0.00029	0.91776	0.00036
			5.06	0.91802	0.00025	0.91852	0.00112
			6.31	0.91851	0.00026	0.91903	0.00163
			7.59	0.91846	0.00025	0.91896	0.00156
			8.74	0.91924	0.00026	0.91976	0.00236
		Uniform Wrap	2.00	0.91822	0.00025	0.91872	0.00132
			4.00	0.91987	0.00023	0.92033	0.00293
			6.00	0.92080	0.00030	0.92140	0.00400
			8.00	0.92235	0.00029	0.92293	0.00553
			10.00	0.92292	0.00025	0.92342	0.00602
		Collected Melt	2.00	0.91846	0.00024	0.91894	0.00154
			4.00	0.92059	0.00026	0.92111	0.00371
			6.00	0.92481	0.00025	0.92531	0.00791
			8.00	0.93252	0.00026	0.93304	0.01564
			10.00	0.94194	0.00028	0.94250	0.02510
17 Bin 1 (4)	XL	**Baseline Case**	0.00	0.93810	0.00023	0.93856	--
		Outer Wrap	1.00	0.93835	0.00028	0.93891	0.00035
			2.00	0.93758	0.00027	0.93812	-0.00044
			3.00	0.93768	0.00026	0.93820	-0.00036

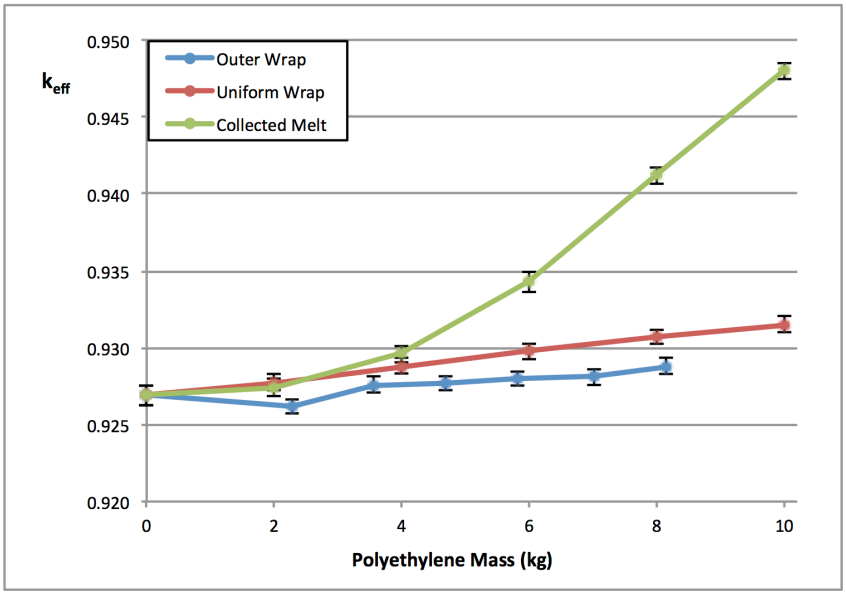

Figure 6-56 Polyethylene Sensitivity Results – HAC Package Array (Group 1)

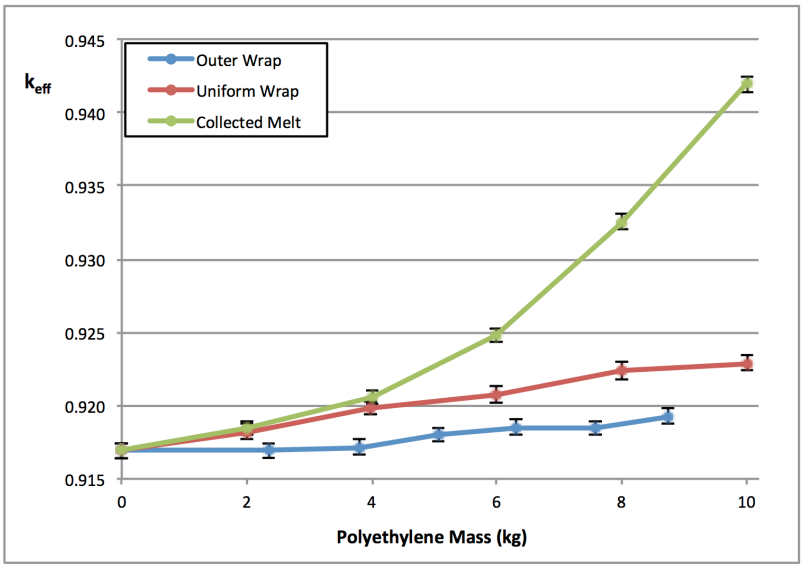

Figure 6-57 Polyethylene Sensitivity Results – HAC Package Array (Group 2)

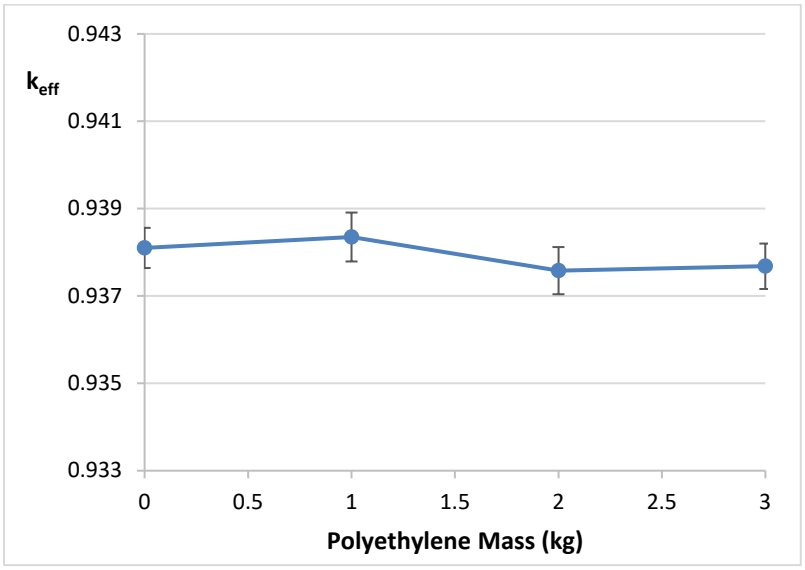

Figure 6-57A Polyethylene Sensitivity Results – HAC Package Array (Group 4)

The axial rod displacement sensitivity study, as defined in Section 6.3.4.3.6, examined the movement of fuel rods upward and out of the lattice during drop testing. Table 6-79 defines the parameters evaluated and the results. Figure 6-58 and Figure 6-59 display the result trends for Groups 1 and 2. The most reactive case is highlighted for each Group.

Table 6-79 Axial Rod Displacement Sensitivity Results – Single Package, HAC, PWR Fuel Assembly Groups

Content (Group)	Traveller Variant	Rod Configuration	Number of Rods	k_{eff}	σ	$k_{eff} + 2\sigma$	$\Delta(k_{eff} + 2\sigma)$
17 Bin 1 (1)	XL	**Baseline**	0	0.92688	0.00031	0.92750	--
		Corner	20	0.91844	0.00026	0.91896	-0.00854
			40	0.91194	0.00024	0.91242	-0.01508
			64	0.90852	0.00027	0.90906	-0.01844
		Random	20	0.92141	0.00025	0.92191	-0.00559
			40	0.91722	0.00026	0.91774	-0.00976
			64	0.91294	0.00024	0.91342	-0.01408
18 Bin 1 (2)	XL	**Baseline**	0	0.91690	0.00025	0.91740	--
		Corner	20	0.91428	0.00024	0.91476	-0.00264
			40	0.91207	0.00029	0.91265	-0.00475
			68	0.90999	0.00025	0.91049	-0.00691
		Random	20	0.91631	0.00024	0.91679	-0.00061
			40	0.91661	0.00030	0.91721	-0.00019
			68	0.91413	0.00026	0.91465	-0.00275

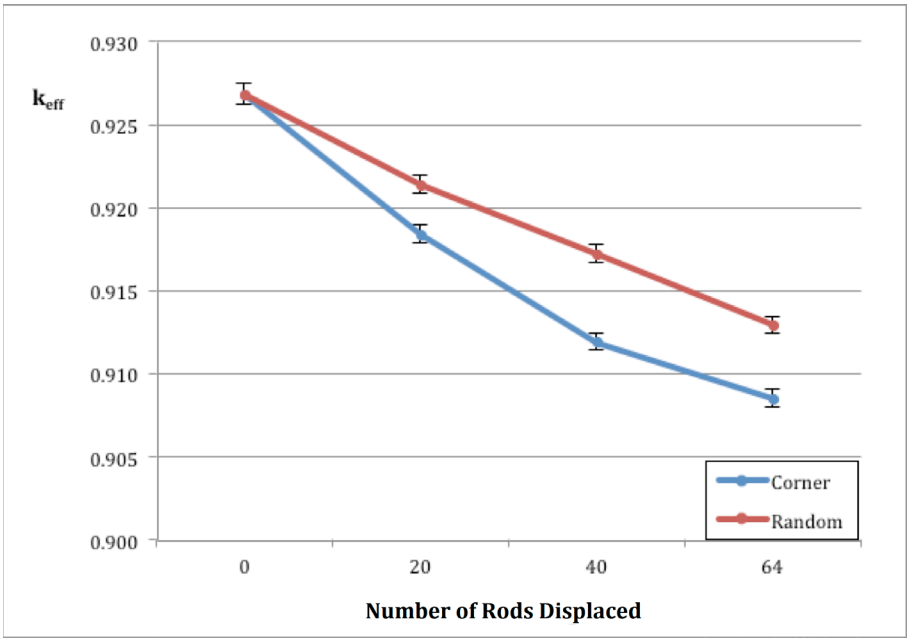

Figure 6-58 Axial Rod Displacement Sensitivity Results – HAC Package Array (Group 1)

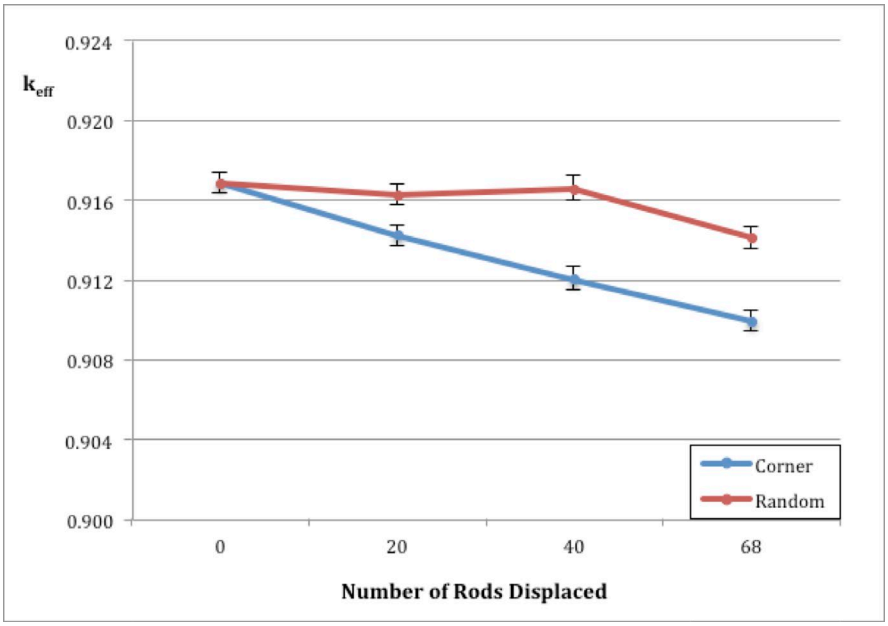

Figure 6-59 Axial Rod Displacement Sensitivity Results – HAC Package Array (Group 2)

The SS replacement rod sensitivity study, as defined in Section 6.3.4.3.7, examined the replacement of fuel rods with SS rods within the fuel assembly. Table 6-80 defines the parameters evaluated and the results. The most reactive case is highlighted for each Group.

Table 6-80 SS Rod Replacement Sensitivity Results – Single Package, HAC, PWR Fuel Assembly Groups

Content (Group)	Traveller Variant	SS Rod Configuration	k_{eff}	σ	$k_{eff} + 2\sigma$	$\Delta(k_{eff} + 2\sigma)$
17 Bin 1 (1)	XL	**Baseline Case**	0.92688	0.00031	0.92750	--
		Corner	0.90189	0.00025	0.90239	-0.02511
		Random	0.86900	0.00022	0.86944	-0.05806
18 Bin 1 (2)	XL	**Baseline Case**	0.91690	0.00025	0.91740	--
		Corner	0.89297	0.00024	0.89345	-0.02395
		Random	0.86274	0.00024	0.86322	-0.05418
17 Bin 1 (4)	XL	**Baseline Case**	0.93810	0.00023	0.93856	--
		Corner	0.89660	0.00027	0.89714	-0.04142
		Random	0.88773	0.00021	0.88815	-0.05041

The tolerance sensitivity studies evaluate cladding dimensions, fuel pellet diameter, and fuel rod pitch, as defined in Section 6.3.4.3.8, 6.3.4.3.9, and 6.3.4.3.10, respectively. Table 6-81 defines the parameter dimensions evaluated and the results. The most reactive case is highlighted for each Group and tolerance parameter.

Table 6-81 Tolerance Sensitivity Results – HAC Package Array, PWR Fuel Assembly Groups

Content (Group)	Traveller Variant	Tolerance Parameter		k_{eff}	σ	$k_{eff} + 2\sigma$	$\Delta(k_{eff} + 2\sigma)$
17 Bin 1 (1)	XL	**Baseline Case**		0.92688	0.00031	0.92750	--
18 Bin 1 (2)	XL	**Baseline Case**		0.91690	0.00025	0.91740	--
17 Bin 1 (4)	XL	**Baseline Case**		0.93810	0.00023	0.93856	--
Cladding Tolerance		**Cladding ID (in.)**	**Cladding OD (in.)**	k_{eff}	σ	$k_{eff} + 2\sigma$	$\Delta(k_{eff} + 2\sigma)$
17 Bin 1 (1)	XL	-0.002	-0.002	0.92688	0.00024	0.92736	-0.00014
			Nominal	0.92498	0.00030	0.92558	-0.00192
			+0.002	0.92359	0.00025	0.92409	-0.00341
		Nominal	-0.002	0.92848	0.00024	0.92896	0.00146
			Nominal	0.92688	0.00031	0.92750	--
			+0.002	0.92504	0.00029	0.92562	-0.00188
		+0.002	-0.002	0.93006	0.00027	0.93060	0.00310
			Nominal	0.92785	0.00025	0.92835	0.00085
			+0.002	0.92614	0.00025	0.92664	-0.00086
18 Bin 1 (1)	XL	-0.002	-0.002	0.91785	0.00026	0.91837	0.00097
			Nominal	0.91516	0.00024	0.91564	-0.00176
			+0.002	0.91223	0.00028	0.91279	-0.00461
		Nominal	-0.002	0.91922	0.00026	0.91974	0.00234
			Nominal	0.91690	0.00025	0.91740	--
			+0.002	0.91504	0.00026	0.91556	-0.00184
		+0.002	-0.002	0.92143	0.00024	0.92191	0.00451
			Nominal	0.91889	0.00030	0.91949	0.00209
			+0.002	0.91647	0.00027	0.91701	-0.00039
Pellet Diameter Tolerance		**Pellet OD (in.)**		k_{eff}	σ	$k_{eff} + 2\sigma$	$\Delta(k_{eff} + 2\sigma)$
17 Bin 1 (1)	XL	-0.0007		0.92689	0.00026	0.92741	-0.00009
		-0.0005		0.92650	0.00023	0.92696	-0.00054
		+0.0005		0.92664	0.00025	0.92714	-0.00036
		+0.0007		0.92723	0.00024	0.92771	0.00021
18 Bin 1 (2)	XL	-0.0007		0.91738	0.00026	0.91790	0.00050
		-0.0005		0.91729	0.00026	0.91781	0.00041
		+0.0005		0.91713	0.00026	0.91765	0.00025
		+0.0007		0.91706	0.00025	0.91756	0.00016
Pitch Tolerance		**Half-pitch (in.)**		k_{eff}	σ	$k_{eff} + 2\sigma$	$\Delta(k_{eff} + 2\sigma)$
17 Bin 1 (1)	XL	-0.005		0.92460	0.00025	0.92510	-0.00240
		-0.001		0.92638	0.00023	0.92684	-0.00070
		+0.001		0.92727	0.00024	0.92775	0.00025
		+0.005		0.92993	0.00024	0.93041	0.00291
18 Bin 1 (2)	XL	-0.0630		0.88930	0.00027	0.88984	-0.02760
		-0.0315		0.89876	0.00027	0.89930	-0.0181
		+0.0059		0.92168	0.00025	0.92218	0.00478
		+0.0118		0.92788	0.00025	0.92838	0.01098
17 Bin 1 (4)	XL	-0.001		0.93659	0.00024	0.93707	-0.00149
		+0.001		0.93895	0.00024	0.93943	0.00087

The steel nozzle reflector sensitivity study, as defined in Section 6.3.4.3.11, examined the presence of a SS304-water mixture and 100% density SS304 blocks at the ends of the fuel assembly, simulating the top and bottom nozzles in two different configurations. Table 6-82 defines the parameter evaluated and the results. The most reactive case is highlighted for each Group.

Table 6-82 Steel Nozzle Reflector Sensitivity Results – HAC Package Array, PWR Fuel Assembly Groups

Contents (Group)	Traveller Variant	Stainless Steel Nozzle Configuration	k_{eff}	σ	$k_{eff} + 2\sigma$	$\Delta(k_{eff} + 2\sigma)$
17 Bin 1 (1)	XL	**Baseline (Water)**	0.92688	0.00031	0.92750	--
		50% SS304 / 50% water	0.92528	0.00024	0.92576	-0.00174
		100% density SS304	0.92601	0.00025	0.92651	-0.00099
18 Bin 1 (2)	XL	**Baseline (Water)**	0.91690	0.00025	0.91740	--
		50% SS304 / 50% water	0.91688	0.00029	0.91746	0.00006
		100% density SS304	0.91669	0.00029	0.91727	-0.00013
17 Bin 1 (4)	XL	**Baseline (Water)**	0.93810	0.00023	0.93856	--
		50% SS304 / 50% water	0.93758	0.00024	0.93806	-0.00050
		100% density SS304	0.93745	0.00024	0.93793	-0.00063

The ADOPT Fuel sensitivity study, as defined in Section 6.3.4.3.13, examined the effect of replacing standard UO_2 fuel with ADOPT fuel. Table 6-82A lists the results of the study. The most reactive case is highlighted.

Table 6-82A ADOPT Fuel Results – HAC Package Array, PWR Fuel Assembly Groups

Contents (Group)	Traveller Variant	Fuel	k_{eff}	σ	$k_{eff} + 2\sigma$	$\Delta(k_{eff} + 2\sigma)$
17 Bin 1 (1)	XL	**Baseline (UO_2)**	0.92688	0.00031	0.92750	--
		ADOPT	0.92656	0.00025	0.92706	-0.00044
18 Bin 1 (2)	XL	**Baseline (UO_2)**	0.91690	0.00025	0.91740	--
		ADOPT	0.91672	0.00030	0.91732	-0.00008
17 Bin 1 (4)	XL	**Baseline (UO_2)**	0.93810	0.00023	0.93856	-
		ADOPT	0.93787	0.00025	0.93837	-0.00019

6.6.2.2.3 Rod Pipe Results Summary

Table 6-83 shows the summary of the penalties assessed for the sensitivity studies evaluated for the Rod Pipe contents. An entry of "0.0" signifies that the study resulted in no positive penalty on reactivity.

Table 6-83 HAC Package Array Assessed Penalties, Δk_u, Rod Pipe

Sensitivity Study	Penalty Assessed	
	UO_2 Fuel Rods	**U_3Si_2 Fuel Rods**
Annular Fuel Pellet Blanket	0.00187	0.0
Rod Pipe Position in Clamshell	0.0	0.0
Moderator Block Density Reduction	0.0	0.00102
Package OD Tolerance	0.00134	0.00101
Polyethylene Packing Materials	0.08270	0.08102
Fuel Pellet Diameter Tolerance	0.0	0.0
Moderator Variation	0.06512	0.06119
ADOPT Fuel	0.0	--
Total Penalty (Δk_u)	**0.15103**	**0.14424**

6.6.2.2.4 Rod Pipe Detailed Results

The annular blanket sensitivity study, as defined in Section 6.3.4.3.1, examined the addition of varying annular fuel pellet ID and lengths of annular fuel pellet blanket lengths equally to the top and bottom of a fuel rod. Table 6-84 defines the parameters evaluated and the results, and Figure 6-60 and Figure 6-61 display the result trends. The most reactive case is highlighted for each package variant.

Table 6-84 Annular Blanket Sensitivity Results – HAC Package Array, Rod Pipe

Contents	Traveller Variant	Annulus Diameter	Annulus Length (cm)	k_{eff}	σ	$k_{eff} + 2\sigma$	$\Delta(k_{eff} + 2\sigma)$
Rod Pipe UO_2 Fuel Rods	XL	**Baseline Case**		0.66385	0.00050	0.66485	--
		0.155 in. (0.3937 cm)	13.0	0.66428	0.00062	0.66552	0.00067
			26.0	0.66460	0.00052	0.66564	0.00079
			39.0	0.66268	0.00052	0.66372	-0.00113
			78.0	0.66562	0.00049	0.66660	0.00175
			250.825	0.66574	0.00049	0.66672	0.00187
		0.183 in. (0.4648 cm)	13.0	0.66298	0.00056	0.66410	-0.00075
			26.0	0.66313	0.00058	0.66429	-0.00056
			39.0	0.66360	0.00056	0.66472	-0.00013
			78.0	0.66380	0.00049	0.66478	-0.00007
			250.825	0.66364	0.00047	0.66458	-0.00027

Table 6-84 Annular Blanket Sensitivity Results – HAC Package Array, Rod Pipe

Contents	Traveller Variant	Annulus Diameter	Annulus Length (cm)	k_{eff}	σ	$k_{eff} + 2\sigma$	$\Delta(k_{eff} + 2\sigma)$
Rod Pipe U_3Si_2 Fuel Rods	STD	**Baseline Case**		0.62316	0.00048	0.62412	--
		0.155 in. (0.3937 cm)	13.0	0.62245	0.00046	0.62337	-0.00075
			26.0	0.62308	0.00048	0.62404	-0.00008
			39.0	0.62329	0.00048	0.62425	0.00013
			78.0	0.62270	0.00053	0.62376	-0.00036
			213.995	0.62294	0.00049	0.62392	-0.00020
		0.183 in. (0.4648 cm)	13.0	0.62274	0.00063	0.62400	-0.00012
			26.0	0.62266	0.00044	0.62354	-0.00058
			39.0	0.62326	0.00052	0.62430	0.00018
			78.0	0.62141	0.00056	0.62253	-0.00159
			213.995	0.62019	0.00058	0.62135	-0.00277

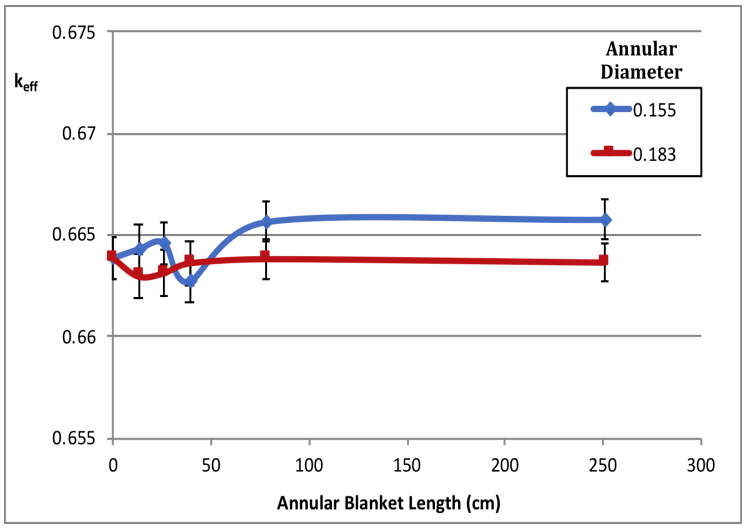

Figure 6-60 Annular Blanket Sensitivity – HAC Package Array (Rod Pipe UO_2 Fuel Rods)

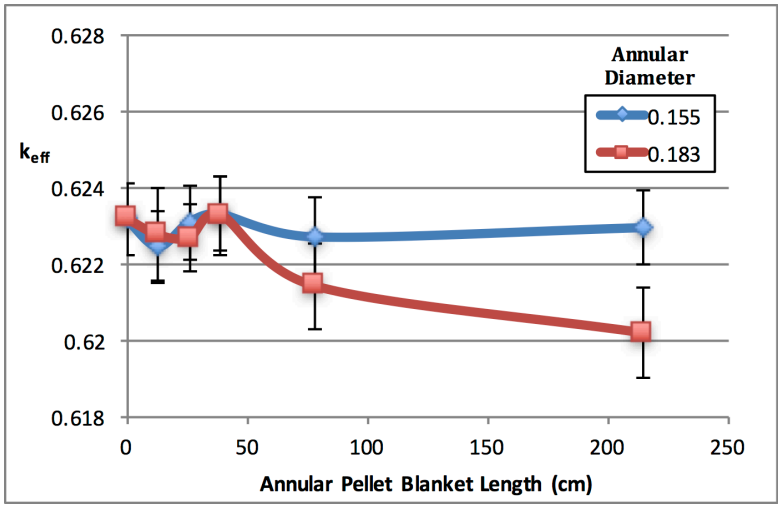

Figure 6-61 Annular Blanket Sensitivity – HAC Package Array (Rod Pipe U_3Si_2 Fuel Rods)

The Rod Pipe position sensitivity study, as defined in Section 6.3.4.3.2, examined the shifting of the Rod Pipe in the Clamshell. Table 6-85 defines the parameter evaluated and the results. The most reactive case is highlighted for each package variant.

Table 6-85 Rod Pipe Position Sensitivity Results – HAC Package Array, Rod Pipe

Contents	Traveller Variant	Rod Pipe Position	k_{eff}	σ	$k_{eff} + 2\sigma$	$\Delta(k_{eff} + 2\sigma)$
Rod Pipe UO_2 Fuel Rods	XL	Up	0.66415	0.00061	0.66537	0.00052
		Baseline Case	0.66385	0.00050	0.66485	--
		Down	0.66449	0.00050	0.66549	0.00064
Rod Pipe U_3Si_2 Fuel Rods	STD	Up	0.62307	0.00047	0.62401	-0.00011
		Baseline Case	0.62316	0.00048	0.62412	--
		Down	0.62337	0.00048	0.62433	0.00021

The moderator block density reduction sensitivity study, as defined in Section 6.3.4.3.3, examined the post-fire condition of the moderator block. Table 6-86 defines the parameter evaluated and the results. The most reactive case is highlighted for each package variant.

Table 6-86 Moderator Block Density Results – HAC Package Array, Rod Pipe

Content	Traveller Variant	Moderator Block Density (g/cm^3)	k_{eff}	σ	$k_{eff} + 2\sigma$	$\Delta(k_{eff} + 2\sigma)$
Rod Pipe UO_2 Fuel Rods	XL	**Baseline Case**	0.66385	0.00050	0.66485	--
		0.9108	0.66471	0.00053	0.66577	0.00092
Rod Pipe U_3Si_2 Fuel Rods	STD	**Baseline Case**	0.62316	0.00048	0.62412	--
		0.9108	0.62422	0.00046	0.62514	0.00102

The package outer diameter tolerance sensitivity study, as defined in Section 6.3.4.3.4, examined the effect of the Traveller outer diameter tolerance, which alters the package spacing in an array, on k_{eff}. Table 6-87 defines the parameter evaluated and the results. The most reactive case is highlighted for each package variant.

Table 6-87 Package Outer Diameter Tolerance Sensitivity Results – HAC Package Array, Rod Pipe

Content (Group)	Traveller Variant	Package Outer Diameter Tolerance (in.)	k_{eff}	σ	$k_{eff} + 2\sigma$	$\Delta(k_{eff} + 2\sigma)$
Rod Pipe UO_2 Fuel Rods	XL	-0.2	0.66513	0.00053	0.66619	0.00134
		Baseline Case	0.66385	0.00050	0.66485	--
		+0.2	0.66305	0.00048	0.66401	-0.00084
Rod Pipe U_3Si_2 Fuel Rods	STD	-0.2	0.62425	0.00044	0.62513	0.00101
		Baseline Case	0.62316	0.00048	0.62412	0
		+0.2	0.62269	0.00049	0.62367	-0.00045

The polyethylene packing materials sensitivity study, as defined in Section 6.3.4.3.5, examined a conservative representation of polyethylene packing materials through HAC. Table 6-88 defines the parameters evaluated and the results, and Figure 6-62 and Figure 6-63 display the result trends. The most reactive case is highlighted.

Table 6-88 Polyethylene Sensitivity Results – HAC Package Array, Rod Pipe

Content	Traveller Variant	Poly Model	Poly Mass (kg)	k_{eff}	σ	$k_{eff} + 2\sigma$	$\Delta(k_{eff} + 2\sigma)$
Rod Pipe UO_2 Fuel Rods	XL	**Baseline Case**	0.0	0.66385	0.00050	0.66485	--
		Uniform Wrap	3.09	0.66719	0.00048	0.66815	0.00330
			4.10	0.66809	0.00052	0.66913	0.00428
			8.60	0.67304	0.00049	0.67402	0.00917
			58.64	0.73889	0.00055	0.73999	0.07514
		Collected Melt	0.60	0.65896	0.00048	0.65992	-0.00493
			1.79	0.66103	0.00052	0.66207	-0.00278
			2.39	0.66085	0.00057	0.66199	-0.00286
			2.99	0.66181	0.00048	0.66277	-0.00208
			4.19	0.67243	0.00052	0.67347	0.00862
			5.98	0.68886	0.00063	0.69012	0.02527
			8.97	0.70544	0.00055	0.70654	0.04169
			11.96	0.71558	0.00047	0.71652	0.05167
			60.00	0.74653	0.00051	0.74755	0.08270
Rod Pipe U_3Si_2 Fuel Rods	STD	**Baseline Case**	0.0	0.62316	0.00048	0.62412	--
		Uniform Wrap	2.64	0.62568	0.00046	0.62660	0.00248
			3.51	0.62667	0.00047	0.62761	0.00349
			7.36	0.63237	0.00053	0.63343	0.00931
			16.09	0.64447	0.00046	0.64539	0.02127
			31.76	0.66735	0.00051	0.66837	0.04425
			50.53	0.69422	0.00053	0.69528	0.07116
		Collected Melt	0.67	0.62368	0.00047	0.62462	0.00050
			2.01	0.62414	0.00044	0.62502	0.00090
			2.68	0.62464	0.00049	0.62562	0.00150
			3.35	0.62713	0.00052	0.62817	0.00405
			4.69	0.63900	0.00046	0.63992	0.01580
			6.70	0.65343	0.00057	0.65457	0.03045
			10.05	0.67179	0.00049	0.67277	0.04865
			13.41	0.68087	0.00046	0.68179	0.05767
			57.38	0.70402	0.00056	0.70514	0.08102

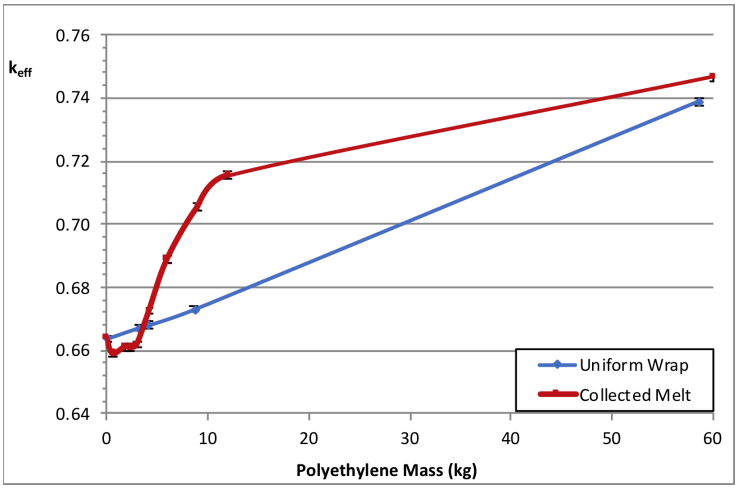

Figure 6-62 Polyethylene Sensitivity Results – HAC Package Array (Rod Pipe UO_2 Fuel Rods)

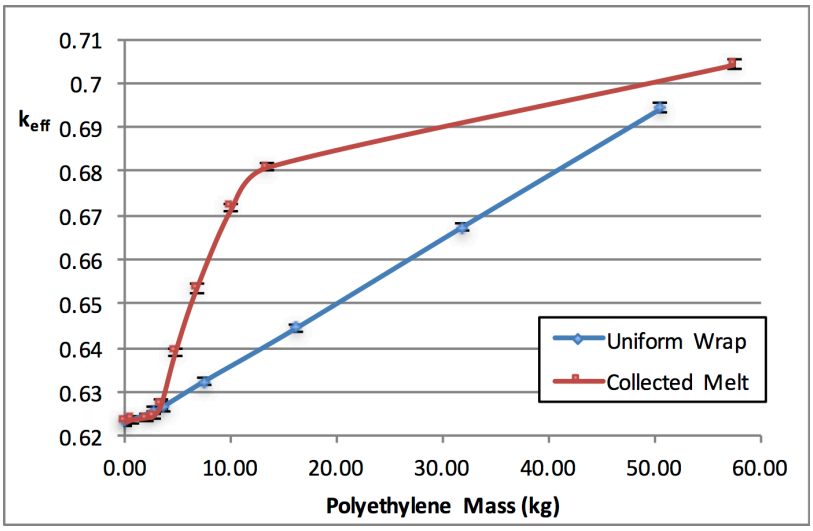

Figure 6-63 Polyethylene Sensitivity Results – HAC Package Array (Rod Pipe U_3Si_2 Fuel Rods)

The tolerance sensitivity study evaluates fuel pellet diameter only, as defined in Section 6.3.4.3.9. The Rod Pipe contents do not credit cladding or have a set pitch, therefore, these parameters are not evaluated. Table 6-89 defines the parameter dimensions evaluated and the results. The most reactive case is highlighted for each package variant and tolerance parameter.

Table 6-89 Tolerance Sensitivity Results – HAC Package Array, Rod Pipe

Content	Traveller Variant	Pellet OD Tolerance (in.)	k_{eff}	σ	$k_{eff} + 2\sigma$	$\Delta(k_{eff} + 2\sigma)$
Rod Pipe UO_2 Fuel Rods	XL	-0.0014	0.66325	0.00047	0.66419	-0.00066
		-0.0010	0.66353	0.00055	0.66463	-0.00022
		Baseline Case	0.66385	0.00050	0.66485	--
		+0.0010	0.66446	0.00054	0.66554	0.00069
		+0.0014	0.66473	0.00049	0.66571	0.00086

Table 6-89 Tolerance Sensitivity Results – HAC Package Array, Rod Pipe

Content	Traveller Variant	Pellet OD Tolerance (in.)	k_{eff}	σ	$k_{eff} + 2\sigma$	$\Delta(k_{eff} + 2\sigma)$
Rod Pipe U_3Si_2 Fuel Rods	STD	-0.0014	0.62335	0.00051	0.62437	0.00025
		-0.0010	0.62335	0.00050	0.62435	0.00023
		Baseline Case	0.62316	0.00048	0.62412	--
		+0.0010	0.62267	0.00047	0.62361	-0.00051
		+0.0014	0.62304	0.00059	0.62422	0.00010

The flooding configuration sensitivity study, as defined in Section 6.3.4.3.12, examined two different flooding scenarios in order to determine which was most reactive. Table 6-90 defines the parameters evaluated and the results, and Figure 6-64 and Figure 6-65 display the result trends. The most reactive case is highlighted.

Table 6-90 Flooding Configuration Results – HAC Package Array, Rod Pipe

Content	Traveller Variant	Flooding Configuration	Moderator Density (g/cm^3)	k_{eff}	σ	$k_{eff} + 2\sigma$	$\Delta(k_{eff} + 2\sigma)$
Rod Pipe UO_2 Fuel Rods	XL	**Baseline Case**	0.0	0.66385	0.00050	0.66485	--
		Clamshell Void (Outerpack Cavity Flooded)	0.001	0.66351	0.00048	0.66447	-0.00038
			0.01	0.65884	0.00068	0.66020	-0.00465
			0.1	0.62875	0.00048	0.62971	-0.03514
			0.5	0.60516	0.00050	0.60616	-0.05869
			0.7	0.60526	0.00052	0.60630	-0.05855
			1.0	0.6075	0.00045	0.60840	-0.05645
		Outerpack Cavity Void (Clamshell Flooded)	0.001	0.66364	0.00055	0.66474	-0.00011
			0.01	0.6643	0.00047	0.66524	0.00039
			0.1	0.66599	0.00050	0.66699	0.00214
			0.5	0.69975	0.00045	0.70065	0.03580
			0.7	0.71337	0.00053	0.71443	0.04958
			1.0	0.72879	0.00059	0.72997	0.06512
Rod Pipe U_3Si_2 Fuel Rods	STD	**Baseline Case**	0.0	0.62316	0.00048	0.62412	--
		Clamshell Void (Outerpack Cavity Flooded)	0.001	0.62245	0.0005	0.62345	-0.00067
			0.01	0.61712	0.00047	0.61806	-0.00606
			0.1	0.58969	0.00048	0.59065	-0.03347
			0.5	0.57012	0.00049	0.5711	-0.05302
			0.7	0.57096	0.00044	0.57184	-0.05228
			1.0	0.57298	0.00052	0.57402	-0.0501
		Outerpack Cavity Void (Clamshell Flooded)	0.001	0.62255	0.00043	0.62341	-0.00071
			0.01	0.62233	0.00049	0.62331	-0.00081
			0.1	0.62469	0.00044	0.62557	0.00145
			0.5	0.65661	0.00045	0.65751	0.03339
			0.7	0.67019	0.00064	0.67147	0.04735
			1.0	0.68433	0.00049	0.68531	0.06119

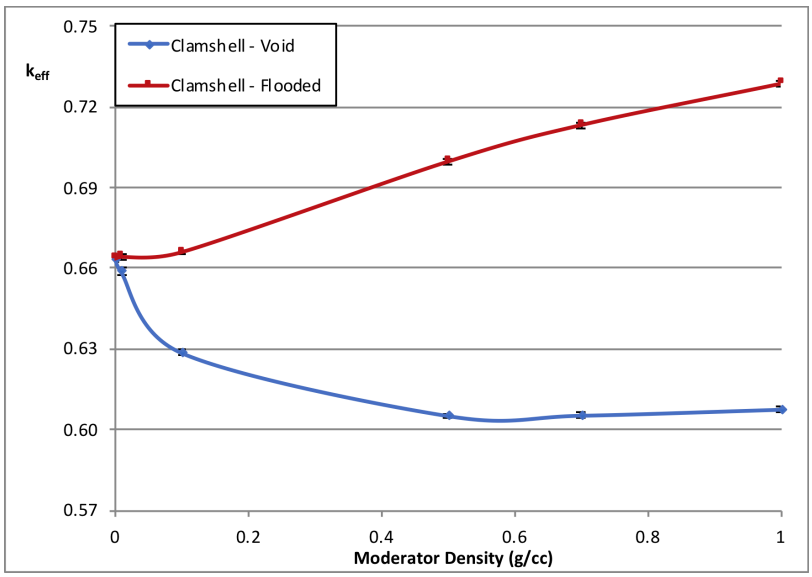

Figure 6-64 Flooding Configuration Sensitivity Results – HAC Package Array (Rod Pipe UO_2 Rods)

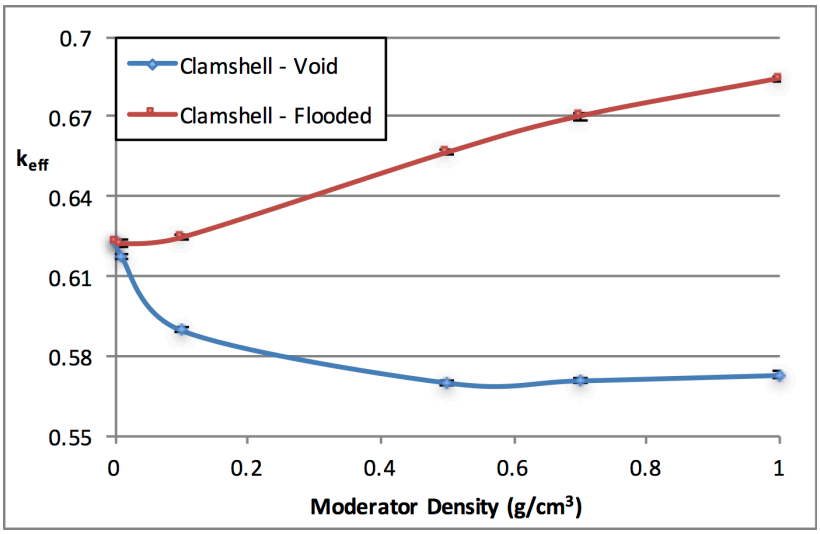

Figure 6-65 Flooding Configuration Sensitivity Results – HAC Package Array (Rod Pipe U_3Si_2 Rods)

The ADOPT Fuel sensitivity study, as defined in Section 6.3.4.3.13, examined the effect of replacing standard UO_2 fuel with ADOPT fuel. Table 6-90A lists the results of the study. The most reactive case is highlighted.

Table 6-90A ADOPT Fuel Results – HAC Package Array, Rod Pipe

Content	Traveller Variant	Fuel	k_{eff}	σ	$k_{eff} + 2\sigma$	$\Delta(k_{eff} + 2\sigma)$
Rod Pipe UO_2 Fuel Rods	XL	**Baseline (UO_2)**	0.66385	0.0005	0.66485	--
		ADOPT	0.66347	0.00047	0.66441	-0.00044

6.7 FISSILE MATERIAL PACKAGES FOR AIR TRANSPORT

The Traveller is not presently authorized for air transport.

6.7.1 Configuration

Not applicable.

6.7.2 Results

Not applicable.

6.8 BENCHMARK EVALUATIONS

6.8.1 Applicability of Benchmark Experiments

Benchmark experiments are selected based on their applicability to the criticality analyses for which the USL function is being generated. Per NUREG/CR-6361, Section 5.1 [7]: "there are three fundamental parameters that should be considered in the selection of suitable experiments for use in the evaluation of transportation and storage package designs. They are the materials of construction (including fissionable material), the geometry of construction, and the inherent neutron energy spectrum affecting the fissionable material(s)." While there are no benchmarks that are entirely alike the application case, benchmark experiments are selected on the basis of being as similar as possible to the Traveller criticality analysis case.

The materials of construction for the Traveller criticality models are low-enriched UO_2 (5-7 wt.% ^{235}U) or U_3Si_2 (5 wt.% ^{235}U) fuel pellets bare or encapsulated by zirconium cladding, surrounded by the aluminum, BORAL, and stainless steel plates that make up the Traveller packaging. Moderation is provided by water that is modeled in the package to consider a flooding event. The geometry of construction for the Traveller criticality safety models are multiple square or hexagonal arrays of fuel rods, separated from each other by the materials of the Traveller packaging. The inherent neutron energy spectrum affecting the fissionable material in the Traveller criticality safety models is a thermalized spectrum, due to the low enrichment of the fuel, and flooding of the package.

In order to generate an applicable USL function for the Traveller criticality safety analysis, a group of benchmarks is selected from the ICSBEP Handbook [8]. All benchmark cases were selected from the series labeled 'LEU-COMP-THERM-XXX' shortened in this report to 'LCT-XXX' with 'XXX' as the identifier of the individual benchmark set. The title of each benchmark experiment is based on its defining characteristics:

LEU – Low-Enriched Uranium
COMP – Compound System (arrays of solid rods)
THERM – Thermal Energy Spectrum

Thus, the 'LCT-XXX' series of experiments is the most similar to the application case of the Traveller packaging transporting a fuel assembly. Within the 'LCT-XXX' series, the experiments most like the application case are selected. The experiments have water-moderated UO_2 fuel rods, with materials of construction similar to the Traveller packaging (aluminum, stainless steel, Zirconium, and BORAL). The experiments are summarized in Table 6-91.

Although the U_3Si_2 loose rod case has a different fuel composition than the UO_2 benchmark experiments, all other aspects of the benchmarks are similar. The U_3Si_2 loose rods are still a low enriched uranium compound system with a thermalized neutron energy spectrum. Thus, the USL function calculated is considered applicable to the U_3Si_2 loose rod analysis. It can also be noted that for both loose rod analyses (UO_2 and U_3Si_2 rods) there is a significant margin between the calculated values for the *Maximum* k_{eff} and USL, making any small change in the USL from rod composition insignificant.

Table 6-91 Benchmark Experiment Summary

Benchmark Group	No. Experiments	Enrichment (wt.% ^{235}U)	Clad Material	Array Shape	Pitch (cm)	Fuel OD [a] (cm)	Clad OD [a] (cm)
LCT-002	5	4.306	Aluminum	Square	2.54	1.265	1.415
LCT-006	18	2.600	Aluminum	Square	Varying	1.250	1.417
LCT-007	10	4.738	Aluminum	Square / Hex	Varying	0.789	0.940
LCT-009	9	4.306	Aluminum	Square	2.54	1.265	1.415
LCT-018	1	7.000	Stainless Steel	Square	1.32	0.743	0.843
LCT-020	7	5.000	Zirconium	Hexagonal	1.3	0.460	0.610
LCT-023	6	10.00	Stainless Steel	Hexagonal	1.4	0.416	0.510
LCT-025	4	7.410	Stainless Steel	Hexagonal	Varying	0.416	0.510
LCT-031	6	5.000	Zirconium	Hexagonal	0.8	0.460	0.610
LCT-034	6	4.738	Aluminum	Square	1.6	0.789	0.940
LCT-080	11	6.903	Aluminum	Square	0.8001	0.526	0.635

Note: [a] Values rounded to indicated precision.

6.8.2 Bias Determination

Using the trending parameter data and the k_{eff} results of the benchmark experiments, correlation coefficients are generated for each of the four trending parameters considered. The calculated correlation coefficients are provided in Table 6-92. A larger correlation coefficient for a parameter indicates a stronger correlation between the parameter and k_{eff}. From this table, it is evident that the trending parameter s with the highest correlation coefficients are EALF and H/X ratio. The correlation coefficients of these parameters are effectively the same, considering that the statistical error in the k_{eff} values used for the trends. Additionally, these two parameters are both used to characterize the same effect in degree of thermalization of the system. Thus, for consistency with the prior revisions of the Traveller criticality safety analysis, the EALF parameter is used to generate the USL with the USLSTATS code.

Table 6-92 Parameter Correlation Coefficient Results

Parameter	R^2	Correlation Coefficient
EALF	0.23237	0.48205
Fuel Enrichment	0.01880	0.13711
WtF Volume Ratio	0.11719	0.34233
H/X Ratio	0.23724	0.48707

The USLSTATS input is produced using the typical values for the problem-specific second-line parameters (as described in Appendix C of NUREG/CR-6361) and the benchmark experiment data used to generate the correlation coefficients of Table 6-92. Using this input, the plot shown in Figure 6-66 is generated.

The USL is equivalent to:

$$USL = 1 - \Delta k_m + \beta - \Delta\beta$$

Where, Δk_m is the administrative margin equivalent to 0.05, β is the bias in the USL(1) calculation, and $\Delta\beta$ is the uncertainty in the USL(1) calculation.

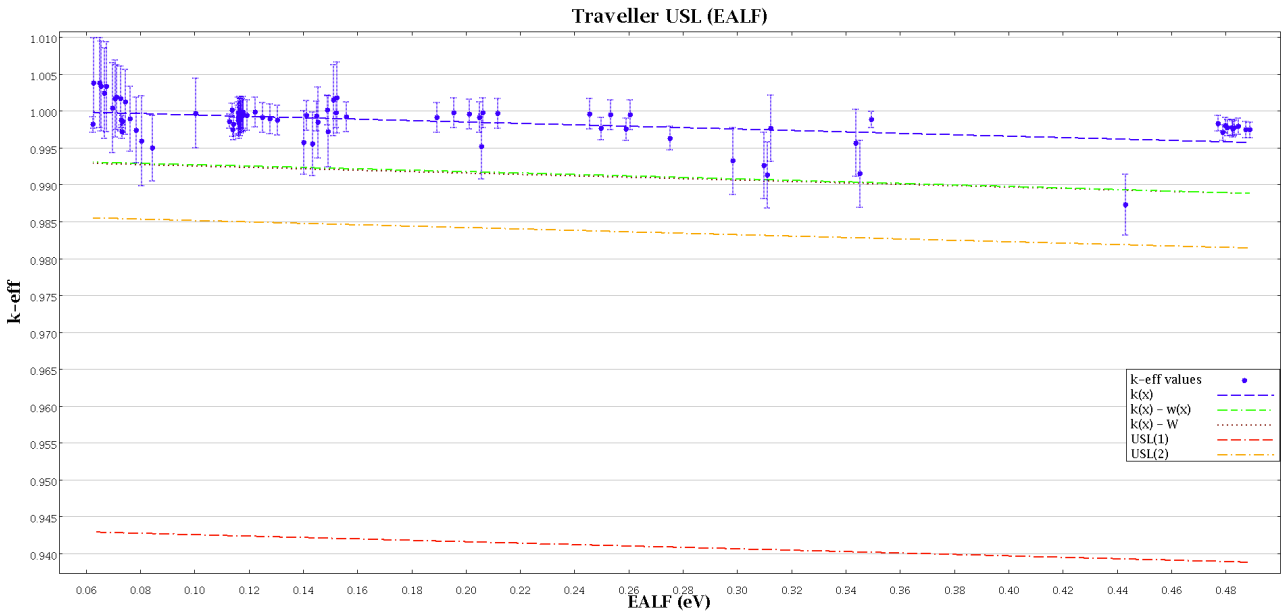

Figure 6-66 EALF USLSTATS Plot

The USLSTATS input also generates USL functions for both Method 1 and Method 2 as described in Appendix C of Reference 6. These USL functions are provided below, where the variable 'X' is the EALF of the system. USL(1) is the USL as calculated with Δk_m equivalent to 0.05. USL(2) is the USL as calculated with a purely statistical margin. If USL(1) is less than USL(2), the adequacy of the value of Δk_m selected is proven. The yellow (USL(2)) and red (USL(1)) curves in Figure 6-66 are generated with these functions. The USLSTATS output states that the data tests normal, verifying the validity of the USL functions generated. In addition, from Figure 6-66 it is clear that USL 1 is always less than USL 2, which verifies the administrative margin applied for Method 1 (Δk_m = 0.05) is sufficient. The Area of Applicability for these USL functions is between the minimum and maximum benchmark experiment EALF values: 0.063 to 0.489 eV.

The USL for the Traveller criticality safety analysis should be calculated by entering the EALF value of the limiting Traveller case in as the value 'X' in the USL1 function, and further reducing the value calculated to account for any additional sensitivity studies.

<u>USL1 Function:</u>
USL1 = 0.9435 + (-9.5714E-03) • X

<u>USL2 Function:</u>
USL2 = 0.9861 + (-9.5714E-03) • X

6.9 APPENDIX

The following appendices are included with Section 6:

6.9.1 References
6.9.2 Categorized Fuel Assembly Analysis
6.9.3 Baseline Detailed Results
6.9.4 Combined Cases

6.9.1 References

[1] U.S. Nuclear Regulatory Commission, "10 CFR Part 71 - Packaging and Transportation of Radioactive Material," 2016.

[2] International Atomic Energy Agency, "Regulations for the Safe Transport of Radioactive Material," 2012 Edition.

[3] R. J. McConn Jr., C. J. Gesh, R. T. Pagh, R. A. Rucker and R. G. Williams III, "Compendium of Material Composition Data for Radiation Transport Modeling," 2011.

[4] H. R. Dyer and C. V. Parks, "Recommendations for Preparing the Criticality Safety Evaluation of Transportation Packages," 1997.

[5] "Scale: A Comprehensive Modeling and Simulation Suite for Nuclear Safety Analysis and Design," SCALE 6.1.2, 2013.

[6] "Scale: A Comprehensive Modeling and Simulation Suite for Nuclear Safety Analysis and Design," SCALE 6.1.3, 2013.

[7] J. J. Licthenwalter, S. M. Bowman, M. D. DeHart and C. M. Hopper, "Criticality Benchmark Guide for Light-Water-Reactor Fuel in Transportation and Storage Packages," 1997.

[8] Organization for Economic Cooperation and Development - Nuclear Energy Agency (OECD-NEA), "International Handbook of Evaluated Criticality Safety Benchmark Experiments," 2014.

6.9.2 Categorized Fuel Assembly Analysis

Three fuel assembly parameters (primary parameters) are used in this analysis to define a bin: array size (e.g. a 17x17 array of lattice cells), fuel rod pattern (i.e. the number and location of fuel rods and non-fuel holes), and nominal fuel rod pitch. A unique combination of primary parameters that are characteristic of a set of fuel assembly designs is called a bin (e.g. 17 Bin 1). The nominal fuel assembly designs that constitute a bin form the basis for its range of secondary parameters (fuel pellet OD, cladding ID, and cladding thickness). The most reactive combination of secondary parameters of a bin is called the categorized fuel assembly (CFA) of that bin. These parameters are verified to be most reactive through a comparison of the variation of secondary parameters among the theoretical fuel assemblies of that bin.

6.9.2.1 CFA Results

For each bin in this analysis, the minimum values of all secondary parameters are determined to be the most reactive. This is primarily due to the fact that fuel assemblies are designed to be under-moderated, so reducing the fuel pellet radius, the fuel-clad gap, and the cladding thickness to their minimum values increases neutron moderation by allowing for the most water possible in the fuel envelope. The CFAs for Groups 1 and 2 are summarized in Table 6-93 and Table 6-94 and the CFAs for Group 4 are summarized in Table 6-94A. The secondary parameter limits for each of the bins in these tables are based on the fuel designs that constitute the respective bin. The maximum fuel length for each bin is set as the maximum length of the fuel designs included in the respective bin, plus one tolerance (0.50 in.).

Table 6-93 Categorized Fuel Assemblies for Input into Package Assessment – Groups 1 and 2

Description	14 Bin 1	14 Bin 2	15 Bin 1	15 Bin 2	16 Bin 1
Array Size	14x14	14x14	15x15	15x15	16x16
Fuel Rods	176	179	204	205	236
Non-Fuel Holes	20	17	21	20	20
Nominal Pitch (in./cm)	0.580 (1.47320)	0.556 (1.41224)	0.563 (1.43002)	0.563 (1.430 cm)	0.563 (1.430 cm)
Minimum Fuel Pellet OD (in./cm)	0.3805 (0.96647)	0.3439 (0.87351)	0.3582 (0.90973)	0.3580 (0.90922 cm)	0.3581 (0.9097 cm)
Minimum Cladding ID (in./cm)	0.3855 (0.97917)	0.3489 (0.88621)	0.3636 (0.92365)	0.3627 (0.92136 cm)	0.3665 (0.9310 cm)
Minimum Cladding Thickness (in./cm)	0.0245 (0.06223)	0.0228 (0.05791)	0.0228 (0.05791)	0.0265 (0.06742 cm)	0.0283 (0.0720 cm)
Cladding Material	Zirconium Alloy	Zirconium Alloy	Zirconium Alloy	Zirconium alloy	Zirconium Alloy
Maximum Active Fuel Length (in./cm)	137.20 (348.49)	144.50 (367.03)	144.50 (367.03)	140.26 (356.27)	154.04 (391.27)

Note: The secondary parameter limits for 16 Bin 1 are slightly different than the minimums listed in Section 6.9.2.6.5 due to unit conversions and rounding.

Table 6-94 Categorized Fuel Assemblies for Input into Package Assessment – Groups 1 and 2

Description	16 Bin 2	16 Bin 3	17 Bin 1	17 Bin 2	18 Bin 1
Array Size	16x16	16x16	17x17	17x17	18x18
Fuel Rods	236	235	264	264	300
Non-Fuel Holes	20	21	25	25	24
Nominal Pitch (in.)	0.506 (1.28524)	0.485 (1.23190)	0.496 (1.25984)	0.502 (1.27508)	0.500 (1.270 cm)
Minimum Fuel Pellet OD (in.)	0.3220 (0.81788)	0.3083 (0.78308)	0.3083 (0.78308)	0.3238 (0.82245)	0.3165 (0.80392 cm)
Minimum Cladding ID (in.)	0.3265 (0.82931)	0.3125 (0.79375)	0.3125 (0.79375)	0.3276 (0.83210)	0.3236 (0.8220 cm)
Minimum Cladding Thickness (in.)	0.0210 (0.05334)	0.0210 (0.05334)	0.0210 (0.05334)	0.0220 (0.05588)	0.0252 (0.0640 cm)
Cladding Material	Zirconium Alloy	Zirconium Alloy	Zirconium Alloy	Zirconium Alloy	Zirconium Alloy
Maximum Active Fuel Length (in.)	150.50 (382.27)	144.50 (367.03)	168.50 (427.99)	144.50 (367.03)	154.04 (391.27)

Note: The secondary parameter limits for 18 Bin 1 are slightly different than the minimums listed in Section 6.9.2.6.10 due to unit conversions and rounding.

Table 6-94A Categorized Fuel Assemblies for Input into Package Assessment – Group 4

Description	14 Bin 1	14 Bin 2	15 Bin 3	16 Bin 2	16 Bin 3	17 Bin 1
Array Size	14x14	14x14	15x15	16x16	16x16	17x17
Fuel Rods	176	179	204	236	235	264
Non-Fuel Holes	20	17	21	20	21	25
GT/IT	5[a]	17	21	5[a]	21	25
Nominal Pitch (in./cm)	0.580 (1.4732)	0.556 (1.4122)	0.563 (1.4300)	0.506 (1.2852)	0.485 (1.2319)	0.496 (1.2598)
Minimum Fuel Pellet OD (in./cm)	0.3805 (0.9665)	0.3439 (0.8735)	0.3654 (0.9281)	0.3220 (0.8179)	0.3083 (0.7831)	0.3083 (0.7831)
Minimum Cladding ID (in./cm)	0.3855 (0.9792)	0.3489 (0.8862)	0.3709 (0.9421)	0.3265 (0.8293)	0.3125 (0.7938)	0.3125 (0.7938)
Minimum Cladding Thickness (in./cm)	0.0245 (0.0622)	0.0228 (0.0579)	0.0228 (0.0579)	0.0210 (0.0533)	0.0210 (0.0533)	0.0210 (0.0533)
Minimum GT/IT ID (in./cm)	0.9630 (2.4460)	0.3720 (0.9449)	0.4970 (1.2624)	0.5450 (1.3843)	0.3810 (0.9677)	0.3950 (1.0033)
Minimum GT/IT Thickness (in./cm)	0.0360 (0.0914)	0.0147 (0.0373)	0.0147 (0.0373)	0.0360 (0.0914)	0.0157 (0.0399)	0.0137 (0.0348)
Cladding Material	Zirconium Alloy	Zirconium Alloy	Zirconium Alloy	Zirconium Alloy	Zirconium Alloy	Zirconium Alloy
Maximum Active Fuel Length (in./cm)	137.20 (348.49)	144.50 (367.03)	144.50 (367.03)	150.00 (381.00)	144.00 (365.76)	168.00 (426.72)

Note: [a] Each GT/IT for this bin occupies a 2x2 array of lattice pins.

6.9.2.2 Organizing Fuel Assemblies into Bins

Table 6-95 and Figure 6-67 present four fuel assembly designs and their relevant primary parameters to show how fuel assembly designs are organized into bins. The [ ]^{a,c} fuel assembly is analyzed by itself in "16 Bin 1," and the [ ]^{a,c} fuel assemblies are analyzed together to create "16 Bin 2" because these three fuel assembly designs have identical array sizes, fuel rod patterns, and pitches. Although [ ]^{a,c} shares the same number of fuel rods and non-fuel holes with the [ ]^{a,c} assemblies, the fuel rod pattern and nominal fuel rod pitch differ. Figure 6-67 is included to demonstrate the

variations in patterns and pitch between fuel assembly designs.

Table 6-95 Bin Organization Example				
Bin	16 Bin 1	16 Bin 2		
Fuel Assembly Type	[			]^{a,c}
Primary Parameters of Fuel Assembly Designs				
Array Size	16 x 16	16 x 16	16 x 16	16 x 16
No. of Fuel Rods per Assembly	236	236	236	236
No. of Non-Fuel Holes	20	20	20	20
Nominal Fuel Rod Pitch (in.)	[			]^{a,c}
Secondary Parameters of Fuel Assembly Designs				
Nominal Fuel Pellet Diameter (in.)	[			]^{a,c}
Nominal Clad Inner Diameter (in.)	[			]^{a,c}
Nominal Clad Outer Diameter (in.)	[			]^{a,c}

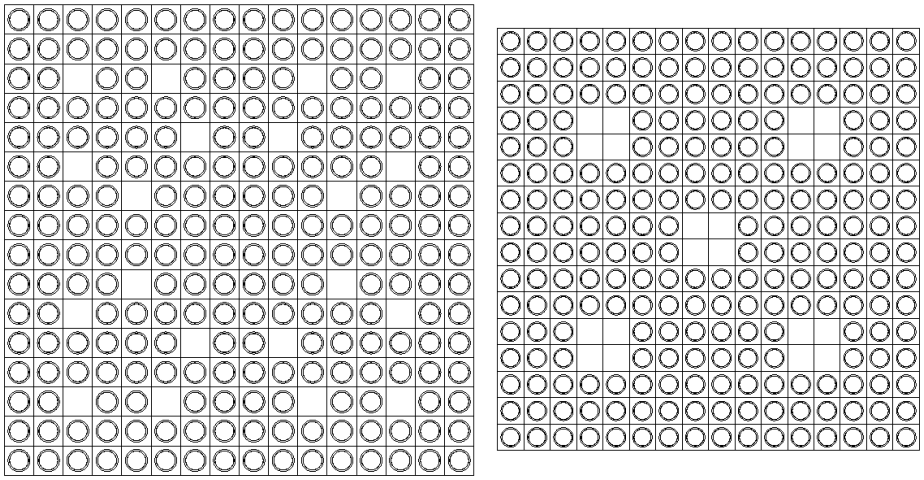

Figure 6-67 Fuel Rod Patterns of 16 Bin 1 (left) and 16 Bin 2 (right) – Not to Scale

6.9.2.3 Determination of Categorized Fuel Assemblies

Upon grouping the nominal fuel assembly designs into bins, the ranges of each secondary parameter (fuel pellet diameter, cladding ID, and cladding thickness) are examined by creating fuel assembly permutations that fully represent the secondary parameter ranges of each bin. For Group 4 contents, the additional secondary parameters of GT/IT ID and GT/IT thickness are examined. Although cladding ID and cladding OD are the dimensions reported for fuel assembly designs, examining the secondary parameters in terms of fuel-clad gap (clad inner radius – fuel pellet radius) and cladding thickness (cladding outer radius – cladding inner radius) results in a more straightforward observation of trends in k_∞. The CFAs analyzed in Section 6.2 are based on secondary parameter limits set from the trends observed for each bin.

6.9.2.3.1 Determining Secondary Parameter Ranges

The fuel pellet radius range of a bin is determined using the nominal fuel pellet diameters of the fuel assemblies of that bin and their respective tolerances. If a bin has only one nominal fuel assembly design, the fuel pellet diameter range consists of the nominal fuel pellet diameter of that design plus or minus the fuel pellet diameter tolerance. If there is more than one fuel assembly design in a bin, the upper limit of the range is the largest nominal fuel pellet diameter of the bin plus one tolerance and the lower limit is the smallest nominal fuel pellet diameter of the bin minus one tolerance. Up to two additional, equally spaced intervals between the upper and lower limits are then added depending on if more than one fuel assembly design applies to a bin. These two scenarios are shown in Table 6-96. This methodology also applies for the fuel-clad gap, the cladding thickness, GT/IT inner diameter, and GT/IT thickness parameter ranges.

Table 6-96 Fuel Pellet Radius Range Determination

Dimensions	16 Bin 2			17 Bin 2
	[			]^{a,c}
Fuel Diameter (in.)	[			]^{a,c}
Fuel Diameter Tolerance (in.)	[			]^{a,c}
Minus Radius (in.)	[			]^{a,c}
Nominal Radius (in.)	[			]^{a,c}
Plus Radius (in.)	[			]^{a,c}
Lower Limit (in.)	[			]^{a,c}
Interval 1 (in.)	[			]^{a,c}
Interval 2 (in.)	[ ]^{a,c}			-
Upper Limit (in.)	[			]^{a,c}

6.9.2.3.2 Case Naming Convention

6.9.2.3.2.1 Bin Permutations

An example of a bin's fuel assembly permutation case name is 14bin1_4_2_3_in. The nomenclature for each case name includes the bin (14bin1), three numbers separated by underscores (4_2_3) that signify which fuel radius (the fourth in the range), fuel-clad gap (the second in the range), and cladding thickness (the third in the range) are modeled, respectively.

6.9.2.3.2.2 Additional Cases

An example additional case name is 14bin1gp_1_in. The first part of this case name (14bin1) is the same as for the bin's original permutations. These cases model additional fuel-clad gaps (gp) that are ± 1 and 2 tolerances from both the minimum and maximum fuel-clad gaps, with the following naming convention: -2 tolerances (1), -1 tolerance (2), +1 tolerance (3), and +2 tolerances (4). The addition of these cases results in a total fuel-clad gap range examined of approximately ± 3 to 4 tolerances. If the most reactive fuel assembly permutation is 14bin1_1_1_1_in, the additional fuel-clad gap cases also model fuel pellet radius 1 and cladding thickness 1. This same methodology is also applied to fuel pellet radius where applicable, replacing "gp" with

"fr" in the case name. The cladding thickness ranges are always sufficiently large as to not require extra cases.

6.9.2.4 Determination of Most Reactive Secondary Parameters

The most reactive combination of secondary parameters of a bin defines the bin's CFA. These parameters are deemed most reactive through comparative analyses of the fuel assembly permutations of a bin, which examine the individual effect of fuel pellet radius, fuel-clad gap, and cladding thickness on k_∞. In order to examine the effect of a secondary parameter on k_∞, the two other secondary parameters are held constant as the parameter of interest is varied. Each permutation models a unique combination of secondary parameters. The most reactive permutation of each bin is selected as the starting point of the comparative analyses of each bin because this permutation is hypothesized to model the most reactive secondary parameters. For PWR Group 4 contents, the case with the bounding secondary parameters of fuel pellet radius, fuel-clad gap, and cladding thickness is then used as the basis to examine the effect of GT/IT inner radius and GT/IT thickness.

Linear regression curves and R^2 values are added to the comparative study plots to better highlight the trends involved and prove the effect relating a secondary parameter to k_∞. The ranges examined are small; therefore, a linear regression was deemed acceptable. For example, fuel-clad gap does not have a strong effect on k_∞. Because of this, additional cases are added to all fuel-clad gap comparative studies. As shown in this appendix, the conclusion of all the studies is that these parameters examined are all negatively correlated to k_∞, proving that the minimum of all the parameters examined is the most reactive.

The figures in this appendix show the three secondary parameter variations of a bin in a single plot. This is accomplished by normalizing the secondary parameters, i.e. representing the secondary parameters as a difference from the minimum value of a secondary parameter range. For example, in Table 6-98, case 14bin1_1_1_1_in's fuel pellet radius of 0.48324 cm is represented as 0 cm in Figure 6-69. In addition, the GT/IT secondary parameters are shown together in a separate plot.

6.9.2.5 Bin Permutation Model

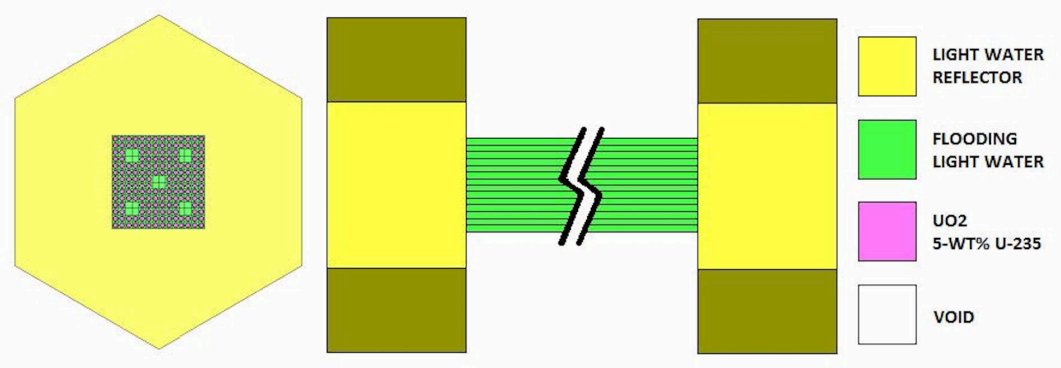

Figure 6-68 x-y (left) and x-z (right) Cross Sections of a Fuel Assembly Permutation. Not to Scale.

Fuel assemblies are modeled in hexagonally pitched arrays that are infinite in the x-y plane. The infinite planar array models white boundary conditions on the lateral faces of the hexagonal prism with 30.48 cm of full-density, light water reflection in the z direction (the long axis of the fuel assembly), and with void between the flooded fuel assembly envelope and the boundaries of the unit, as shown in Figure 6-68. No packaging

materials are modeled in this analysis. However, the pitch of the fuel assemblies in the infinite array takes credit for the spacing afforded by the Traveller packaging outer diameter, but no credit is taken for any spacing provided by handling and stacking features. The fuel assemblies are centered in this spacing.

Several modeling conditions were chosen for this analysis that are bounding of actual conditions:

1. UO_2 is modeled at theoretical density (10.96 g/cm^3) and at an enrichment of 5 wt.% ^{235}U for Groups 1 and 2 and 6 wt.% ^{235}U for Group 4 with the remaining uranium modeled solely as ^{238}U, as this is the bounding configuration permitted in the Traveller.
2. All water is modeled as full density light water at room temperature.
3. All fuel cladding and GT/IT for Group 4 CFAs are modeled as the built-in Zircaloy-4 material of SCALE 6.1.2.
4. Active fuel length is modeled at 168.5 in. for all fuel assembly permutations, as this is the maximum active fuel length of all fuel assembly designs considered, with the largest tolerance of the active fuel length applied, 0.5 in. No credit is taken for fuel pellet dishing or chamfering in this analysis as no individual fuel pellets are modeled. Instead, the fuel is modeled as one continuous cylinder of UO_2.
5. The entire fuel assembly envelope is modeled as flooded with light water, including all fuel-clad gaps.

6.9.2.6 CFA Most Reactive Secondary Parameters

For all bins analyzed, the minimum fuel pellet diameter, fuel-clad gap, and cladding thickness are bounding for each bin. The ranges of secondary fuel assembly parameters for each bin of Groups 1 and 2 are listed in Table 6-97 and the ranges for Group 4 are listed in Table 6-97A.

Table 6-97 Secondary Fuel Assembly Parameter Ranges – Groups 1 and 2

Bin		Parameter		
		Fuel Pellet OD	Cladding ID	Cladding OD
14 Bin 1	Maximum in. (cm)	[		]^{a,c}
	Minimum in. (cm)	[		]^{a,c}
14 Bin 2	Maximum in. (cm)	[		]^{a,c}
	Minimum in. (cm)	[		]^{a,c}
15 Bin 1	Maximum in. (cm)	[		]^{a,c}
	Minimum in. (cm)	[		]^{a,c}
15 Bin 2	Maximum in. (cm)	[		]^{a,c}
	Minimum in. (cm)	[		]^{a,c}
16 Bin 1	Maximum in. (cm)	[		]^{a,c}
	Minimum in. (cm)	[		]^{a,c}

Table 6-97 Secondary Fuel Assembly Parameter Ranges – Groups 1 and 2

Bin		Parameter		
		Fuel Pellet OD	Cladding ID	Cladding OD
16 Bin 2	Maximum in. (cm)	[		]a,c
	Minimum in. (cm)	[		]a,c
16 Bin 3	Maximum in. (cm)	[		]a,c
	Minimum in. (cm)	[		]a,c
17 Bin 1	Maximum in. (cm)	[		]a,c
	Minimum in. (cm)	[		]a,c
17 Bin 2	Maximum in. (cm)	[		]a,c
	Minimum in. (cm)	[		]a,c
18 Bin 1	Maximum in. (cm)	[		]a,c
	Minimum in. (cm)	[		]a,c

Table 6-97A Secondary Fuel Assembly Parameter Ranges – Group 4

Bin		Secondary Parameter				
		Fuel Pellet OD	Cladding ID	Cladding OD	GT/IT ID	GT/IT OD
14 Bin 1	Maximum in. (cm)	[				]a,c
	Minimum in. (cm)	[				]a,c
14 Bin 2	Maximum in. (cm)	[				]a,c
	Minimum in. (cm)	[				]a,c
15 Bin 3	Maximum in. (cm)	[				]a,c
	Minimum in. (cm)	[				]a,c
16 Bin 2	Maximum in. (cm)	[				]a,c
	Minimum in. (cm)	[				]a,c

Table 6-97A Secondary Fuel Assembly Parameter Ranges – Group 4						
Bin		**Secondary Parameter**				
		Fuel Pellet OD	**Cladding ID**	**Cladding OD**	**GT/IT ID**	**GT/IT OD**
16 Bin 3	**Maximum in. (cm)**	[				]a,c
	Minimum in. (cm)	[				]a,c
17 Bin 1	**Maximum in. (cm)**	[				]a,c
	Minimum in. (cm)	[				]a,c

6.9.2.6.1 14 Bin 1

The following comparative analyses, shown in Table 6-98 and Figure 6-69, demonstrate the effect of fuel pellet radius, fuel-clad gap, and cladding thickness on k_∞ for 14 Bin 1 and verify that the minimum dimension is the most reactive for all three secondary parameters. The minimum value of each secondary parameter range is shaded in gray in Table 6-98.

Table 6-98 Effect of Secondary Parameters on k-inf - 14 Bin 1				
Case	**Fuel Pellet Radius (cm)**	**Delta from Minimum (cm)**	k_∞	**σ**
14bin1fr_1_in	[ ]a,c	-0.00127	1.40062	0.00026
14bin1fr_2_in	[ ]a,c	-0.00064	1.40053	0.00027
14bin1_1_1_1_in	[ ]a,c	0.0	1.40061	0.00026
14bin1_2_1_1_in	[ ]a,c	0.00063	1.40061	0.00033
14bin1_3_1_1_in	[ ]a,c	0.00127	1.39959	0.00028
14bin1fr_3_in	[ ]a,c	0.00190	1.39897	0.00027
14bin1fr_4_in	[ ]a,c	0.00254	1.39959	0.00031
Case	**Fuel-Clad Gap Thickness (cm)**	**Delta from Minimum (cm)**	k_∞	**σ**
14bin1gp_1_in	[ ]a,c	-0.00508	1.40084	0.00031
14bin1gp_2_in	[ ]a,c	-0.00254	1.40068	0.00027
14bin1_1_1_1_in	[ ]a,c	0.0	1.40061	0.00026
14bin1_1_2_1_in	[ ]a,c	0.00254	1.40019	0.00029
14bin1_1_3_1_in	[ ]a,c	0.00508	1.39982	0.00027
14bin1gp_3_in	[ ]a,c	0.00762	1.39980	0.00026
14bin1gp_4_in	[ ]a,c	0.01016	1.39987	0.00029
Case	**Clad Thickness (cm)**	**Delta from Minimum (cm)**	k_∞	**σ**
14bin1_1_1_1_in	[ ]a,c	0.0	1.40061	0.00026
14bin1_1_1_2_in	[ ]a,c	0.00423	1.39826	0.00029
14bin1_1_1_3_in	[ ]a,c	0.00847	1.39655	0.00028

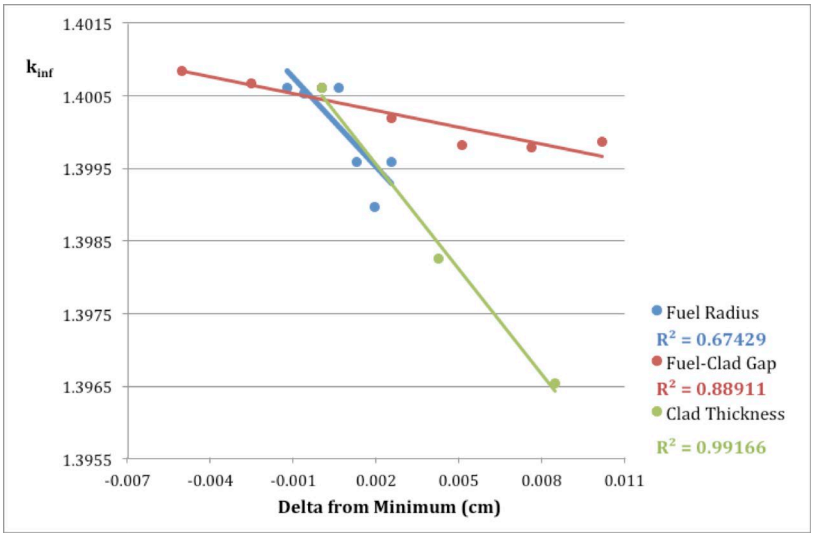

Figure 6-69 Trend Plot of Effect of Secondary Parameters on k-inf – 14 Bin 1

6.9.2.6.2 14 Bin 2

The following comparative analyses, shown in Table 6-99 and Figure 6-70, demonstrate the effect of fuel pellet radius, fuel-clad gap, and cladding thickness on k_∞ for 14 Bin 2 and verify that the minimum dimension is the most reactive for all three secondary parameters. The minimum value of each secondary parameter range is shaded in gray in Table 6-99.

Table 6-99 Effect of Secondary Parameters on 14 Bin 2

Case	Fuel Pellet Radius (cm)	Delta from Minimum (cm)	k_∞	σ
14bin2_1_1_1_in	[ ]^{a,c}	0.0	1.41129	0.00027
14bin2_2_1_1_in	[ ]^{a,c}	0.00953	1.40719	0.00030
14bin2_3_1_1_in	[ ]^{a,c}	0.01905	1.40301	0.00030
14bin2_4_1_1_in	[ ]^{a,c}	0.02858	1.39757	0.00028
Case	**Fuel-Clad Gap Thickness (cm)**	**Delta from Minimum (cm)**	**k_∞**	**σ**
14bin2gp_1_in	[ ]^{a,c}	-0.00508	1.41176	0.00030
14bin2gp_2_in	[ ]^{a,c}	-0.00254	1.41163	0.00031
14bin2_1_1_1_in	[ ]^{a,c}	0.0	1.41129	0.00027
14bin2_1_2_1_in	[ ]^{a,c}	0.00191	1.41139	0.00032
14bin2_1_3_1_in	[ ]^{a,c}	0.00381	1.41089	0.00026
14bin2_1_4_1_in	[ ]^{a,c}	0.00572	1.41136	0.00028
14bin2gp_3_in	[ ]^{a,c}	0.00826	1.41073	0.00031
14bin2gp_4_in	[ ]^{a,c}	0.01080	1.41091	0.00027
Case	**Clad Thickness (cm)**	**Delta from Minimum (cm)**	**k_∞**	**σ**
14bin2_1_1_1_in	[ ]^{a,c}	0.0	1.41129	0.00027
14bin2_1_1_2_in	[ ]^{a,c}	0.00381	1.40960	0.00029
14bin2_1_1_3_in	[ ]^{a,c}	0.00762	1.40802	0.00034

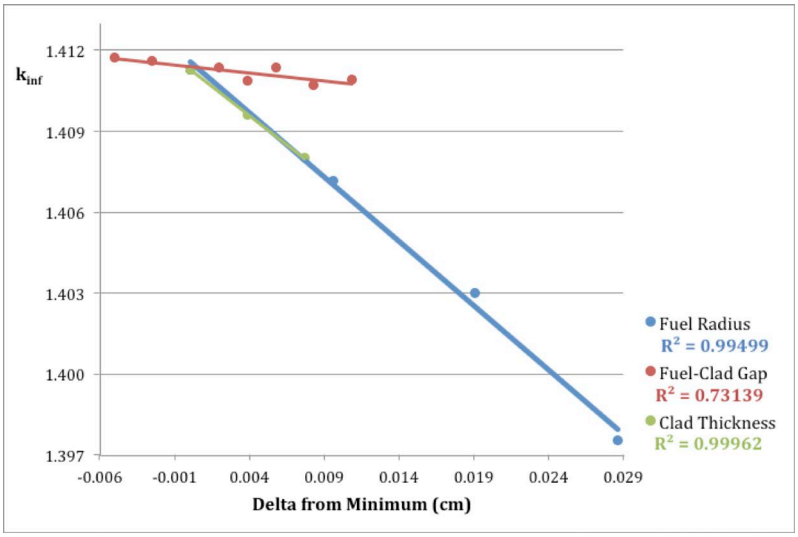

Figure 6-70 Trend Plot of Effect of Secondary Parameters on k-inf – 14 Bin 2

6.9.2.6.3 15 Bin 1

The following comparative analyses, shown in Table 6-100 and Figure 6-71, demonstrate the effect of fuel pellet radius, fuel-clad gap, and cladding thickness on k_∞ for 15 Bin 1 and verify that the minimum dimension is the most reactive for all three secondary parameters. The minimum value of each secondary parameter range is shaded in gray in Table 6-100.

Table 6-100 Effect of Secondary Parameters on 15 Bin 1

Case	Fuel Pellet Radius (cm)	Delta from Minimum (cm)	k_∞	σ
15bin1_1_1_1_in	[ ]a,c	0	1.42514	0.00029
15bin1_2_1_1_in	[ ]a,c	0.00348	1.42381	0.00026
15bin1_3_1_1_in	[ ]a,c	0.00697	1.42180	0.00026
15bin1_4_1_1_in	[ ]a,c	0.01046	1.42039	0.00031
Case	**Fuel-Clad Gap Thickness (cm)**	**Delta from Minimum (cm)**	**k_∞**	**σ**
15bin1gp_1_in	[ ]a,c	-0.00508	1.42573	0.00028
15bin1gp_2_in	[ ]a,c	-0.00254	1.42528	0.00025
15bin1_1_1_1_in	[ ]a,c	0	1.42514	0.00029
15bin1_1_2_1_in	[ ]a,c	0.00170	1.42504	0.00026
15bin1_1_3_1_in_more [1]	[ ]a,c	0.00340	1.42493	0.00027
15bin1_1_4_1_in	[ ]a,c	0.00511	1.42465	0.00031
15bin1gp_3_in	[ ]a,c	0.00765	1.42437	0.00035
15bin1gp_4_in	[ ]a,c	0.01019	1.42406	0.00026
Case	**Clad Thickness (cm)**	**Delta from Minimum (cm)**	**k_∞**	**σ**
15bin1_1_1_1_in	[ ]a,c	0	1.42514	0.00029
15bin1_1_1_2_in	[ ]a,c	0.00613	1.42294	0.00024
15bin1_1_1_3_in	[ ]a,c	0.01227	1.41969	0.00032
15bin1_1_1_4_in	[ ]a,c	0.01840	1.41615	0.00026

Note: [1] More histories were modeled to improve source convergence.

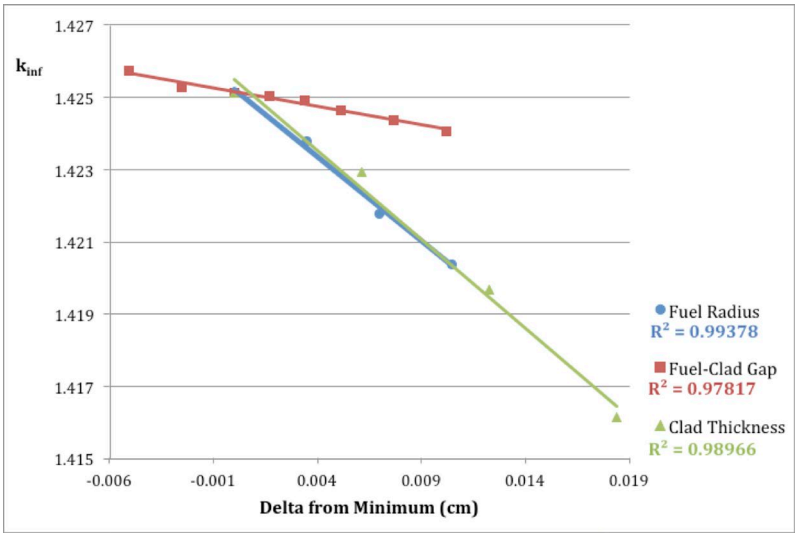

Figure 6-71 Trend Plot of Effect of Secondary Parameters on k-inf – 15 Bin 1

6.9.2.6.4 15 Bin 2

The following comparative analyses, shown in Table 6-101 and Figure 6-72, demonstrate the effect of fuel pellet radius, fuel-clad gap, and cladding thickness on k_∞ for 15 Bin 2 and verify that the minimum dimension is the most reactive for all three secondary parameters. The minimum value of each secondary parameter range is shaded in gray in Table 6-101.

Table 6-101 Effect of Secondary Parameters on 15 Bin 2

Case	Fuel Pellet Radius (cm)	Delta from Minimum (cm)	k_∞	σ
15bin2fr_1_in	[ ]^{a,c}	-0.00178	1.42131	0.00026
15bin2fr_2_in	[ ]^{a,c}	-0.00089	1.42082	0.00028
15bin2_1_1_1_in	[ ]^{a,c}	0.0	1.42018	0.00029
15bin2_2_1_1_in	[ ]^{a,c}	0.00089	1.4199	0.00032
15bin2_3_1_1_in	[ ]^{a,c}	0.00178	1.41932	0.00029
15bin2fr_3_in	[ ]^{a,c}	0.00267	1.41933	0.00025
15bin2fr_4_in	[ ]^{a,c}	0.00356	1.41857	0.00026
Case	**Fuel-Clad Gap Thickness (cm)**	**Delta from Minimum (cm)**	**k_∞**	**σ**
15bin2gp_1_in	[ ]^{a,c}	-0.00607	1.42142	0.00027
15bin2gp_2_in	[ ]^{a,c}	-0.00343	1.4205	0.00036
15bin2_1_1_1_in	[ ]^{a,c}	0.0	1.42018	0.00029
15bin2_1_2_1_in	[ ]^{a,c}	0.00343	1.42024	0.00026
15bin2_1_3_1_in	[ ]^{a,c}	0.00686	1.41958	0.00025
15bin2gp_3_in	[ ]^{a,c}	0.01029	1.41944	0.00026
15bin2gp_4_in [1]	[ ]^{a,c}	0.01372	1.41899	0.00026
Case	**Clad Thickness (cm)**	**Delta from Minimum (cm)**	**k_∞**	**σ**
15bin2_1_1_1_in	[ ]^{a,c}	0.0	1.42018	0.00029
15bin2_1_1_2_in	[ ]^{a,c}	0.00508	1.41822	0.00027
15bin2_1_1_3_in	[ ]^{a,c}	0.01016	1.41463	0.00029

Note: [1] More histories were modeled to improve source convergence.

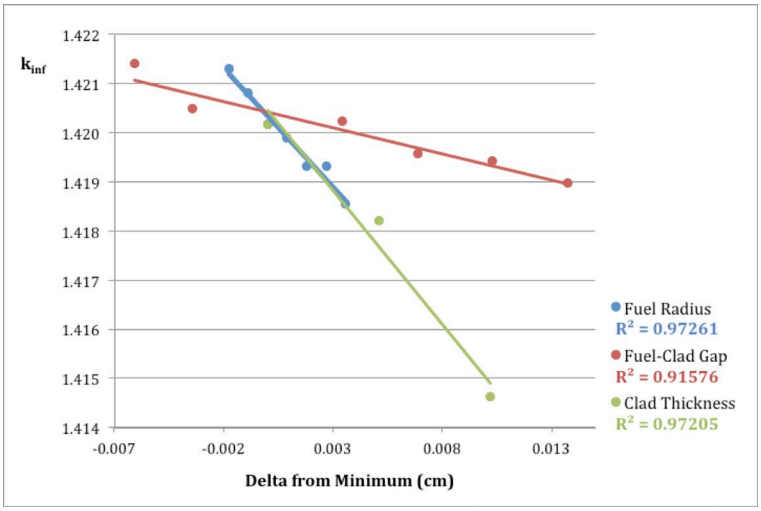

Figure 6-72 Trend Plot of Effect of Secondary Parameters on k-inf – 15 Bin 2

6.9.2.6.5 16 Bin 1

The following comparative analyses, shown in Table 6-102 and Figure 6-73, demonstrate the effect of fuel pellet radius, fuel-clad gap, and cladding thickness on k_∞ for 16 Bin 1 and verify that the minimum dimension is the most reactive for all three secondary parameters. The minimum value of each secondary parameter range is shaded in gray in Table 6-102.

Table 6-102 Effect of Secondary Parameters on 16 Bin 1

Case	Fuel Pellet Radius (cm)	Delta from Minimum (cm)	k_∞	σ
16bin1fr_1_in	[ ]a,c	-0.00127	1.43165	0.00029
16bin1fr_2_in	[ ]a,c	-0.00064	1.43083	0.00027
16bin1_1_1_1_in	[ ]a,c	0.0	1.43101	0.00026
16bin1_2_1_1_in	[ ]a,c	0.00063	1.43050	0.00032
16bin1_3_1_1_in	[ ]a,c	0.00127	1.43020	0.00027
16bin1fr_3_in	[ ]a,c	0.00190	1.42978	0.00026
16bin1fr_4_in	[ ]a,c	0.00254	1.42961	0.00033
Case	**Fuel-Clad Gap Thickness (cm)**	**Delta from Minimum (cm)**	k_∞	**σ**
16bin1gp_1_in	[ ]a,c	-0.00508	1.43156	0.00026
16bin1gp_2_in	[ ]a,c	-0.00254	1.43089	0.00025
16bin1_1_1_1_in	[ ]a,c	0.0	1.43101	0.00026
16bin1_1_2_1_in	[ ]a,c	0.00254	1.43074	0.00031
16bin1_1_3_1_in	[ ]a,c	0.00508	1.43009	0.00025
16bin1gp_3_in	[ ]a,c	0.00762	1.42970	0.00027
16bin1gp_4_in	[ ]a,c	0.01016	1.42918	0.00027
Case	**Clad Thickness (cm)**	**Delta from Minimum (cm)**	k_∞	**σ**
16bin1_1_1_1_in	[ ]a,c	0.0	1.43101	0.00026
16bin1_1_1_2_in	[ ]a,c	0.00381	1.42896	0.00032
16bin1_1_1_3_in	[ ]a,c	0.00762	1.42678	0.00025

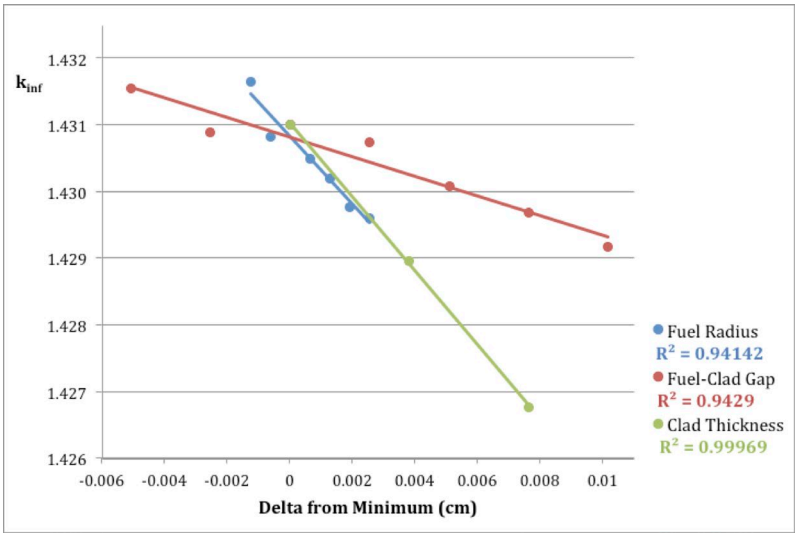

Figure 6-73 Trend Plot of Effect of Secondary Parameters on k-inf – 16 Bin 1

6.9.2.6.6 16 Bin 2

The following comparative analyses, shown in Table 6-103 and Figure 6-74, demonstrate the effect of fuel pellet radius, fuel-clad gap, and cladding thickness on k_∞ for 16 Bin 2 and verify that the minimum dimension is the most reactive for all three secondary parameters. The minimum value of each secondary parameter range is shaded in gray in Table 6-103.

Table 6-103 Effect of Secondary Parameters on 16 Bin 2

Case	Fuel Pellet Radius (cm)	Delta from Minimum (cm)	k_∞	σ
16bin2_1_1_1_in	[ ]^{a,c}	0.0	1.40585	0.00032
16bin2_2_1_1_in	[ ]^{a,c}	0.00169	1.40476	0.00028
16bin2_3_1_1_in	[ ]^{a,c}	0.00339	1.40361	0.00031
16bin2_4_1_1_in	[ ]^{a,c}	0.00508	1.40339	0.00031
Case	**Fuel-Clad Gap Thickness (cm)**	**Delta from Minimum (cm)**	**k_∞**	**σ**
16bin2gp_1_in	[ ]^{a,c}	-0.00508	1.40650	0.00028
16bin2gp_2_in	[ ]^{a,c}	-0.00254	1.40585	0.00026
16bin2_1_1_1_in	[ ]^{a,c}	0.0	1.40585	0.00032
16bin2_1_2_1_in	[ ]^{a,c}	0.00190	1.40513	0.00028
16bin2_1_3_1_in	[ ]^{a,c}	0.00381	1.40540	0.00036
16bin2_1_4_1_in	[ ]^{a,c}	0.00571	1.40501	0.00034
16bin2gp_3_in	[ ]^{a,c}	0.00825	1.40510	0.00030
16bin2gp_4_in	[ ]^{a,c}	0.01079	1.40506	0.00031
Case	**Clad Thickness (cm)**	**Delta from Minimum (cm)**	**k_∞**	**σ**
16bin2_1_1_1_in	[ ]^{a,c}	0.0	1.40585	0.00032
16bin2_1_1_2_in	[ ]^{a,c}	0.00487	1.40297	0.00026
16bin2_1_1_3_in	[ ]^{a,c}	0.00974	1.40048	0.00026
16bin2_1_1_4_in	[ ]^{a,c}	0.01461	1.39717	0.00030

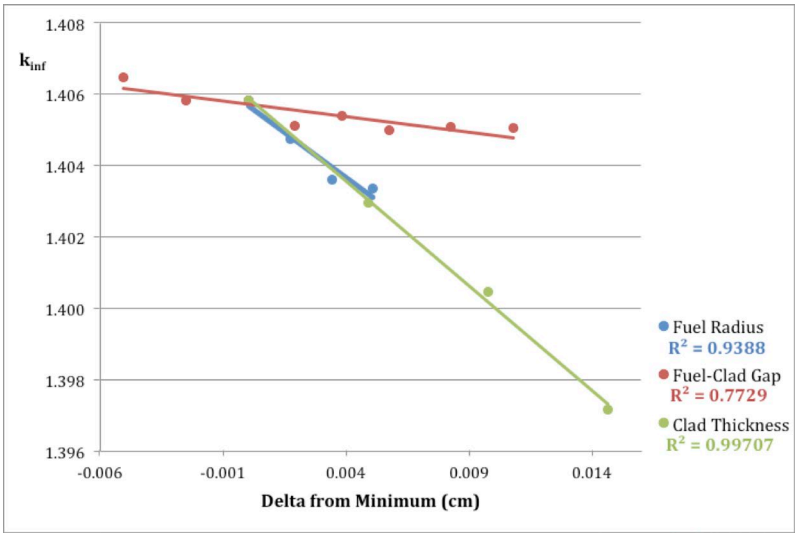

Figure 6-74 Trend Plot of Effect of Secondary Parameters on k-inf – 16 Bin 2

6.9.2.6.7 16 Bin 3

The following comparative analyses, shown in Table 6-104 and Figure 6-75, demonstrate the effect of fuel pellet radius, fuel-clad gap, and cladding thickness on k_∞ for 16 Bin 3 and verify that the minimum dimension is the most reactive for all three secondary parameters. The minimum value of each secondary parameter range is shaded in gray in Table 6-104.

Table 6-104 Effect of Secondary Parameters on 16 Bin 3

Case	Fuel Pellet Radius (cm)	Delta from Minimum (cm)	k_∞	σ
16bin3_1_1_1_in	[ ]^{a,c}	0.0	1.40154	0.00028
16bin3_2_1_1_in	[ ]^{a,c}	0.00622	1.39711	0.00027
16bin3_3_1_1_in	[ ]^{a,c}	0.01245	1.39245	0.00029
16bin3_4_1_1_in	[ ]^{a,c}	0.01867	1.38813	0.00027
Case	**Fuel-Clad Gap Thickness (cm)**	**Delta from Minimum (cm)**	**k_∞**	**σ**
16bin3gp_1_in	[ ]^{a,c}	-0.00508	1.40173	0.00029
16bin3gp_2_in	[ ]^{a,c}	-0.00254	1.40181	0.00028
16bin3_1_1_1_in	[ ]^{a,c}	0.0	1.40154	0.00028
16bin3_1_2_1_in	[ ]^{a,c}	0.00182	1.40128	0.00026
16bin3_1_3_1_in	[ ]^{a,c}	0.00364	1.40070	0.00025
16bin3_1_4_1_in	[ ]^{a,c}	0.00547	1.40020	0.00030
16bin3gp_3_in	[ ]^{a,c}	0.00801	1.40038	0.00030
16bin3gp_4_in	[ ]^{a,c}	0.01055	1.40003	0.00027
Case	**Clad Thickness (cm)**	**Delta from Minimum (cm)**	**k_∞**	**σ**
16bin3_1_1_1_in	[ ]^{a,c}	0.0	1.40154	0.00028
16bin3_1_1_2_in	[ ]^{a,c}	0.00381	1.39948	0.00028
16bin3_1_1_3_in	[ ]^{a,c}	0.00762	1.39686	0.00028

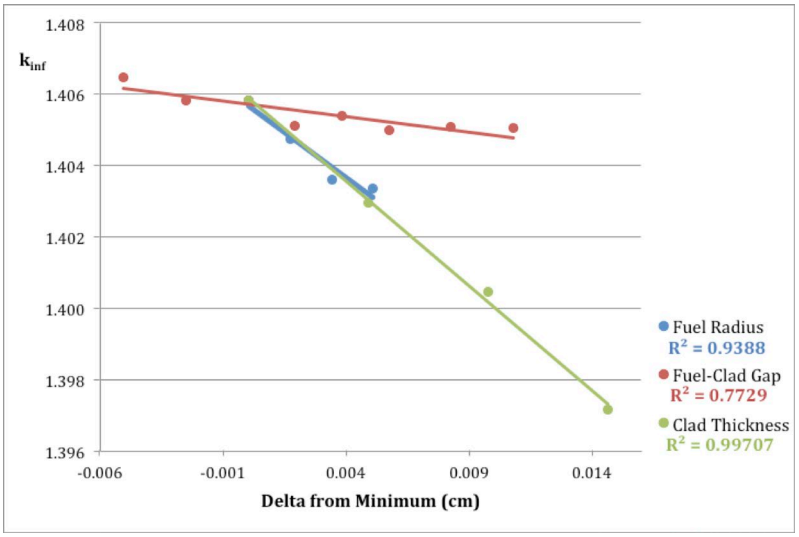

Figure 6-75 Trend Plot of Effect of Secondary Parameters on k-inf – 16 Bin 3

6.9.2.6.8 17 Bin 1

The following comparative analyses, shown in Table 6-105 and Figure 6-76, demonstrate the effect of fuel pellet radius, fuel-clad gap, and cladding thickness on k_∞ for 17 Bin 1 and verify that the minimum dimension is the most reactive for all three secondary parameters. The minimum value of each secondary parameter range is shaded in gray in Table 6-105.

Table 6-105 Effect of Secondary Parameters on 17 Bin 1

Case	Fuel Pellet Radius (cm)	Delta from Minimum (cm)	k_∞	σ
17bin1_1_1_1_in	[ ]^{a,c}	0.0	1.42552	0.00027
17bin1_2_1_1_in	[ ]^{a,c}	0.00622	1.42288	0.00027
17bin1_3_1_1_in	[ ]^{a,c}	0.01245	1.41930	0.00025
17bin1_4_1_1_in	[ ]^{a,c}	0.01867	1.41459	0.00030
Case	**Fuel-Clad Gap Thickness (cm)**	**Delta from Minimum (cm)**	**k_∞**	**σ**
17bin1gp_1_in	[ ]^{a,c}	-0.00508	1.42622	0.00024
17bin1gp_2_in	[ ]^{a,c}	-0.00254	1.42604	0.00029
17bin1_1_1_1_in	[ ]^{a,c}	0.0	1.42552	0.00027
17bin1_1_2_1_in	[ ]^{a,c}	0.00182	1.42531	0.00026
17bin1_1_3_1_in	[ ]^{a,c}	0.00364	1.42570	0.00031
17bin1_1_4_1_in_more [1]	[ ]^{a,c}	0.00547	1.42501	0.00029
17bin1gp_3_in	[ ]^{a,c}	0.00801	1.42535	0.00027
17bin1gp_4_in	[ ]^{a,c}	0.01055	1.42506	0.00026
Case	**Clad Thickness (cm)**	**Delta from Minimum (cm)**	**k_∞**	**σ**
17bin1_1_1_1_in	[ ]^{a,c}	0.0	1.42552	0.00027
17bin1_1_1_2_in	[ ]^{a,c}	0.00381	1.42391	0.00026
17bin1_1_1_3_in	[ ]^{a,c}	0.00762	1.42198	0.00035

Note: [1] More histories were modeled to improve source convergence.

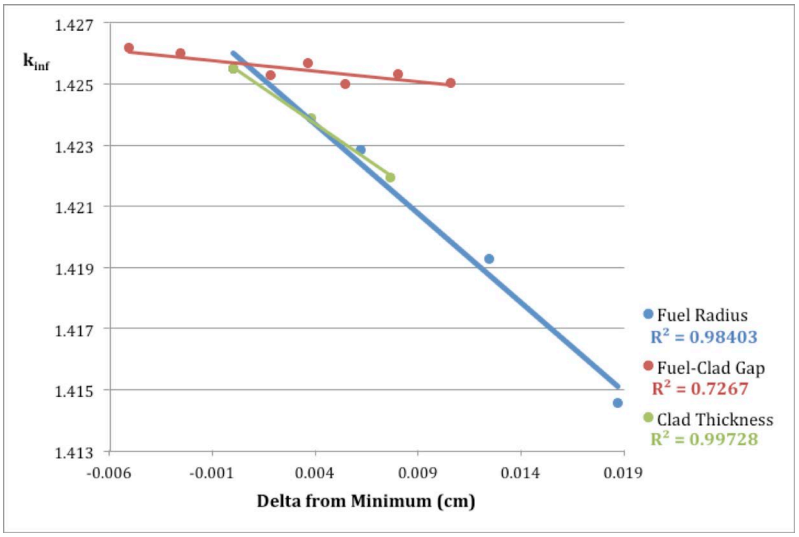

Figure 6-76 Trend Plot of Effect of Secondary Parameters on k-inf – 17 Bin 1

6.9.2.6.9 17 Bin 2

The following comparative analyses, shown in Table 6-106 and Figure 6-77, demonstrate the effect of fuel pellet radius, fuel-clad gap, and cladding thickness on k_∞ for 17 Bin 2 and verify that the minimum dimension is the most reactive for all three secondary parameters. The minimum value of each secondary parameter range is shaded in gray in Table 6-106.

Table 6-106 Effect of Secondary Parameters on 17 Bin 2

Case	Fuel Pellet Radius (cm)	Delta from Minimum (cm)	k_∞	σ
17bin2fr_1_in	[ ]^{a,c}	-0.00178	1.42032	0.00031
17bin2fr_2_in	[ ]^{a,c}	-0.00089	1.41992	0.00026
17bin2_1_1_1_in	[ ]^{a,c}	0.0	1.41936	0.00029
17bin2_2_1_1_in	[ ]^{a,c}	0.00089	1.41834	0.00028
17bin2_3_1_1_in	[ ]^{a,c}	0.00177	1.41802	0.00024
17bin2fr_3_in	[ ]^{a,c}	0.00266	1.41771	0.00029
17bin2fr_4_in	[ ]^{a,c}	0.00355	1.41661	0.00027
Case	**Fuel-Clad Gap Thickness (cm)**	**Delta from Minimum (cm)**	k_∞	σ
17bin2gp_1_in	[ ]^{a,c}	-0.00483	1.41964	0.00026
17bin2gp_2_in	[ ]^{a,c}	-0.00343	1.41969	0.00028
17bin2_1_1_1_in	[ ]^{a,c}	0.0	1.41936	0.00029
17bin2_1_2_1_in	[ ]^{a,c}	0.00343	1.41891	0.00028
17bin2_1_3_1_in	[ ]^{a,c}	0.00685	1.41849	0.00028
17bin2gp_3_in	[ ]^{a,c}	0.01028	1.41784	0.00026
17bin2gp_4_in	[ ]^{a,c}	0.01371	1.41771	0.00028
Case	**Clad Thickness (cm)**	**Delta from Minimum (cm)**	k_∞	σ
17bin2_1_1_1_in	[ ]^{a,c}	0.0	1.41936	0.00029
17bin2_1_1_2_in	[ ]^{a,c}	0.00508	1.41665	0.00031
17bin2_1_1_3_in	[ ]^{a,c}	0.01016	1.41308	0.00025

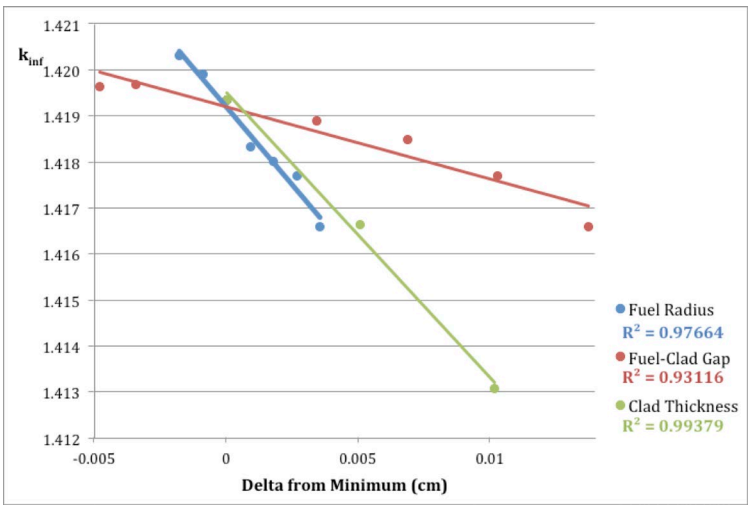

Figure 6-77 Trend Plot of Effect of Secondary Parameters on k-inf – 17 Bin 2

6.9.2.6.10 18 Bin 1

The following comparative analyses, shown in Table 6-107 and Figure 6-78, demonstrate the effect of fuel pellet radius, fuel-clad gap, and cladding thickness on k_∞ for 18 Bin 1 and verify that the minimum dimension is the most reactive for all three secondary parameters. The minimum value of each secondary parameter range is shaded in gray in Table 6-107.

Table 6-107 Effect of Secondary Parameters on 18 Bin 1

Case	Fuel Pellet Radius (cm)	Delta from Minimum (cm)	k_∞	σ
18bin1fr_1_in	[ ]^{a,c}	-0.00127	1.43029	0.00026
18bin1fr_2_in	[ ]^{a,c}	-0.00064	1.42971	0.00031
18bin1_1_1_1_in	[ ]^{a,c}	0.0	1.42963	0.00036
18bin1_2_1_1_in	[ ]^{a,c}	0.00063	1.42865	0.00027
18bin1_3_1_1_in	[ ]^{a,c}	0.00127	1.42825	0.00025
18bin1fr_3_in	[ ]^{a,c}	0.00190	1.42784	0.00028
18bin1fr_4_in	[ ]^{a,c}	0.00254	1.42743	0.00025
Case	**Fuel-Clad Gap Thickness (cm)**	**Delta from Minimum (cm)**	k_∞	σ
18bin1gp_1_in	[ ]^{a,c}	-0.00508	1.42943	0.00030
18bin1gp_2_in	[ ]^{a,c}	-0.00254	1.42970	0.00028
18bin1_1_1_1_in	[ ]^{a,c}	0.0	1.42963	0.00036
18bin1_1_2_1_in	[ ]^{a,c}	0.00254	1.42885	0.00029
18bin1_1_3_1_in	[ ]^{a,c}	0.00508	1.42858	0.00027
18bin1gp_3_in	[ ]^{a,c}	0.00762	1.42807	0.00032
18bin1gp_4_in	[ ]^{a,c}	0.01016	1.42803	0.00026
Case	**Clad Thickness (cm)**	**Delta from Minimum (cm)**	k_∞	σ
18bin1_1_1_1_in	[ ]^{a,c}	0.0	1.42963	0.00036
18bin1_1_1_2_in	[ ]^{a,c}	0.00381	1.42606	0.00025
18bin1_1_1_3_in	[ ]^{a,c}	0.00762	1.42493	0.00029

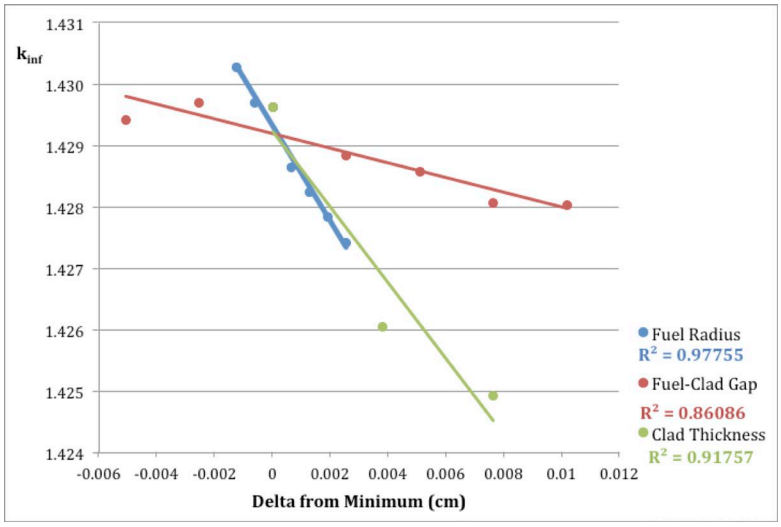

Figure 6-78 Trend Plot of Effect of Secondary Parameters on k-inf – 18 Bin 1

6.9.2.6.11 14 Bin 1, Group 4

The following comparative analyses, shown in Table 6-107A, Table 6-107 B, Figure 6-78A, and Figure 6-78B, demonstrate that as any dimension is minimized, k_∞ decreases for 14 Bin 1. The minimum value of each secondary parameter range is shaded in gray in Table 6-107A and Table 6-107B.

Table 6-107A Effect of Secondary Parameters on k-inf - 14 Bin 1, Group 4

Case	Fuel Pellet Radius (cm)	Delta from Minimum (cm)	k_∞	σ
14bin1fr_1_in	[ ]a,c	-0.00254	1.42949	0.00026
14bin1fr_2_in	[ ]a,c	-0.00127	1.42882	0.00017
14bin1_1_1_1_in	[ ]a,c	0.0	1.42797	0.00016
14bin1_2_1_1_in	[ ]a,c	0.00063	1.42761	0.00017
14bin1_3_1_1_in	[ ]a,c	0.00127	1.42722	0.00019
14bin1fr_3_in	[ ]a,c	0.00254	1.42662	0.00018
14bin1fr_4_in	[ ]a,c	0.00381	1.42568	0.00019
Case	**Fuel-Clad Gap Thickness (cm)**	**Delta from Minimum (cm)**	k_∞	**σ**
14bin1gp_1_in	[ ]a,c	-0.00508	1.42882	0.00021
14bin1gp_2_in	[ ]a,c	-0.00254	1.42858	0.00017
14bin1_1_1_1_in	[ ]a,c	0.0	1.42797	0.00016
14bin1_1_2_1_in	[ ]a,c	0.00254	1.42810	0.00018
14bin1_1_3_1_in	[ ]a,c	0.00508	1.42783	0.00019
14bin1gp_3_in	[ ]a,c	0.01016	1.42661	0.00019
14bin1gp_4_in	[ ]a,c	0.01524	1.42688	0.00016
Case	**Clad Thickness (cm)**	**Delta from Minimum (cm)**	k_∞	**σ**
14bin1_1_1_1_in	[ ]a,c	0.0	1.42797	0.00016
14bin1_1_1_2_in	[ ]a,c	0.00381	1.42589	0.00023
14bin1_1_1_3_in	[ ]a,c	0.00762	1.42440	0.00019

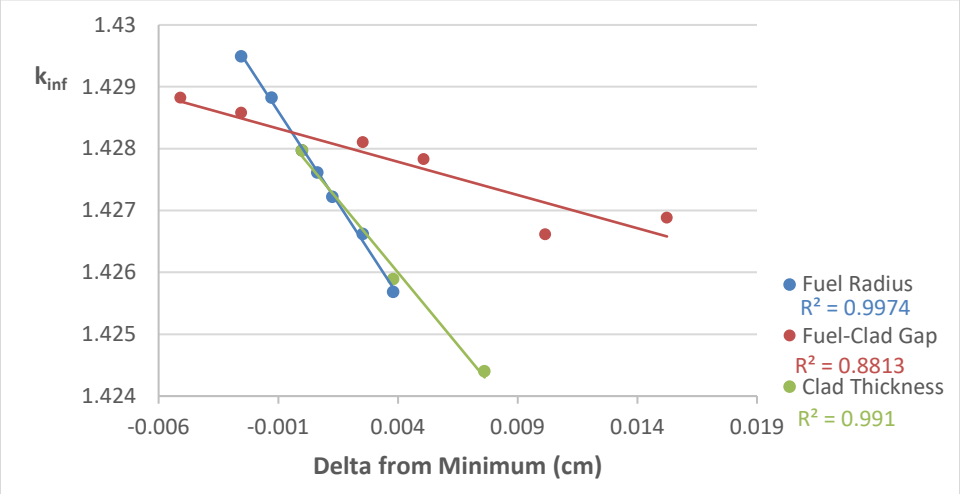

Figure 6-78A Trend Plot of Effect of Secondary Parameters on k-inf – 14 Bin 1, Group 4

Table 6-107B Effect of GT/IT Secondary Parameters on k-inf – 14 Bin 1, Group 4				
Case	**GT/IT Inner Radius (cm)**	**Delta from Minimum (cm)**	**k_∞**	**σ**
14bin1_GTITir_1_in	[ ]^{a,c}	-0.32301	1.42881	0.00021
14bin1_GTITir_2_in	[ ]^{a,c}	-0.22301	1.42802	0.00019
14bin1_GTITir_3_in	[ ]^{a,c}	-0.12301	1.42851	0.00018
14bin1_GTIT_1_1_in	[ ]^{a,c}	0.0	1.42797	0.00016
14bin1_GTIT_2_1_in	[ ]^{a,c}	0.03260	1.42827	0.00019
14bin1_GTIT_3_1_in	[ ]^{a,c}	0.06519	1.42812	0.00022
14bin1_GTIT_4_1_in	[ ]^{a,c}	0.09779	1.42785	0.00017
14bin1_GTITir_4_in	[ ]^{a,c}	0.15875	1.42766	0.00020
Case	**GT/IT Thickness (cm)**	**Delta from Minimum (cm)**	**k_∞**	**σ**
14bin1_GTITt_1_in	[ ]^{a,c}	-0.05080	1.42901	0.00019
14bin1_GTITt_2_in	[ ]^{a,c}	-0.02540	1.42846	0.00017
14bin1_GTIT_1_1_in	[ ]^{a,c}	0.0	1.42797	0.00016
14bin1_GTIT_1_2_in	[ ]^{a,c}	0.00762	1.42802	0.00022
14bin1_GTIT_1_3_in	[ ]^{a,c}	0.01524	1.42756	0.00021
14bin1_GTIT_1_4_in	[ ]^{a,c}	0.02286	1.42802	0.00017
14bin1_GTITt_3_in	[ ]^{a,c}	0.04826	1.42709	0.00018
14bin1_GTITt_4_in	[ ]^{a,c}	0.07366	1.42662	0.00020

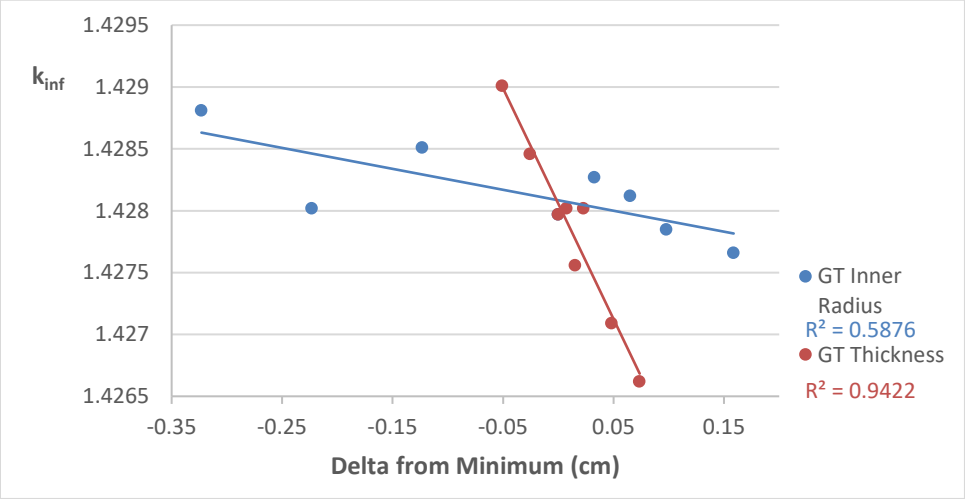

Figure 6-78B Trend Plot of Effect of GT/IT Secondary Parameters on k-inf – 14 Bin 1, Group 4

6.9.2.6.12 14 Bin 2, Group 4

The following comparative analyses, shown in Table 6-107C, Table 6-107D, Figure 6-78C, and Figure 6-78D demonstrate that as any dimension is minimized, k_∞ decreases for 14 Bin. The minimum value of each secondary parameter range is shaded in gray in Table 6-107C and Table 6-107D.

Table 6-107C Effect of Secondary Parameters on k-inf – 14 Bin 2, Group 4

Case	Fuel Pellet Radius (cm)	Delta from Minimum (cm)	k_∞	σ
14bin2_1_1_1_in	[ ]^{a,c}	0.0	1.44088	0.00021
14bin2_2_1_1_in	[ ]^{a,c}	0.00953	1.43630	0.00019
14bin2_3_1_1_in	[ ]^{a,c}	0.01905	1.43024	0.00020
14bin2_4_1_1_in	[ ]^{a,c}	0.02858	1.42448	0.00019
Case	**Fuel-Clad Gap Thickness (cm)**	**Delta from Minimum (cm)**	k_∞	**σ**
14bin2gp_1_in	[ ]^{a,c}	-0.00508	1.44162	0.00018
14bin2gp_2_in	[ ]^{a,c}	-0.00254	1.44075	0.00019
14bin2_1_1_1_in	[ ]^{a,c}	0.0	1.44088	0.00021
14bin2_1_2_1_in	[ ]^{a,c}	0.00191	1.44042	0.00019
14bin2_1_3_1_in	[ ]^{a,c}	0.00381	1.44020	0.00018
14bin2_1_4_1_in	[ ]^{a,c}	0.00572	1.44026	0.00020
14bin2gp_3_in	[ ]^{a,c}	0.01080	1.43936	0.00019
14bin2gp_4_in	[ ]^{a,c}	0.01588	1.43955	0.00021
Case	**Clad Thickness (cm)**	**Delta from Minimum (cm)**	k_∞	**σ**
14bin2_1_1_1_in	[ ]^{a,c}	0.0	1.44088	0.00021
14bin2_1_1_2_in	[ ]^{a,c}	0.00381	1.43922	0.00022
14bin2_1_1_3_in	[ ]^{a,c}	0.00762	1.43738	0.00019

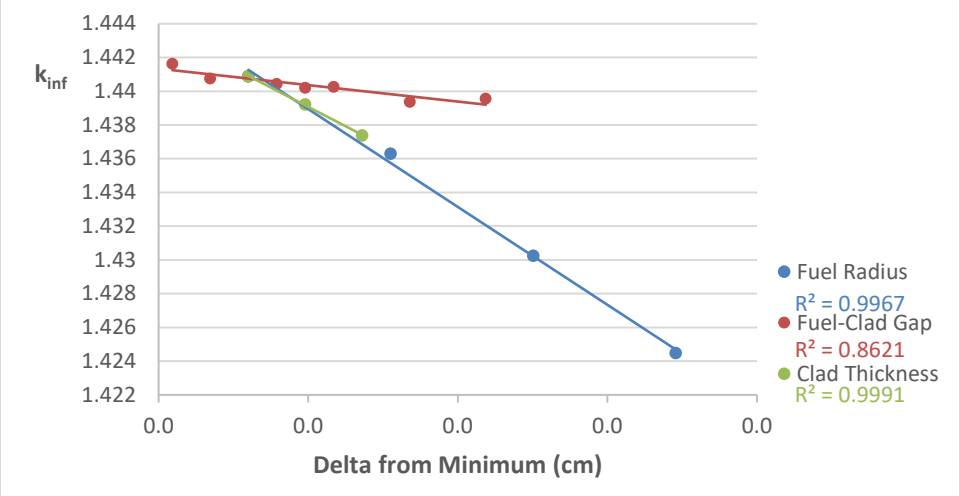

Figure 6-78C Trend Plot of Effect of Secondary Parameters on k-inf – 14 Bin 2, Group 4

Table 6-107D Effect of GT/IT Secondary Parameters on k-inf – 14 Bin 2, Group 4				
Case	**GT/IT Inner Radius (cm)**	**Delta from Minimum (cm)**	**k_∞**	**σ**
14bin2_GTITir_1_in	[ ]^{a,c}	-0.30244	1.44155	0.00023
14bin2_GTITir_2_in	[ ]^{a,c}	-0.20244	1.44135	0.00018
14bin2_GTITir_3_in	[ ]^{a,c}	-0.10244	1.44106	0.00020
14bin2_GTIT_1_1_in	[ ]^{a,c}	0.0	1.44088	0.00021
14bin2_GTIT_2_1_in	[ ]^{a,c}	0.05165	1.44046	0.00026
14bin2_GTIT_3_1_in	[ ]^{a,c}	0.10329	1.44051	0.00017
14bin2_GTIT_4_1_in	[ ]^{a,c}	0.15494	1.44032	0.00019
14bin2_GTITir_4_in	[ ]^{a,c}	0.19634	1.44014	0.00021
Case	**GT/IT Thickness (cm)**	**Delta from Minimum (cm)**	**k_∞**	**σ**
14bin2_GTITt_1_in	[ ]^{a,c}	-0.02540	1.44184	0.00019
14bin2_GTITt_2_in	[ ]^{a,c}	-0.01270	1.44114	0.00019
14bin2_GTIT_1_1_in	[ ]^{a,c}	0.0	1.44088	0.00021
14bin2_GTIT_1_2_in	[ ]^{a,c}	0.00999	1.44010	0.00022
14bin2_GTIT_1_3_in	[ ]^{a,c}	0.01998	1.43957	0.00024
14bin2_GTIT_1_4_in	[ ]^{a,c}	0.02997	1.43932	0.00018
14bin2_GTITt_3_in	[ ]^{a,c}	0.04267	1.43845	0.00021
14bin2_GTITt_4_in	[ ]^{a,c}	0.05537	1.43820	0.00020

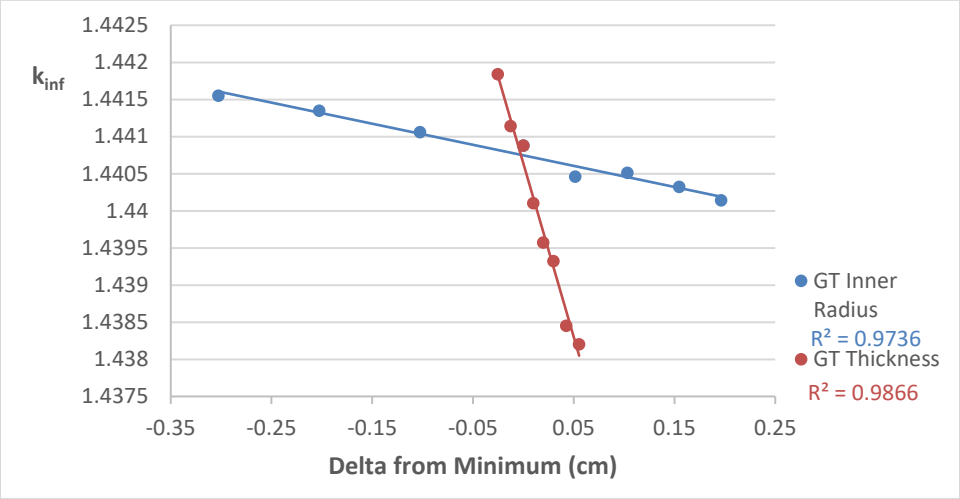

Figure 6-78D Trend Plot of Effect of GT/IT Secondary Parameters on k-inf – 14 Bin 2, Group 4

6.9.2.6.13 15 Bin 3, Group 4

The following comparative analyses, shown in Table 6-107E, Table 6-107F, Figure 6-78E, and Figure 6-78F, demonstrate that as any dimension is minimized, k_∞ decreases for 15 Bin 3. The minimum value of each secondary parameter range is shaded in gray in Table 6-107E and Table 6-107F.

Table 6-107E Effect of Secondary Parameters on k-inf – 15 Bin 3, Group 4

Case	Fuel Pellet Radius (cm)	Delta from Minimum (cm)	k_∞	σ
15bin3fr_1_in	[ ]a,c	-0.00254	1.44931	0.00021
15bin3fr_2_in	[ ]a,c	-0.00127	1.44828	0.00019
15bin3_1_1_1_in	[ ]a,c	0.0	1.44727	0.00028
15bin3_2_1_1_in	[ ]a,c	0.00063	1.44750	0.00019
15bin3_3_1_1_in	[ ]a,c	0.00127	1.44663	0.00019
15bin3fr_3_in	[ ]a,c	0.00254	1.44604	0.00018
15bin3fr_4_in	[ ]a,c	0.00381	1.44523	0.00029
Case	**Fuel-Clad Gap Thickness (cm)**	**Delta from Minimum (cm)**	k_∞	σ
15bin3gp_1_in	[ ]a,c	-0.00508	1.44783	0.00017
15bin3gp_2_in	[ ]a,c	-0.00254	1.44810	0.00016
15bin3_1_1_1_in	[ ]a,c	0	1.44727	0.00028
15bin3_1_2_1_in	[ ]a,c	0.00254	1.44732	0.00018
15bin3_1_3_1_in	[ ]a,c	0.00508	1.44702	0.00017
15bin3gp_3_in	[ ]a,c	0.01016	1.44684	0.00019
15bin3gp_4_in	[ ]a,c	0.01524	1.44583	0.00023
Case	**Clad Thickness (cm)**	**Delta from Minimum (cm)**	k_∞	σ
15bin3_1_1_1_in	[ ]a,c	0	1.44727	0.00028
15bin3_1_1_2_in	[ ]a,c	0.00381	1.44587	0.00017
15bin3_1_1_3_in	[ ]a,c	0.00762	1.44361	0.00022

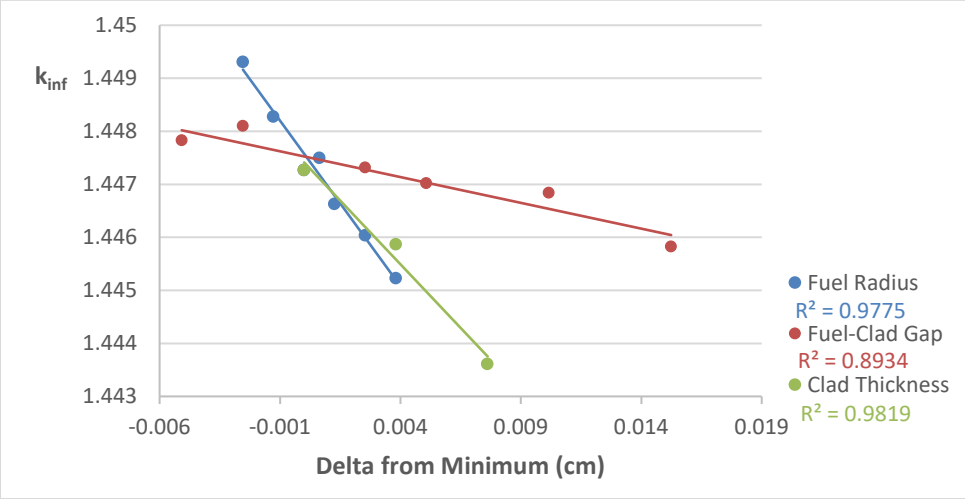

Figure 6-78E Trend Plot of Effect of Secondary Parameters on k-inf – 15 Bin 3, Group 4

Table 6-107F Effect of GT/IT Secondary Parameters on k-inf – 15 Bin 3, Group 4				
Case	**GT/IT Inner Radius (cm)**	**Delta from Minimum (cm)**	**k_∞**	**σ**
15bin3_GTITir_1_in	[ ]^{a,c}	-0.30119	1.44874	0.00017
15bin3_GTITir_2_in	[ ]^{a,c}	-0.20119	1.44874	0.00019
15bin3_GTITir_3_in	[ ]^{a,c}	-0.10119	1.44799	0.00017
15bin3_GTIT_1_1_in	[ ]^{a,c}	0.0	1.44727	0.00028
15bin3_GTIT_2_1_in	[ ]^{a,c}	0.00169	1.44732	0.00022
15bin3_GTIT_3_1_in	[ ]^{a,c}	0.00339	1.44702	0.00025
15bin3_GTIT_4_1_in	[ ]^{a,c}	0.00508	1.44788	0.00019
15bin3_GTITir_4_in	[ ]^{a,c}	0.04648	1.44764	0.00018
Case	**GT/IT Thickness (cm)**	**Delta from Minimum (cm)**	**k_∞**	**σ**
15bin3_GTITt_1_in	[ ]^{a,c}	-0.02032	1.44886	0.00019
15bin3_GTITt_2_in	[ ]^{a,c}	-0.01016	1.44828	0.00018
15bin3_GTIT_1_1_in	[ ]^{a,c}	0.0	1.44727	0.00028
15bin3_GTIT_1_2_in	[ ]^{a,c}	0.00364	1.44746	0.00018
15bin3_GTIT_1_3_in	[ ]^{a,c}	0.00728	1.44702	0.00018
15bin3_GTIT_1_4_in	[ ]^{a,c}	0.01092	1.44698	0.00021
15bin3_GTITt_3_in	[ ]^{a,c}	0.02108	1.44647	0.00019
15bin3_GTITt_4_in	[ ]^{a,c}	0.03124	1.44538	0.00018

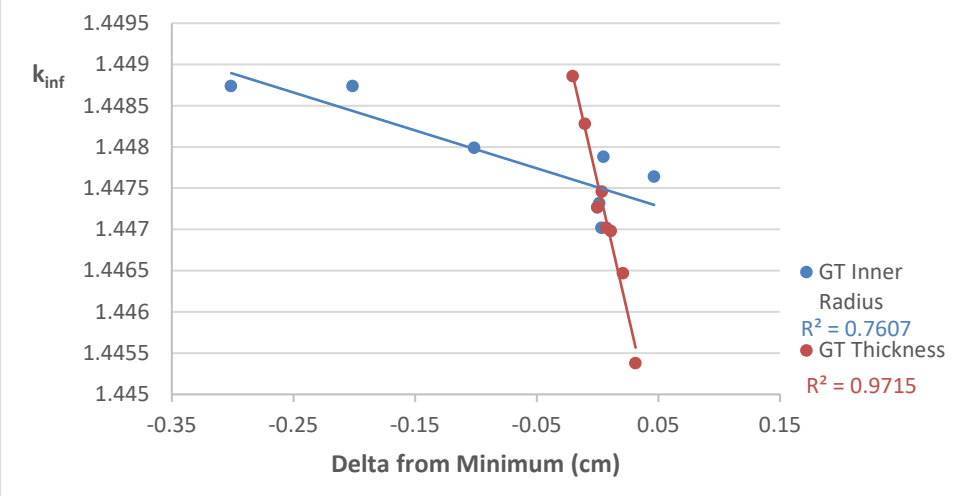

Figure 6-78F Trend Plot of Effect of GT/IT Secondary Parameters on k-inf – 15 Bin 3, Group 4

6.9.2.6.14 16 Bin 2, Group 4

The following comparative analyses, shown in Table 6-107G, Table 6-107H, Figure 6-78G, and Figure 6-78H, demonstrate that as any dimension is minimized, k_∞ decreases for 16 Bin 2. The minimum value of each secondary parameter range is shaded in gray in Table 6-107G and Table 6-107H.

Table 6-107G Effect of Secondary Parameters on k-inf – 16 Bin 2, Group 4

Case	Fuel Pellet Radius (cm)	Delta from Minimum (cm)	k_∞	σ
16bin2_1_1_1_in	[ ]^{a,c}	0.0	1.43424	0.00018
16bin2_2_1_1_in	[ ]^{a,c}	0.00169	1.43331	0.00019
16bin2_3_1_1_in	[ ]^{a,c}	0.00339	1.43200	0.00022
16bin2_4_1_1_in	[ ]^{a,c}	0.00508	1.43091	0.00019
Case	**Fuel-Clad Gap Thickness (cm)**	**Delta from Minimum (cm)**	k_∞	σ
16bin2gp_1_in	[ ]^{a,c}	-0.00508	1.43495	0.00020
16bin2gp_2_in	[ ]^{a,c}	-0.00254	1.43478	0.00021
16bin2_1_1_1_in	[ ]^{a,c}	0.0	1.43424	0.00018
16bin2_1_2_1_in	[ ]^{a,c}	0.00191	1.43402	0.00022
16bin2_1_3_1_in	[ ]^{a,c}	0.00381	1.43417	0.00020
16bin2_1_4_1_in	[ ]^{a,c}	0.00572	1.43384	0.00020
16bin2gp_3_in	[ ]^{a,c}	0.01080	1.43325	0.00018
16bin2gp_4_in	[ ]^{a,c}	0.01588	1.43284	0.00020
Case	**Clad Thickness (cm)**	**Delta from Minimum (cm)**	k_∞	σ
16bin2_1_1_1_in	[ ]^{a,c}	0.0	1.43424	0.00018
16bin2_1_1_2_in	[ ]^{a,c}	0.00487	1.43162	0.00017
16bin2_1_1_3_in	[ ]^{a,c}	0.00974	1.42843	0.00017
16bin2_1_1_4_in	[ ]^{a,c}	0.01461	1.42581	0.00019

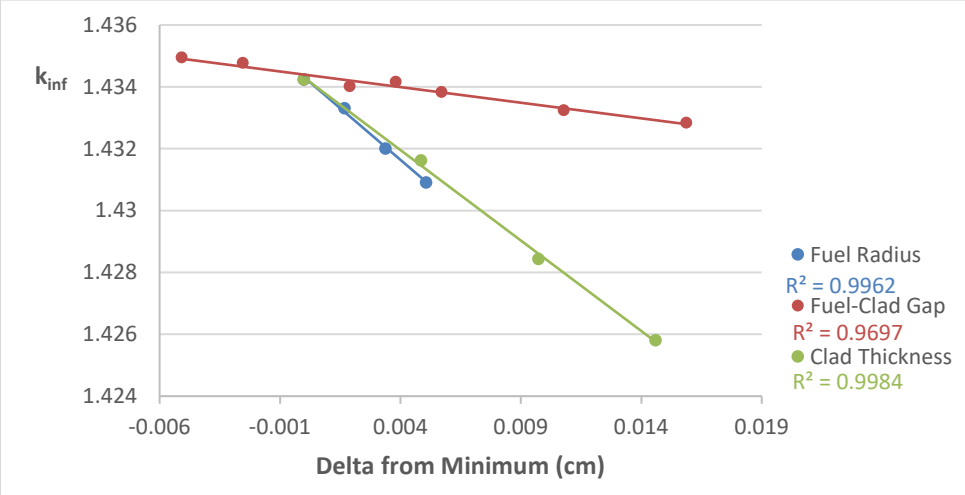

Figure 6-78G Trend Plot of Effect of Secondary Parameters on k-inf – 16 Bin 2, Group 4

Table 6-107H Effect of GT/IT Secondary Parameters on k-inf – 16 Bin 2, Group 4				
Case	**GT/IT Inner Radius (cm)**	**Delta from Minimum (cm)**	k_∞	**σ**
16bin2_GTITir_1_in	[ ]^{a,c}	-0.39215	1.43471	0.00023
16bin2_GTITir_2_in	[ ]^{a,c}	-0.29215	1.43496	0.00023
16bin2_GTITir_3_in	[ ]^{a,c}	-0.19215	1.43466	0.00021
16bin2_GTIT_1_1_in	[ ]^{a,c}	-0.09215	1.43471	0.00017
16bin2_GTIT_2_1_in	[ ]^{a,c}	0.0	1.43424	0.00018
16bin2_GTIT_3_1_in	[ ]^{a,c}	0.16722	1.43414	0.00018
16bin2_GTIT_4_1_in	[ ]^{a,c}	0.33443	1.43377	0.00027
16bin2_GTITir_4_in	[ ]^{a,c}	0.50165	1.43378	0.00018
Case	**GT/IT Thickness (cm)**	**Delta from Minimum (cm)**	k_∞	**σ**
16bin2_GTITt_1_in	[ ]^{a,c}	-0.07620	1.43511	0.00020
16bin2_GTITt_2_in	[ ]^{a,c}	-0.03810	1.43479	0.00021
16bin2_GTIT_1_1_in	[ ]^{a,c}	0.0	1.43424	0.00018
16bin2_GTIT_1_2_in	[ ]^{a,c}	0.02413	1.43391	0.00018
16bin2_GTIT_1_3_in	[ ]^{a,c}	0.04826	1.43391	0.00022
16bin2_GTIT_1_4_in	[ ]^{a,c}	0.07239	1.43378	0.00019
16bin2_GTITt_3_in	[ ]^{a,c}	0.11049	1.43283	0.00020
16bin2_GTITt_4_in	[ ]^{a,c}	0.14859	1.43261	0.00018

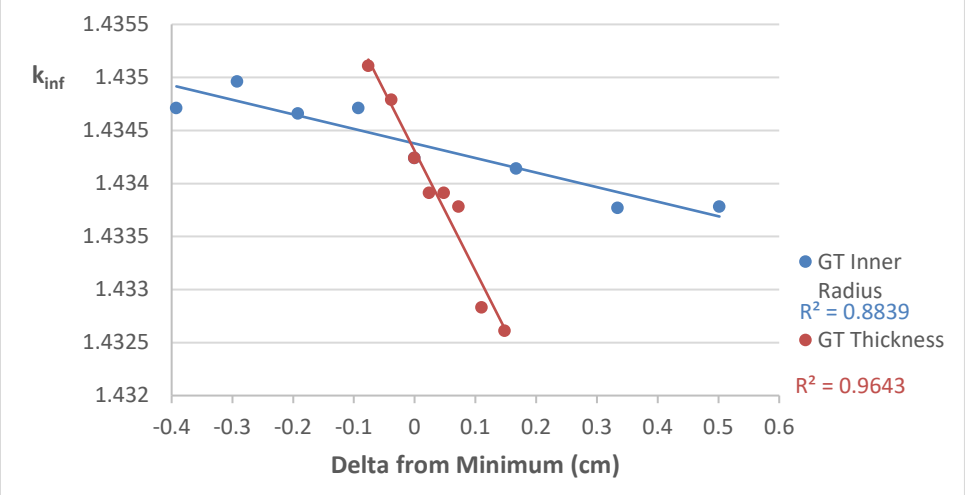

Figure 6-78HTrend Plot of Effect of GT/IT Secondary Parameters on k-inf – 16 Bin 2, Group 4

6.9.2.6.15 16 Bin 3, Group 4

The following comparative analyses, shown in Table 6-107I, Table 6-107J, Figure 6-78I, and Figure 6-78J, demonstrate that as any dimension is minimized, k_∞ decreases for 16 Bin 3. The minimum value of each secondary parameter range is shaded in gray in Table 6-107I and Table 6-107J.

Table 6-107I Effect of Secondary Parameters on k-inf – 16 Bin 3, Group 4

Case	Fuel Pellet Radius (cm)	Delta from Minimum (cm)	k_∞	σ
16bin3_1_1_1_in	[ ]^{a,c}	0.0	1.42822	0.00022
16bin3_2_1_1_in	[ ]^{a,c}	0.00622	1.42341	0.00021
16bin3_3_1_1_in	[ ]^{a,c}	0.01245	1.41832	0.00022
16bin3_4_1_1_in	[ ]^{a,c}	0.01867	1.41284	0.00021
Case	**Fuel-Clad Gap Thickness (cm)**	**Delta from Minimum (cm)**	k_∞	σ
16bin3gp_1_in	[ ]^{a,c}	-0.00508	1.42836	0.00019
16bin3gp_2_in	[ ]^{a,c}	-0.00254	1.42828	0.00020
16bin3_1_1_1_in	[ ]^{a,c}	0.0	1.42822	0.00022
16bin3_1_2_1_in	[ ]^{a,c}	0.00182	1.42763	0.00019
16bin3_1_3_1_in	[ ]^{a,c}	0.00364	1.42762	0.00019
16bin3_1_4_1_in	[ ]^{a,c}	0.00546	1.42739	0.00019
16bin3gp_3_in	[ ]^{a,c}	0.01054	1.42685	0.00024
16bin3gp_4_in	[ ]^{a,c}	0.01562	1.42633	0.00017
Case	**Clad Thickness (cm)**	**Delta from Minimum (cm)**	k_∞	σ
16bin3_1_1_1_in	[ ]^{a,c}	0.0	1.42822	0.00022
16bin3_1_1_2_in	[ ]^{a,c}	0.00381	1.42566	0.00023
16bin3_1_1_3_in	[ ]^{a,c}	0.00762	1.42305	0.00022

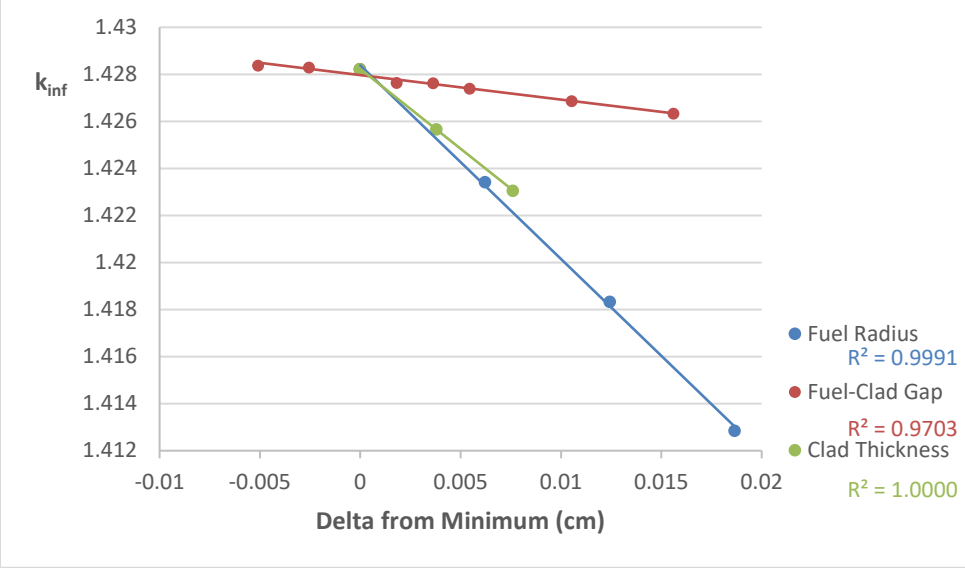

Figure 6-78I Trend Plot of Effect of Secondary Parameters on k-inf – 16 Bin 3, Group 4

Table 6-107J Effect of GT/IT Secondary Parameters on k-inf – 16 Bin 3, Group 4				
Case	**GT/IT Inner Radius (cm)**	**Delta from Minimum (cm)**	**k_∞**	**σ**
16bin3_GTITir_1_in	[ ]^{a,c}	-0.30387	1.42971	0.00018
16bin3_GTITir_2_in	[ ]^{a,c}	-0.20387	1.42891	0.00019
16bin3_GTITir_3_in	[ ]^{a,c}	-0.10387	1.42842	0.00019
16bin3_GTIT_1_1_in	[ ]^{a,c}	0.0	1.42822	0.00022
16bin3_GTIT_2_1_in	[ ]^{a,c}	0.02371	1.42833	0.00021
16bin3_GTIT_3_1_in	[ ]^{a,c}	0.04741	1.42815	0.00021
16bin3_GTIT_4_1_in	[ ]^{a,c}	0.07112	1.42802	0.00022
16bin3_GTITir_4_in	[ ]^{a,c}	0.09220	1.42777	0.00019
Case	**GT/IT Thickness (cm)**	**Delta from Minimum (cm)**	**k_∞**	**σ**
16bin3_GTITt_1_in	[ ]^{a,c}	-0.02540	1.42963	0.00021
16bin3_GTITt_2_in	[ ]^{a,c}	-0.01270	1.42868	0.00019
16bin3_GTIT_1_1_in	[ ]^{a,c}	0.0	1.42822	0.00022
16bin3_GTIT_1_2_in	[ ]^{a,c}	0.00449	1.42755	0.00018
16bin3_GTIT_1_3_in	[ ]^{a,c}	0.00897	1.42717	0.00020
16bin3_GTIT_1_4_in	[ ]^{a,c}	0.01346	1.42688	0.00019
16bin3_GTITt_3_in	[ ]^{a,c}	0.02616	1.42633	0.00022
16bin3_GTITt_4_in	[ ]^{a,c}	0.03886	1.42498	0.00022

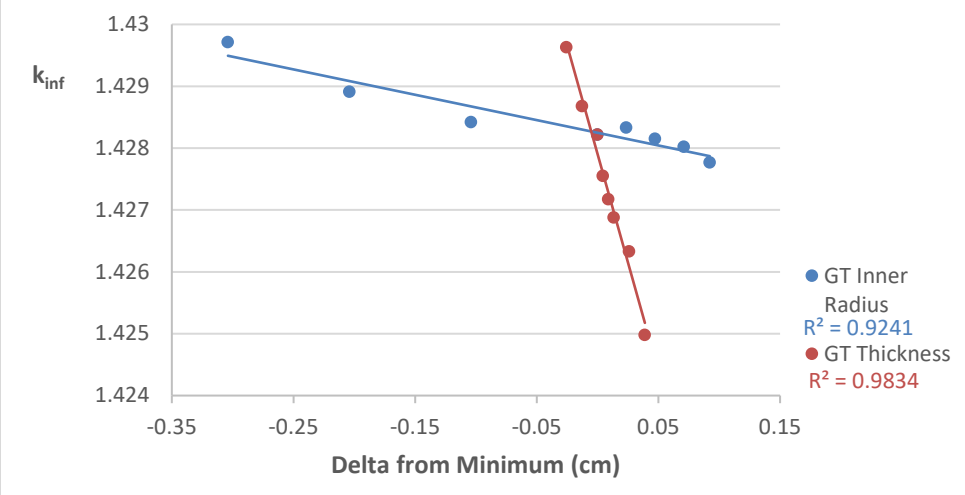

Figure 6-78J Trend Plot of Effect of GT/IT Secondary Parameters on k-inf – 16 Bin 3, Group 4

6.9.2.6.16 17 Bin 1, Group 4

The following comparative analyses, shown in Table 6-107K, Table 6-107L, Figure 6-78K, and Figure 6-78L, demonstrate that as any dimension is minimized, k_∞ decreases for 17 Bin 1. The minimum value of each secondary parameter range is shaded in gray in Table 6-107K and Table 6-107L.

Table 6-107K Effect of Secondary Parameters on k-inf – 17 Bin 1, Group 4

Case	Fuel Pellet Radius (cm)	Delta from Minimum (cm)	k_∞	σ
17bin1_1_1_1_in	[ ]a,c	0.0	1.45416	0.00018
17bin1_2_1_1_in	[ ]a,c	0.00622	1.45035	0.00018
17bin1_3_1_1_in	[ ]a,c	0.01245	1.44567	0.00019
17bin1_4_1_1_in	[ ]a,c	0.01867	1.44100	0.00018
Case	**Fuel-Clad Gap Thickness (cm)**	**Delta from Minimum (cm)**	k_∞	σ
17bin1gp_1_in	[ ]a,c	-0.00508	1.45486	0.00020
17bin1gp_2_in	[ ]a,c	-0.00254	1.45438	0.00019
17bin1_1_1_1_in	[ ]a,c	0.0	1.45416	0.00018
17bin1_1_2_1_in	[ ]a,c	0.00182	1.45430	0.00022
17bin1_1_3_1_in	[ ]a,c	0.00364	1.45374	0.00021
17bin1_1_4_1_in	[ ]a,c	0.00546	1.45346	0.00018
17bin1gp_3_in	[ ]a,c	0.00800	1.45316	0.00023
17bin1gp_4_in	[ ]a,c	0.01054	1.45319	0.00019
Case	**Clad Thickness (cm)**	**Delta from Minimum (cm)**	k_∞	σ
17bin1_1_1_1_in	[ ]a,c	0.0	1.45416	0.00018
17bin1_1_1_2_in	[ ]a,c	0.00381	1.45214	0.00020
17bin1_1_1_3_in	[ ]a,c	0.00762	1.45006	0.00020

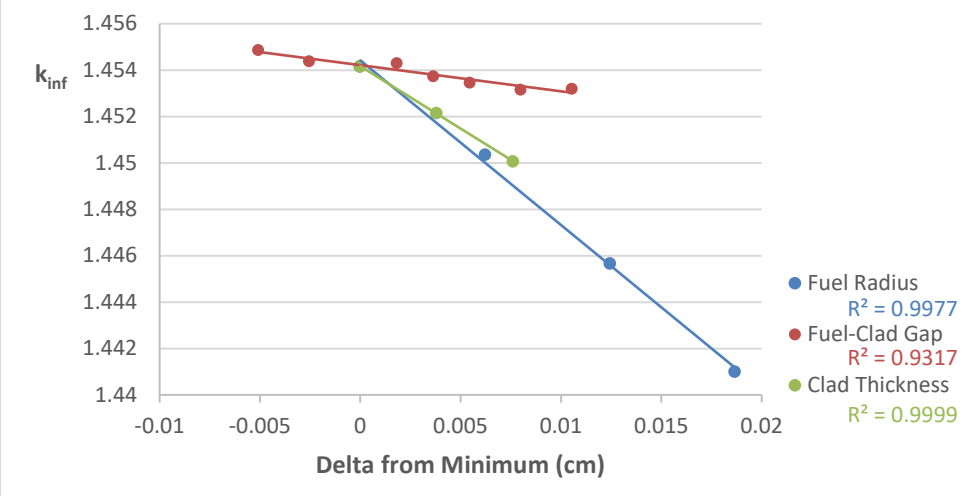

Figure 6-78K Trend Plot of Effect of Secondary Parameters on k-inf – 17 Bin 1, Group 4

Table 6-107L Effect of GT/IT Secondary Parameters on k-inf – 17 Bin 1, Group 4				
Case	**GT/IT Inner Radius (cm)**	**Delta from Minimum (cm)**	**k_∞**	**σ**
17bin1_GTITir_1_in	[ ]^{a,c}	-0.30165	1.45537	0.00018
17bin1_GTITir_2_in	[ ]^{a,c}	-0.20165	1.45469	0.00018
17bin1_GTITir_3_in	[ ]^{a,c}	-0.10165	1.45478	0.00026
17bin1_GTIT_1_1_in	[ ]^{a,c}	0.0	1.45416	0.00018
17bin1_GTIT_2_1_in	[ ]^{a,c}	0.02074	1.45419	0.00018
17bin1_GTIT_3_1_in	[ ]^{a,c}	0.04149	1.45377	0.00019
17bin1_GTIT_4_1_in	[ ]^{a,c}	0.06223	1.45419	0.00020
17bin1_GTITir_4_in	[ ]^{a,c}	0.09347	1.45384	0.00019
Case	**GT/IT Thickness (cm)**	**Delta from Minimum (cm)**	**k_∞**	**σ**
17bin1_GTITt_1_in	[ ]^{a,c}	-0.02540	1.45573	0.00020
17bin1_GTITt_2_in	[ ]^{a,c}	-0.01270	1.45518	0.00027
17bin1_GTIT_1_1_in	[ ]^{a,c}	0.0	1.45416	0.00018
17bin1_GTIT_1_2_in	[ ]^{a,c}	0.00830	1.45381	0.00022
17bin1_GTIT_1_3_in	[ ]^{a,c}	0.01659	1.45330	0.00019
17bin1_GTIT_1_4_in	[ ]^{a,c}	0.02489	1.45276	0.00021
17bin1_GTITt_3_in	[ ]^{a,c}	0.03759	1.45195	0.00022
17bin1_GTITt_4_in	[ ]^{a,c}	0.05029	1.45090	0.00018

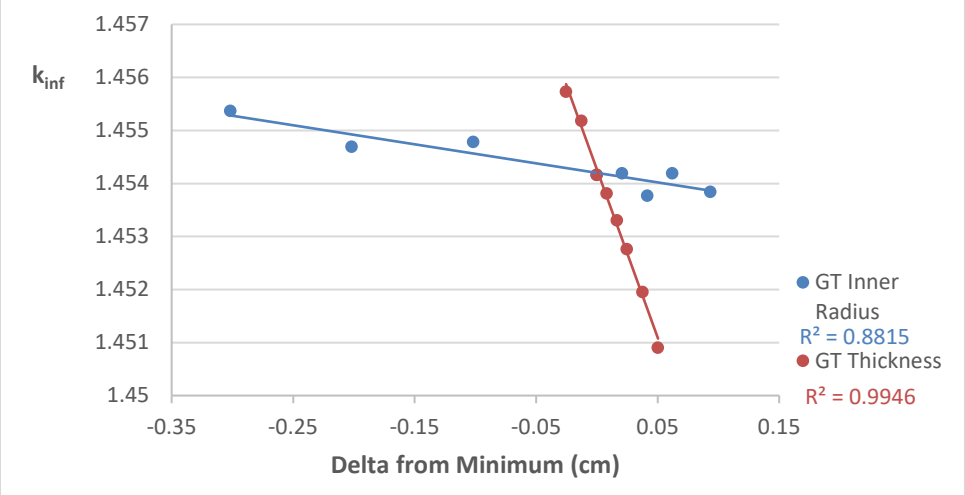

Figure 6-78L Trend Plot of Effect of GT/IT Secondary Parameters on k-inf – 17 Bin 1, Group 4

6.9.3 Baseline Detailed Results

6.9.3.1 Single Package, Fuel Assembly

6.9.3.1.1 CFA Package Variant Comparison Results

For the bins 16 Bin 2 and 17 Bin 1, the maximum active fuel length can only fit in the Traveller XL. For this reason in the CFA-package variant comparison, these bins are broken up into 2 CFAs. The longer CFA (with suffix 'a') is the maximum fuel length for the bin, which only fits in the Traveller XL. The shorter CFA (no suffix) is the fuel length of an existing fuel design in the bin that fits in both the STD and XL. For the Groups 1 & 2 Single Package evaluation under NCT, 16 Bin 1 and 18 Bin 1 in the Traveller XL are selected as the most reactive CFA-package variants for evaluation in the baseline case determination. For Group 1 and 2 single package HAC, 17 Bin 1, 17 Bin 1a, and 17 Bin 2 in the Traveller XL are selected as the most reactive CFA-package variants for evaluation in the baseline case determination. As the XL is always bounding of the STD for Groups 1 & 2, the STD is not analyzed for Group 4. For Group 4 single package, 17 Bin 1 in the Traveller XL is the bounding CFA. The results are tabulated in Table 6-108.

Table 6-108 Single Package, CFA-Package Variant Comparison Results

Traveller Variant	CFA	Active Fuel Length (in.)	NCT			HAC		
			k_{eff}	σ	$k_{eff} + 2\sigma$	k_{eff}	σ	$k_{eff} + 2\sigma$
STD (Groups 1 & 2)	14 Bin 1	137.20	0.82687	0.00057	0.82801	0.85417	0.00063	0.85543
	14 Bin 2	144.50	0.82905	0.00055	0.83015	0.85961	0.00059	0.86079
	15 Bin 1	144.50	0.85594	0.00050	0.85694	0.87093	0.00074	0.87241
	15 Bin 2	140.26	0.84727	0.00085	0.84897	0.86367	0.00053	0.86473
	16 Bin 2	137.20	0.83498	0.00048	0.83594	0.86204	0.00057	0.86318
	16 Bin 3	144.50	0.82091	0.00055	0.82201	0.86419	0.00062	0.86543
	17 Bin 1	144.50	0.85691	0.00048	0.85787	0.87226	0.00053	0.87332
	17 Bin 2	144.50	0.85304	0.00048	0.85400	0.86943	0.00053	0.87049
XL (Groups 1 & 2)	14 Bin 1	137.20	0.84081	0.00051	0.84183	0.88205	0.00050	0.88305
	14 Bin 2	144.50	0.83904	0.00062	0.84028	0.88247	0.00054	0.88355
	15 Bin 1	144.50	0.87324	0.00049	0.87422	0.90031	0.00048	0.90127
	15 Bin 2	140.26	0.86513	0.00087	0.86687	0.89637	0.00050	0.89737
	16 Bin 1	154.04	0.88423	0.00055	0.88533	0.89874	0.00050	0.89974
	16 Bin 2	137.20	0.84900	0.00053	0.85006	0.88942	0.00049	0.89040
	16 Bin 2a *	150.50	0.84815	0.00047	0.84909	0.88881	0.00054	0.88989
	16 Bin 3	144.50	0.83133	0.00047	0.83227	0.89059	0.00050	0.89159
	17 Bin 1	144.50	0.87474	0.00049	0.87572	0.90301	0.00052	0.90405
	17 Bin 1a *	168.50	0.87576	0.00060	0.87696	0.90347	0.00051	0.90449
	17 Bin 2	144.50	0.87033	0.00055	0.87143	0.90188	0.00049	0.90286
	18 Bin 1	154.04	0.88464	0.00053	0.88570	0.90069	0.00054	0.90177
XL (Group 4)	14 Bin 1	137.20	--	--	--	0.87477	0.00025	0.87527
	14 Bin 2	144.50	--	--	--	0.88435	0.00026	0.88487
	15 Bin 3	144.50	--	--	--	0.89686	0.00031	0.89748
	16 Bin 2	150.50	--	--	--	0.88471	0.00023	0.88517
	16 Bin 3	144.50	--	--	--	0.87370	0.00025	0.87420
	17 Bin 1	168.50	--	--	--	0.90483	0.00026	0.90535

Note: * These cases model an active fuel length that cannot be shipped in the STD and are therefore only modeled in the XL.

6.9.3.1.2 Baseline Determination Results

For Groups 1 & 2 under NCT, the baseline case is chosen as 18 Bin 1 in the Traveller XL with an axial displacement of the fuel of 72.583 cm. As there is no statistically significant trend between the selected baseline case and the axial position "peak" baseline case (Table 6-109), it was determined for these cases that the difference in k_{eff} was based on the statistical nature of the Monte Carlo code rather than a true physical effect of repositioning the fuel assembly (See Figure 6-79). Thus, the case with the fuel assembly centered in the Clamshell was selected to promote axial reflection for the fuel assembly in the Clamshell.

Table 6-109 Axial Position Baseline Results – Single Package, NCT, PWR Fuel Assembly Groups

Group	Content	Traveller Variant	Axial Position (cm)	k_{eff}	σ	$k_{eff} + 2\sigma$
1 & 2	16 Bin 1	XL	2.540	0.88423	0.00055	0.88533
			25.888	0.88384	0.00050	0.88484
			49.235	0.88456	0.00055	0.88566
			72.583	0.88481	0.00055	0.88591
			95.931	0.88427	0.00048	0.88523
			119.278	0.88509	0.00048	0.88605
	18 Bin 1	XL	2.540	0.88464	0.00053	0.88570
			25.888	0.88555	0.00052	0.88659
			49.235	0.88520	0.00053	0.88626
			72.583	0.88499	0.00059	0.88617
			95.931	0.88594	0.00053	0.88700
			119.278	0.88601	0.00048	0.88697

For Groups 1 & 2 under HAC, the baseline case is chosen as 17 Bin 1 in the Traveller XL with an axial displacement of the fuel of 87.122 cm. As there is no statistically significant trend between the selected baseline case and the axial position "peak" baseline case, it was determined for these cases that the difference in k_{eff} was based on the statistical nature of the Monte Carlo code rather than a true physical effect of repositioning the fuel assembly (See Figure 6-80). Thus, the case with the fuel assembly centered in the Clamshell was selected to promote axial reflection for the fuel assembly in the Clamshell.

For Group 4, the baseline case modeled the fuel assembly as axially centered (axial position = 42.545 cm). As there is no statistically significant trend in the data, it was determined for these cases that the difference in k_{eff} was based on the statistical nature of the Monte Carlo code rather than a true physical effect of repositioning the fuel assembly (See Figure 6-80A). Thus, the case with the fuel assembly centered in the Clamshell was selected to promote axial reflection for the fuel assembly in the Clamshell.

Table 6-110 Axial Position Baseline Results – Single Package, HAC, PWR Fuel Assembly Groups

Group	Content	Traveller Variant	Axial Position (cm)	k_{eff}	σ	$k_{eff} + 2\sigma$
1 & 2	17 Bin 1	XL	2.540	0.90301	0.00052	0.90405
			30.734	0.90320	0.00055	0.90430
			58.928	0.90219	0.00052	0.90323
			87.122	0.90209	0.00049	0.90307
			115.316	0.90340	0.00056	0.90452
			143.510	0.90368	0.00056	0.90480
	17 Bin 1a	XL	2.540	0.90347	0.00051	0.90449
			18.542	0.90372	0.00048	0.90468
			34.544	0.90347	0.00054	0.90455
			50.546	0.90364	0.00051	0.90466
			66.548	0.90222	0.00049	0.90320
			82.550	0.90304	0.00064	0.90432
	17 Bin 2	XL	2.540	0.90188	0.00049	0.90286
			30.734	0.90268	0.00055	0.90378
			58.928	0.90374	0.00046	0.90466
			87.122	0.90228	0.00059	0.90346
			115.316	0.90249	0.00056	0.90361
			143.510	0.90300	0.00055	0.90410
4	17 Bin 1	XL	2.540	0.90453	0.00027	0.90507
			15.875	0.90487	0.00025	0.90537
			29.210	0.90518	0.00026	0.90570
			42.545	0.90483	0.00026	0.90535
			55.880	0.90534	0.00027	0.90588
			69.215	0.90502	0.00026	0.90554
			82.550	0.90465	0.00024	0.90513

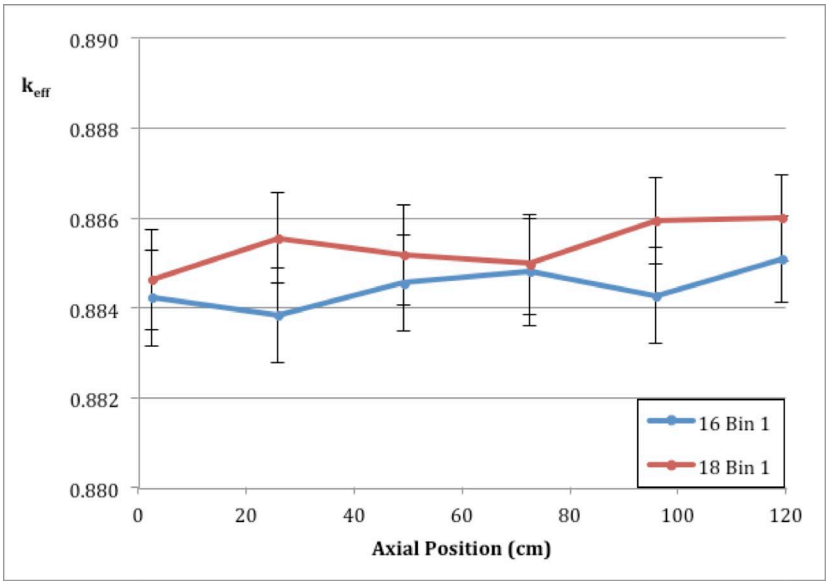

Figure 6-79 Axial Position Baseline Results – Single Package, NCT, Groups 1 and 2

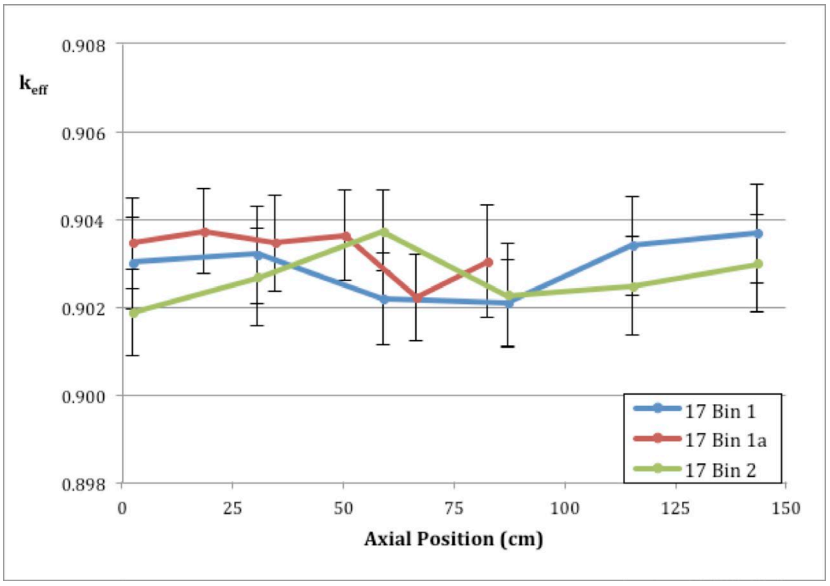

Figure 6-80 Axial Position Baseline Results – Single Package, HAC, Groups 1 and 2

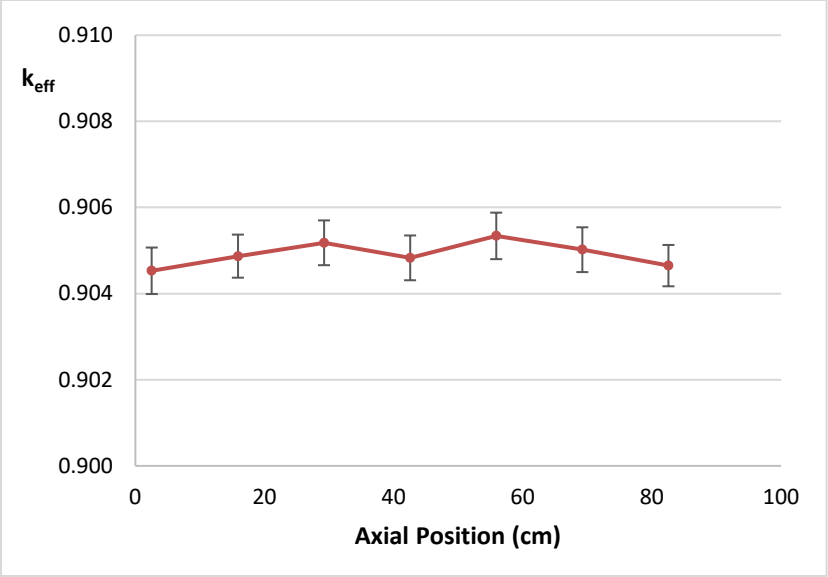

Figure 6-80A Axial Position Baseline Results – Single Package, HAC, Group 4

6.9.3.2 Single Package, Rod Pipe

6.9.3.2.1 Baseline Determination Results

The bounding fuel OR data for each baseline configuration is shown in Table 6-111 for Single Package NCT. Only the square pitch-type was examined beyond a fuel OR of 0.65 cm, as square pitch was more reactive than hexagonal pitch. For UO_2 fuel rods, the resultant bounding fuel OR is much larger than a standard LWR fuel pellet, with a fuel OR of 3.5 cm and an equivalent half-pitch of 3.5 cm. For U_3Si_2 fuel rods, the bounding fuel OR is the upper limit of examination, 0.4851 cm, with an equivalent square half-pitch of 0.4851 cm.

Table 6-111 Single Package, NCT, Rod Pipe Package Variant Results

Content	Traveller Variant	Fuel OR (cm)	Half-Pitch (cm)	Hexagonal Pitch-Type			Square Pitch-Type		
				k_{eff}	σ	$k_{eff} + 2\sigma$	k_{eff}	σ	$k_{eff} + 2\sigma$
UO_2 Fuel Rods	STD	0.39	0.39	0.46567	0.00063	0.46693	0.51224	0.00079	0.51382
		0.425	0.425	0.46632	0.00061	0.46754	0.51370	0.00067	0.51504
		0.45	0.45	0.46553	0.00060	0.46673	0.51232	0.00062	0.51356
		0.475	0.475	0.46678	0.00055	0.46788	0.51263	0.00066	0.51395
		0.5	0.5	0.46598	0.00070	0.46738	0.51231	0.00061	0.51353
		0.55	0.55	0.46567	0.00059	0.46685	0.51453	0.00070	0.51593
		0.6	0.6	0.46620	0.00059	0.46738	0.51496	0.00069	0.51634
		0.65	0.65	0.46713	0.00065	0.46843	0.51540	0.00064	0.51668
	XL	0.39	0.39	0.47715	0.00058	0.47831	0.52178	0.00063	0.52304
		0.425	0.425	0.47613	0.00063	0.47739	0.52237	0.00068	0.52373
		0.45	0.45	0.47609	0.00059	0.47727	0.52128	0.00070	0.52268
		0.475	0.475	0.47754	0.00060	0.47874	0.52267	0.00066	0.52399
		0.5	0.5	0.47638	0.00059	0.47756	0.52236	0.00063	0.52362
		0.55	0.55	0.47840	0.00064	0.47968	0.52426	0.00063	0.52552
		0.6	0.6	0.47755	0.00063	0.47881	0.52416	0.00065	0.52546
		0.65	0.65	0.47703	0.00063	0.47829	0.52432	0.00064	0.52560

Table 6-111 Single Package, NCT, Rod Pipe Package Variant Results

Content	Traveller Variant	Fuel OR (cm)	Half-Pitch (cm)	Hexagonal Pitch-Type			Square Pitch-Type		
				k_{eff}	σ	$k_{eff} + 2\sigma$	k_{eff}	σ	$k_{eff} + 2\sigma$
		0.7	0.7	--	--	--	0.52673	0.0007	0.52813
		0.75	0.75	--	--	--	0.52715	0.00068	0.52851
		0.8	0.8	--	--	--	0.52535	0.00071	0.52677
		0.85	0.85	--	--	--	0.52505	0.00069	0.52643
		0.9	0.9	--	--	--	0.52908	0.00069	0.53046
		1.0	1.0	--	--	--	0.52906	0.00072	0.53050
		1.2	1.2	--	--	--	0.53460	0.00067	0.53594
		1.5	1.5	--	--	--	0.52953	0.00068	0.53089
		2.0	2.0	--	--	--	0.54344	0.00071	0.54486
		2.5	2.5	--	--	--	0.52381	0.00062	0.52505
		3.0	3.0	--	--	--	0.54699	0.00067	0.54833
		3.5	3.5	--	--	--	0.56435	0.00086	0.56607
		4.0	4.0	--	--	--	0.55588	0.00074	0.55736
		4.5	4.5	--	--	--	0.52236	0.00068	0.52372
		5.0	5.0	--	--	--	0.50621	0.00064	0.50749
		5.5	5.5	--	--	--	0.48890	0.00066	0.49022
		6.0	6.0	--	--	--	0.47085	0.00056	0.47197
		6.5	6.5	--	--	--	0.45437	0.00068	0.45573
		7.0	7.0	--	--	--	0.44140	0.00058	0.44256
U_3Si_2 Fuel Rods	STD	0.3909	0.3909	0.37181	0.00042	0.37265	0.39207	0.00042	0.39291
		0.4145	0.4145	0.38052	0.00036	0.38124	0.40264	0.00036	0.40336
		0.438	0.438	0.39037	0.0004	0.39117	0.41198	0.00041	0.41280
		0.4616	0.4616	0.39893	0.00035	0.39963	0.42104	0.00037	0.42178
		0.4851	0.4851	0.40592	0.00035	0.40662	0.42948	0.00037	0.43022

For the Rod Pipe Single Package under HAC, a full study was done that examined several pitch values for each fuel OR listed in order to determine the peak reactivity. For each fuel OR value, five half-pitch values were examined such that a curve was developed for each fuel OR. Table 6-112 lists the peak value of each of these curves, with the overall maximum shaded in gray. Table 6-113 and Table 6-114 show the fuel pitch variation curve for the most reactive fuel OR of each package variant and pitch type. The full range of fuel OR and half-pitch values examined are listed in Table 6-15. Table 6-115 takes the overall most reactive UO_2 fuel rod case (the Traveller XL with fuel OR = 0.55 cm and half-pitch = 1.05 cm with a hexagonal pitch-type) and examines finer pitch values for fuel OR of 0.50, 0.55, and 0.60 cm in order to better determine the optimum fuel OR-fuel pitch combination. The Rod Pipe, UO_2 Fuel Rod, Single Package, HAC baseline case models the Traveller XL with a fuel OR of 0.55 cm and a hexagonal half-pitch of 1.00 cm. The Rod Pipe, U_3Si_2 Fuel Rod, Single Package, HAC baseline case models the Traveller STD with a fuel OR of 0.4851 cm and a square half-pitch of 1.0101 cm.

Table 6-112 Single Package, HAC, Rod Pipe Fuel OR-Pitch Combination – Maximum Results

Contents	Traveller Variant	Fuel OR (cm)	Hexagonal Pitch-Type				Square Pitch-Type			
			Half-Pitch (cm)	k_{eff}	σ	$k_{eff} + 2\sigma$	Half-Pitch (cm)	k_{eff}	σ	$k_{eff} + 2\sigma$
UO_2 Fuel Rods	STD	0.390	0.640	0.70158	0.00084	0.70326	0.640	0.71305	0.00091	0.71487
		0.425	0.675	0.69713	0.00095	0.69903	0.675	0.70660	0.00100	0.70860
		0.450	0.700	0.70226	0.00086	0.70398	0.700	0.70507	0.00087	0.70681
		0.475	0.975	0.70917	0.00085	0.71087	0.725	0.70577	0.00085	0.70747
		0.500	1.000	0.71458	0.00088	0.71634	0.750	0.70148	0.00097	0.70342
		0.550	1.050	0.71759	0.00088	0.71935	1.050	0.69789	0.00074	0.69937
		0.600	1.100	0.70806	0.00088	0.70982	1.100	0.70211	0.00084	0.70379
		0.650	1.150	0.69349	0.00084	0.69517	1.150	0.70220	0.00082	0.70384
	XL	0.390	0.640	0.70650	0.00100	0.70850	0.640	0.71643	0.00090	0.71823
		0.425	0.675	0.70070	0.00080	0.70230	0.675	0.71244	0.00086	0.71416
		0.450	0.700	0.70703	0.00080	0.70863	0.700	0.71048	0.00079	0.71206
		0.475	0.975	0.71213	0.00092	0.71397	0.725	0.71372	0.00086	0.71544
		0.500	1.000	0.71842	0.00084	0.72010	0.750	0.70775	0.00091	0.70957
		0.550	1.050	0.72148	0.00091	0.72330	1.050	0.70213	0.00081	0.70375
		0.600	1.100	0.71222	0.00084	0.71390	1.100	0.70750	0.00079	0.70908
		0.650	1.150	0.69830	0.00084	0.69998	1.150	0.70862	0.00093	0.71048
U_3Si_2 Fuel Rods	STD	0.3909	0.9409	0.64433	0.00047	0.64527	0.8909	0.64625	0.00043	0.64711
		0.4145	0.9645	0.65555	0.00050	0.65655	0.8895	0.65556	0.00051	0.65658
		0.4380	0.9880	0.66260	0.00044	0.66348	0.8880	0.66275	0.00048	0.66371
		0.4616	1.0116	0.66958	0.00045	0.67048	0.8866	0.66790	0.00051	0.66892
		0.4851	1.0101	0.67492	0.00049	0.67590	0.9101	0.67170	0.00044	0.67258

Table 6-113 UO_2 Single Package, HAC, Rod Pipe Fuel OR-Pitch Combination – Pitch Variation

Traveller Variant	Hexagonal Pitch-Type Fuel OR = 0.55 cm				Square Pitch-Type Fuel OR = 0.39 cm			
	Half-Pitch (cm)	k_{eff}	σ	$k_{eff} + 2\sigma$	Half-Pitch (cm)	k_{eff}	σ	$k_{eff} + 2\sigma$
STD	0.550	0.46567	0.00059	0.46685	0.39	0.51224	0.00079	0.51382
	0.650	0.57384	0.00070	0.57524	0.49	0.64028	0.00080	0.64188
	0.800	0.67225	0.00078	0.67381	0.64	0.71305	0.00091	0.71487
	1.050	0.71759	0.00088	0.71935	0.89	0.69093	0.00080	0.69253
	1.300	0.67762	0.00091	0.67944	1.14	0.60186	0.00077	0.60340
XL	0.550	0.47840	0.00064	0.47968	0.39	0.52178	0.00063	0.52304
	0.650	0.58179	0.00070	0.58319	0.49	0.64570	0.00085	0.64740
	0.800	0.67945	0.00084	0.68113	0.64	0.71643	0.00090	0.71823
	1.050	0.72148	0.00091	0.72330	0.89	0.69441	0.00083	0.69607
	1.300	0.68201	0.00082	0.68365	1.14	0.60238	0.00074	0.60386

Table 6-114 U_3Si_2 Single Package, HAC, Rod Pipe Fuel OR-Pitch Combination – Pitch Variation

Traveller Variant	Hexagonal Pitch-Type Fuel OR = 0.4851 cm				Square Pitch-Type Fuel OR = 0.4851 cm			
	Half-Pitch (cm)	k_{eff}	σ	$k_{eff} + 2\sigma$	Half-Pitch (cm)	k_{eff}	σ	$k_{eff} + 2\sigma$
STD	0.6351	0.50275	0.00039	0.50353	0.6351	0.53921	0.00044	0.54009
	0.6851	0.53725	0.00043	0.53811	0.6851	0.57200	0.00043	0.57286
	0.7351	0.57009	0.00044	0.57097	0.7351	0.60327	0.00047	0.60421
	0.7851	0.59831	0.00047	0.59925	0.7851	0.63083	0.00048	0.63179
	0.8351	0.62586	0.00048	0.62682	0.8351	0.65343	0.00051	0.65445
	0.8851	0.64822	0.00051	0.64924	0.8851	0.66937	0.00049	0.67035
	0.9351	0.66411	0.00051	0.66513	0.9101	0.67170	0.00044	0.67258
	0.9601	0.66978	0.00046	0.67070	0.9351	0.66719	0.00049	0.66817
	0.9851	0.67377	0.0005	0.67477	0.9601	0.65913	0.00046	0.66005
	1.0101	0.67492	0.00049	0.67590	0.9851	0.65365	0.00047	0.65459
	1.0351	0.67343	0.00047	0.67437	1.0351	0.64914	0.00046	0.65006
	1.0851	0.65959	0.00048	0.66055	1.0851	0.63989	0.00046	0.64081
	1.1351	0.63237	0.00051	0.63339	1.1351	0.62649	0.00040	0.62729
	1.1851	0.62553	0.00044	0.62641	1.1851	0.61949	0.00048	0.62045
	1.2351	0.62486	0.00046	0.62578	1.2351	0.59977	0.00046	0.60069
	1.2851	0.61578	0.00068	0.61714	1.2851	0.57214	0.00047	0.57308
	1.3351	0.60152	0.00043	0.60238	1.3351	0.55316	0.00038	0.55392

Table 6-115 UO_2 Single Package, HAC, Rod Pipe Fuel OR-Pitch Combination – Refined Parameter Study

Fuel OR (cm)	Half-Pitch (cm)	k_{eff}	σ	$k_{eff} + 2\sigma$
0.50	0.50	0.47715	0.00038	0.47791
	0.60	0.59249	0.00041	0.59331
	0.75	0.68716	0.00048	0.68812
	0.90	0.71225	0.00053	0.71331
	0.95	0.71069	0.00053	0.71175
	1.00	0.71899	0.00056	0.72011
	1.05	0.71636	0.00054	0.71744
	1.10	0.69702	0.00051	0.69804
	1.15	0.67265	0.00044	0.67353
	1.20	0.67062	0.00049	0.67160
	1.25	0.66829	0.00049	0.66927
0.55	0.55	0.47725	0.00033	0.47791
	0.65	0.58184	0.00038	0.58260
	0.80	0.67930	0.00044	0.68018
	0.95	0.70537	0.00045	0.70627
	1.00	0.72106	0.00047	0.72200
	1.05	0.72104	0.00046	0.72196
	1.10	0.70821	0.00056	0.70933
	1.15	0.68711	0.00047	0.68805
	1.20	0.68673	0.00051	0.68775
	1.25	0.68652	0.00050	0.68752
	1.30	0.68179	0.00047	0.68273
0.60	0.60	0.47726	0.00039	0.47804
	0.70	0.57688	0.00040	0.57768
	0.85	0.67549	0.00055	0.67659
	1.00	0.71384	0.00047	0.71478
	1.05	0.71834	0.00051	0.71936
	1.10	0.71201	0.00052	0.71305
	1.15	0.69473	0.00051	0.69575
	1.20	0.69488	0.00050	0.69588
	1.25	0.69882	0.00048	0.69978
	1.30	0.69745	0.00046	0.69837
	1.35	0.69157	0.00051	0.69259

6.9.3.3 Package Array, NCT, Fuel Assembly

6.9.3.3.1 CFA-Package Variant Comparison Results

Table 6-116 details the results of the Package Array, NCT evaluation for Groups 1, 2, and 4. For Group 1, the most reactive CFA-Package Variant combination is the Traveller XL with 17 Bin 2 and an array stack height of 2 packages. For Group 2, the most reactive CFA-Package Variant combination is the Traveller XL with 16 Bin 1 and an array stack height of 1 package. For Group 4, the most reactive CFA is the Traveller XL with 15 Bin 3 and an array stack height of 1 package. A stack height of two packages was not examined for Group 4 as a stack height of one is bounding for smaller array sizes (<100 packages).

Table 6-116 Package Array, NCT, CFA Package Variant Results

Traveller Variant	Group	CFA	Active Fuel Length (in.)	Array Stack Height = 2			Array Stack Height = 1		
				k_{eff}	σ	$k_{eff} + 2\sigma$	k_{eff}	σ	$k_{eff} + 2\sigma$
STD	1	14 Bin 1	137.20	0.28743	0.00024	0.28791	0.27923	0.00024	0.27971
		14 Bin 2	144.50	0.26258	0.00032	0.26322	0.25522	0.00027	0.25576
		15 Bin 1	144.50	0.29497	0.00029	0.29555	0.28814	0.00026	0.28866
		15 Bin 2	140.26	0.29413	0.00026	0.29465	0.28671	0.00025	0.28721
		16 Bin 2	137.20	0.28149	0.00023	0.28195	0.27367	0.00024	0.27415
		16 Bin 3	144.50	0.26860	0.00028	0.26916	0.26127	0.00023	0.26173
		17 Bin 1	144.50	0.28916	0.00025	0.28966	0.28211	0.00026	0.28263
		17 Bin 2	144.50	0.30307	0.00028	0.30363	0.29554	0.00025	0.29604
XL	1	14 Bin 1	137.20	0.29419	0.00037	0.29493	0.28865	0.00026	0.28917
		14 Bin 2	144.50	0.27142	0.00026	0.27194	0.26686	0.00026	0.26738
		15 Bin 1	144.50	0.30100	0.00025	0.30150	0.29587	0.00025	0.29637
		15 Bin 2	140.26	0.29981	0.00032	0.30045	0.29434	0.00022	0.29478
		16 Bin 2	137.20	0.28892	0.00024	0.28940	0.28302	0.00024	0.28350
		16 Bin 2a *	150.50	0.28997	0.00026	0.29049	0.28544	0.00025	0.28594
		16 Bin 3	144.50	0.27758	0.00029	0.27816	0.27242	0.00023	0.27288
		17 Bin 1	144.50	0.29550	0.00030	0.29610	0.29036	0.00024	0.29084
		17 Bin 1a *	168.50	0.29696	0.00026	0.29748	0.29368	0.00030	0.29428
		17 Bin 2	144.50	0.30888	0.00027	0.30942	0.30338	0.00024	0.30386
	2	16 Bin 1	154.04	0.29991	0.00026	0.30043	0.30847	0.00031	0.30909
		18 Bin 1	154.04	0.29864	0.00026	0.29916	0.30660	0.00026	0.30712
XL	4	14 Bin 1	137.20				0.28727	0.00019	0.28765
		14 Bin 2	144.50				0.26196	0.00024	0.26244
		15 Bin 3	144.50				0.30347	0.00018	0.30383
		16 Bin 2	150.50				0.28449	0.00023	0.28495
		16 Bin 3	144.50				0.26733	0.0002	0.26773
		17 Bin 1	168.50				0.29654	0.00022	0.29698

Note: * these cases model an active fuel length that cannot be shipped in the STD and are therefore only modeled in the XL.

6.9.3.3.2 Baseline Determination Results

For Group 1, the baseline case has a most reactive axial fuel position of 2.54 cm, modeling the CFA of 17 Bin 2 at the bottom of the Clamshell. The axial positions listed in Table 6-117 represent the axial positions of the fuel assemblies in the top package. An axial position of 2.54 cm represents the fuel assemblies of the top and bottom package as close to one another as possible, which is the most reactive configuration, whereas an axial position of 143.51 cm represents the fuel assemblies as far from each other as possible. For Group 2, the baseline case has a most reactive axial fuel position of 119.278 cm, modeling the CFA of 16 Bin 1 at the top of the Clamshell. For Group 4, the bounding axial fuel position is 143.510 cm, modeling the 15 Bin 3 CFA at the top of the Clamshell.

Table 6-117 Axial Position Baseline Results –Package Array, NCT, PWR Fuel Assembly Groups

Content (Group)	Traveller Variant	Axial Position (cm)	k_{eff}	σ	$k_{eff} + 2\sigma$
17 Bin 2 (1)	XL	2.540	0.30888	0.00027	0.30942
		30.734	0.29814	0.00025	0.29864
		58.928	0.29714	0.00029	0.29772
		87.122	0.29670	0.00035	0.29740
		115.316	0.29660	0.00027	0.29714
		143.510	0.30040	0.00024	0.30088
16 Bin 1 (2)	XL	2.540	0.30847	0.00031	0.30909
		25.888	0.30664	0.00028	0.30720
		49.235	0.30649	0.00023	0.30695
		72.583	0.30664	0.00025	0.30714
		95.931	0.30652	0.00025	0.30702
		119.278	0.30950	0.00026	0.31002
15 Bin 3 (4)	XL	2.540	0.30547	0.00020	0.30587
		26.035	0.30377	0.00019	0.30415
		49.530	0.30347	0.00018	0.30383
		73.025	0.30347	0.00018	0.30383
		96.520	0.30371	0.00019	0.30409
		120.015	0.30386	0.00019	0.30424
		143.510	0.30731	0.00020	0.30771

6.9.3.4 Package Array, NCT, Rod Pipe

6.9.3.4.1 Baseline Determination Results

The bounding fuel OR data for each baseline configuration is shown in Table 6-118 for Package Array, NCT. For UO_2 fuel rods, only the square pitch-type was examined beyond a fuel OR of 0.65 cm, as it was evident that the square pitch-type was more reactive than the hexagonal pitch-type. The resultant bounding fuel OR is much larger than a standard LWR fuel pellet, with peak reactivity at a fuel OR of 3.5 cm with an equivalent half-pitch of 3.5 cm. For U_3Si_2 fuel rods, the bounding fuel OR is 0.4851 cm with an equivalent square half-pitch of 0.4851 cm.

Table 6-118 Package Array, NCT, Rod Pipe-Package Variant Comparison Results

Contents	Traveller Variant	Fuel OR (cm)	Half-Pitch (cm)	Hexagonal Pitch-Type			Square Pitch-Type		
				k_{eff}	σ	$k_{eff} + 2\sigma$	k_{eff}	σ	$k_{eff} + 2\sigma$
UO_2 Fuel Rods	STD	0.390	0.390	0.36250	0.00074	0.36398	0.41675	0.00052	0.41779
		0.450	0.450	0.36264	0.00052	0.36368	0.41782	0.00070	0.41922
		0.475	0.475	0.36306	0.00056	0.36418	0.41960	0.00066	0.42092
		0.500	0.500	0.36204	0.00057	0.36318	0.41929	0.00059	0.42047
		0.550	0.550	0.36251	0.00048	0.36347	0.42081	0.00053	0.42187
		0.600	0.600	0.36337	0.00049	0.36435	0.41983	0.00065	0.42113
		0.650	0.650	0.36451	0.00049	0.36549	0.42114	0.00061	0.42236
		0.700	0.700	0.36401	0.00048	0.36497	0.42225	0.00058	0.42341
		0.750	0.750	0.36380	0.00054	0.36488	0.42248	0.00059	0.42366
	XL	0.390	0.390	0.36722	0.00049	0.36820	0.42171	0.00059	0.42289
		0.450	0.450	0.36710	0.00046	0.36802	0.42188	0.00060	0.42308
		0.475	0.475	0.36664	0.00048	0.36760	0.42174	0.00061	0.42296
		0.500	0.500	0.36601	0.00051	0.36703	0.42209	0.00056	0.42321
		0.550	0.550	0.36709	0.00050	0.36809	0.42317	0.00055	0.42427
		0.600	0.600	0.36795	0.00052	0.36899	0.42435	0.00062	0.42559
		0.650	0.650	0.36697	0.00049	0.36795	0.42515	0.00060	0.42635
		0.700	0.700	0.36813	0.00051	0.36915	0.42507	0.00058	0.42623
		0.750	0.750	0.36709	0.00049	0.36807	0.42608	0.00060	0.42728
		0.800	0.800	--	--	--	0.42641	0.00056	0.42753
		0.950	0.950	--	--	--	0.42861	0.0006	0.42981
		1.000	1.000	--	--	--	0.42964	0.00057	0.43078
		1.500	1.500	--	--	--	0.43248	0.00061	0.4337
		2.000	2.000	--	--	--	0.44342	0.00055	0.44452
		2.500	2.500	--	--	--	0.43539	0.00069	0.43677
		3.000	3.000	--	--	--	0.45212	0.00064	0.4534
		3.500	3.500	--	--	--	0.46675	0.00067	0.46809
		4.000	4.000	--	--	--	0.45741	0.00075	0.45891

Table 6-118 Package Array, NCT, Rod Pipe-Package Variant Comparison Results

Contents	Traveller Variant	Fuel OR (cm)	Half-Pitch (cm)	Hexagonal Pitch-Type			Square Pitch-Type		
				k_{eff}	σ	$k_{eff} + 2\sigma$	k_{eff}	σ	$k_{eff} + 2\sigma$
U_3Si_2	STD	0.3909	0.3909	0.36594	0.00036	0.36666	0.38418	0.00046	0.3851
		0.4145	0.4145	0.37462	0.00035	0.37532	0.39369	0.00042	0.39453
		0.438	0.438	0.38208	0.00038	0.38284	0.40172	0.00035	0.40242
		0.4616	0.4616	0.38886	0.00037	0.38960	0.40923	0.00041	0.41005
		0.4851	0.4851	0.39364	0.00044	0.39452	0.41633	0.00035	0.41703

6.9.3.5 Package Array, HAC, Fuel Assembly

6.9.3.5.1 CFA-Package Variant Comparison Results

Table 6-119 details the results of the Package Array, HAC evaluation for Groups 1 and 2. For Group 1, the most reactive CFA-Package Variant combinations model the Traveller XL with 17 Bin 1, 17 Bin 1a, and 17 Bin 2, and an array stack height of 1 package. For Group 2, the most reactive CFA-Package Variant combination is the Traveller XL with 18 Bin 1 and an array stack height of 1 package. For Group 4, the most reactive CFA is 17 Bin 1. Note that the Traveller XL bounds the STD and an array height of one bounds two for smaller arrays (<100 packages). Therefore, the Traveller STD and an array height of two were not analyzed.

Table 6-119 Package Array, HAC, CFA Package Variant Results

Group	Traveller Variant	Content	Active Fuel Length (in.)	Array Stack Height = 2			Array Stack Height = 1		
				k_{eff}	σ	$k_{eff} + 2\sigma$	k_{eff}	σ	$k_{eff} + 2\sigma$
1	STD	14 Bin 1	137.20	0.87847	0.00024	0.87895	0.88074	0.00024	0.88122
		14 Bin 2	144.50	0.88017	0.00027	0.88071	0.88301	0.00024	0.88349
		15 Bin 1	144.50	0.90231	0.00025	0.90281	0.90515	0.00026	0.90567
		15 Bin 2	140.26	0.89559	0.00024	0.89607	0.89775	0.00029	0.89833
		16 Bin 2	137.20	0.88621	0.00035	0.88691	0.88900	0.00024	0.88948
		16 Bin 3	144.50	0.88231	0.00025	0.88281	0.88517	0.00032	0.88581
		17 Bin 1	144.50	0.90404	0.00026	0.90456	0.90726	0.00026	0.90778
		17 Bin 2	144.50	0.90015	0.00026	0.90067	0.90314	0.00027	0.90368
	XL	14 Bin 1	137.20	0.89879	0.00027	0.89933	0.90104	0.00024	0.90152
		14 Bin 2	144.50	0.89606	0.00026	0.89658	0.89901	0.00024	0.89949
		15 Bin 1	144.50	0.92220	0.00027	0.92274	0.92413	0.00026	0.92465
		15 Bin 2	140.26	0.91581	0.00026	0.91633	0.91885	0.00026	0.91937
		16 Bin 2	137.20	0.90670	0.00024	0.90718	0.90894	0.00026	0.90946
		16 Bin 2a *	150.50	0.90602	0.00031	0.90664	0.90850	0.00027	0.90904
		16 Bin 3	144.50	0.90457	0.00029	0.90515	0.90676	0.00025	0.90726
		17 Bin 1	144.50	0.92391	0.00026	0.92443	0.92612	0.00026	0.92664
		17 Bin 1a *	168.50	0.92377	0.00027	0.92431	0.92646	0.00027	0.92700
		17 Bin 2	144.50	0.92331	0.00027	0.92385	0.92573	0.00026	0.92625

Table 6-119 Package Array, HAC, CFA Package Variant Results

Group	Traveller Variant	Content	Active Fuel Length (in.)	Array Stack Height = 2			Array Stack Height = 1		
				k_{eff}	σ	$k_{eff} + 2\sigma$	k_{eff}	σ	$k_{eff} + 2\sigma$
2	XL	16 Bin 1	154.04	0.90565	0.00024	0.90613	0.91484	0.00024	0.91532
		18 Bin 1	154.04	0.90697	0.00026	0.90749	0.91633	0.00026	0.91685
4	XL	14 Bin 1	137.20	--	--	--	0.81618	0.00023	0.81664
		14 Bin 2	144.50	--	--	--	0.80532	0.00024	0.80580
		15 Bin 3	144.50	--	--	--	0.86157	0.00027	0.86211
		16 Bin 2	150.50	--	--	--	0.82668	0.00025	0.82718
		16 Bin 3	144.50	--	--	--	0.79166	0.00027	0.79220
		17 Bin 1	168.50	--	--	--	0.86948	0.00024	0.86996

Note: * these cases model an active fuel length that cannot be shipped in the STD and are therefore only modeled in the XL.

6.9.3.5.2 Baseline Determination Results

Table 6-120 details the results of the Package Array, HAC evaluation for Groups 1 and 2. For Group 1, the baseline case models the 17 Bin 1 CFA with a most reactive axial fuel position of 87.122 cm, approximately centered in the Clamshell. For Group 2, the baseline case has a most reactive axial fuel position of 72.583 cm, modeling the CFA of 16 Bin 1 approximately centered. For Group 4, the baseline case has the bounding axial fuel position of 65.405 cm, modeling the 17 Bin 1 CFA centered, as the off-centered positions are within statistical differences.

Table 6-120 Axial Position Baseline Results –Package Array, HAC, PWR Fuel Assembly Groups

Group	Traveller Variant	Content	Axial Position (cm)	k_{eff}	σ	$k_{eff} + 2\sigma$
1	XL	17 Bin 1	2.540	0.92612	0.00026	0.92664
			30.734	0.92410	0.00026	0.92462
			58.928	0.92563	0.00027	0.92617
			87.122	0.92688	0.00031	0.92750
			115.316	0.92566	0.00028	0.92622
			143.510	0.92574	0.00028	0.92630
		17 Bin 1a	2.540	0.92646	0.00027	0.92700
			18.542	0.92524	0.00023	0.92570
			34.544	0.92375	0.00023	0.92421
			50.546	0.92486	0.00027	0.92540
			66.548	0.92605	0.00024	0.92653
			82.550	0.92665	0.00024	0.92713
		17 Bin 2	2.540	0.92573	0.00026	0.92625
			30.734	0.92375	0.00027	0.92429
			58.928	0.92492	0.00025	0.92542
			87.122	0.92590	0.00027	0.92644
			115.316	0.92567	0.00027	0.92621

Table 6-120 Axial Position Baseline Results –Package Array, HAC, PWR Fuel Assembly Groups						
Group	**Traveller Variant**	**Content**	**Axial Position (cm)**	**k_{eff}**	**σ**	**$k_{eff} + 2\sigma$**
			143.510	0.92507	0.00029	0.92565
2	XL	18 Bin 1	2.540	0.91633	0.00026	0.91685
			25.888	0.91629	0.00032	0.91693
			49.235	0.91633	0.00024	0.91681
			72.583	0.91690	0.00025	0.91740
			95.931	0.91628	0.00024	0.91676
			119.278	0.91603	0.00029	0.91661
4	XL	17 Bin 1	2.540	0.93736	0.00022	0.93780
			23.495	0.93805	0.00025	0.93855
			44.450	0.93826	0.00024	0.93874
			65.405	0.93810	0.00023	0.93856
			86.360	0.93769	0.00025	0.93819
			107.315	0.93797	0.00025	0.93847
			128.270	0.93728	0.00026	0.93780

Table 6-121 displays the results of the partial flooding baseline study. For all Groups, the highest water level is the most reactive, but the preferential flooding study presented in Table 6-122 is ultimately more reactive. For all Groups, a fully flooded Clamshell with all other package regions, and the package exterior, modeled as dry results in the most reactive flooding configuration, as shown in Figure 6-81, Figure 6-82, and Figure 6-82A, respectively. For all Groups, this is the baseline flooding configuration.

Table 6-121 Partial Flooding Baseline Results – Package Array, HAC, PWR Fuel Assembly Groups					
Content (Group)	**Traveller Variant**	**Water Level ***	**k_{eff}**	**σ**	**$k_{eff} + 2\sigma$**
17 Bin 1 (1)	XL	1	0.28275	0.00014	0.28303
		2	0.27528	0.00016	0.27560
		3	0.51721	0.00022	0.51765
		4	0.79216	0.00030	0.79276
		5	0.90268	0.00032	0.90332
		6	0.91304	0.00030	0.91364
18 Bin 1 (2)	XL	1	0.28637	0.00014	0.28665
		2	0.28263	0.00014	0.28291
		3	0.52063	0.00022	0.52107
		4	0.76388	0.00031	0.76450
		5	0.89435	0.00029	0.89493
		6	0.90525	0.00025	0.90575

Table 6-121 Partial Flooding Baseline Results – Package Array, HAC, PWR Fuel Assembly Groups

Content (Group)	Traveller Variant	Water Level *	k_{eff}	σ	$k_{eff} + 2\sigma$
17 Bin 1 (4)	XL	1	0.28341	0.00016	0.28373
		2	0.27617	0.00015	0.27647
		3	0.51661	0.00024	0.51709
		4	0.77811	0.00025	0.77861
		5	0.90668	0.00027	0.90722
		6	0.91414	0.00028	0.91470

Note: * Water Levels 1 – 6 represent water rising diagonally through the Clamshell as shown in Figure 6-11, where Water Level 1 is empty and Water Level 6 is full.

Table 6-122 Preferential Flooding Baseline Results – Package Array, HAC, PWR Fuel Assembly Groups				
Preferential Flooding Configuration	**Water Density (g/cm^3)**	**Group 1**	**Group 2**	**Group 4**
		Traveller XL		
		$k_{eff} + 2\sigma$		
Outerpack Inner Cavity	0.0000	0.90967	0.89848	0.86996
	0.0010	0.90920	0.89921	0.86940
	0.0100	0.90896	0.89840	0.86950
	0.1000	0.90673	0.89726	0.86326
	0.5000	0.90133	0.89418	0.84523
	0.7000	0.89971	0.89328	0.84025
	0.9982	0.89790	0.89239	0.83464
Clamshell	0.0000	0.90967	0.89848	0.86996
	0.0010	0.90859	0.89838	0.87041
	0.0100	0.90940	0.89878	0.87094
	0.1000	0.91182	0.90137	0.87751
	0.5000	0.91975	0.90916	0.90619
	0.7000	0.92310	0.91150	0.91985
	0.9982	0.92750	0.91740	0.93856
Outerpack Outer Cavity	0.0000	0.90967	0.89848	0.86996
	0.0010	0.90922	0.89843	0.87021
	0.0100	0.90798	0.89727	0.86705
	0.1000	0.89574	0.88772	0.84697
	0.5000	0.87478	0.86863	0.81302
	0.7000	0.87227	0.86691	0.80817
	0.9982	0.87039	0.86501	0.80625
Entire Package	0.0000	0.90967	0.89848	0.86996
	0.0010	0.90907	0.89907	0.87051
	0.0100	0.90790	0.89728	0.86789
	0.1000	0.89745	0.88912	0.85081
	0.5000	0.89509	0.88805	0.86523
	0.7000	0.89862	0.89160	0.88181
	0.9982	0.90418	0.89688	0.90589
Interspersed Moderation	0.0000	0.90967	0.89848	0.86996
	0.0010	0.90888	0.89899	0.86945
	0.0100	0.90899	0.89797	0.86972
	0.1000	0.90670	0.89712	0.86479
	0.5000	0.89696	0.88904	0.84961
	0.7000	0.89420	0.88684	0.84475
	0.9982	0.89039	0.88318	0.83897

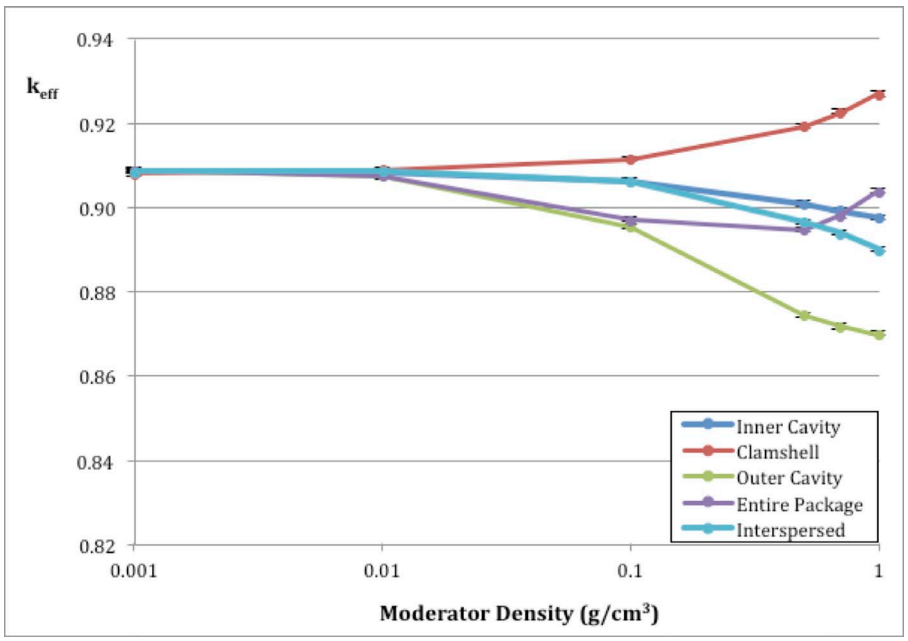

Figure 6-81 Effect of Preferential Flooding Configuration on k_{eff} (Group 1)

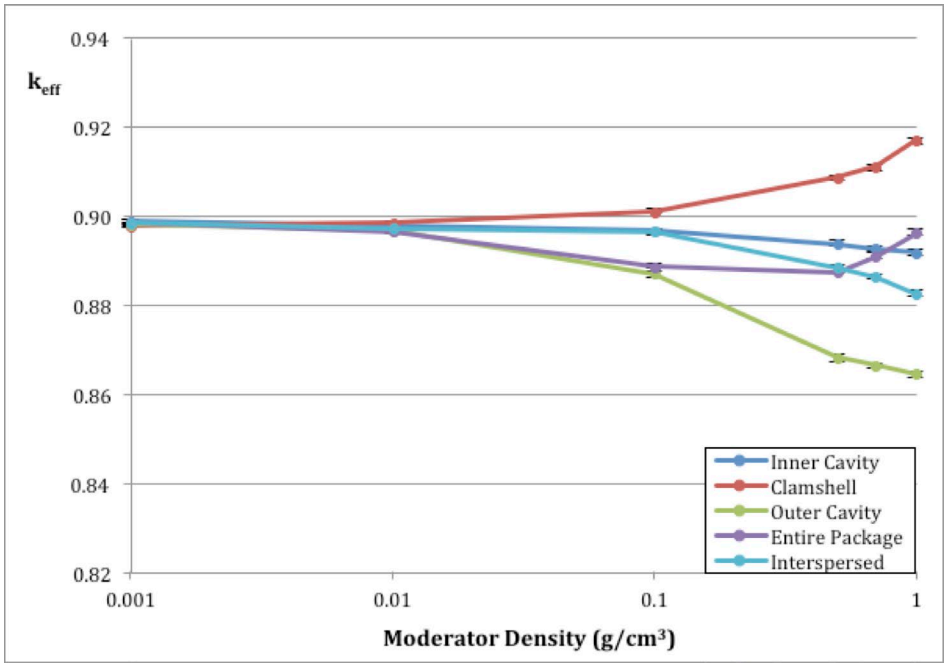

Figure 6-82 Effect of Preferential Flooding Configuration on k_{eff} (Group 2)

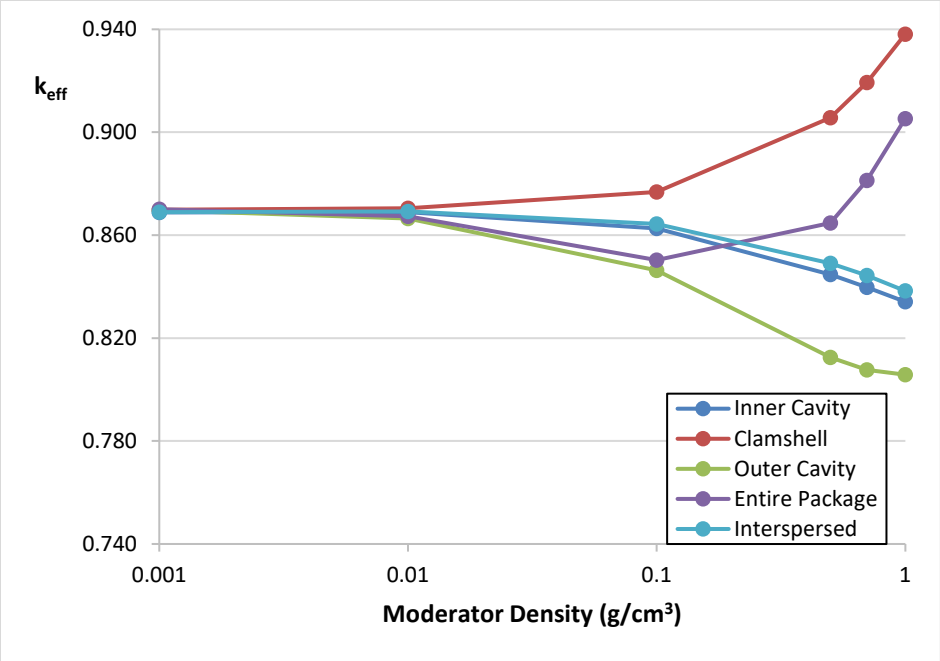

Figure 6-82A Effect of Preferential Flooding Configuration on k_{eff} (Group 4)

6.9.3.6 Package Array, HAC, Rod Pipe

6.9.3.6.1 Baseline Determination Results

For the Rod Pipe Package Array under HAC, a full study was done that examined several pitch values for each fuel OR listed in order to determine the peak reactivity. Table 6-123 lists the peak value of each of these curves, with the overall maximum shaded in gray. Table 6-123, Table 6-124, and Table 6-125 show the fuel pitch variation curve for the most reactive fuel OR of each package variant and pitch type. The full range of fuel OR and half-pitch values examined are listed in Table 6-15. Table 6-126 takes the overall most reactive UO_2 fuel rod case (the Traveller XL with fuel OR = 0.5 cm and half-pitch = 1.0 cm with a hexagonal pitch-type) and examines finer pitch values for fuel OR of 0.45, 0.5, and 0.55 cm in order to better determine the optimum fuel OR-fuel pitch combination. The Rod Pipe UO_2 Fuel Rods Package Array, HAC baseline case models the Traveller XL with a fuel OR of 0.5 cm and a hexagonal half-pitch of 1.00 cm. The Rod Pipe U_3Si_2 Fuel Rods Package Array, HAC baseline case models the Traveller STD with a fuel OR of 0.4851 cm and a square half-pitch of 0.9851 cm.

Table 6-123 Package Array, HAC, Rod Pipe Fuel OR-Pitch Combination – Maximum Results

Contents	Traveller Variant	Fuel OR (cm)	Hexagonal Pitch-Type				Square Pitch-Type			
			Half-Pitch (cm)	k_{eff}	σ	$k_{eff} + 2\sigma$	Half-Pitch (cm)	k_{eff}	σ	$k_{eff} + 2\sigma$
UO_2 Fuel Rods	STD	0.39	0.89	0.65080	0.00100	0.65280	0.64	0.65546	0.00082	0.65710
		0.45	0.95	0.65670	0.00100	0.65870	0.7	0.64712	0.00079	0.64870
		0.475	0.975	0.65896	0.00084	0.66064	0.725	0.64482	0.00096	0.64674
		0.5	1.0	0.66131	0.00088	0.66307	1.0	0.64560	0.00100	0.64760
		0.55	1.05	0.65958	0.00080	0.66118	1.05	0.65110	0.00092	0.65294
		0.6	1.1	0.65142	0.00092	0.65326	1.1	0.65190	0.00100	0.65390
		0.65	1.15	0.64336	0.00096	0.64528	1.15	0.64818	0.00087	0.64992
		0.7	1.2	0.64161	0.00078	0.64317	1.2	0.64719	0.00086	0.64891
		0.75	1.25	0.64006	0.00085	0.64176	1.25	0.64409	0.00078	0.64565
	XL	0.39	0.89	0.65219	0.00091	0.65401	0.64	0.65671	0.00086	0.65843
		0.45	0.95	0.65800	0.00100	0.66000	0.7	0.64847	0.00089	0.65025
		0.475	0.975	0.66092	0.00084	0.66260	0.725	0.64641	0.00082	0.64805
		0.5	1.0	0.66404	0.00090	0.66584	1.0	0.65015	0.00089	0.65193
		0.55	1.05	0.66278	0.00088	0.66454	1.05	0.65587	0.00084	0.65755
		0.6	1.1	0.65487	0.00083	0.65653	1.1	0.65278	0.00081	0.65440
		0.65	1.15	0.64503	0.00081	0.64665	1.15	0.65232	0.00080	0.65392
		0.7	1.2	0.64394	0.00084	0.64562	1.2	0.65153	0.00081	0.65315
		0.75	1.25	0.64204	0.00078	0.64360	1.25	0.64680	0.00093	0.64866
U_3Si_2 Fuel Rods	STD	0.3909	0.9159	0.60523	0.00055	0.60633	0.8659	0.60508	0.00047	0.60602
		0.4145	0.9395	0.61310	0.00045	0.61400	0.8645	0.61139	0.00048	0.61235
		0.4380	0.9380	0.61677	0.00068	0.61813	0.8630	0.61641	0.00050	0.61741
		0.4616	0.9866	0.62163	0.00044	0.62251	0.8866	0.61943	0.00056	0.62055
		0.4851	0.9851	0.62316	0.00048	0.62412	0.9101	0.61984	0.00049	0.62082

Table 6-124 UO_2 Package Array, HAC, Rod Pipe Fuel OR-Pitch Combination – Pitch Variation

Traveller Variant	Hexagonal Pitch-Type Fuel OR = 0.50 cm				Square Pitch-Type Fuel OR = 0.39 cm			
	Half-Pitch (cm)	k_{eff}	σ	$k_{eff} + 2\sigma$	Half-Pitch (cm)	k_{eff}	σ	$k_{eff} + 2\sigma$
STD	0.5	0.36030	0.00051	0.36132	0.39	0.41473	0.00057	0.41587
	0.6	0.49679	0.00077	0.49833	0.49	0.56512	0.00085	0.56682
	0.75	0.61458	0.00079	0.61616	0.64	0.65546	0.00082	0.65710
	1.0	0.66131	0.00088	0.66307	0.89	0.64367	0.00090	0.64547
	1.25	0.62189	0.00084	0.62357	1.14	0.56496	0.00081	0.56658
XL	0.5	0.36481	0.00051	0.36583	0.39	0.41863	0.00055	0.41973
	0.6	0.50205	0.00070	0.50345	0.49	0.56960	0.00087	0.57134
	0.75	0.61877	0.00078	0.62033	0.64	0.65671	0.00086	0.65843
	1.0	0.66404	0.00090	0.66584	0.89	0.64537	0.00092	0.64721
	1.25	0.62488	0.00091	0.62670	1.14	0.56566	0.00091	0.56748

Table 6-125 U_3Si_2 Package Array, HAC, Rod Pipe Fuel OR-Pitch Combination – Pitch Variation

Traveller Variant	Hexagonal Pitch-Type Fuel OR = 0.4851 cm				Square Pitch-Type Fuel OR = 0.4851 cm			
	Half-Pitch (cm)	k_{eff}	σ	$k_{eff} + 2\sigma$	Half-Pitch (cm)	k_{eff}	σ	$k_{eff} + 2\sigma$
STD	0.6351	0.48303	0.00040	0.48383	0.6351	0.51485	0.00040	0.51565
	0.6851	0.51369	0.00056	0.51481	0.6851	0.54510	0.00049	0.54608
	0.7351	0.54171	0.00052	0.54275	0.7351	0.57244	0.00044	0.57332
	0.7851	0.56883	0.00047	0.56977	0.7851	0.59382	0.00042	0.59466
	0.8351	0.59099	0.00050	0.59199	0.8351	0.60970	0.00046	0.61062
	0.8851	0.60725	0.00053	0.60831	0.8851	0.61963	0.00057	0.62077
	0.9351	0.61865	0.00048	0.61961	0.9101	0.61984	0.00049	0.62082
	0.9601	0.62188	0.00048	0.62284	0.9351	0.61657	0.00046	0.61749
	0.9851	0.62316	0.00048	0.62412	0.9601	0.61307	0.00051	0.61409
	1.0101	0.62295	0.00053	0.62401	0.9851	0.60988	0.00046	0.61080
	1.0351	0.62181	0.00048	0.62277	1.0351	0.60517	0.00046	0.60609
	1.0851	0.61007	0.00046	0.61099	1.0851	0.59670	0.00049	0.59768
	1.1351	0.59411	0.00052	0.59515	1.1351	0.58495	0.00048	0.58591
	1.1851	0.58921	0.00051	0.59023	1.1851	0.57452	0.00049	0.57550
	1.2351	0.5839	0.00046	0.58482	1.2351	0.55718	0.00042	0.55802
	1.2851	0.57329	0.00050	0.57429	1.2851	0.53699	0.00043	0.53785
	1.3351	0.55946	0.00044	0.56034	1.3351	0.52171	0.00043	0.52257

Table 6-126 UO_2 Package Array, HAC, Rod Pipe Fuel OR-Pitch Combination – Refined Parameter Study

Fuel OR (cm)	Half-Pitch (cm)	k_{eff}	σ	$k_{eff} + 2\sigma$
0.475	0.475	0.36435	0.00029	0.36493
	0.575	0.50652	0.00038	0.50728
	0.725	0.62531	0.00045	0.62621
	0.875	0.66157	0.00043	0.66243
	0.925	0.65967	0.00066	0.66099
	0.975	0.66217	0.00044	0.66305
	1.025	0.65971	0.00050	0.66071
	1.075	0.65040	0.00061	0.65162
	1.125	0.63150	0.00054	0.63258
	1.175	0.62186	0.00046	0.62278
	1.225	0.61769	0.00063	0.61895
0.5	0.5	0.36489	0.00030	0.36549
	0.6	0.50025	0.00041	0.50107
	0.75	0.61898	0.00045	0.61988
	0.9	0.65602	0.00052	0.65706
	0.95	0.65915	0.00049	0.66013
	1	0.66385	0.00050	0.66485
	1.05	0.66147	0.00057	0.66261
	1.1	0.64822	0.00048	0.64918
	1.15	0.63379	0.00050	0.63479
	1.2	0.62922	0.00047	0.63016
	1.25	0.62453	0.00056	0.62565
0.550	0.55	0.36474	0.00033	0.36540
	0.65	0.49089	0.00039	0.49167
	0.8	0.60868	0.00049	0.60966
	0.95	0.65168	0.00051	0.65270
	1	0.66151	0.00054	0.66259
	1.05	0.66253	0.00047	0.66347
	1.1	0.65524	0.00048	0.65620
	1.15	0.64444	0.00052	0.64548
	1.2	0.64255	0.00050	0.64355
	1.25	0.64131	0.00051	0.64233
	1.3	0.63354	0.00057	0.63468

6.9.4 Combined Cases

For each content type, an individual "worst-case" HAC array model was generated combining all the positive penalty model results and its SCALE 6.1.2 case was analyzed, as shown in Table 6-127. Only the HAC array cases were analyzed because these cases are the closest to the USL for each content type. For all contents, the combined penalty case's $k_{eff} + 2\sigma$ was either less than the *Maximum* k_{eff} values listed in Table 6-2, or the difference in k_{eff} was statistically insignificant. This result is primarily because penalties from each study are indiscriminately summed for a total penalty, while for multiple studies the penalty is due to the same effect (e.g. increased moderation). Thus, the increase in k_{eff} from independently adding penalties from separate studies is either greater than the cumulative effect from modeling all positive penalty parameters in a single model or has no difference in effect. PWR Group 4 was not analyzed because this section has shown that the *Maximum* k_{eff} method bounds the combined cases and Group 4 has a relatively low Total Penalty when compared to Groups 1 and 2.

Table 6-127 *Maximum* k_{eff} vs. Combined Case Results

Case	Content	k_{eff}	σ	$k_{eff} + 2\sigma$
CSI 1.0				
--	Table 6-2 *Maximum* k_{eff}	--		0.93783
17 Bin 1	Combined Model	0.93732	0.00024	0.93780
CSI 4.2				
--	Table 6-2 *Maximum* k_{eff}	--		0.93945
18 Bin 1	Combined Model	0.93618	0.00027	0.93672
UO_2 Rod Pipe				
--	Table 6-2 *Maximum* k_{eff}	--		0.76784
UO_2 Rod Pipe	Combined Model	0.72230	0.00048	0.72326
U_3Si_2 Rod Pipe				
--	Table 6-2 *Maximum* k_{eff}	--		0.76836
U_3Si_2 Rod Pipe	Combined Model	0.74746	0.00056	0.74858

TABLE OF CONTENTS

7.0 PACKAGE OPERATIONS 7-1
7.1 PACKAGE LOADING 7-1
7.1.1 Preparation for Loading 7-1
7.1.1.1 Receive Shipping Package 7-1
7.1.1.2 Clean Shipping Package 7-2
7.1.1.3 Refurbish Shipping Package 7-2
7.1.1.4 Configure Package for Fuel Assembly Loading 7-2
7.1.1.5 Inspection 7-2
7.1.2 Loading Contents and Closing Package 7-3
7.1.2.1 Fuel Assemblies 7-3
7.1.2.2 Rod Pipe 7-4
7.1.3 Preparation for Transport 7-5
7.1.3.1 Conveyance Loading of Shipping Packages 7-5
7.1.3.2 Regulatory 7-5
7.1.3.3 Inspection 7-5
7.2 PACKAGE UNLOADING 7-6
7.2.1 Receipt of Package from Carrier 7-6
7.2.2 Removal of Contents 7-6
7.2.2.1 Fuel Assemblies 7-6
7.2.2.2 Rod Pipe 7-7
7.3 PREPARATION OF EMPTY PACKAGE FOR TRANSPORT 7-8
7.4 APPENDICES 7-8
7.4.1 References 7-8

7.0 PACKAGE OPERATIONS

The following information contains the significant actions relating to the routine use of fuel assembly shipping packages. Complete detailed instructions are outlined within the individual site operating procedures and quality control instructions pertinent to each specific operation at each site. It should be considered that in this section the term "Traveller package" refers to the STD and XL. The requirements listed below are for both Type A and Type B contents unless content Type is explicitly stated.

7.1 PACKAGE LOADING

Operations at the loading site include the span of activities from receiving and inspecting the package to loading and preparing the loaded package for transport. Each loading site must provide fully trained personnel and operating procedures to cover all of the activities.

7.1.1 Preparation for Loading

For contents to be acceptable for shipment in the Traveller package as Type A material, without the additional configuration requirements for Type B material, the requirements of (a) or (b) shall be met (as described in Section 1.2.2.2):

a. The uranium content meets the "unirradiated uranium" definition of SSR-6 para. 527 [1] and 10 CFR 71.4 [2]:

> *Unirradiated uranium* means uranium containing not more than 2 x 10^3 Bq of plutonium per gram of uranium-235, not more than 9 x 10^6 Bq of fission products per gram of uranium-235, and not more than 5 x 10^{-3} g of uranium-236 per gram of uranium-235.

b. If the ^{236}U requirement of the unirradiated definition is not met, the content may still be shipped if the following criteria are met:
   1) The contents meet the requirements of the Enriched Commercial Grade specification of ASTM C 996 [3], specifically the ^{236}U limit (250 $\mu g^{236}U/gU$), as outlined in Table 1-2.
   2) There is less than a Type A quantity of material in the content.
      - For an A_2 calculation, the *U (enriched to 20% or less) - Unlimited* value may not be used.
      - The A_2 calculation must be completed using the A_2 values in 10 CFR 71 Appendix A, Table A-1 for the individual isotopes in the fuel content, using the "slow lung absorption" values for uranium isotopes (i.e. for a UO_2 or U_3Si_2 compound).

Contents that exceed the quantities to be defined as Type A material may be transported as Type B material, as long as the limits of contaminated uranium, as defined in Table 1-2, Section 1.2.2.2, are not exceeded.

Loose fuel rods in the Rod Pipe may only be transported in the Type A configuration.

7.1.1.1 Receive Shipping Package

- Unload the shipping package from the truck.
- Report any obvious damage to the package engineer.
- Prepare a package identification route card.

7.1.1.2 Clean Shipping Package

- Use soap or a suitable detergent and/or water to clean the package, as required.
- Move the package to the refurbishing or lay down areas.

7.1.1.3 Refurbish Shipping Package

- Check package upper and lower Outerpack exterior for damage.
- Open Outerpack and check for internal damage or excessive wear.
- Repair/rework as required.
- Check Clamshell for loose parts, and if found, secure per specifications and drawings.
- Check the Clamshell for any mechanical damage or excessive wear.
- Vacuum package to collect foreign debris.

7.1.1.4 Configure Package for Fuel Assembly Loading

- For Type A Configuration: Configure (install) top axial restraint(s) and axial spacer (as needed) for specific fuel assembly type.
- For Type B Configuration: Configure (install) top axial restraint(s) and bottom support component for the specific fuel assembly type. For a fuel assembly with corner support legs on the bottom nozzle the bottom support spacer is utilized, and for a fuel assembly with a bottom nozzle without corner support legs the combination of the bottom axial spacer and the bottom support plate are utilized. (Note: no other axial spacer component may be solely utilized for the Type B configuration)
- Install accelerometers as required per site procedure.
- Check installed accelerometers for QC seal, calibration, and tripped condition. If found in tripped condition, replace with un-tripped and calibrated accelerometer.

7.1.1.5 Inspection

- Verify that the package interior/exterior Outerpack and Clamshell are clean, and in good condition.
- For Type A Configuration: Verify that the top axial restraint(s), axial spacer (as needed) and grids pads are present and in good working condition.
- For Type B Configuration: Verify that the top axial restraint(s), grid pads, and bottom support component for the specific fuel assembly type are present and in good working condition. For a fuel assembly with corner support legs on the bottom nozzle the bottom support spacer is utilized, and for a fuel assembly with a bottom nozzle without corner support legs the combination of the bottom axial spacer and the bottom support spacer plate are utilized. (Note: no other axial spacer component may be solely utilized for the Type B configuration)
- Verify that the BORAL neutron absorber plates are present and in good visual condition.
- Verify that outstanding applicable package non-conformances have been closed prior to release for loading.

7.1.2 Loading Contents and Closing Package

7.1.2.1 Fuel Assemblies

- Secure Outerpack in Upender by engaging lock pins or latch.
- Remove all but at least one of the upper Outerpack bolts on one side of the package. (All other hinge bolts remain in place).
- Raise shipping package to vertical position. Lockout support arms when using mechanical Upenders.
- Remove the remaining hinge bolt(s) from the one side.
- Loosen Outerpack swing bolts and rotate away from package.
- Open upper Outerpack door and fully rotate away from package.
- Remove the hinge pin and open Clamshell top door.
- Loosen and remove Clamshell top axial restraint assembly.
- Open lower Clamshell doors by turning latches to open position.
- Install Clamshell door stop.
- Check upper and lower accelerometers are not tripped. If found in tripped condition, replace with un-tripped and calibrated accelerometer.
- For Type B Configuration: Verify that the proper axial fuel restraints, including the bottom support component and top axial restraint assembly for the specific fuel design, are in place prior to installing the fuel assembly.
    - For any fuel assembly with a bottom nozzle corner support legs, the bottom support spacer is utilized, and for a fuel assembly with a bottom nozzle without corner support legs the combination of the bottom fuel axial spacer and the bottom support plate are utilized.
    - For any fuel assembly with a top nozzle with an open center, the top axial restraint (i.e., center post) plus axial clamping studs are utilized, and for a fuel assembly with a flat top nozzle, the circular/square base plate plus clamping stud is utilized.
- Verify that the fuel assembly has been released by Quality Assurance. Install fuel assembly by resting it on Clamshell bottom plate.
- Verify that the fuel assembly is properly oriented in the package.
- For Type B Configuration: Tighten the top axial restraint(s) using hand tools and the lock nut(s). Torque to 4.2 ft-lb (5.7 N-m) nominally.
- For Type B Configuration: Verify proper fit of the fuel assembly and axial fuel restraints with a visual and physical hand check of the arrangement. The visual inspection shall verify a tight fit and that there are no gaps between the fuel assembly, axial restraints, and Clamshell top and bottom ends. A tight fit of the axial components shall be physically verified by grasping the bottom support spacer and ensuring that it does not move independently.
- Check that grid pads are positioned at fuel assembly structural grids and nozzles.
- Remove door stop.
- Close lower Clamshell doors and secure latches by turning to lock position.
- Remove fuel tool.
- Install Clamshell top axial restraint assembly and secure axial restraint.

- Close Clamshell top door and install hinge pin.
- Close the upper Outerpack.
- Rotate Outerpack swing bolts into bracket and secure.
- Install at least one Outerpack bolt.
- Disengage upper support arm lock pins on mechanical Upender. Lower package to horizontal position. Disengage latch on powered Upender.
- Verify general cleanliness and absence of debris on the Outerpack after closing the upper Outerpack door.
- Torque the swing bolts to 20 ± 1 ft-lb (27.1 ± 1.4 N-m) and torque the Outerpack bolts to 60 ± 5 ft-lb (81.3 +7/–6 N-m).
- Verify one approved tamper proof security seal is installed on each opposite side of the package.
- Verify that the required decals, labels, stencil markings, etc. are present and legible.

7.1.2.2 Rod Pipe

- Secure open Rod Pipe to the horizontal position and load rods into pipe.
- Install the ½-13 UNC bolts into the desired flange end and torque bolts to 20 ± 1 ft·lb [27 ± 1 N·m].
- Remove the 24 upper Outerpack hinge bolts and lift upper Outerpack off the package.
- Unlock the quarter turn Clamshell latches and open the Clamshell main doors.
- Place the pipe into the Clamshell trough. Attach lateral flange pads as needed.
- Install shipping insert/spacer at the Rod Pipe top end. For Traveller STD, place foam between the Clamshell top plate assembly and Rod Pipe top end. For Traveller XL, attach shim plate to Rod Pipe top end and install Clamshell top plate assembly, ensure adjustable jackscrew is tightened down to touch the Rod Pipe.
- Close Clamshell top door, secure, and install hinge pin.
- Check that upper and lower accelerometers are not tripped. If found in the tripped condition, replace with un-tripped and calibrated accelerometer.
- Verify general cleanliness of Clamshell interior and Outerpack interior.
- Close Clamshell main doors, and then secure by turning the quarter turn Clamshell latches to the lock position.
- Place the upper Outerpack onto the lower Outerpack.
- Install all 24 upper hinge bolts and torque bolts to 60 ± 5 ft·lb [81 +7/–6 N-m].
- Rotate swing bolts onto upper Outerpack and torque nuts 20 ± 1 ft·lb [27 ± 1 N-m].
- Verify general cleanliness of Outerpack exterior.
- Verify on approved tamper proof security seal is installed on each opposite side of the package.
- Verify that the required decals, labels, stencil markings, etc. are present and legible.

7.1.3 Preparation for Transport

7.1.3.1 Conveyance Loading of Shipping Packages

- Place shipping package on conveyance equipped to permit chaining and strapping package securely.
    - When lifting by four (4) upper Outerpack lift eyes:
        - A maximum of two (2) stacked Traveller STDs may be lifted at a time
        - A maximum of one (1) Traveller XL may be lifted at a time.
- Center and place package lengthwise on conveyance.
- Install spacer bars, if required, and install quick release lockout pin.
- Secure packages to conveyance with stops or locating pins.
- Chain or strap the packages to conveyance using "come along" tighteners with chains of 3/8 in (0.95 cm) minimum diameter and/or nylon straps with a minimum 5000 lb (22.24 kN) Working Load Limit (WLL).
- Place webbing swings over spacer bars, if required, and secure to conveyance.

7.1.3.2 Regulatory

- Conduct direct alpha surveys on both the package(s) and the accessible areas of the flatbed.
- Conduct radiation survey of the package(s) and transport vehicle consistent with 10 CFR 71.47 and SSR-6 para. 527. Note: A neutron and gamma radiation survey shall be performed.
- Perform the removable alpha and beta-gamma external smear surveys on both the package(s) and the accessible areas of the flatbed. If any of the following measurements are met or exceeded, notify Regulatory Engineering or appropriate site personnel for instructions on decontamination:
    - 0.4 Bq/cm^2 (1×10^{-5} µCi/cm^2 or 2400 dpm/100 cm^2) for beta and gamma emitters and low toxicity alpha emitters
    - 0.04 Bq/cm^2 (1×10^{-6} µCi/cm^2 or 240 dpm/100 cm^2) for all other alpha emitters

7.1.3.3 Inspection

- Verify that package(s) are properly stacked and secured.
- Verify that required Health Physics, Radioactive, and any other placards or labels have been properly placed.
- Verify that two tamper proof security seals have been properly placed on each package.

7.2 PACKAGE UNLOADING

Operations at the unloading site include receipt and inspection of the loaded package and removal of contents. Each unloading facility must provide fully trained personnel and will be supplied with detailed operating procedures to cover all activities as required by 10 CFR 71.89.

7.2.1 Receipt of Package from Carrier

- Conduct contamination surveys of the package(s) and transport vehicle as outlined in site-specific procedures, consistent with Section 7.1.3.2.
- Conduct radiation survey of the package(s) and transport vehicle as outlined in site-specific procedures, consistent with Section 7.1.3.2.
- Perform an external inspection of the unopened package and record any significant observations.
- Verify that two tamper proof security seals have been properly placed on each package. If either seal is missing or damaged, record the damage and follow site procedures for possible security issues.
- When lifting by four (4) upper Outerpack lift eyes, a maximum of two (2) stacked Traveller STDs may be lifted and a maximum of one (1) Traveller XL may be lifted at a time.

7.2.2 Removal of Contents

7.2.2.1 Fuel Assemblies

- Secure Outerpack in Upender by engaging lock pins, or a latch on a Powered Upender.
- Remove all but at least one of the upper Outerpack bolts on one side of the package. (All other hinge bolts remain in place).
- Raise shipping package to vertical position. Lockout support arms when using mechanical Upenders.
- Remove the remaining hinge bolt(s) from the one side.
- Loosen Outerpack swing bolts and rotate away from package.
- Open upper Outerpack door and fully rotate away from package.
- Check upper and lower accelerometers for tripped condition. If in tripped condition, disposition fuel assembly per applicable Field Specification.
- Remove the Clamshell top hinge pin and open Clamshell top door.
- Loosen and remove Clamshell top axial restraint assembly.
- Install and latch the plant fuel tool to the fuel assembly/component.
- Tension crane cable between 100 to 1,000 lb (0.44 kN to 4.45 kN), as needed, to take load off Clamshell bottom plate.
- Turn lower Clamshell door latches to open position and open main doors.
- Install Clamshell door stop.
- Lift fuel assembly at least 1.5 in (3.81 cm) above Clamshell bottom plate or bottom support component.
- Carefully remove fuel assembly from Clamshell.
- Move fuel assembly to dry storage or other desired location.
- Prepare to close Clamshell by removing Clamshell door stop.

- Close main Clamshell doors and secure latches.
- Install Clamshell top axial restraint assembly.
- Close Clamshell top door and install hinge pin.
- Rotate Outerpack swing bolts into bracket and install at least one Outerpack bolt.
- Verify the swing bolts and Outerpack bolts are at least hand tight using standard hand tools.
- Disengage upper support arm lock pins on mechanical Upender. Lower package to horizontal position. Disengage latch if using a powered Upender.

7.2.2.2 Rod Pipe

- Remove tamper seals located on each opposite side of the package.
- Remove the 24 upper Outerpack hinge bolts.
- Loosen the swing bolts and remove the upper Outerpack.
- Check the upper and lower accelerometers for their tripped condition. If found tripped, disposition rods per applicable Field Specification or instruction from Westinghouse Fuel Engineering.
- Remove the Clamshell top door hinge pin and open the top door assembly.
- For Traveller STD, remove foam between the Clamshell top plate and Rod Pipe top end; for Traveller XL, remove shim plate at Rod Pipe top end and remove Clamshell top plate.
- Open the quarter turn Clamshell latches and then open the Clamshell main doors.
- Lift pipe out of Clamshell and transfer to desired location.
- Remove the ½-13 UNC bolts from the desired flange end.
- Remove the flange and remove fuel rods.
- Re-assemble the flange and bolts, then verify that the flange bolts are at least hand tight using standard hand tools.
- Place the pipe into the Clamshell trough.
- Close Clamshell main doors, and then secure by turning the quarter turn Clamshell latches to the lock position.
- Place the upper Outerpack onto the lower Outerpack.
- Install all 24 upper hinge bolts and verify that all bolts are at least hand tight using standard hand tools.
- Rotate swing bolts onto upper Outerpack and verify that all bolts are at least hand tight using standard hand tools.

7.3 PREPARATION OF EMPTY PACKAGE FOR TRANSPORT

The requirements for preparing an empty Traveller package for transport are intended to meet the relevant requirements for shipping an empty radioactive material package (49 CFR 173 [4] and SSR-6 paras. 422 and 427 [1]).

- Verify the package is empty of contents.
- Verify radiation levels do not exceed limits prescribed in 49 CFR 173.421(b).
- Verify non-fixed radioactive surface contamination does not exceed limits prescribed in 49 CFR 173.421(c).
- Verify the package does not contain fissile material unless an exception of 49 CFR 173.453 is met.
- Verify the packaging is in unimpaired condition and is securely closed.
- Verify the internal contamination does not exceed 100 times the limits as prescribed by 49 CFR 173.428(d).
- Remove any previously applied labels affixed for fuel shipments.
- Affix an “Empty” label.

7.4 APPENDICES

7.4.1 References

[1] International Atomic Energy Agency, "Regulations for the Safe Transport of Radioactive Material," Specific Safety Requirements No. SSR-6, 2012.

[2] U.S. Nuclear Regulatory Commission Code of Federal Regulations, Title 10 Part 71, "Packaging and Transport of Radioactive Material," 10 CFR 71, 2018.

[3] American Society for Testing and Materials, "Standard Specification for Uranium Hexafluoride Enriched to Less Than 5% 235U," ASTM C996-15, 2015.

[4] U.S. Department of Transportation Code of Federal Regulations, Title 49 Subchapter C, "Hazardous Materials Regulations," 2016.

TABLE OF CONTENTS

8.0 ACCEPTANCE TESTS AND MAINTENANCE PROGRAM 8-1
8.1 ACCEPTANCE TESTS 8-1
8.1.1 Visual Inspections and Measurements 8-1
8.1.2 Weld Examinations 8-1
8.1.3 Structural and Pressure Tests 8-2
8.1.4 Leakage Tests 8-2
8.1.5 Component and Material Tests 8-2
8.1.5.1 Polyurethane Foam 8-2
8.1.5.2 Neutron Absorber Plates 8-6
8.1.5.3 Polyethylene Moderator Blocks 8-9
8.1.6 Shielding Tests 8-9
8.1.7 Thermal Tests 8-9
8.2 MAINTENANCE PROGRAM 8-9
8.2.1 Structural and Pressure Tests 8-9
8.2.2 Leakage Tests 8-9
8.2.3 Component and Material Tests 8-10
8.2.3.1 Fasteners 8-10
8.2.3.2 Weather Gasket 8-10
8.2.3.3 Shock Mounts 8-10
8.2.4 Thermal 8-10
8.2.5 Neutron Absorber Plates 8-10
8.2.6 Periodic Weld Examinations 8-11
8.2.7 Periodic Acetate Plug Examinations 8-11
8.3 APPENDICES 8-12
8.3.1 References 8-12

LIST OF TABLES

Table 8-1 Packaging Rigid Polyurethane Foam Density Requirements 8-3
Table 8-2 Packaging Rigid Polyurethane Foam Property Compressive Strength Range 8-3
Table 8-3 Packaging Rigid Polyurethane Foam Thermal Conductivity Properties 8-5
Table 8-4 Packaging Material Test Methods 8-8

8.0 ACCEPTANCE TESTS AND MAINTENANCE PROGRAM

It should be considered that in this section the term "Traveller package" refers to the STD and XL. The requirements listed below are for both Type A and Type B contents unless content Type is explicitly stated.

8.1 ACCEPTANCE TESTS

Per the requirements of 10 CFR 71.85 [1] and SSR-6 para. 501 [2], this section discusses the inspections and acceptance tests to be performed prior to first use of the Traveller package. The Traveller package is procured under an NRC approved Quality Assurance (QA) program meeting the requirements of 10 CFR 71 Subpart H.

8.1.1 Visual Inspections and Measurements

The Traveller STD and Traveller XL packages have manufacturing drawings that are controlled within a quality assurance program. The drawings have quality control characteristics that must be inspected during the manufacturing process. Source inspection and final release of the package will be performed by Westinghouse to verify the quality characteristics were inspected and that the package is acceptable. Any characteristic that is out of specification must be reported. It will then be dispositioned according to Westinghouse procedure.

8.1.2 Weld Examinations

All Traveller packaging welds shall be examined to verify conformance with all applicable codes, standards and notes on each applicable drawing or specification. Nondestructive examination procedures and acceptance standards are based on the ASME Code, Section III, Subsection NF-5000 (Reference [3] or a later edition as approved by Engineering at the time of manufacturing). For the Support Shelf Welds and the Fork Lift Leg Sub-Assembly, the non-destructive examination technique, such as liquid penetrant testing, is required to verify the integrity of these welds.

Weld examination verifies that locations, types and sizes of welds match drawing specifications. Further, it must be verified that there are no cracks, incomplete fusion or lack of penetration. Parts that do not meet their respective specification are repaired or replaced in accordance with Westinghouse procedure and re-inspected.

For Type B contents, the fuel rod weld joints are examined at the time of fuel fabrication and leak tested to ensure that they are sealed. The welding and leak testing of fuel rods is performed during manufacturing using a qualified process. This process assures that the fuel is acceptable for use in a nuclear reactor core and is tightly controlled. The welds between the cladding tube and end caps on every fuel rod shall be 100% visually and radiographically or ultrasonically inspected per qualified procedures, and the following minimum requirements:

Visual Inspections – Shall confirm that there are no visual unacceptable defects or abnormalities (e.g., blow holes, cracks, non-fusion areas, inclusions, irregular contours, O.D. undercuts, or discoloration). No melt back (melting of a portion of the top end plug during seal welding) extending beyond the chamfer and affecting the rod diameter or an allowable depth defined by process controls.

Radiographic Inspections – Shall verify that there are no areas showing unacceptable defects (e.g., a lack of penetration, weld porosity, or inclusions), and the maximum allowed undercut of the wall thickness is

specified by process controls. For girth welds containing porosity, underpenetration, ID undercut and inclusions have less than a combined circumferential cross-section defined by process controls and are detectable with level 2-2T radiography or Engineering approved equivalent.

Ultrasonic Inspections – For weld penetrations with porosity or inclusions, the ultrasonic response shall be less than received from a measurement defined by process controls with Level 2-2T radiography or Engineering approved equivalent.

8.1.3 Structural and Pressure Tests

The Traveller packaging includes hoist rings, which require acceptance inspection. Prior to first-time use, the hoist rings need to be tested at 150% of their maximum rated loading for a minimum of ten minutes.

The Traveller packaging is not pressurized, therefore no pressure testing of the packaging is required.

Additionally, for Type B contents, the fuel rods which form the containment boundary are designed to withstand the pressures found within a reactor, which are significantly greater than the pressure the Traveller package could ever credibly experience. Therefore, no additional pressure testing is required of the fuel rods for transport packaging acceptance tests prior to first-use.

8.1.4 Leakage Tests

The Traveller packaging does not have any requirements for leak testing. The packaging Outerpack and Clamshell are not relied on for containment, and do not require leak testing.

For Type B contents, the fuel rod weld joints are examined at the time of fuel fabrication and leak tested to ensure that they are sealed. The welding and leak testing of fuel rods is performed during manufacturing using a qualified process. This process assures that the fuel is acceptable for use in a nuclear reactor core and is tightly controlled. Leak testing of 100% of Type B contents is required of all fuel rods to the leak tight criteria: a leakage rate less than or equal to $1x10^{-7}$ ref·cm^3/s, with a sensitivity less than or equal to $5x10^{-8}$ ref·cm^3/s, in compliance with American National Standards Institute (ANSI) N14.5 [4].

8.1.5 Component and Material Tests

8.1.5.1 Polyurethane Foam

The Traveller packaging utilizes a closed-cell, polyurethane foam and must be certified to meet the requirements and acceptance criteria for installation, inspection, and testing as defined in this section.

The finished foam product shall be greater than 85% closed-cell polyurethane plastic foam of the self-extinguishing variety of the density specified. The closed-cell configuration will ensure that the foam will not be susceptible to significant water absorption.

If the polyurethane foam doesn't meet the required mechanical, thermal and water absorption properties, the material will be rejected.

8.1.5.1.1 Density

Rigid polyurethane foam shall have a density per Table 8-1.

Table 8-1 Packaging Rigid Polyurethane Foam Density Requirements

Part	lb/ft^3 (pcf)
Endcap Impact Limiters	20.0 ± 2.0
Outerpack Package Body	10.0 ± 1.0
Inner Pillow Impact Limiters	6.0 ± 1.0

Density shall be determined in accordance with ASTM D-1622 with the following exceptions:

a) A minimum of one specimen per pour shall be taken, distributed regularly throughout the batch.

b) Conditioning shall be 70°F to 80°F and 40% – 60% relative humidity for 12 hours minimum.

c) Test conditions shall be 70°F to 80°F and 30% – 70% relative humidity.

d) Length, width, and thickness measurements shall be made with a 6-inch digital or dial caliper.

e) Measurements shall be made and reported to the nearest 0.001 inches.

f) Density shall be reported in pounds per cubic foot (pcf) and no correction is made for the (negligible) buoyant effect of air.

g) The standard deviation of the three density determinations need not be calculated or reported.

8.1.5.1.2 Mechanical Properties

Exhibited foam compressive strength for 10% strain parallel to foam rise shall be determined in accordance with ASTM D-1621, with the exceptions noted below, and shall fall within the range of values presented in Table 8-2.

Table 8-2 Packaging Rigid Polyurethane Foam Property Compressive Strength Range

Part	Density (pcf)	Compressive Strength	
		Min	Max
Endcap Impact Limiters	20.0 ± 2.0	888 psi	1332 psi
Outerpack Package Body	10.0 ± 1.0	262 psi	393 psi
Inner Pillow Impact Limiters	6.0 ± 1.0	132 psi	198 psi

Specimen shall be right rectangular prisms 1.0 ± 0.1 inches thick x 2.0 ± 0.1 inches x 2.0 ± 0.1 inches with the 1.0 ± 0.1 inch dimension parallel to the direction of foam rise.

a) A specimen from each batch shall be tested.

b) Conditioning shall be 70°F to 80°F and 40% – 60% relative humidity for 12 hours minimum.

c) Test conditions shall be 70°F to 80°F and 30% – 70% relative humidity.

d) Length, width, and thickness measurements shall be made with a 6-inch digital or dial caliper.

e) Measurements shall be made and reported to the nearest 0.001 inches.

f) Strain rate shall be 0.1 ± 0.05 in/in – min.

g) Only actual values (not averages or standard deviations) need be reported.

8.1.5.1.3 Flame Retardant Characteristics

Flame retardant characteristics shall be qualified by demonstrating compliance with the following requirements. The requirements shall be demonstrated by flame testing described in FAA Powerplant Engineering Report No. 3A. Additional certification testing to validate the flame-retardant characteristics shall also be performed in accordance with ASTM F-501-93. The test described in b) below is not applicable to the 6 pcf foam.

a) Foam shall not be capable of sustaining a flame for a period greater than five (5) minutes, following the removal of the heat source and after being exposed to temperatures up to 1,500°F. A heat source with a flame temperature of at least 1,500°F is applied until the foam is ignited. The heat source is removed after ignition of the foam and the time until self-extinguishment of the flame (absence of flame) will be monitored and compared against the 5-minute acceptance criteria.

b) Prepare a representative sample of the foam material and test in accordance with the following:

   1) Cut two pieces of sheet metal (16 gauge maximum/25 gauge minimum) to a size sufficient to cover a 10 inch diameter test sample.

   2) Attach a thermocouple at the approximate center of one side of each piece of sheet metal.

   3) Prepare a representative sample of the foam material inside a 10-inch inner diameter by 6-inch long steel cylinder. Foam to fill the entire length of the cylinder and the full 10-inch diameter.

   4) Sandwich the sample between the two pieces of sheet metal, with the thermocouples in contact with the foam.

   5) Expose one end of the foam sample (sheet metal) to a heat source. Apply enough heat to cause the indicated thermocouple temperature to increase from ambient temperature to 1,475°F minimum on the exposed side.

   6) Hold the sample at a minimum of 1,475°F for a minimum period of thirty (30) minutes.

Acceptance criteria shall be as follows:

During the period that heat is applied, the thermocouple on the non-exposed end of the sample shall not exceed 180°F. The thermocouple on the back side (away from the flame) shall be isolated from the sheet metal to prevent heat from radiating from the metal instead of traversing the foam core. The thermocouple can be isolated using a piece of Nomex cloth or approved equivalent.

8.1.5.1.4 Thermal Properties

The foam shall exhibit the following nominal thermal characteristics for the 6 pcf, 10 pcf, and 20 pcf nominal density pours, minimum of three specimens per qualification:

a) Thermal Conductivity (Table 8-3)

Table 8-3 Packaging Rigid Polyurethane Foam Thermal Conductivity Properties

Part	**Thermal Conductivity** (Test Method – ASTM C-177 at 75°F mean temperature)	**Density (pcf)**	**k-factor** (BTU/Hr-ft^2-F/inch)
Inner Pillow Impact Limiters	LAST-A-FOAM® FR-3706	6.0 +/- 1.0	0.240
Outerpack Package Body	LAST-A-FOAM® FR-3710	10.0 +/- 1.0	0.279
Endcap Impact Limiters	LAST-A-FOAM® FR-3720	20.0 +/- 2.0	0.376

b) Specific Heat

0.353 BTU/lb-°F (Test Method – ASTM E-1269)

8.1.5.1.5 Water Absorption Properties

The average water absorption by the foam observed through testing using ASTM D-2842, with the following testing exceptions, shall not be more than 5% by volume. The construction of the Traveller will further ensure that, in actual operation, significantly lower water absorption rate would be observed.

a) Length, width and thickness measurements shall be made with a digital or dial caliper.

b) Measurements shall be made and reported to the nearest 0.001 inches.

c) A single specimen of the qualifying material shall be molded to the density range as stated in the density chart above.

d) The specimen shall consist of a single 3.0 inches x 6.0 inches x 6.0 inches (tolerance on dimensions is 0.5 inches) block of foam.

e) No correction shall be made for cut or open cells in the specimen's volume calculations.

8.1.5.1.6 Chemical Composition

The chemical composition of the foam shall be as follows:

C: 50% – 70%
O: 14% – 34%
N: 4% – 12%
H: 4% – 10%
P: 0% – 2%
Si: < 1%
Cl: < 1800 PPM
Leachable Chlorides: < 1 PPM
Other: < 1%

The foam is a rigid polyether polyurethane formed as reaction product of the primary chemicals: polyphenylene, polymethylene, polyisocyanate (polymeric isocyanate) and polyoxypropylene glycols (polyether polyols). These materials react to produce a rigid, polyether, polyurethane foam. The foam will not contain halogen containing flame retardant or trichloromonoflouromethane (Freon 11).

Leachable chloride testing is required when using stainless steel as the container structure because free chloride ions in contact with the container sides have been faulted as a contributor to stress corrosion cracking. Leachable chlorides will not be greater than 1 ppm when tested in accordance with either (1) GP-TM9510: Method for Sample Preparation and Determination of Leachable Chlorides in Rigid Polyurethane Foam or (2) EPA 300.0: Determination of Inorganic Anions by Ion Chromatography.

8.1.5.2 Neutron Absorber Plates

Neutron absorber plates are installed along the four faces of the Clamshell to meet the requirements specified in Section 6 of this document. The neutron absorber material, BORAL, is a hot-rolled composite aluminum sheet consisting of a core of uniformly distributed boron carbide and aluminum particles, which is enclosed within layers of pure aluminum forming a solid barrier against the environment. The plates are used to ensure sub-criticality during transportation as a neutron absorber and are not relied upon for the conductivity or mechanical properties. The service conditions are not so severe as to promote significant alterations of these plates. Therefore, durability of these neutron absorbing materials is regarded to meet or exceed the service requirements of this application.

To ensure the BORAL meets the drawing requirements, the plates will be inspected on a periodic basis not to exceed five years per Section 8.2.5. This will ensure that the BORAL maintains its durability throughout its service lifetime. The visual inspection will verify that the plates are present and in good condition. This includes inspection of the BORAL core for chipping or flaking resulting from brittleness. There are no significant routine loads applied to the BORAL plates, therefore no durability problems should arise during normal conditions of transport.

No processing changes are anticipated for the production of BORAL since the established process will be used to produce the packages.

8.1.5.2.1 Boron-10 Areal Density

The BORAL neutron absorber plate minimum ^{10}B areal density for the final thickness of [ ]^{a,c} is [ ]^{a,c}. Acceptance testing to ensure that the manufacturing process is operating in a satisfactory manner may be conducted using neutronics transmission or chemical analysis to ensure an effective minimum ^{10}B areal density of [ ]^{a,c}.

Neutron Transmittance is a neutron counting testing technique performed to determine the concentration of an isotope in a material. Testing involves placement of test coupons in a calibrated neutron source beam and measuring the number of neutrons allowed to pass through the test material. Based on the neutron count, the areal density of the coupon can be calculated and compared to certified standards. Chemical analysis is assay testing performed on a sample taken from test coupons to determine the boron content.

8.1.5.2.2 Neutron Absorption Testing Requirements

Neutron Transmittance testing shall be performed at thermal neutron energies per approved test method to verify the minimum required ^{10}B concentration. Test coupons are considered acceptable when the transmittance data indicates a ^{10}B areal density equal to or greater than [ ]^{a,c}. Statistical data on transmissivity may be coupled with luminescence test data to demonstrate uniformity of the boron material.

Neutron Radiograph testing shall be performed for each selected sample with a luminance test or approved equivalent to verify the uniformity of the ^{10}B distribution in the sheet at thermal neutron energies. Neutron Radiograph (luminance) testing is a non-destructive imaging technique for the internal evaluation of materials. It involves attenuation of a neutron beam by an object to be radiographed, and registration of the attenuation process (as an image) on film or video. Inspection results shall be recorded using the appropriate data recording method by the testing facility.

8.1.5.2.3 Chemical Testing Requirements

Chemical testing may be employed as an acceptable substitute to the neutronics testing to verify the minimum areal density of ^{10}B is present in the neutron absorber plate. Prior to ^{10}B verification by chemical testing, the process shall be demonstrated to be equivalent to the neutronics testing described with respect to ^{10}B uniformity and isotopic composition. Test coupons are considered acceptable when the calculated ^{10}B areal density is equal to or greater than [ ]^{a,c}.

8.1.5.2.4 Sampling Rates and Test Methods

The inspection levels shall be as stipulated in the supplier-submitted process specification(s). Test methods, when not referenced herein, shall be reviewed by Westinghouse Engineering. Sample coupons shall be randomly selected and be representative of the configuration, material, and lot being evaluated. The test methods are outlined in Table 8-4.

Table 8-4 Packaging Material Test Methods

Requirement	Number of Tests Per Lot	Test Method
Aluminum Alloy Compositions	1 per Heat	ASTM B209/B221 and Approved Procedure
Neutron Radiograph	100%(1)	WEC Approved Procedure
Neutron Transmittance for ^{10}B Areal Density	100%(1)	WEC Approved Procedure
Chemical Testing	100%(2)	WEC Approved Procedure

Notes:

(1) For every lot, initial sampling of coupons for neutron transmission measurements and radiograph/ radioscopy shall be 100%, which shall be considered normal sampling. Rejection of a given coupon shall result in rejection of any contiguous plate(s). Reduced sampling (50%) may be introduced based upon acceptance of all coupons in the first 25% of the lot. The approved process specification shall reflect the use of reduced sampling, as applicable. A rejection during reduced inspection will require a return to 100% inspection of the lot.

(2) For every lot, initial sampling of coupons for chemical testing shall be 100%, which shall be considered normal sampling. Rejection of a given coupon shall result in rejection of any contiguous plate(s). Reduced sampling of the lot to 95/95 confidence sampling is acceptable based upon acceptance of all coupons in the first 25% of the lot. The approved process specification shall reflect the use of reduced sampling, as applicable. A rejection during reduced inspection will require a return to 100% inspection of the lot.

8.1.5.2.5 Mechanical Tests

The neutron absorber plates perform a neutronic function of the Traveller package. Thus, no mechanical testing is required.

8.1.5.2.6 Visual Inspection

For all plates, the finished plate shall be free of visual surface cracks, blisters, pores, or foreign inclusions.

Evidence of foreign material shall be cause for rejection (embedded pieces of B_4C matrix are not considered foreign material). Creases or other surface discontinuities are acceptable on the cladding of the BORAL provided the core is not exposed. If necessary, the plate shall be examined by visual inspection per approved procedure(s) to determine if a surface indication is a crease or a crack. Surface roughness shall not exceed 125 RMS roughness maximum.

8.1.5.2.7 Test Terminology

Acceptance test criteria are as follows:

a) Lot Definition – A lot shall consist of all plate of the same nominal size, condition and finish that is produced from the same heat, processed in the same manner, and presented for inspection at the same time.

b) Heat Definition – A heat shall consist of the total molten metal output from a single heating in a batch melting process or the total metal output from essentially a single heating in a continuous melting

operation and targeted at a fixed metal chemistry at the furnace spout.

c) Coupon (BORAL) – A selected sample of the thinnest section of a lot of the neutron absorber used for acceptance testing of the candidate material.

8.1.5.3 Polyethylene Moderator Blocks

This section establishes the requirements and acceptance criteria for inspection and testing of Ultra High Molecular Weight (UHMW) Polyethylene moderator blocks utilized within the Traveller packaging.

The supplier shall certify that the polyethylene is Ultra High Molecular Weight (UHMW) complies with ASTM D4020 including a specific gravity greater than 0.93.

8.1.6 Shielding Tests

The Traveller package does not contain any purpose-built shielding components. Therefore, shielding tests are not required.

8.1.7 Thermal Tests

The material properties utilized in Chapter 3, Thermal Evaluation, are consistently conservative for the Normal Conditions of Transport (NCT) thermal analysis performed. The Hypothetical Accident Condition (HAC) fire certification testing of the Traveller package (see Section 3.4.3) verified material performance in the HAC thermal environment. As such, with the exception of the tests required for specific packaging components as discussed in Section 8.1.5, Component and Material Tests, specific acceptance tests for material thermal properties are not required or performed.

8.2 MAINTENANCE PROGRAM

This section describes the maintenance program used to ensure continued performance of the Traveller package.

Visual inspection for damage of all exposed surfaces will be performed before each use. Individual components will also be inspected as described in the sections below. If any defects are found during inspection, the package will be segregated and dispositioned by standard site procedure before its next use.

8.2.1 Structural and Pressure Tests

The Traveller packaging does not contain any structural or lifting/tie-down devices that require testing.

The Traveller packaging is not pressurized, therefore no pressure testing of the packaging is required.

8.2.2 Leakage Tests

The Traveller packaging does not have any requirements for leak testing. The packaging Outerpack and Clamshell are not relied on for containment, and do not require leak testing.

For Type B contents, each fuel rod is leak tested prior to transport (per Section 8.1.4) to assure it is leaktight

in compliance with ANSI N14.5 [4]. The leak testing assures each fuel rod has satisfactorily passed the leak rate requirements defined by 10 CFR 71.51 and SSR-6 para. 659. Fuel assemblies are intended for one-time contents in the Traveller packaging, and thus maintenance is not provided.

The Traveller packaging is not credited with providing leak protection. Therefore, no leak test of the packaging is required.

8.2.3 Component and Material Tests

8.2.3.1 Fasteners

Threaded components shall be inspected prior to each use for deformed or stripped threads. Damaged components shall be repaired or replaced prior to further use.

8.2.3.2 Weather Gasket

Prior to each use, visual inspection of the silicone rubber or fiberglass weather gasket shall be performed for tears, damage, or deterioration. Unacceptable gaskets shall be replaced.

8.2.3.3 Shock Mounts

Prior to first use and at an interval not to exceed five years or 50 cycles, whichever is more limiting, each Lord Sandwich Shock Mount (Part Number J-5425-275 or engineering approved equivalent) shall be visually inspected. The inspection shall verify the condition of the shock mount for tears, missing material or deterioration from aging. A load shall be placed on the Clamshell to tension the shock mounts to visually inspect. A light source with a videoscope is used to inspect the full circumference of each shock mount. Damaged or suspect shock mounts shall be replaced with Lord Sandwich Shock Mount Part Number J-5425-275, or engineering approved equivalent.

8.2.4 Thermal

Because the Outerpack of the Traveller package is constructed of rigid polyurethane foam encapsulated in stainless steel, no degradation of heat transfer capability will occur during normal conditions of transport. Therefore, routine thermal tests are not necessary to ensure continued thermal performance of the Traveller packaging.

8.2.5 Neutron Absorber Plates

On a periodic basis (not to exceed five years or 50 cycles, whichever is more limiting), packages will be inspected to verify the neutron absorber plate configuration complies with the drawing requirements. Quality Control Instructions and Mechanical Operating Procedures will define the specific inspection requirements. In accordance with established site procedures, a visual inspection will be conducted of the visible side of the neutron absorber plates. Personnel will visually verify that the plates are present and in good condition. Any neutron absorber plate with deep scratches or gouges, which expose the inner boron carbide center, shall be replaced. Neutron absorber plates covered with cork rubber shall be visually inspected at each screw location and the cork rubber inspected for signs of tampering. Documentation relating to these inspections, repairs, and part replacements will be produced and maintained.

8.2.6 Periodic Weld Examinations

During routine, scheduled maintenance not to exceed two (2) years, external Outerpack and internal Clamshell structural welds are inspected visually per ASME Section III, subsection NF-5221 Class 2 (c), NF-5222, or an approved Engineering equivalent standard including European EN standard. The lifting eye and forklift leg sub-assembly leg welds, in lieu of visual inspections, may be inspected by non-destructive test methods, such as liquid dye penetrant or magnetic particle, per ASME Section III, subsection NF-5221 Class 2 (a), or an approved Engineering equivalent standard including European EN standard.

8.2.7 Periodic Acetate Plug Examinations

During routine, scheduled maintenance not to exceed two (2) years, the Outerpack acetate plugs are inspected visually for obvious physical damage. The visual and functional inspection requires that acetate plugs be replaced if any of the following conditions are found:

- Thru-the-wall cracks are present or cracking along full length/width of the plug.
- During tightening (hand tool, 9/16 inch or 15 mm ratchet wrench), cracking is observed.
- During tightening (hand tool, 9/16 inch or 15 mm ratchet wrench), the acetate plug will not thread into the threaded vent port.

8.3 APPENDICES

8.3.1 References

[1] U.S. Nuclear Regulatory Commission Code of Federal Regulations, Title 10 Part 71, "Packaging and Transport of Radioactive Material," 2016.

[2] International Atomic Energy Agency, "Regulations for the Safe Transport of Radioactive Material," Specific Safety Requirements No. SSR-6, 2012.

[3] American Socity of Mechanical Engineers, "ASME Boiler and Pressure Vessel Code, Rules for Construction of Nuclear Power Plant Components, Section III," 2001 with 2003 Addenda.

[4] American National Standards Institute, "Leakage Tests on Packages for Shipment," ANSI N14.5-2014, 2014.